KINGSTON UNIVERSITY

BIOCHEMICAL EVALUATION OF POTENTIAL ENZYME INHIBITORS

A THESIS SUBMITTED IN ACCORDANCE WITH THE CONDITIONS GOVERNING CANDIDATES FOR THE DEGREE OF DOCTOR OF PHILOSOPHIAE

BY

SACHIN PARYANTRAY DHANANI

SCHOOL OF LIFE SCIENCES
PENRHYN ROAD
KINGSTON-UPON-THAMES
LONDON
KT1 2EE

August 2006

Acknowledgements

I am deeply indebted to Prof. Sabbir Ahmed, my second supervisor, for his assistance, guidance, advice and encouragement throughout this project and the opportunity to carry out this project at Kingston University.

This acknowledgement would not be complete without, mentioning the invaluable technical assistance provided by all of the technicians in the Schools of Life Sciences. I would like to extend my thanks to the Sabbir Ahmed research group, with a special thanks to Dr. Chirag H. Patel, Mr. Imran Shahid and Miss Rupinder Lota. In addition I would like to extend my thanks to my colleagues of Lab EM212 and Dr. Michael Tsang for their continued support, friendship, encouragement and help.

I would like to thank my family especially for all the support they have given me in my time at University and for helping me through the times of pressure. My appreciation goes to my friends for their continued encouragement and for helping me to keep the goals in sight.

Abstract

A high proportion of prostate cancer and benign prostatic hyperplasia (BPH) have been shown to be dependent on androgen biosynthesis. The biosynthesis of androgens is undertaken by a number of important enzymes such as 17α-hydroxylase/17,20-lyase and 17β-hydroxysteroid dehydrogenase. Through the inhibition of these enzymes it is possible to reduce the amount of androgens present, which in turn reduces the stimulation of androgen-dependent prostatic diseases. Within the current study, we have undertaken the biochemical evaluation of a number of compounds of varying structural features and which were synthesised within our group as potential enzyme inhibitors in the tretament of androgen-dependent diseases.

In general, the results from the current study show that the compounds evaluated against the enzyme complex 17α-hydroxylase/17,20-lyase possessed good inhibitory activity. In particular, the imidazole-based inhibitors were found to be more potent against 17,20-lyase in comparison to 17α-hydroxylase, and were more potent than the triazole-based compounds. The most potent compounds within the current study include: 1-(7-phenyl-heptyl)-1H-imidazole (**171**) (IC_{50}=98.5±15.6nM, K_i=55.3±3.4nM against 17,20-lyase and IC_{50}=0.32±0.05μM, K_i=0.21±0.01μM against 17α-hydroxylase), 1-[7-(4-fluoro-phenyl)-heptyl]-1H-imidazole (**179**) (IC_{50}=57.5±1.5nM, K_i=21.5±0.1nM against 17,20-lyase and IC_{50}=173.62±7.00nM, K_i=77.5±2.5nM against 17α-hydroxylase) and 1-[5-(4-bromo-phenyl)-pentyl]-1H-imidazole (**187**) (IC_{50}=58.1±5.2nM against 17,20-lyase and IC_{50}=0.50±0.04μM against 17α-hydroxylase), these compounds were all potent inhibitors compared to the standard inhibitor ketoconazole (**1**) (IC_{50}=1.66±0.15μM, K_i=0.67±0.02μM against 17,20-lyase and IC_{50}=3.76±0.01μM, K_i=1.24±0.01μM against 17α-hydroxylase).

In an effort to discover lead compounds in the inhibition of the 17β-hydroxysteroid dehydrogenase (17β-HSD) family of enzymes, a range of commercially available compounds based on phenyl ketones were initially evaluated against type 1 (17β-HSD1) and 3 (17β-HSD3) of 17β-HSD which are responsible for the reduction of estrone and androstenedione to estradiol and testosterone respectively. The majority of these compounds were found to possess weak inhibitory activity, however, some were found to possess good inhibitory activity. As such, a number of compounds were synthesised within our group as potential inhibitors of 17β-HSD1 and 17β-HSD3. The results show that the 4-hydroxyphenyl ketone-based compounds were found to be highly potent against type 3 in comparison to type 1. For example, 1-(4-hydroxy-phenyl)-nonan-1-one (**254**) was found to possess (against type 3) inhibitory activity of 83.53±0.48% (at [I]=100μM) (IC_{50} of 2.86 ± 0.03μM). Under similar conditions, **254** was found to possess 36.32±0.33% (at [I]=100μM) inhibitory activity against type1. A range of compounds were also synthesised based on the biphenyl ketones, however, these were found to be weaker inhibitors of type 3 in comparison to the 4-hydroxyphenyl ketones although they possessed greater inhibitory activity against type 1. In an effort to determine the selectivity of these compounds against the overall class of HSD enzymes, all inhibitors were evaluated for 3β-hydroxysteroid dehydrogenase (3β-HSD) inhibitory activity. We discovered that in general, all of the synthesised compounds possessed weak inhibitory activity against this enzyme at inhibitor concentration of 100μM and 500μM, as such, these synthesised compounds could be considered to be good lead compounds for the inhibition of 17β-HSD.

Chapter 1

1.0 INTRODUCTION

1.1 Cancer

The word cancer is used to describe a group of diseases in which cell reproduction has malfunctioned, leading to uncontrolled cell division, resulting in the eventual loss of specificity of the cell (Eales et al, 1997). Cancer does not only exist as a single disease but as part of a family of diseases, consisting of over 200 different types, which respond to different treatments.

During the development of cancers, four main features have been noted:

- **Excessive cell proliferation:** resulting in the formation of the tumour.

- **Loss of tissue specific characteristics:** in the early stages, cancer cells that are formed appear and function similarly to the original cells from which they are derived, but as the tumour progresses, the tumour cells begin to differ functionally, as well as in appearance.

- **Invasiveness:** the tumour begins to spread into adjacent tissues, and is the point at which it begins to become malignant. [Some tumours, however, may exist as benign growths (tumours which do not have the ability to damage tissue or spread to distant sites in the body)].

- **Metastasis:** the tumour begins to establish itself in sites distant from the initial site of the growth. Most patients who die of cancer usually do so as a result of metastasis to vital organs such as the brain or liver; there are only a limited number of cases where the patient dies due to the primary tumour, as they can usually be removed surgically (Rang et al, 1996).

1.2 The prostate gland

The prostate is composed of tubular and alveolar glands arranged in lobules surrounded by a stroma. It is positioned deep within the pelvis, and is rich in nerves, smooth muscle, connective tissue and lymphatic vessels. This surrounding stroma not only physically supports the glandular epithelium but also contributes to the endocrine and paracrine microenvironment. The fibromuscular and glandular organ is made up of four regions: three glandular zones and a fibromuscular stroma (Figure 1.1).

The three glandular zones are the transition zone, the central zone and the peripheral zone (McNeal, 1981). The transition zone surrounds the prostatic urethra, the central zone surrounds the ejaculatory ducts from the base of the prostate to the verumontanum, whilst the peripheral zone is posterior and lateral to the prostate.

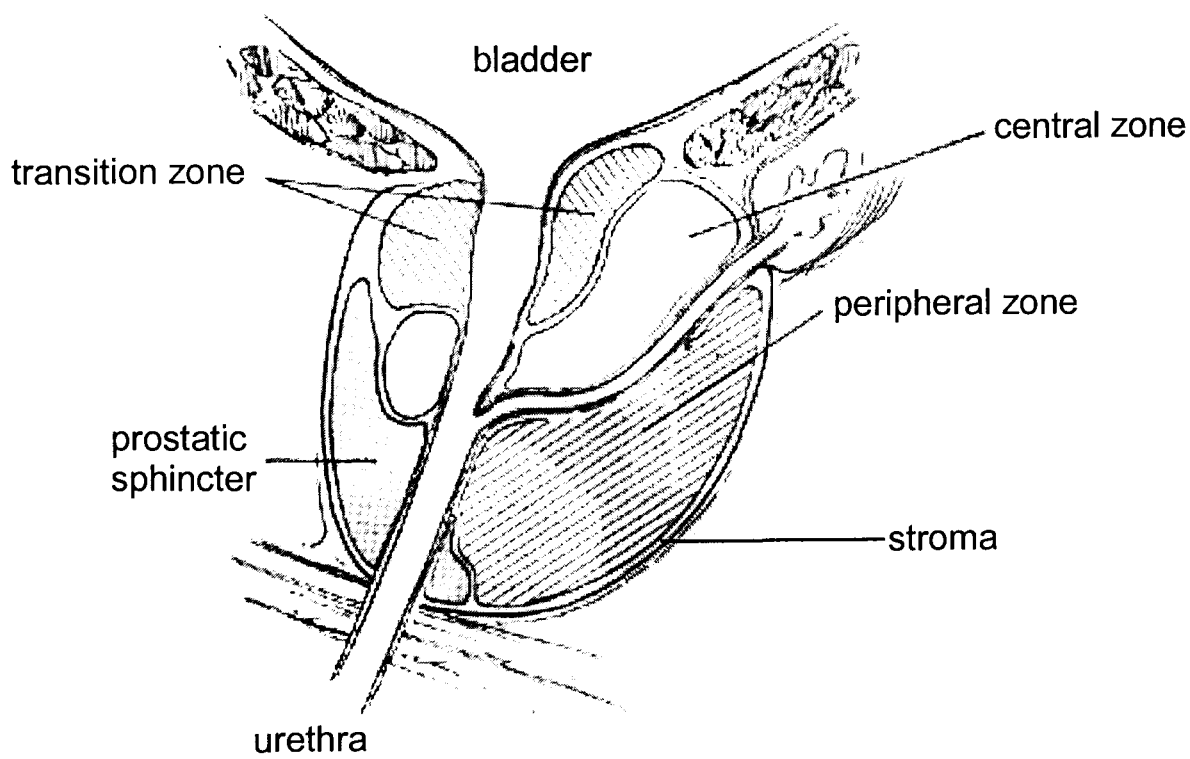

Figure 1.1 Glandular zones of the prostate (Shen et al, 2001)

The composition of the glandular component is mainly of two types of epithelial cells: luminal and basal, and is interspersed with occasional neuroendocrine cells.

The basal layer is made up of cuboidal cells and the luminal layer is made up of a layer of columnar secretory cells. The basal cells next to the basement membrane include the stem cells that form the proliferative compartment of the prostate epithelium. The luminal cells synthesise and secrete the products of the seminal fluid, including prostate-specific antigen (PSA) and prostate-specific acid phosphatase, polyamines and prostaglandins (Allsbrook and Simms, 1992; Leong et al, 1988). The luminal cells express androgen receptors (AR) and are dependent on androgenic stimulation for their viability and secretory ability.

The prostatic stroma is a mixture of smooth muscle cells, fibroblasts, blood vessels and nerves within the intervening extracellular matrix. Prostate growth and differentiation is critically dependent on highly complex but poorly understood epithelial-stromal interactions (Pentyala et al, 1998; Chung et al, 1991; Cunha et al, 1983).

1.3 Endocrinology of the prostate

At puberty, when the testes begin to secrete large quantities of testosterone (T), there is a large increase in prostate growth (Nnane et al, 1999b; Suzuki et al, 2001). Up to the age of forty-five, the size of the prostate stays constant, but at approximately fifty years, there is often another increase in prostate growth, despite levels of T decreasing and it is postulated therefore, that an unknown factor is involved in the continued growth of benign prostate hyperplasia (BPH, Section 1.4) and prostate cancer (Section 1.5) in older men (Mahapokai et al, 2000; Long et al, 2000).

The majority of circulating T is synthesised within the testes, although approximately 10% is produced from adrenal precursors. The hypothalamus releases luteinizing hormone releasing hormone (LHRH) in pulses, which in turn results in the pulsatile release of follicle stimulating hormone (FSH) and luteinizing hormone (LH). There is promotion of T production by the attachment of LH to receptors on the Leydig cells of the testes (Gregory et al, 2001; Landis et al, 1999; Lin et al, 1993; Linja et al, 2001; Pentyala et al, 2000).

The T produced by the testes is transported in the blood bound to steroid hormone binding globulin; it enters the prostate cell and is converted by 5α-reductase (5AR) to dihydrotestosterone (DHT). This conversion promotes further passive diffusion of T into the cell. DHT then binds to the AR in the cytoplasm and this DHT-AR complex moves into the nucleus where, after binding to a nuclear acceptor site, stimulates the synthesis of proteins. Synthesised proteins promote further cellular division, along with synthesis of 5AR. It is the preferential binding of DHT to the AR rather than T that produces the given effect in the prostatic epithelial cells (Bratoeff at al, 1999).

1.3.1 Androgen Receptors (AR)

AR are specific androgen-binding proteins (termed androphilin) and are located in the cytoplasm and nucleus of androgen responsive prostate cells. In order for androgens to influence the biological activity and growth rate of prostate cells the presence of androgen receptors is necessary. As T levels decline during the normal ageing process the number of AR would be expected to decline, however the reverse is observed, utilising a greater percentage of the T and DHT, which is hypothesised for the resulting growth of the prostate.

Molecular biology has shown the importance of the DHT-AR complex in the regulation of gene expression. The other major influence on cellular homeostasis and regulation of prostatic growth is exercised by a number of intrinsic factors (e.g. peptide growth regulatory factors) through various paracrine, autocrine or intracrine interactions (Quigley et al, 1995).

1.4 Benign Prostate Hyperplasia (BPH)

BPH is a non-malignant enlargement which is due to the growth of the stromal and glandular components of the prostate (Frye, 1996). There are two major factors associated with BPH: the presence of testes and ageing (Denis and Mahler, 1990). The prostate reaches its full adult size by the age of twenty and remains constant until fifty years of age (Siiteri and Wilson, 1970), when there is

a 75% probability of the male population experiencing BPH. The detection of hyperplasia is difficult before the age of forty but by the age of forty-five, 50% of the male population demonstrates histological hyperplasia on autopsy, and by the age of ninety, it is proposed that most men will have histologic BPH (Isaacs, 1990; Arrighi et al, 1991).

BPH is the formation of nodules, which increase the size of the gland and, as the prostate is located below the bladder surrounding the urethra, consequently results in the obstruction of the urinary tract (Isaacs, 1990; Arrighi et al, 1991). It has been shown that BPH depends on testicular androgens and that the absence of functioning testes before the age of forty prevents both BPH and prostate cancer (Huggins and Hodges, 1941; Geller, 1993). BPH is caused by increased levels of DHT (Imperato-McGinley et al, 1974; Siiteri and Wilson, 1970), the most potent androgen. DHT is necessary for the development of male characteristics (e.g. thick hair growth, acne, baldness), external genitalia and as mentioned, the prostate (Imperato-McGinley et al, 1974).

1.5 Prostate Cancer

Prostate cancer is the most common malignancy in men over the age of forty years (Frye et al, 1996) and can be of two types: hormone-dependent or hormone-independent. It has been established that the level of circulating androgens is very important to the growth and spread of prostate cancer (Huggins and Hodges, 1941). The chances of developing prostate cancer and the mortality rate increase in relation to age, peaking in those over the age of eighty-five.

1.5.1 Risk factors for prostate cancer

The initiation and promotion of prostate cancer has been linked to environmental factors such as: damaging radiation, chemical, as well as oncogenic viruses. Genetic factors, race, age, hormonal factors and family

history are also recognised risk factors (Catalona et al, 1986; Gormley, 1996). Some of these risk-factors are discussed below.

a Age

As previously discussed, age is a major contributing factor to prostate cancer. As men pass the age of fifty, the prostate gland begins to enlarge. This enlargement is generally benign and may cause slight elevations in the PSA level. Due to the growth of the prostate with increasing age the prostate gland becomes susceptible to malignancies or abnormalities (Crawford, 2003).

b Race and ethnicity

It has been shown that prostate cancer varies widely between race and ethnic groups, for example, African-Americans have the highest incidence rate, whereas native Japanese have amongst the lowest. The reason for these risk differences are not clearly understood but dietary and other culturally-mediated differences have been suspected to play important roles. It has been shown that 5AR activity is higher in Caucasian and Black men compared to Japanese subjects (Ross et al, 1992), which may explain the geographical variations in risk not explained by environmental exposure and cultural differences. The differences may also be due to AR polymorphism (Sartora et al, 1999; Chang et al, 2002).

c Diet

The importance of dietary factors for prostate carcinogenesis has been shown by epidemiological studies. Intake of foods rich in fat including meat, are suggested to be risk factors. It was shown experimentally that high fat intake promoted rat prostate carcinogenesis (Pollard and Luckert, 1986; Kondo et al, 1994; Gann et al, 1994; Giovannucci et al, 1993; Harvei et al, 1997), however, other studies revealed no enhancing effect by high and low fat intake (Pour et al, 1991; Shirai et al, 1991).

Other dietary factors that possibly play a modulatory role in prostate cancer risk are vitamin E [shown to reduce risk (Zhang et al, 2002)], lycopene [shown to reduce risk (Chen et al, 2001)], dairy products/calcium [shown to increase risk (Chan et al, 2001)], vitamin D [shown to reduce risk (Peehl et al, 2003)], selenium [shown to reduce risk (Duffield-Lillico et al, 2003)] and phytochemicals [shown to reduce risk (Giovannucci et al, 2002)].

1.5.2 PSA

It has been postulated that PSA regulates the invasiveness and metastatic potential in prostate cancer pathogenesis (Stenman et al, 1999; Leinonen et al, 2000). PSA is a serine proteinase produced mainly by epithelial cells that line the acini and ducts of the prostate gland (Zhang et al, 2000). Its main biological function is liquefaction of the seminal gel formed after ejaculation. Normal prostate cells produce a PSA count of between 2 and 4ng/mL of blood, however, in prostate cancer over 1000ng/mL PSA can be observed - this is ten to a hundred times more PSA per volume of tumour in comparison to BPH cells (Tortora and Anagnostakos, 1990).

1.5.3 Molecular genetics of prostate cancer

The molecular mechanics for the development and progression of prostate cancer is poorly understood despite its substantial clinical importance. Prostate cancer susceptibility genes may be harboured by four chromosomal loci which have been implicated by linkage analyses. Comparative genomic hybridisation studies have been used to study chromosomal alteration in prostate tumours. These analyses have commonly indicated losses of chromosomes 6q, 8p, 10q, 13q and 16q, as well as gains of 7, 8q and Xq (Laitinen et al, 2002). Gain of 13q12-q13 and loss of 4, 6q24-qter, 20p and 21q have been associated with the acquisition of androgen independence (Hyytinen et al, 1997).

Multicentre linkage studies have associated numerous chromosomal loci with prostate cancer, and epidemiological studies have also suggested that 5-10% of all prostate cancers are familial (Simard et al, 2002).

1.6 Steroid biosynthesis

Steroid hormones are synthesised from cholesterol within the mitochondria. The steroidogenic acute regulatory protein (StAR) mediates the acute stimulation of steroid synthesis, which is an active transporter of cholesterol through the inner mitochondrial membrane.

The majority of the enzymes involved in the synthesis of steroids from cholesterol are from the cytochrome P450 family. Cytochrome P450s are haem-containing proteins which when combined with carbon monoxide possess a characteristic absorption maximum at 450nm. They are part of a family of enzymes known as oxygenases, that is they are able to incorporate/insert an oxygen atom of an oxygen molecule into the substrate (see equation 1.1), whilst the other oxygen atom is reduced to water. The stoichiometry of the monooxygenation is one mole of substrate, one mole of oxygen and one mole of reduced nicotinamide adenine dinucleotide phosphate (NADPH), resulting in one mole of product, one mole of $NADP^+$ and one mole of water (Mason, 1957).

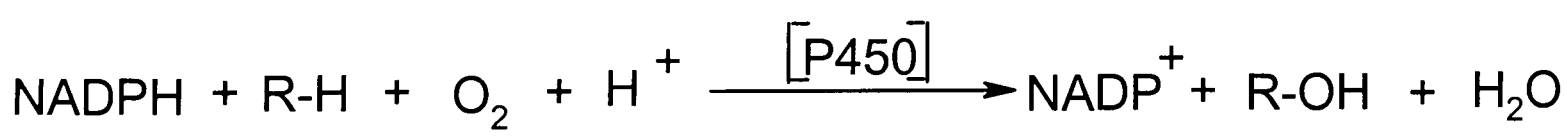

Equation 1.1 Enzymatic reaction for cytochrome P450 monooxygenases.

Proteins with protoporphyrin as cofactor are components of cytochrome P450 (Figure 1.2). It is thought that the haem of cytochrome P450 is not covalently bound to the protein, unlike other haem-containing proteins. The haem iron has the capability of forming a total of six co-ordinate bonds and is located at the centre of the porphyrin nucleus. Pyrrole nitrogen atoms occupy four of its co-ordinate valencies and as they lie in the plane of the haem ring they are

considered planar. The fifth and sixth co-ordination sites are available for binding of two axial ligands, the fifth ligand involving a thiolate ion from a cysteine residue of the apoprotein, which attaches the haem to the protein and is responsible for many of the characteristic properties of cytochrome P450s. The sixth co-ordination site is occupied by a weaker ligand (possibly water or some amino acid side-chain) and can be displaced by substrates or alternative ligands. In addition to these features of the cytochrome P450 molecule, the protein moiety of the enzyme includes a hydrophobic pocket, in which the haem is situated, and a substrate-binding region. However, due to difficulty crystallising these membrane-bound enzymes, specific information regarding the active site still remains unclear.

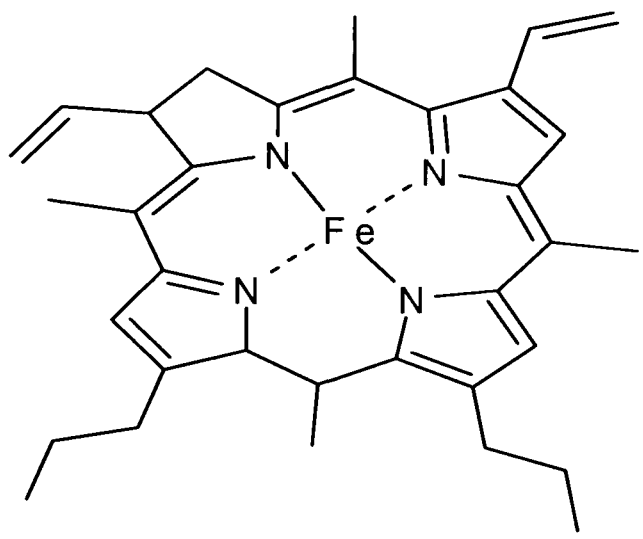

Figure 1.2 Active site of P450 – a single protoporphyrin IX prosthetic group (Oritz de Montellano, 1986, Rovira et al, 1997).

In order for molecules (for example oxygen or carbon monoxide) to bind to the haem iron, it must be reduced from the ferric to the ferrous state. This change also occurs in the presence of substrate which also causes a conformational change, resulting in the loss of the sixth axial bond and a displacement of the iron from the plane of the ring towards the thiolate sulphur (a penta co-ordinate state) (Figure 1.3).

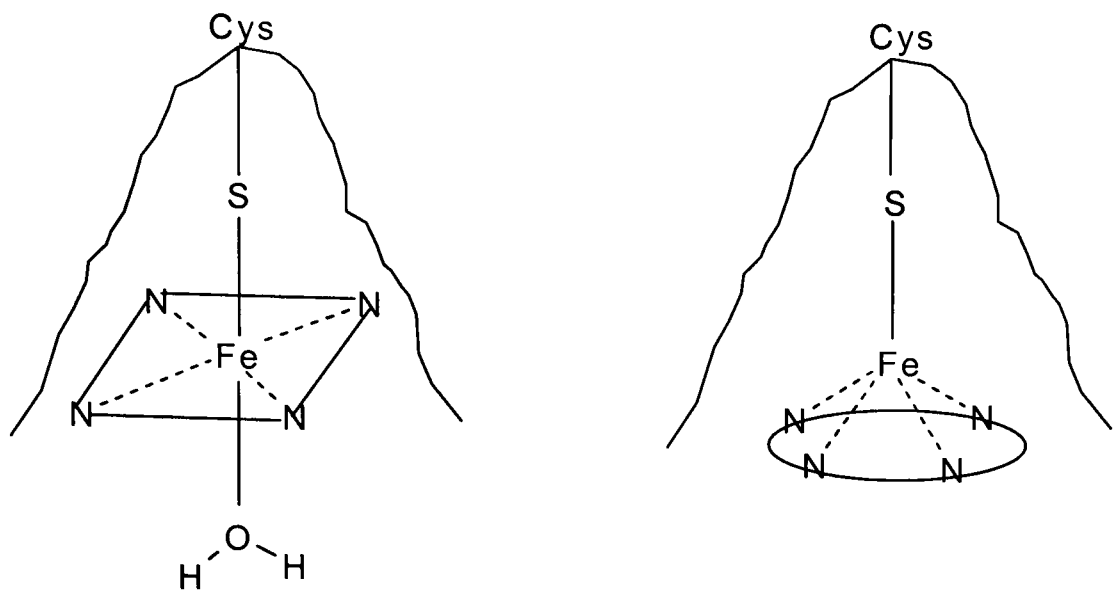

Figure 1.3 Conformational change induced in the P450 active site by the loss of the sixth ligand (Hall, 1986).

The catalytic cycle of cytochrome P450 is depicted by the hypothetical mechanism outlined in Figure 1.4.

1. Substrate binding

The binding of a substrate to a P450 causes a lowering of the redox potential which makes the transfer of an electron favourable from NADH or NADPH, resulting in the low spin hexa co-ordinate iron (**1**) losing the sixth ligand (a water molecule or hydroxyl group from a serine, tyrosine, or threonine residue) to form the penta co-ordinated high spin iron (**2**).

2. The first reduction

The next stage in the cycle involves the reduction of the Fe^{3+} ion by an electron transferred from NAD(P)H which forms a complex with the enzyme, resulting in the uptake of one electron by the iron, resulting in the reduction of the ferric to the high-spin Fe^{2+} state (**3**).

3. Oxygen binding

The reduced Fe^{2+} configuration is now able to co-ordinate one oxygen molecule, promoted by the loss of the sixth ligand, to form a ferric-oxy intermediate (**5**).

4. Second reduction

A second reduction is required by the stoichiometry of the reaction. A second electron is transferred to the ferric-oxy intermediate reducing it to a ferric-peroxy state (**6**) observed from resonance Raman spectroscopy (Egawa et al, 1991).

5. Oxygen cleavage

Cleavage and separation of the two oxygen atoms occurs influenced by the strong electron-pushing ability of the fifth ligand (cysteine), resulting in the release of water and the formation of a ferryl-oxy intermediate (**7**).

6. Oxygen insertion:

It is thought that the oxygen atom (containing only seven electrons) exerts a strong electrophilic activity and abstracts a hydrogen atom or electron from the nearby bound substrate, producing a carbon radical and an Fe^{3+}-bound hydroxyl radical. This latter radical, then recombines with the carbon radical to form the Fe^{3+}-bound hydroxylated substrate.

7. Dissociation:

Dissociation of the hydroxylated product and enzyme occurs.

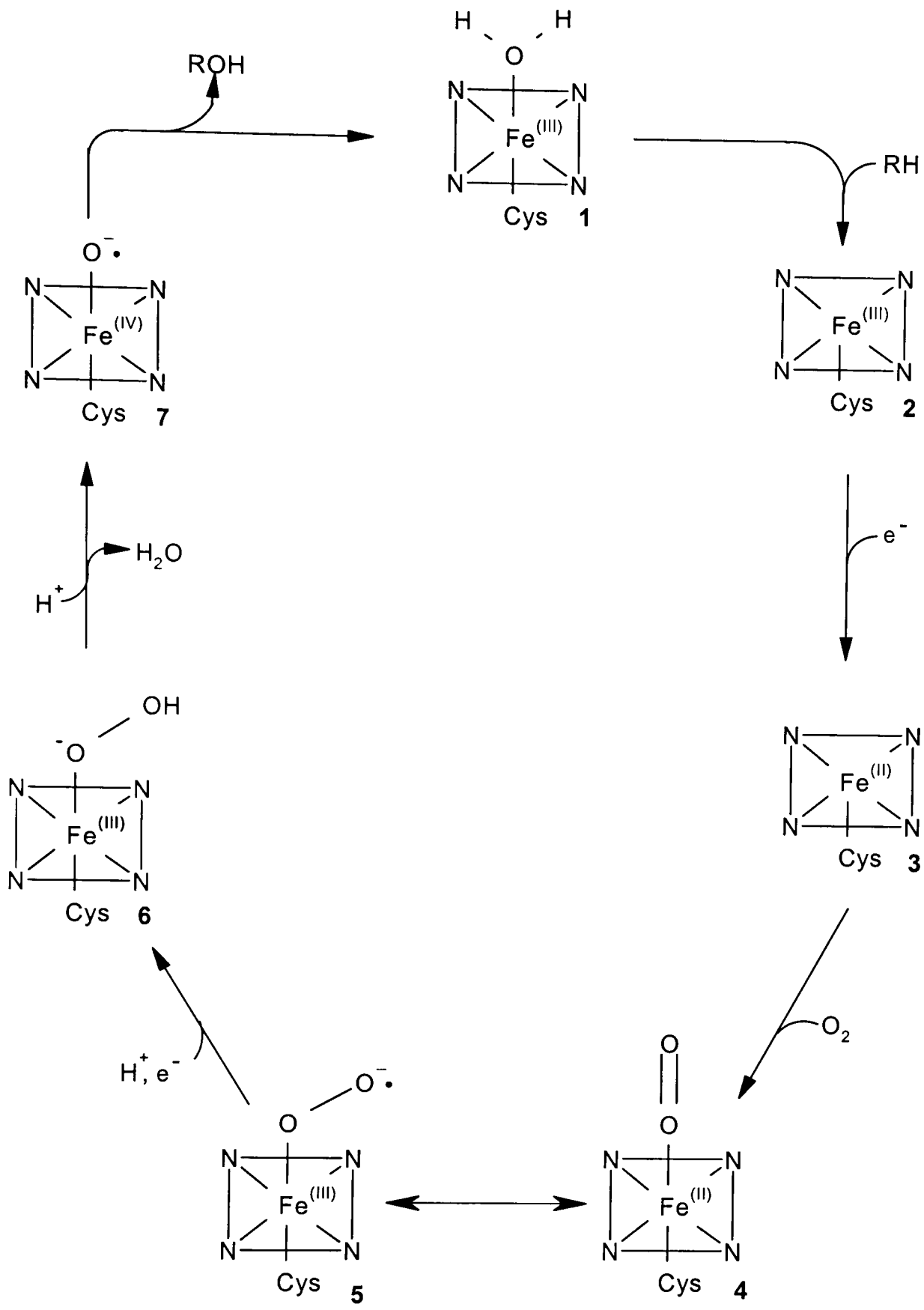

Figure 1.4 The catalytic cycle of cytochrome P-450 (Van Wauwe and Janssen, 1989).

Cytochrome P450s involved in steroidogenesis may be microsomal or mitochondrial. Microsomal cytochrome P450s are insoluble in water and are difficult to remove from the microsomal membrane, whereas mitochondrial enzymes are soluble in aqueous buffer and are associated with the inner mitochondrial membrane. The steroidogenic cellular location of enzymes can be illustrated diagrammatically as in Figure 1.5.

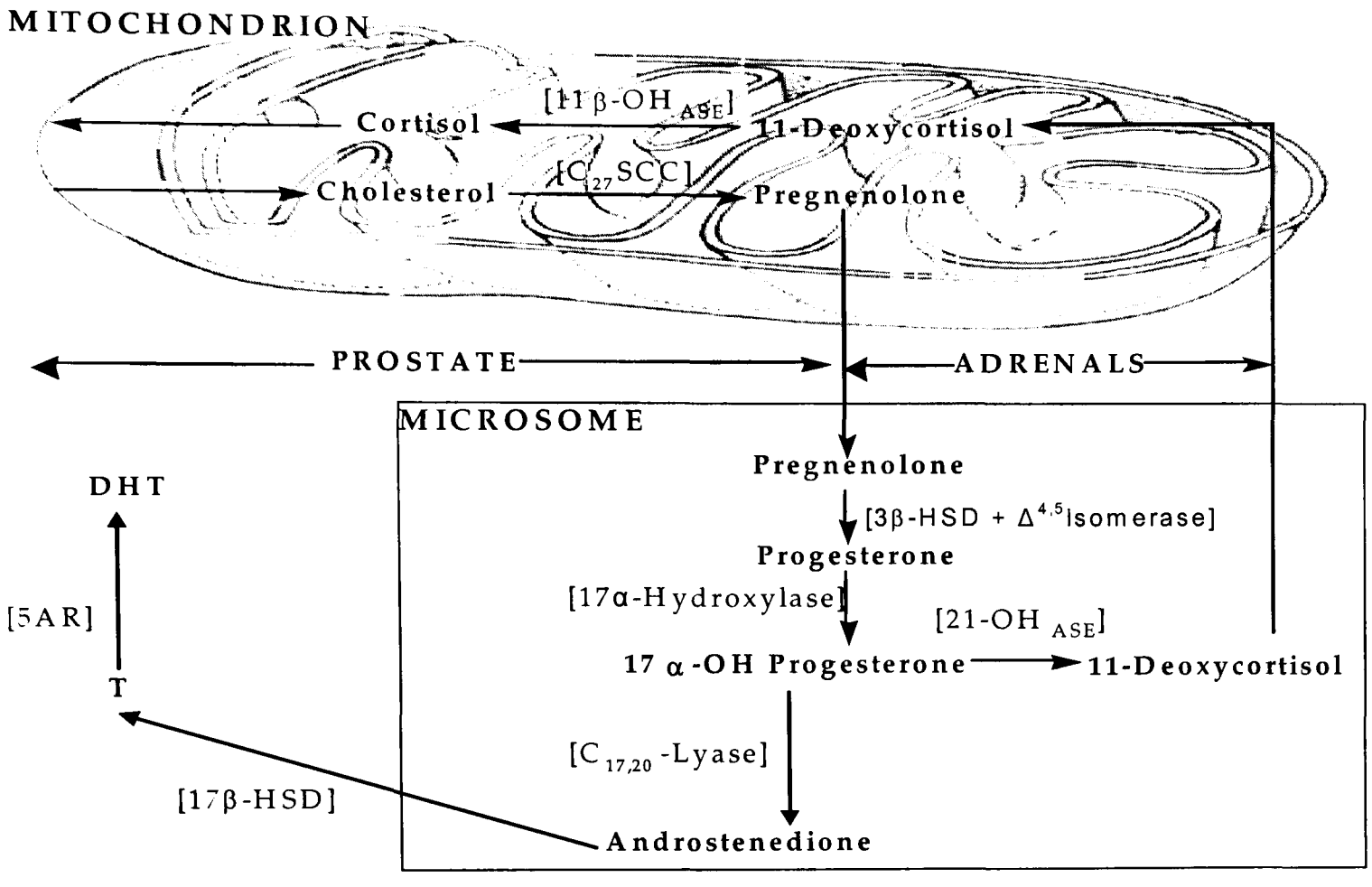

Figure 1.5 Subcellular location of steroidogenesis enzymes within steroidogenic cells (Hall, 1986; Auzeby et al, 1995).

The first enzymatic step in the steroidal cascade from cholesterol to pregnenolone (Preg) is mediated by the cytochrome P450 enzyme cholesterol side chain cleavage ($P450_{scc}$) (Figure 1.6). The 3β-hydroxysteroid dehydrogenase (3β-HSD) enzyme catalyses the oxidation of the 3β-hydroxide converting Preg to progesterone (P) while isomerisation of the double bond of the steroid B ring to the steroid A ring occurs by the action of the isomerase enzyme. Androgen biosynthesis involves the conversion of P to androstenedione (A) by the action of 17α-hydroxylase/17,20-lyase ($P450_{17\alpha}$). This is then converted to the more potent androgen T by the action of 17β-hydroxysteroid dehydrogenase (17β-HSD) which is converted further to the most potent androgen DHT by the action of 5AR (Figure 1.6).

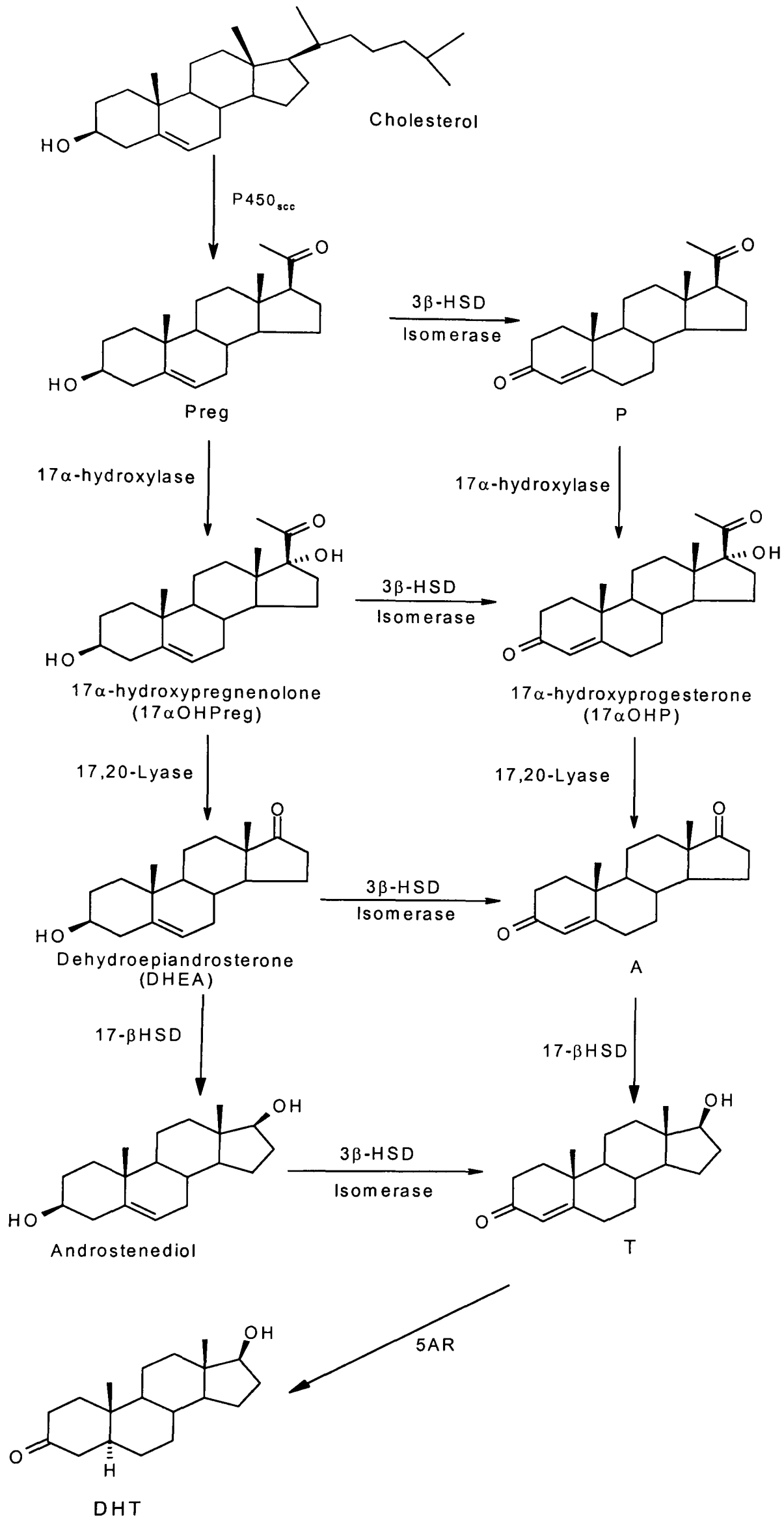

Figure 1.6 Steroidal cascade from cholesterol to DHT

1.6.1 17α-Hydroxylase/17,20-lyase ($P450_{17\alpha}$)

As shown in Figure 1.6, cholesterol is converted to Preg and P, which undergo further conversion by $P450_{17\alpha}$ to dehydroepiandrosterone (DHEA) and A respectively. This conversion occurs in two steps by two separate components, the first being the hydroxylation of Preg and P by 17α-hydroxylase to form 17α-hydroxypregnenolone (17αOHPreg) and 17α-hydroxyprogesterone (17αOHP) respectively. The second step involves the cleavage of the C(17)-C(20) bond by 17,20-lyase, resulting in the formation of the C(17) carbonyl functionality. Both of these reactions are undertaken by a single enzyme, which is expressed in both adrenal and testicular human tissues.

The enzyme is encoded for by the CYP17 gene located on human chromosome 10 (Matteson et al, 1986; Sparkes et al, 1991). In the testes this enzyme is localised on the endoplasmic reticulum of the Leydig cells, in the ovaries it is localised on the theca interna region and in the adrenals it is localised on the zona reticularis (Chan et al, 1996; Kühn-velten and Staib, 1983; Mesiano et al, 1993; Sasano et al, 1989).

The activity of both 17α-hydroxylase and 17,20-lyase is decreased upon disruption of the lipid environment (Perrin et al, 1995). The activity of the enzyme requires the presence of NADPH and NADPH cytochrome P450 reductase (Barrie et al, 1996), as well as cytochrome b_5 which acts as an alternative electron donor in the donation of the second electron in the P450 cycle. The 17α-hydroxylation catalysis of the steroids P and Preg occurs to produce their 17α-hydroxy derivatives, which in turn is followed by the cleavage of the C17,20 carbon-carbon bond to give A and DHEA respectively (Nakajin et al, 1981). It was reported by both Chabre et al (1993) and Georgiou et al (1987) that 17α-hydroxylase and 17,20-lyase activity are both sensitive to effects of low oxygen, whereby 17,20-lyase is more sensitive than 17α-hydroxylase. A similar effect was noticed in the case of the amount of NADPH cytochrome P450 reductase present (Lin et al, 1993).

The postulated catalytic cycle for 17α-hydroxylase is shown in Figure 1.7: the hydroxylation is believed to occur via an iron-monooxygen (feroxy) species (Akhtar et al, 1997; Lee-Robichaud et al, 1998).

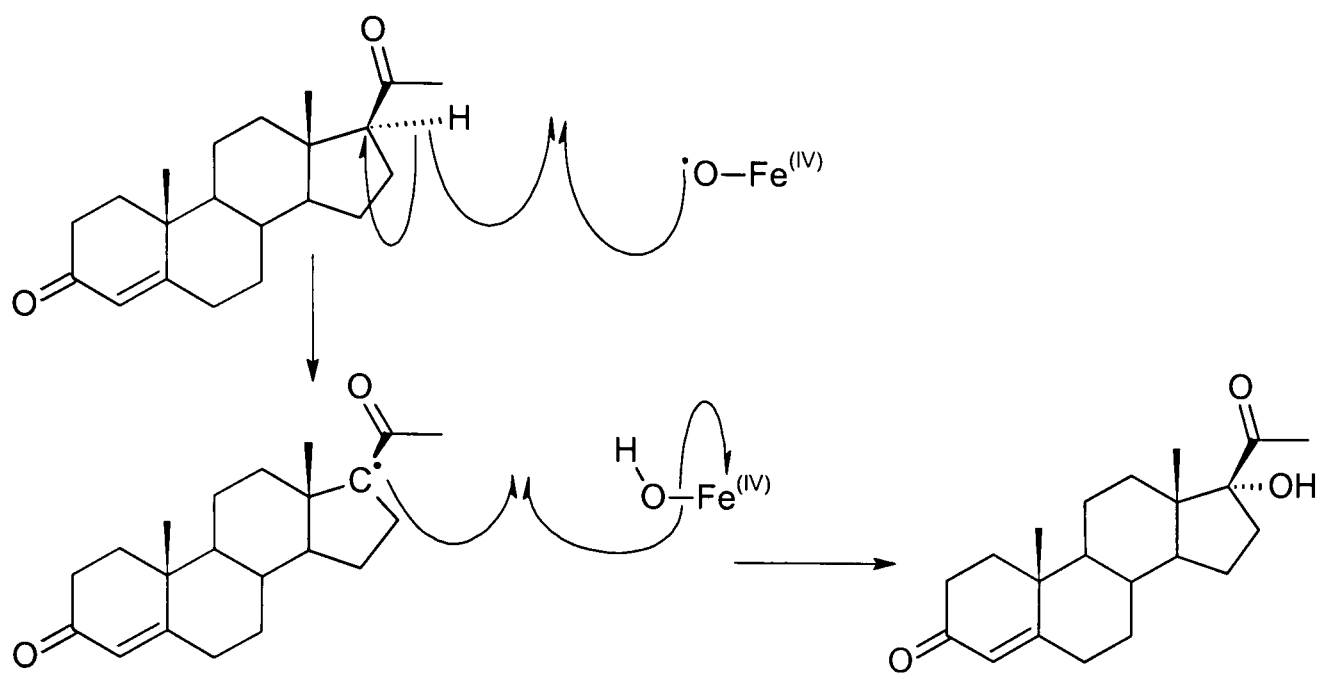

Figure 1.7 The postulated mechanism for the hydroxylation of P by 17α-hydroxylase (Akhtar et al, 1997; Lee-Robichaud et al, 1998).

Several mechanisms have been suggested for the 17,20-lyase step, some involving attack by a ferroxy species (Ahmed and Owen, 1998), others by a peroxy species (Akhtar et al, 1997). Workers within our group have suggested a mechanism involving the ferroxy species rather than both the ferroxy and peroxy species in the mechanism where attack on the C(20) carbonyl group takes place prior to the attack on the C(17). This postulated catalytic cycle for 17,20-lyase is shown in Figure 1.8

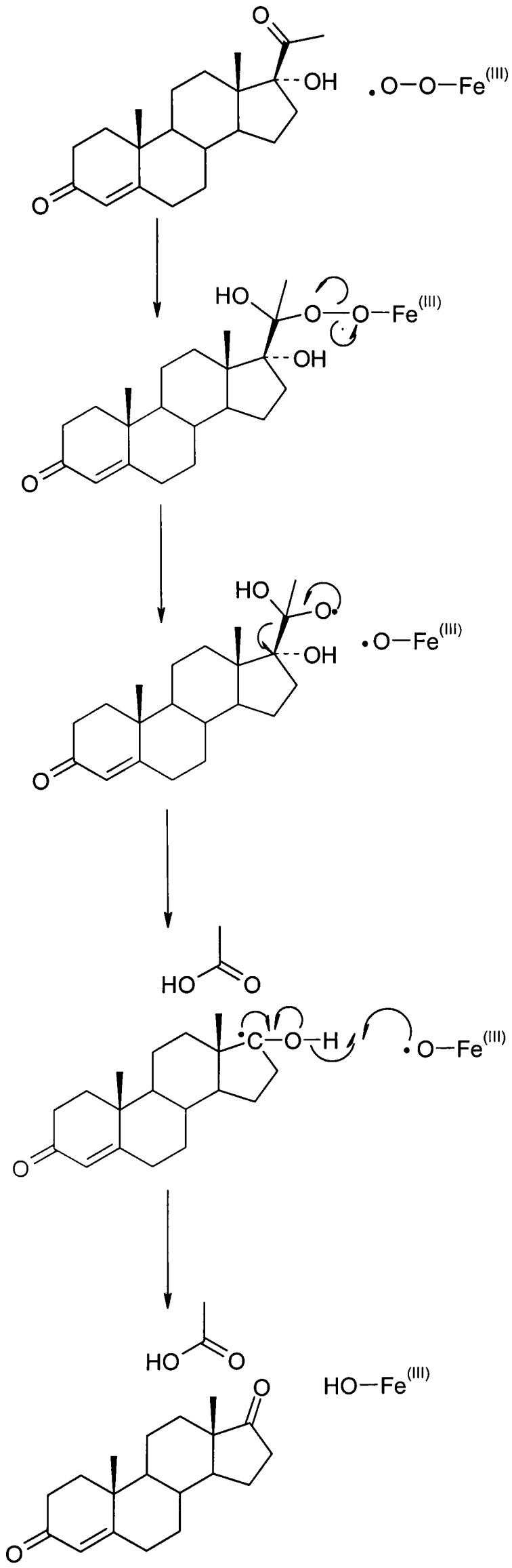

Figure 1.8 A postulated mechanism for 17,20-Lyase (Ahmed, 1999)

1.6.2 17β-Hydroxysteroid dehydrogenase (17β-HSD)

The 17β-HSD family of enzymes plays a pivotal role in the formation and inactivation of active androgens and estrogens from circulating steroid precursors. This enzyme can thus regulate tumoural cell proliferation in androgen- or estrogen-dependent cancers. 17β-HSD catalyses the reduction of 17-ketosteroids or the oxidation of 17β-hydroxysteroids using NAD(P)H/ $NAD(P)^+$ as a cofactor (Figure 1.9). The actual size of the enzymes is not known but they are predicted to have 327 amino acids (Luu-The et al, 1989; Luu-The et al, 1990).

Nine types of 17β-HSD isozymes have been isolated to date in humans, the mouse and rat. Types 1, 3, 5 and 7 show 17-ketosteroid reductase activity of which only types 1, 3 and 5 can utilise A as a substrate, whereas types 2, 4 and 8 catalyse the oxidative reaction (Luu-The, 2001). It is believed that in the testes type 3 has a major involvement in T biosynthesis because loss of this isozyme results in the failure of masculinisation during development and a rise in circulating A along with reduction in circulating T in the adult (Maltais et al, 2001).

The substrate specificity and steroid biosynthesis by the isozymes is summarised in Figure 1.9.

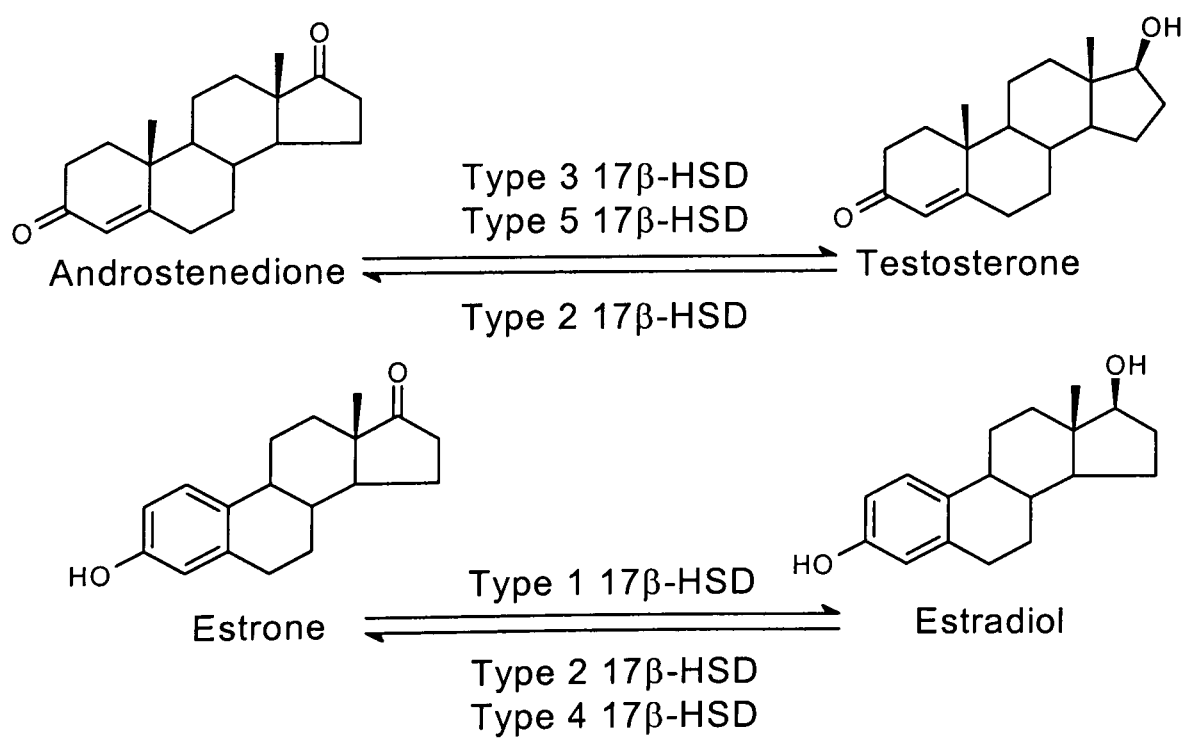

Figure 1.9 Steroid biosynthesis and isozyme specificity (Tremblay et al 1999).

The catalytic mechanisms, both oxidative and reductive, are shown in Figures 1.10a and 1.10b (Penning et al, 1999).

The catalytic mechanism for HSDs involves a 'push-pull' mechanism, in which a conserved catalytic tyrosine (Tyr55) functions as a general acid–base. This bifunctionality requires participation from other groups in the tetrad (involving Tyr55, His117, Asp50 and Lys84). In the reduction process of HSDs, Tyr55 has its acidity enhanced by the adjacent histidine (His117), which is achieved by a hydride transfer facilitated by a proton relay to a delocalised positive charge on the imidazole ring of His117. In the oxidation process of HSDs, Tyr55 has its basicity enhanced by the adjacent Lysine (Lys84), achieved by a phenolate anion deprotonating the steroid alcohol so that the hydride ion can be transferred back to the cofactor.

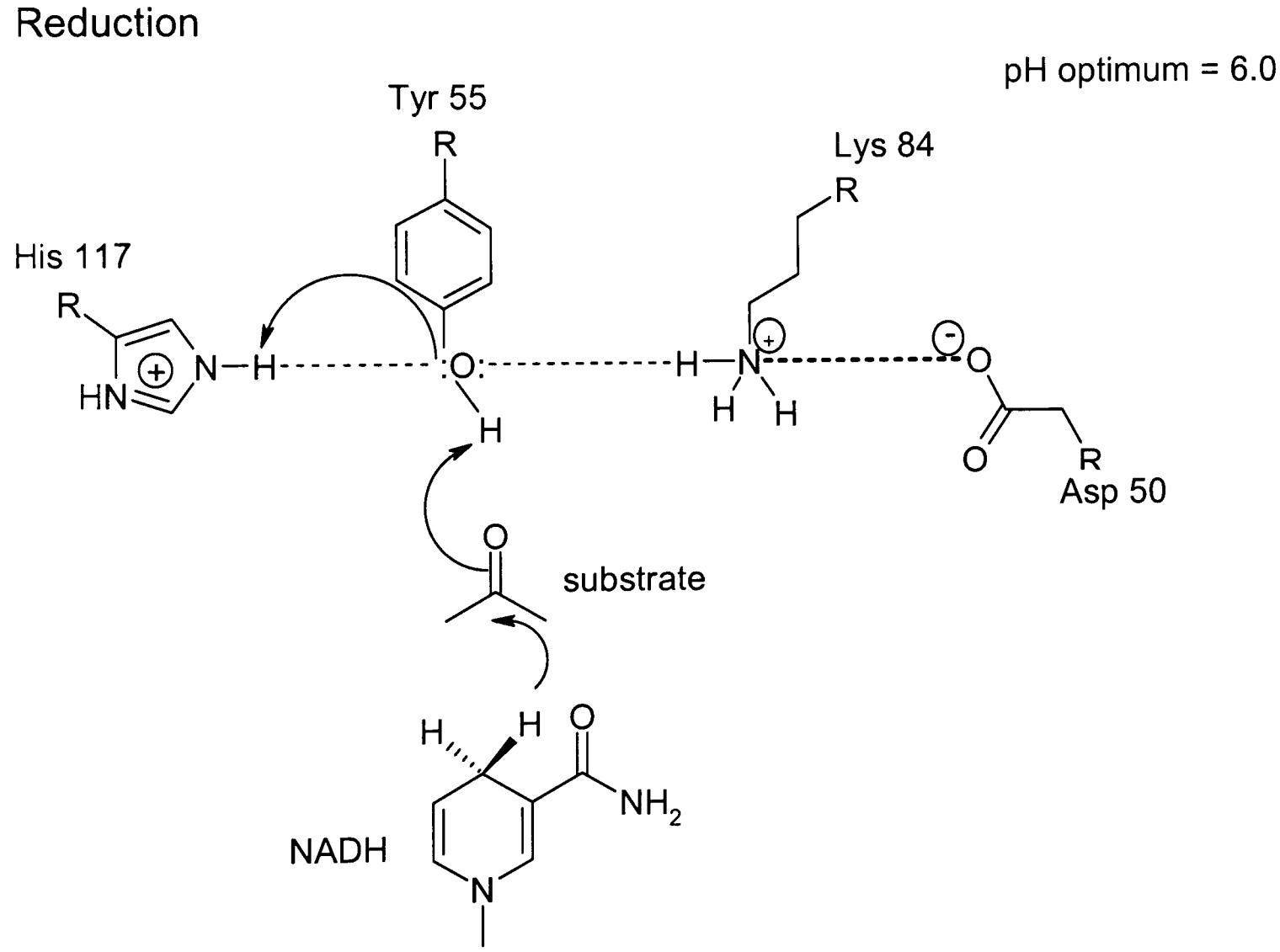

Figure 1.10a The postulated reduction cycle for 17β-HSD (Penning et al, 1999).

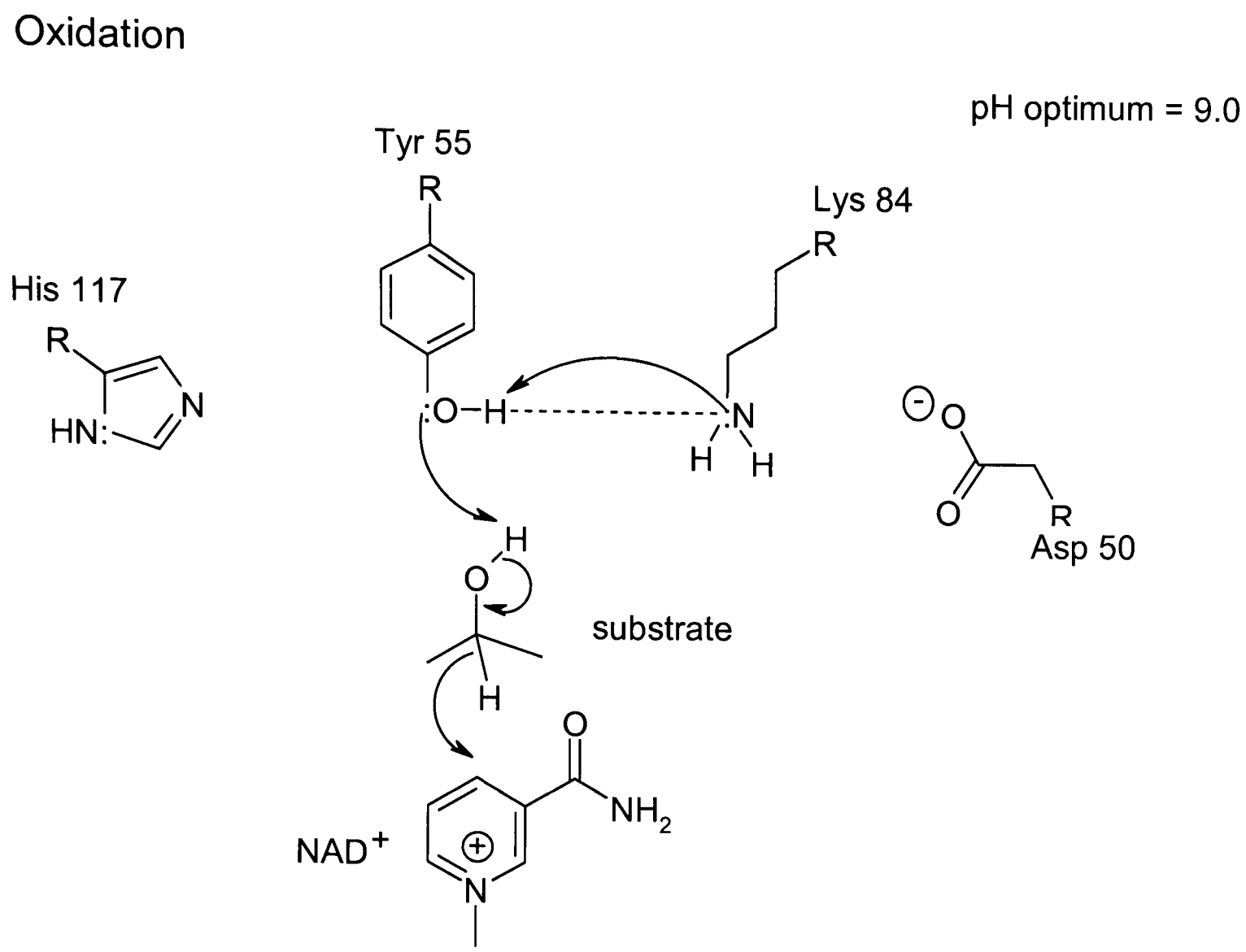

Figure 1.10b The postulated oxidation cycle for 17β-HSD (Penning et al, 1999).

1.7 Treatments for prostate cancer

There are several treatments for prostate cancer in use at present, including chemotherapy, surgery, radiation and hormonal therapy. These will be discussed below.

1.7.1 Surgery

This is the most common treatment for early stage prostate cancer. This involves the partial or total removal of the prostate. The surgery for total removal of the prostate is known as radical prostatectomy, and is further described in terms of the incisions used. The main risks of surgery are incontinence (caused by damage to the bladder sphincter) and impotence (caused by the damage or removal of nerves). Another method for surgery is surgical castration also known as orchiectomy which is the removal of the

testicles which causes a lowering of T levels thereby reducing or stopping cancer cell growth, and thus can also be considered as hormonal therapy.

1.7.2 Radiation therapy

This is of two types: the use of high energy x-rays to destroy cancer cells, and the use of radioactive pellets (called "seeds"), and like surgery it can only affect cancer cells in the treated area. It can be used in the early stages of cancer, instead of surgery or after surgery to destroy any cancer cells that may remain in the area. In advanced stages, it can help to reduce tumour size and relieve pain. Both types of radiation therapy obtain similar results in curing prostate cancer.

1.7.3 Chemotherapy

This method is less commonly used to treat hormone-dependent prostate cancer or BPH, however, it is more frequently used in advanced prostate cancer where the tumour has become hormone-independent. Some stabilisation is provided by doxorubicin (an anthracycline which works by intercalating the DNA) but its use is limited due to systemic toxicities, primarily cardiotoxicity and immunosuppression (Garsky et al, 2001).

Potent inhibitors of microtubule function, paclitaxel and docetaxel, were the first taxanes to enter the clinic and had important activity against several common human solid tumours. They both play an important role in the chemotherapy of hormone-refractory prostate cancer (Obasaju and Hudes, 2001).

1.7.4 Hormonal therapy

This is the systemic ablation of the body's T which, for a period of time, will slow or stop the growth and spread of prostate cancer. Hormone therapy may also be called androgen deprivation or androgen ablation. There are several forms of hormonal therapy:

i LHRH agonists

LHRH agonists induce a transient rise in pituitary LH which interacts with receptors on the interstitial Leydig cells of the testis leading to the synthesis and release of T (see Section 1.3). If T levels increase, T itself regulates the negative feedback loop and inhibits the release of further LHRH from the hypothalamus as well as the release of LH from the pituitary. This results in a decrease in the synthesis and release of T from the Leydig cells. When treated for the first time there is a surge in T plasma levels to concentrations far above pre-treatment values (known as the flare phenomenon). This causes worsening of bone pain, urinary obstruction, or other symptoms attributable to rapid cancer growth among some patients. However, continuous administration results in the receptors for LHRH becoming less responsive and results in a reduction in the release of LH, and therefore suppresses androgen production. LHRH agonists used include leuprolide, goserelin and triptorelin and side-effects associated with these agents can include fluid retention, thromboembolism, gynaecomastia and myocardial ischaemia.

ii Anti-androgens

The primary target in the treatment of prostate cancer and BPH is the reduction of T levels by surgical castration or its medical equivalent (administration of LHRH agonists). These methods eliminate T production from the testes, but not that produced from the adrenals. The importance of the requirement of androgens in maintaining tumour growth has been shown by improved therapeutic benefits, such as the survival advantage seen in patients treated with the combination of LHRH agonists and anti-androgens, compared with those given LHRH agonists alone (Labrie et al, 1983).

Compounds that cause an antagonistic response by binding to AR are known as anti-androgens. It has been postulated that anti-androgens act by counteracting the stimulant action of residual adrenal androgens on AR in prostate cancer (Kim et al, 2002). The most commonly used drugs are flutamide, bicalutamide and nilutamide and the most common side-effects

seen from the use of anti-androgens are due to the decreased levels of hormones, for example, loss of sex drive, and impotence. Other side-effects include mild nausea, vomiting, diarrhoea, loss of appetite, skin reactions, muscle aches, liver problems, blood in the urine and generalised pain and decrease in blood counts.

1.7.5 Enzyme inhibitors

It has been postulated that compounds that can inhibit the formation of androgens by blocking enzymes such as $P450_{17\alpha}$ and 17β-HSD can reduce the formation of the androgens and thus reduce BPH or androgen-dependent prostate cancer.

1.7.6 Inhibitors of $P450_{17\alpha}$

Inhibitors of this enzyme can be divided into two categories: non-steroidal and steroidal. These categories can be further subdivided according to their mode of action (reversible or irreversible). In the various studies undertaken, different sources of enzymes were used to test the inhibitors as they are species dependent, whereby the source of enzyme determines the pathway the cascade follows (Δ^4 or Δ^5). In rats, the Δ^4 pathway is predominant whereas in humans, it is the Δ^5 pathway, while for pigs, both pathways are viable.

i Non-steroidal inhibitors

The majority of non-steroidal inhibitors exhibit a basic functionality which is capable of co-ordinating with the haem residue of $P450_{17\alpha}$. They include groups such as azoles, pyridyls and phenylamines. However, there are other non-steroidal inhibitors that bind to other sites of the enzyme and do not contain these functionalities.

a Imidazole and triazole based compounds

Ketoconazole **(1)** (Table 1.1a) is an oral antifungal agent of the imidazole class, which contains two nitrogen atoms in the five membered azole ring.

It is almost insoluble in water except at low pH, therefore any conditions that increase the acidity or decrease the pH of the stomach will decrease the absorption and hence reduce the bioavailability of this compound. Ketoconazole has been used in clinical trials in patients with advanced prostate cancer. The major drawback is that it is not very potent or specific, and has a number of significant side-effects the most notable being hepatotoxicity (Trachtenberg and Zadra, 1988).

The discovery of ketoconazole as a $P450_{17\alpha}$ inhibitor led to the development of other imidazole derivatives and also triazole derivatives. It has been postulated using superimpositioning studies that the nitrogen of the imidazole derivatives forms a dative covalent bond with the iron of the haem then positioning itself within the active site of $P450_{17\alpha}$, and this is thought to lead to the inhibitory activity observed with these compounds. Triazole compounds have a similar mode of action, but have lower inhibitory activity in comparison. Tables 1.1a-1.1c outline the structures and biological activity of some of these azole based compounds.

NO.	Structure	Biological Activity	Enzyme	Source of Enzyme	Reference
1	Ketoconazole	2.4μM (IC_{50}) 2.6μM (K_i)	17,20-Lyase 17,20-Lyase	Human Porcine	Rotstein et al, 1992 Nagai et al, 1987
2	Econazole	0.3μM (IC_{50})	17α-Hydroxylase	Human	Mason et al, 1987
3	Miconazole	0.3μM (IC_{50})	17α-Hydroxylase	Human	Mason et al, 1987
4	Tioconazole	0.5μM (K_i) 0.9μM (K_i)	17,20-Lyase 17α-Hydroxylase	Rat	Ayub and Levell, 1987a
5	Bifonazole	56.5nM (K_i) 86nM (K_i)	17,20-Lyase 17α-Hydroxylase	Rat	Ayub and Levell, 1987a
6	Clotrimazole	81.5nM (K_i) 0.17μM (K_i)	17,20-Lyase 17α-Hydroxylase	Rat	Ayub and Levell, 1987a
7	YM116	4.2nM (IC_{50})	17,20-Lyase	Human	Ideyama et al, 1999
8	Etomidate	16μM (K_i)	17,20-Lyase	Porcine	Nagai et al, 1987

Table 1.1a Some azole-based inhibitors of 17α-hydroxylase and 17,20-lyase.

NO.	Structure	Biological Activity IC_{50}	Enzyme
9	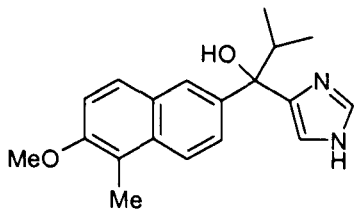	[a]28nM	17,20-Lyase
10	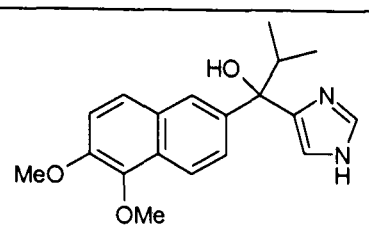	[a]29nM	17,20-Lyase
11	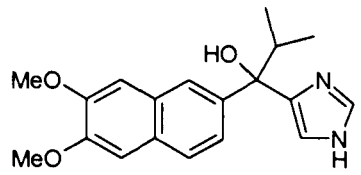	[a]29nM	17,20-Lyase
12	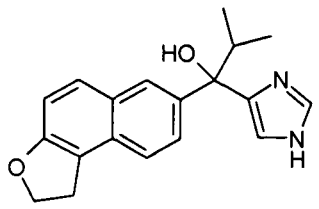	[a]25nM	17,20-Lyase
13	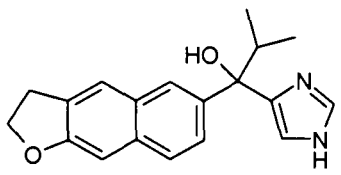	[a]23nM	17,20-Lyase
14	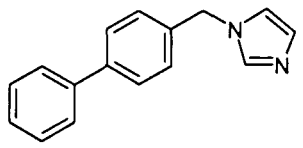	[b]0.98μM	17α-Hydroxylase
15	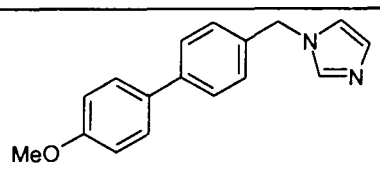	[b]3.7μM	17α-Hydroxylase
16	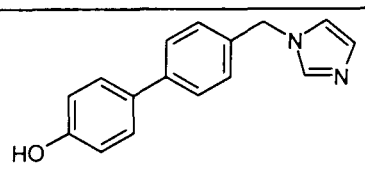	[b]0.31μM	17α-Hydroxylase
17	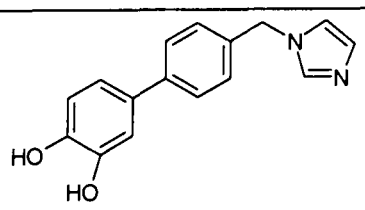	[b]87nM	17α-Hydroxylase
18	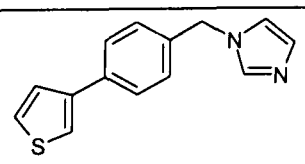	[b]0.33μM	17α-Hydroxylase

Table 1.1b Some azole-based inhibitors of 17α-hydroxylase and 17,20-lyase tested against human source of enzyme ([a]Matsunaga et al, 2004; [b]Wachall et al, 1999).

NO.	Structure	Biological Activity	Enzyme
19	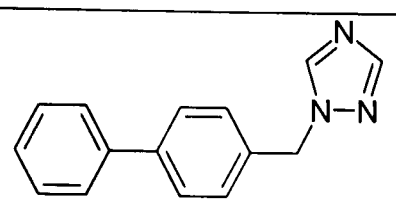	[a]48% inhibition at 2.5μM	17α-Hydroxylase
20	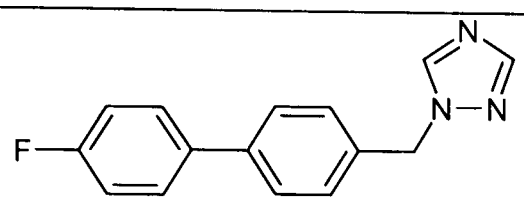	[a]37% inhibition at 2.5μM	17α-Hydroxylase
21	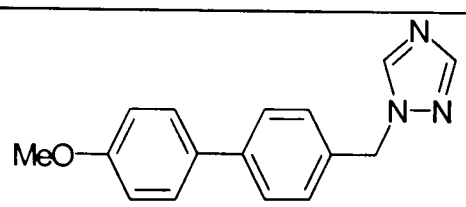	[a]30% inhibition at 2.5μM	17α-Hydroxylase
22	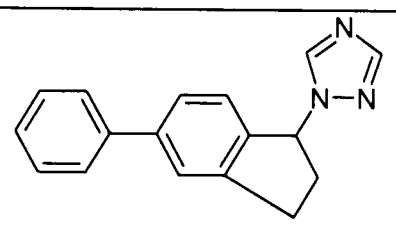	[a]35% inhibition at 2.5μM	17α-Hydroxylase
23	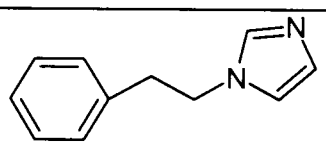	[b]46μM (IC_{50})	17,20-Lyase
24	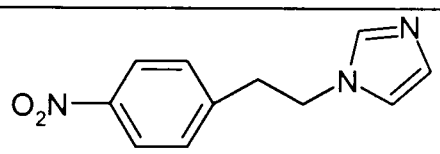	[b]30μM (IC_{50})	17,20-Lyase
25	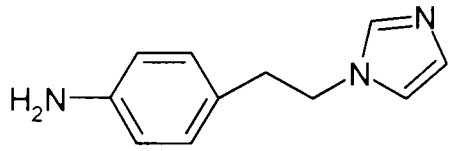	[b]28μM (IC_{50})	17,20-Lyase
26	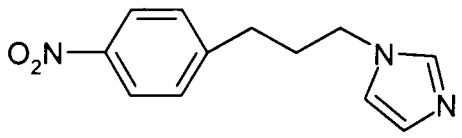	[b]25μM (IC_{50})	17,20-Lyase
27	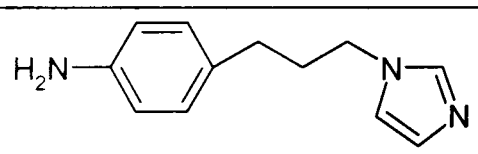	[b]22μM (IC_{50})	17,20-Lyase
28	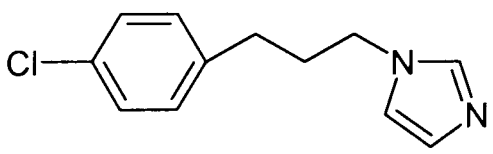	[b]29μM (IC_{50})	17,20-Lyase

Table 1.1d Some azole-based inhibitors of 17α-hydroxylase and 17,20-lyase tested against rat source of enzyme ([a]Zhuang et al, 2000; [b]Ahmed et al, 1995).

b Pyridyl Derivatives

These compounds have a similar mode of action to azole-based compounds, whereby the nitrogen of the pyridyl ring co-ordinates with the heam at the active site of $P450_{17\alpha}$ leading to competitive reversible inhibition. Some of these have been shown to be more potent inhibitors

than ketoconazole and more selective, for example cyclohexyl derivatives of 4-pyridylacetic acid showed more potent inhibition than ketoconazole. These compounds are good mimics of the natural substrate, which was found by superimpositioning studies on Preg (Laughton et al, 1990). Their potential to be used clinically is limited due to their susceptibility to esterases, but the tertiary ester derivatives have been shown to be more stable than the secondary ester derivatives. Tables 1.2a-1.2b outline the structure and biological activity of some of these pyridyl based compounds.

NO.	Structure	Biological Activity	Enzyme
29		[a]20μM (IC_{50}) [a]15μM (IC_{50})	17,20-Lyase 17α-Hydroxylase
30		[a]2.7μM (IC_{50}) [a]2.0μM (IC_{50})	17,20-Lyase 17α-Hydroxylase
31		[a]2.2μM (IC_{50}) [a]2.0μM (IC_{50})	17,20-Lyase 17α-Hydroxylase
32		[b]13μM (IC_{50})	17α-Hydroxylase
33		[b]19μM (IC_{50})	17α-Hydroxylase
34		[b]13μM (IC_{50})	17α-Hydroxylase
35		[b]6.3μM (IC_{50})	17α-Hydroxylase
36		[b]36% inhibition at 125μM	17α-Hydroxylase

Table 1.2a Some pyridyl-based inhibitors of 17α-hydroxylase and 17,20-lyase tested against rat source of enzyme ([a]Laughton et al, 1990; [b]Wächter et al, 1996).

NO.	Structure	Biological Activity IC_{50}	Enzyme	Source of Enzyme
37		[a]1.8nM [a]3.3nM	17,20-Lyase 17α-Hydroxylase	Human
38		[a]2.7nM [a]8.8nM	17,20-Lyase 17α-Hydroxylase	Human
39		[a]18nM [a]43nM	17,20-Lyase 17α-Hydroxylase	Human
40		[a]74nM [a]340nM	17,20-Lyase 17α-Hydroxylase	Human
41		[b]5nM [b]14nM	17,20-Lyase 17α-Hydroxylase	Human
42		[b]6nM [b]19nM	17,20-Lyase 17α-Hydroxylase	Human
43		[b]10nM [b]26nM	17,20-Lyase 17α-Hydroxylase	Human

Table 1.2b Some pyridyl-based inhibitors of 17α-hydroxylase and 17,20-lyase ([a]Chan et al, 1996, [b]Rowlands et al, 1995).

c **Phenylamines**

Pyrrolidine-2,5-diones containing an aniline ring functionality have been shown to inhibit $P450_{17\alpha}$ with potencies comparable to ketoconazole (Table 1.3). They also have a similar mode of action to the azole-based compounds, whereby the nitrogen of the phenylamine ring co-ordinates with the haem at the active site of $P450_{17\alpha}$, leading to competitive reversible inhibition.

NO.	Structure	Biological Activity % inhibition at 100μM	Enzyme
44	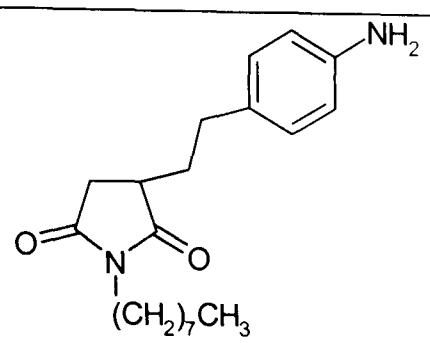	88	17,20-Lyase
45	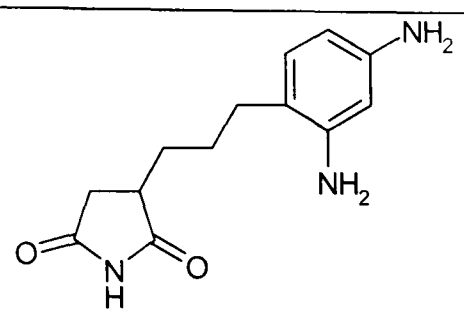	95	17,20-Lyase
46	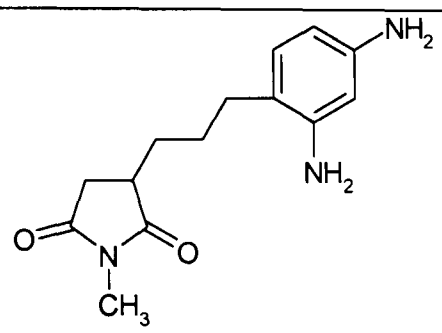	81	17,20-Lyase
47	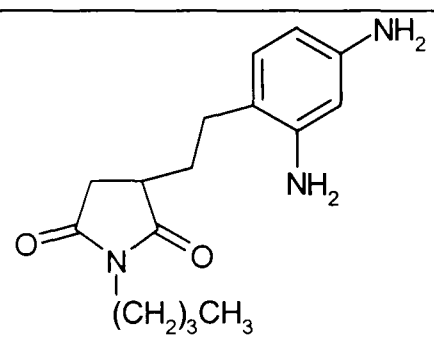	75	17,20-Lyase
48	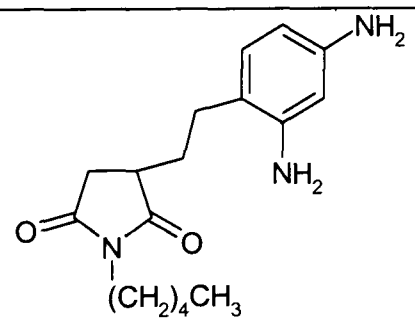	89	17,20-Lyase

Table 1.3 Some phenylamine-based inhibitors of 17α-hydroxylase and 17,20-lyase tested against rat source of enzyme (Ahmed et al, 1995).

ii Steroidal Inhibitors

Modifications of the natural substrates, mainly at the 17,20 side chain and the D-ring, are the basis for the design of steroidal inhibitors. The functional groups present on the inhibitor interact at positions at the active site that would normally interact with the natural substrate.

a **Mechanism-based (Irreversible) inhibitors**

These inhibitors work by mimicking the natural substrate or transition states involved in the conversion of progestins to androgens. The inhibition is irreversible which is made possible by the inclusion of a group capable of reacting with the active site. Mechanism-based inhibitors are activated by the normal catalytic activity of the enzyme to produce a species capable of forming a covalent bond with the active site (Angelastro et al, 1989). Examples of such inhibitors are shown in Table 1.4.

NO.	Structure	Biological Activity IC_{50} (μM)	Enzyme
49	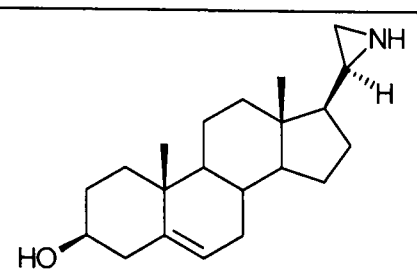	0.21	17α-Hydroxylase
50	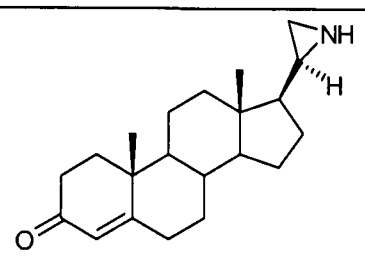	1.2	17α-Hydroxylase
51	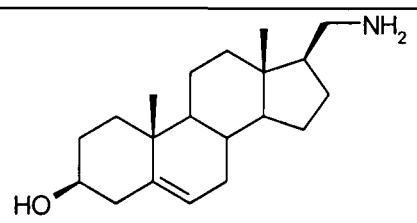	>125	17α-Hydroxylase
52	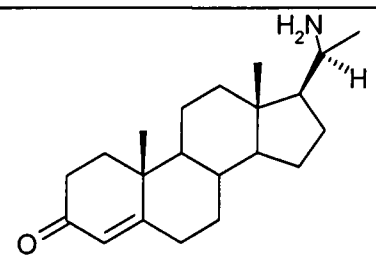	>125	17α-Hydroxylase
53	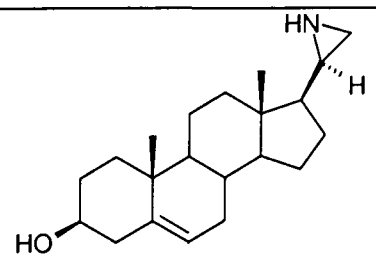	34	17α-Hydroxylase
54	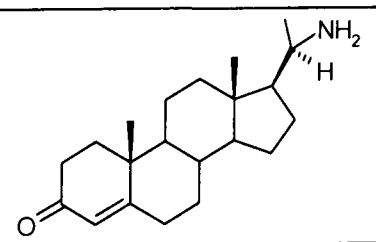	>125	17α-Hydroxylase

Table 1.4 Some steroidal irreversible inhibitors of 17α-hydroxylase and 17,20-lyase tested against rat source of enzyme (Njar et al, 1996).

b Substrate Analogues (Reversible)

These compounds are structurally similar to the natural substrate, like the mechanism-based (irreversible) steroidal inhibitors, but they do not undergo irreversible reaction with the active site. They bind reversibly to the active site, thus preventing the natural substrate from binding, and therefore inhibiting the production of androgens. The mode of action is the same as the non-steroidal imidazole- and triazole-based compounds. Tables 1.5a and 1.5b summarise the azole-based substrate analogues whilst Table 1.6 summarises the pyridyl-based substrate analogues.

NO.	Structure	Biological Activity IC_{50} (nM)	Enzyme
55		90	17,20-Lyase
56		8	17,20-Lyase
57		13	17,20-Lyase
58		55	17,20-Lyase
59		7	17,20-Lyase

Table 1.5a Some steroidal azole-based inhibitors of 17α-hydroxylase and 17,20-lyase tested against human source of enzyme (Nnane et al, 1999a).

NO.	Structure	Biological Activity IC_{50} (nM)
60	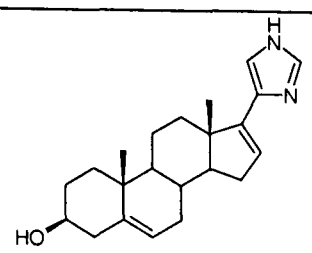	24
61	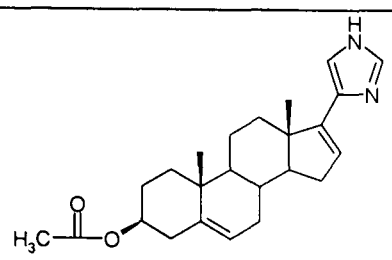	75
62	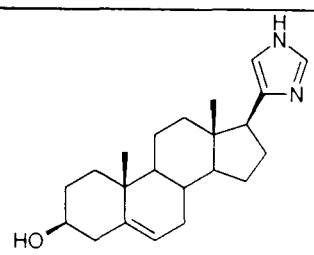	66
63	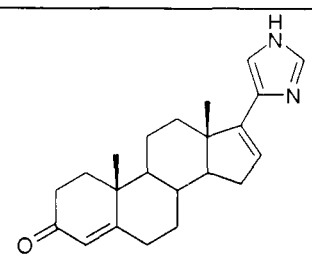	50
64	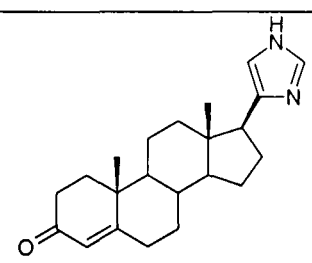	58
65	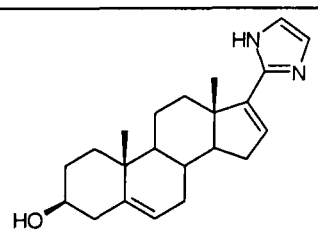	21
66	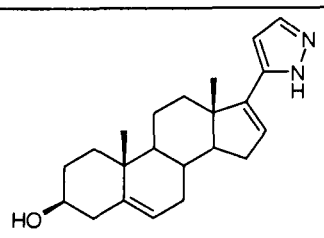	42
67	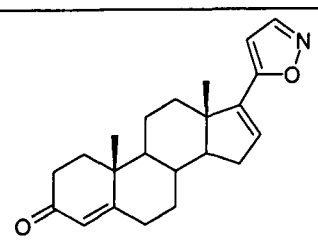	39

Table 1.5b Some steroidal azole-based inhibitors of 17α-hydroxylase and 17,20-lyase tested against human source of enzyme (Jarman et al, 1998).

NO.	Structure	Biological Activity IC_{50} (nM)	Enzyme
68	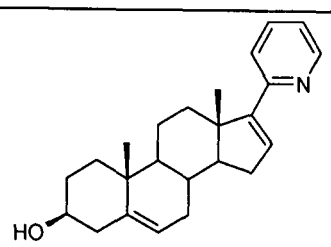	76 270	17,20-Lyase 17α-Hydroxylase
69	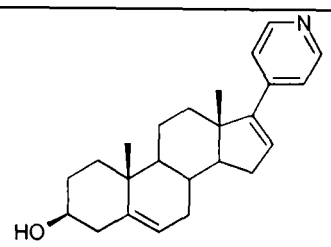	1000 4000	17,20-Lyase 17α-Hydroxylase
70	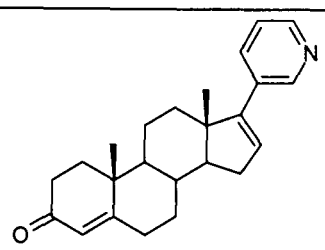	2.1 2.8	17,20-Lyase 17α-Hydroxylase
71	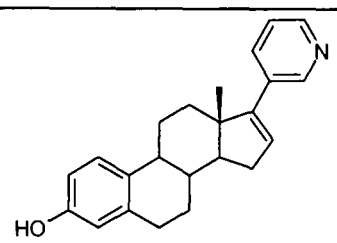	1.8 2.6	17,20-Lyase 17α-Hydroxylase
72	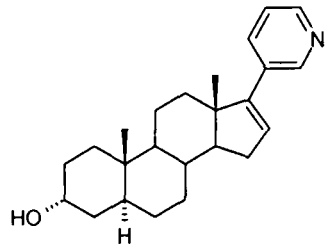	2.5 4.3	17,20-Lyase 17α-Hydroxylase
73	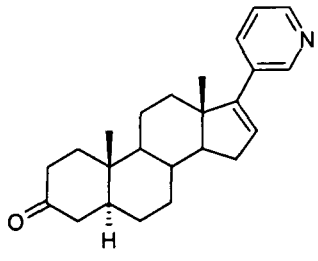	3.0 4.7	17,20-Lyase 17α-Hydroxylase
74	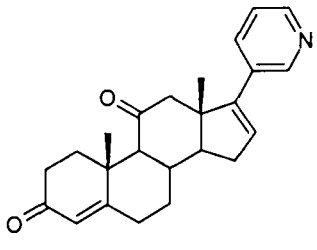	2.9 13	17,20-Lyase 17α-Hydroxylase
75	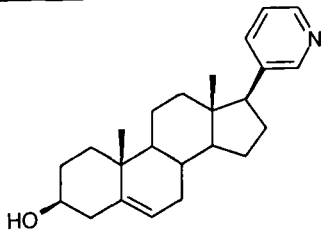	23 47	17,20-Lyase 17α-Hydroxylase

Table 1.6 Some steroidal pyridyl-based inhibitors of 17α-hydroxylase and 17,20-lyase tested against human source of enzyme (Potter et al, 1995).

1.7.7 Inhibitors of 17β-HSD

i Steroidal Inhibitors

a Isoxazoles and Pyrazoles

Competitive inhibition of type 1 17β-HSD was reported by Sweet et al (1991) using estrone (E1) derivatives with pyrazole or isoxazole fused to the 16,17 position on the D-ring, whereas for inhibition of type 3 17β-HSD, Levy et al (1987) reported steroidal derivatives with pyrazole or isoxazole fused to the 2,3 or 3,4 position on the A-ring. It was noticed in both cases that the pyrazole derivative was a better inhibitor than the isoxazole analogue. It was suggested that specific intramolecular hydrogen bonds between the pyrazole fused to the D-ring and the phenol groups of the hydroxysteroid and three specific histidyl residues stabilised the enzyme-inhibitor complex resulting in a good enzyme affinity for type 1 17β-HSD. Tables 1.7a and table 1.7b summarise the isoxazole and pyrazole-based inhibitors.

NO.	Structure	Biological Activity K_i (μM)
76	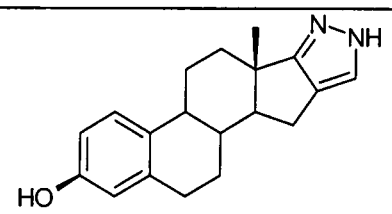	4.1
77	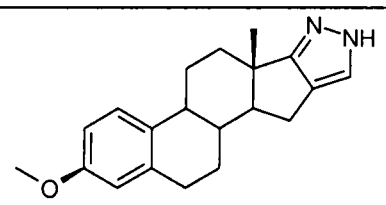	12.8
78	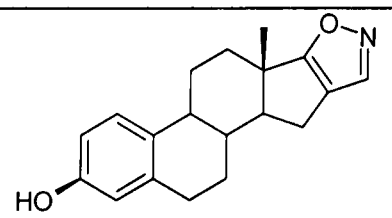	69.4
79	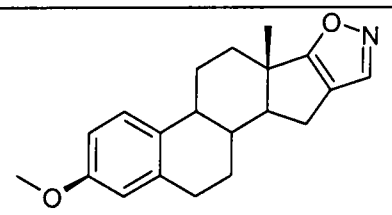	424.5

Table 1.7a Some pyrazole- and isoxazole-based inhibitors of type 1 17β-HSD tested against human source of enzyme using estradiol as substrate (Sweet et al, 1991).

NO.	Structure	Biological Activity K_i (nM)
80	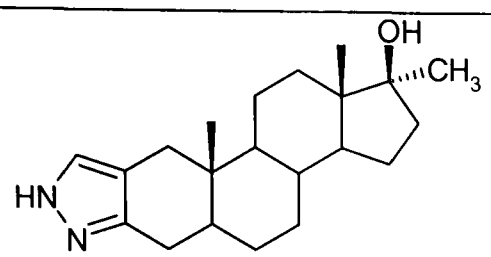	20
81	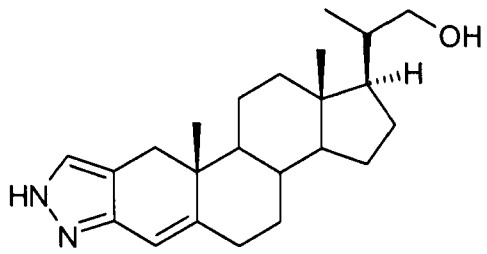	15
82	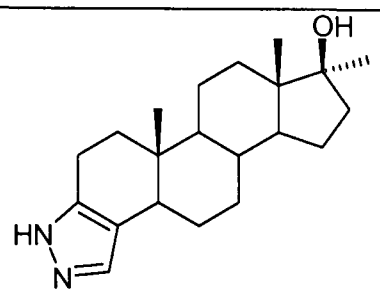	6
83	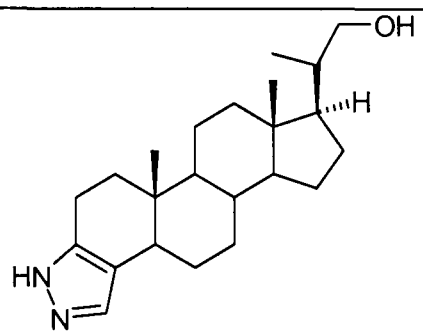	7
84	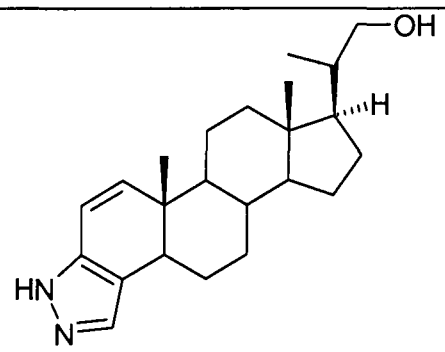	100
85	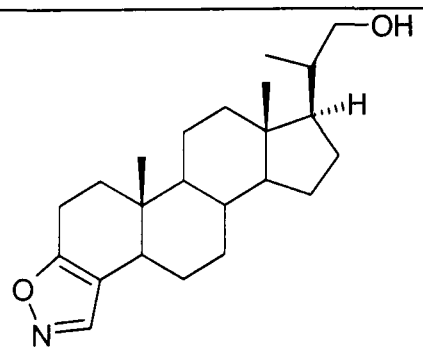	190

Table 1.7b Some pyrazole- or isoxazole-based inhibitors of 17β-HSD for isozyme type 3 tested against bacterial source of enzyme using T as substrate (Levy et al, 1987).

b Estradiol (E2) derivatives

A series of E2 derivatives bearing a thia-alkanamide side chain at position C6 was developed to inhibit 17β-HSD type 1. The compounds showed agonistic activity against estrogen-sensitive ZR-75-1 cells. However, as they showed interesting screening data they were explored further and showed some potency when tested against human placental cytosolic 17β-HSD (type 1) transformation of E1 to E_2. Table 1.8 summarises some antiestrogen inhibitors.

NO.	Structure	Biological Activity IC_{50} (μM)
86	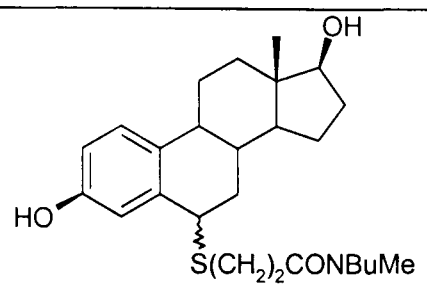	0.30
87	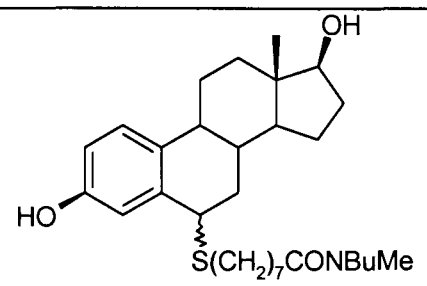	7.80
88	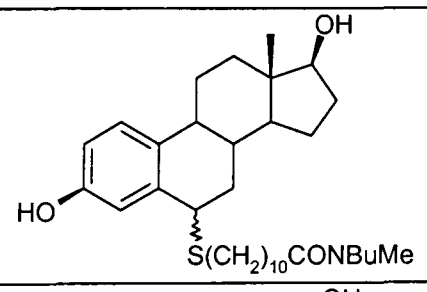	11.20
89	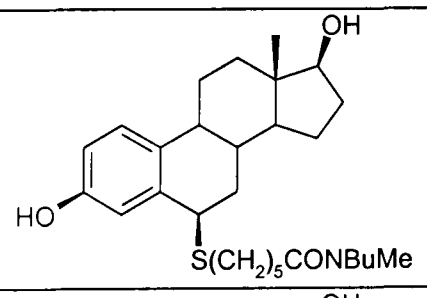	0.17
90	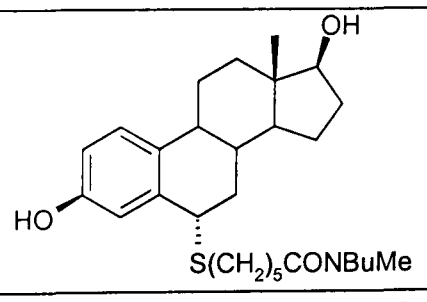	12.00

Table 1.8 Some antiestrogen inhibitors of 17β-HSD for isozyme type 1 tested against human source of enzyme using E1 as substrate (Poirier et al, 1998).

c Androsterone derivatives

A range of 3β-substituted androsterone derivatives were produced and tested for type 3 17β-HSD inhibition. The compounds proved more potent than A, the natural substrate, when used as an inhibitor (IC_{50} - 489±112nM). Table 1.9 summarises some androsterone derivative inhibitors.

NO.	Structure	Biological Activity IC_{50} (nM)
91	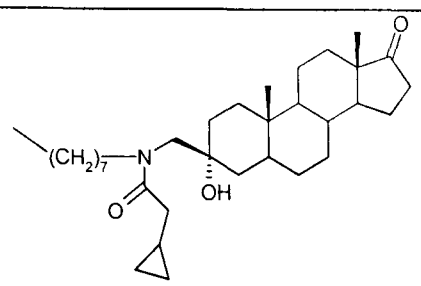	57
92	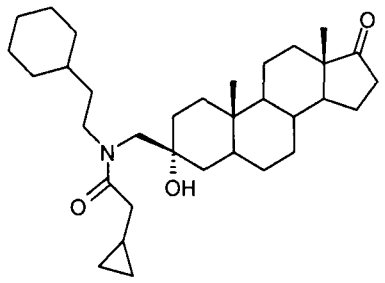	85
93	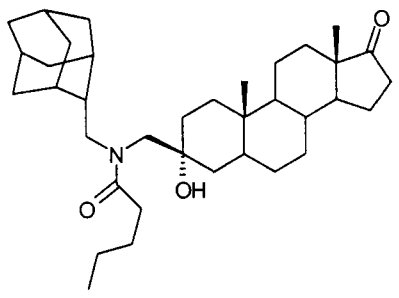	35
94	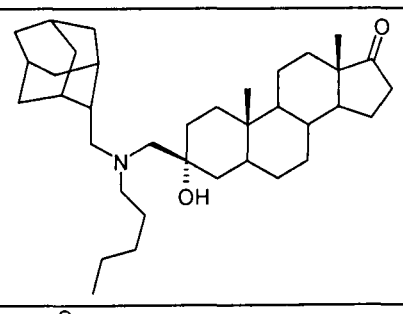	80
95	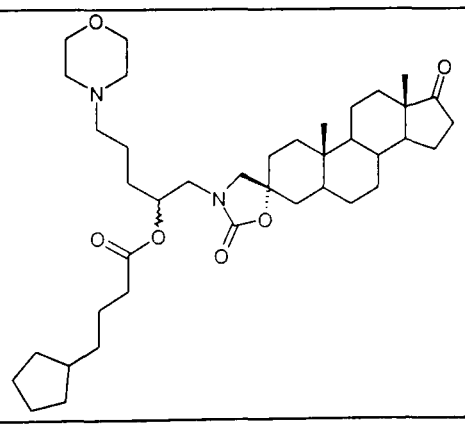	74

Table 1.9 Some androsterone derivatives as inhibitors of 17β-HSD tested against human HEK-293 cells transfected with vectors encoding for type 3 17β-HSD using A as substrate (Maltais et al, 2002).

ii Non-steroidal Inhibitors

a Phytoestrogens

Phytoestrogens are plant-derived, non-steroidal compounds with estrogenic activity. Phytoestrogens possess antiviral, anti-inflammatory, antimutagenic and anticarcinogenic activities (Le Bail et al, 2000) with different mechanisms of action, including inhibition of 17β-HSD. Tables 1.10a and 1.10b summarise some phytoestrogenic inhibitors of type1 17β-HSD, and Table 1.10c summarises some inhibitors of type 3 17β-HSD.

NO.	Structure	Biological Activity IC_{50} (μM)
96	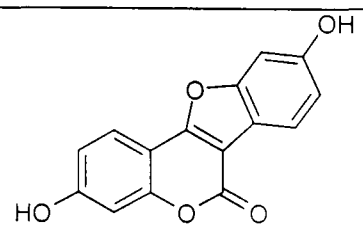	0.2
97	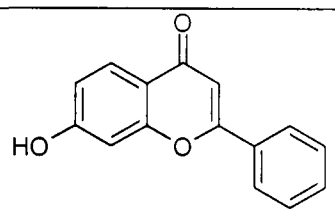	0.9
98	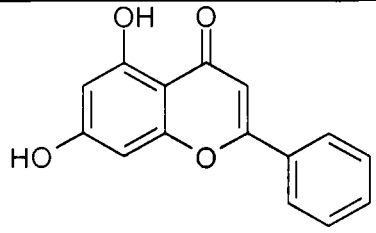	0.3
99	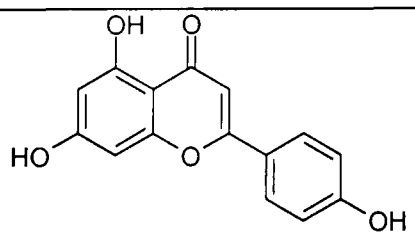	3.6
100	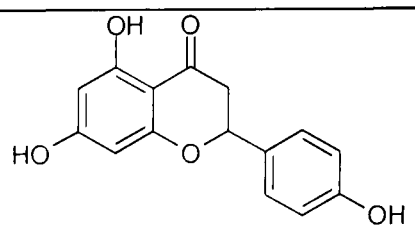	15.0
101	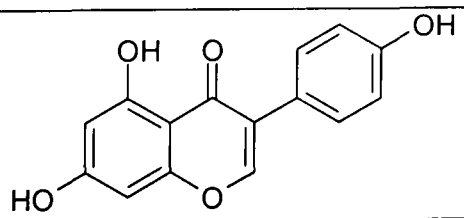	1.0

Table 1.10a Some phytoestrogens as inhibitors of 17β-HSD for isozyme type 1 tested against human source of enzyme using E1 as substrate (Le Bail et al, 1998).

NO.	Structure	Biological Activity IC_{50} (μM)
102	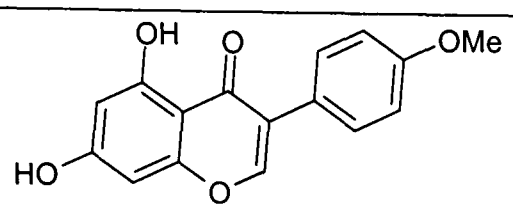	4.9
103	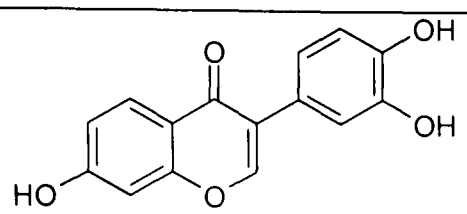	5.2
104	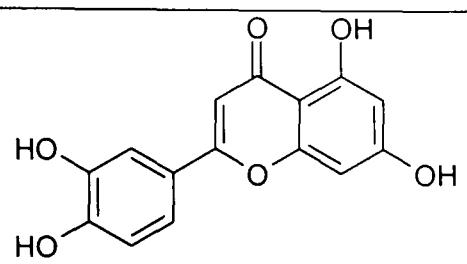	1.2
105	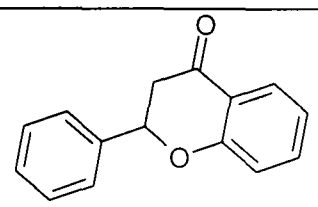	13.8
106	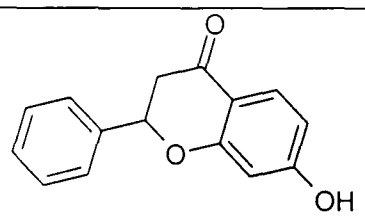	2.4
107	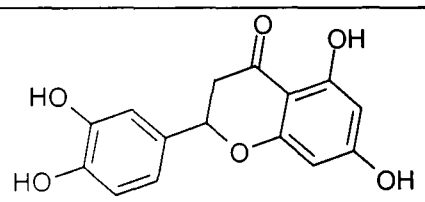	0.6
108	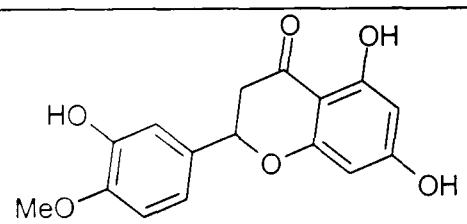	3.3
109	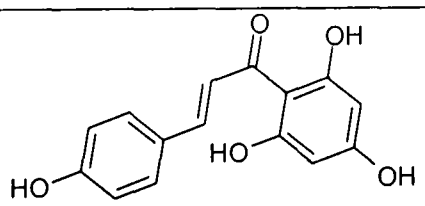	2.6
110	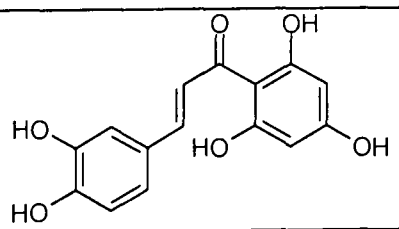	2.8

Table 1.10b Some phytoestrogens as inhibitors of 17β-HSD for isozyme type 1 tested against human source of enzyme using E1 as substrate (Le Bail et al, 2001).

NO.	Structure	Biological Activity IC_{50} (μM)
111	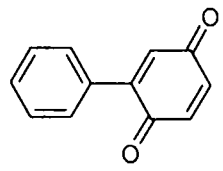	[a]5.7
112	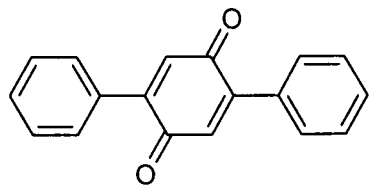	[a]2.7
97	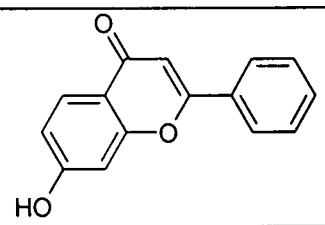	[a]9.0
113	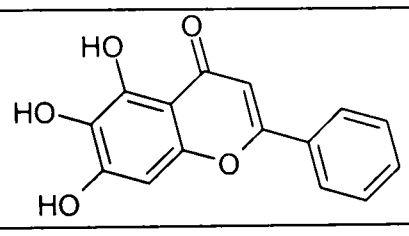	[a]9.3
114	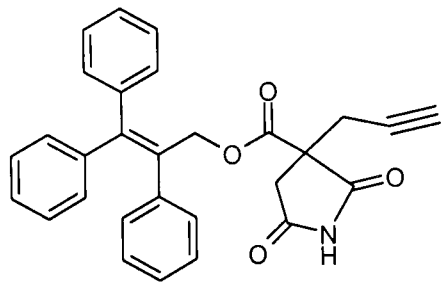	[a]9.1
115	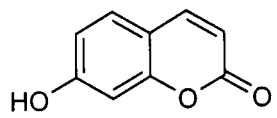	[b]1.4
116	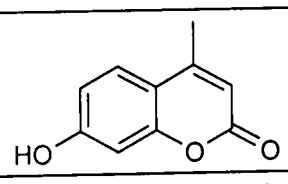	[b]0.9

Table 1.10c Some phytoestrogens as inhibitors of 17β-HSD for isozyme type 3 tested against human source of enzyme using A as substrate ([a]Le Lain et al, 2001, [b]Le Lain et al, 2002).

b Cinnamic acid analogues

The biosynthesis of flavanoids proceeds via cinnamic acid or related phenolic acids. As flavanoids and their analogues have proved to be good inhibitors, cinnamic acid analogues were tested and the results are shown in Tables 1.11a and 1.11b

NO.	Structure	Biological Activity IC_{50} (μM)		Isozyme type
		Oxidation	Reduction	
117		26	>200	1,3 & 5
118		13	No Inhibition	1,3 & 5
119		135	No Inhibition	1,3 & 5
120		0.7	7	1,3 & 5
121		14	No Inhibition	1,3 & 5
122		130	No Inhibition	1,3 & 5
123		10	No Inhibition	1,3 & 5
124		5	90	1,3 & 5

Table 1.11a Some cinnamic acid analogues as inhibitors of 17β-HSD tested against fungal source of enzyme (Gobec et al, 2004).

NO.	Structure	Biological Activity IC_{50} (μM)		Isozyme type
		Oxidation	Reduction	
125	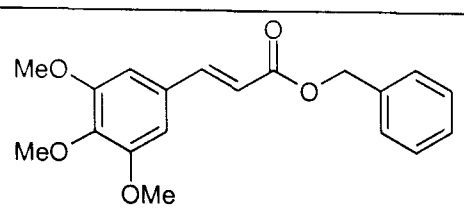	11	144	1,3 & 5
126	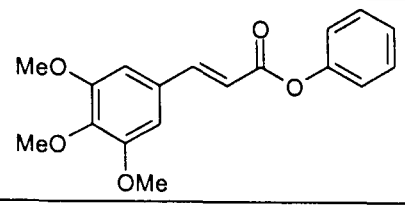	7	17	1,3 & 5
127	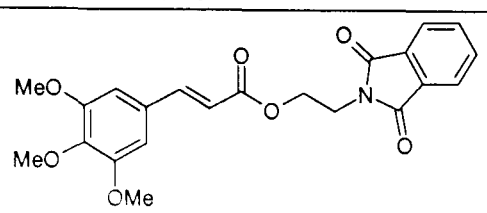	57	>200	1,3 & 5
128	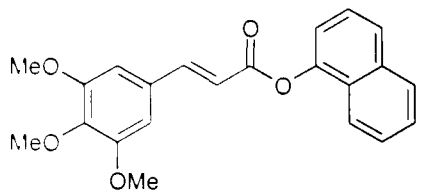	160	No Inhibition	1,3 & 5
129	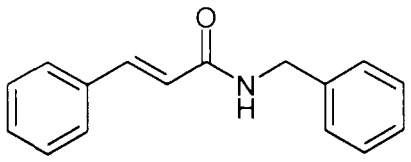	125	>200	1,3 & 5
130	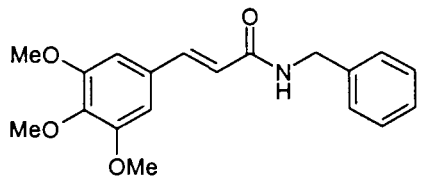	110	>200	1,3 & 5
131	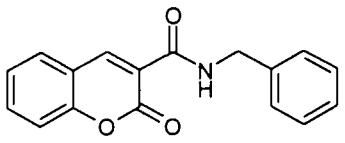	3	32	1,3 & 5

Table 1.11b Some cinnamic acid analogues as inhibitors of 17β-HSD tested against fungal source of enzyme (Kristan et al, 2006).

c Other 17β-HSD inhibitors

A novel range of compounds has been discovered by high-throughput screening. They have shown very high potency towards the type 3 form of the enzyme. Some have shown picomolar potency and nanomolar potency against the enzymatic activity and cellular activity respectively. Tables 1.12a to 1.12e summarise some novel inhibitors.

NO.	Structure	Biological Activity IC_{50} (nM)	
		Enzyme	Cellular
132	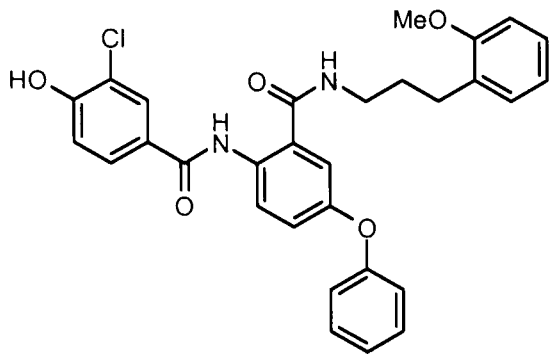	60	300
133	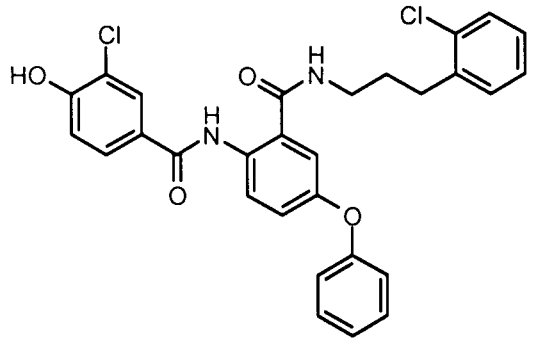	40	710
134	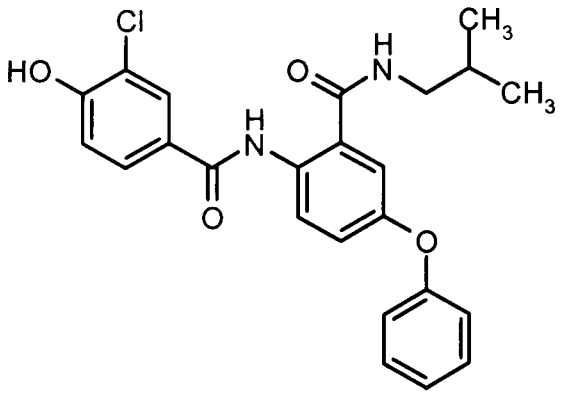	1	1200
135	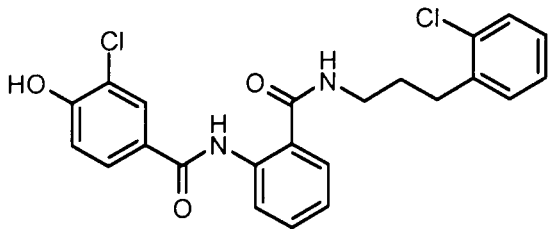	170	1600

Table 1.12a Some novel compounds as inhibitors of 17β-HSD tested against human source of enzyme for isozyme type 3 using A as substrate (Spires et al, 2005).

NO.	Structure	Biological Activity IC_{50} (nM)	
		Enzyme	Cellular
136	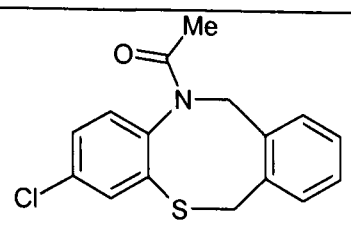	100	160
137	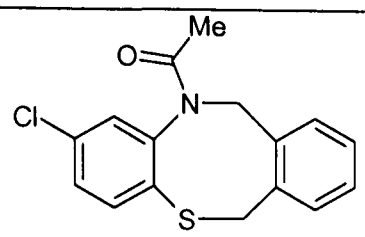	30	170
138	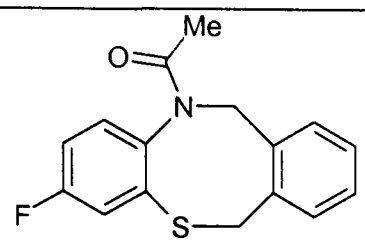	90	290
139	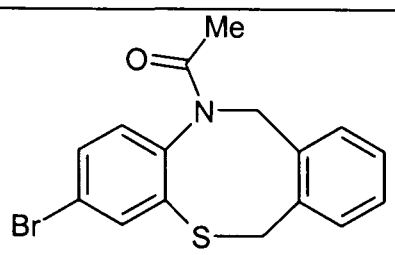	250	120
140	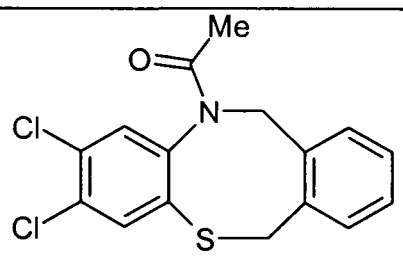	10	130
141	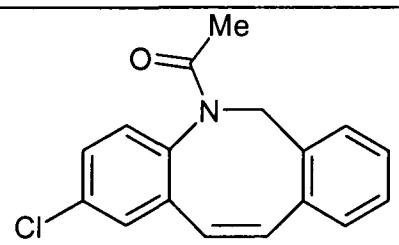	240	500
142	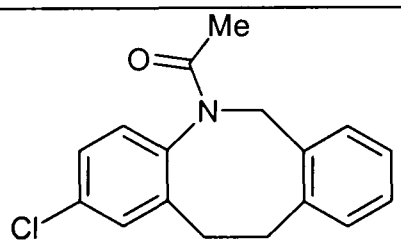	70	630
143	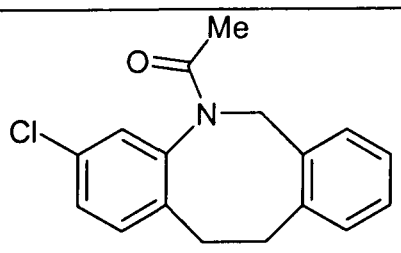	50	130

Table 1.12b Some tetrahydrobenzazocines as inhibitors of 17β-HSD tested against human source of enzyme for isozyme type 3 using A as substrate (Fink et al, 2006).

NO.	Structure	Biological Activity IC_{50} (nM)	
		Enzyme	Cellular
144	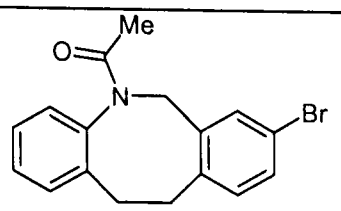	9	32
145	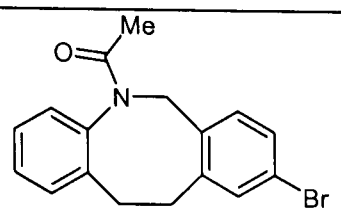	7	36
146	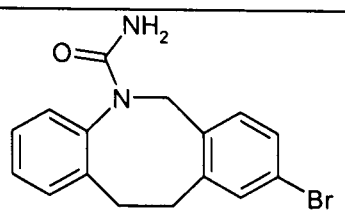	280	930
147	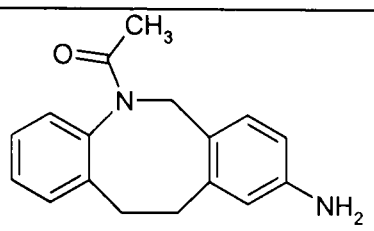	490	490
148	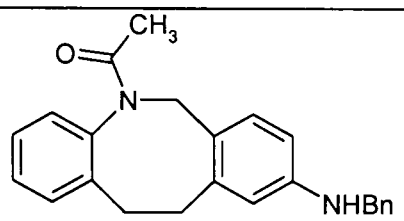	8	4
149	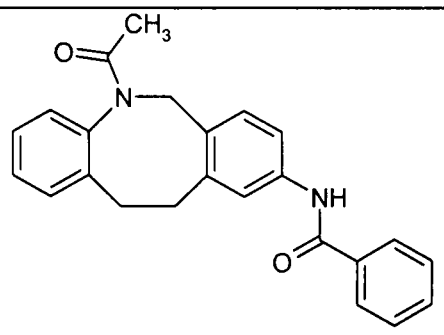	160	260
150	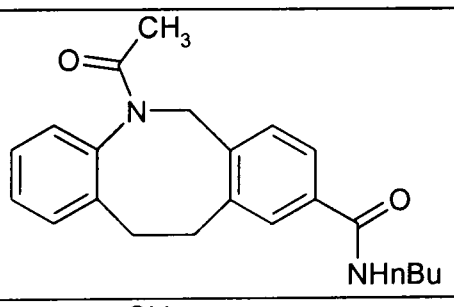	35	52
151	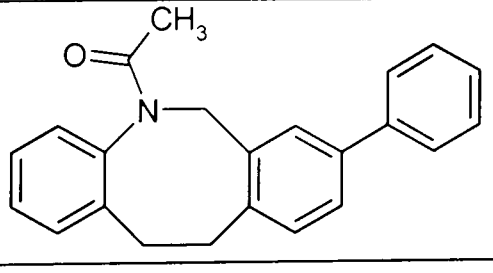	0.02	4

Table 1.12c Some tetrahydrobenzazocines as inhibitors of 17β-HSD tested against human source of enzyme for isozyme type 3 using A as substrate (Fink et al, 2006).

NO.	Structure	Biological Activity IC_{50} (nM)	
		Enzyme	Cellular
152	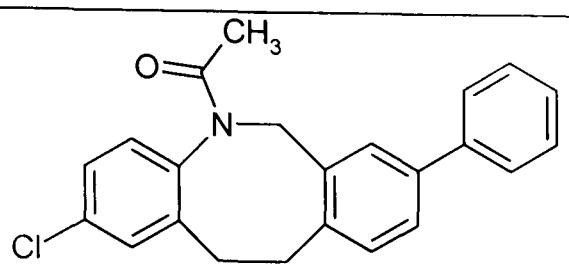	4	18
153	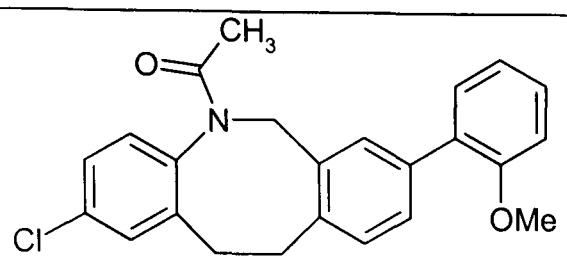	2	5
154	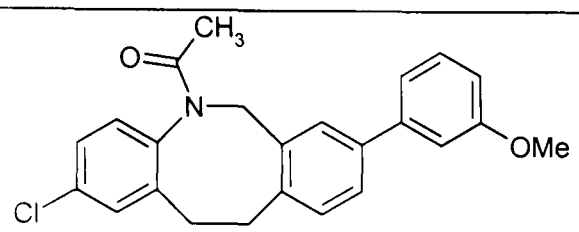	8	53
155	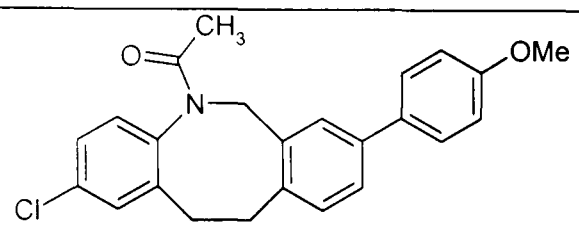	3	48
156	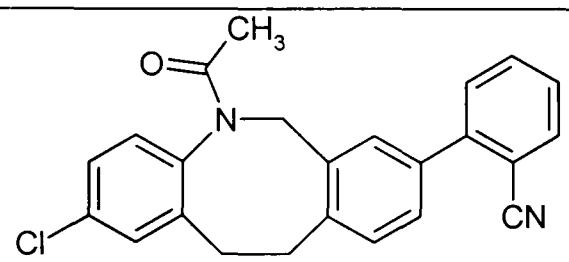	5	62
157	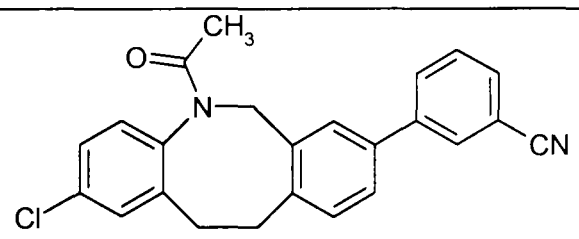	3	15
158	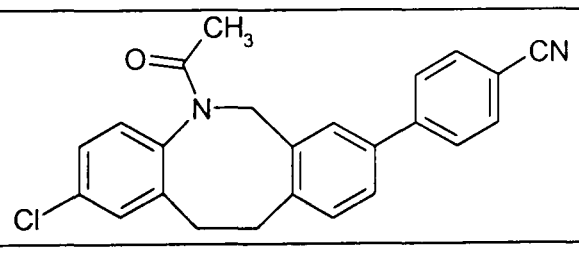	3	19

Table 1.12d Some tetrahydrobenzazocines as inhibitors of 17β-HSD tested against human source of enzyme for isozyme type 3 using A as substrate (Fink et al, 2006)

NO.	Structure	Biological Activity IC_{50} (nM)	
		Enzyme	Cellular
159	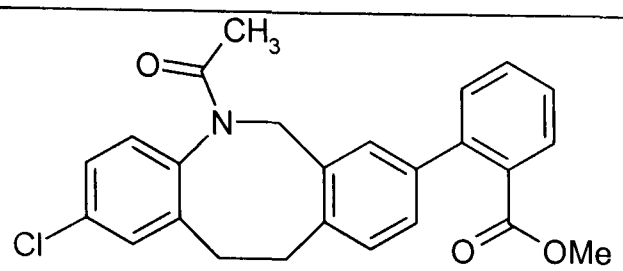	0.02	0.5
160	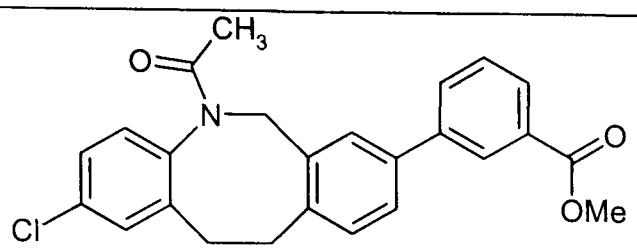	1.4	2
161	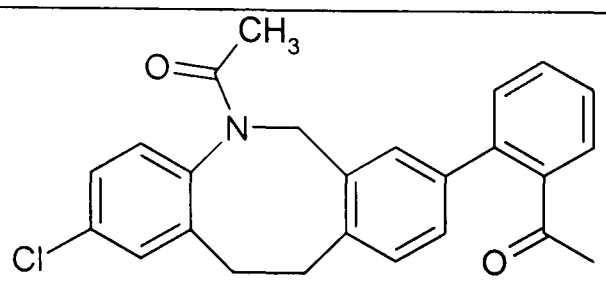	0.02	0.5
162	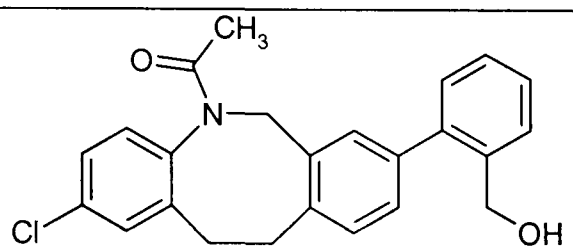	0.9	2
163	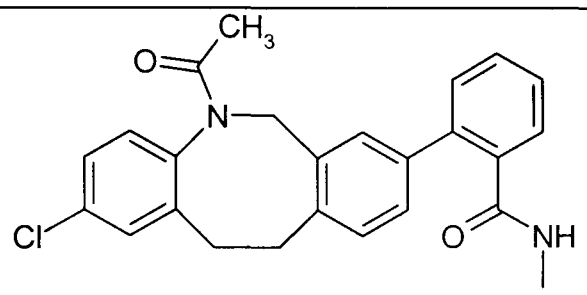	25	25
164	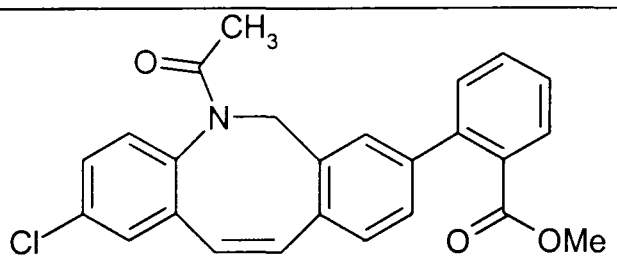	0.7	1

Table 1.12e Some tetrahydrobenzazocines as inhibitors of 17β-HSD tested against human source of enzyme for isozyme type 3 using A as substrate (Fink et al, 2006)

1.8 Enzyme Kinetics

Kinetics is the study of the rate of change of reactants to products. An enzyme catalysed reaction is dependent upon the formation of product by the breakdown of an enzyme-substrate complex. The first time an enzyme-substrate complex was deduced from the kinetics of an enzyme reaction was in

1902 by Brown. In 1913 Michaelis and his assistant, Menten derived an equation which is crucial in enzyme studies. The basic concepts of Michaelis and Menten were confirmed by several other workers who approached the problem from different viewpoints, and their work was particularly useful in advanced kinetic and mechanistic studies. The dissociation constant is known as the Michaelis constant, K_m.

$$E + S \underset{k_{-1}}{\overset{k_1}{\rightleftharpoons}} ES \underset{k_{-2}}{\overset{k_2}{\rightleftharpoons}} E + P \qquad \therefore \quad K_m = \frac{k_1 + k_2}{k_{-1} + k_{-2}}$$

Where:-

E = Enzyme concentration

S = Substrate concentration

P = Product concentration

ES = Concentration of enzyme-substrate complex

k_1, k_{-1}, k_2, k_{-2} = rate constants for each step

When complex concentration is constant the rate of formation equals the rate of disappearance. There cannot be any measurement of product if the reverse reaction from product to enzyme-substrate complex occurs, thus for the reaction to proceed to product formation the rate constant k_{-2} is assumed to be negligible and is omitted, generating the following equation:

$$K_m = \frac{k_1 + k_2}{k_{-1}}$$

Measuring total activity of enzyme is possible, whilst measuring relative amounts of free and complexed enzyme is extremely difficult. Representation of the proportion of free enzyme is shown by the difference between total enzyme (E) and substrate-enzyme complex (ES), thus:-

Rate of ES formation $= k_1[E - ES][S]$

Rate of ES removal $= k_{-1}[ES] + k_2[ES]$

Therefore:-

$$\frac{k_1 + k_2}{k_{-1}} = \frac{[E - ES]\,[S]}{[ES]} = K_m$$

Rearranging the equation results in:-

$$K_m = \frac{[E]\,[S]}{[ES]} - \frac{[ES]\,[S]}{[ES]}$$

$$K_m = \frac{[E]\,[S]}{[ES]} - [S]$$

$$[ES] = \frac{[E]\,[S]}{K_m + [S]}$$

By definition, the observable rate of product formation (v) is proportional to the concentration of the enzyme substrate complex, ES.

$$v = k_2\,[ES]$$

Thus substituting it into the previous equation:-

$$v = \frac{k_2\,[E]\,[S]}{K_m + [S]}$$

Measuring the true concentration of enzyme in terms of molar concentration is difficult but if the substrate concentration is large in comparison to that of enzyme, all of the enzyme will be present as the ES complex and the reaction will proceed at maximum velocity. Under these conditions of excess substrate and maximum velocity (V_{max}):-

$$V_{max} = k_2\,[E]$$

Substituting into the previous equation results in the common form of the Michaelis equation:

$$v = \frac{V_{max} \times [S]}{K_m + [S]}$$

The equation gives a measure of the Michaelis constant (K_m) in terms of the measured velocity of the reaction (v) which results from a substrate concentration ([S]) and maximum velocity (V_{max}) which can be achieved using a very high concentration of substrate.

The value for the maximum velocity is related to the amount of enzyme used but the Michaelis constant is peculiar to the enzyme and is a measure of the activity of the enzyme. Enzymes with large values for K_m show a reluctance to dissociate from the substrate and hence are often less active than enzymes with low K_m values.

The determination of the Michaelis constant is achieved by plotting the two variables with fixed amount of enzyme, producing a characteristic shape. Substrate concentration at half the maximum velocity is numerically equal to the Michaelis constant:

$$\frac{V_{max}}{2} = \frac{V_{max} \times [S]}{K_m + [S]}$$

$$[S] = K_m$$

Although this method is extremely simple, it is experimentally inaccurate. Due to the hyperbolic nature of the relationship, the curve approaches maximum velocity asymptotically making the deduction of a value for V_{max} difficult. Any errors in assessing this value gets reflected in the value ascribed to K_m.

Due to the reason of poor deduction using the Michaelis graph, other methods are used which give a linear graph. They are derived from the rearrangement of the original equation and are as follows:-

Lineweaver-Burk equation:

$$v = \frac{V_{max} \times [S]}{K_m + [S]}$$

$$\frac{1}{v} = \frac{K_m + [S]}{V_{max} \times [S]}$$

$$\frac{1}{v} = \frac{K_m}{V_{max}\ [S]} + \frac{1}{V_{max}}$$

Hanes Woolf equation:

$$\frac{1}{v} = \frac{K_m}{V_{max}\ [S]} + \frac{1}{V_{max}}$$

multiply both sides by [S]

$$\frac{[S]}{v} = \frac{K_m\ \cancel{[S]}}{V_{max}\ \cancel{[S]}} + \frac{[S]}{V_{max}}$$

$$\frac{[S]}{v} = \frac{K_m}{V_{max}} + \frac{1}{V_{max}}[S]$$

Eadie-Hofstee equation:

$$\frac{1}{v} = \frac{K_m}{V_{max}}\ \frac{1}{[S]} + \frac{1}{V_{max}}$$

multiply both sides by v x V_{max}

$$\frac{\cancel{v} \times V_{max}}{\cancel{v}} = \frac{K_m}{\cancel{V_{max}}}\ \frac{v \times \cancel{V_{max}}}{[S]} + \frac{v \times \cancel{V_{max}}}{\cancel{V_{max}}}$$

$$V_{max} = K_m \frac{v}{[S]} + v$$

$$\therefore\ v = V_{max} - K_m \frac{v}{[S]}$$

These plots are a perfectly good method for determining kinetic parameters when experimental data does not contain errors but it is well known that every experiment will contain errors and this will affect the results gained in each case. In the cases of Lineweaver-Burk plot and Eadie-Hofstee the points furthest from the axis tend to skew the graphs the most as these points are for low substrate concentrations which are more prone to errors due to velocities being much slower making measurements less accurate. The Hanes-Woolf plot is a bit more accurate than the other two methods due to less scatter but still inaccurate when compared to another method - direct linear plots (Eisenthal, Cornish-Bowden). The direct linear plot is a simple method which plots negative substrate concentration and velocity and involves drawing a straight line between the points. This is done for each concentration of substrate giving a set of lines that cross at a point which is read as K_m. Errors not seen on the other plots are easily seen in this plot showing outlying points. This method is much more accurate for the determination of Km for the substrate (Eisenthal and Cornish-Bowden, 1974).

1.8.1 Enzyme Inhibition

Substances that decrease the rate of an enzyme catalysed reaction are known as inhibitors and their effects may be permanent or transient. There are three basic types of inhibition which can be seen by the Lineweaver-Burk plots they produce:

Competitive Inhibition

Competitive inhibition occurs when a compound has a similar chemical structure to the enzyme substrate. The inhibitor interacts with the enzyme to form an unproductive enzyme-competitive inhibitor complex. The Lineweaver-Burk plot showing competitive inhibition is shown in Figure 1.11. Another method used is the Dixon plot which involves plotting the reciprocal of velocity against the inhibitor concentration at each substrate concentration and the K_i value is read from the point at which they intersect. The Dixon plot showing competitive inhibition is shown in Figure 1.12.

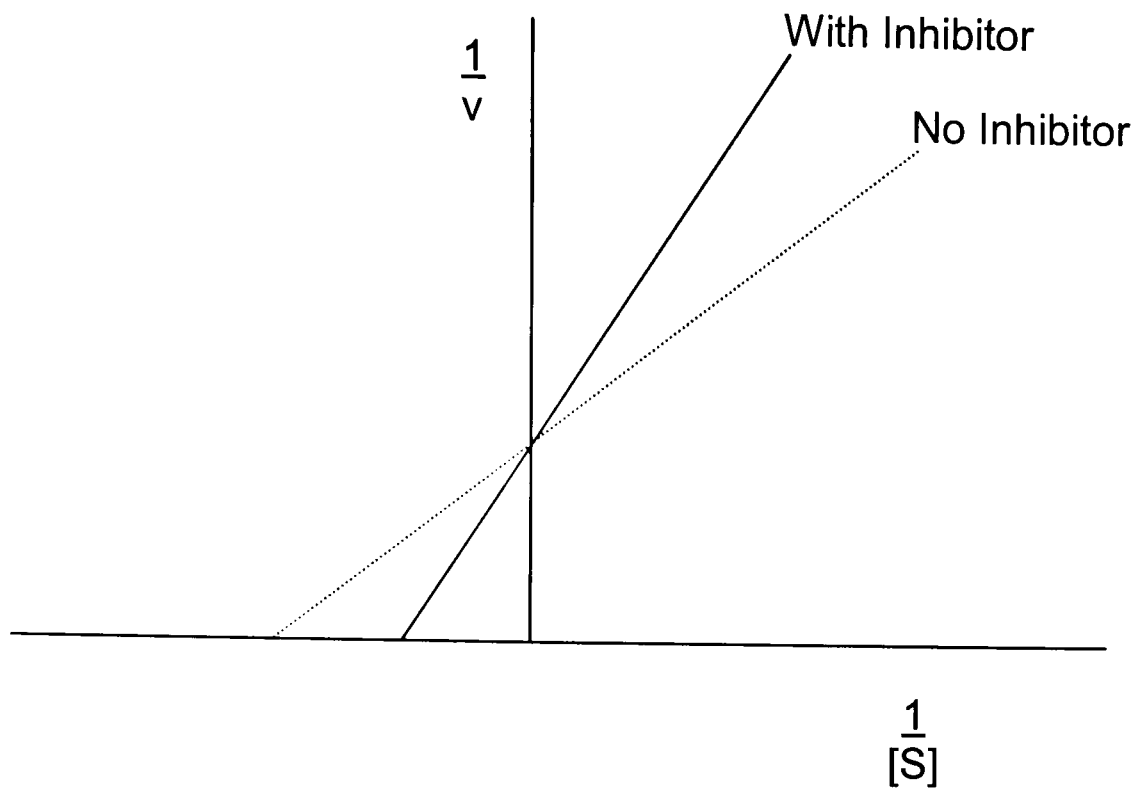

Figure 1.11 Lineweaver-Burk plot showing competitive inhibition

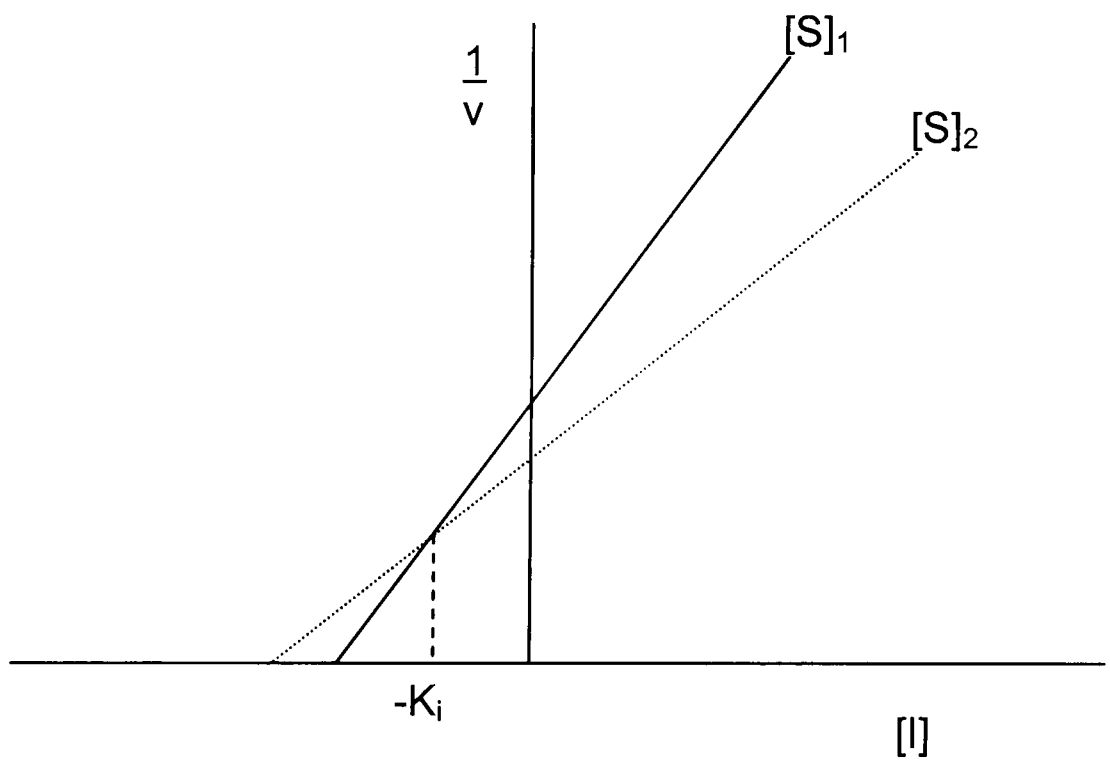

Figure 1.12 Dixon plot showing competitive inhibition

Non-competitive Inhibition

Non-competitive inhibitors bind to sites different from the substrate binding site and result in the inhibition of the formation of product by the breakdown of the enzyme-substrate complex. Such inhibition cannot be reversed by the addition of excess substrate and generally the inhibitor shows no structural similarity to

the substrate. The Lineweaver-Burk plot and Dixon plot showing non-competitive inhibition are shown in Figures 1.13 and 1.14.

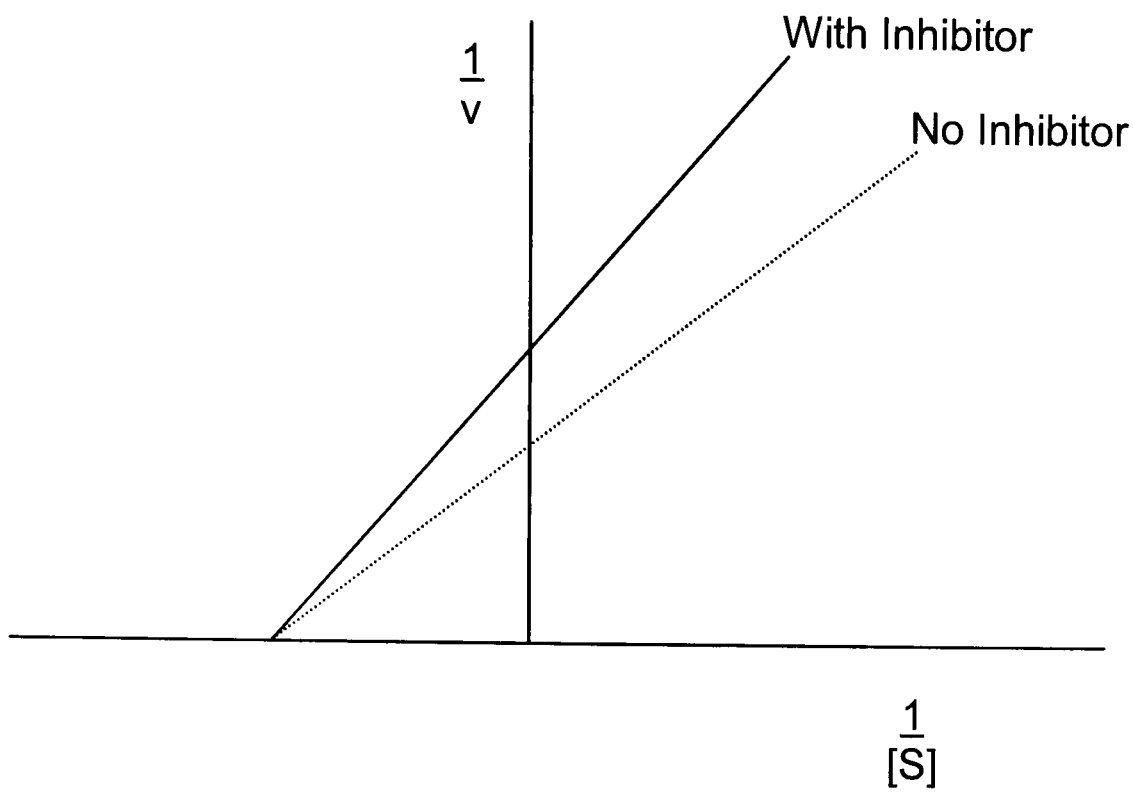

Figure 1.13 Lineweaver-Burk plot showing non-competitive inhibition

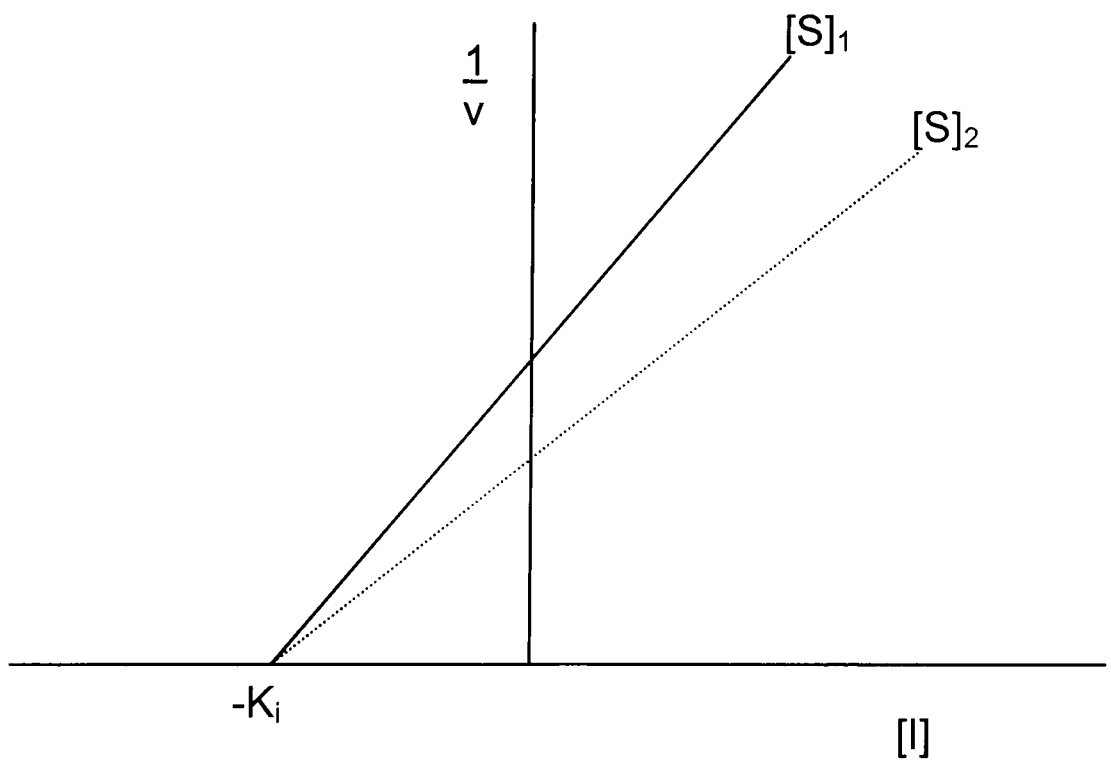

Figure 1.14 Dixon plot showing non-competitive inhibition

Uncompetitive Inhibition

Uncompetitive inhibitors bind only to the enzyme-substrate complex, and not to the free enzyme, thus reducing the formation of products. The Lineweaver-Burk plot showing uncompetitive inhibition is shown in Figure 1.15. It is not possible

to plot a Dixon plot for uncompetitive inhibition as the lines would be parallel, and since there is no intersection K_i cannot be determined.

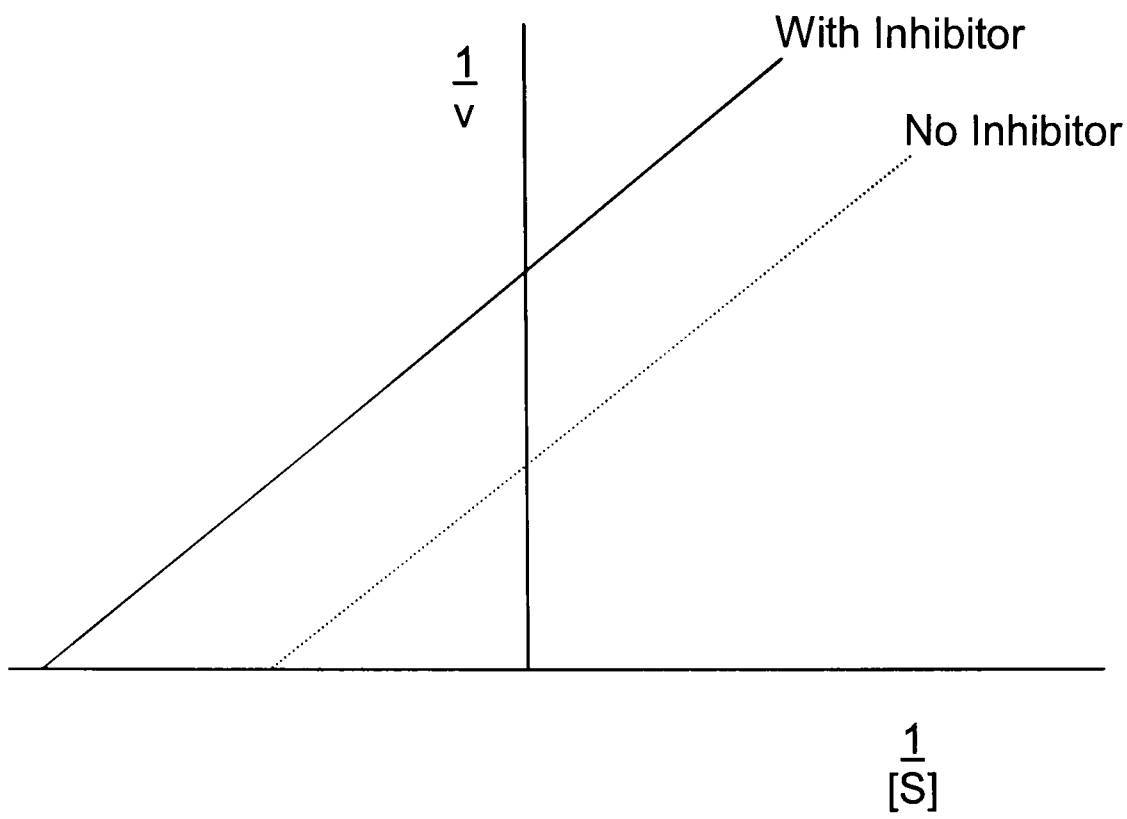

Figure 1.15 Lineweaver-Burk plot showing uncompetitive inhibition

1.9 Basis of present investigation

Androgens have been proposed as key endocrine factors for the initiation and progression of androgen-dependent diseases such as BPH and prostate cancer. One of the methods of treatment is the deprivation of androgens by the inhibition of enzymes involved in androgen biosynthesis including $P450_{17\alpha}$ and the 17β-HSD family of enzymes.

Extensive work has been carried out to develop highly potent and selective inhibitors of these enzymes. It is thought that the development of inhibitors for these enzymes may lead to an improvement in the treatment for hormone-dependent prostate cancer and BPH. Although extensive work has been undertaken in this area, there is a need for further development, since only a few compounds have been shown to be suitable for clinical trials.

The aim of the present investigation is to investigate the inhibitory activity of compounds previously designed and synthesised within the medicinal chemistry research group at Kingston University. The study aims to undertake initial screening of a range of compounds and the determination of their full biochemical profiles against both $P450_{17\alpha}$ and the 17β-HSD family of enzymes (in particular, types 1 and 3). In an effort to determine the selectivity of the compounds against the general HSD family of enzymes, the compounds designed as inhibitors of types 1 and 3 of 17β-HSD were also evaluated against 3β-HSD.

Chapter 2

2.0 $P450_{17\alpha}$

2.1 Introduction:

Several methods for assessing the activity of $P450_{17\alpha}$ have been developed which have used human, rat or pig testicular microsomal preparation to provide the major source of the enzyme (Rowlands et al, 1995; Chan et al, 1996; McCague et al, 1990; Nagai et al, 1987). Preparations from cattle, dog and monkey testes and adrenals have also been utilised. It has been found that P and Preg are each converted to A and DHEA respectively via their corresponding 17α-hydroxy intermediates (Lynn and Brown, 1958). As the enzyme catalyses two enzymatic activities, the assay procedures for each of the activities have been developed separately. Generally, the assay for the 17α-hydroxylase component involves the use of either radiolabelled P (for rat enzyme) or radiolabelled Preg (for human enzyme) as substrate. The substrate used for the 17,20-lyase component is either radiolabelled 17αOHP (for rat enzyme) or radiolabelled 17αOHPreg (for human enzyme).

Also, there has been some work carried out using non-radiolabelled substrate (Sergejew and Hartmann, 1994). This assay was specific for the 17α-hydroxylase component as P was used as a substrate and the source used was rat testis. The assay measured the absorbance of all the products at 240nm.

Initially separation and identification of the radiolabelled steroids used thin layer chromatography (TLC) (Betz and Michels, 1973; Li et al, 1992; Ayub and Levell, 1987a), after the assay procedure, however HPLC is now more commonly used (Barrie et al, 1989). Also for the non-radiolabelled assay, the method for the separation of steroids involved HPLC as the preferred method, as it has a better accuracy as well as it can detect much lower concentrations.

Another method that has been employed has been an acetic acid release assay which was originally designed by Chasalow et al (1982), but has been developed by Njar et al (1997). This method used 17αOHPreg labelled at the

21 position of the substrate and measured the amount of acetic acid released during the assay.

2.2 $P450_{17\alpha}$ Enzyme Assay: 17α-Hydroxylase Component

Compounds synthesised within the research group (by Dr. Chirag Patel and Mr. Imran Shahid) were evaluated for $P450_{17\alpha}$ (17α-hydroxylase) inhibitory activity, using the microsomal fraction obtained from rat testicular tissue (Sprague-Dawley). The assay was based on that of Owen (1995) and measures the effect of the novel compounds on the rate of conversion of radiolabelled P to 17αOHP then to A mediated by the action of $P450_{17\alpha}$ (17,20-lyase). However, since A is converted to T [mediated by the action of 17β-HSD (type 3)], as such so as to take into consideration this conversion of A, we also measured the production of T, thereby taking into consideration the majority of products and by-products resulting from the action of 17α-hydroxylase.

The assay reaction is quenched by the addition of diethyl ether (2mL), which is then extracted into a clean tube, followed by a further extraction with diethyl ether (2x2mL), which then provides the necessary solvent for extraction of the radiolabelled substrate and products.

The reaction products (17αOHP, A and T) along with the starting material (P), are separated using TLC. The extracts are applied to TLC plates (POLYGRAM® SIL G/UV_{254} silica gel with fluorescent indicator UV_{254} pre-coated on plastic sheets), together with non-radiolabelled carrier steroids (P, 17αOHP, A and T) which are used for the identification of the radiolabelled steroids from the assay mixture. The TLC plates are developed using a mixture of dichloromethane (70mL) and ethyl acetate (30mL).

After developing the plates, each steroid spot is identified under UV light and cut out, placed in individual scintillation tubes and counted for 3min in a cocktail of scintillation fluid (Optiscint HiSafe, 3mL) and acetone (1mL). The percentage conversion of P to 17αOHP, A and T is then determined by dividing the counts

per minute (CPM) for both products by the total CPM for all three steroids (equation 2.1).

$$\% \text{ Conversion} = \frac{A + T + 17\alpha OHP}{A + T + 17\alpha OHP + P} \times 100$$

Equation 2.1 Percentage conversion of P.

The method outlined in this study does not therefore require a quantitative recovery of all reactants and products from the assay mixture.

2.3 Methods, Materials and Instrumentation

All non-radioactive steroids and laboratory reagents were analar grade; β-NADP (mono sodium salt), D-glucose-6-phosphate (mono sodium salt), D-glucose-6-phosphate dehydrogenase (suspension in ammonium sulphate) were obtained from Roche Diagnostics, Lewes, East Sussex and ketoconazole was obtained from Sigma-Aldrich Company, Poole, Dorset. [1,2,6,7-^{3}H]P was obtained from Amersham Pharmacia Biotech UK Limited, Buckinghamshire.

Radioactivity was measured using a 1217 Rackbeta Scintillation Counter (LKB Wallac). Scintillation fluid was Optiscint HiSafe and was obtained from PerkinElmer Life and Analytical Sciences, Beaconsfield, Bucks.

Homogenisation of the rat testicular tissue was carried out using an Ultra-Turrax homogeniser (Janke & Kunkel, Germany). Excess tissue and the microsomal fraction was further homogenised with a Potter-Elvehjem homogeniser. Centrifugation was carried out using a MSE Europa 65M Ultracentrifuge at 10,000 × g (12,000RPM) and at 100,000 × g (35,000RPM).

All assays were carried out in triplicate – each value is therefore the mean of nine determinations.

2.4 Buffer, Solution and Substrate Preparation

Buffers and solutions used in the assay were as follows:

Potassium Phosphate Buffer pH7.4 (50mM)

A: 13.61g Potassium dihydrogen orthophosphate (KH_2PO_4, mW=136.09) dissolved in distilled water (500mL)

B: 34.84g Dipotassium hydrogen orthophosphate (K_2HPO_4, mW=174.18) dissolved in distilled water (1L)

Solution B was added to solution A until a pH of 7.4 was reached, to give a 0.2M buffer. The buffer (250mL) was diluted with distilled water (750mL) to give a concentration of 50mM.

Sodium Phosphate Buffer pH7.4 (50mM)

A: 3.90g Sodium dihydrogen orthophosphate ($NaH_2PO_4.2H_2O$, mW=156.01) dissolved in distilled water (500mL)

B: 4.45g Disodium hydrogen orthophosphate ($Na_2HPO_4.2H_2O$, mW=177.99) dissolved in distilled water (500mL)

Solution A was added to solution B until a pH of 7.4 was reached.

Sucrose Phosphate Buffer pH7.4 (50mM)

Sucrose (0.25M) in potassium phosphate buffer (50mM, pH7.4). 21.39g sucrose (mW= 342.30) was dissolved in potassium phosphate buffer (50mM, pH7.4, 250mL).

NADPH-generating System

D-glucose-6-phosphate (0.0282g, 0.1M)

NADP as the monosodium salt (0.0086g, 0.1M)

D-glucose-6-phosphate dehydrogenase (15μL, 4iu/mL)

Phosphate buffer pH7.4 (1mL, 50mM)

The generating system was kept on ice until required for use.

Substrate preparation of [1,2,6,7-^{3}H]P (100μM)

A stock solution was prepared by transferring radiolabelled [1,2,6,7-^{3}H]P (0.22μM, 50μL) to a glass vial and removing the toluene under a stream of nitrogen. Unlabelled substrate in propane-1,2-diol (99.78μM, 1 mL) was added to the radiolabelled residue and mixed thoroughly to give a final concentration of 100μM.

2.5 Preparation of Testicular Microsomes

Mature male rat testes (Sprague-Dawley) were obtained from Charles Rivers, Margate, Kent. The capsule was dissected out and the tissue was homogenised in phosphate buffer pH7.4 containing sucrose (50mM, 15mL) using a Potter homogeniser and then centrifuged for 20min at 12,000RPM (10,000 x g) at 4°C. The pellet was discarded and the supernatant spun at 35,000RPM (100,000 x g) for 1h. The pellet (microsomal fraction) was suspended in sodium phosphate buffer pH7.4 (15mL) using a Potter homogeniser and aliquots (500μL) pipetted into capped 1.5mL plastic tubes, snap-frozen in liquid nitrogen and stored at -70°C until required for use.

2.6 Protein Assay

The protein content of the microsomal fraction was determined using the Folin-Lowry assay (Lowry et al, 1951). This assay depends on the presence of aromatic amino acids in the protein. A cupric/peptide bond complex (between the alkaline copper-phenol reagent used and the tyrosine and tryptophan residues of the protein) is formed and then this is enhanced by a phosphomolybdate complex with the aromatic amino acids (Young et al, 2001). The protein content is determined colourimetrically with reference to a standard curve of bovine serum albumin (Gibson and Skett, 1994). The optimum absorbance was found to be λ_{max} 750nm.

Protein standard solutions (0-200μg/mL, 1mL) were prepared in test tubes (in triplicate), containing varying amounts of bovine serum albumin protein standard (200μg/mL). The microsomes were diluted by a factor of 100 (50μL/5mL), and 1mL (in triplicate) tested alongside the standards.

Anhydrous sodium carbonate (2%), in sodium hydroxide (0.1M, 200mL) was added to copper sulphate (1%, 2mL), and sodium potassium tartrate (2%, 2mL). Aliquots (5mL) were added at 30s intervals to each of the test tubes. After standing for 10min, a 50% diluted solution of Folin-Ciocalteu's phenol reagent (0.5mL) was added to each tube. The tubes were immediately vortexed and allowed to stand at room temperature (30min). The optical density (λ_{max} 750nm) of each solution was measured (UNICAM 8700 series UV/VIS) against the blank.

The protein concentration of the testicular microsomes was determined from the standard protein calibration curve (Figure 2.1), and was found to be 15.64mg/mL.

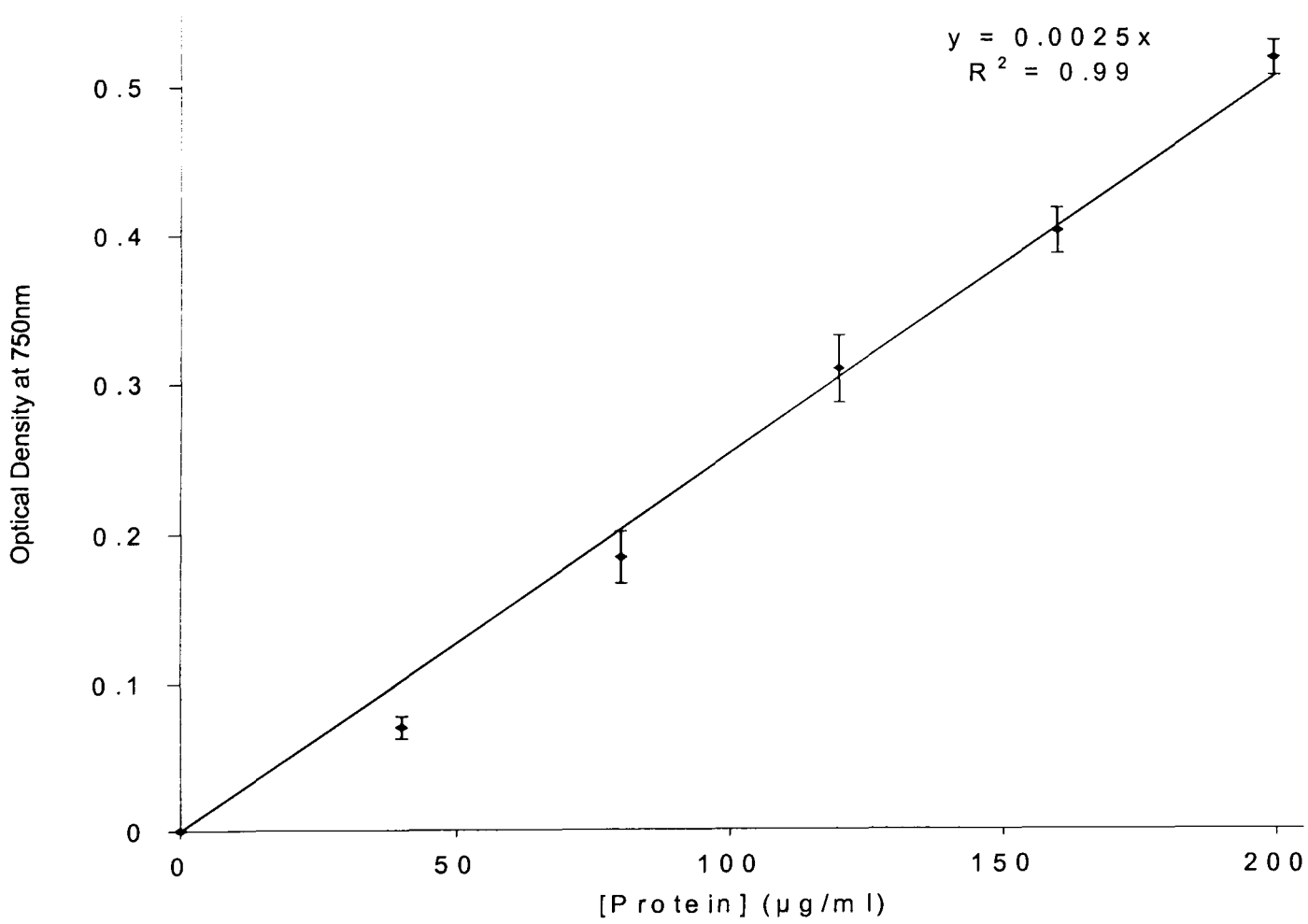

Figure 2.1 Calibration graph for protein assay for 17α-hydroxylase

2.7 Validation of the 17α-Hydroxylase Assay

To validate the 17α-hydroxylase assay, it was necessary to determine the quantity of non-enymatic product formation. Assay conditions were set so that the prepared substrate, P (1μM final concentration), was incubated for 30min at 37°C in the following solutions:

i. Sodium phosphate buffer (50mM, pH7.4)
ii. Testicular microsomes (0.16mg/mL, 10μL) and sodium phosphate buffer, lacking NADPH-generating system
iii. Testicular microsomes, denatured by addition of ether (2mL), sodium phosphate buffer and NADPH-generating system

After incubation, the assay mixtures were treated, except (iii), with ether (2mL). The solutions were vortexed, then left to stand over ice for 15min. The organic phase was extracted into a separate clean tube. The assay mixture was further extracted with ether (2x2mL), and the organic layers combined. The solvent was removed under a stream of nitrogen, acetone (30μl) was added to each tube and the solution spotted onto silica based TLC plates along with carrier steroids (P, 17αOHP, A and T, 5mg/mL). The plates were developed using the mobile phase which consisted of dichloromethane (70mL) and ethyl acetate (30mL). After development, the separated steroids were identified, using an UV lamp, cut from the plate and placed into a scintillation tube. Acetone (1mL) was added to dissolve the steroid from the silica plate and scintillation fluid (Optiscint HiSafe, 3mL) was then added. The samples were vortexed and then read for radioactivity (3min). None of the samples showed detectable quantities of 17αOHP, A or T, indicating that (a) testicular microsomes and (b) NADPH are both essential requirements for the conversion of P to its subsequent products.

2.8 Protein-dependency Assay for 17α-Hydroxylase

An assay was carried out to establish whether the rate of appearance of 17αOHP, A and T produced during the enzymatic reaction, was proportional to the protein concentration.

Incubations were carried out (in triplicate) using protein concentrations 0.1564, 0.3128, 0.4692, 0.6256 and 0.7820mg/mL (final concentration), prepared substrate P (1.5μM final concentration, 15μl), NADPH-generating system (50μL) and sodium phosphate buffer (pH7.4, made up to 1mL). The solutions were incubated for 15min at 37°C and the reaction was quenched by the addition of ether (2mL). The assay was completed as previously described (Section 2.7) and the percentage conversions determined using equation 2.1. The results are shown in Figure 2.2.

At 1.5μM substrate concentration, it can be concluded that the kinetics of the reaction are linear for concentrations up to 0.47mg/mL protein.

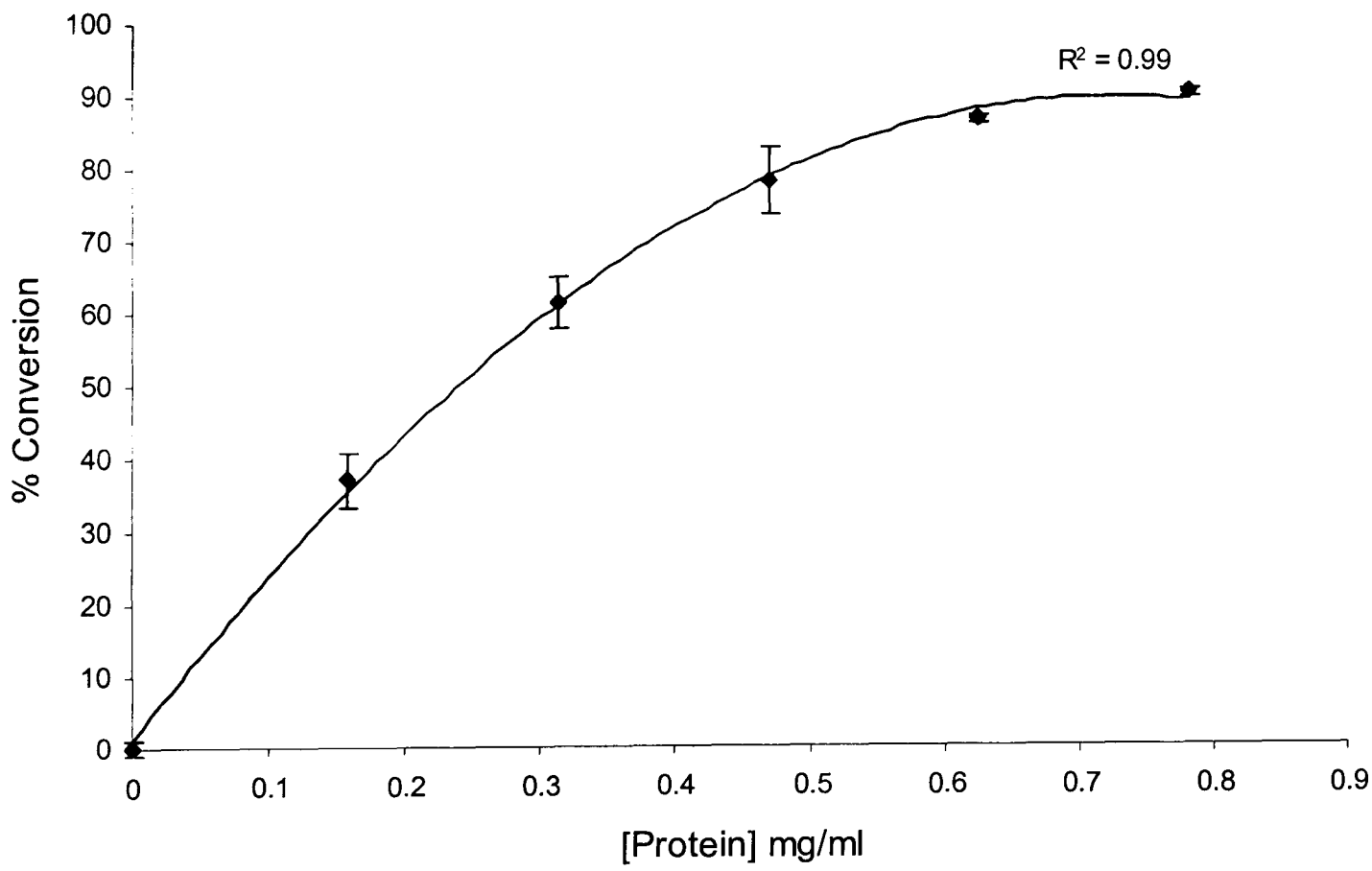

Figure 2.2 Plot to show percentage conversion of P at varying protein concentrations.

2.9 Time Validation Assay for 17α-Hydroxylase

A time dependency assay was carried out to ensure that the assay was within the linear phase of the enzyme reaction.

The prepared substrate, P (1.5μM, 15μL), NADPH-generating system (50μL) and sodium phosphate buffer (pH7.4, 925μL) were incubated in triplicate at 37°C in a shaking water bath for 5min. The assay was initiated by the addition of testicular microsomes (final assay concentration 0.16mg/mL, 10μL). After 15, 30, 45, 60, 75 and 90min of incubation the assay tubes were quenched by the addition of ether (2mL) and placed on ice. The assay was completed as previously described (Section 2.7). A graph was then plotted for percentage conversion versus time (Figure 2.3).

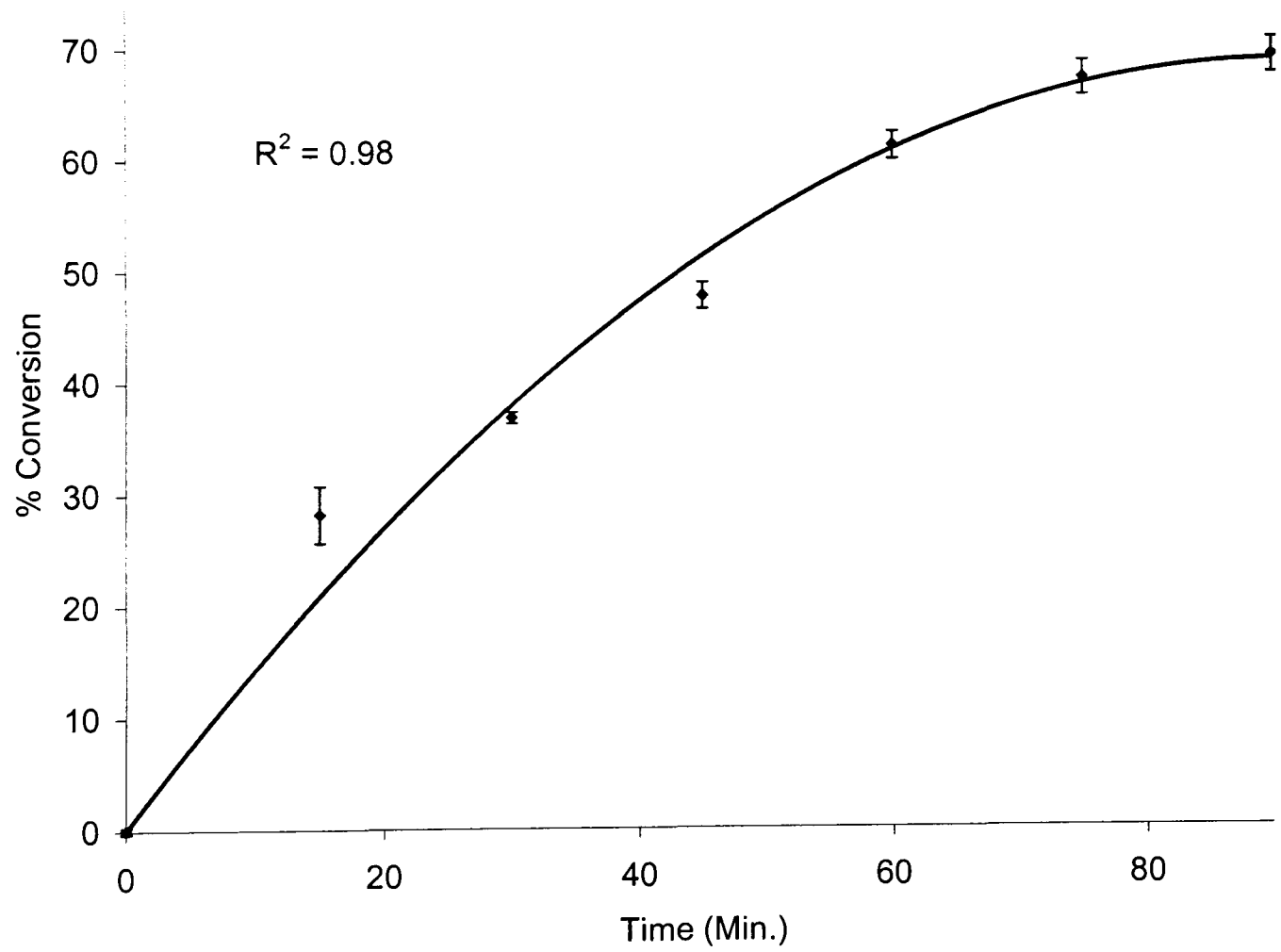

Figure 2.3 Plot to show percentage conversion of P at varying time intervals.

At 0.16mg/mL protein concentration and 1.5μM substrate concentration, it can be concluded that the kinetics of the reaction are linear up to 60 min.

2.10 Determination of the Michaelis Constant (K_m) for 17α-Hydroxylase

The assay was carried out in triplicate. The prepared substrate was serially diluted with propane-1,2-diol, to give a range of final incubation concentrations of 0.1 to 1μM. All incubations were carried out at 37°C in a shaking water bath. Incubation mixtures (1mL), containing NADPH-generating system (50μL) and prepared substrate, P (of varying concentrations, 10μL), in phosphate buffer (930μL, pH7.4) were incubated for 5min. The testicular microsomes (10μL, final assay concentration 0.16mg/mL) were thawed and warmed to 37°C before addition to the assay mixture. The assay was initiated by the addition of the microsomes. After 15min incubation at 37°C, the assay tubes were quenched by the addition of ether (2mL) and placed on ice. The assay was completed as previously described (Section 2.7).

The velocity, v, for each substrate concentration was calculated using the following equation, where units for v are: μM/min/mg.

$$v = \frac{\text{CPM (A + T + 17}\alpha\text{OHP) x Substrate conc. [S] (}\mu\text{M)}}{\text{CPM (A + T + 17}\alpha\text{OHP + P) x protein conc. (mg/ml) x time (min)}}$$

Equation 2.2 Velocity calculation for each substrate concentration

2.11 Results: Determination of K_m

The K_m and maximum velocity (V_{max}) were determined from five different general methods for P and are shown in Figures 2.4 to 2.8.

I. Michaelis Menten plot: v vs [S] where K_m = [S] at ½ V_{max} (Figure 2.4)
II. Lineweaver-Burk plot: 1/v vs 1/[S] where $-1/K_m$ = x intercept, $1/V_{max}$ = y intercept, and K_m/V_{max} = slope (Figure 2.5)
III. Hanes-Woolf plot: [S]/v vs [S] where K_m/V_{max} = y intercept, $1/V_{max}$ = slope and $-K_m$ = x intercept (Figure 2.6)

IV. Eadie-Hofstee plot: v vs v/[S] where $-K_m$ = gradient, and V_{max} = y intercept (Figure 2.7)

V. Direct linear plot where K_m and V_{max}= intercept of plot lines. (Figure 2.8)

The K_m values obtained from the graphical methods are summarised in Table 2.1.

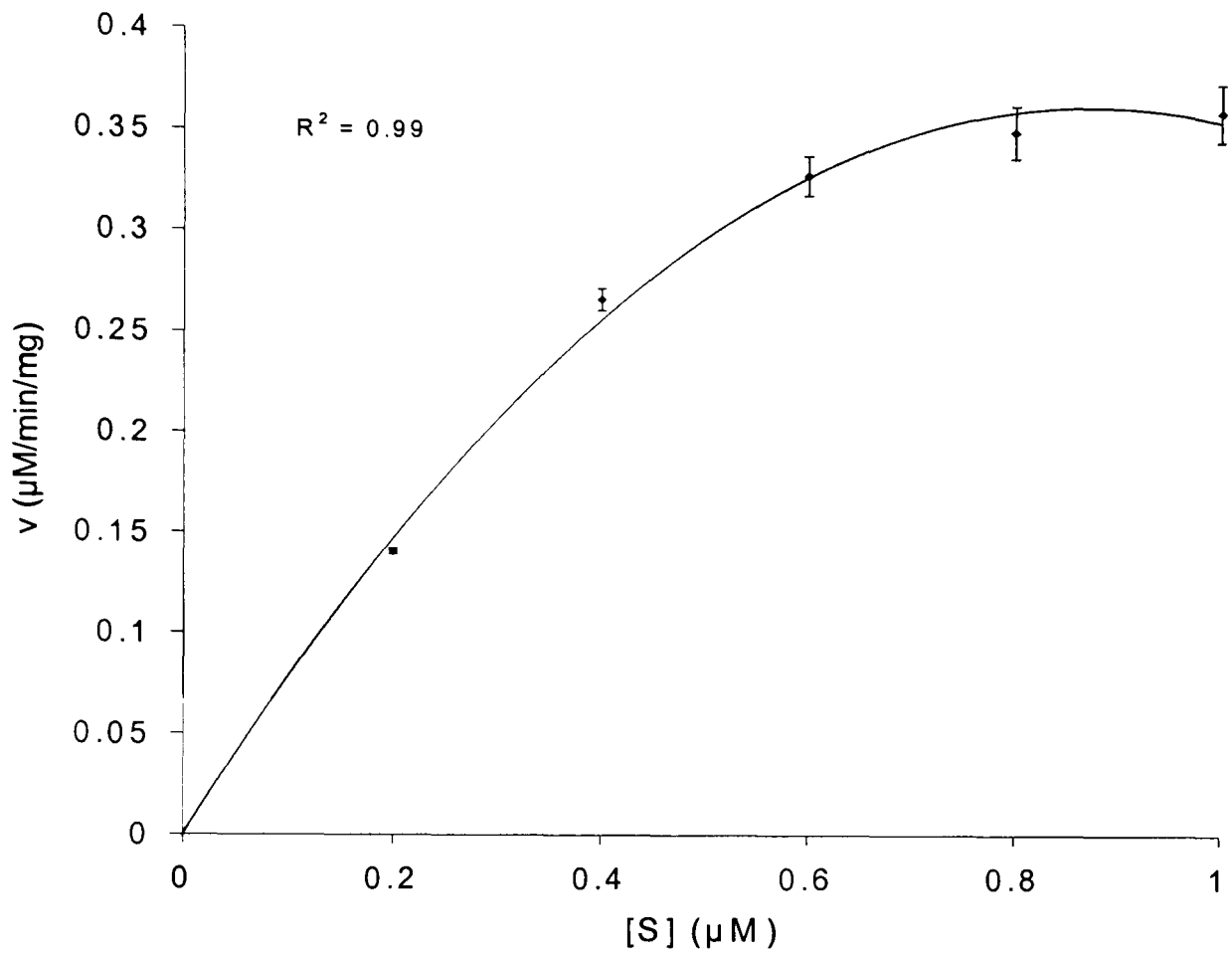

Figure 2.4 Michaelis Menten plot for 17α-hydroxylase.

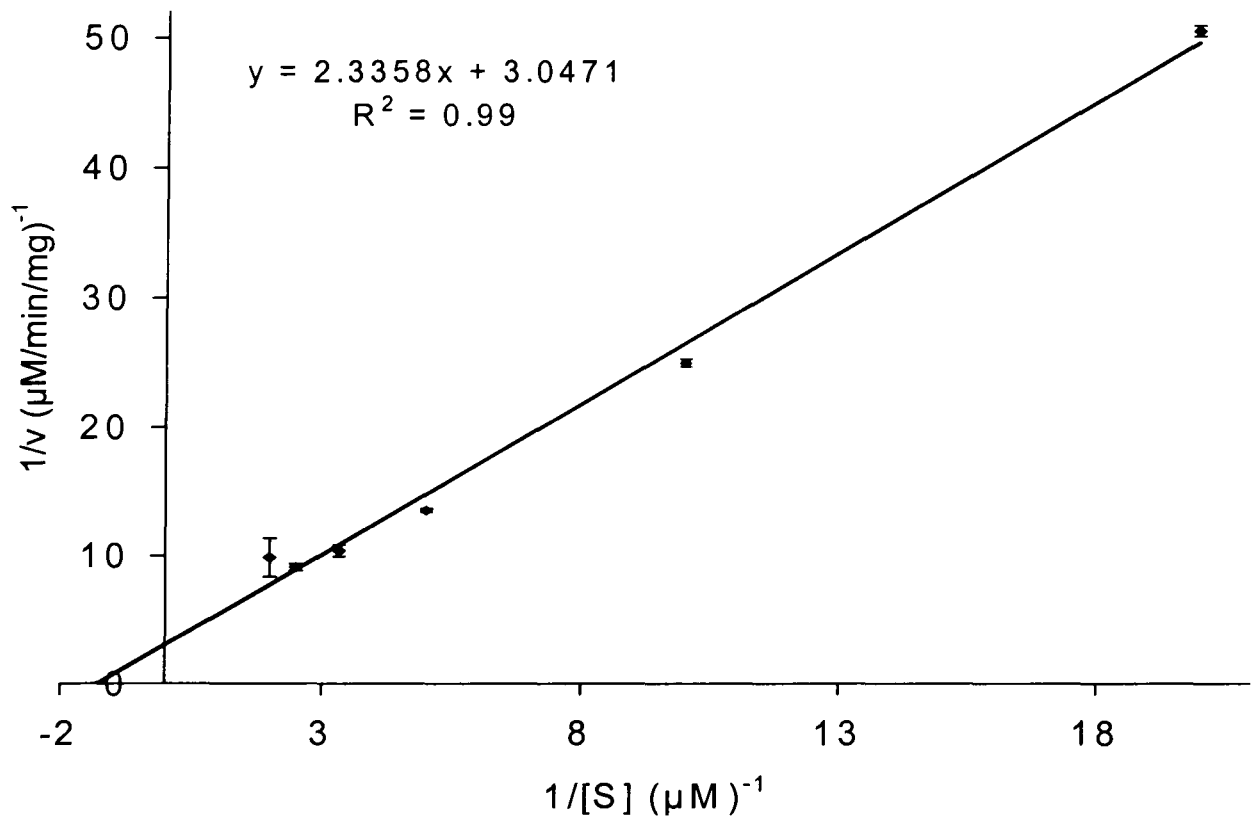

Figure 2.5 Lineweaver-Burk plot for 17α-hydroxylase.

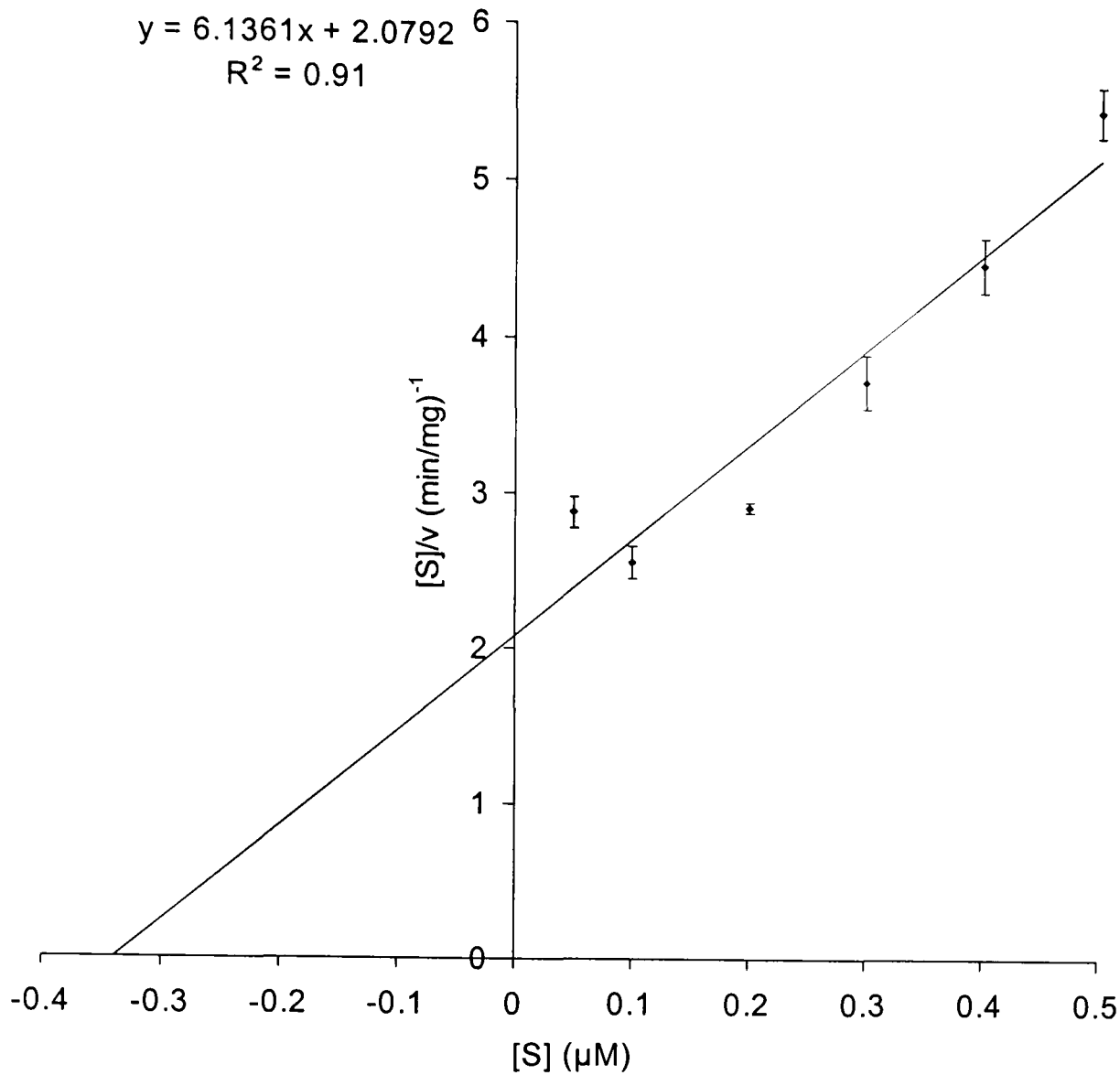

Figure 2.6 Hanes-Woolf plot for 17α-hydroxylase.

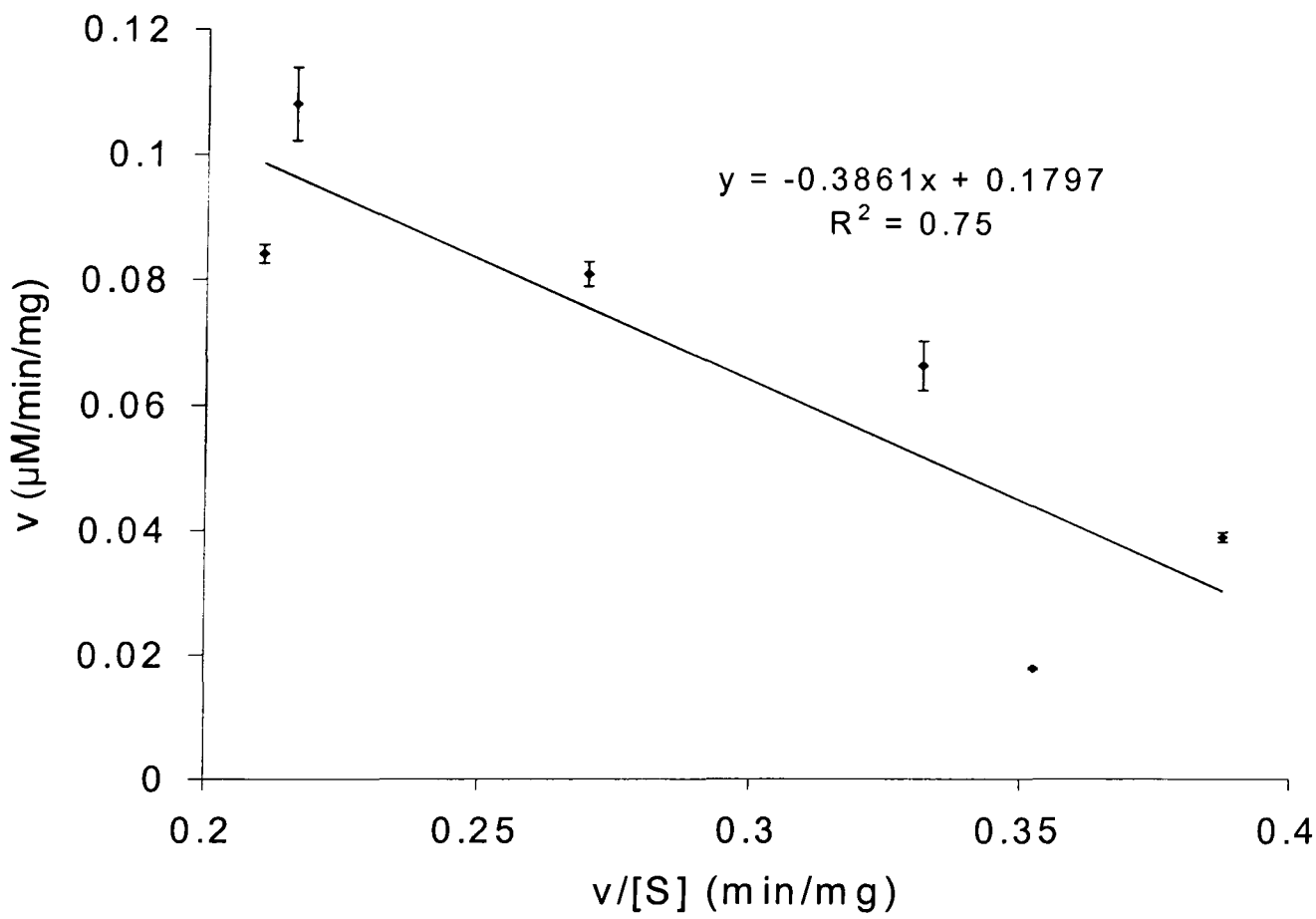

Figure 2.7 Eadie-Hofstee plot for 17α-hydroxylase.

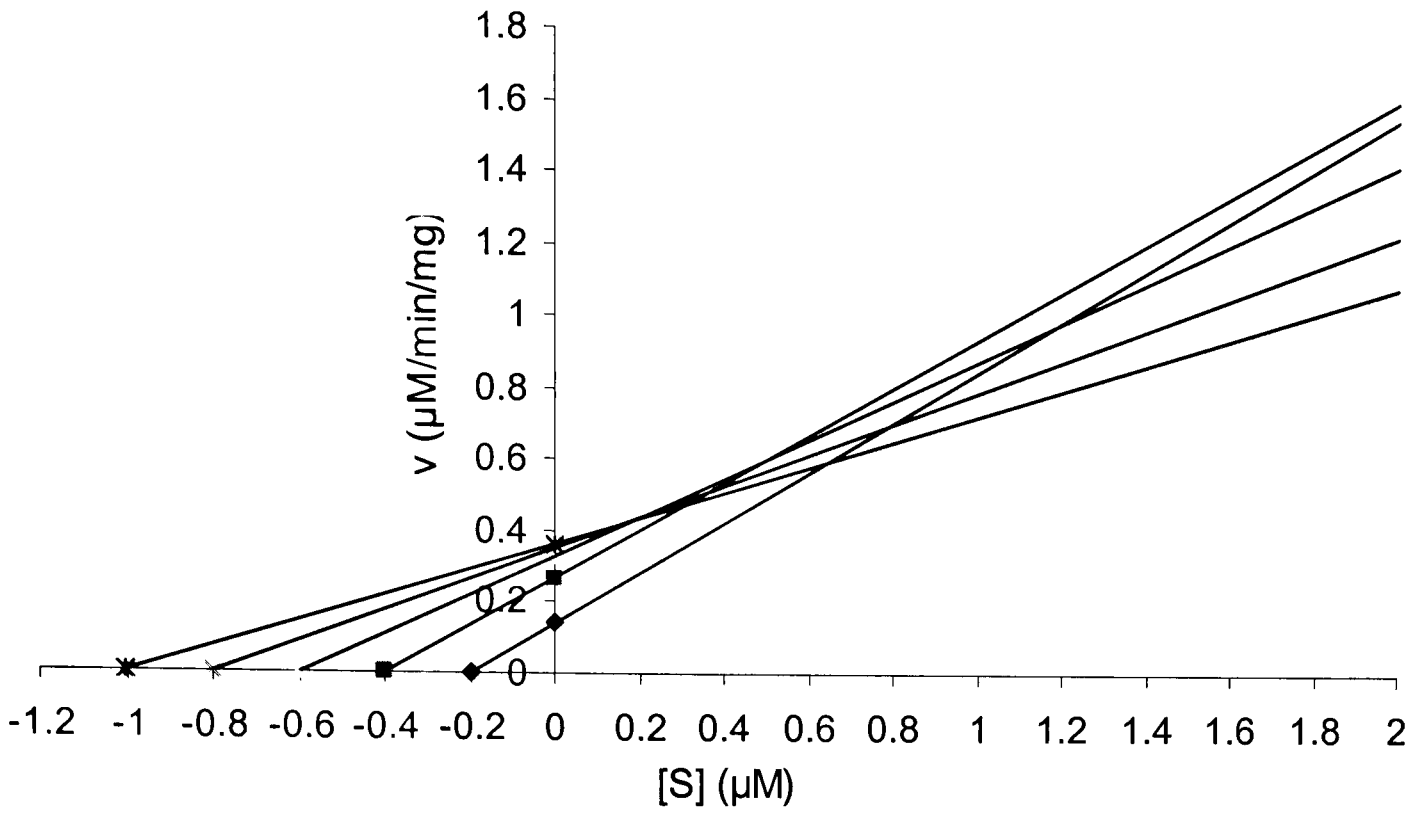

Figure 2.8 Direct linear plot for 17α-hydroxylase.

Plot	K_m (μM)
Michaelis Menten plot	0.25 ± 0.05
Lineweaver-Burk plot	0.77 ± 0.18
Hanes-Woolf plot	0.34 ± 0.02
Eadie-Hofstee plot	0.39 ± 0.03
Direct linear plot	0.39 ± 0.02
Average K_m	0.43 ± 0.06

Table 2.1 Summary of K_m plots for 17α-hydroxylase. Results are expressed as mean ± SD.

2.12 Discussion

The average K_m value for 17α-hydroxylase with the substrate P using Sprague-Dawley testicular microsomes was found to be 0.43 ± 0.06μM, compared to K_m values obtained by other workers against rat testicular microsomes, i.e., K_m = 1.4μM (Hartmann et al, 2000) and K_m = 4.3nM (Barrie et al, 1997). Evidence of inhibition at high substrate concentration is seen by the upward curve on the Lineweaver-Burk plot. Non-linearity is seen for the Lineweaver-Burk plot which explains the poor R^2 values for the Hanes-Woolf and Eadie-Hofstee plots.

2.13 Preliminary Screening of Synthesised Compounds for 17α-Hydroxylase Inhibitory Activity

The assay procedure for screening involved inhibitors and standard (ketoconazole) dissolved in absolute ethanol and diluted to give the required final incubation concentration. The assay was carried out (in triplicate) at 37°C in a shaking water bath. The total assay volume was 1mL. Prepared substrate, P (15μL, 1.5μM/tube), inhibitors (20μL, in ethanol), NADPH-generating system (50μL) and sodium phosphate buffer (pH7.4, 905μL) was added to each tube. The testicular microsomes and assay tubes were pre-incubated for 5min at 37°C in a shaking water bath prior to the addition of the microsomes (10μL, final assay concentration 0.16mg/mL) to the tubes. After 15min incubation at 37°C, the assay tubes were quenched by the addition of ether (2mL) and placed on ice. The assay was completed as previously described (Section 2.7). Control samples with no inhibitor were incubated simultaneously. The results were determined by using equation 2.1 to determine the percentage conversion of P and then comparing the conversion in the presence of inhibitors to that of the controls. Results are shown in Tables 2.3a – 2.10c.

2.14 Determination of IC_{50}

IC_{50} is the inhibitor concentration required for 50% inhibition of the enzyme. IC_{50} determination was carried out on ketoconazole and all inhibitors which showed significant 17α-hydroxylase inhibitory activity. The assay was carried out in the same manner as described in Section 2.13, except that a single inhibitor (20μL) was tested over a range of final assay concentrations depending on their preliminary screening result. The IC_{50} was determined from plots of percentage inhibition versus Log [I] (Figures 2.17 – 2.26; Figures 2.37 – 2.41; Figures 2.46 – 2.49; Figures 2.53 – 2.56 and Figures 2.69 – 2.72).

2.15 $P450_{17\alpha}$ Enzyme Assay: 17,20-Lyase Component

The compounds tested for 17α-hydroxylase activity were also tested for 17,20-lyase inhibitory activity, using the microsomal fraction obtained from rat testicular tissue (Sprague-Dawley). The assay was based on that of Owen (1995) and measures the effect of the novel compounds on the rate of conversion of radiolabelled 17αOHP to A mediated by the action of $P450_{17\alpha}$ (17,20-lyase), and also considering the conversion to T mediated by the action of 17β-HSD (type 3) as mentioned in Section 2.2. The assay reaction is quenched and the extraction carried out in a similar manner to the 17α-hydroxylase assay.

The reaction products (A and T) along with the substrate (17αOHP) are separated using TLC. The TLC plates are developed using a mixture modified from that of Owen (1995), ie. dichloromethane (70mL) and ethyl acetate (30mL).

The percentage conversion of 17αOHP to A and T is then determined by dividing the CPM for both products by the total CPM for all three steroids (equation 2.3).

$$\% \text{ Conversion} = \frac{A + T}{A + T + 17\alpha OHP} \times 100$$

Equation 2.3 Percentage conversion of 17αOHP.

As with the 17α-hydroxylase assay the method outlined does not require a quantitative recovery of all reactants and products from the assay mixture.

2.16 Methods, Materials and Instrumentation

Methods, materials and instruments were, in general, as described in Section 2.3 except that [1,2,6,7-^{3}H]17αOHP was obtained from Amersham Pharmacia Biotech UK Limited, Buckinghamshire and was used in place of P.

2.17 Buffer, Solution and Substrate Preparation

Buffers and solutions used in the assay were prepared as for the 17α-hydroxylase assay (Section 2.4).

Substrate preparation of [1,2,6,7-^{3}H]17αOHP (100μM)

A stock solution was prepared by transferring radiolabelled 17α-hydroxy[1,2,6,7-^{3}H]progesterone (0.27μM, 50μL) to a glass vial and removing the toluene under a stream of nitrogen. Unlabelled substrate in propane-1,2-diol (99.73μM, 1mL) was added to the radiolabelled residue and mixed thoroughly to give a final concentration of 100μM.

2.18 Preparation of Testicular Microsomes

The testicular microsomes were prepared as described in Section 2.5.

2.19 Protein Assay

The protein content of the microsomal fraction was determined as previously described in Section 2.6. The results are shown in Figure 2.9 below.

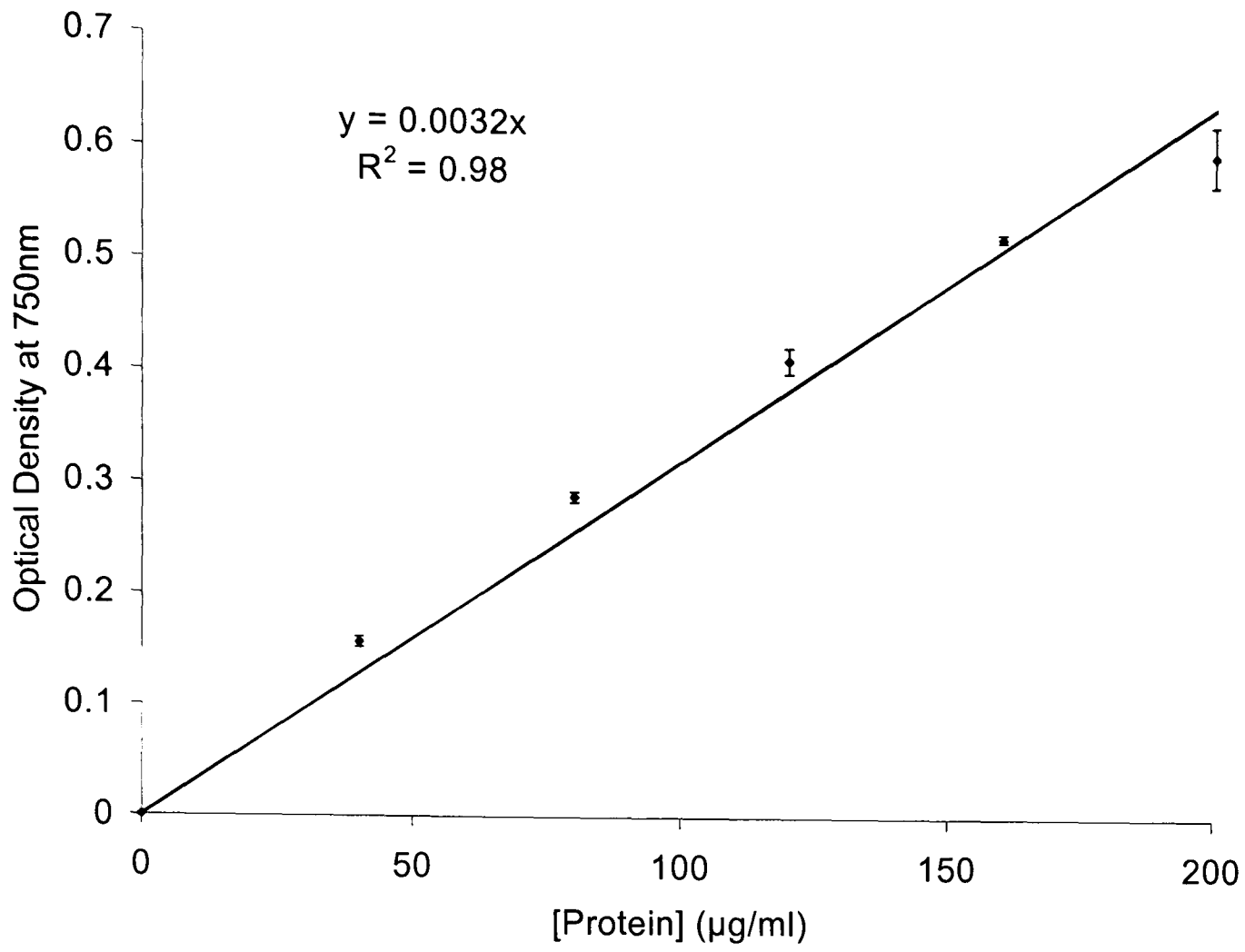

Figure 2.9 Calibration graph for protein assay for 17,20-lyase

The protein concentration of the testicular microsomes was determined from the standard protein calibration curve (Figure 2.9) and was found to be 15.37mg/mL.

2.20 Validation of the 17,20-Lyase Assay

To validate the 17,20-lyase assay, it was necessary to determine the quantity of non-enymatic product formation. Assay conditions were set so that the prepared substrate, 17αOHP (1µM final concentration), was incubated for 30min at 37°C in the following solutions:

i. Sodium phosphate buffer (50mM, pH7.4)
ii. Testicular microsomes (0.15mg/mL, 10µl) and sodium phosphate buffer, lacking NADPH-generating system
iii. Testicular microsomes, denatured by addition of ether (2mL), sodium phosphate buffer and NADPH-generating system

After incubation, the assay mixtures were treated, except (iii), with ether (2mL). The solutions were vortexed, then left to stand over ice for 15min. The organic phase was extracted into a separate clean tube. The assay mixture was further extracted with ether (2x2mL), and the organic layers combined. The solvent was removed under a stream of nitrogen, acetone (30μl) was added to each tube and the solution spotted onto silica based TLC plates along with carrier steroids (17αOHP, A and T, 5mg/mL). The TLC plates were developed using a mobile phase consisting of dichloromethane (70mL) and ethyl acetate (30mL). After development, the separated steroids were identified, using an UV lamp, cut from the plate and placed into a scintillation tube. Acetone (1mL) was added to dissolve the steroid from the silica plate and scintillation fluid (Optiscint HiSafe, 3mL) was then added. The samples were vortexed and then read for radioactivity (3min). None of the samples showed detectable quantities of A or T, indicating that (a) testicular microsomes and (b) NADPH are both essential requirements for the conversion of 17αOHP to its subsequent products.

2.21 Protein-dependency Assay for 17,20-Lyase

An assay was carried out to establish whether the rate of appearance of A and T produced during the enzymatic reaction, was proportional to the protein concentration.

Incubations were carried out (in triplicate) using protein concentrations 0.0767, 0.1534, 0.3068, 0.4602, 0.6136mg/mL (final concentration), prepared substrate, 17αOHP (1μM final concentration, 10μL), NADPH-generating system (50μL) and sodium phosphate buffer (pH7.4, made up to 1mL). The solutions were incubated for 30min at 37°C and the reaction was quenched by the addition of ether (2mL) and placed on ice. The assay was completed as previously described (Section 2.20) and the percentage conversions determined using equation 2.3. The results are shown in Figure 2.10.

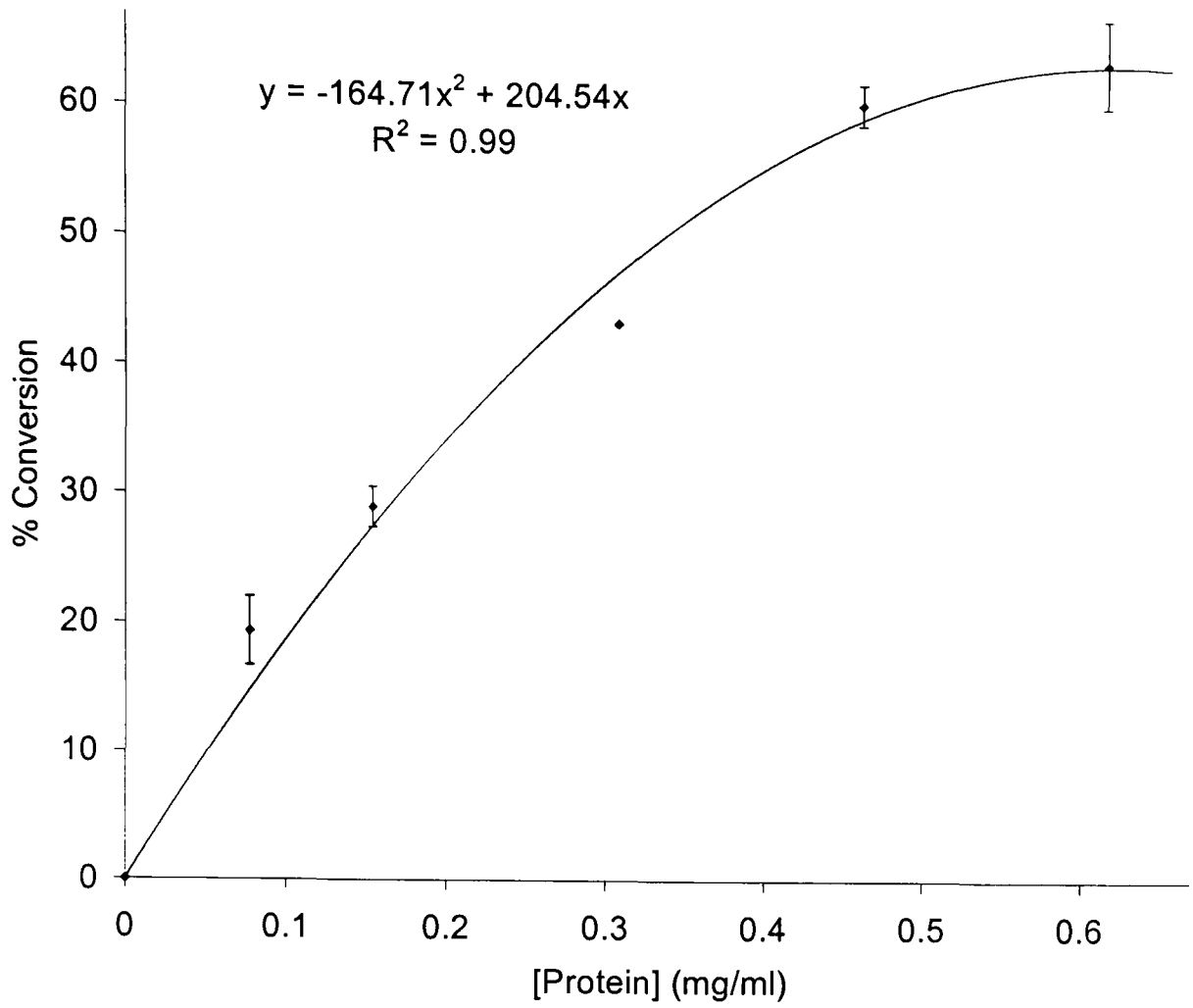

Figure 2.10 Plot to show percentage conversion of 17αOHP at varying protein concentrations.

At 1μM substrate concentration, it can be concluded that the kinetics of the reaction are linear for protein concentrations below 0.31mg/mL.

2.22 Time Validation Assay for 17,20-Lyase

A time dependency assay was carried out to ensure that the assay was within the linear phase of the enzyme reaction.

The prepared substrate, 17αOHP (1μM, 10μL), NADPH-generating system (50μL) and sodium phosphate buffer (pH7.4, 930μL) were incubated in triplicate at 37°C in a shaking water bath for 5min. The assay was initiated by the addition of testicular microsomes (final assay concentration 0.15mg/mL, 10μL). After 10, 20, 30, 40 and 50min of incubation the assay tubes were quenched by the addition of ether (2mL) and placed on ice. The assay was completed as previously described (Section 2.20). A graph was then plotted for percentage conversion versus time (Figure 2.11).

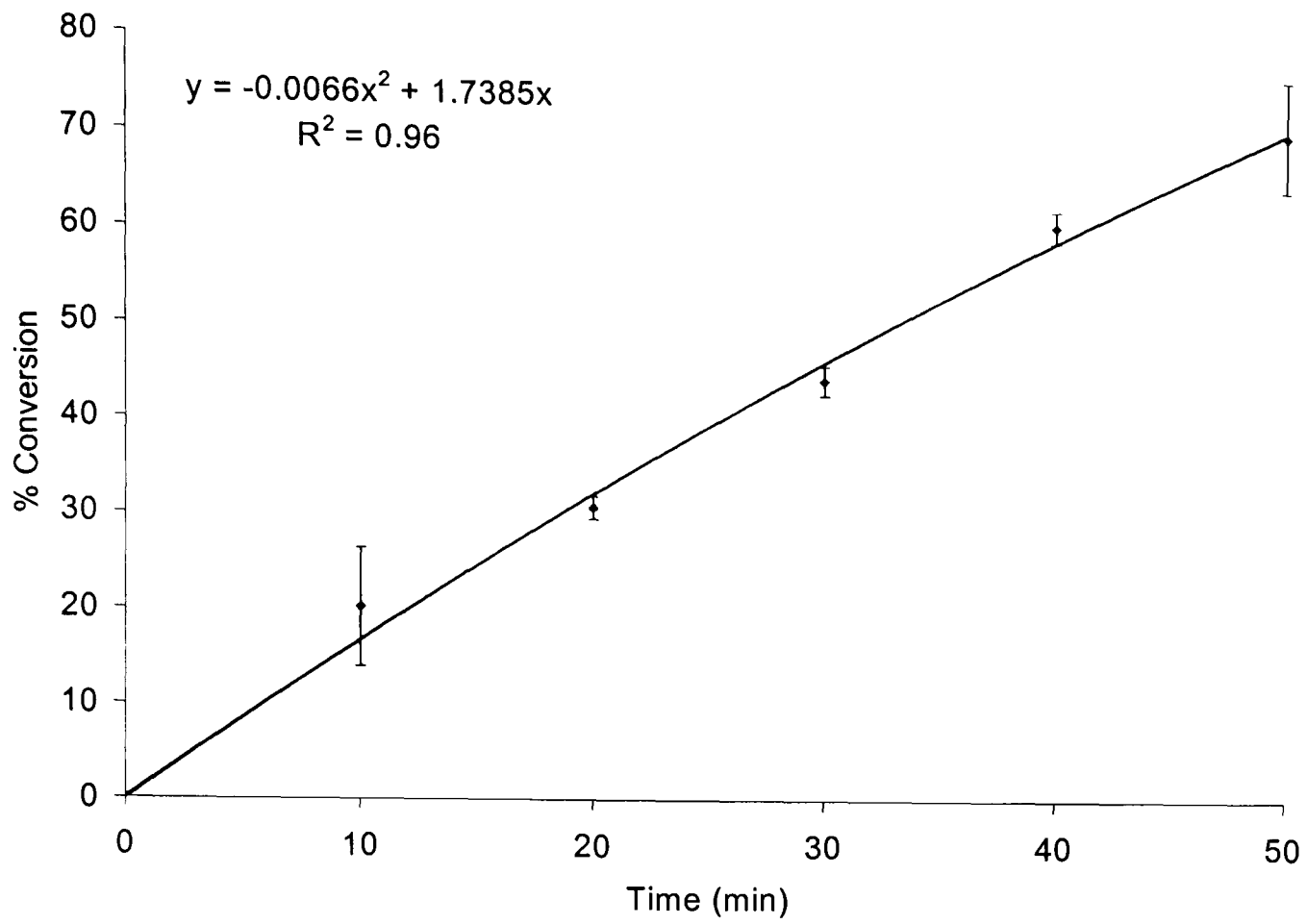

Figure 2.11 Plot to show percentage conversion of 17αOHP at varying time intervals.

At 0.15mg/mL protein concentration and 1μM substrate concentration, it can be concluded that the kinetics of the reaction are linear up to 50min.

2.23 Determination of K_m for 17,20-Lyase

The assay was carried out in triplicate. The prepared substrate was serially diluted with propane-1,2-diol, to give a range of final incubation concentrations of 0.25 to 1μM. All incubations were carried out at 37°C in a shaking water bath. Incubation mixtures (1mL), containing NADPH-generating system (50μL) and prepared substrate, 17αOHP (of varying concentrations, 10μL), in phosphate buffer (930μL, pH7.4) were incubated for 5min. The testicular microsomes (10μL, final assay concentration 0.15mg/mL) were thawed and warmed to 37°C before addition to the assay mixture. The assay was initiated by the addition of the microsomes. After 30min incubation at 37°C, the assay tubes were quenched by the addition of ether (2mL) and placed on ice. The assay was completed as previously described (Section 2.20).

The velocity, v, for each substrate concentration was calculated using the following equation, where units for v are: μM/min/mg.

$$v = \frac{\text{CPM (A + T) x Substrate conc. [S] (}\mu\text{M)}}{\text{CPM (A + T + 17}\alpha\text{-OHP) x protein conc. (mg/ml) x time (min)}}$$

Equation 2.4 Velocity calculation for each substrate concentration

The K_m and V_{max} were determined from five different general methods (see Section 2.11) for 17αOHP and are shown in Figures 2.12 to 2.16.

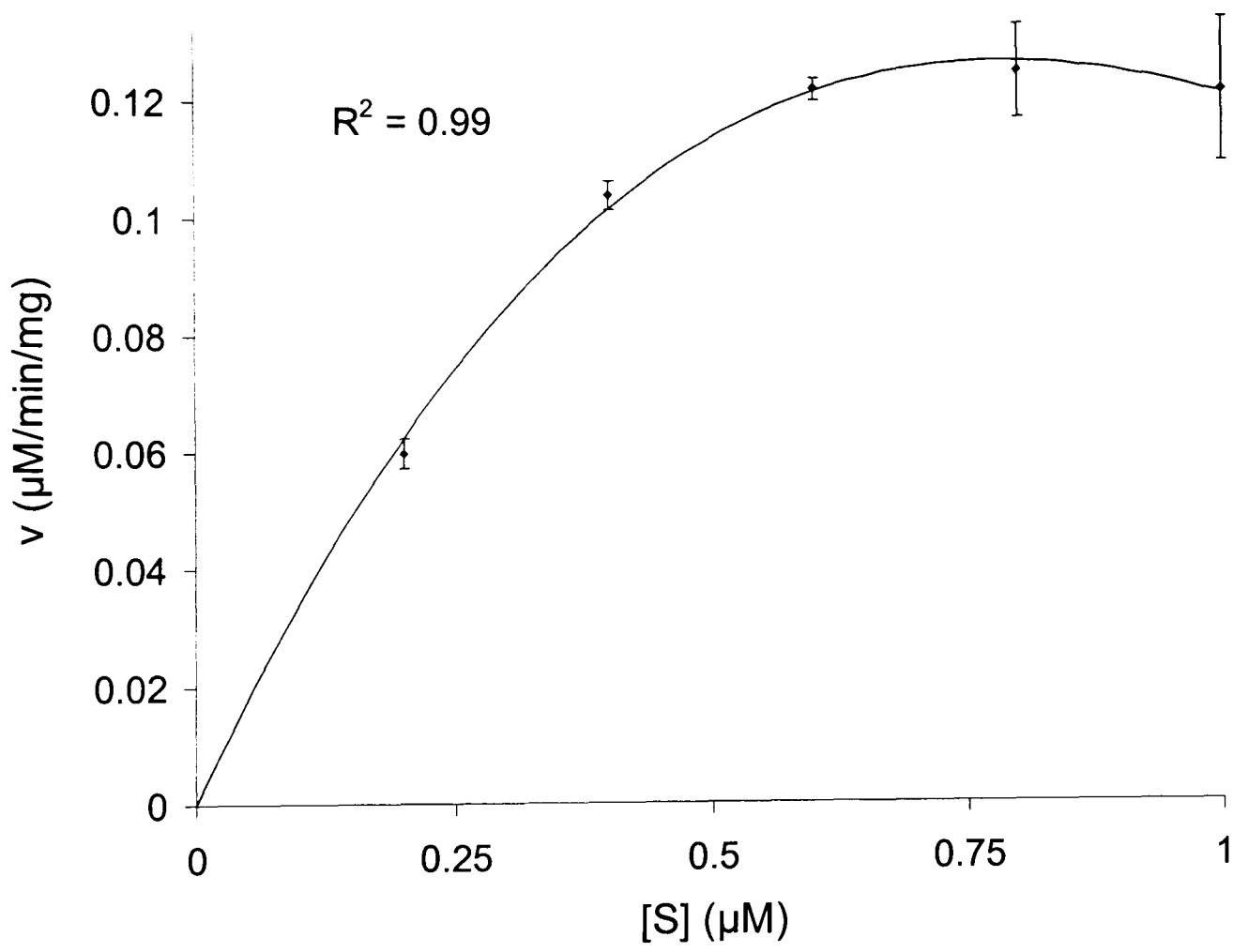

Figure 2.12 Michaelis Menten plot for 17,20-lyase.

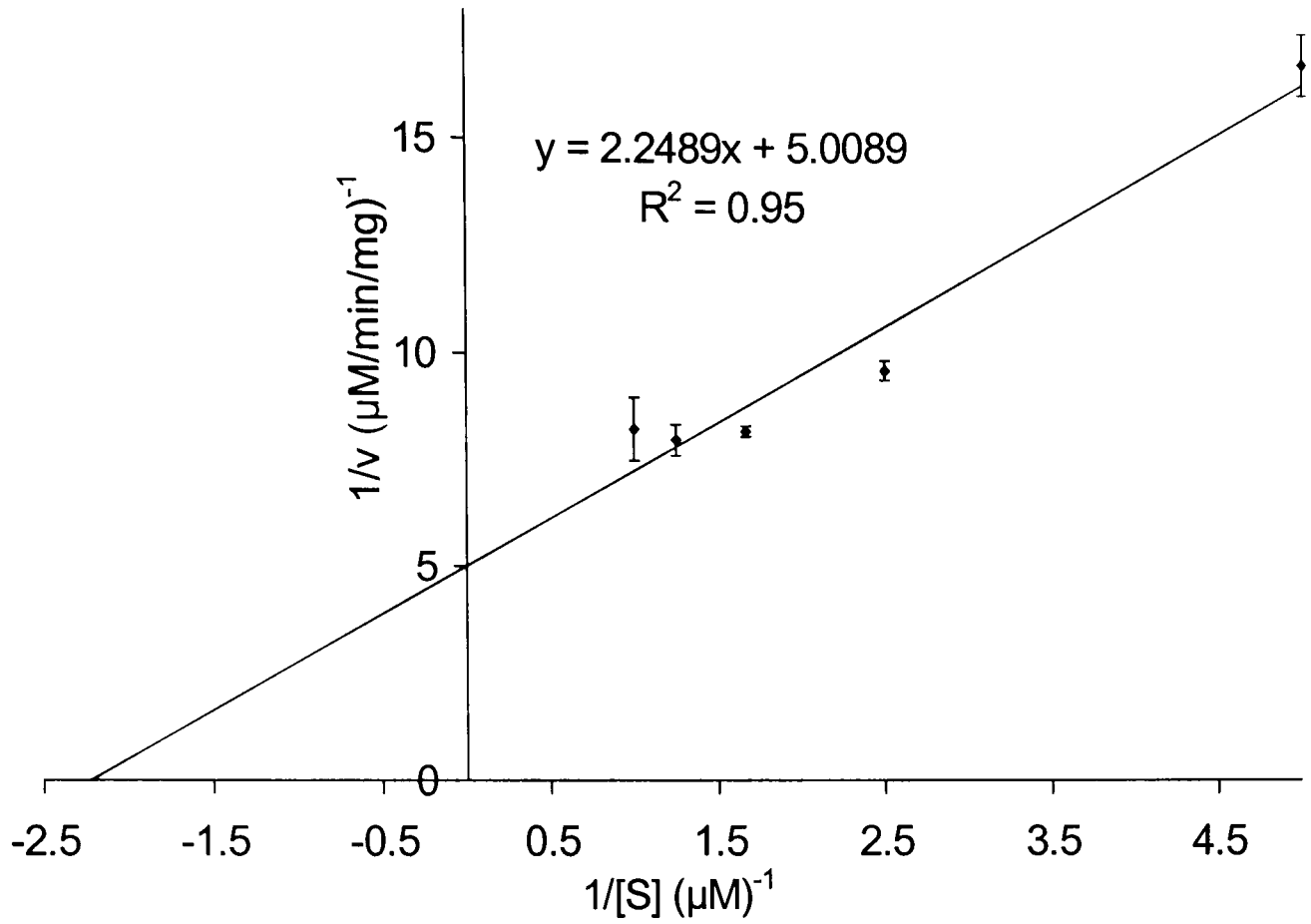

Figure 2.13 Lineweaver-Burk plot for 17,20-lyase.

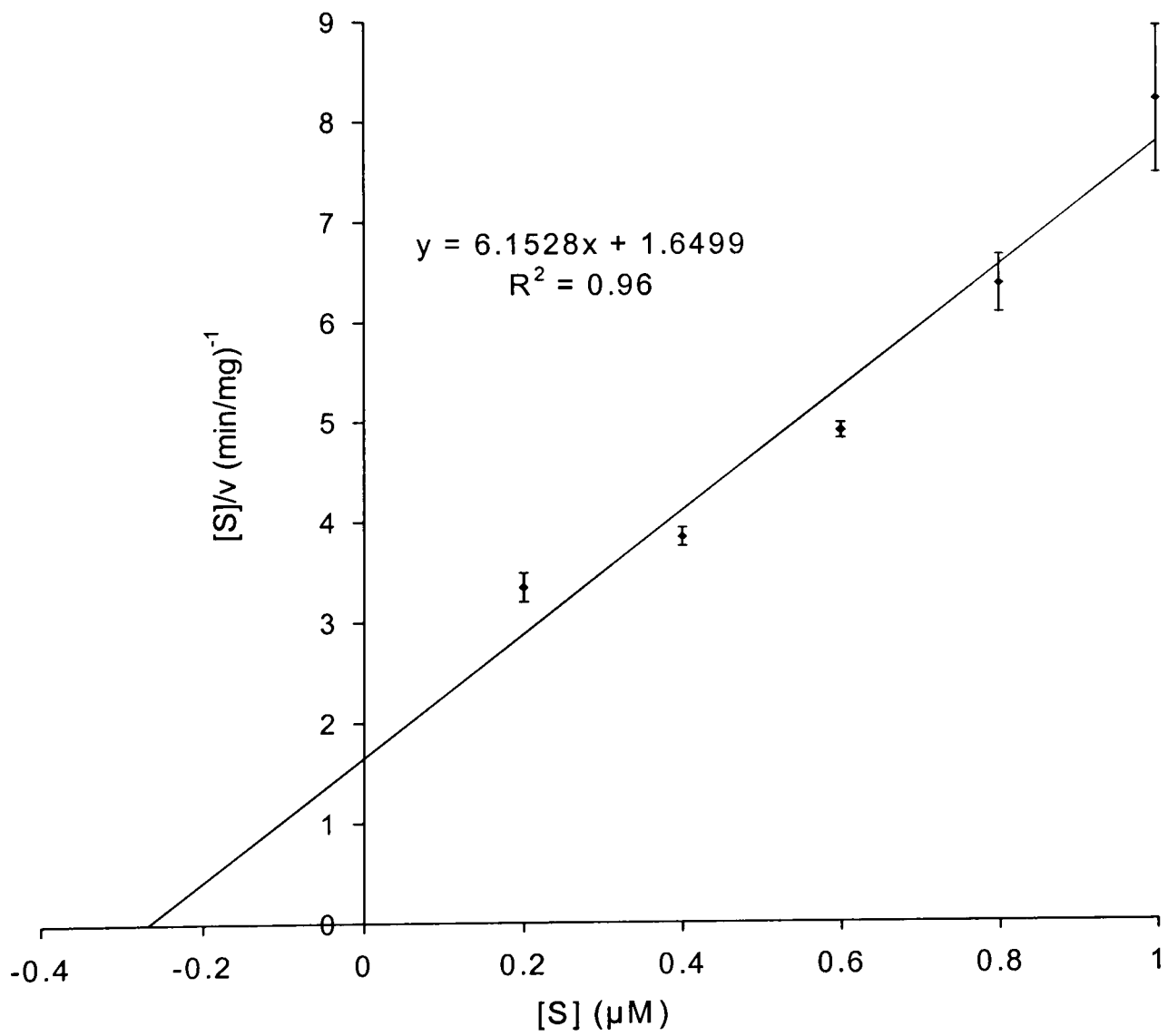

Figure 2.14 Hanes-Woolf plot for 17,20-lyase.

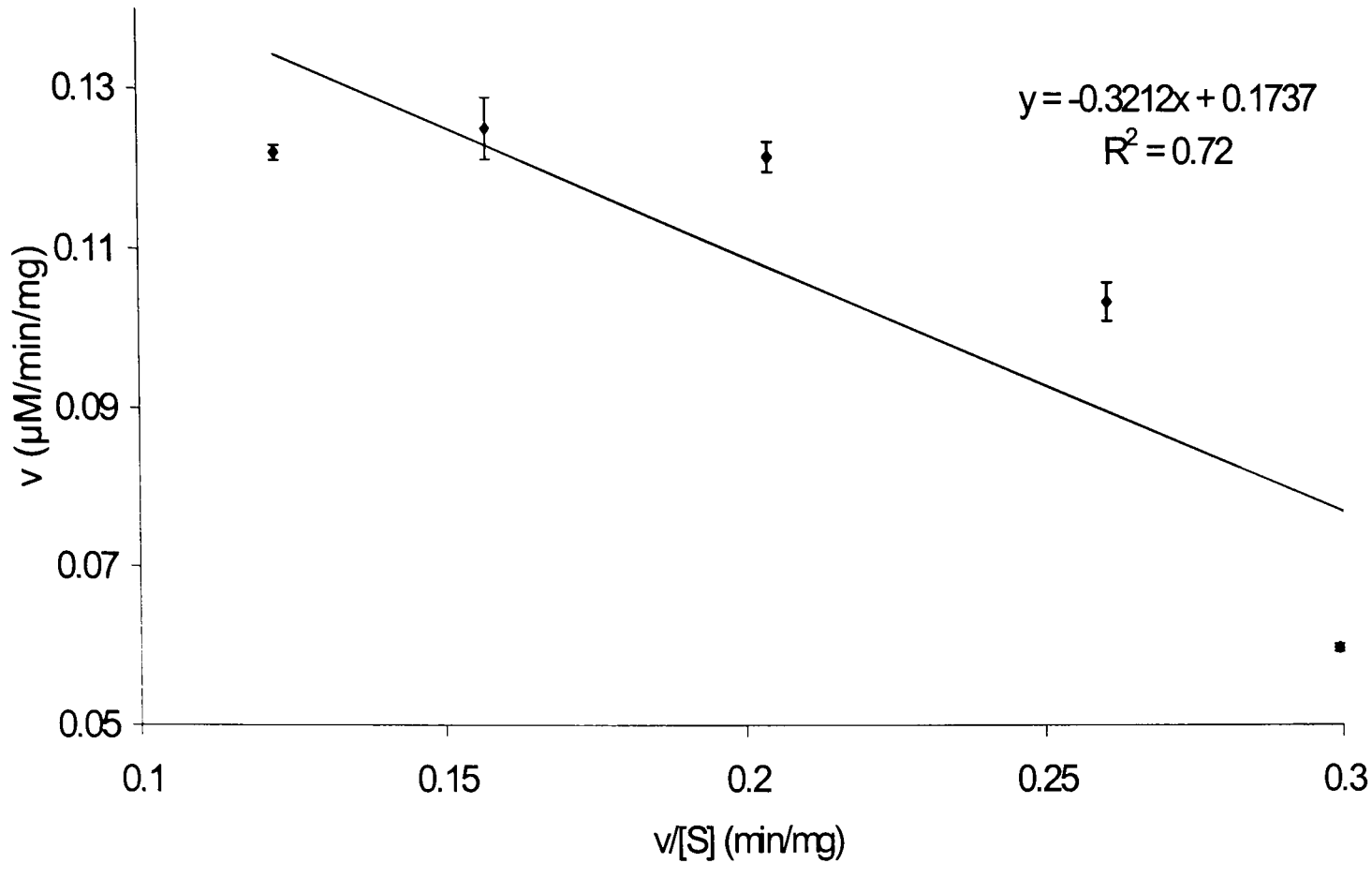

Figure 2.15 Eadie-Hofstee plot for 17,20-lyase.

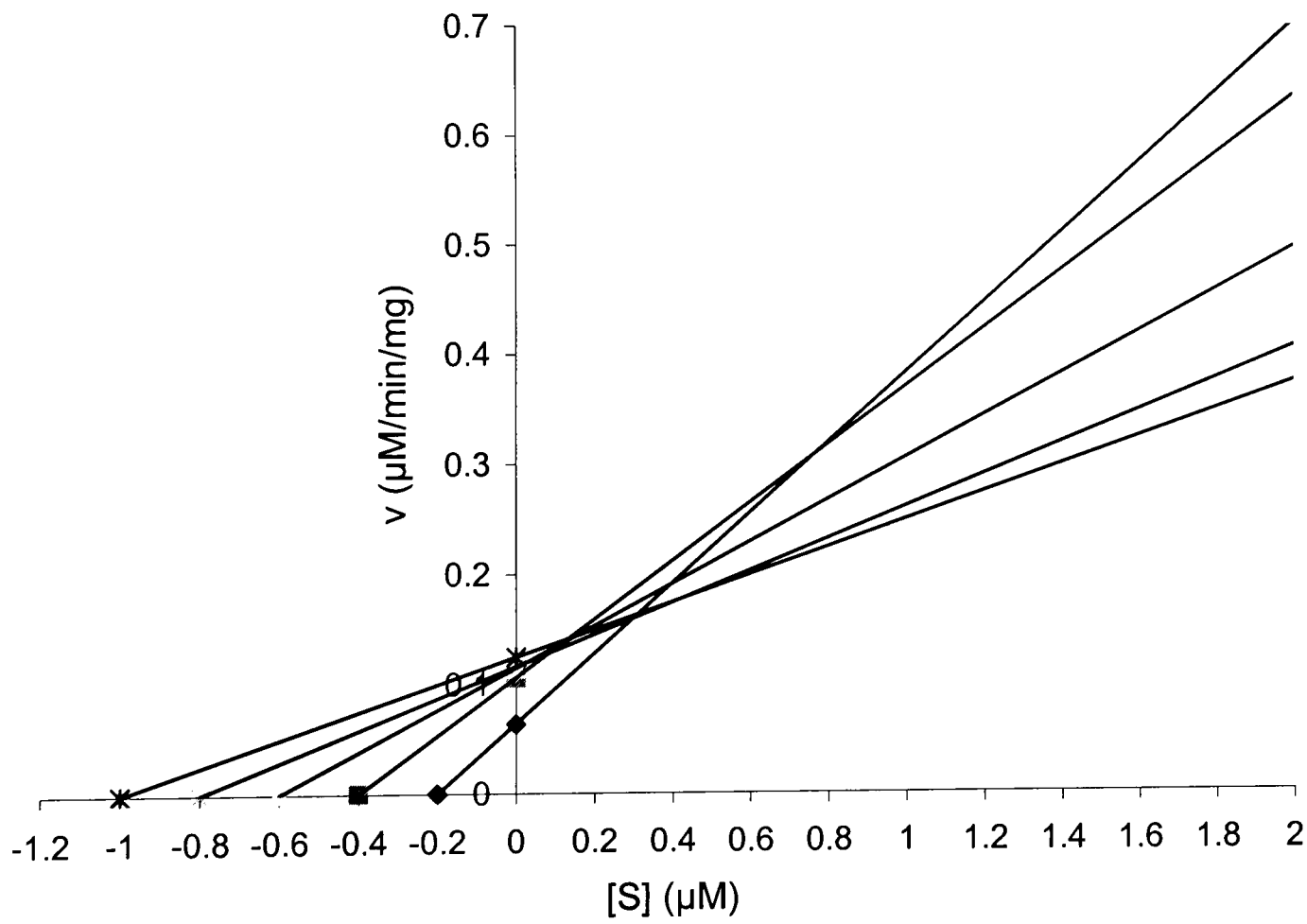

Figure 2.16 Direct linear plot for 17,20-lyase

Plot	K_m (μM)
Michaelis Menten plot	0.20 ± 0.03
Lineweaver Burk plot	0.45 ± 0.08
Hanes-Woolf plot	0.27 ± 0.02
Eadie-Hofstee plot	0.32 ± 0.04
Direct linear plot	0.28 ± 0.02
Average K_m	0.30 ± 0.04

Table 2.2 Summary of K_m plots for 17,20-lyase.

2.24 Discussion

The average K_m value for 17,20-lyase with the substrate 17αOHP using Sprague-Dawley testicular microsomes was found to be 0.30 ± 0.04μM, compared to K_m values obtained by other workers against rat testicular microsomes i.e., K_m = 192 ± 0.42nM (Ayub and Levell, 1987b), K_m = 4.55μM (Li et al, 1992) and K_m = 524.9 ± 174.52nM (Dalla Valle et al, 1996). Evidence of inhibition at high substrate concentration is seen by the upward curve on the Lineweaver-Burk plot. Non-linearity is seen for the Lineweaver-Burk plot which explains the poor R^2 values for the Hanes-Woolf and Eadie-Hofstee plots.

2.25 Preliminary Screening of Synthesised Compounds for 17,20-Lyase Inhibitory Activity

The assay procedure for screening involved inhibitors and standard (ketoconazole) dissolved in absolute ethanol and diluted to give the required final incubation concentration. The assay was carried out (in triplicate) at 37°C in a shaking water bath. The total assay volume was 1mL. Prepared substrate, 17αOHP (10μL, 1.0μM/tube), inhibitors (20μL, in ethanol), sodium phosphate buffer (pH7.4, 910μL), NADPH-generating system (50μL) were incubated at 37°C. The testicular microsomes were thawed and warmed to 37°C before addition (0.15mg/mL final concentration, 10μL) to the assay mixture. The assay was incubated at 37°C for 30min and then quenched by the addition of ether (2mL) and placed on ice. The assay was completed as previously described (Section 2.20). Control samples with no inhibitor were incubated

simultaneously. The results were determined by using equation 2.3 to determine the percentage conversion of 17αOHP and then comparing the conversion in the presence of inhibitors to that of the controls. Results are shown in Table 2.3a – 2.10c.

2.26 Determination of IC_{50}

IC_{50} determination was carried out on ketoconazole and all inhibitors which showed significant 17,20-lyase inhibitory activity. The assay was carried out in the same manner as described in Section 2.25, except that a single inhibitor was tested over a range of final assay concentrations depending on the initial screening results. The IC_{50} was determined from plots of percentage inhibition versus Log [I] (Figures 2.27 – 2.36; Figures 2.42 – 2.45; Figures 2.50 – 2.52 and Figures 2.57 – 2.68).

2.27 Results for Unsubstituted Phenyl Alkyl-*1H*-imidazoles against $P450_{17\alpha}$

The results are shown in Tables 2.3a and 2.3b

2.27.1 Discussion

The IC_{50} was conducted on ketoconazole for comparison. Compounds **165** and **167** were both less potent than ketoconazole for both 17α-hydroxylase as well as 17,20-lyase. Compounds **169** – **174** were all more potent than ketoconazole against both components. Compound **168** however was found to be weaker than ketoconazole against the 17α-hydroxylase component but equipotent against the 17,20-lyase component.

Compound No.	Structure	17α-hydroxylase		17,20-lyase	
		% Inhibition at 10μM	IC_{50} Values (μM)	% Inhibition at 10μM	IC_{50} Values (μM)
1	Ketoconazole	61.54 ± 1.53	3.76 ± 0.01	78.69 ± 2.44	1.66 ± 0.15
165		13.51 ± 0.65	154.20 ± 7.93	12.64 ± 0.65	50.90 ± 0.86
166		10.56 ± 1.76	N/A	6.36 ± 0.65	N/A
167		23.35 ± 0.97	30.95 ± 0.68	39.95 ± 0.89	6.14 ± 1.21
168		40.69 ± 0.72	8.65 ± 1.37	65.95 ± 0.25	2.23 ± 0.38
169		59.74 ± 0.63	2.20 ± 0.25	72.59 ± 0.31	1.31 ± 0.21

Table 2.3a Results from preliminary screening and IC_{50} data of some unsubstituted phenyl alkyl-*1H*-imidazoles and ketoconazole for 17α-hydroxylase/17,20-lyase activity.

Compound No.	Structure	17α-hydroxylase		17,20-lyase	
		% Inhibition at 10μM	IC_{50} Values (μM)	% Inhibition at 10μM	IC_{50} Values (μM)
170	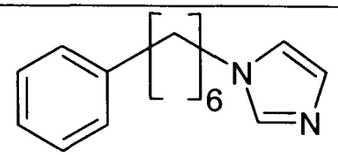	61.28 ± 0.58	0.87 ± 0.03	86.99 ± 1.29	0.51 ± 0.03
171	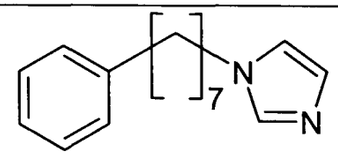	67.45 ± 0.48	0.32 ± 0.05	88.67 ± 0.32	0.099 ± 0.016
172	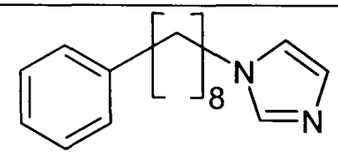	70.17 ± 0.63	0.25 ± 0.01	88.38 ± 0.14	0.21 ± 0.02
173	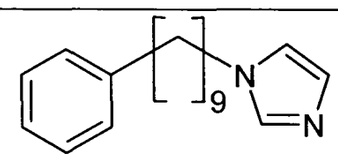	64.52 ± 0.29	1.06 ± 0.03	89.06 ± 2.68	0.35 ± 0.01
174	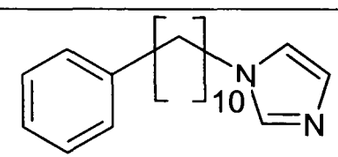	65.20 ± 0.71	1.75 ± 0.02	79.63 ± 0.89	1.04 ± 0.06

Table 2.3b Results from preliminary screening and IC_{50} data of some unsubstituted phenyl alkyl-*1H*-imidazoles for 17α-hydroxylase/17,20-lyase activity.

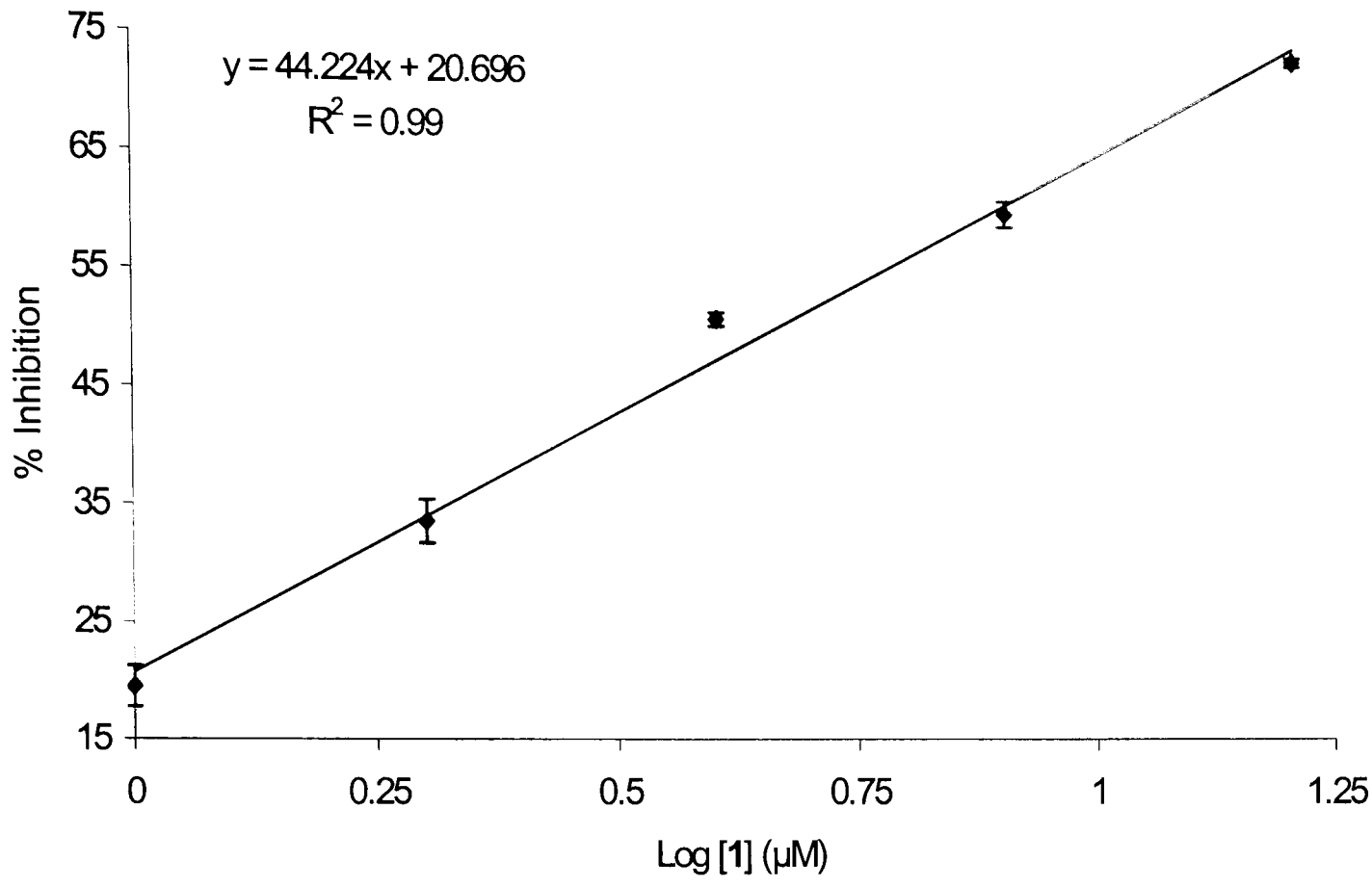

Figure 2.17 Plot of percentage inhibition versus log [**1**] for ketoconazole (**1**) against 17α-hydroxylase.

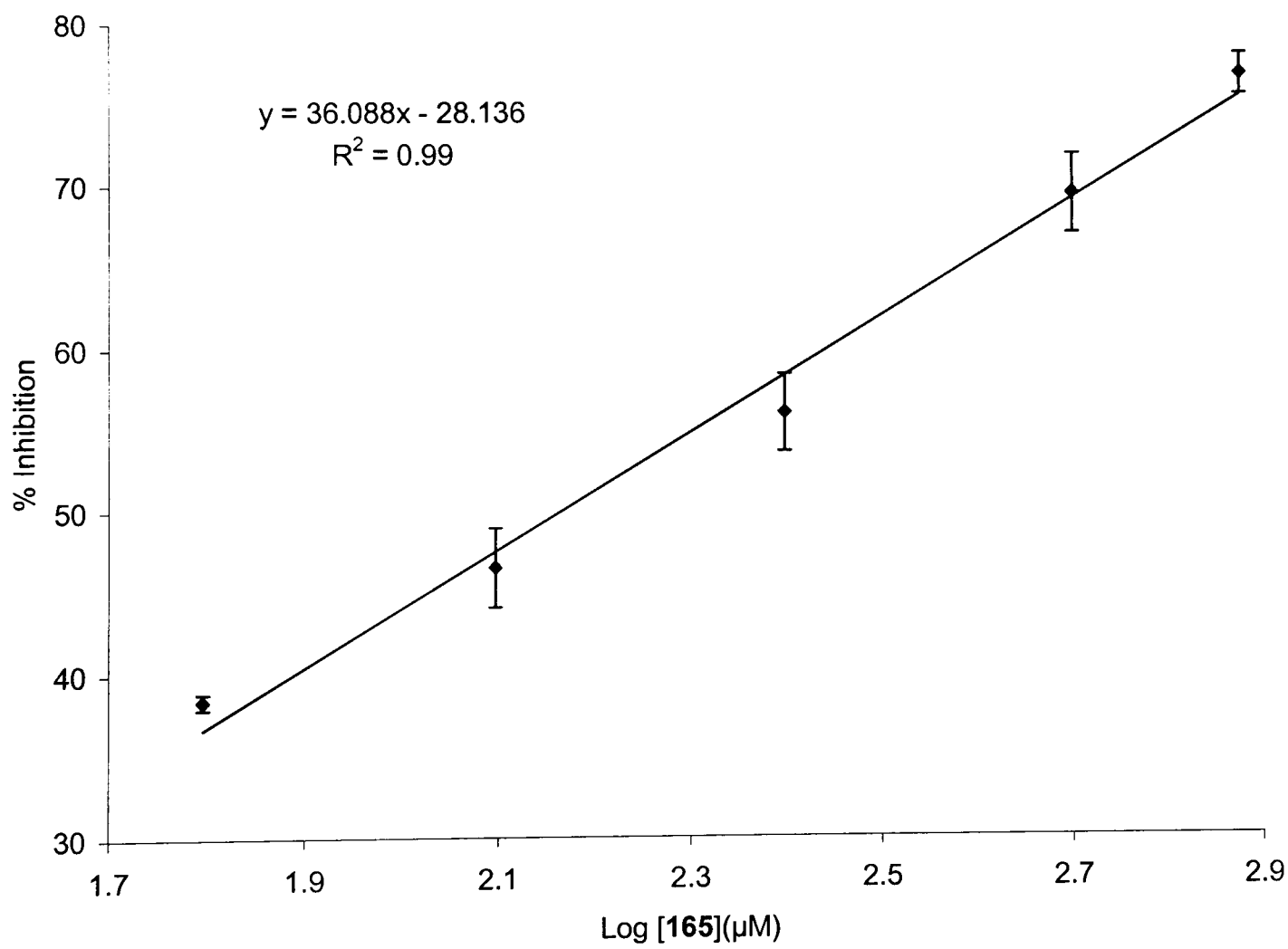

Figure 2.18 Plot of percentage inhibition versus log [**165**] for 1-benzyl-1*H*-imidazole (**165**) against 17α-hydroxylase.

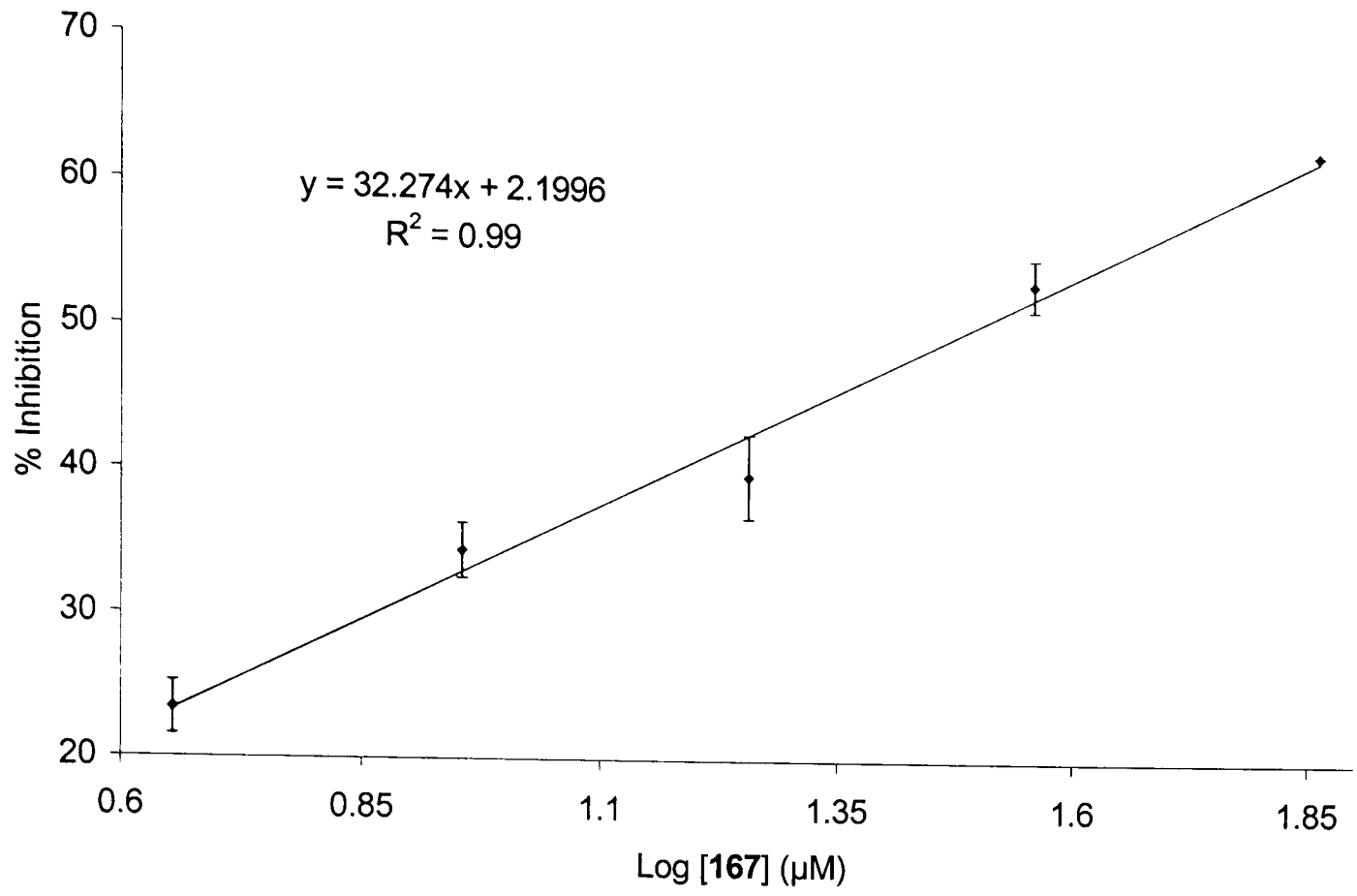

Figure 2.19 Plot of percentage inhibition versus log [**167**] for 1-(3-phenyl-propyl)-1*H*-imidazole (**167**) against 17α-hydroxylase.

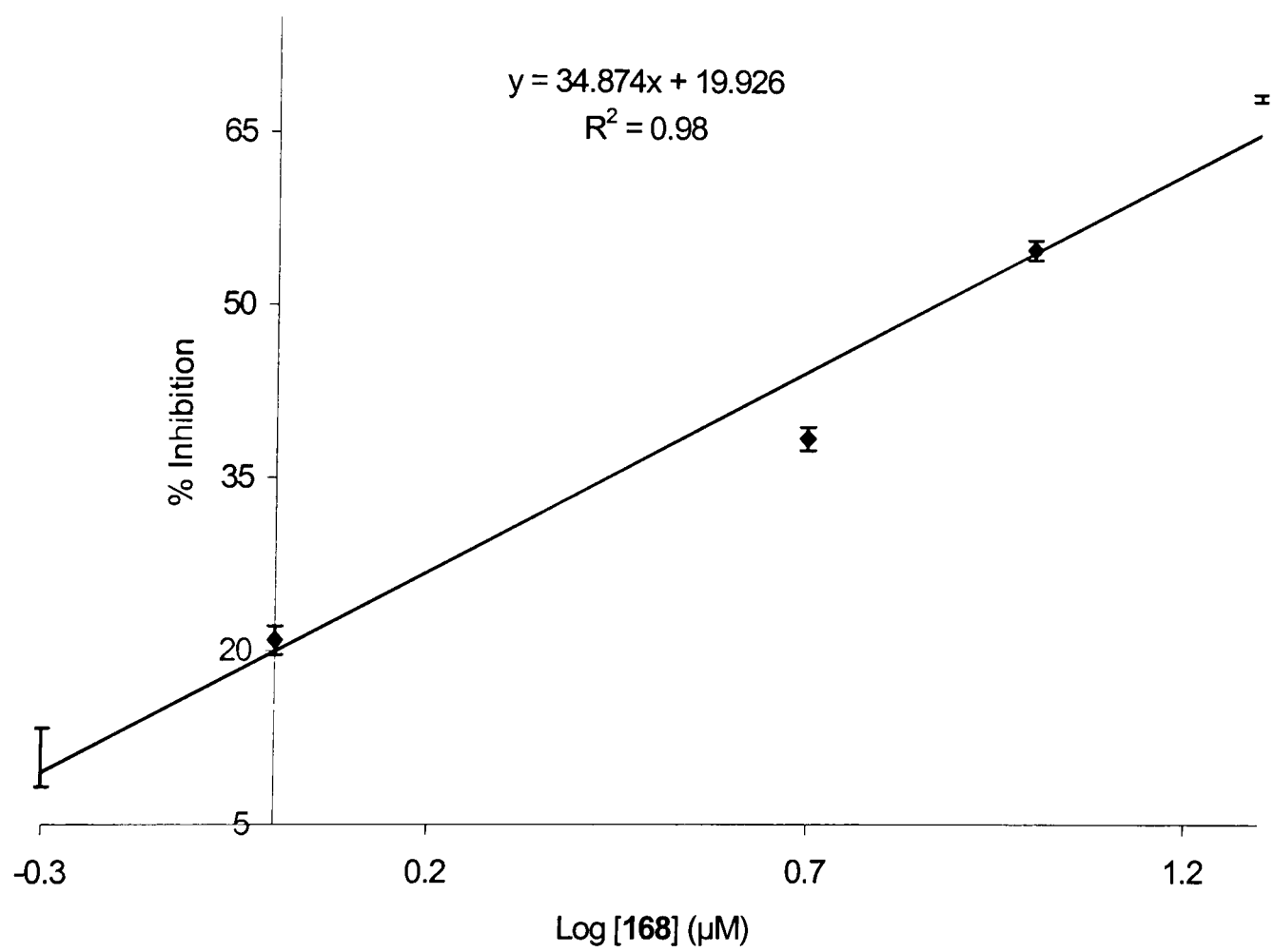

Figure 2.20 Plot of percentage inhibition versus log [**168**] for 1-(4-phenyl-buyl)-1*H*-imidazole (**168**) against 17α-hydroxylase.

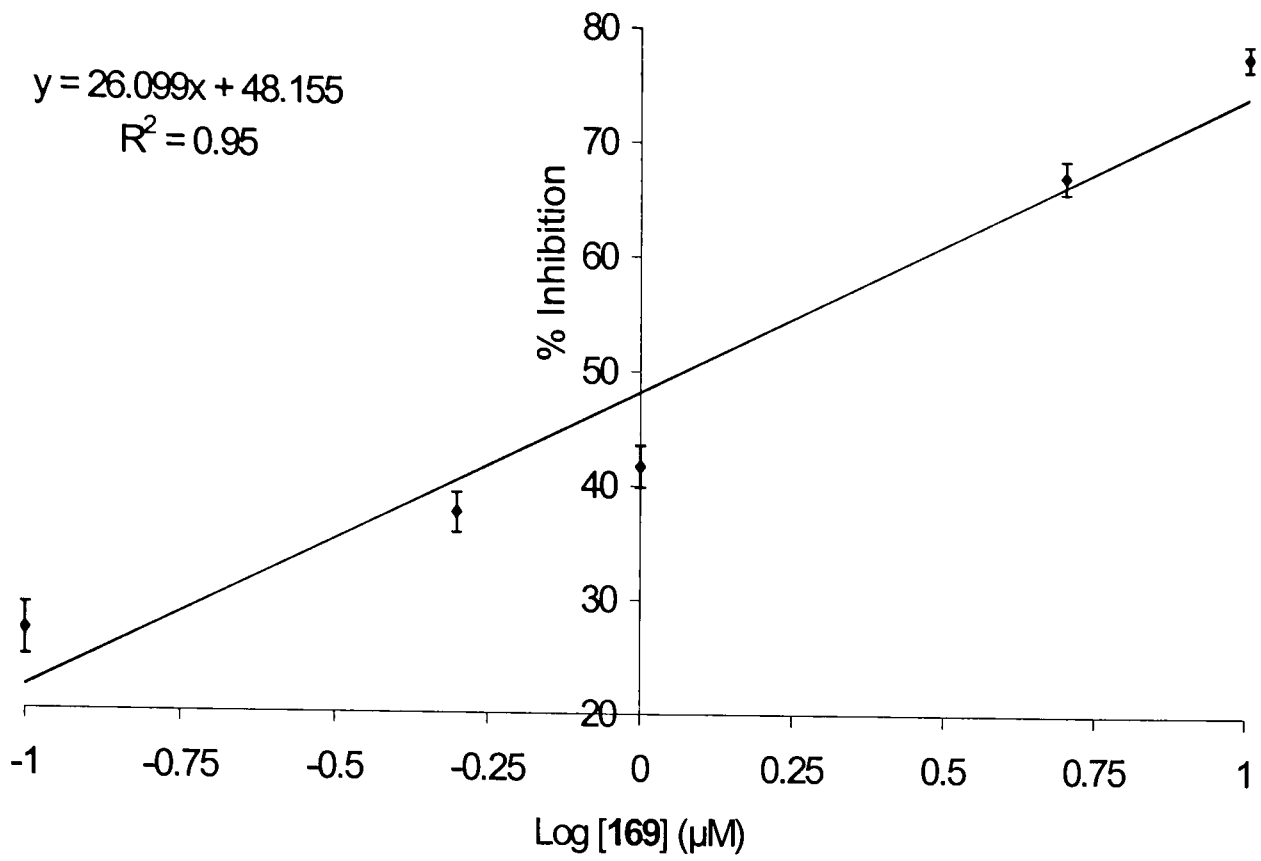

Figure 2.21 Plot of percentage inhibition versus log [**169**] for 1-(5-phenyl-pentyl)-1*H*-imidazole (**169**) against 17α-hydroxylase.

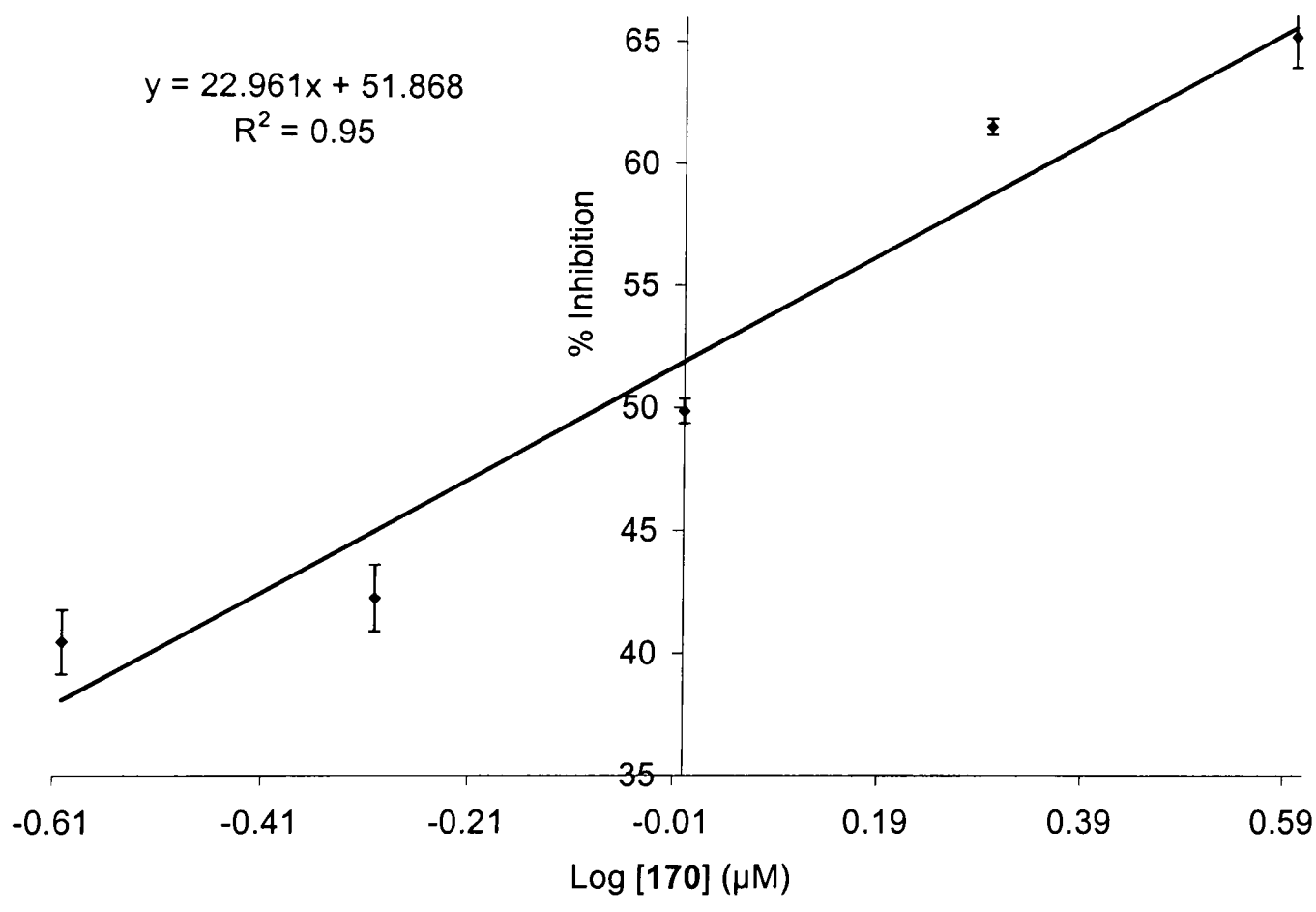

Figure 2.22 Plot of percentage inhibition versus log [**170**] for 1-(6-phenyl-hexyl)-1*H*-imidazole (**170**) against 17α-hydroxylase.

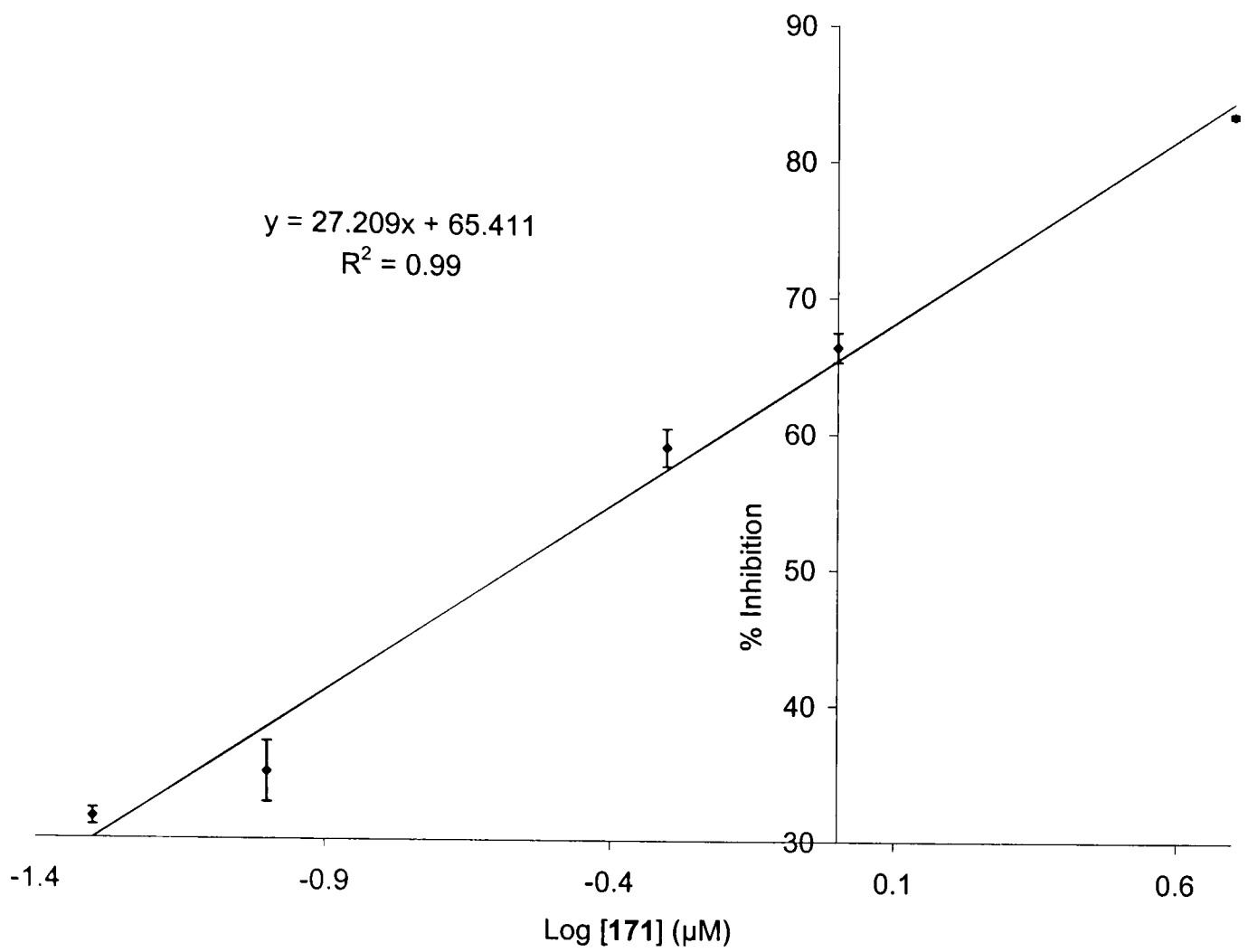

Figure 2.23 Plot of percentage inhibition versus log [**171**] for 1-(7-phenyl-heptyl)-1*H*-imidazole (**171**) against 17α-hydroxylase.

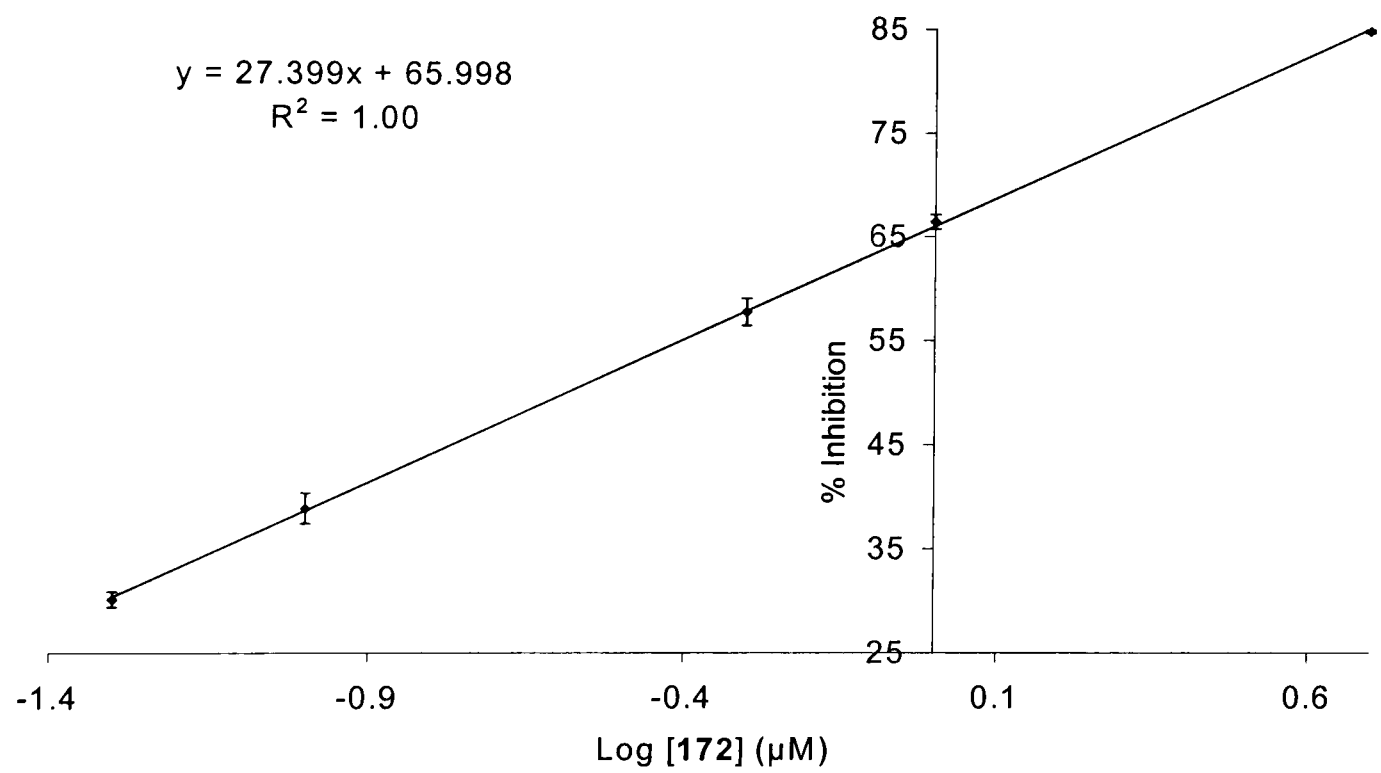

Figure 2.24 Plot of percentage inhibition versus log [**172**] for 1-(8-phenyl-octyl)-1*H*-imidazole (**172**) against 17α-hydroxylase.

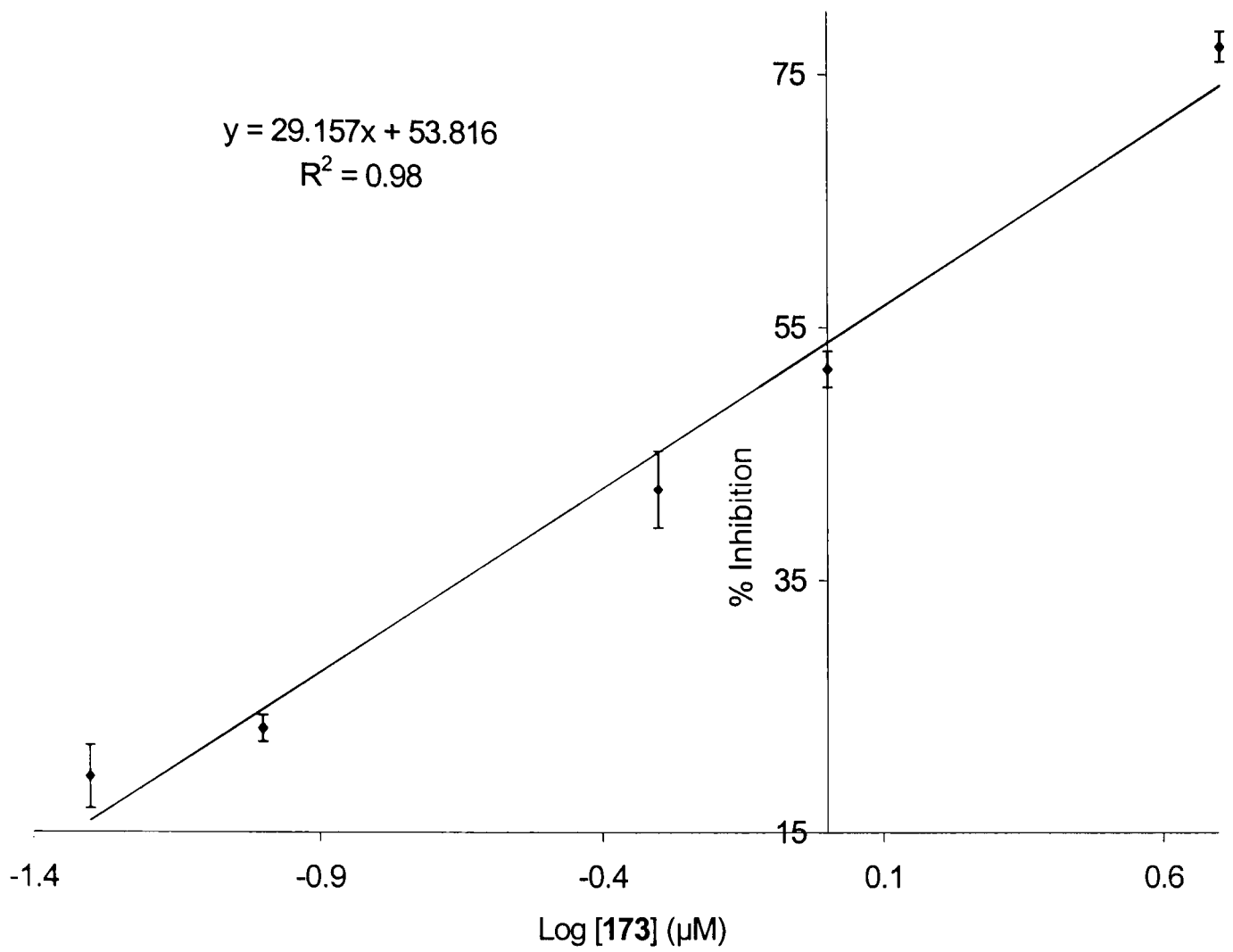

Figure 2.25 Plot of percentage inhibition versus log [**173**] for 1-(9-phenyl-nonyl)-1*H*-imidazole (**173**) against 17α-hydroxylase.

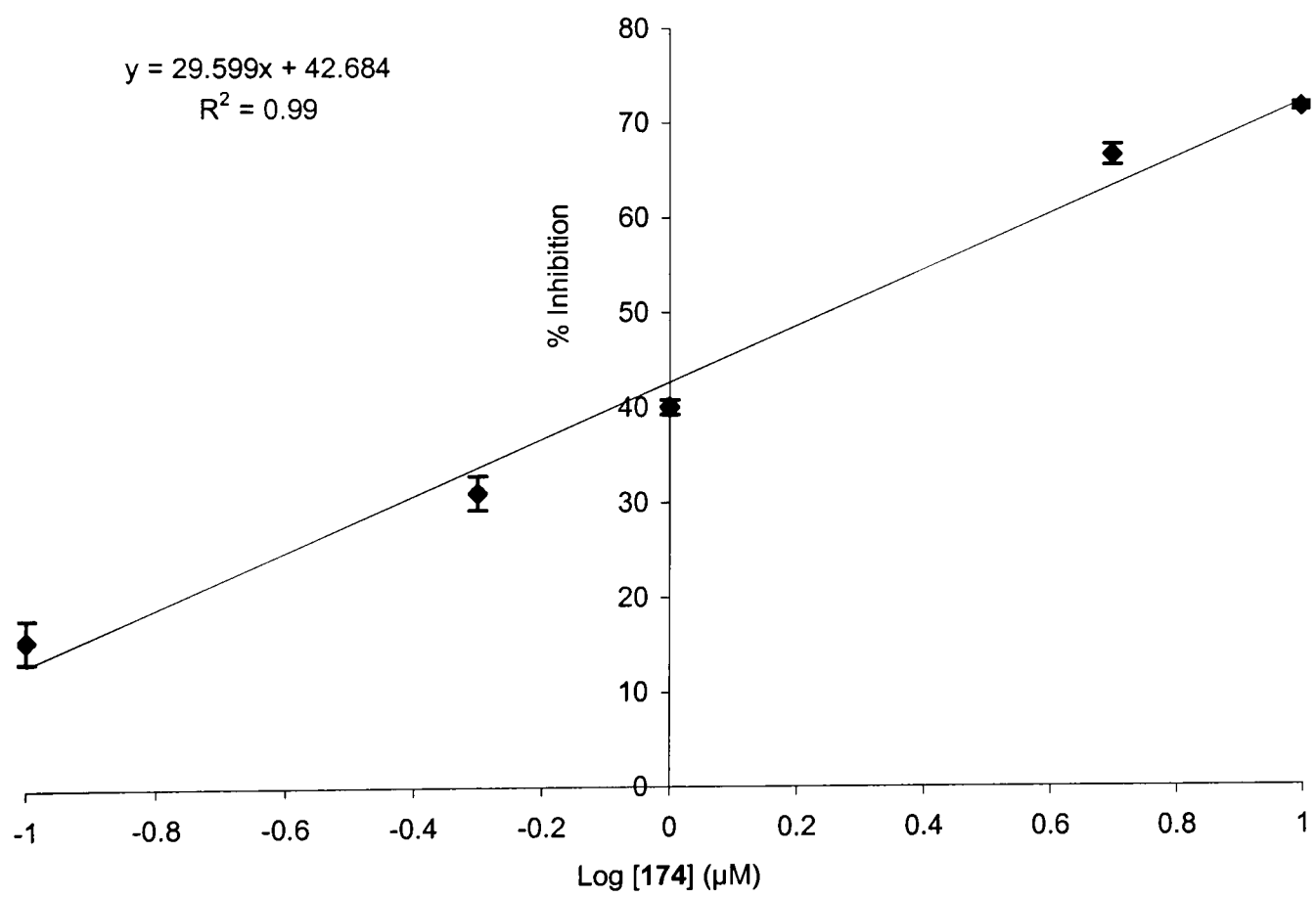

Figure 2.26 Plot of percentage inhibition versus log [**174**] for 1-(10-phenyl-decyl)-1*H*-imidazole (**174**) against 17α-hydroxylase.

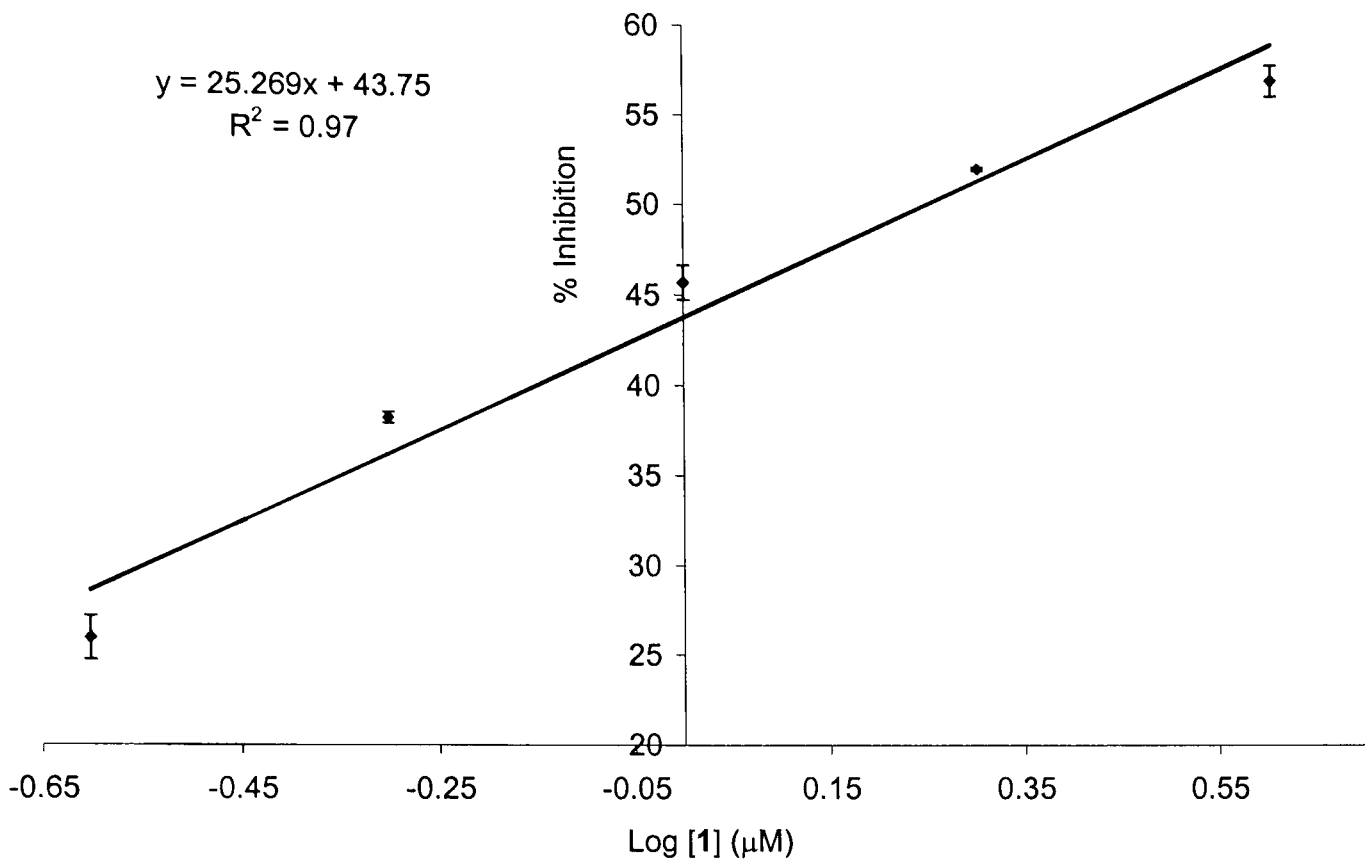

Figure 2.27 Plot of percentage inhibition versus log [**1**] for ketoconazole (**1**) against 17,20-lyase.

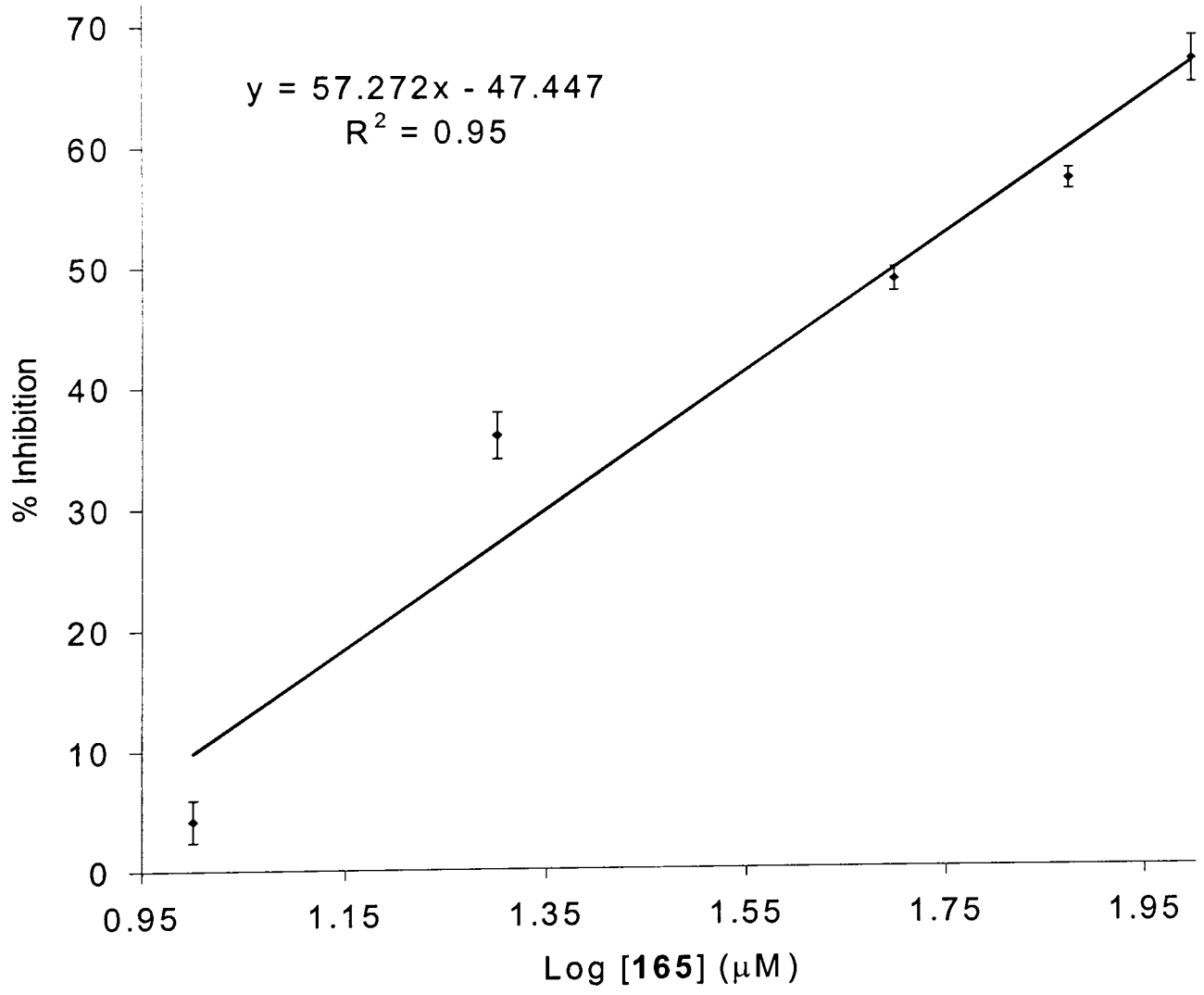

Figure 2.28 Plot of percentage inhibition versus log [**165**] for 1-benzyl-1*H*-imidazole (**165**) against 17,20-lyase.

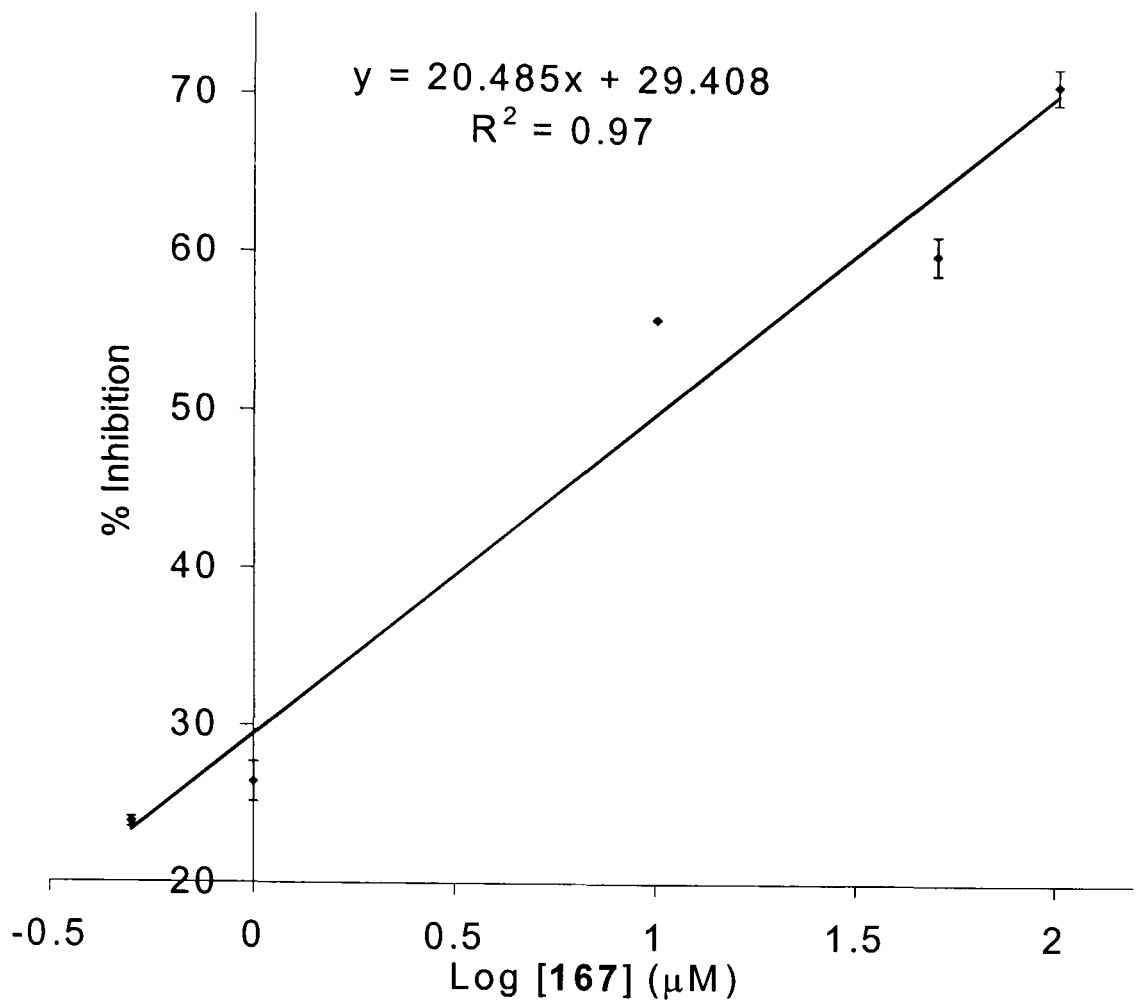

Figure 2.29 Plot of percentage inhibition versus log [**167**] for 1-(3-phenyl-propyl)-1*H*-imidazole (**167**) against 17,20-lyase.

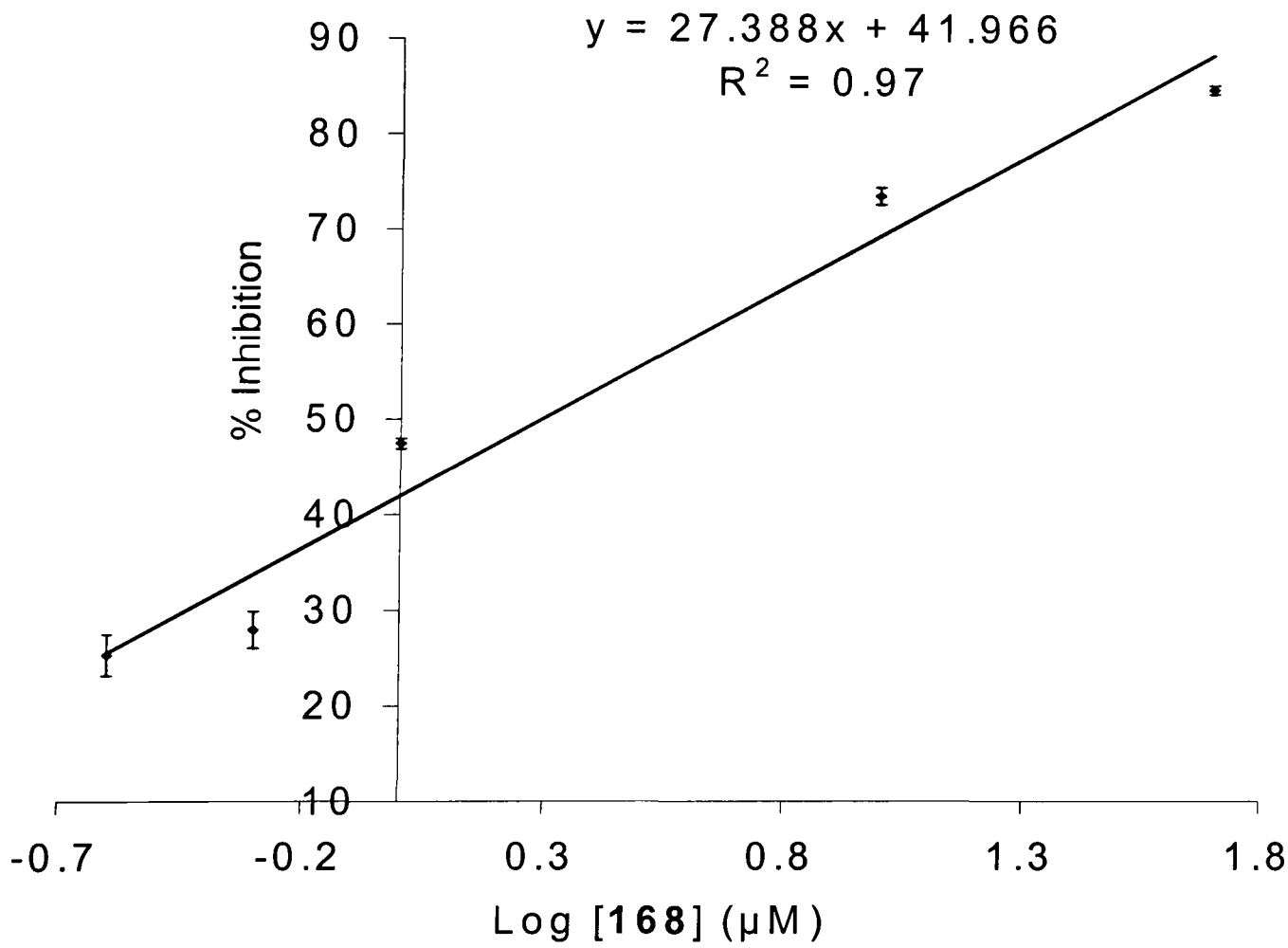

Figure 2.30 Plot of percentage inhibition versus log [**168**] for 1-(4-phenyl-butyl)-1*H*-imidazole (**168**) against 17,20-lyase.

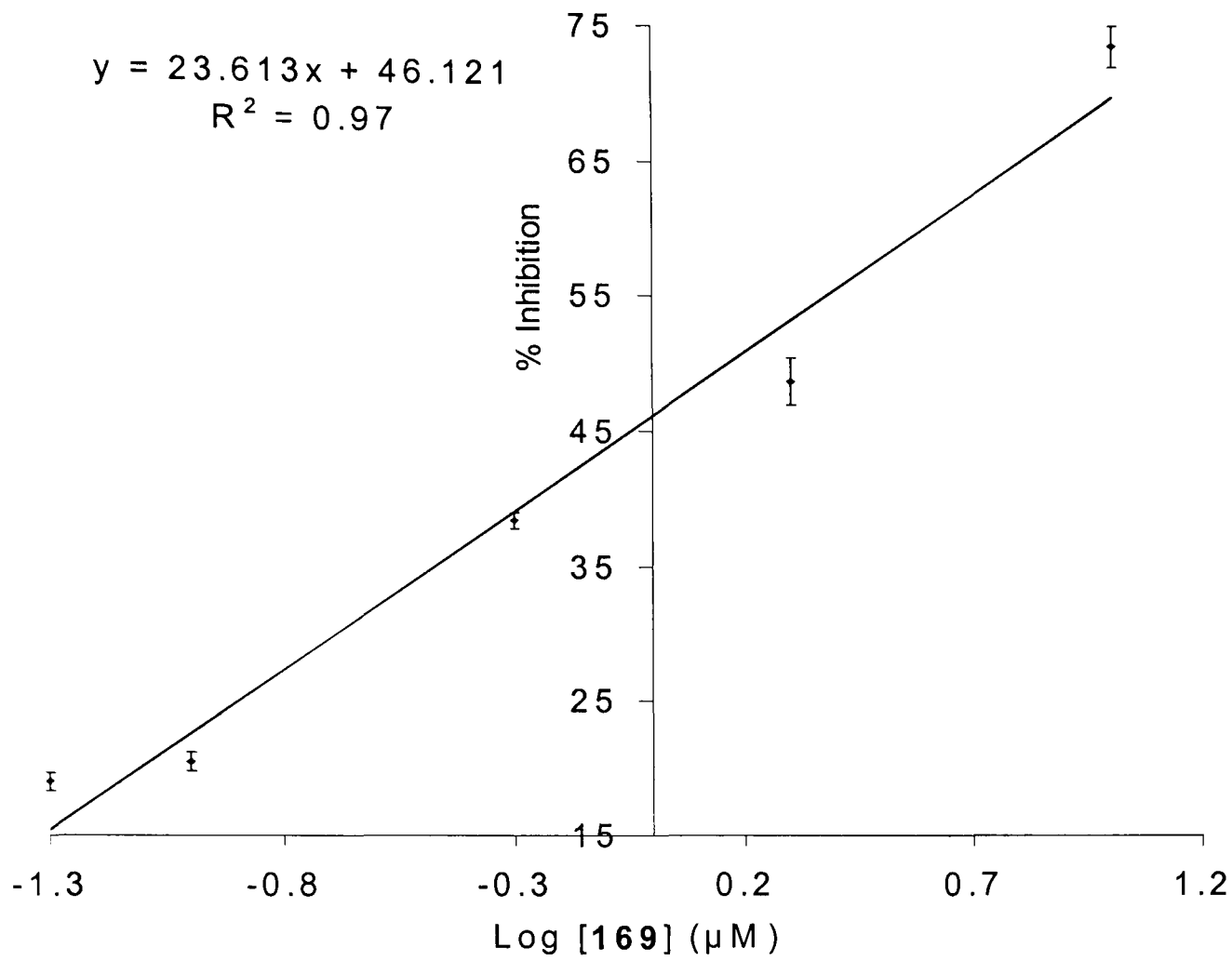

Figure 2.31 Plot of percentage inhibition versus log [**169**] for 1-(5-phenyl-pentyl)-1*H*-imidazole (**169**) against 17,20-lyase.

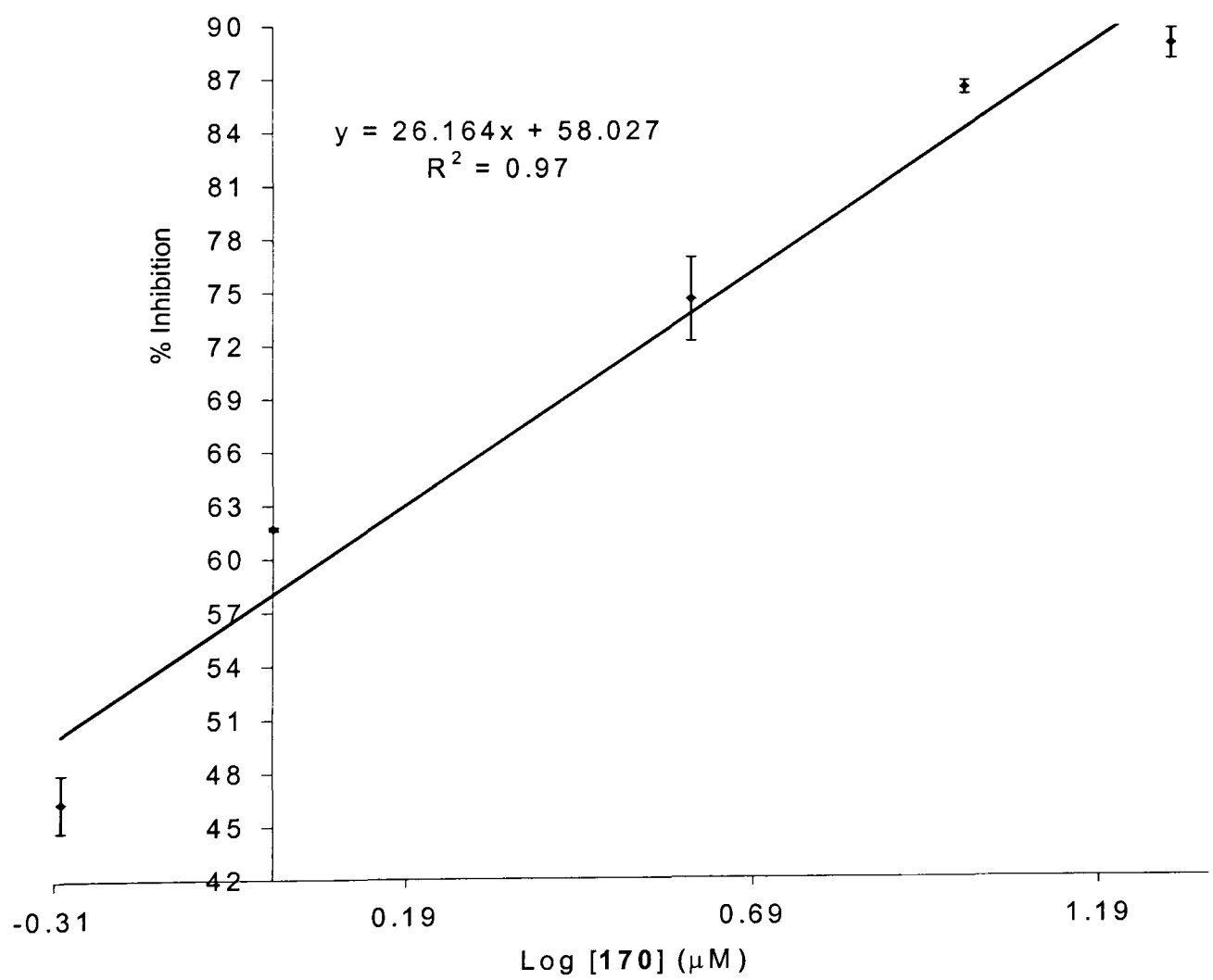

Figure 2.32 Plot of percentage inhibition versus log [**170**] for 1-(6-phenyl-hexyl)-1*H*-imidazole (**170**) against 17,20-lyase.

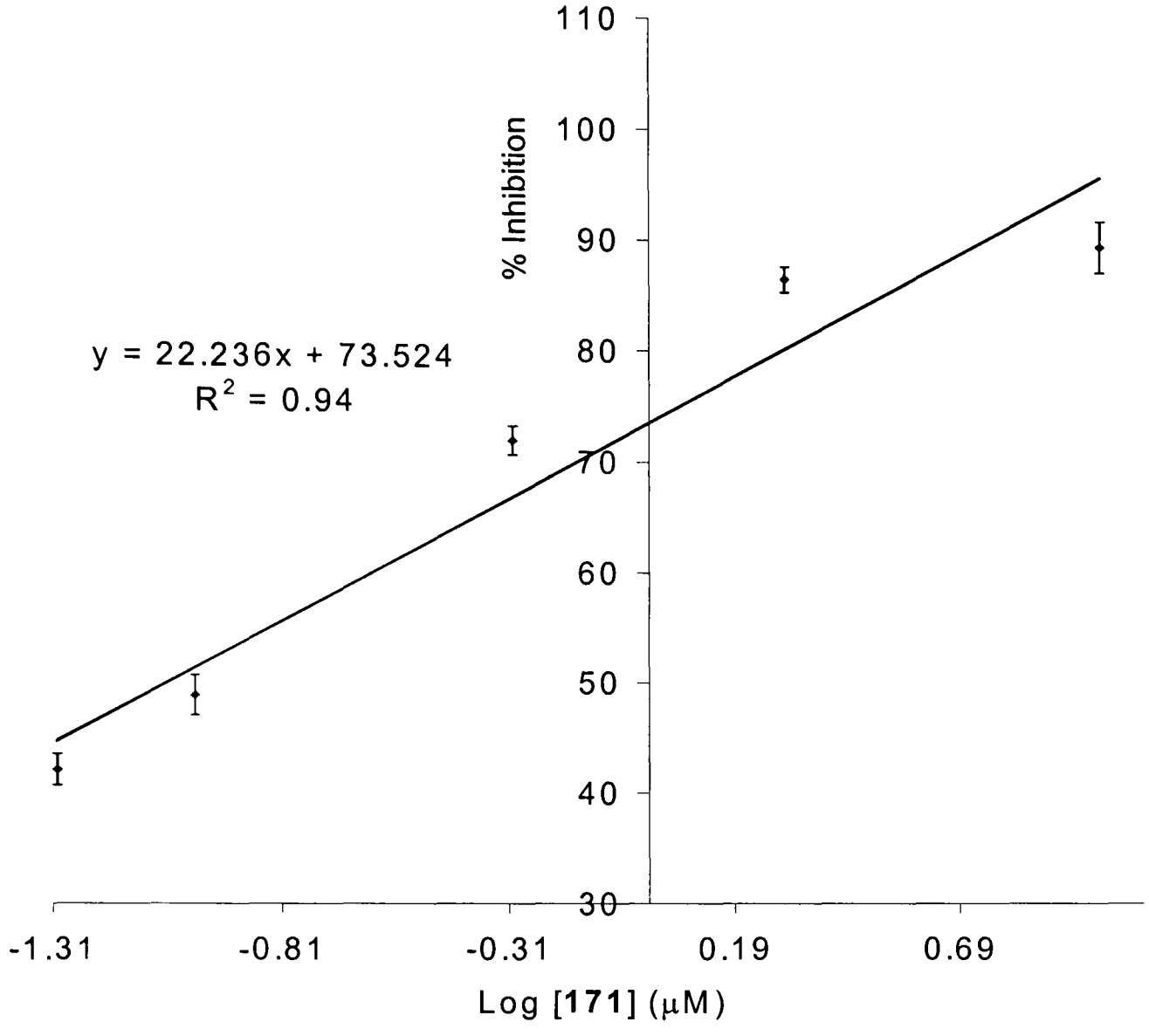

Figure 2.33 Plot of percentage inhibition versus log [**171**] for 1-(7-phenyl-heptyl)-1*H*-imidazole (**171**) against 17,20-lyase.

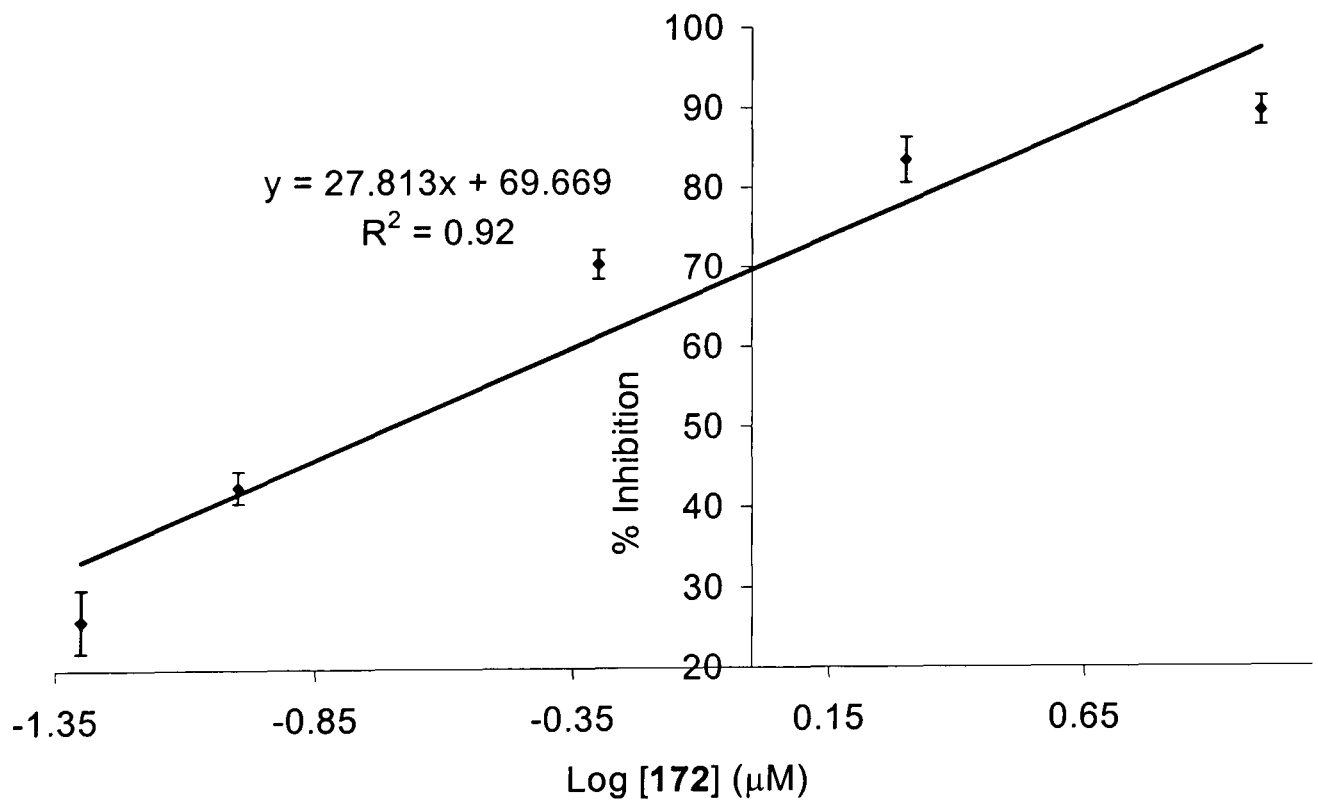

Figure 2.34 Plot of percentage inhibition versus log [**172**] for 1-(8-phenyl-octyl)-1*H*-imidazole (**172**) against 17,20-lyase.

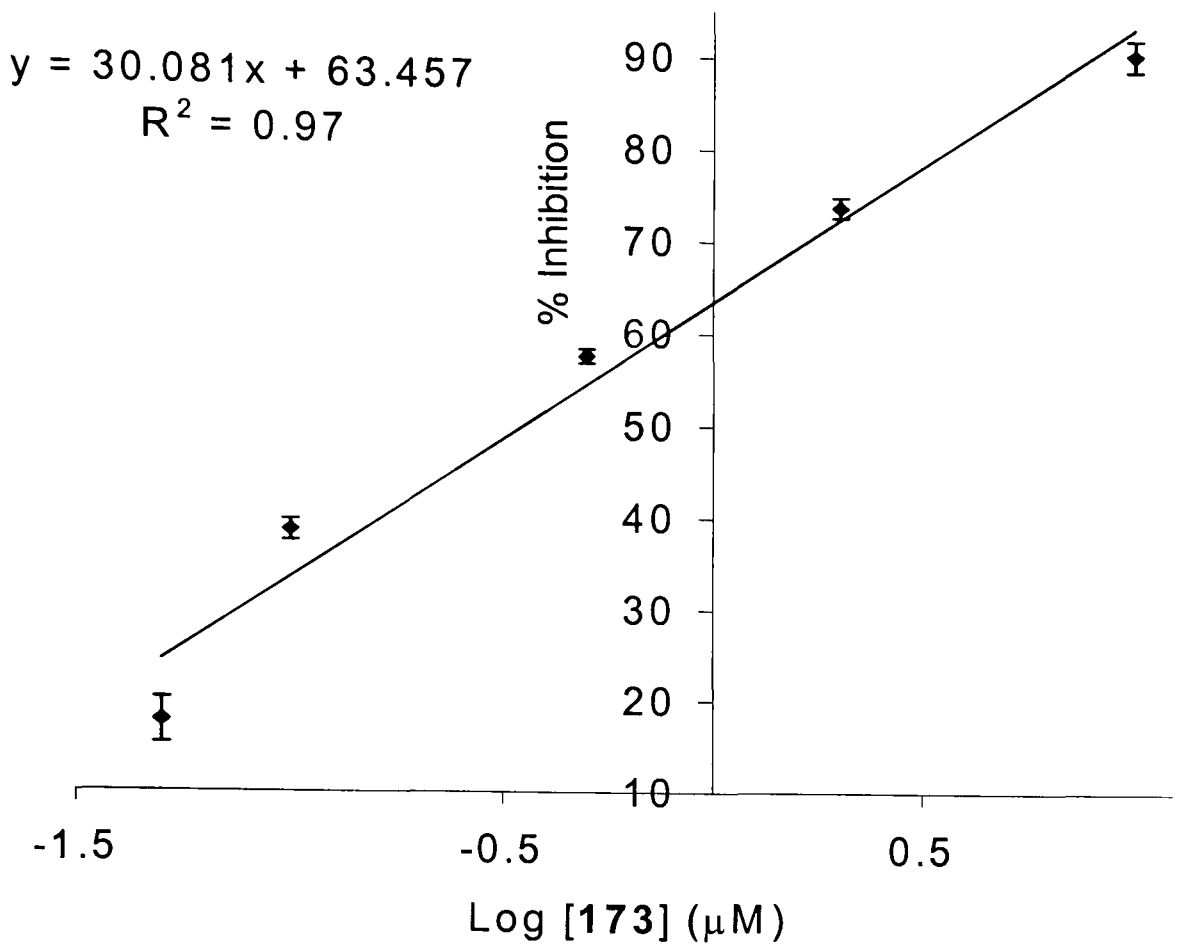

Figure 2.35 Plot of percentage inhibition versus log [**173**] for 1-(9-phenyl-nonyl)-1*H*-imidazole (**173**) against 17,20-lyase.

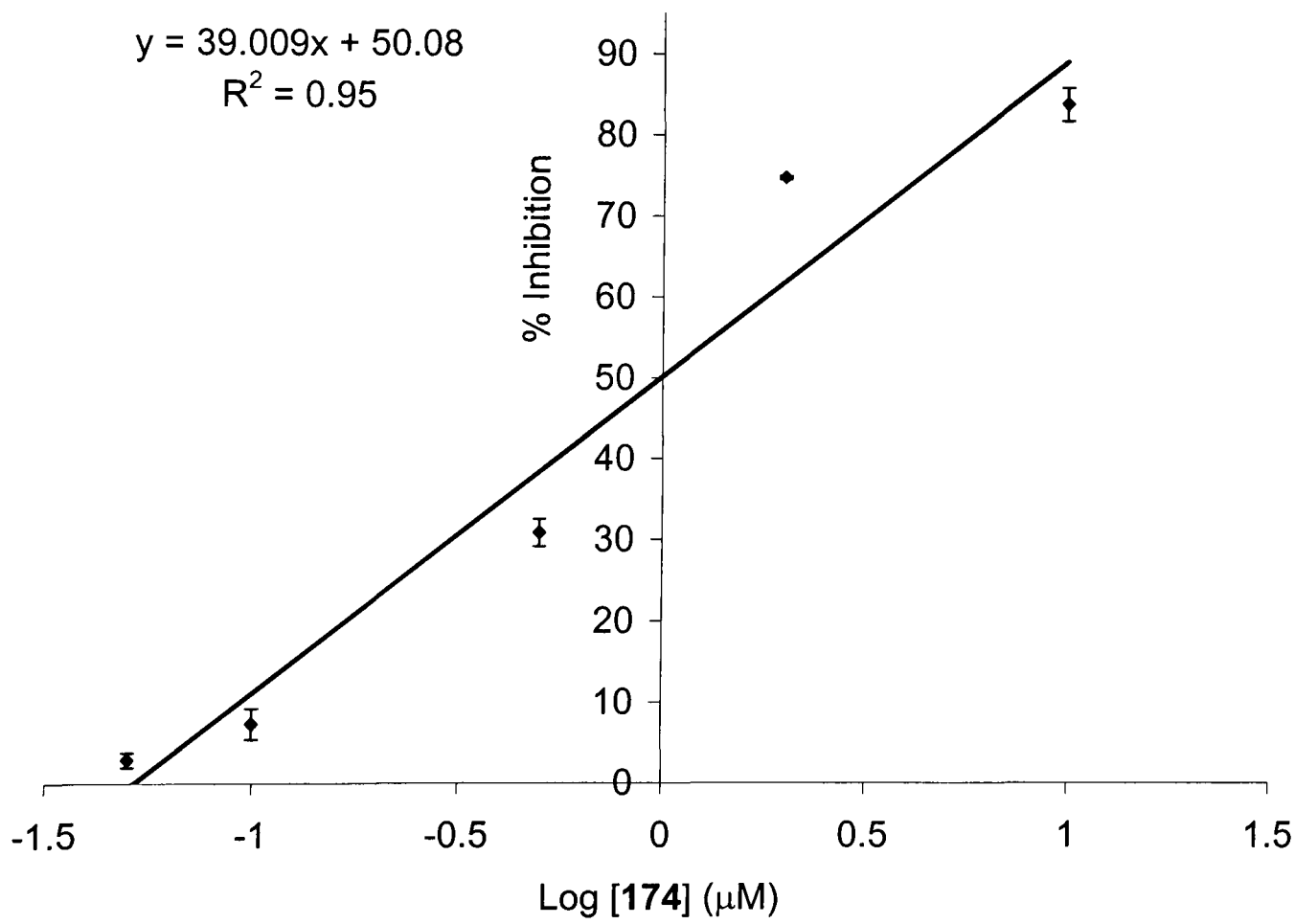

Figure 2.36 Plot of percentage inhibition versus log [**174**] for 1-(10-phenyl-decyl)-1*H*-imidazole (**174**) against 17,20-lyase.

2.28 Results of 4-Fluoro-substituted Phenyl Alkyl-*1H*-imidazoles against $P450_{17\alpha}$

The results are shown in Table 2.4

2.28.1 Discussion

Compound **175** was less potent than ketoconazole for both 17α-hydroxylase and 17,20-lyase. Compounds **178** and **179** were both more potent than ketoconazole against both components. Compound **177** however was found to be much weaker than ketoconazole against the 17α-hydroxylase component but equipotent against the 17,20-lyase component. Compound **176** was found to show much less potency against 17α-hydroxylase and thus was not tested against 17,20-lyase.

Compound No.	Structure	17α-hydroxylase		17,20-lyase	
		% Inhibition at 10μM	IC_{50} Values (μM)	% Inhibition at 10μM	IC_{50} Values (μM)
175	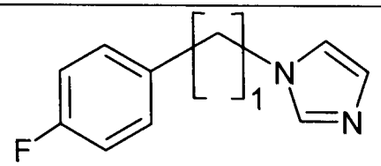	20.47 ± 1.79	96.46 ± 0.20	50.98 ± 1.36	11.26 ± 0.22
176	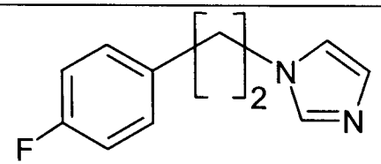	22.48 ± 1.84	120.20 ± 7.74	45.07 ± 1.21	N/A
177	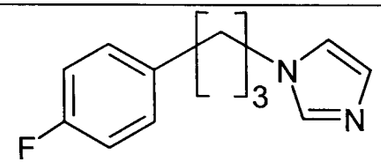	40.77 ± 0.53	27.81 ± 1.44	73.15 ± 0.33	1.96 ± 0.01
178	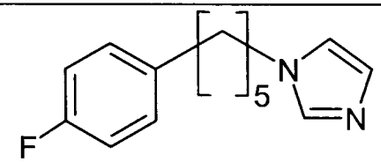	84.89 ± 1.82	0.75 ± 0.005	84.07 ± 0.58	0.10 ± 0.01
179	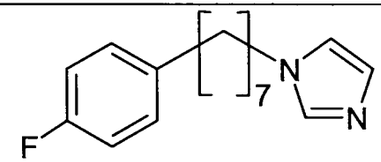	88.04 ± 0.52	0.174 ± 0.00	90.45 ± 0.68	0.058 ± 0.002

Table 2.4 Results from preliminary screening and IC_{50} data of some 4-fluro-substituted phenyl alkyl-*1H*-imidazoles for 17α-hydroxylase/17,20-lyase activity.

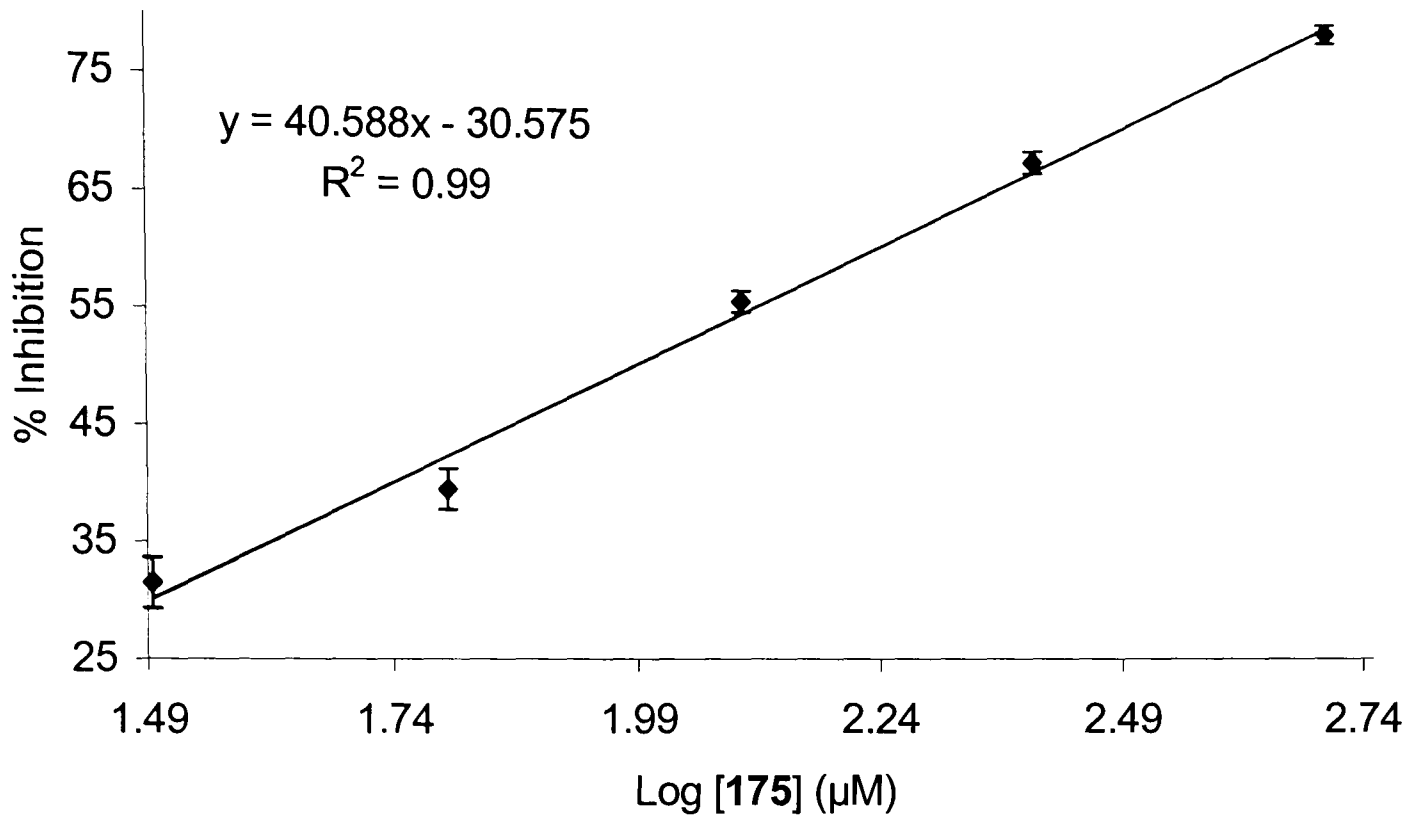

Figure 2.37 Plot of percentage inhibition versus log [**175**] for 1-(4-fluoro-benzyl)-1*H*-imidazole (**175**) against 17α-hydroxylase.

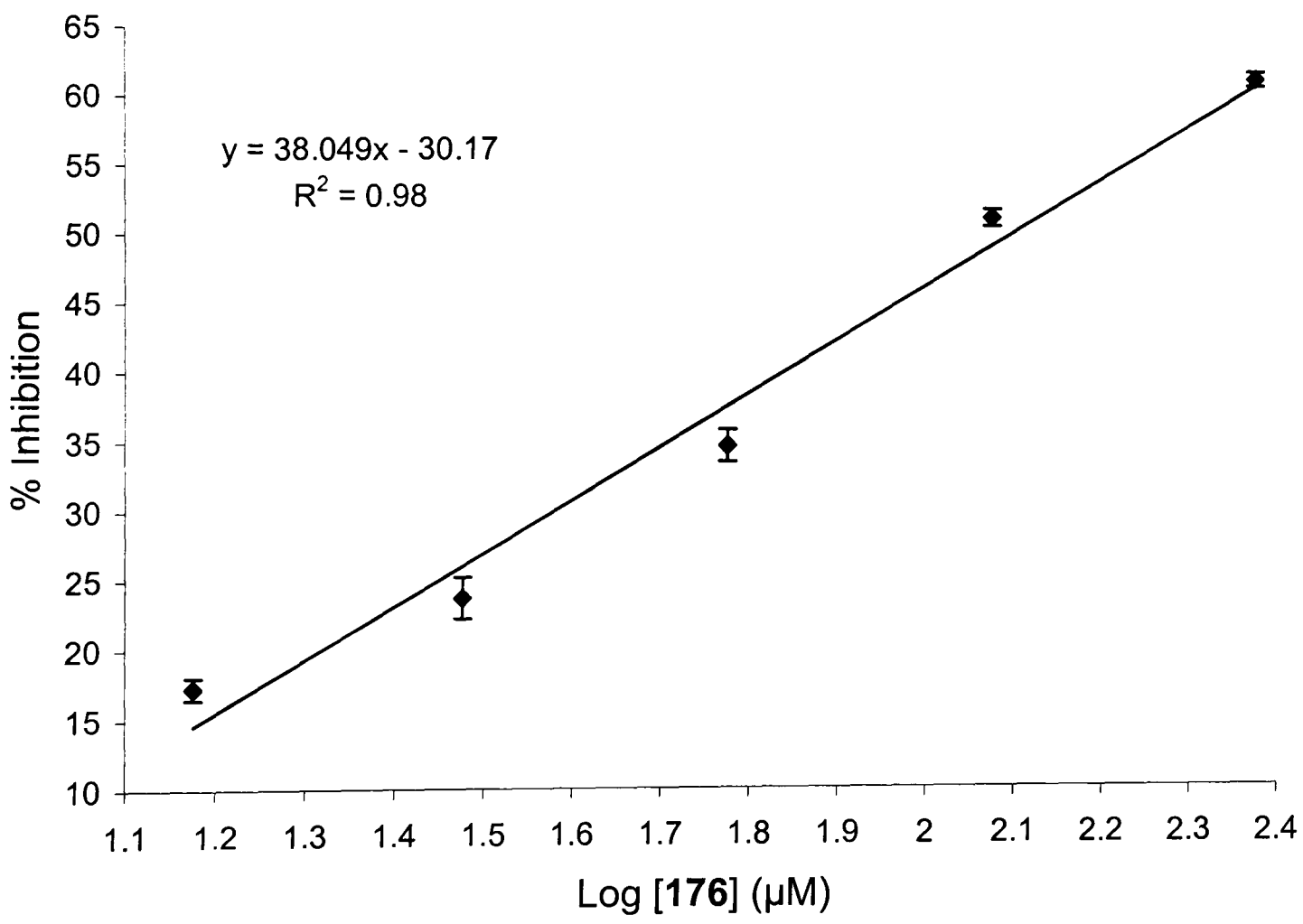

Figure 2.38 Plot of percentage inhibition versus log [**176**] for 1-[2-(4-fluoro-phenyl)-ethyl]-1*H*-imidazole (**176**) against 17α-hydroxylase.

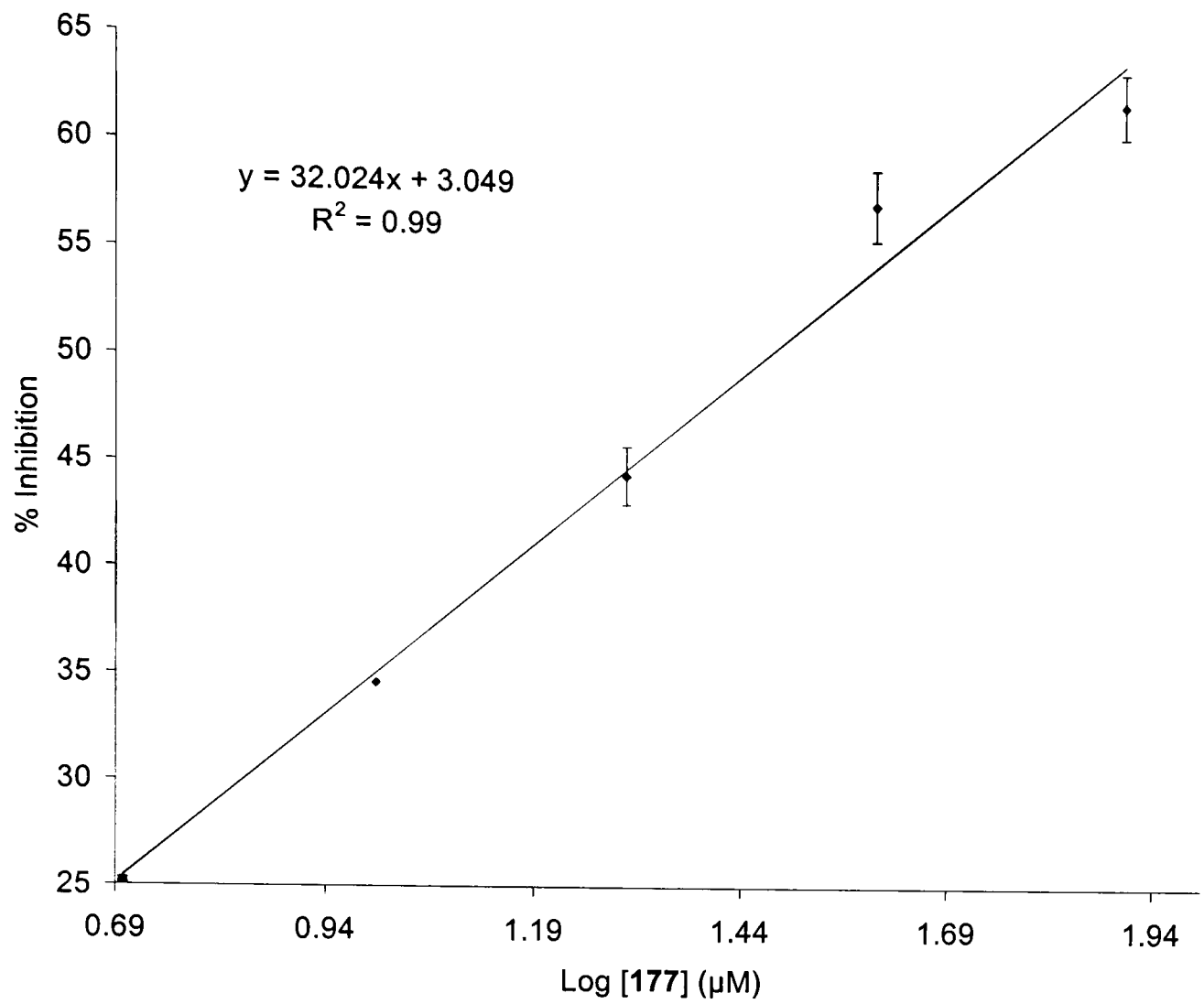

Figure 2.39 Plot of percentage inhibition versus log [**177**] for 1-[3-(4-fluoro-phenyl)-propyl]-1*H*-imidazole (**177**) against 17α-hydroxylase.

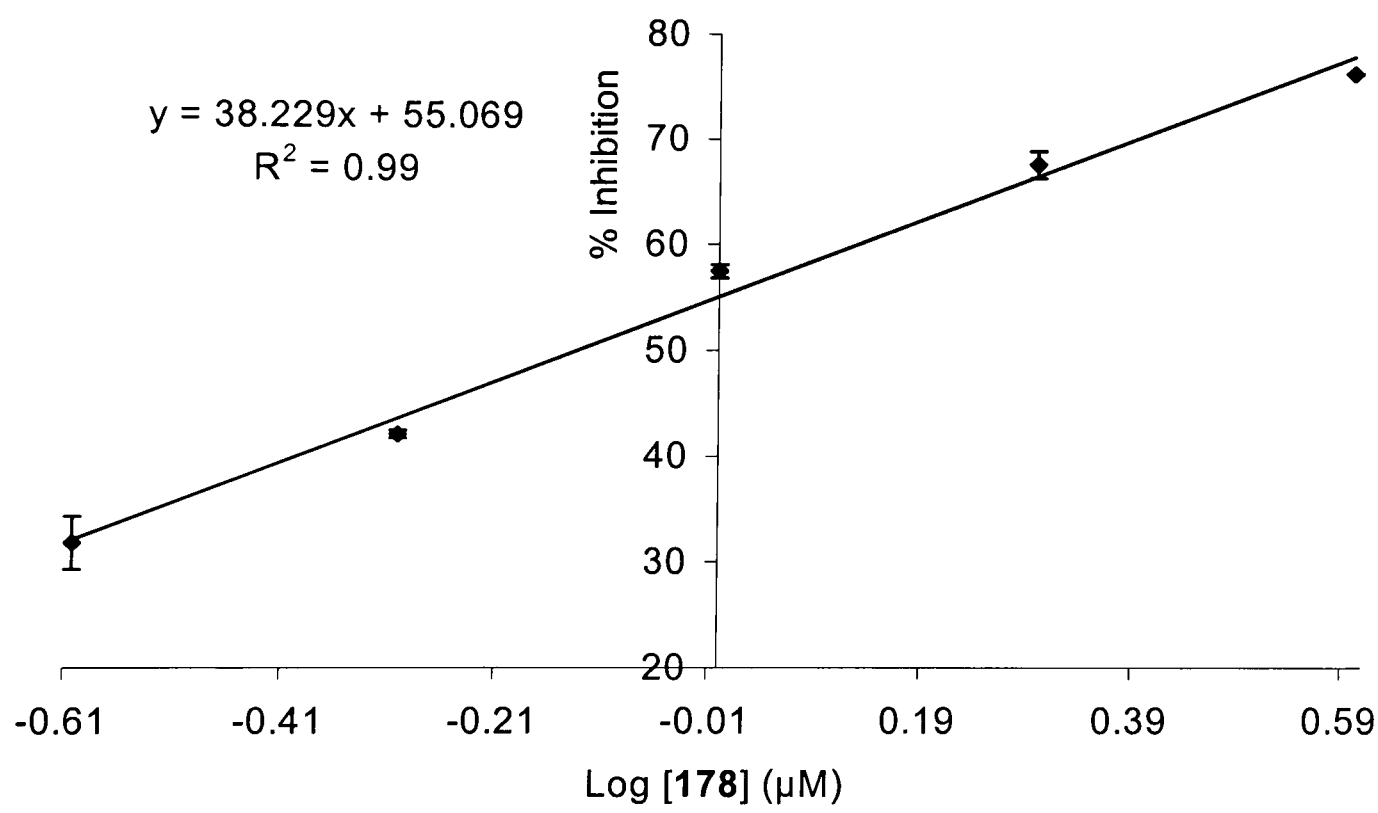

Figure 2.40 Plot of percentage inhibition versus log [**178**] for 1-[5-(4-fluoro-phenyl)-pentyl]-1*H*-imidazole (**178**) against 17α-hydroxylase.

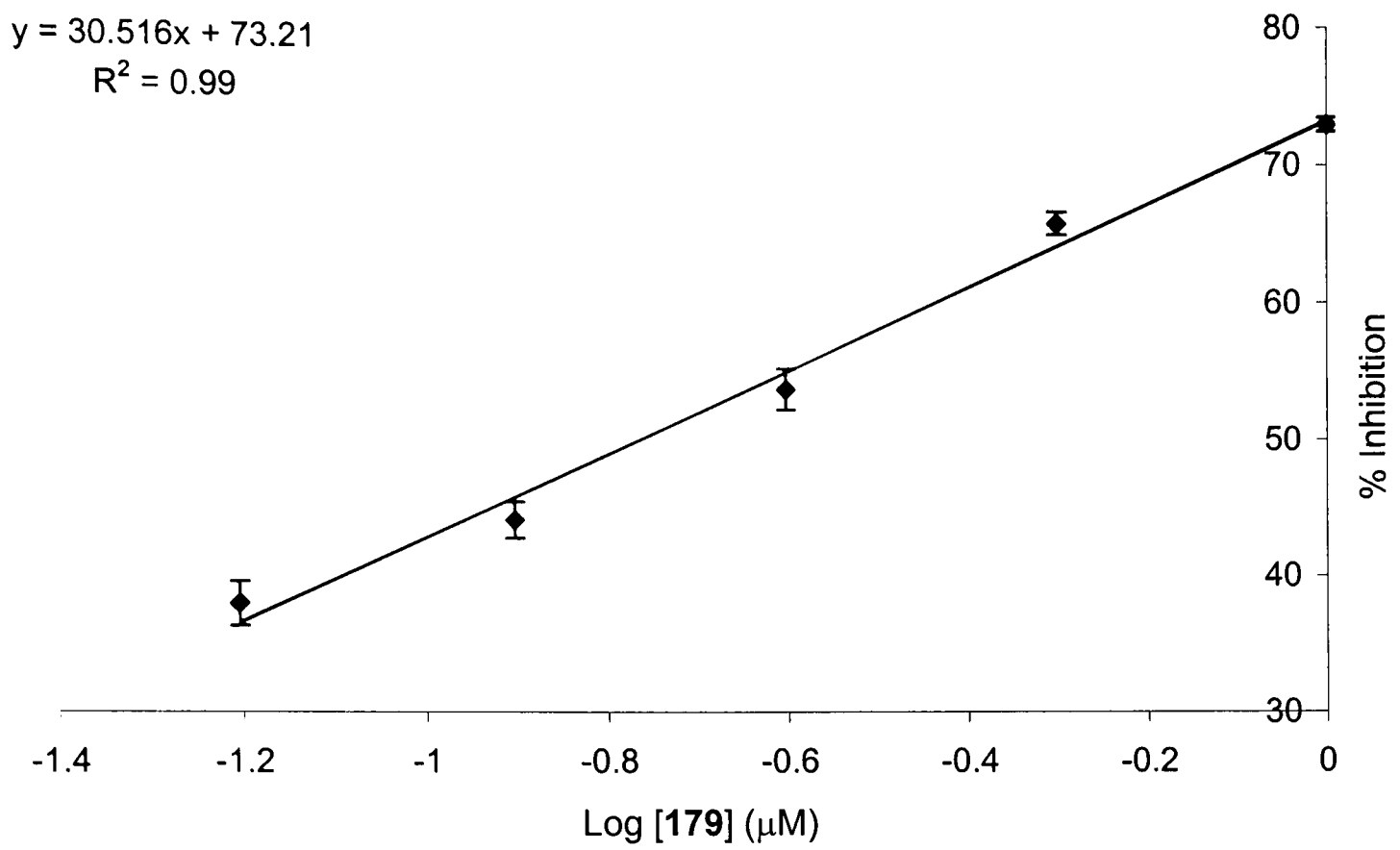

Figure 2.41 Plot of percentage inhibition versus log [**179**] for 1-[3-(4-fluoro-phenyl)-heptyl]-1*H*-imidazole (**179**) against 17α-hydroxylase.

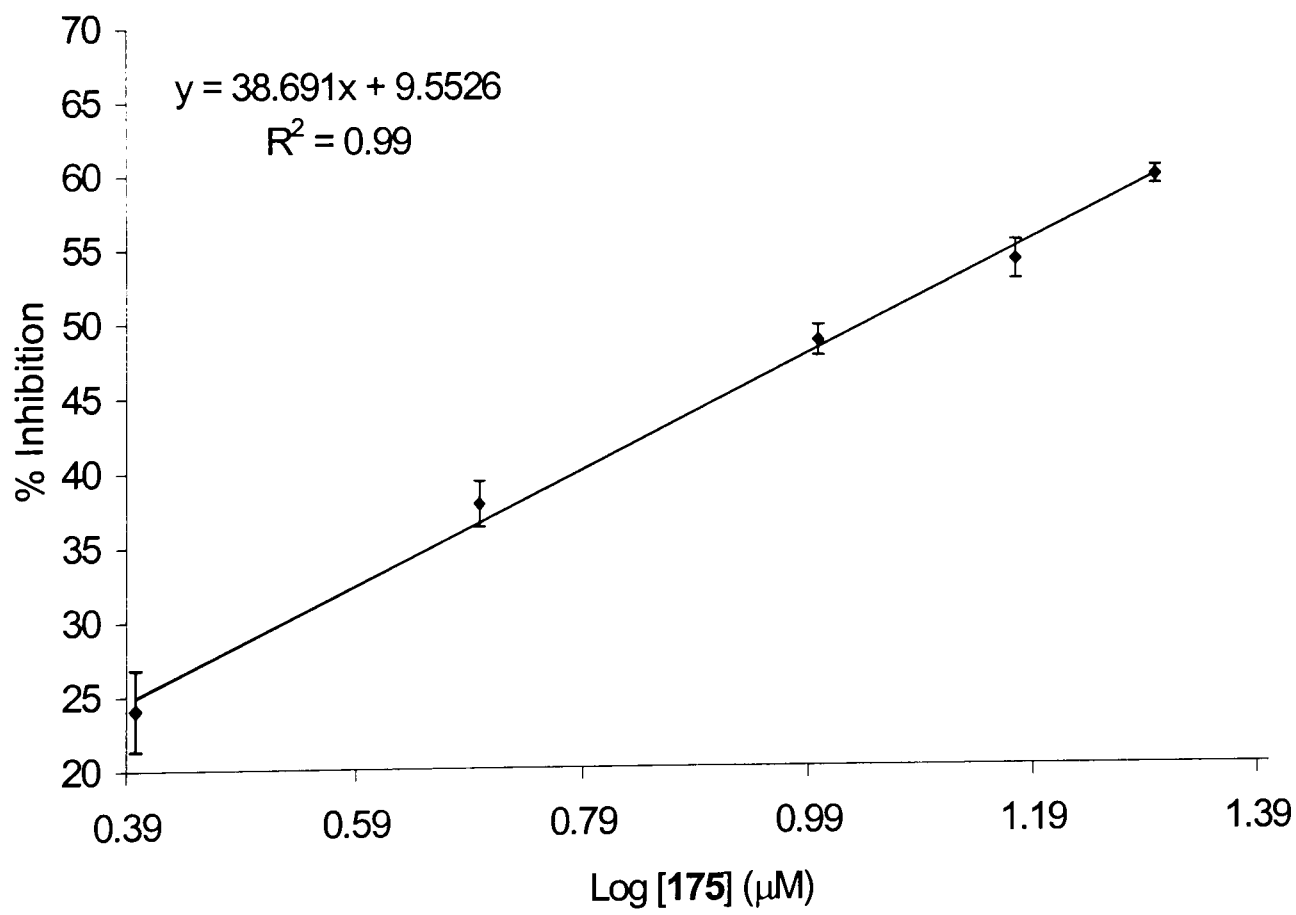

Figure 2.42 Plot of percentage inhibition versus log [**175**] for 1-(4-fluoro-benzyl)-1*H*-imidazole (**175**) against 17,20 lyase.

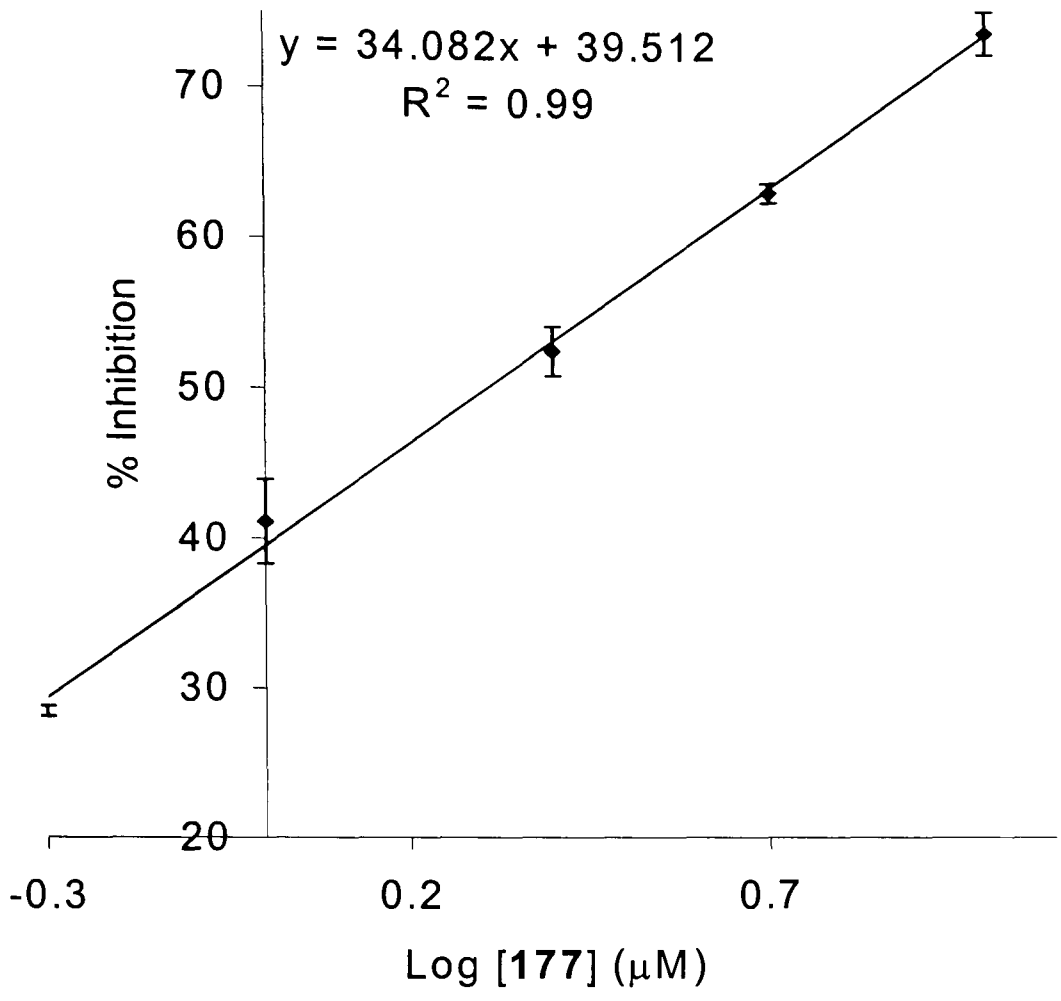

Figure 2.43 Plot of percentage inhibition versus log [**177**] for 1-[3-(4-fluoro-phenyl)-propyl]-1*H*-imidazole (**177**) against 17,20 lyase.

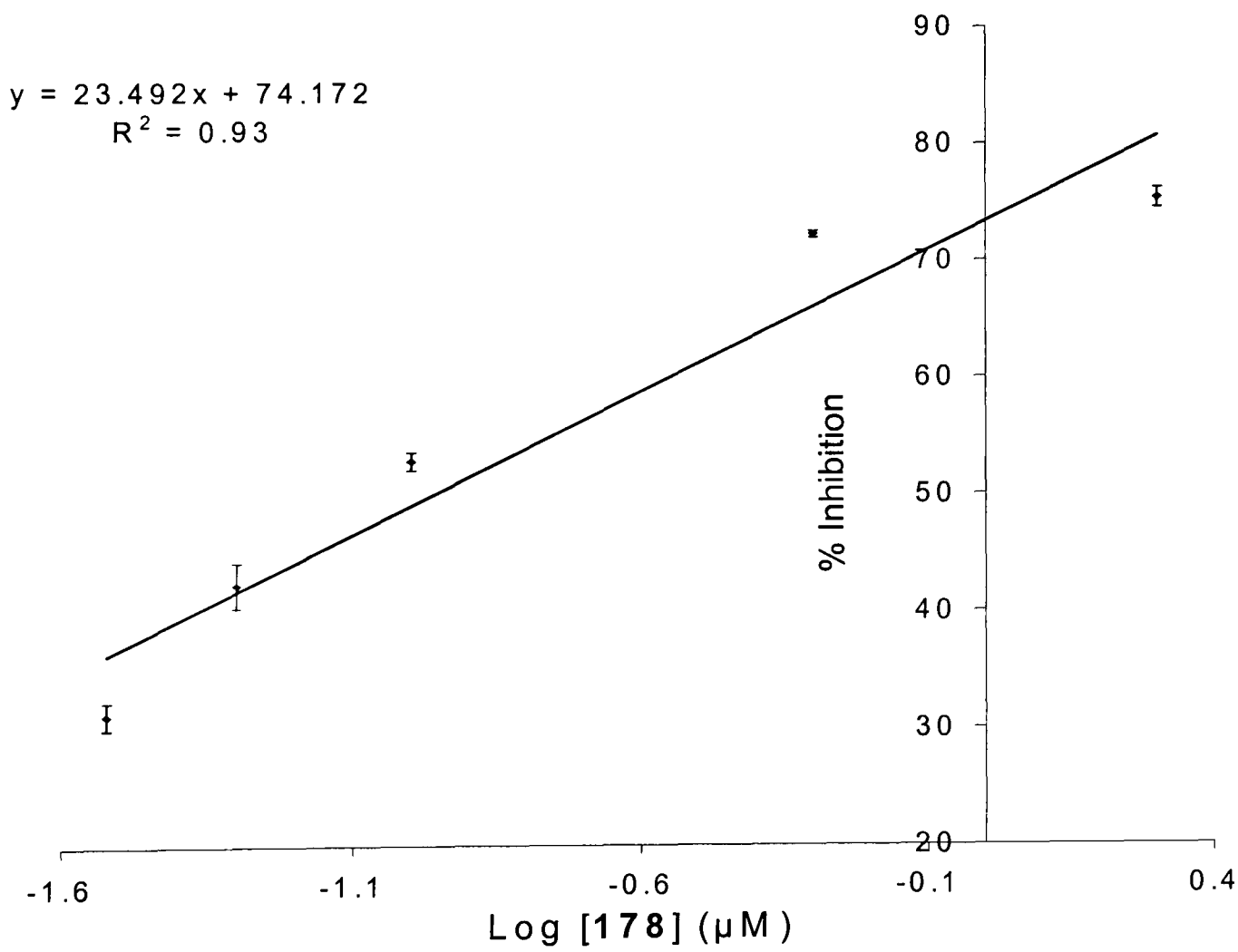

Figure 2.44 Plot of percentage inhibition versus log [**178**] for 1-[5-(4-fluoro-phenyl)-pentyl]-1*H*-imidazole (**178**) against 17,20 lyase.

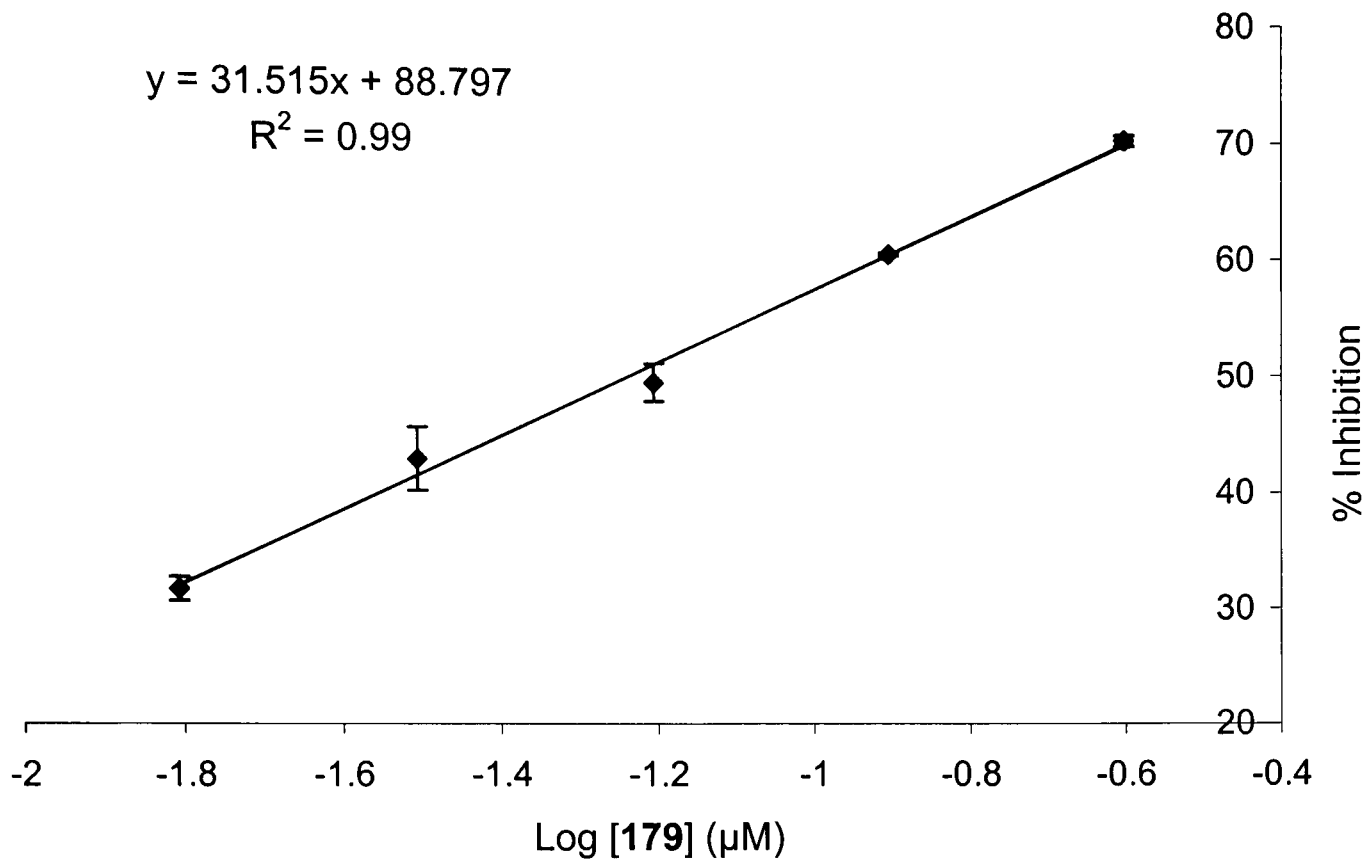

Figure 2.45 Plot of percentage inhibition versus log [**179**] for 1-[7-(4-fluoro-phenyl)-heptyl]-1*H*-imidazole (**179**) against 17,20 lyase.

2.29 Results of 4-Chloro-substituted Phenyl Alkyl-*1H*-imidazoles against $P450_{17\alpha}$

The results are shown in Table 2.5

2.29.1 Discussion

Compound **180** was less potent than ketoconazole for both 17α-hydroxylase and 17,20-lyase. Compound **183** was more potent than ketoconazole against both components. Compound **182** however was found to be weaker than ketoconazole against the 17α-hydroxylase component but more potent against the 17,20-lyase component. Compound **181** was found to show much less potency against 17α-hydroxylase and thus was not tested against 17,20-lyase.

Compound No.	Structure	17α-hydroxylase		17,20-lyase	
		% Inhibition at 10μM	IC_{50} Values (μM)	% Inhibition at 10μM	IC_{50} Values (μM)
180	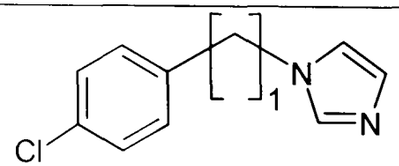	45.70 ± 0.98	29.84 ± 0.27	73.65 ± 0.99	4.94 ± 0.17
181	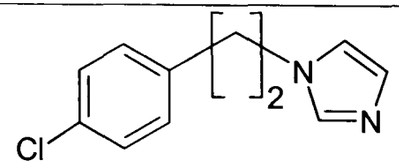	28.42 ± 2.92	49.64 ± 1.48	57.38 ± 2.50	N/A
182	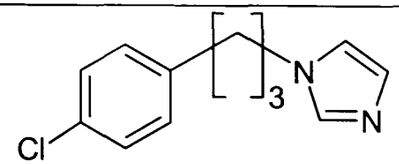	71.00 ± 0.53	5.85 ± 0.19	80.85 ± 1.28	0.55 ± 0.07
183	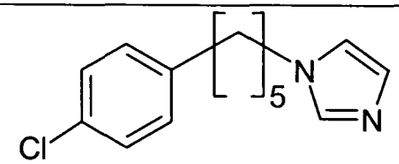	84.93 ± 0.27	0.57 ± 0.03	84.84 ± 1.33	0.086 ± 0.006

Table 2.5 Results from preliminary screening and IC_{50} data of some 4-chloro-substituted phenyl alkyl-*1H*-imidazoles for 17α-hydroxylase/17,20-lyase activity.

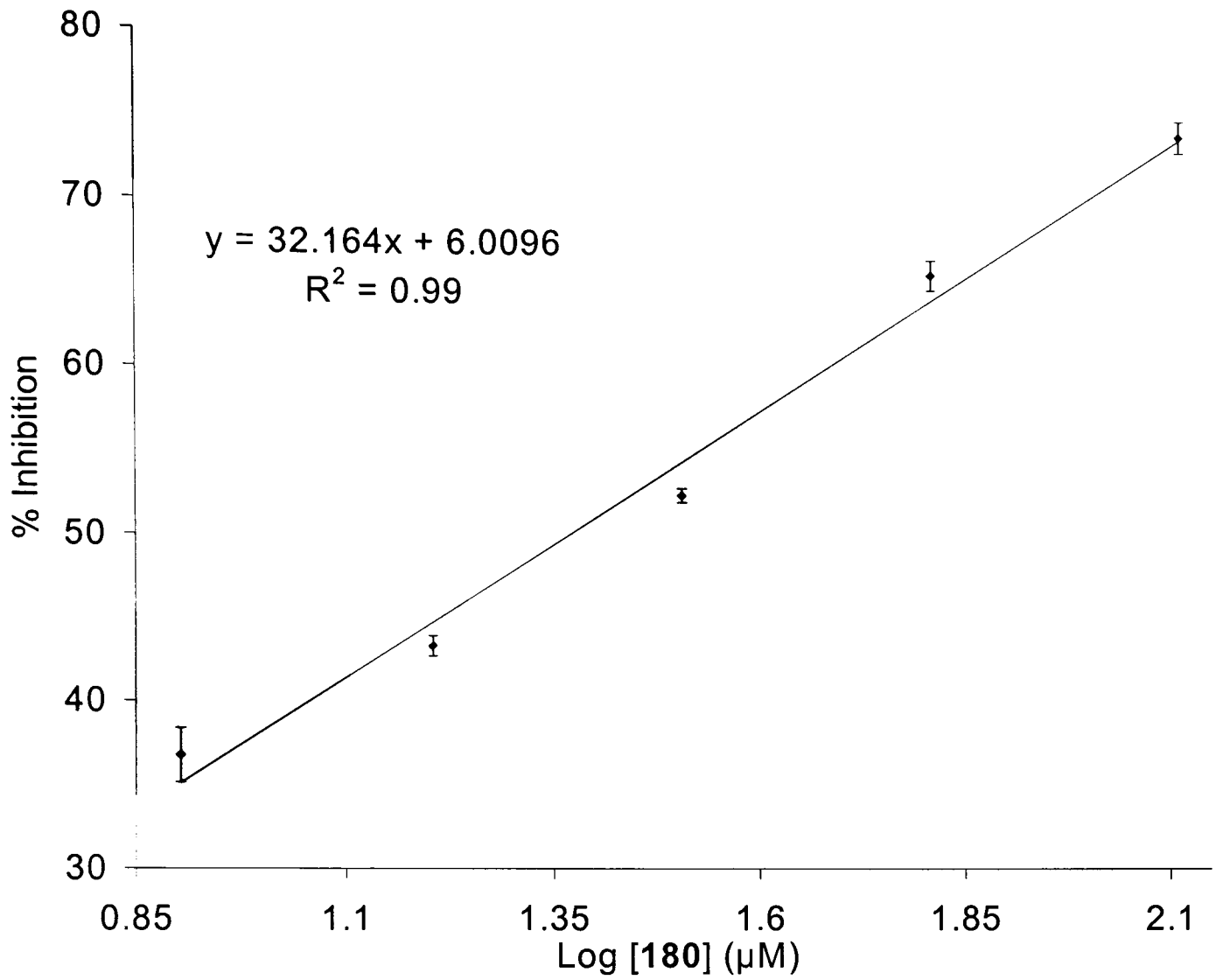

Figure 2.46 Plot of percentage inhibition versus log [**180**] for 1-(4-chloro-benzyl)-1*H*-imidazole (**180**) against 17α-hydroxylase.

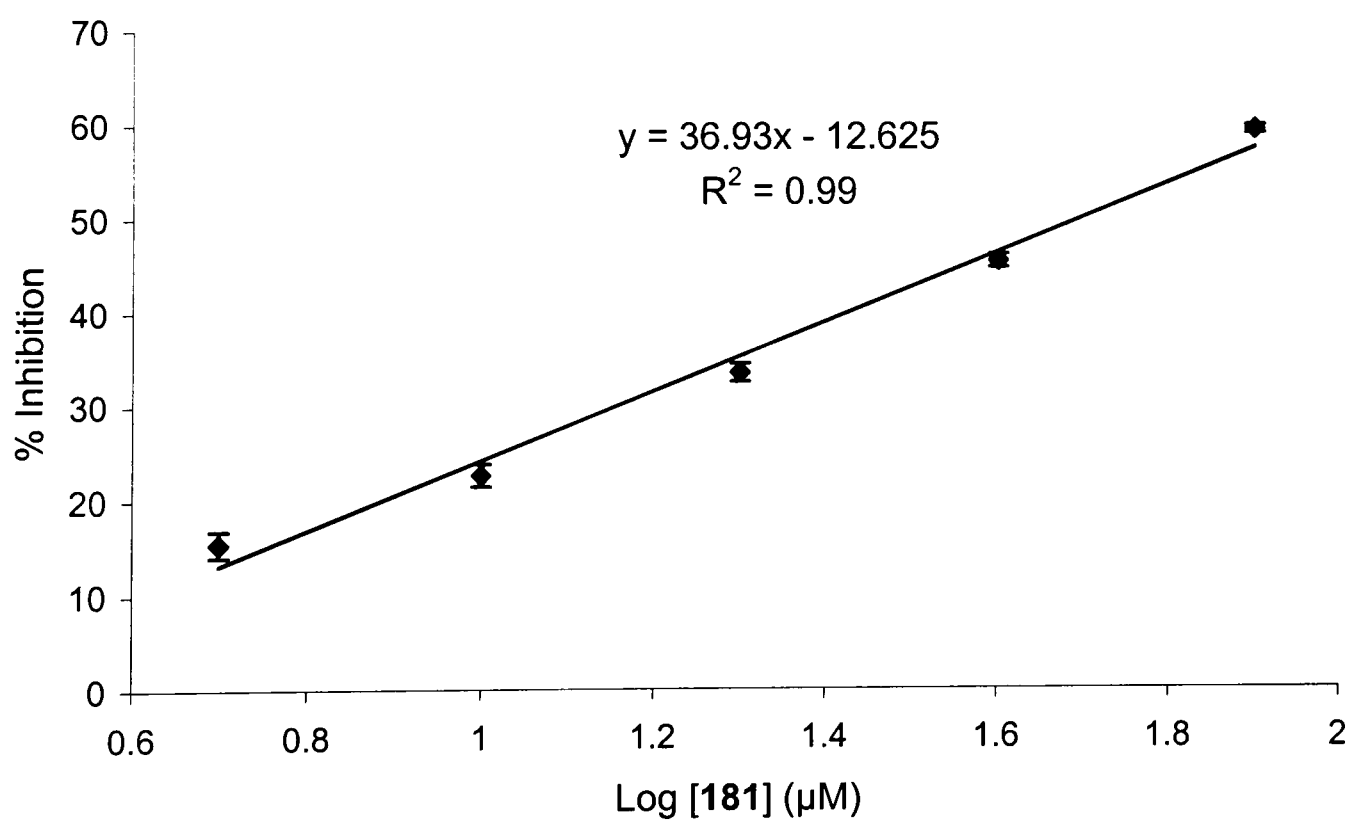

Figure 2.47 Plot of percentage inhibition versus log [**181**] for 1-[2-(4-chloro-phenyl)-ethyl]-1*H*-imidazole (**181**) against 17α-hydroxylase.

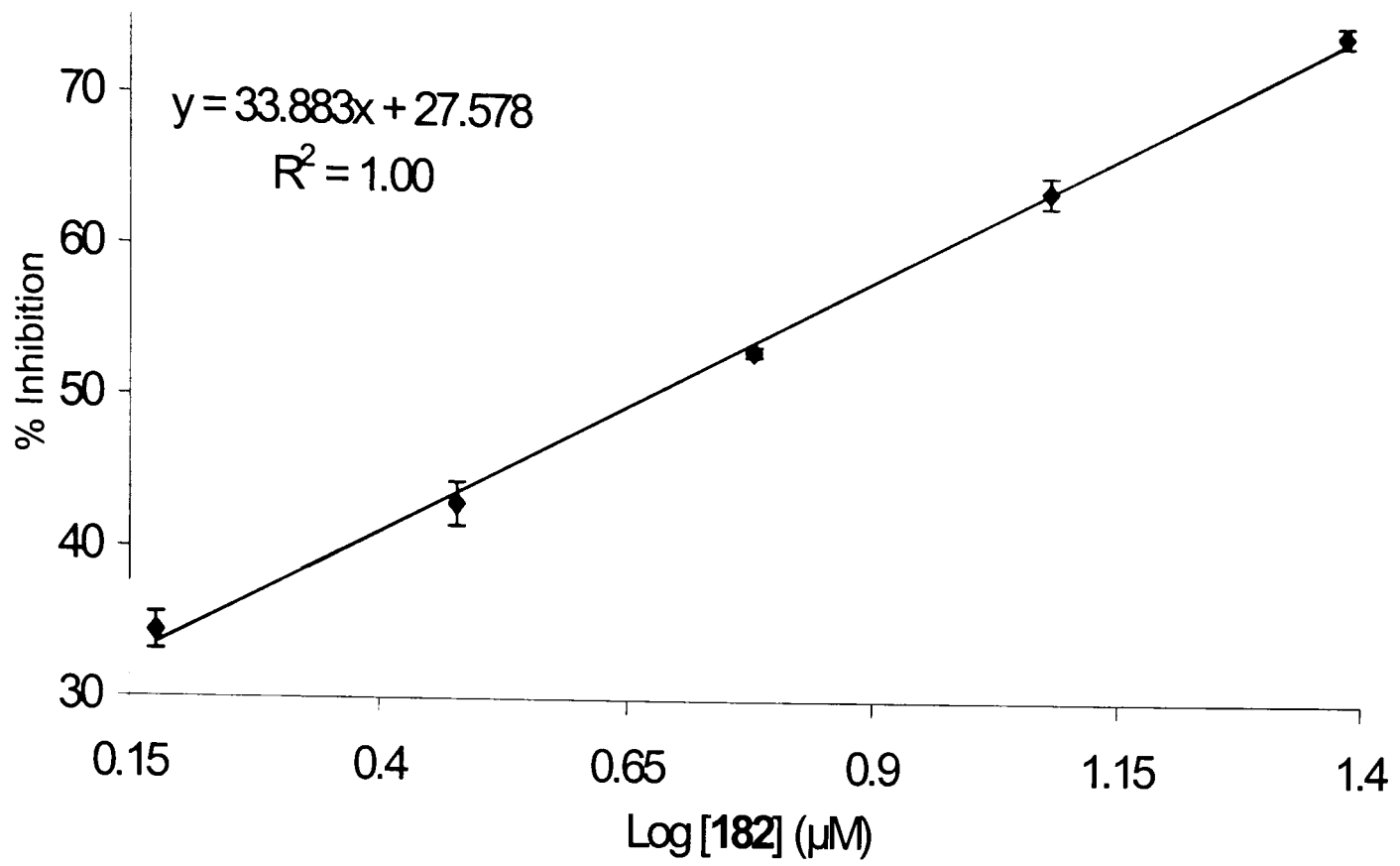

Figure 2.48 Plot of percentage inhibition versus log [**182**] for 1-[3-(4-chloro-phenyl)-propyl]-1*H*-imidazole (**182**) against 17α-hydroxylase.

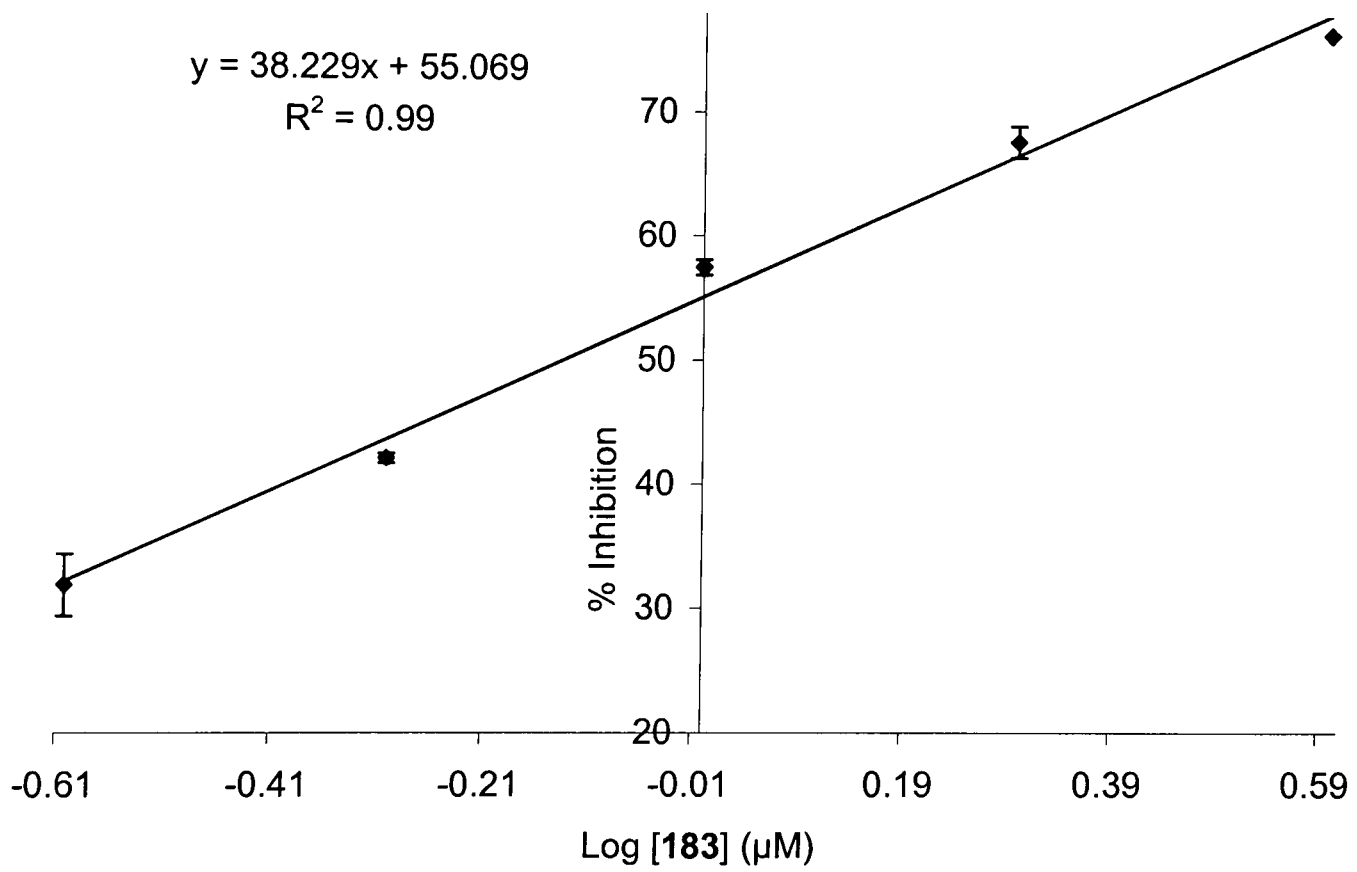

Figure 2.49 Plot of percentage inhibition versus log [**183**] for 1-[5-(4-chloro-phenyl)-pentyl]-1*H*-imidazole (**183**) against 17α-hydroxylase.

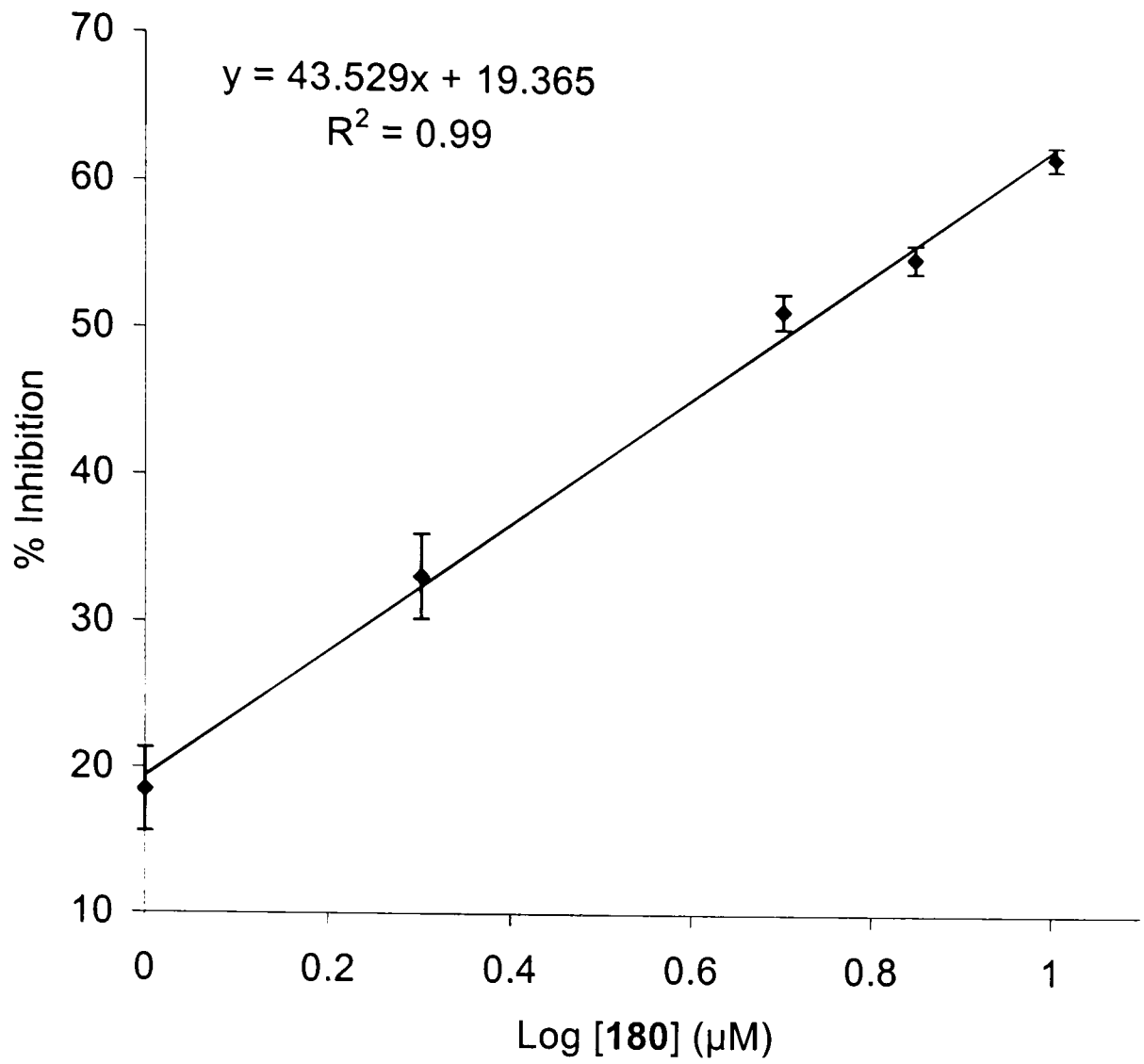

Figure 2.50 Plot of percentage inhibition versus log [**180**] for 1-(4-chloro-benzyl)-1*H*-imidazole (**180**) against 17,20 lyase.

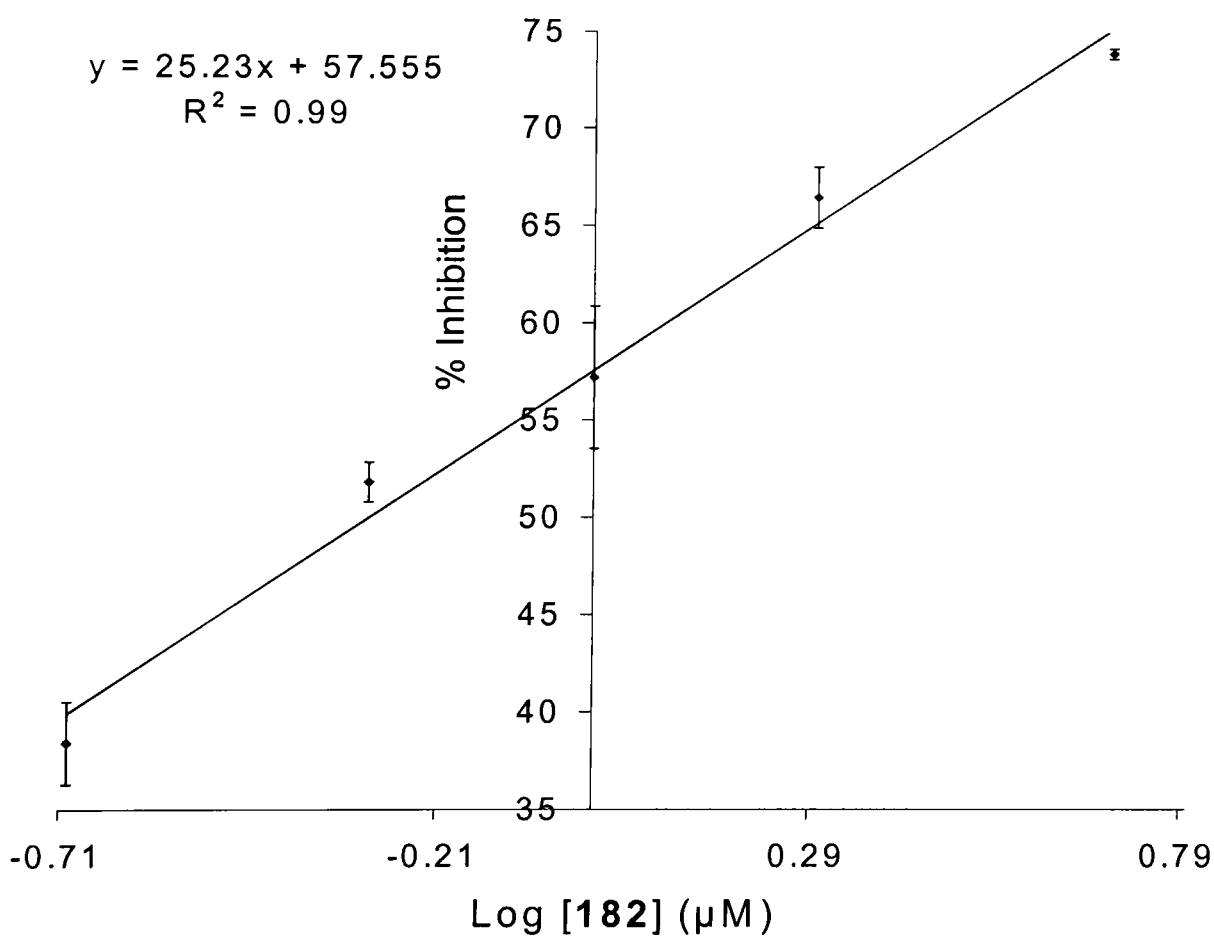

Figure 2.51 Plot of percentage inhibition versus log [**182**] for 1-[3-(4-chloro-phenyl)-propyl]-1*H*-imidazole (**182**) against 17,20 lyase.

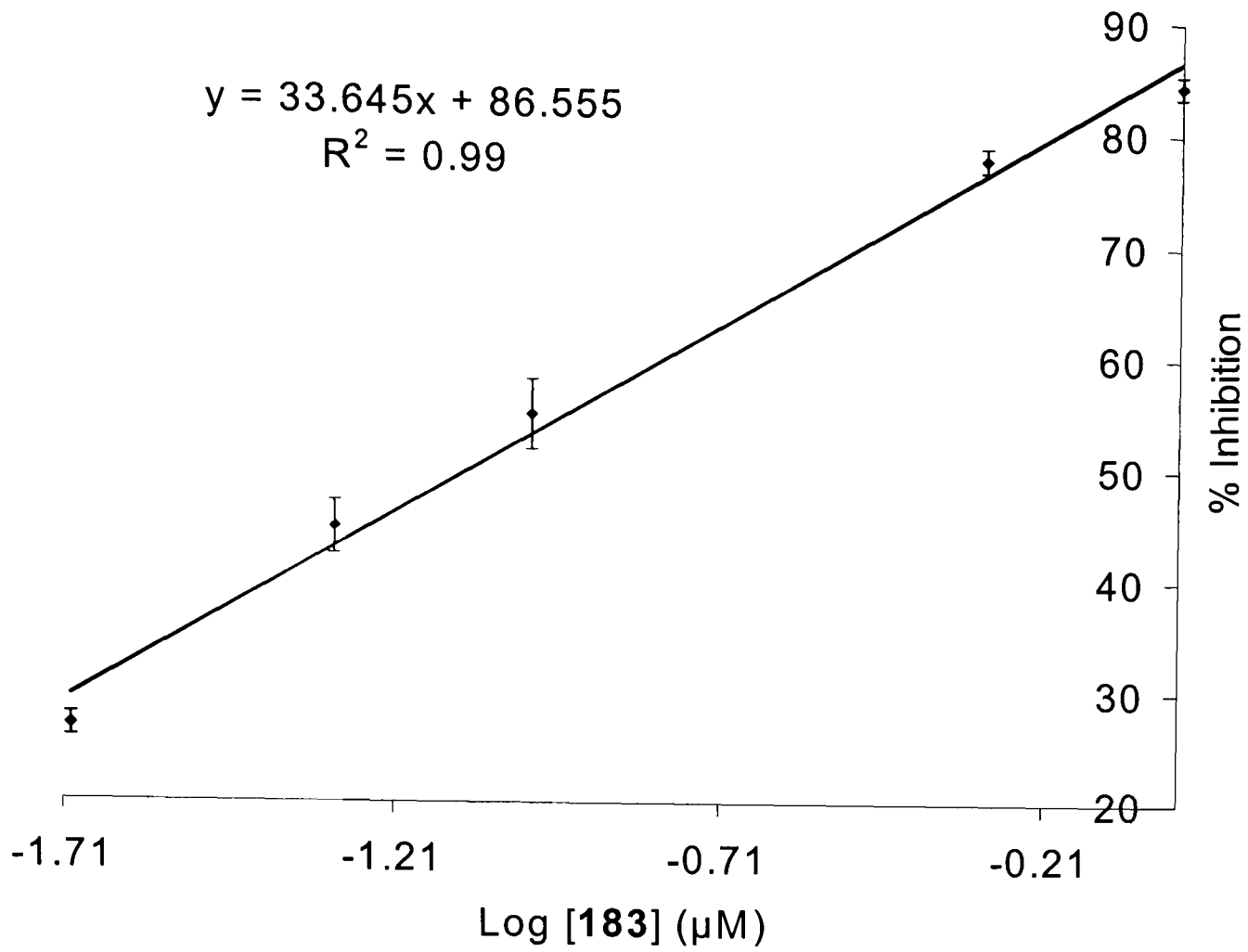

Figure 2.52 Plot of percentage inhibition versus log [**183**] for 1-[5-(4-chloro-phenyl)-pentyl]-1*H*-imidazole (**183**) against 17,20 lyase.

2.30 Results of 4-Bromo-substituted Phenyl Alkyl-*1H*-imidazoles against $P450_{17\alpha}$

The results are shown in Table 2.6

2.30.1 Discussion

Compound **184** was less potent than ketoconazole for both 17α-hydroxylase and 17,20-lyase. Compounds **186** and **187** were both more potent than ketoconazole against both components. Compound **185** was found to show much less potency against 17α-hydroxylase and thus was not tested against 17,20-lyase.

Compound No.	Structure	17α-hydroxylase		17,20-lyase	
		% Inhibition at 10μM	IC_{50} Values (μM)	% Inhibition at 10μM	IC_{50} Values (μM)
184	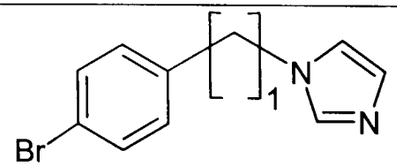	49.29 ± 1.97	16.55 ± 0.23	76.25 ± 0.65	2.85 ± 0.08
185	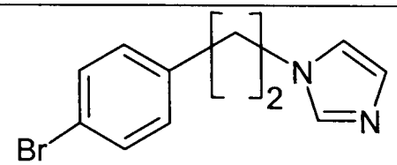	37.54 ± 0.60	30.66 ± 0.13	61.52 ± 2.49	N/A
186	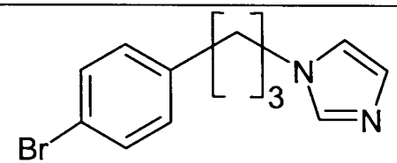	70.15 ± 0.94	2.95 ± 0.03	86.29 ± 0.3	0.33 ± 0.02
187	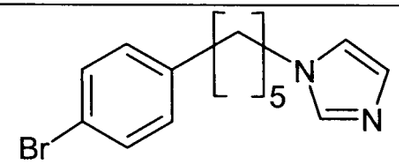	89.22 ± 0.31	0.50 ± 0.04	81.34 ± 3.85	0.058 ± 0.005

Table 2.6 Results from preliminary screening and IC_{50} data of some 4-bromo-substituted phenyl alkyl-*1H*-imidazoles for 17α-hydroxylase/17,20-lyase activity.

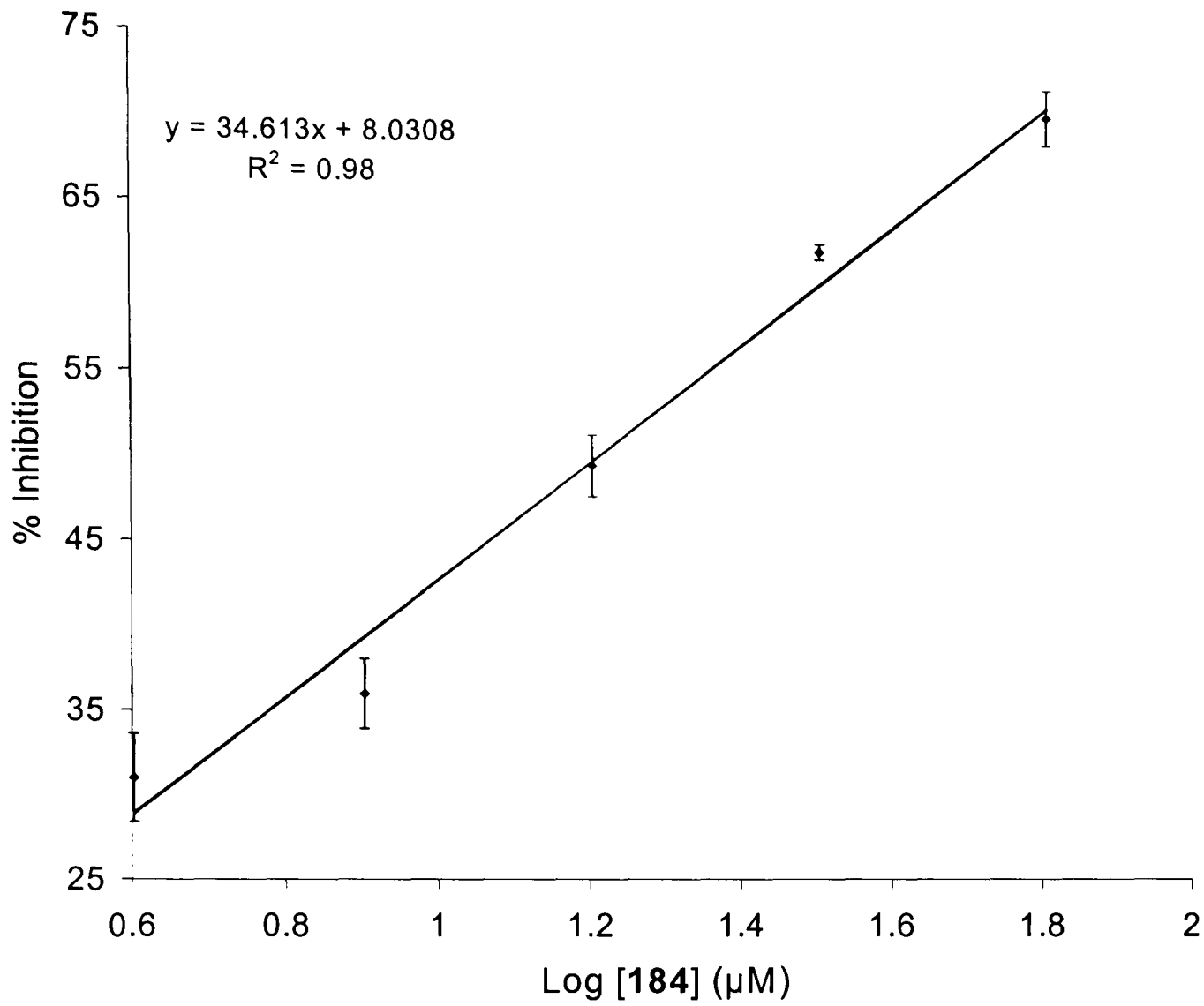

Figure 2.53 Plot of percentage inhibition versus log [**184**] for 1-(4-bromo-benzyl)-1*H*-imidazole (**184**) against 17α-hydroxylase.

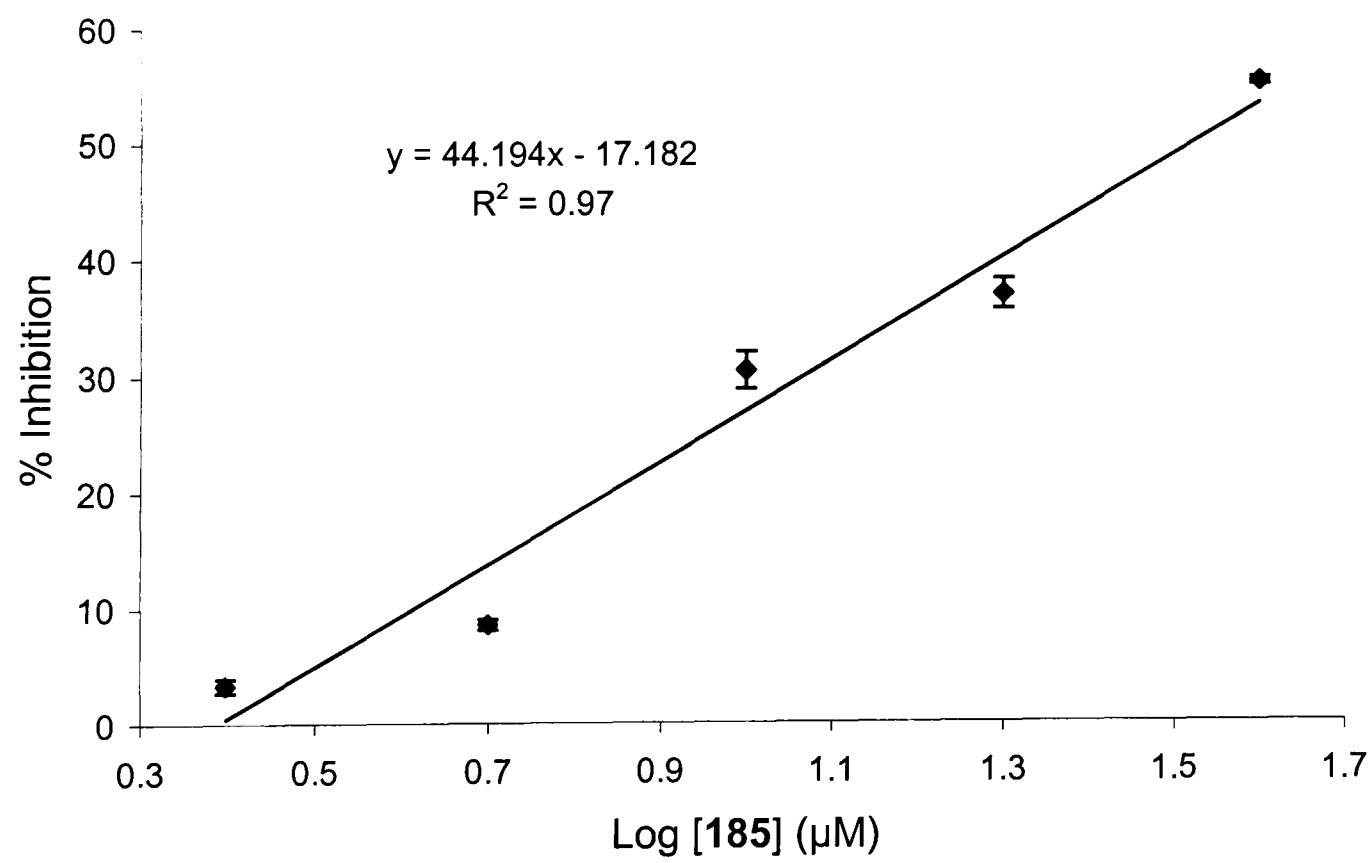

Figure 2.54 Plot of percentage inhibition versus log [**185**] for 1-[2-(4-bromo-phenyl)-ethyl]-1*H*-imidazole (**185**) against 17α-hydroxylase.

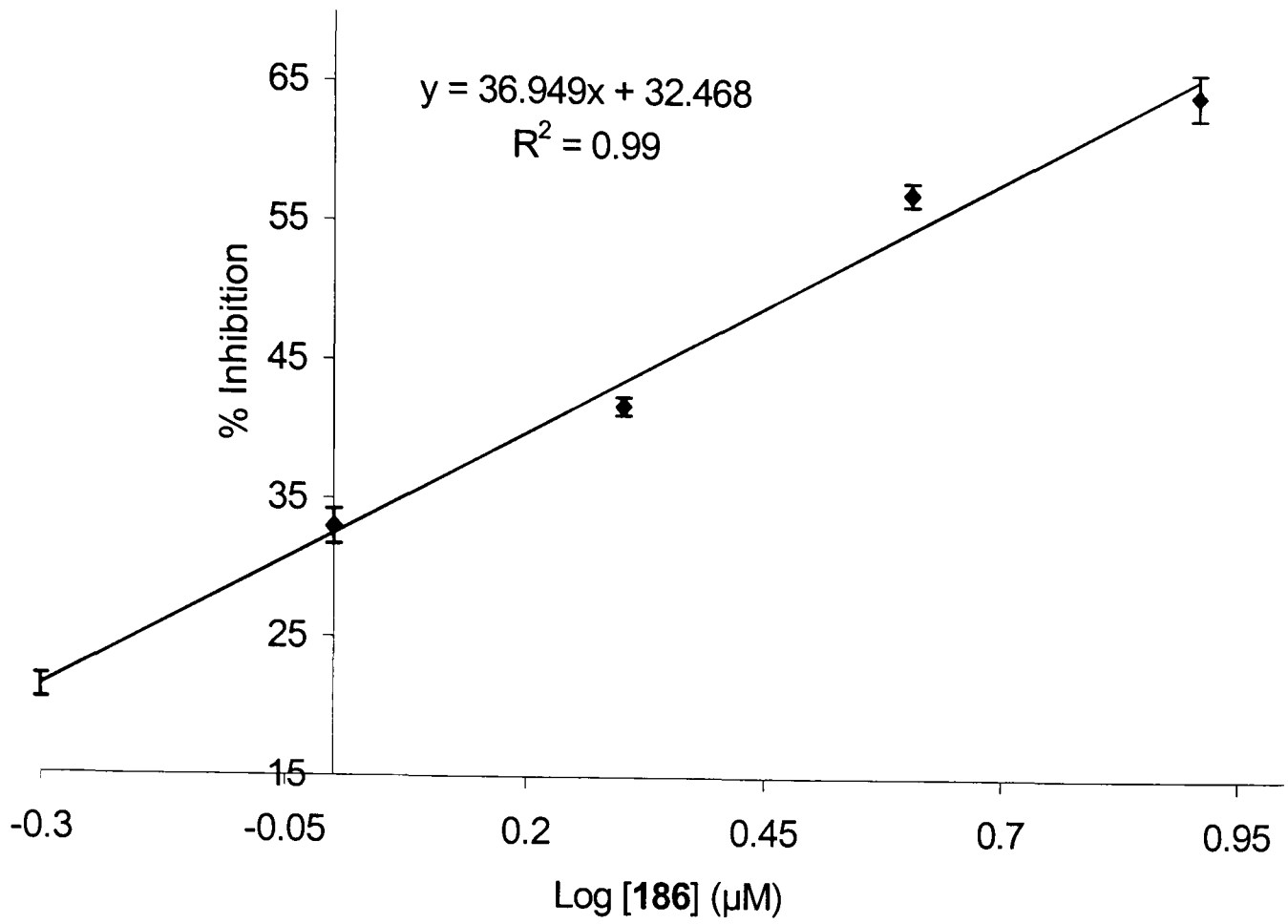

Figure 2.55 Plot of percentage inhibition versus log [**186**] for 1-[3-(4-bromo-phenyl)-propyl]-1*H*-imidazole (**186**) against 17α-hydroxylase.

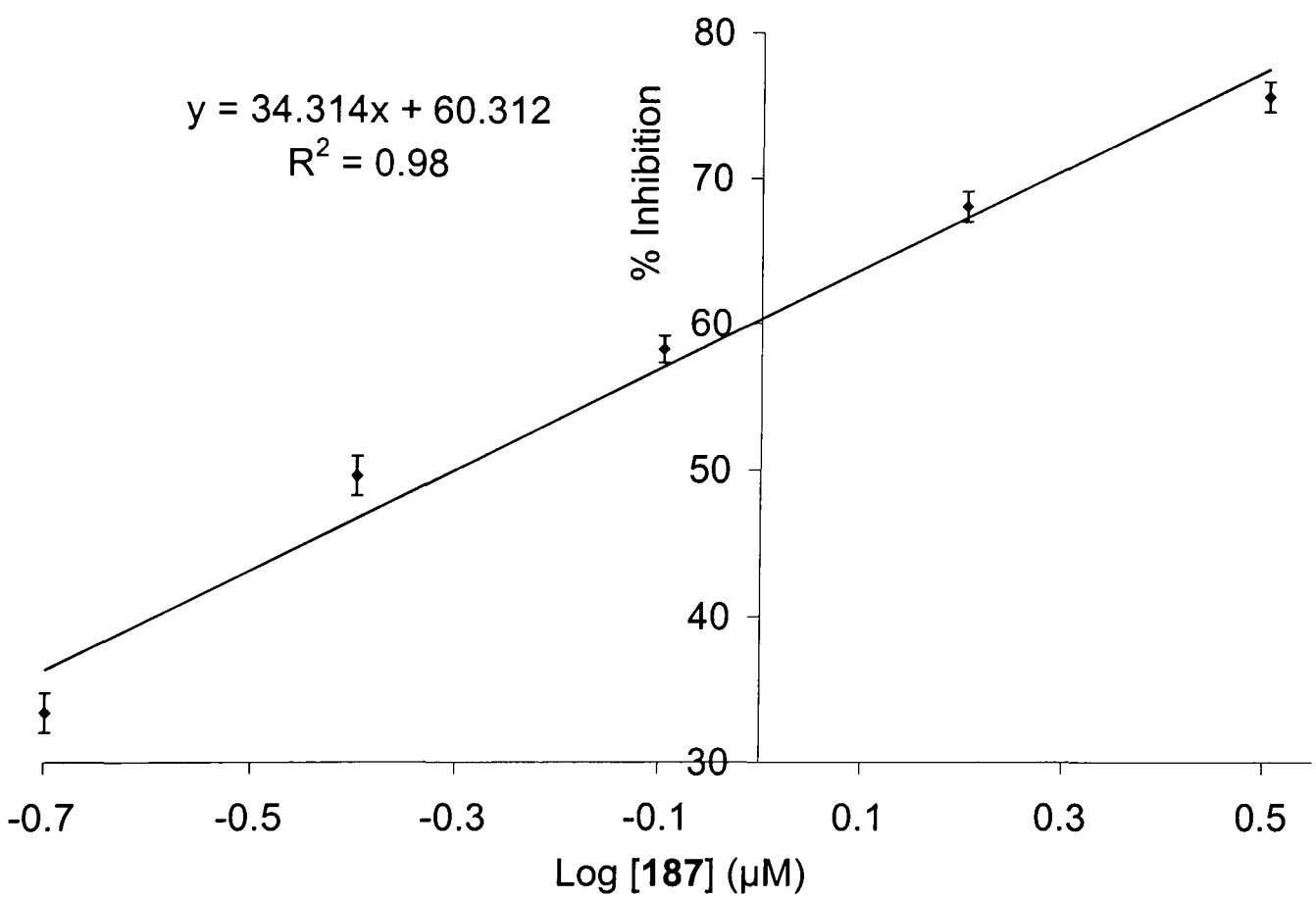

Figure 2.56 Plot of percentage inhibition versus log [**187**] for 1-[5-(4-bromo-phenyl)-pentyl]-1*H*-imidazole (**187**) against 17α-hydroxylase.

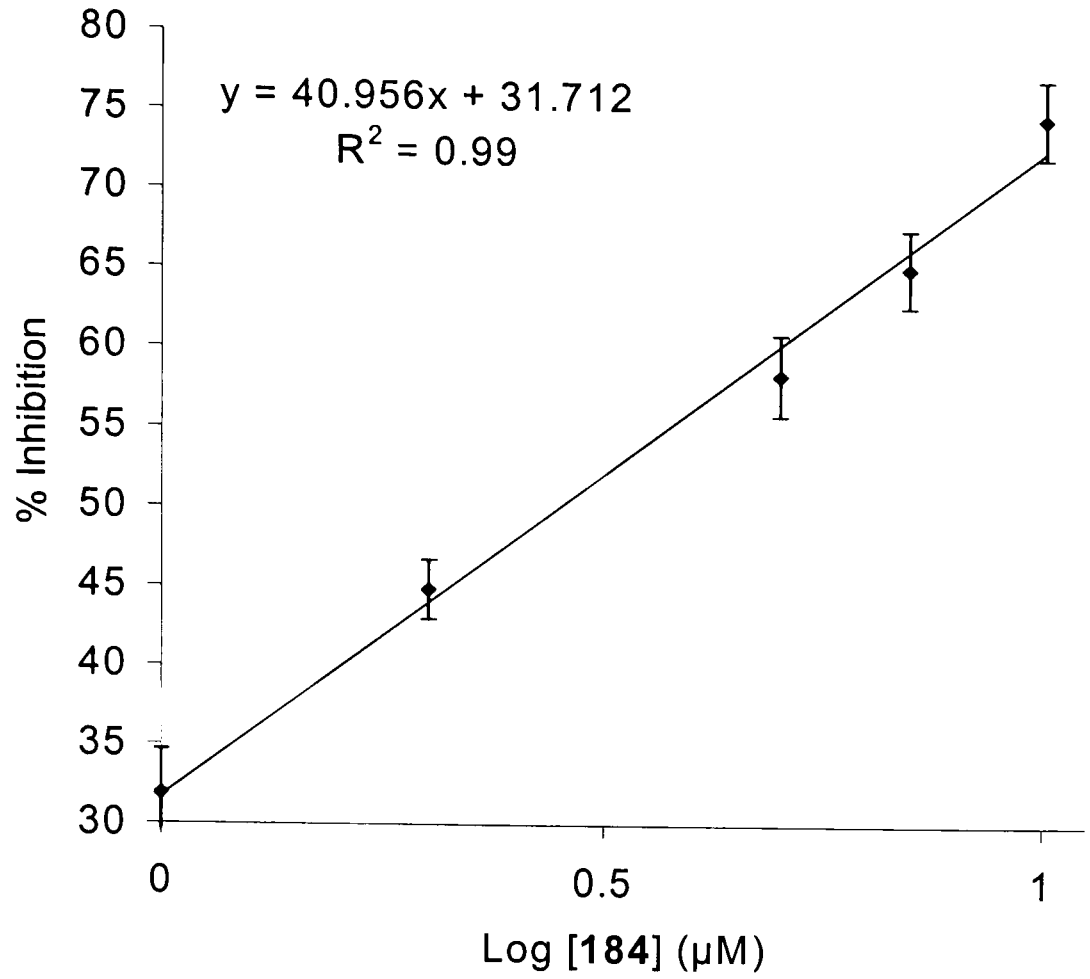

Figure 2.57 Plot of percentage inhibition versus log [**184**] for 1-(4-bromo-benzyl)-1*H*-imidazole (**184**) against 17,20 lyase.

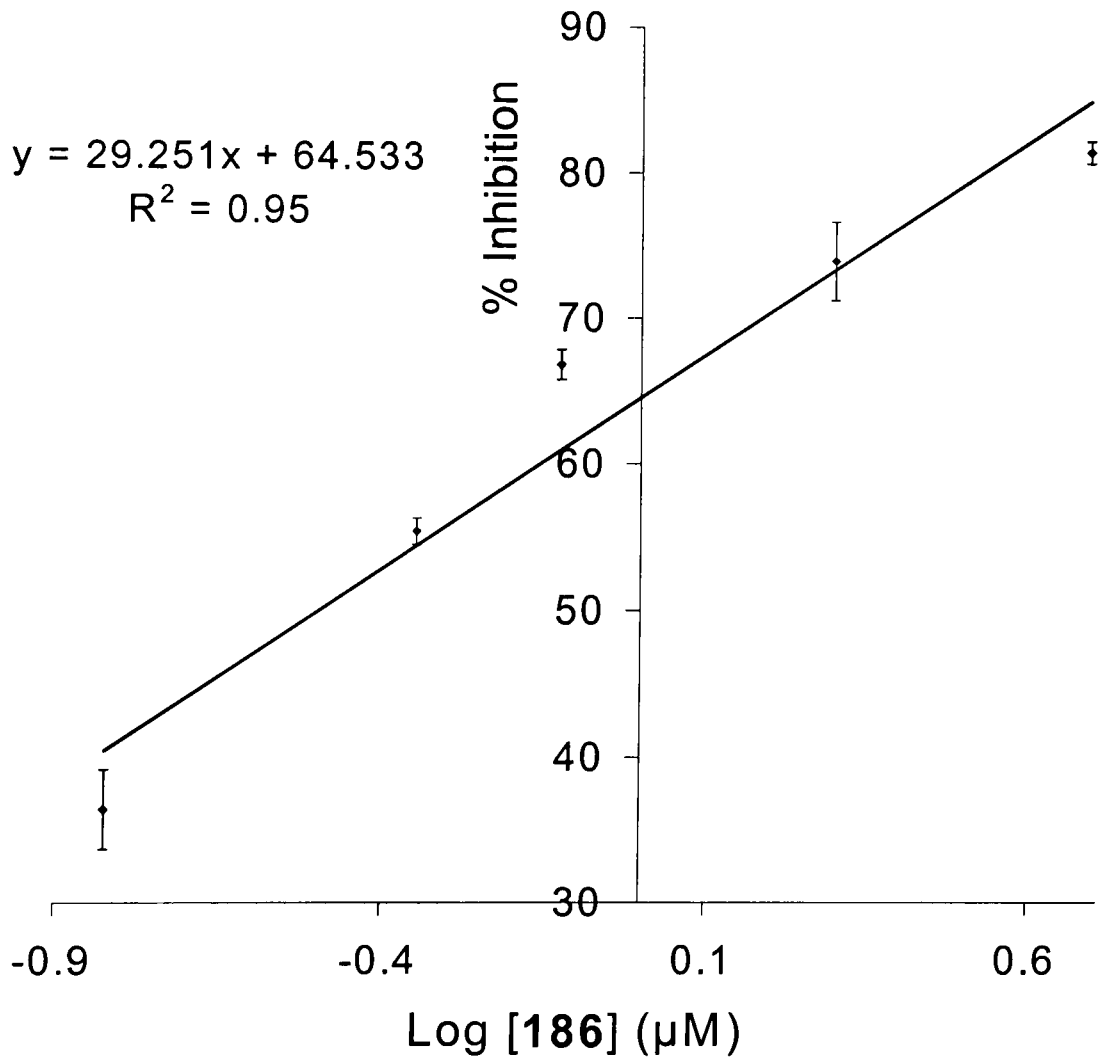

Figure 2.58 Plot of percentage inhibition versus log [**186**] for 1-[3-(4-bromo-phenyl)-propyl]-1*H*-imidazole (**186**) against 17,20 lyase.

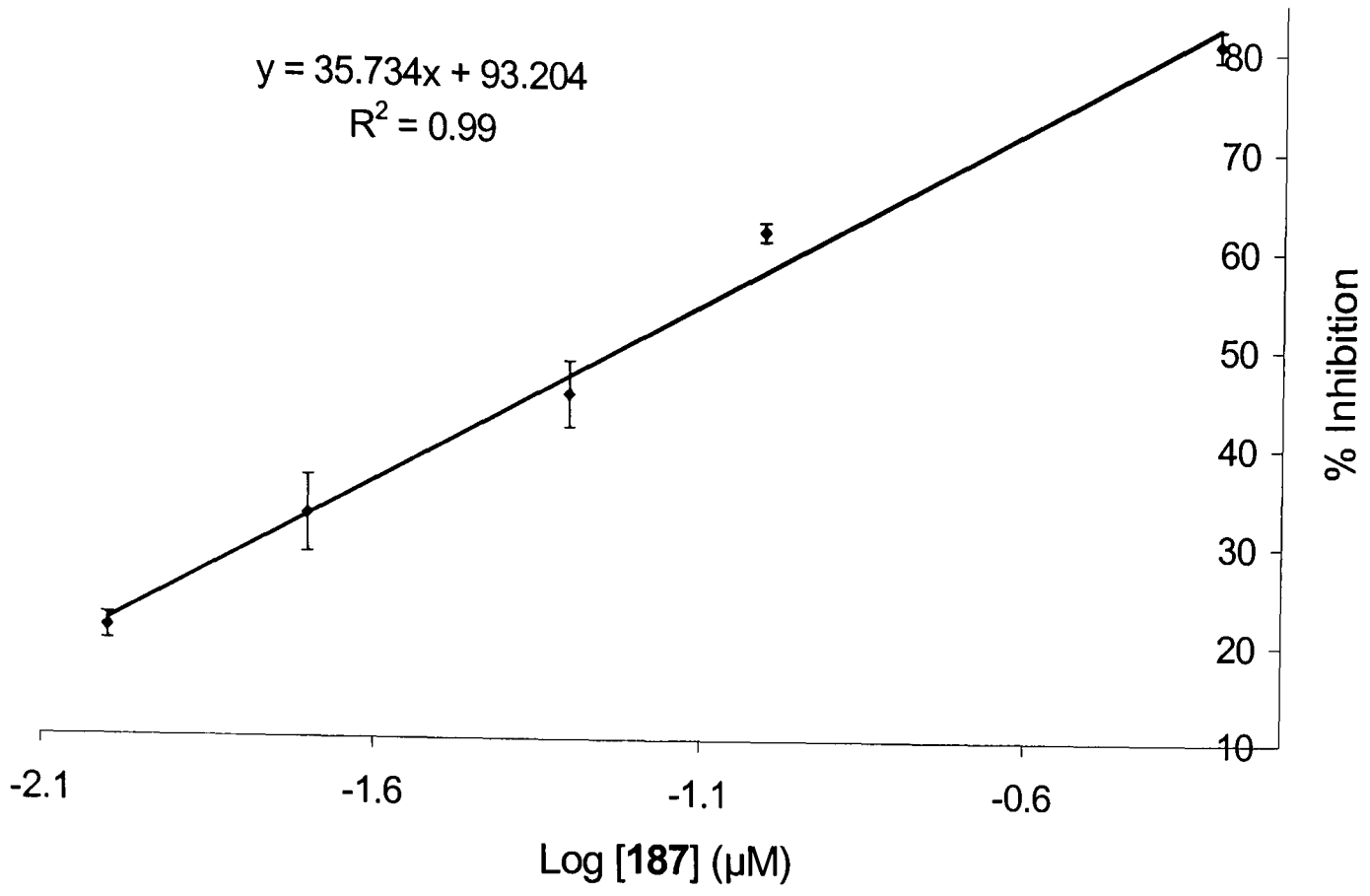

Figure 2.59 Plot of percentage inhibition versus log [**187**] for 1-[5-(4-bromo-phenyl)-pentyl]-1*H*-imidazole (**187**) against 17,20 lyase.

2.31 Results of Phenyl Alkyl-*1H*-triazoles against $P450_{17\alpha}$

The results are shown in Tables 2.7a – 2.7b

2.31.1 Discussion

The compounds were screened against both components but the IC_{50} was carried out against the 17,20-lyase component only, as, in general, they showed weak inhibition against 17α-hydroxylase. They were in general weaker in comparison to ketoconazole, except compound **194** which showed similar potency to ketoconazole for the lyase component.

Compound No.	Structure	17α-hydroxylase	17,20-lyase	
		% Inhibition at 100μM	% Inhibition at 100μM	IC_{50} Values (μM)
188	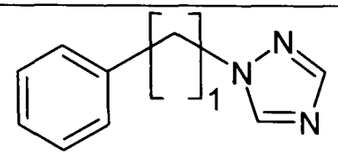	6.84 ± 0.86	2.71 ± 0.20	680.02 ± 7.72
189	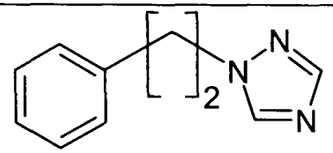	10.92 ± 1.94	0	N/A
190	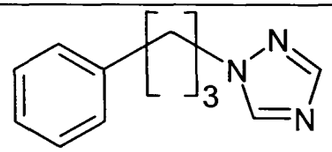	17.22 ± 1.28	37.46 ± 0.93	151.79 ± 2.90
191	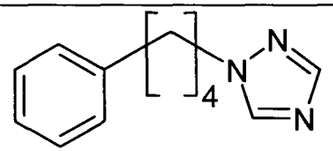	28.99 ± 0.99	63.65 ± 0.77	39.56 ± 0.24
192	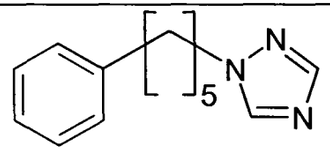	55.00 ± 0.36	81.20 ± 0.31	9.53 ± 0.48

Table 2.7a Results from preliminary screening and IC_{50} data of some unsubstituted phenyl alkyl-*1H*-[1,2,4,]triazoles for 17α-hydroxylase/17,20-lyase activity.

Compound No.	Structure	17α-hydroxylase	17,20-lyase	
		% Inhibition at 100μM	% Inhibition at 100μM	IC_{50} Values (μM)
193	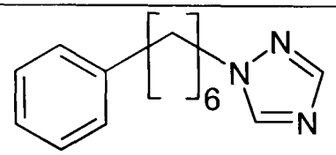	60.39 ± 0.57	89.56 ± 0.35	8.15 ± 0.85
194	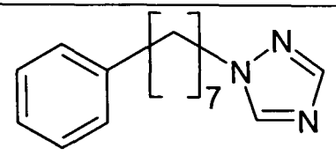	73.17 ± 1.23	93.88 ± 0.20	2.17 ± 0.01
195	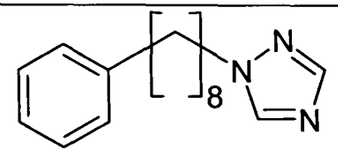	76.56 ± 0.03	94.38 ± 0.20	2.69 ± 0.01
196	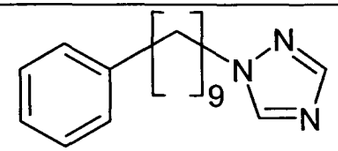	79.10 ± 0.24	94.51 ± 0.37	2.87 ± 0.17
197	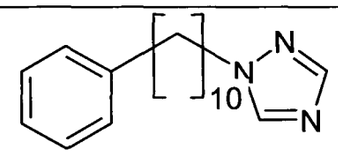	79.58 ± 1.48	91.68 ± 0.39	3.07 ± 0.12

Table 2.7b Results from preliminary screening and IC_{50} data of some unsubstituted phenyl alkyl-*1H*-[1,2,4,]triazole for 17α-hydroxylase/17,20-lyase activity continued.

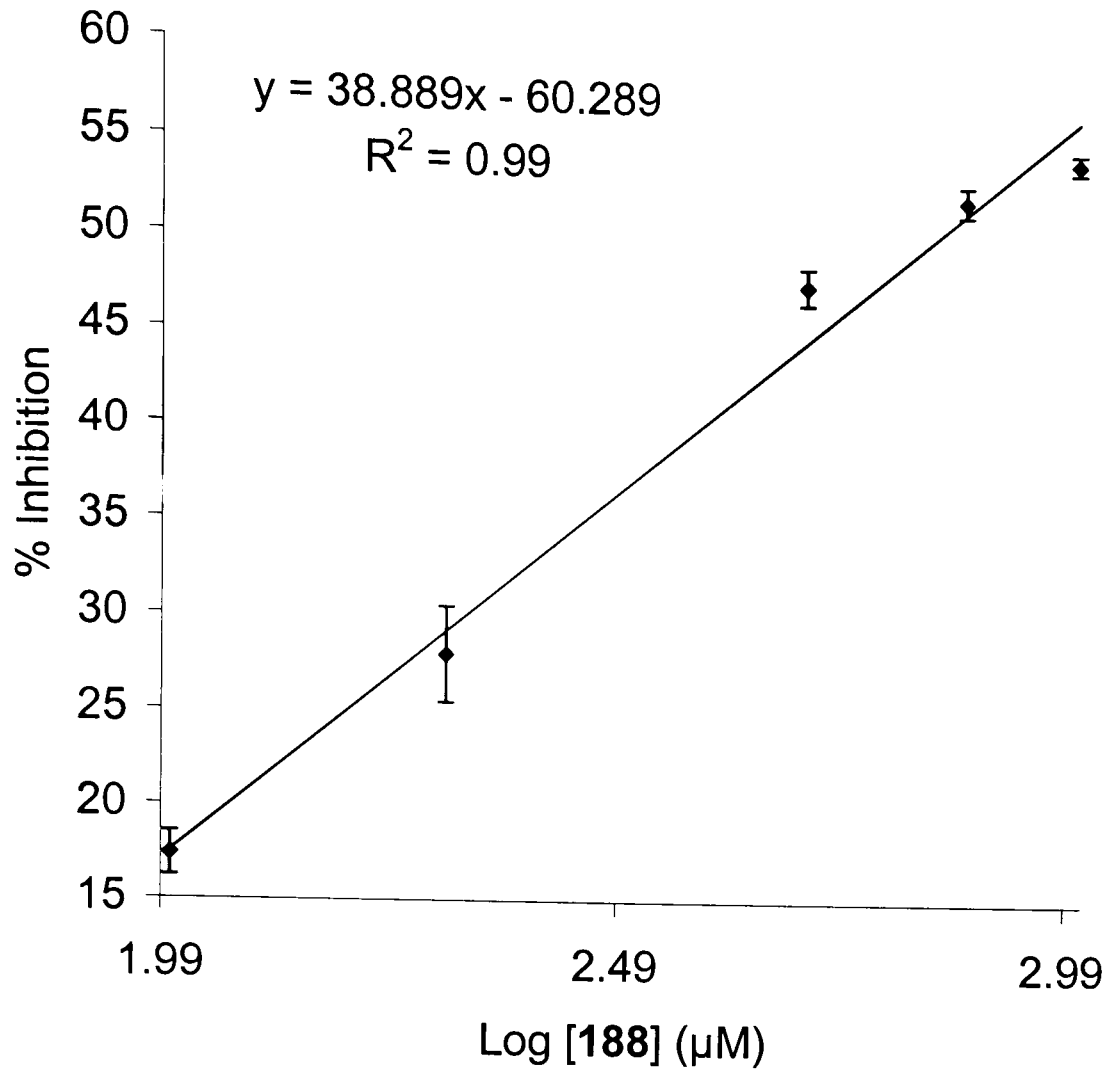

Figure 2.60 Plot of percentage inhibition versus log [**188**] for 1-benzyl-1*H*-[1,2,4]triazole (**188**) against 17,20-lyase.

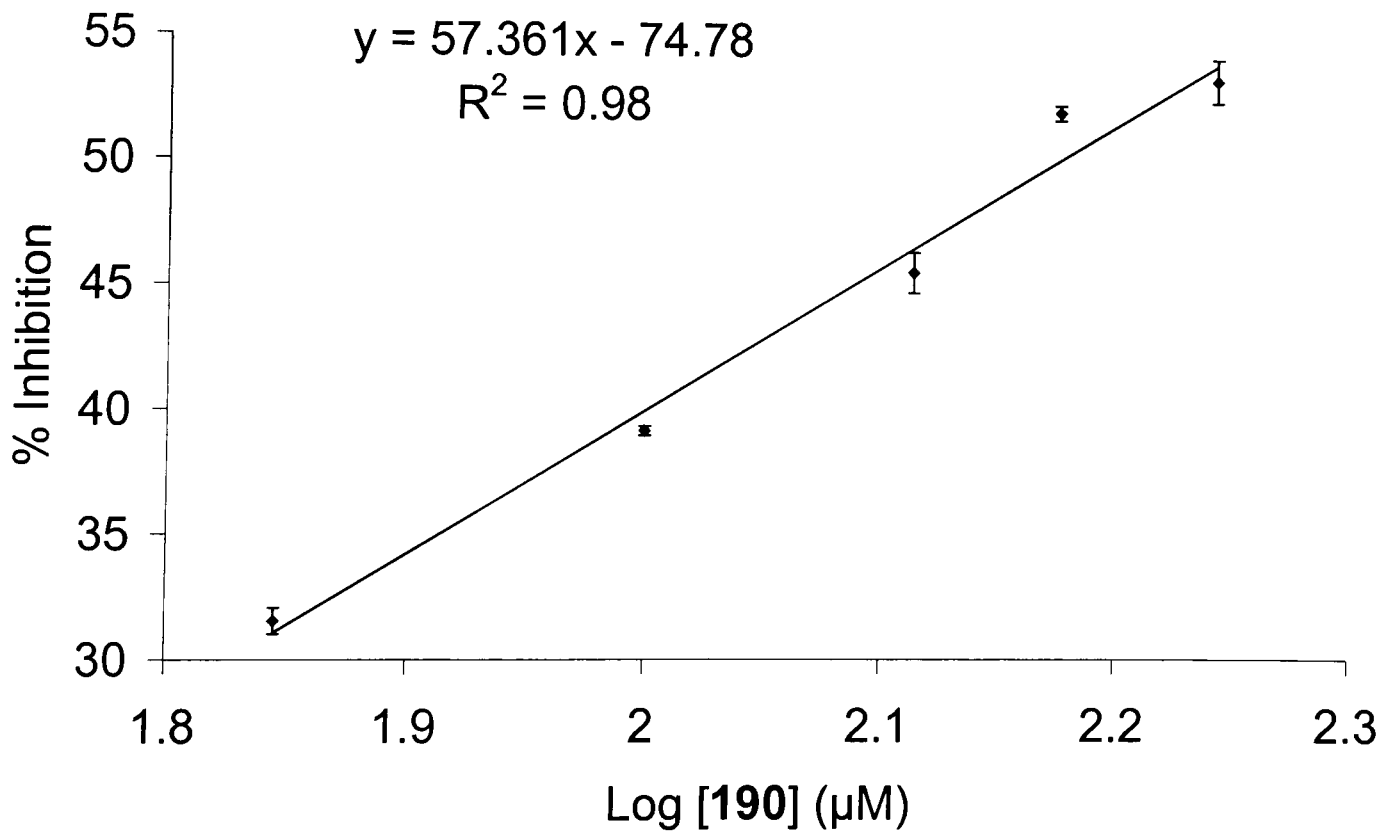

Figure 2.61 Plot of percentage inhibition versus log [**190**] for 1-(3-phenyl-propyl)-1*H*-[1,2,4]triazole (**190**) against 17,20-lyase.

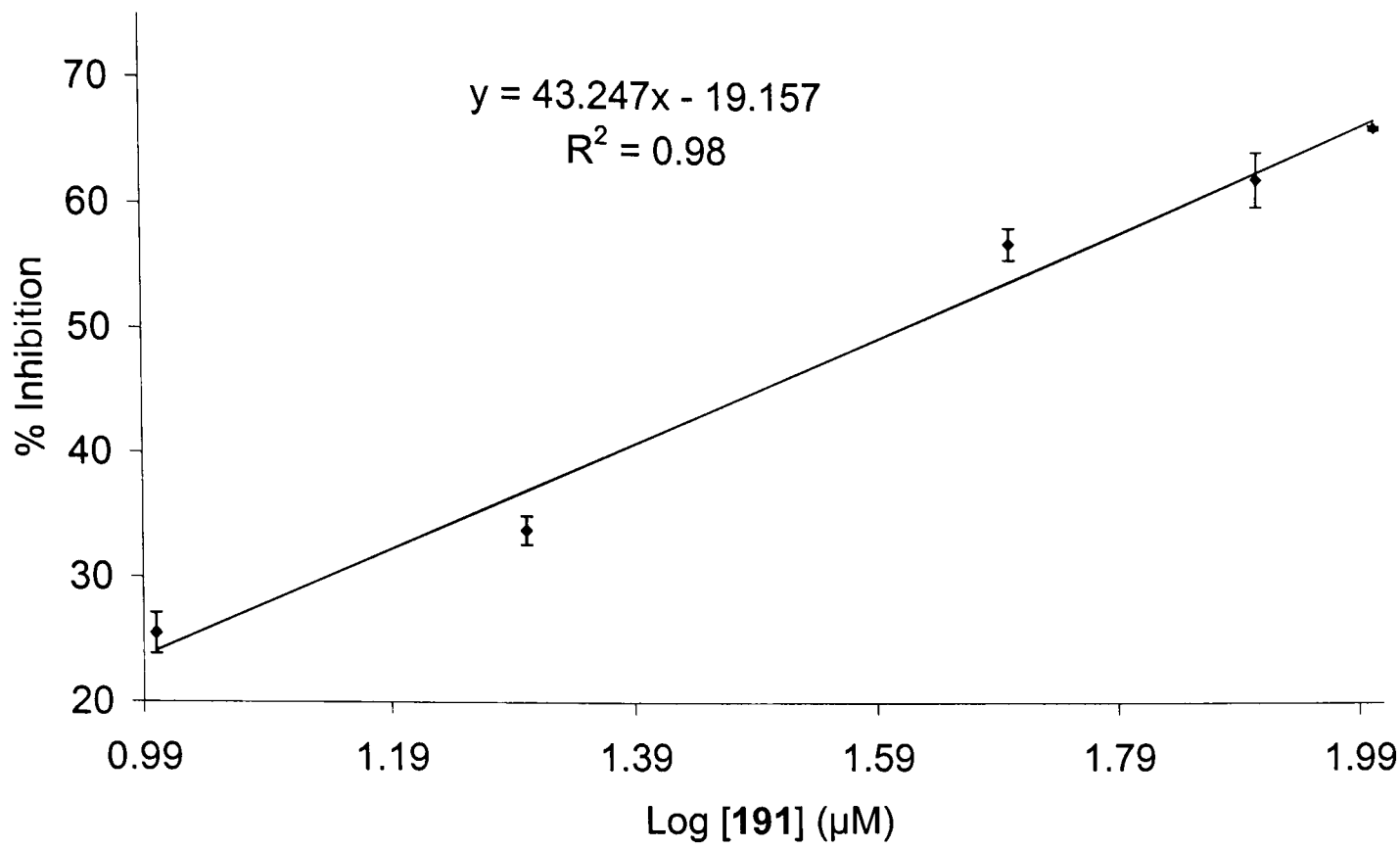

Figure 2.62 Plot of percentage inhibition versus log [**191**] for 1-(4-phenyl-butyl)-1*H*-[1,2,4]triazole (**191**) against 17,20-lyase.

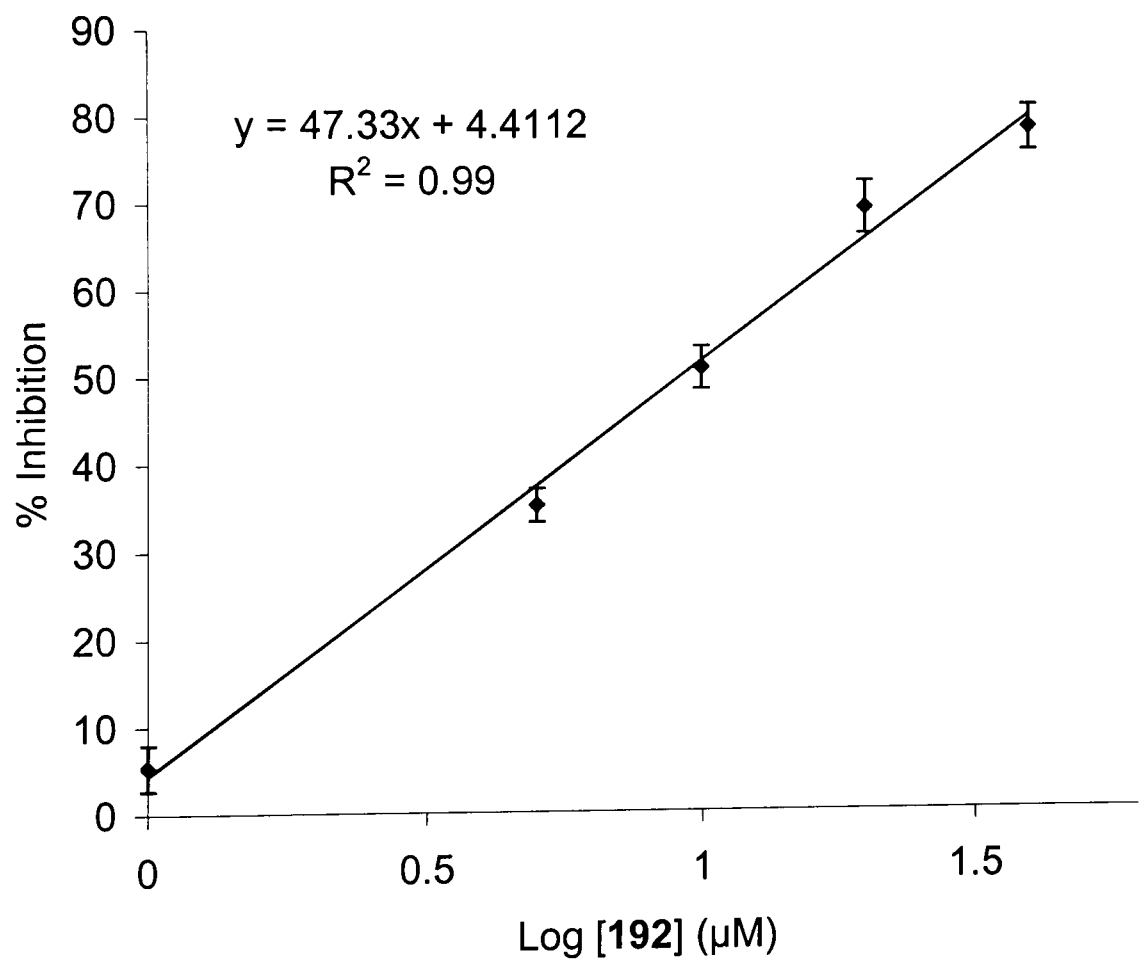

Figure 2.63 Plot of percentage inhibition versus log [**192**] for 1-(5-phenyl-pentyl)-1*H*-[1,2,4]triazole (**192**) against 17,20-lyase.

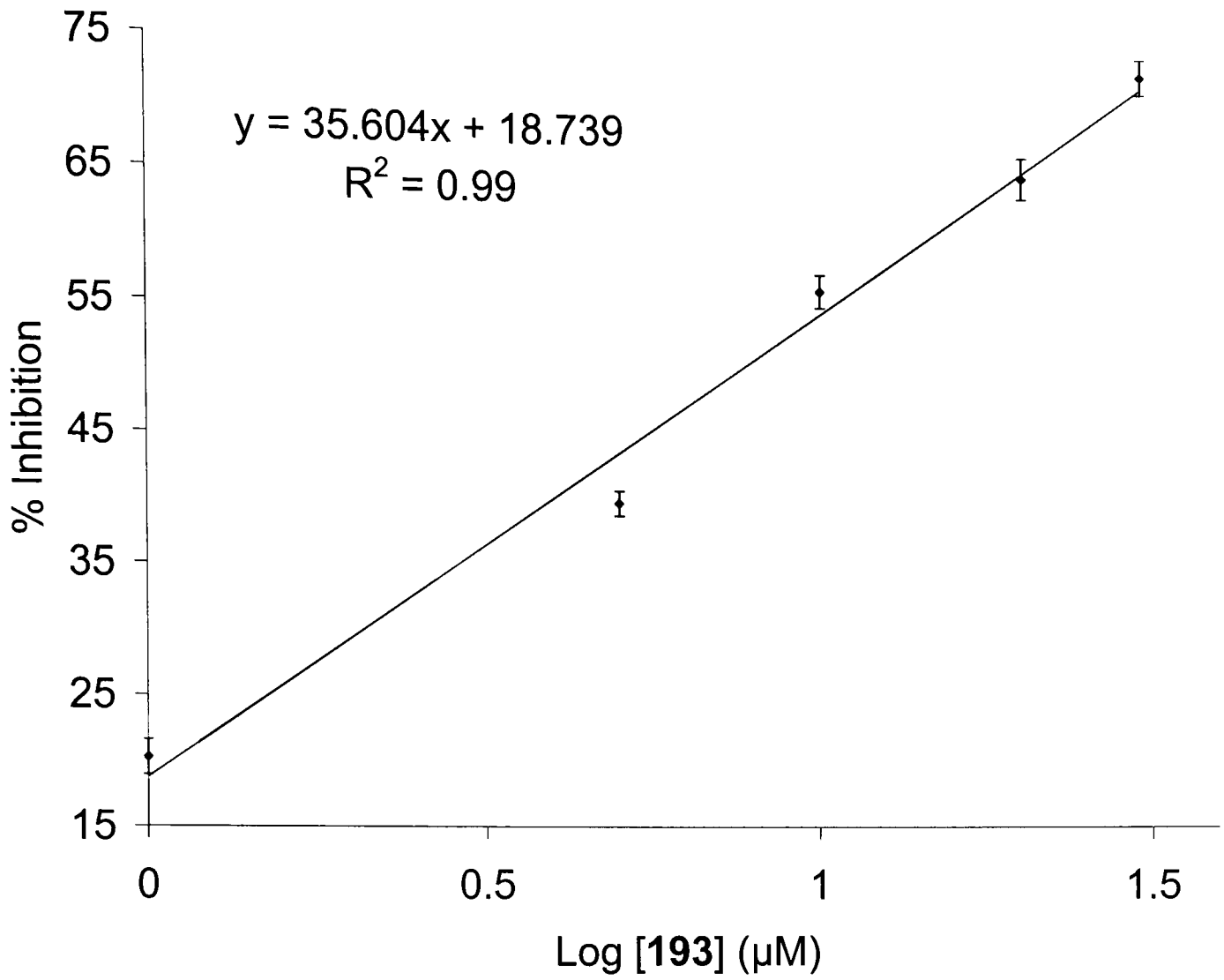

Figure 2.64 Plot of percentage inhibition versus log [**193**] for 1-(6-phenyl-hexyl)-1*H*-[1,2,4]triazole (**193**) against 17,20-lyase.

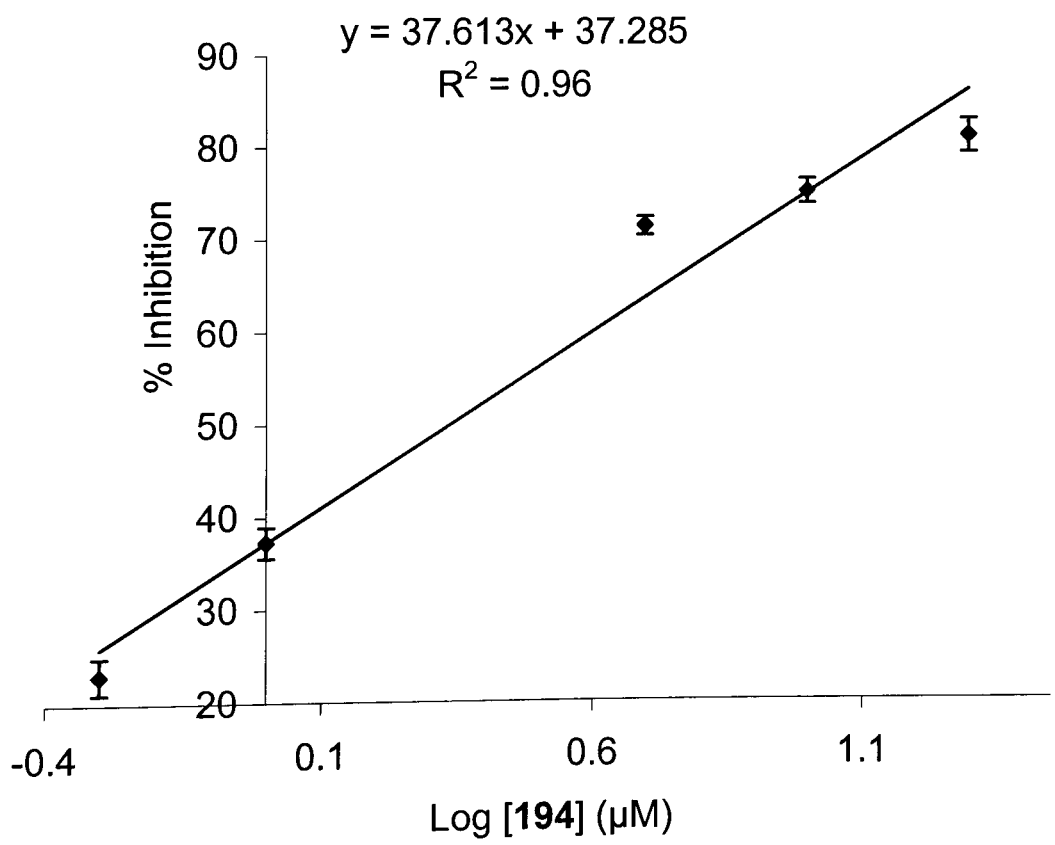

Figure 2.65 Plot of percentage inhibition versus log [**194**] for 1-(7-phenyl-heptyl)-1*H*-[1,2,4]triazole (**194**) against 17,20-lyase.

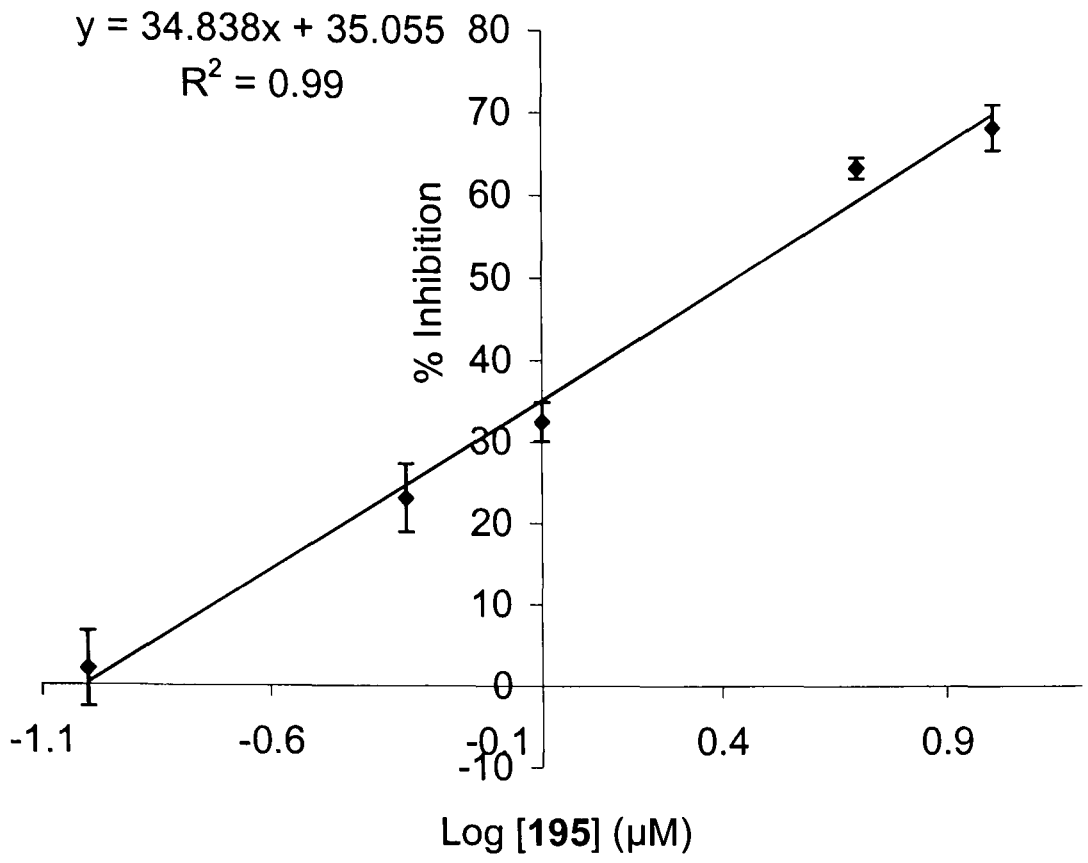

Figure 2.66 Plot of percentage inhibition versus log [**195**] for 1-(8-phenyl-octyl)-1*H*-[1,2,4]triazole (**195**) against 17,20-lyase.

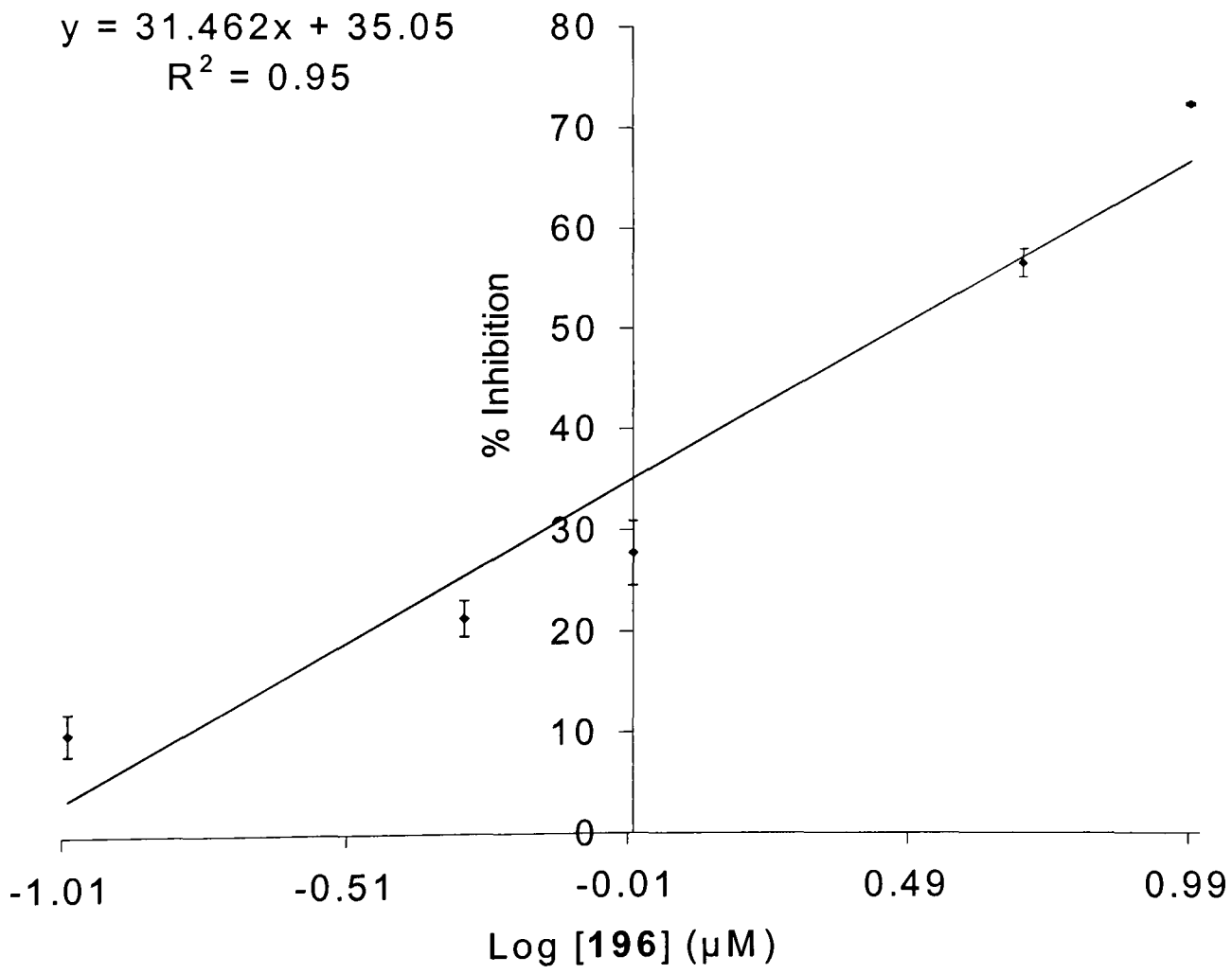

Figure 2.67 Plot of percentage inhibition versus log [**196**] for 1-(9-phenyl-nonyl)-1*H*-[1,2,4]triazole (**196**) against 17,20-lyase.

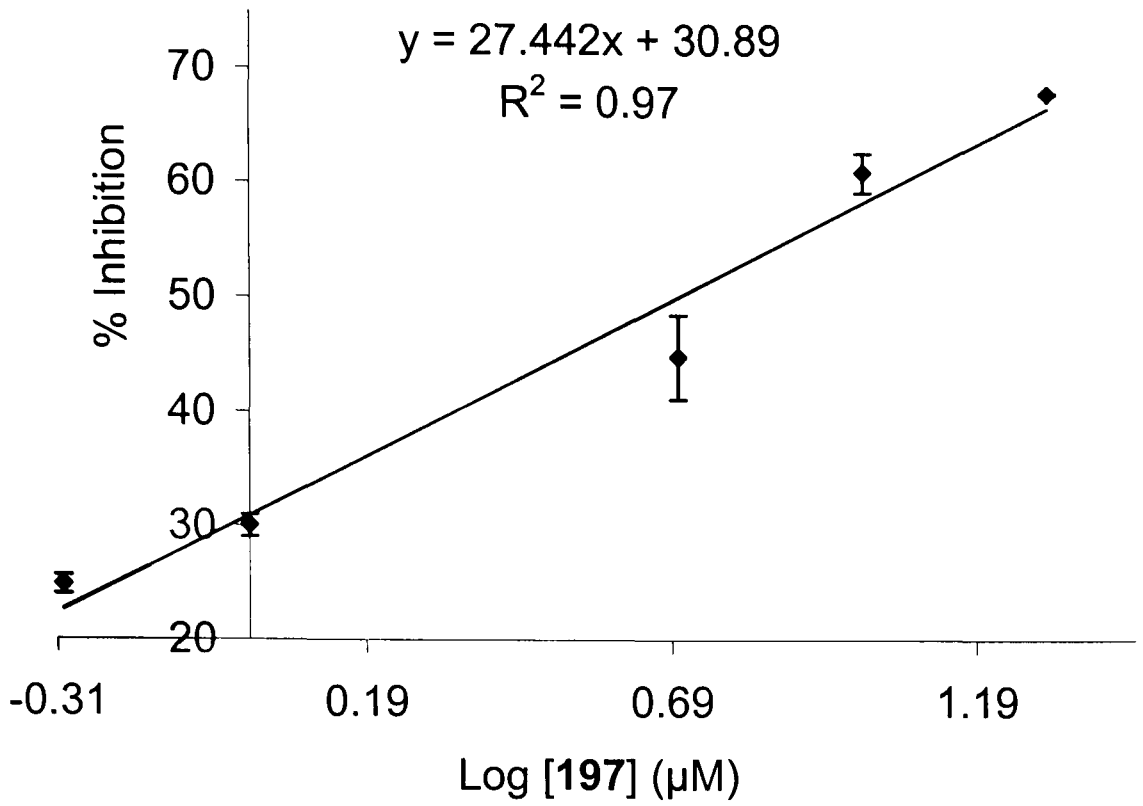

Figure 2.68 Plot of percentage inhibition versus log [**197**] for 1-(10-phenyl-decyl)-1*H*-[1,2,4]triazole (**197**) against 17,20-lyase.

2.32 Results of Substituted Phenyl Alkyl-*1H*-triazoles against $P450_{17\alpha}$

The results are shown in Tables 2.8 – 2.9

2.32.1 Discussion

The compounds were screened for both components; those showing good inhibition were tested for IC_{50} against the 17α-hydroxylase component (shown in table 2.9, Figures 2.69 – 2.72). All the compounds tested were shown to be much weaker than ketoconazole, including compound **194** which had shown equipotency when tested for 17,20-lyase inhibition.

Compound No.	Structure	17α-hydroxylase % Inhibition at 100μM	17,20-lyase % Inhibition at 100μM
198	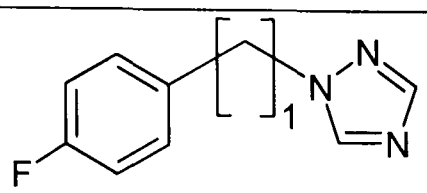	16.25 ± 1.13	31.46 ± 2.41
199	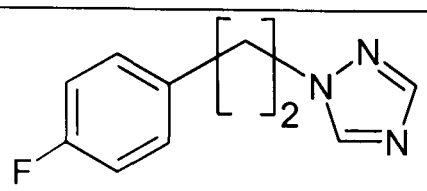	13.58 ± 0.58	25.21 ± 3.29
200	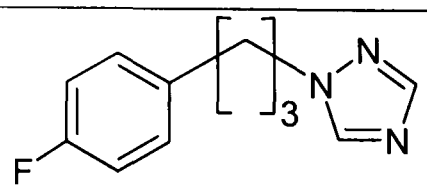	24.70 ± 0.54	45.90 ± 0.12
201	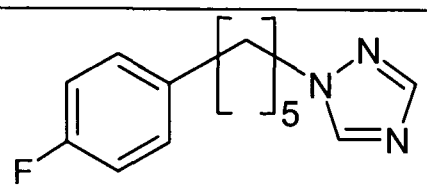	70.96 ± 0.53	81.82 ± 1.40
202	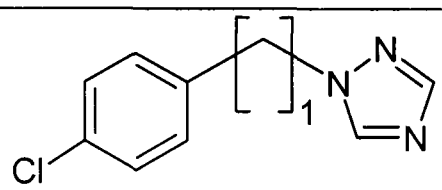	26.93 ± 2.90	45.70 ± 1.11
203	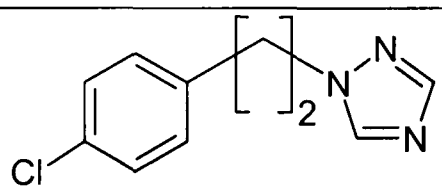	16.93 ± 0.31	31.72 ± 0.6
204	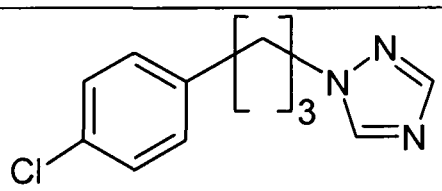	39.50 ± 0.61	74.38 ± 1.40
205	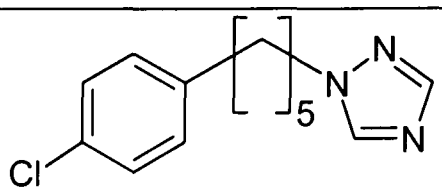	57.33 ± 4.98	84.41 ± 0.85

Table 2.8a Results from preliminary screening data of some *para*-substituted phenyl alkyl-*1H*-[1,2,4]triazoles for 17α-hydroxylase and 17,20-lyase activity.

Compound No.	Structure	17α-hydroxylase % Inhibition at 100μM	17,20-lyase % Inhibition at 100μM
206	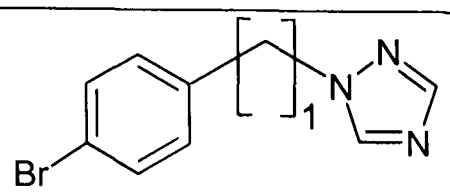	24.92 ± 1.06	50.65 ± 1.24
207	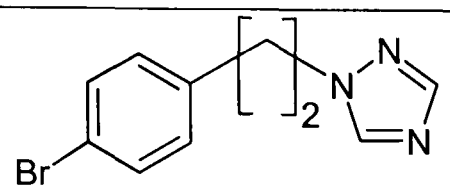	22.79 ± 0.80	39.42 ± 2.68
208	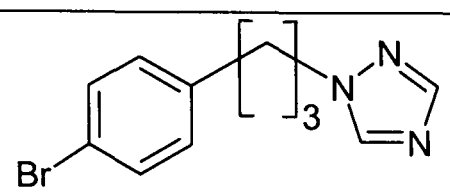	24.11 ± 1.91	50.87 ± 1.16
209	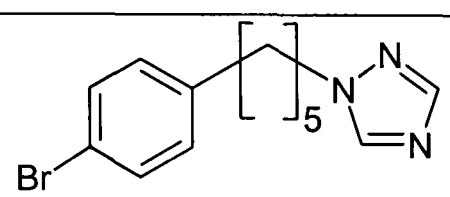	79.07 ± 0.35	85.97 ± 0.53
210	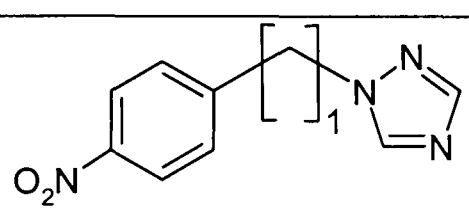	28.56 ± 0.76	47.67 ± 1.11

Table 2.8b Results from preliminary screening data of some *para*-substituted phenyl alkyl-*1H*-[1,2,4]triazoles for 17α-hydroxylase/17,20-lyase activity.

Compound No.	Structure	17α-hydroxylase IC_{50} Values (μM)
194	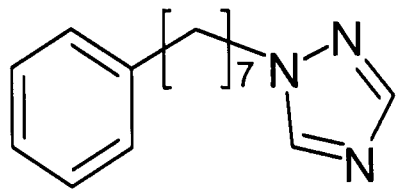	32.22 ± 2.64
201	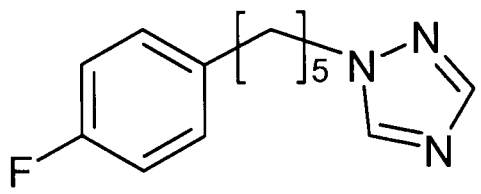	43.74 ± 3.51
205	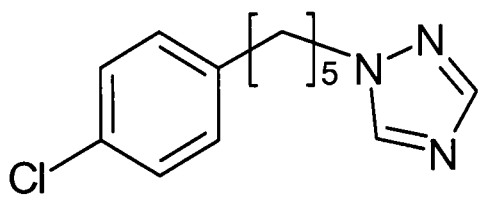	45.52 ± 6.01
209	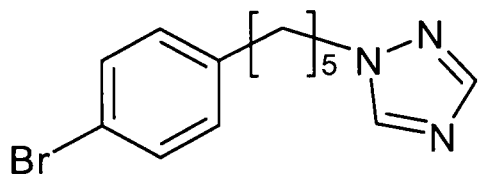	37.79 ± 3.65

Table 2.9 Results from preliminary screening and IC_{50} data of some phenyl alkyl-*1H*-[1,2,4]triazoles for 17α-hydroxylase activity.

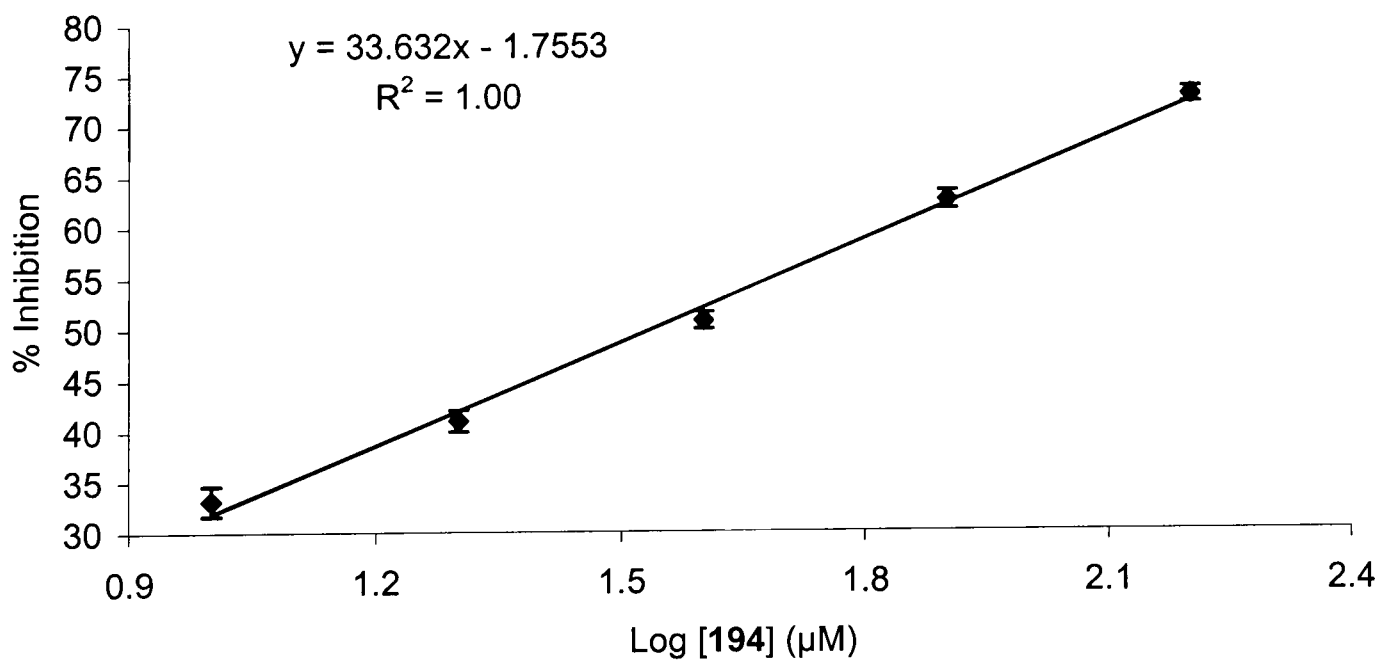

Figure 2.69 Plot of percentage inhibition versus log **[194]** for 1-(7-phenyl-heptyl)-1*H*-[1,2,4]triazole (**194**) against 17α-hydroxylase.

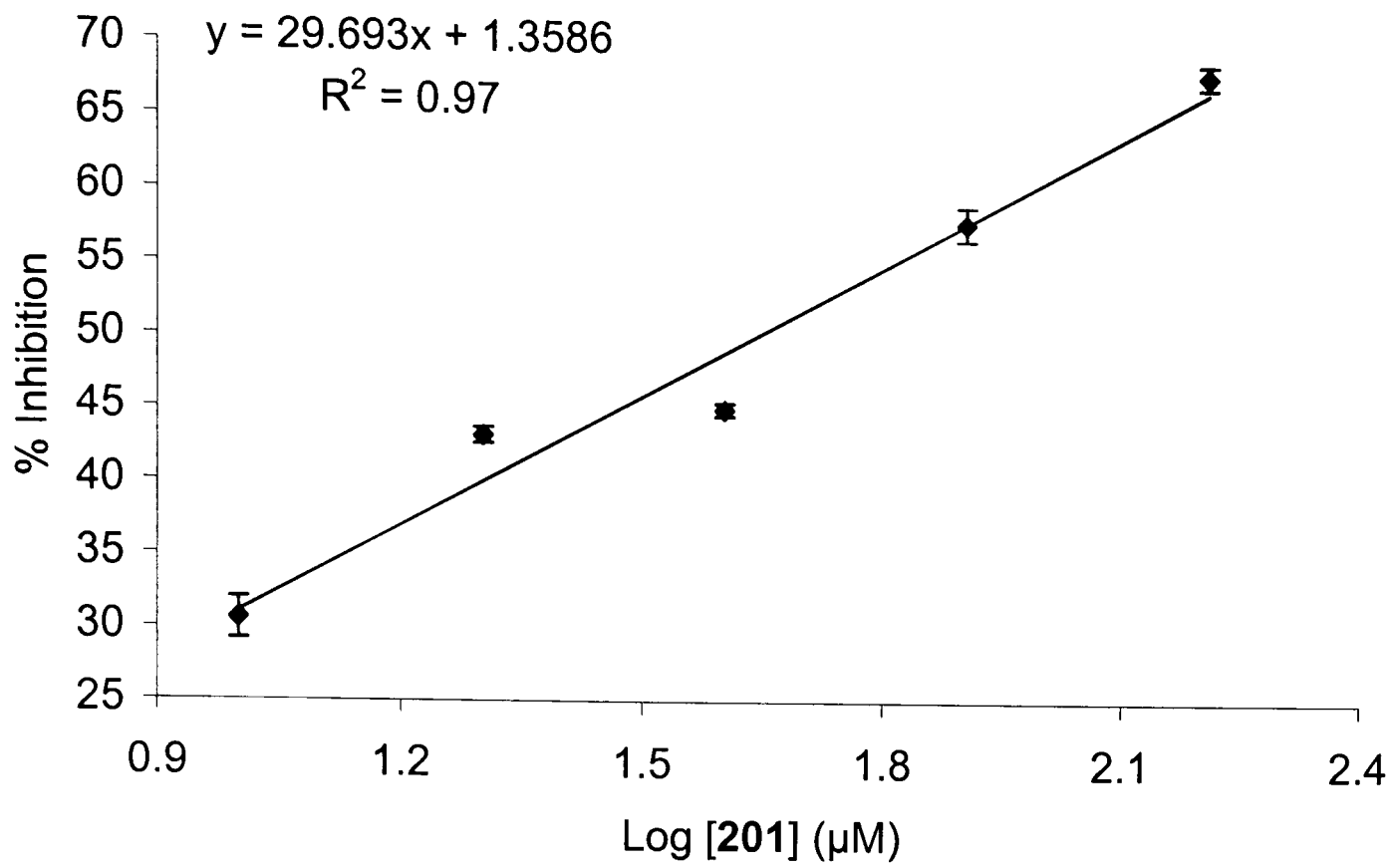

Figure 2.70 Plot of percentage inhibition versus log [**201**] for 1-[5-(4-fluoro-phenyl)-pentyl)-1*H*-[1,2,4]triazole (**201**) against 17α-hydroxylase.

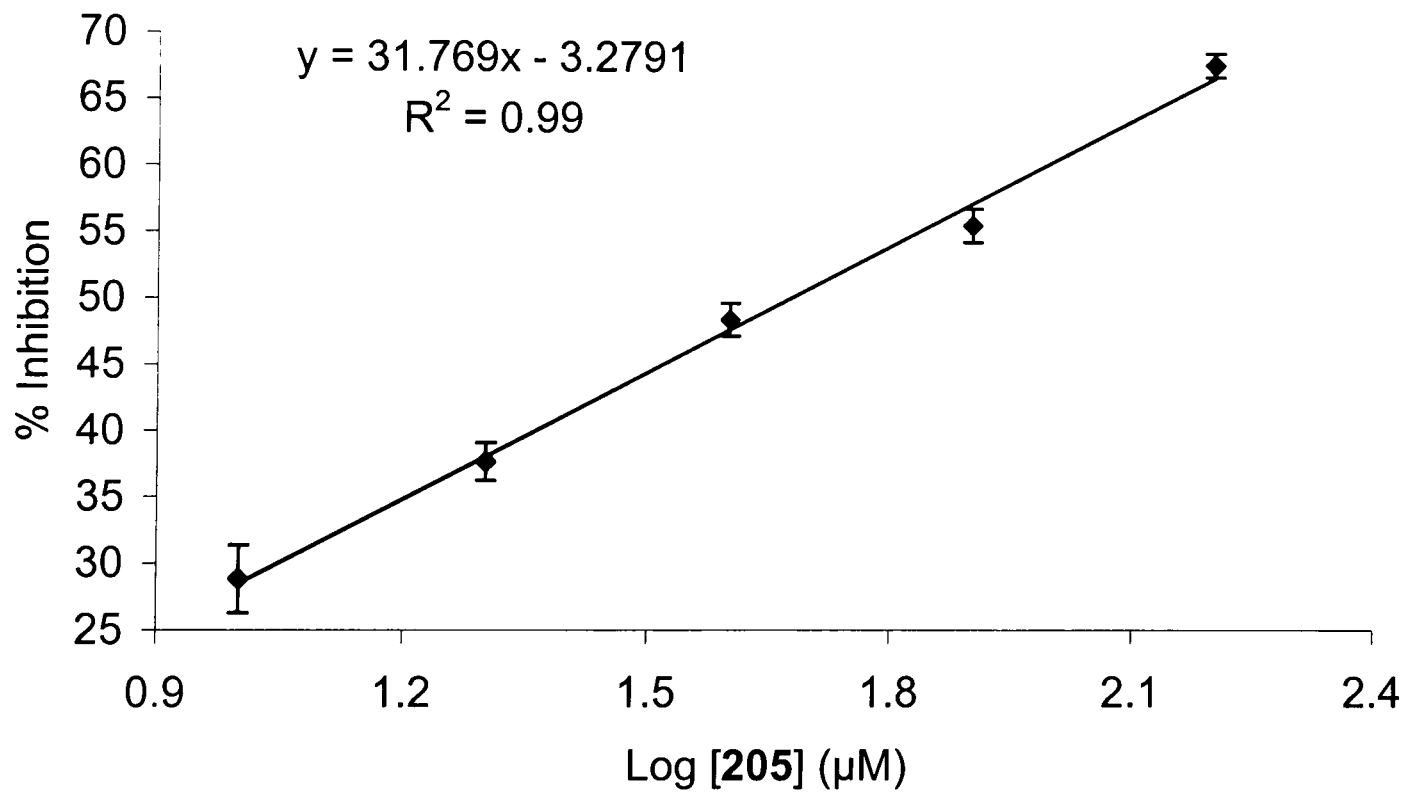

Figure 2.71 Plot of percentage inhibition versus log [**205**] for 1-[5-(4-chloro-phenyl)-pentyl)-1*H*-[1,2,4]triazole (**205**) against 17α-hydroxylase.

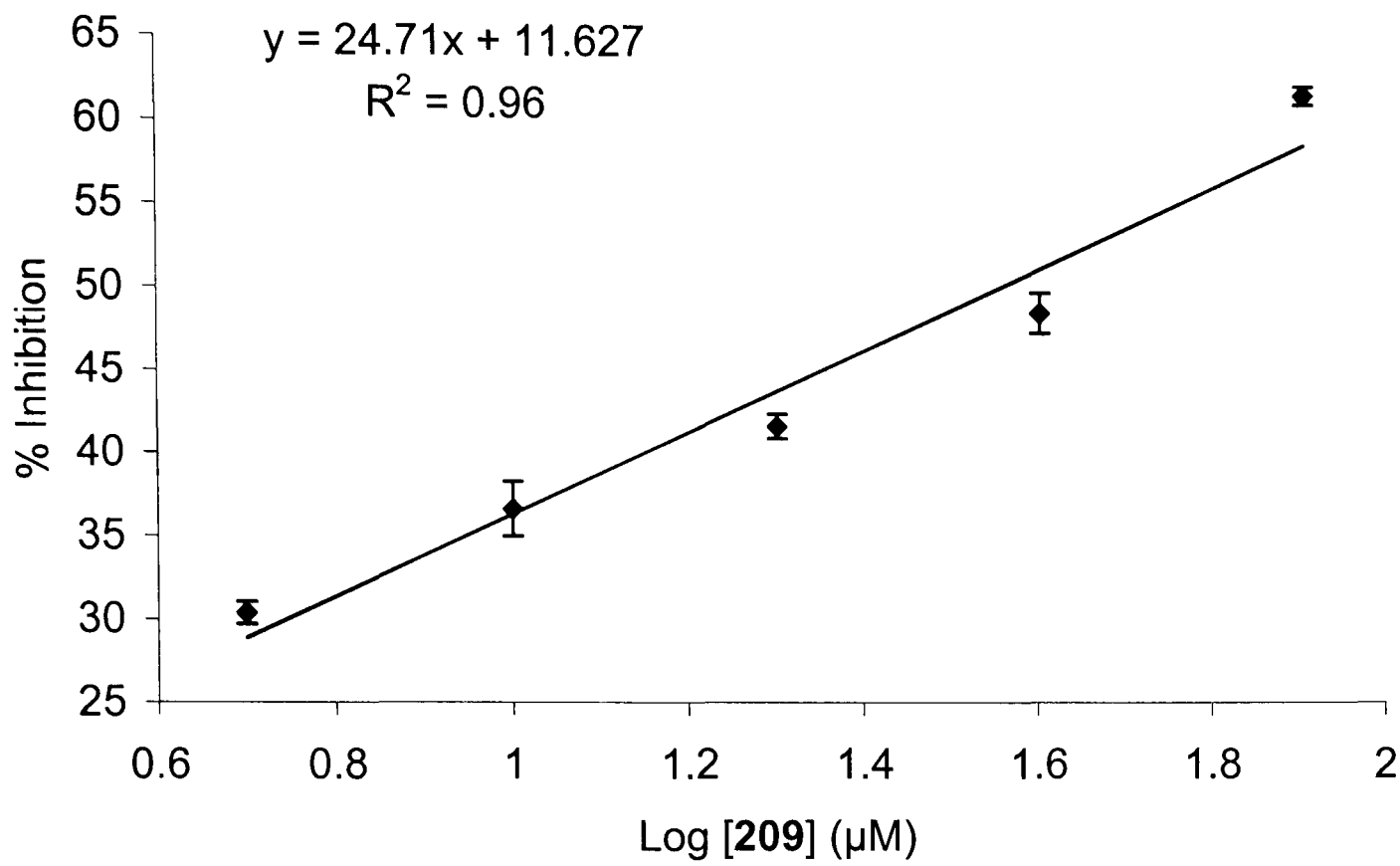

Figure 2.72 Plot of percentage inhibition versus log [**209**] for 1-[5-(4-bromo-phenyl)-pentyl)-1*H*-[1,2,4]triazole (**209**) against 17α-hydroxylase.

2.33 Results of Phenylamine Derivatives against $P450_{17\alpha}$

The results are shown in Tables 2.10a – 2.10c.

2.33.1 Discussion

The compounds were screened against both components and were found to be much weaker than ketoconazole.

Compound No.	Structure	17α-hydroxylase	17,20-lyase
		% Inhibition	% Inhibition
211	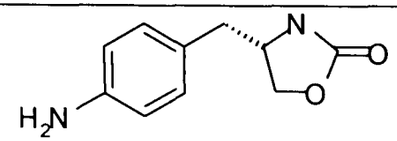	3.80 ± 0.91[b]	15.06 ± 2.59[b]
212	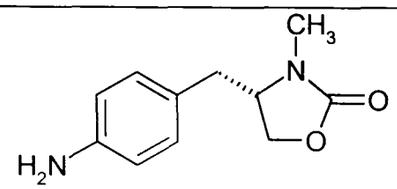	8.18 ± 2.51[b]	16.14 ± 1.97[b]
213	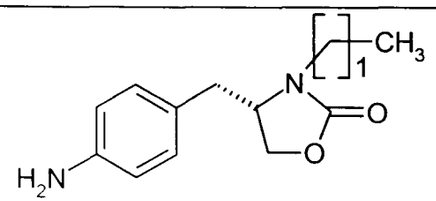	4.82 ± 1.60[a] 16.35 ± 3.32[b]	30.00 ± 1.44[b]
214	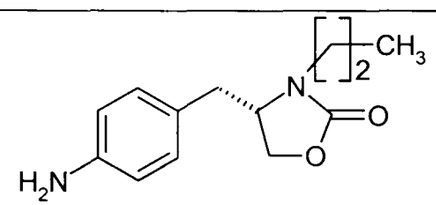	4.87 ± 4.11[b]	32.94 ± 4.44[b]

Table 2.10a Results from preliminary screening and IC_{50} data of some *para*-substituted 4-*(S)*-(4-amino-benzyl)-oxazolidin-2-one for 17α-hydroxylase/17,20-lyase activity. (Where [a] [I] = 500μM, [b] [I] = 1000μM).

Compound No.	Structure	17α-hydroxylase	17,20-lyase
		% Inhibition	% Inhibition
215	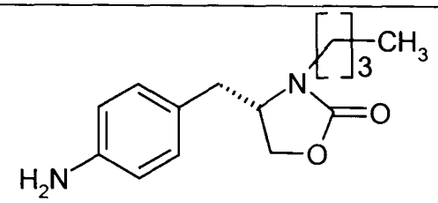	12.83 ± 0.01[b]	31.63 ± 3.49[b]
216	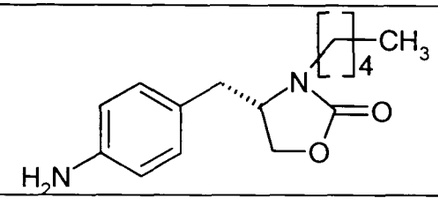	5.93 ± 1.45[b]	24.12 ± 1.63[b]
217	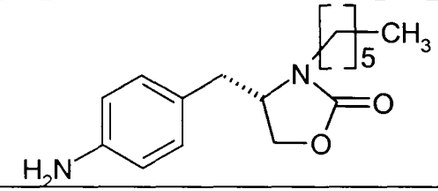	15.72 ± 3.87[b]	24.27 ± 1.36[b]
218	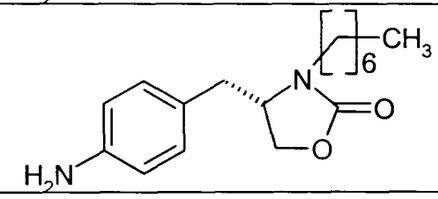	12.76 ± 7.40[b]	7.84 ± 0.79[a]

Table 2.10b Results from preliminary screening and IC_{50} data of some *para*-substituted 4-*(S)*-(4-amino-benzyl)-oxazolidin-2-one for 17α-hydroxylase/17,20-lyase activity. (Where [a] [I] = 500μM, [b] [I] = 1000μM).

Compound No.	Structure	17α-hydroxylase	17,20-lyase
		% Inhibition	% Inhibition
219	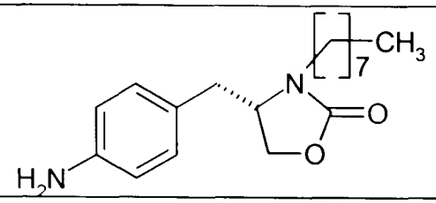	10.24 ± 7.28[b]	13.26 ± 1.04[a] 40.97 ± 0.66[b]
220	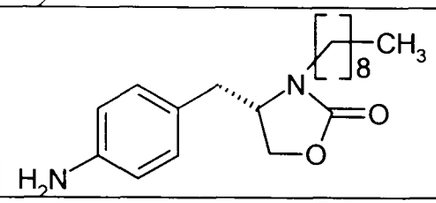	11.30 ± 0.27[b]	9.80 ± 0.14[a] 39.73 ± 0.50[b]
221	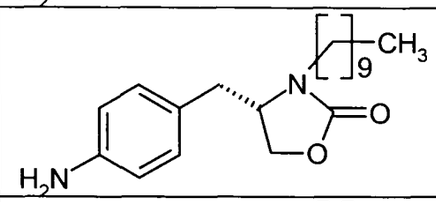	14.98 ± 0.54[b]	0[b]
222	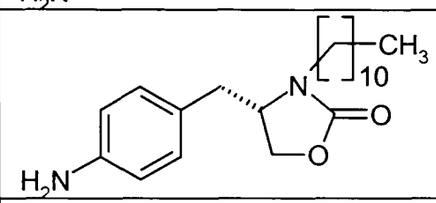	7.11 ± 1.15[b]	0[b]
223	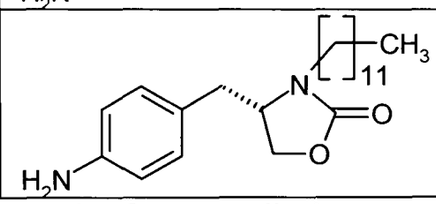	0[b]	15.13 ± 4.64[b]

Table 2.10c Results from preliminary screening and IC_{50} data of some *para*-substituted 4-*(S)*-(4-amino-benzyl)-oxazolidin-2-one for 17α-hydroxylase/17,20-lyase activity. (Where [a] [I] = 500μM, [b] [I] = 1000μM).

2.34 Protein Assay for 17α-Hydroxylase

Due to the number of assays carried out, it was necessary to prepare a new batch of enzymes for testing. This was carried out as previously described in Section 2.5.

The protein concentration of the testicular microsomes was determined as previously discussed in Section 2.6. The protein concentration was found to be 10.47mg/mL.

2.35 Protein-dependency Assay for 17α-Hydroxylase

The protein-dependency assay was determined as previously mentioned in Section 2.8. The reaction was found to be linear for concentrations below 0.21mg/mL.

2.36 Time Validation Assay for 17α-Hydroxylase

The time validation assay was determined as previously mentioned in Section 2.9. The reaction was found to be linear for time intervals up to 45min.

2.37 Determination of K_m for 17α-Hydroxylase

The determination of the Michaelis constant was carried out as previously mentioned in Section 2.10, The K_m values obtained from the graphical methods are summarised in Table 2.11, and the average K_m was found to be 0.87 ± 0.04μM

Plot	K_m (μM)
Michalis Menten plot	0.34 ± 0.015
Lineweaver-Burk plot	1.46 ± 0.34
Hanes-Woolf plot	1.08 ± 0.99
Eadie-Hofstee plot	1.06 ± 0.12
Direct linear plot	0.37 ± 0.03
Average K_m	0.87 ± 0.04

Table 2.11 Summary of K_m plots for 17α-hydroxylase.

2.38 Preliminary Screening of Synthesised Compounds for 17α-Hydroxylase Inhibitory Activity

The preliminary screening assay was carried out as previously mentioned in Section 2.13, except that the substrate concentration used was 3μM (15μL), inhibitor (10μL), NADPH-generating system (25μL), protein (0.10mg/mL, 5μL) and buffer (445μL). The results are shown in Tables 2.13a – 2.13e.

2.39 Determination of IC_{50} for 17α-Hydroxylase

The IC_{50} was determined as previously mentioned in Section 2.14 except the concentrations and volumes used were as mentioned in Section 2.38. The results and plots are shown in Tables 2.13a – 2.13e and Figures 2.73 – 2.99.

2.40 Protein Assay for 17,20-Lyase

Due to the number of assays carried out, it was necessary to prepare a new batch of enzymes for testing. This was carried out as previously described in Section 2.5.

The protein concentration of the testicular microsomes was determined as previously discussed in Section 2.19. The protein concentration was found to be 18.93mg/mL.

2.41 Protein-dependency Assay for 17,20-Lyase

The protein-dependency assay was determined as previously mentioned in Section 2.21. The reaction was found to be linear for concentrations below 0.379mg/mL.

2.42 Time Validation Assay for 17,20-Lyase

The time validation assay was determined as previously mentioned in Section 2.22. The reaction was found to be linear for time intervals prior to 50min.

2.43 Determination of K_m for 17,20-Lyase

The determination of the Michaelis constant was carried out as previously mentioned in Section 2.23, The K_m values obtained from the graphical methods are summarised in Table 2.12, and the average K_m was found to be 1.66 ± 0.10μM

Plot	K_m (μM)
Michalis Menten plot	2.86 ± 0.18
Lineweaver-Burk plot	1.87 ± 0.09
Hanes-Woolf plot	1.61 ± 0.07
Eadie-Hofstee plot	0.40 ± 0.01
Direct linear plot	1.58 ± 0.11
Average K_m	1.66 ± 0.10

Table 2.12 Summary of K_m plots for 17,20-lyase.

2.44 Preliminary Screening of Synthesised Compounds for 17,20-Lyase Inhibitory Activity

The preliminary screening assay was carried out as previously mentioned in Section 2.25, except that the substrate concentration used was 5μM (10μL), inhibitor (4μL), NADPH-generating system (10μL), protein (0.19mg/mL, 2μL) and buffer (174μL). The results are shown in Tables 2.13a – 2.13e.

2.45 Determination of IC_{50} for 17,20-lyase

The IC_{50} was determined as previously mentioned in Section 2.26 except the concentrations and volumes used were as mentioned in Section 2.44. The results and plots are shown in Tables 2.13a – 2.13e and Figures 2.100 – 2.126.

2.46 Results of Substituted Benzyl-*1H*-imidazoles against $P450_{17\alpha}$

The results are shown in Tables 2.13a – 2.13e

2.46.1 Discussion

In general most compounds were poorer inhibitors in comparison to ketoconazole for both components, except compounds **234** and **241** which showed equipotency to ketoconazole for 17,20-lyase component.

Compound No.	Structure	17α-hydroxylase		17,20-lyase	
		% Inhibition at 10μM	IC_{50} Values (μM)	% Inhibition at 10μM	IC_{50} Values (μM)
165	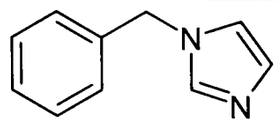	13.95 ± 2.15	214.58 ± 19.67	31.81 ± 0.77	39.06 ± 1.22
224	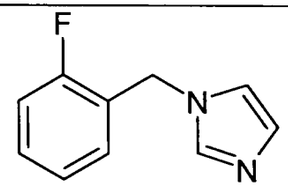	13.56 ± 0.64	139.51 ± 13.43	37.66 ± 0.89	30.26 ± 1.90
225	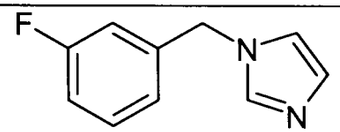	11.97 ± 1.35	101.42 ± 6.16	32.90 ± 0.79	30.02 ± 1.43
175	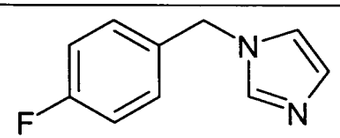	12.76 ± 1.87	99.37 ± 8.82	38.00 ± 0.98	18.44 ± 0.17
226	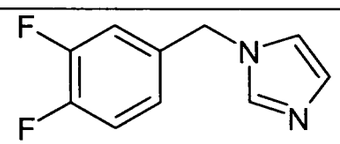	18.64 ± 0.51	70.66 ± 6.72	44.99 ± 0.92	9.60 ± 0.14
227	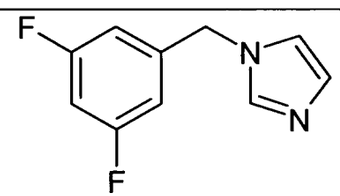	23.26 ± 0.41	83.10 ± 7.05	41.94 ± 0.68	11.80 ± 0.41

Table 2.13a Results from preliminary screening and IC_{50} data of some substituted benzyl-*1H*-imidazoles for 17α-hydroxylase/17,20-lyase activity.

Compound No.	Structure	17α-hydroxylase		17,20-lyase	
		% Inhibition at 10μM	IC_{50} Values (μM)	% Inhibition at 10μM	IC_{50} Values (μM)
228	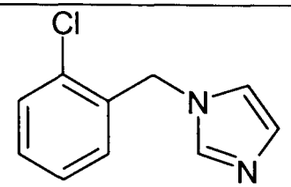	33.21 ± 0.69	96.71 ± 13.20	52.94 ± 0.39	8.27 ± 0.80
229	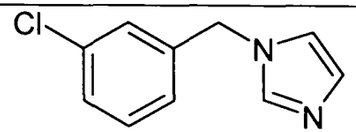	26.54 ± 2.25	43.08 ± 2.21	44.03 ± 0.88	10.61 ± 0.39
180	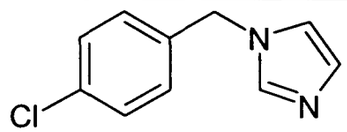	23.81 ± 0.54	31.63 ± 3.86	56.41 ± 0.46	8.98 ± 0.57
230	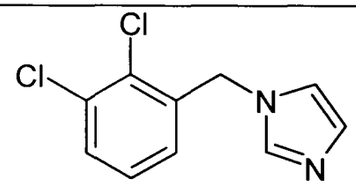	39.19 ± 0.46	13.80 ± 1.15	58.69 ± 1.13	4.28 ± 0.27
231	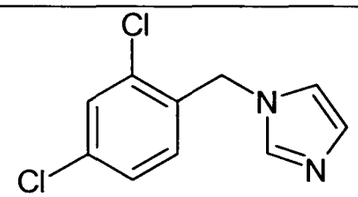	39.66 ± 0.59	21.99 ± 0.96	62.64 ± 0.94	3.90 ± 0.18

Table 2.13b Results from preliminary screening and IC_{50} data of some substituted benzyl-*1H*-imidazoles for 17α-hydroxylase/17,20-lyase activity.

Compound No.	Structure	17α-hydroxylase		17,20-lyase	
		% Inhibition at 10μM	IC_{50} Values (μM)	% Inhibition at 10μM	IC_{50} Values (μM)
232	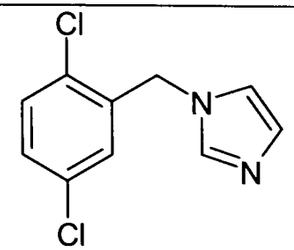	30.94 ± 1.30	19.95 ± 1.88	57.31 ± 0.07	4.50 ± 0.20
233	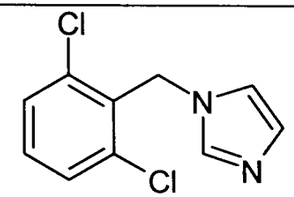	24.68 ± 0.72	32.27 ± 1.27	54.17 ± 0.22	13.25 ± 0.74
234	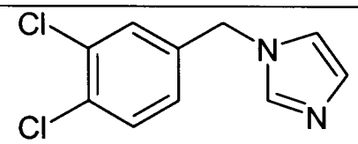	39.29 ± 0.96	12.22 ± 0.88	60.68 ± 1.04	2.07 ± 0.07
235	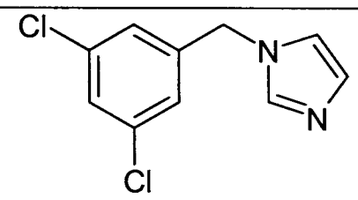	35.44 ± 1.28	22.56 ± 0.34	56.42 ± 1.31	3.34 ± 0.11
236	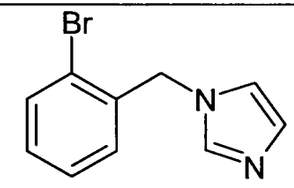	29.70 ± 0.88	15.45 ± 0.98	57.32 ± 0.50	5.17 ± 0.57

Table 2.13c Results from preliminary screening and IC_{50} data of some substituted benzyl-*1H*-imidazoles for 17α-hydroxylase/17,20-lyase activity.

Compound No.	Structure	17α-hydroxylase		17,20-lyase	
		% Inhibition at 10μM	IC_{50} Values (μM)	% Inhibition at 10μM	IC_{50} Values (μM)
237	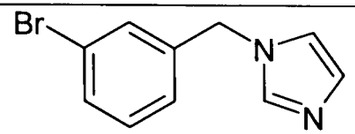	26.46 ± 1.83	21.25 ± 1.71	54.42 ± 0.47	6.29 ± 0.53
184	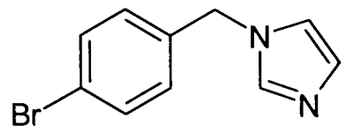	41.58 ± 1.28	23.47 ± 1.90	59.68 ± 0.46	3.77 ± 0.28
238	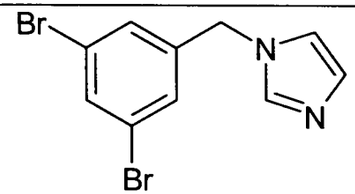	36.29 ± 0.34	23.62 ± 2.00	59.00 ± 0.90	3.16 ± 0.11
239	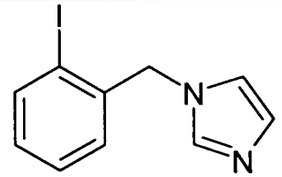	34.56 ± 0.37	22.67 ± 1.18	59.86 ± 1.14	2.96 ± 0.26
240	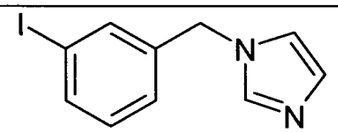	37.38 ± 1.42	16.56 ± 1.05	60.75 ± 0.28	3.51 ± 0.23
241	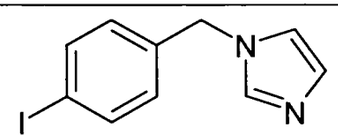	47.72 ± 0.56	10.06 ± 0.96	63.74 ± 0.26	1.58 ± 0.17

Table 2.13d Results from preliminary screening and IC_{50} data of some substituted benzyl-*1H*-imidazoles for 17α-hydroxylase/17,20-lyase activity.

Compound No.	Structure	17α-hydroxylase		17,20-lyase	
		% Inhibition at 10μM	IC_{50} Values (μM)	% Inhibition at 10μM	IC_{50} Values (μM)
242	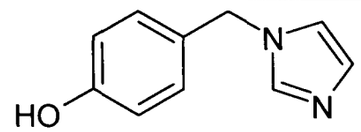	16.30 ± 1.90	72.05 ± 3.95	43.25 ± 0.56	8.22 ± 0.97
243	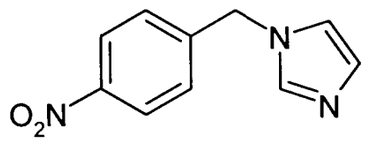	27.39 ± 1.33	25.38 ± 1.65	57.30 ± 0.99	7.17 ± 0.13
244	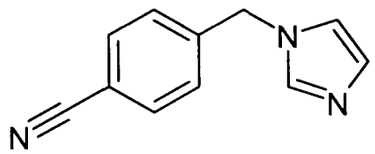	29.07 ± 0.50	40.26 ± 3.49	54.64 ± 0.20	7.67 ± 0.05
245	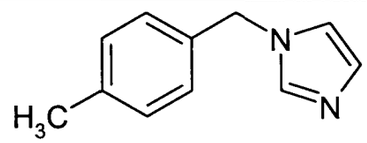	24.20 ± 0.54	50.56 ± 8.01	55.43 ± 1.03	8.81 ± 0.43
246	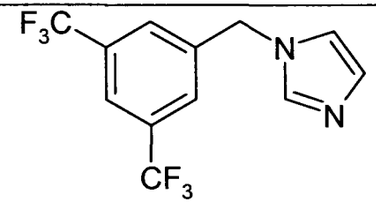	5.90 ± 1.33	244.85 ± 24.45	25.39 ± 1.16	19.46 ± 0.75

Table 2.13e Results from preliminary screening and IC_{50} data of some substituted benzyl-*1H*-imidazoles for 17α-hydroxylase/17,20-lyase activity.

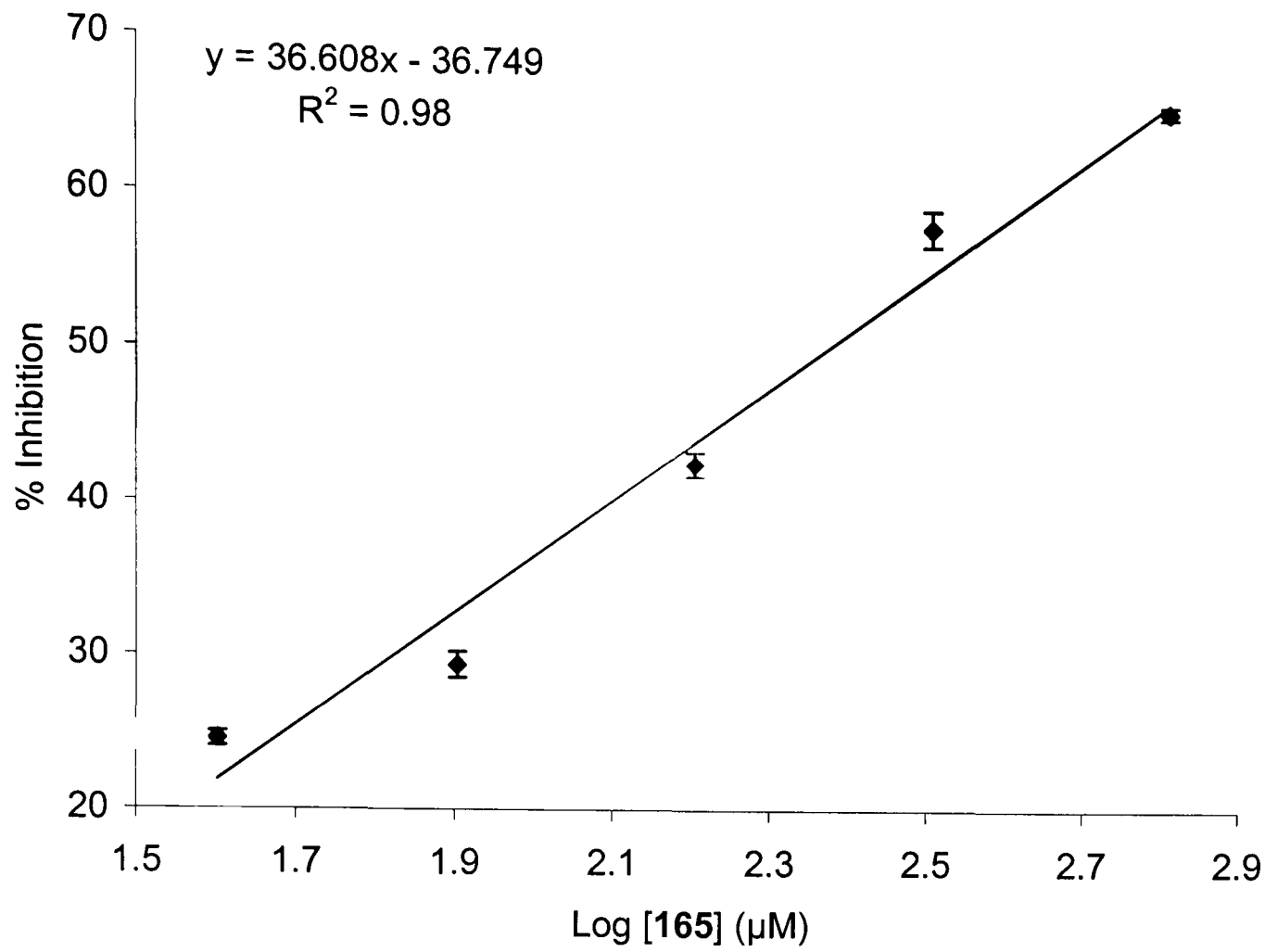

Figure 2.73 Plot of percentage inhibition versus log [**165**] for 1-benzyl-1*H*-imidazole (**165**) against 17α-hydroxylase.

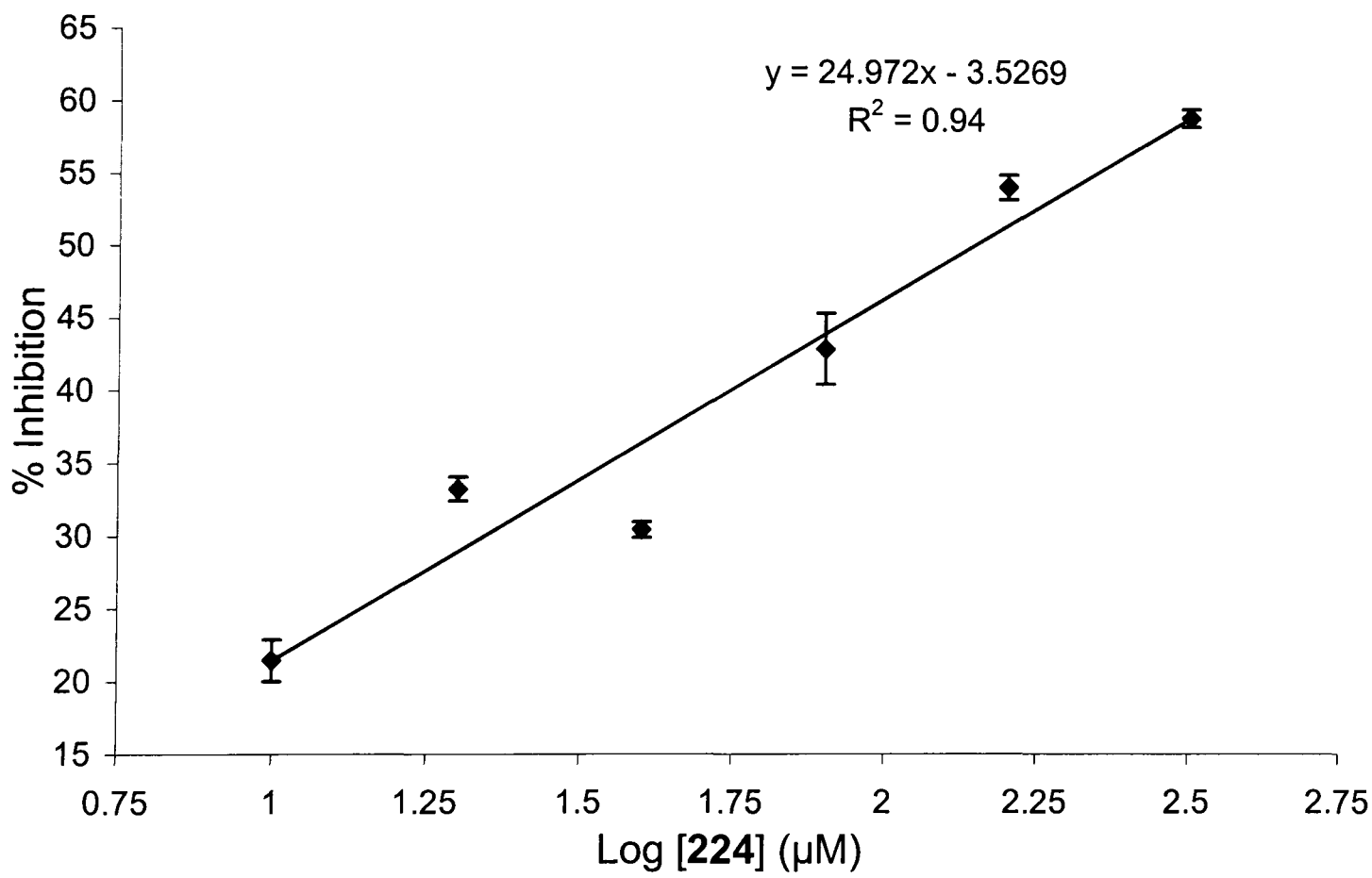

Figure 2.74 Plot of percentage inhibition versus log [**224**] for 1-(2-fluoro-benzyl)-1*H*-imidazole (**224**) against 17α-hydroxylase.

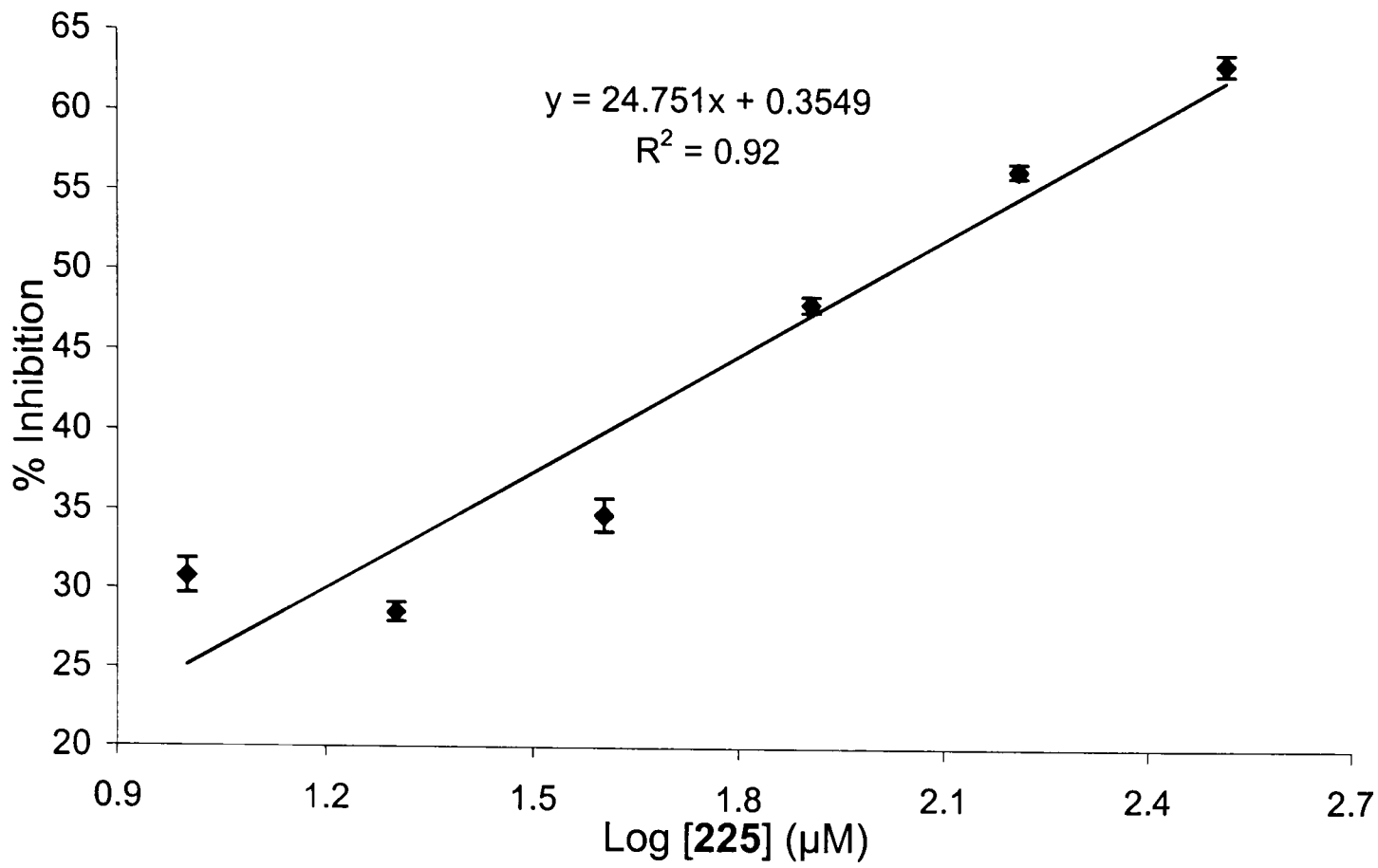

Figure 2.75 Plot of percentage inhibition versus log [**225**] for 1-(3-fluoro-benzyl)-1*H*-imidazole (**225**) against 17α-hydroxylase.

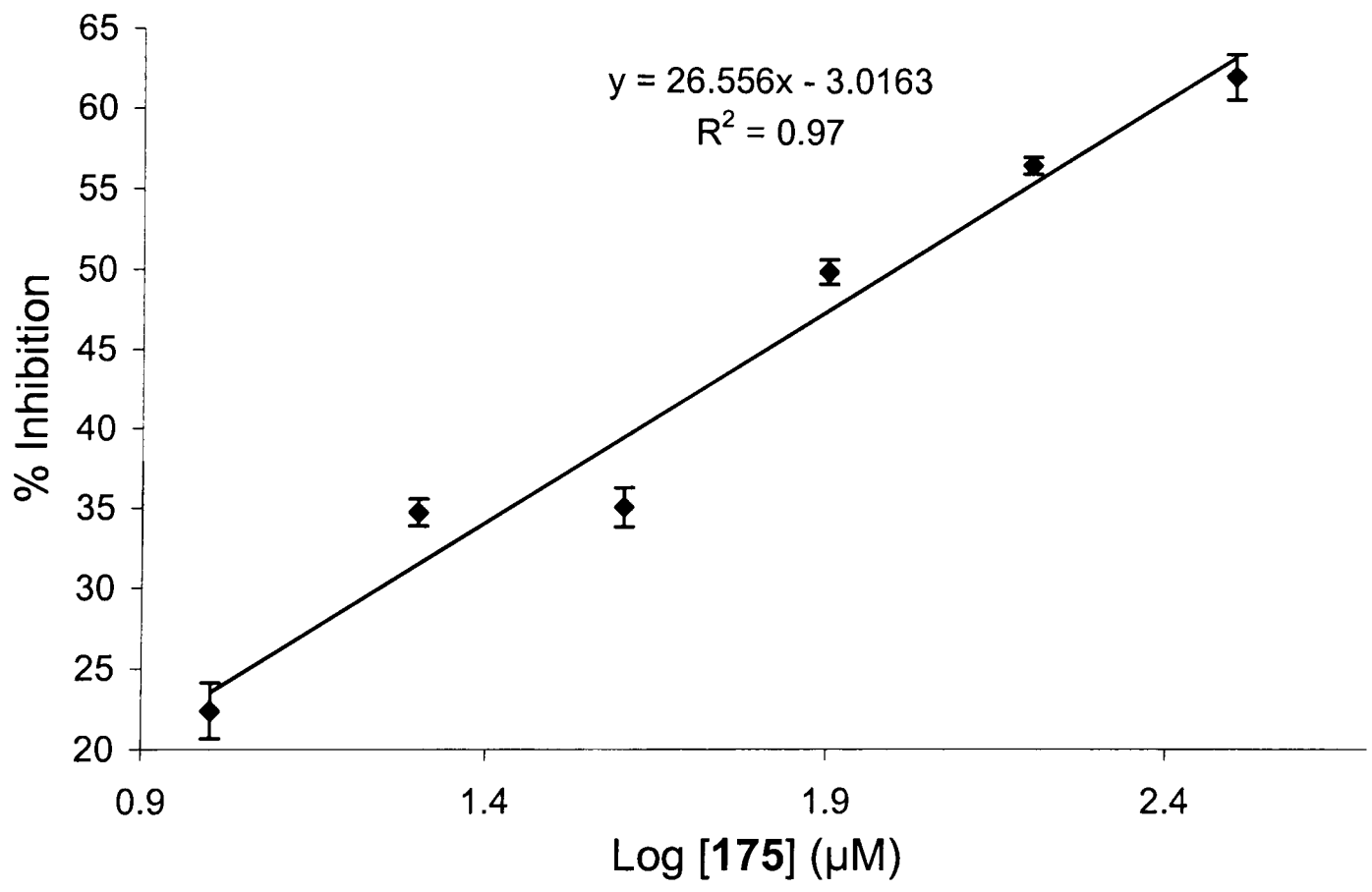

Figure 2.76 Plot of percentage inhibition versus log [**175**] for 1-(4-fluoro-benzyl)-1*H*-imidazole (**175**) against 17α-hydroxylase.

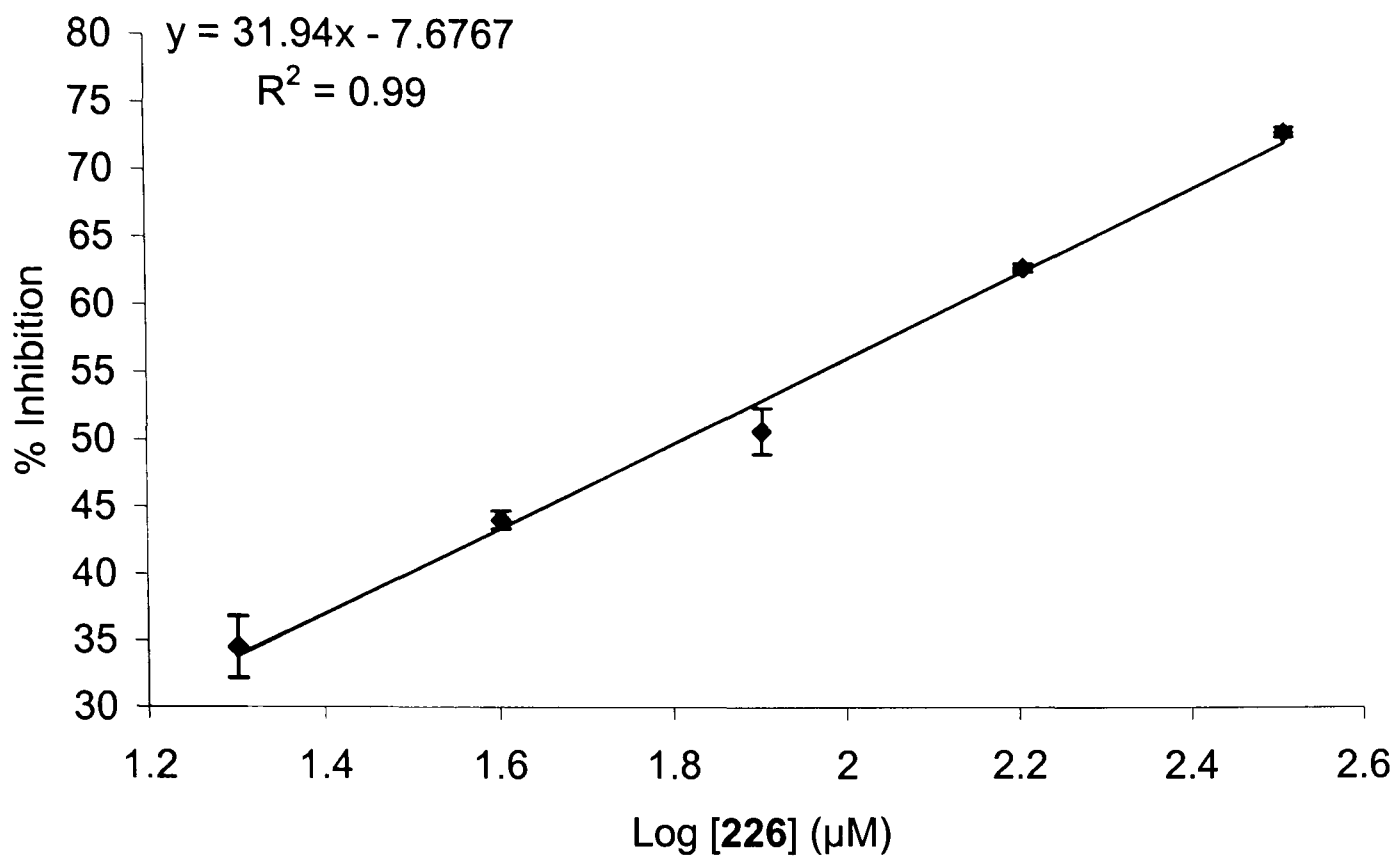

Figure 2.77 Plot of percentage inhibition versus log [**226**] for 1-(3,4-difluoro-benzyl)-1*H*-imidazole (**226**) against 17α-hydroxylase.

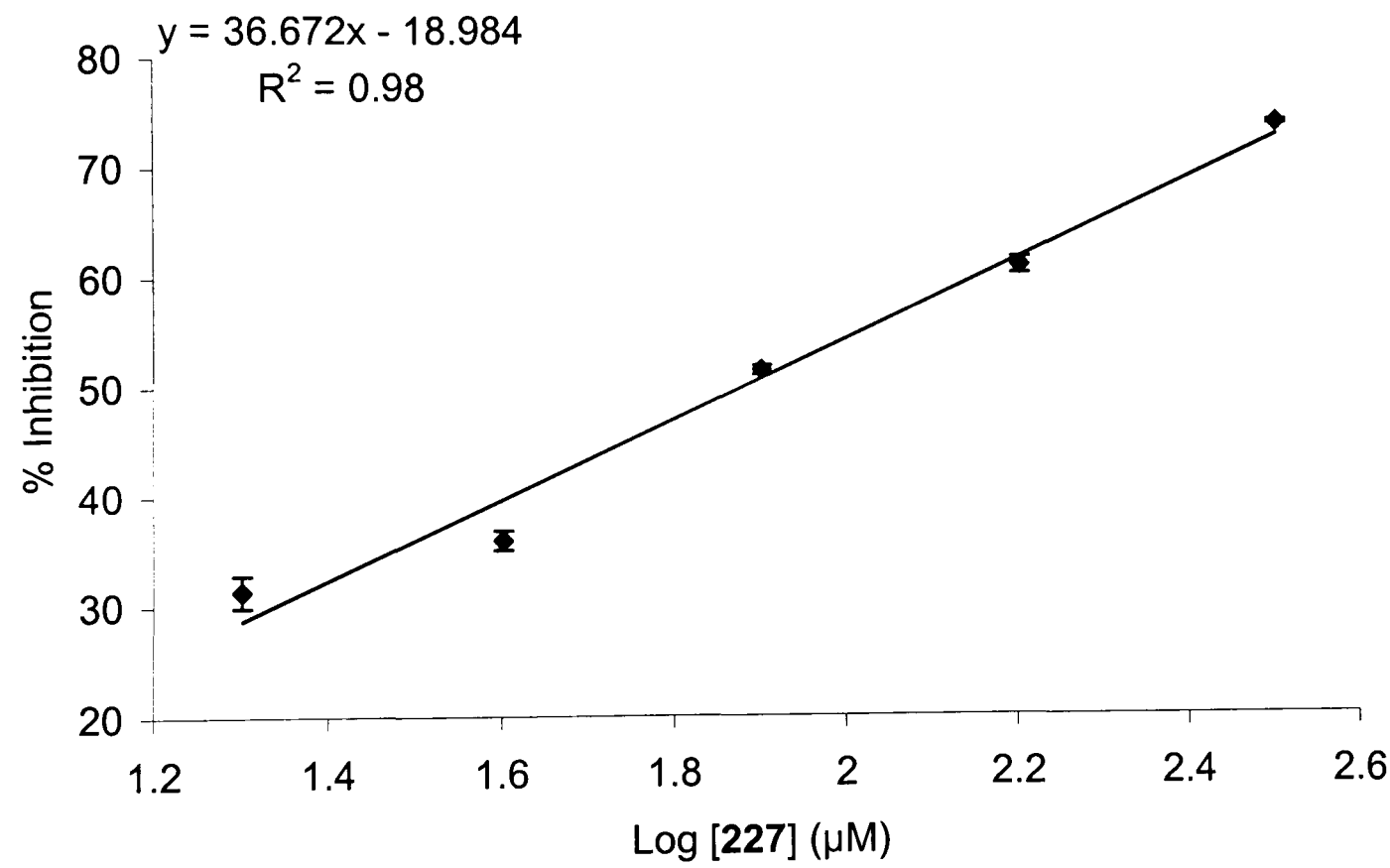

Figure 2.78 Plot of percentage inhibition versus log [**227**] for 1-(3,5-difluoro-benzyl)-1*H*-imidazole (**227**) against 17α-hydroxylase.

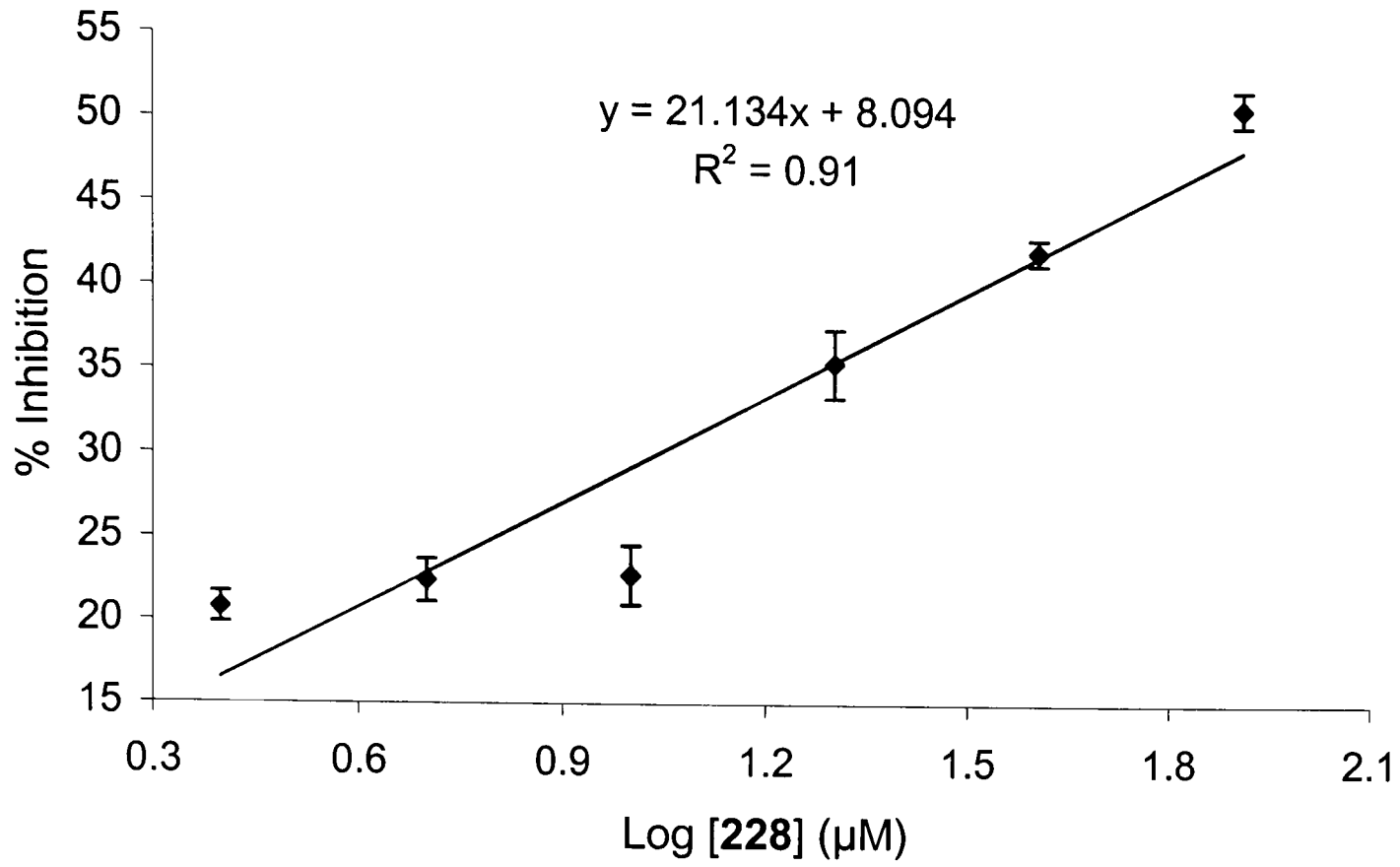

Figure 2.79 Plot of percentage inhibition versus log [**228**] for 1-(2-chloro-benzyl)-1*H*-imidazole (**228**) against 17α-hydroxylase.

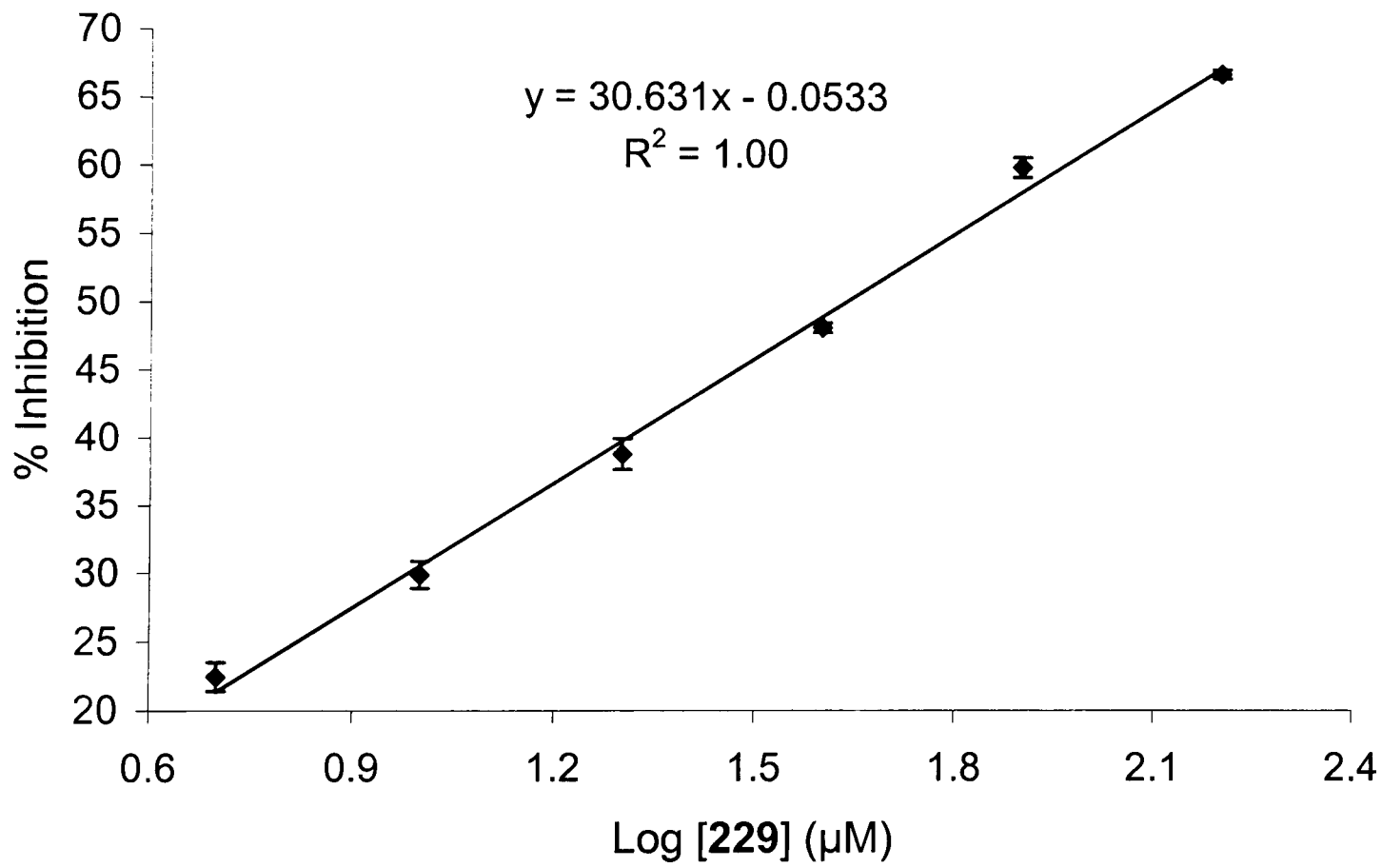

Figure 2.80 Plot of percentage inhibition versus log [**229**] for 1-(3-chloro-benzyl)-1*H*-imidazole (**229**) against 17α-hydroxylase.

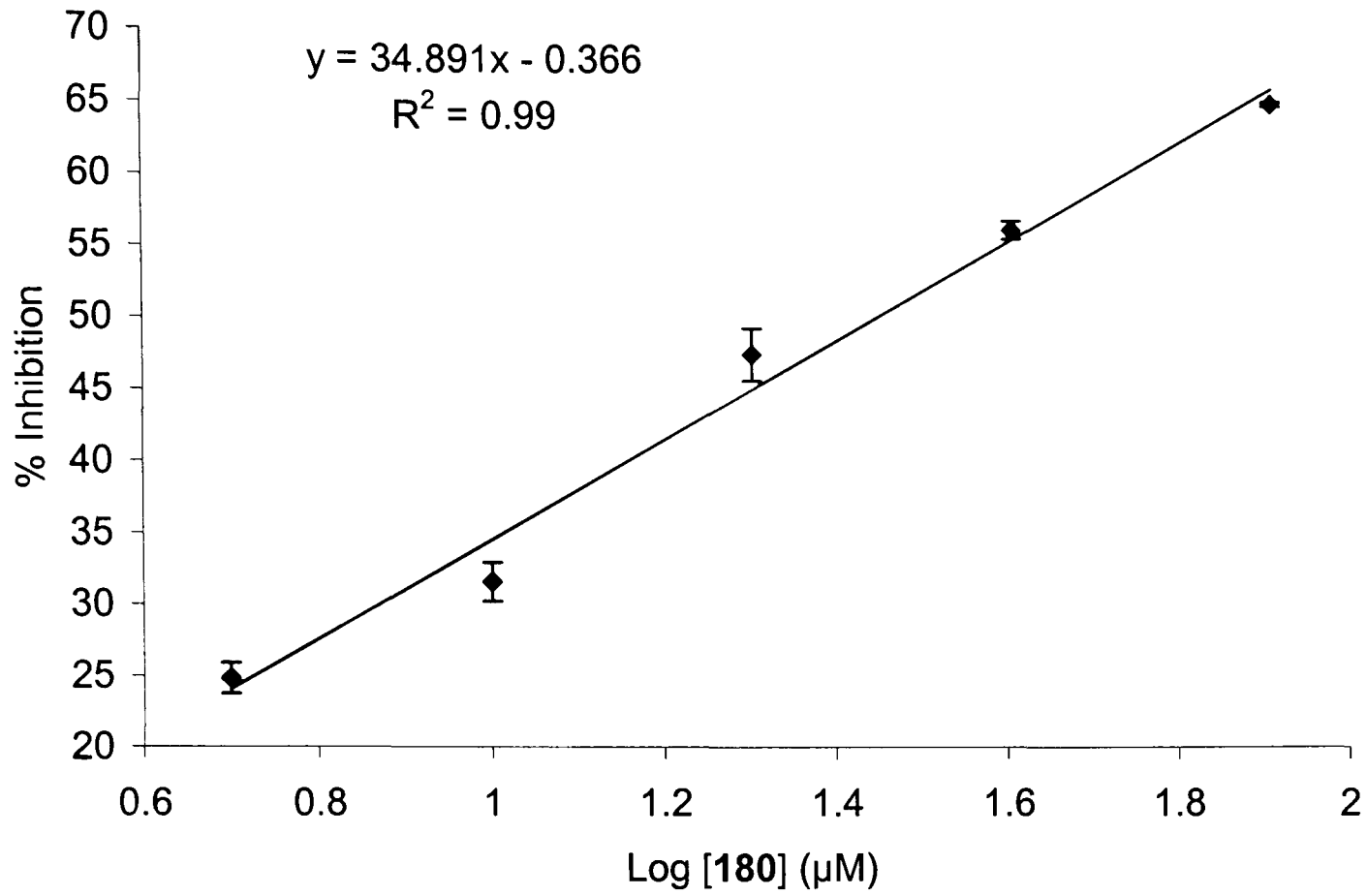

Figure 2.81 Plot of percentage inhibition versus log [**180**] for 1-(4-chloro-benzyl)-1*H*-imidazole (**180**) against 17α-hydroxylase.

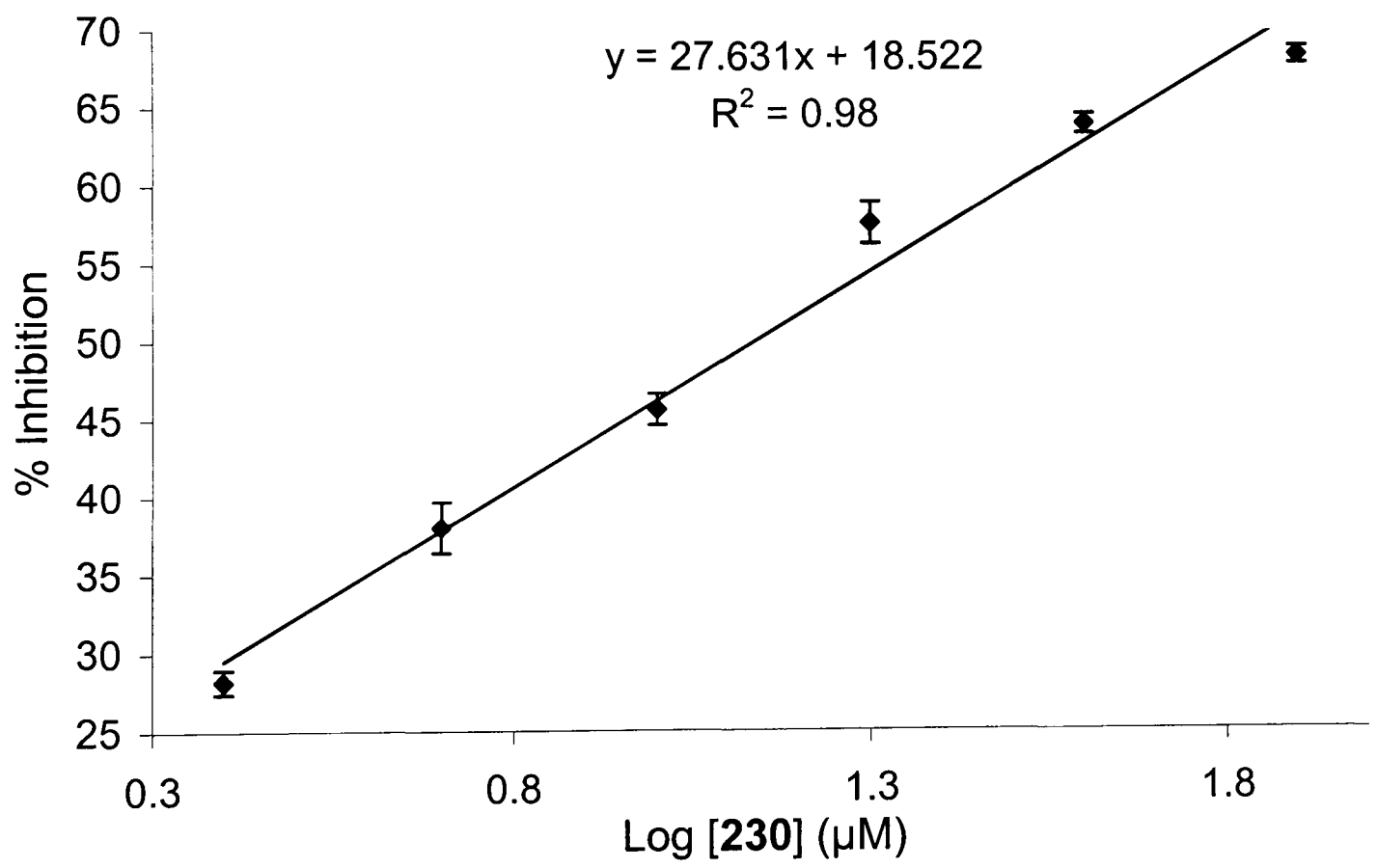

Figure 2.82 Plot of percentage inhibition versus log [**230**] for 1-(2,3-dichloro-benzyl)-1*H*-imidazole (**230**) against 17α-hydroxylase.

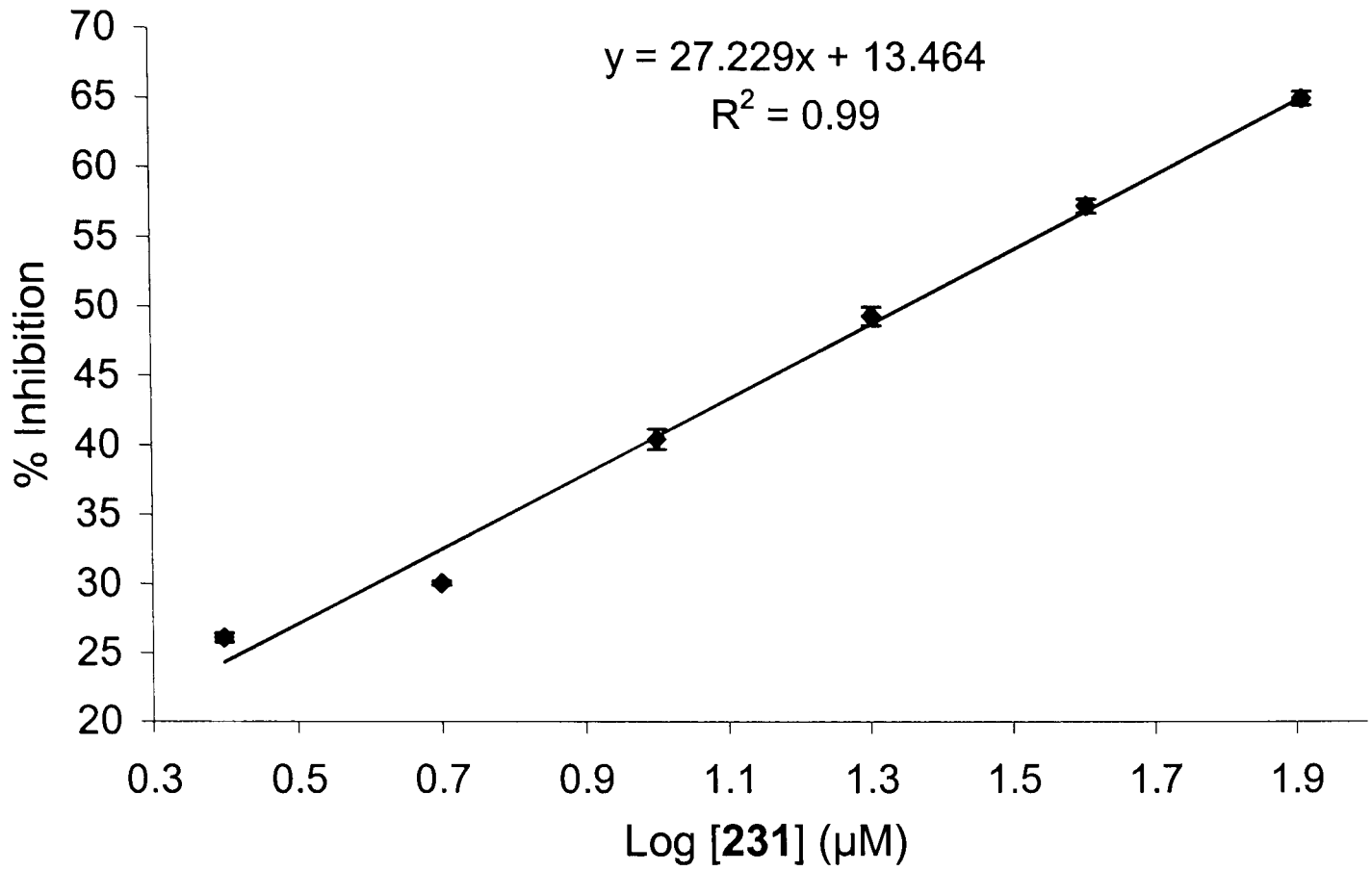

Figure 2.83 Plot of percentage inhibition versus log [**231**] for 1-(2,4-dichloro-benzyl)-1*H*-imidazole (**231**) against 17α-hydroxylase.

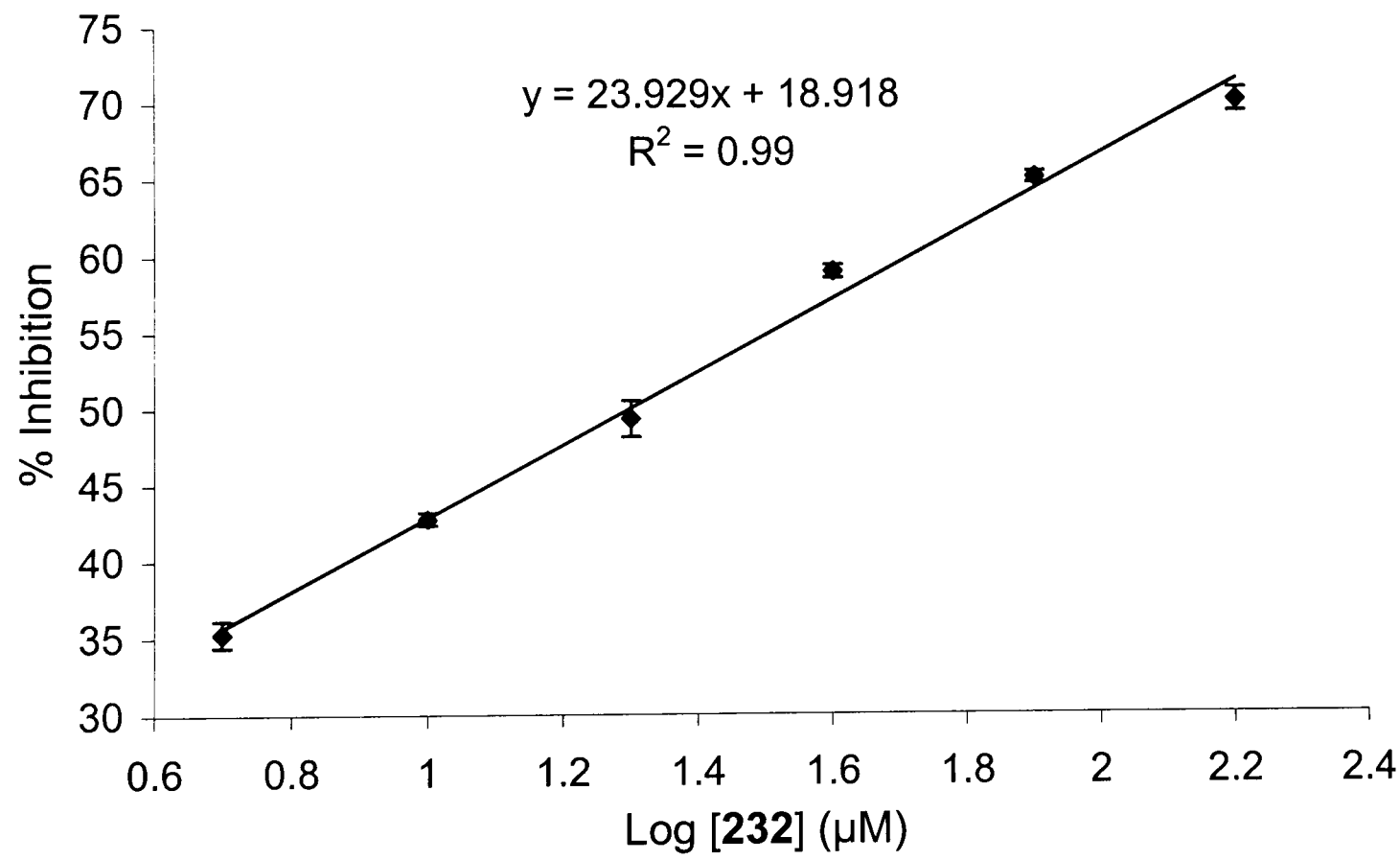

Figure 2.84 Plot of percentage inhibition versus log [**232**] for 1-(2,5-dichloro-benzyl)-1*H*-imidazole (**232**) against 17α-hydroxylase.

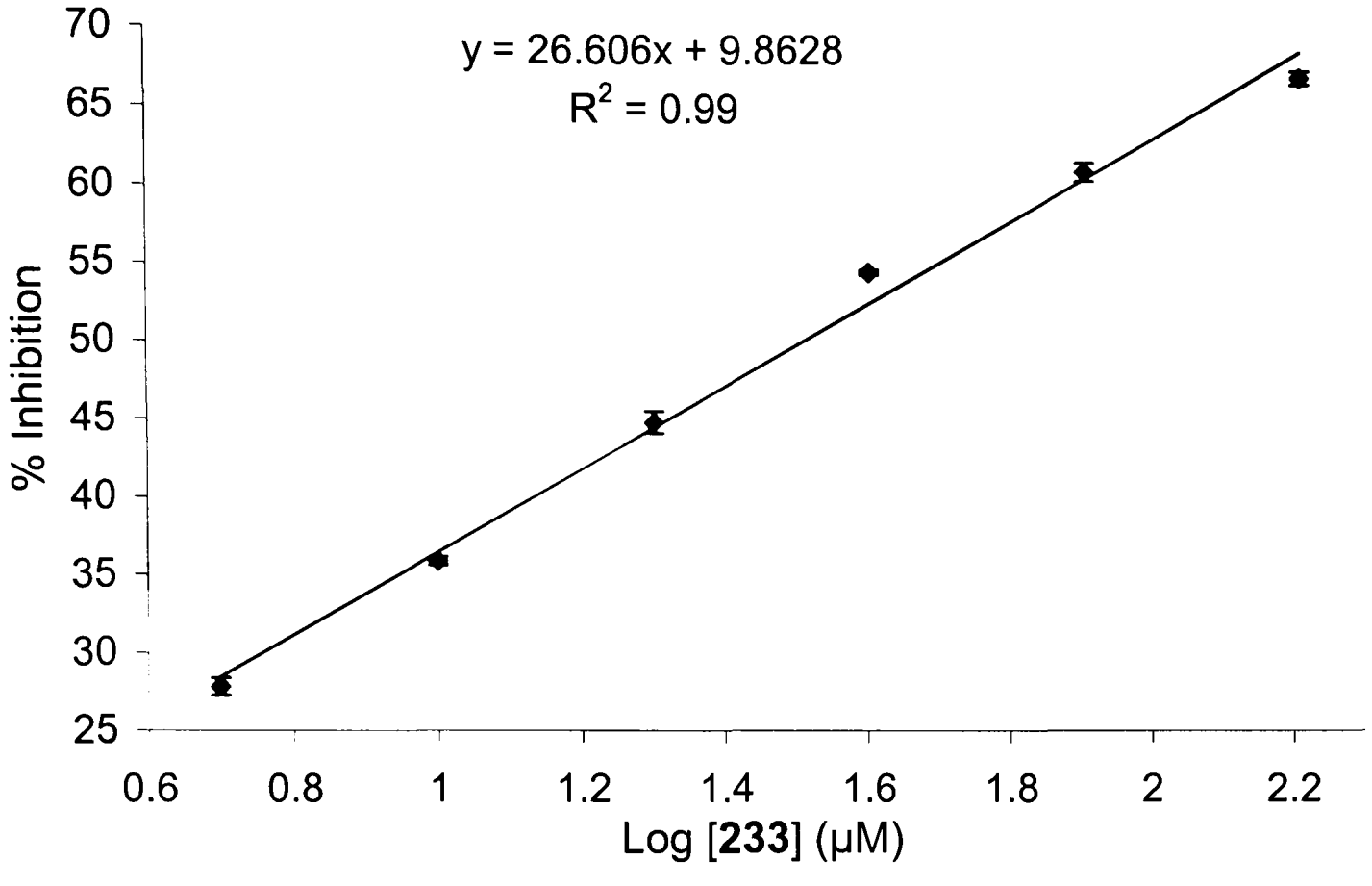

Figure 2.85 Plot of percentage inhibition versus log [**233**] for 1-(2,6-dichloro-benzyl)-1*H*-imidazole (**233**) against 17α-hydroxylase.

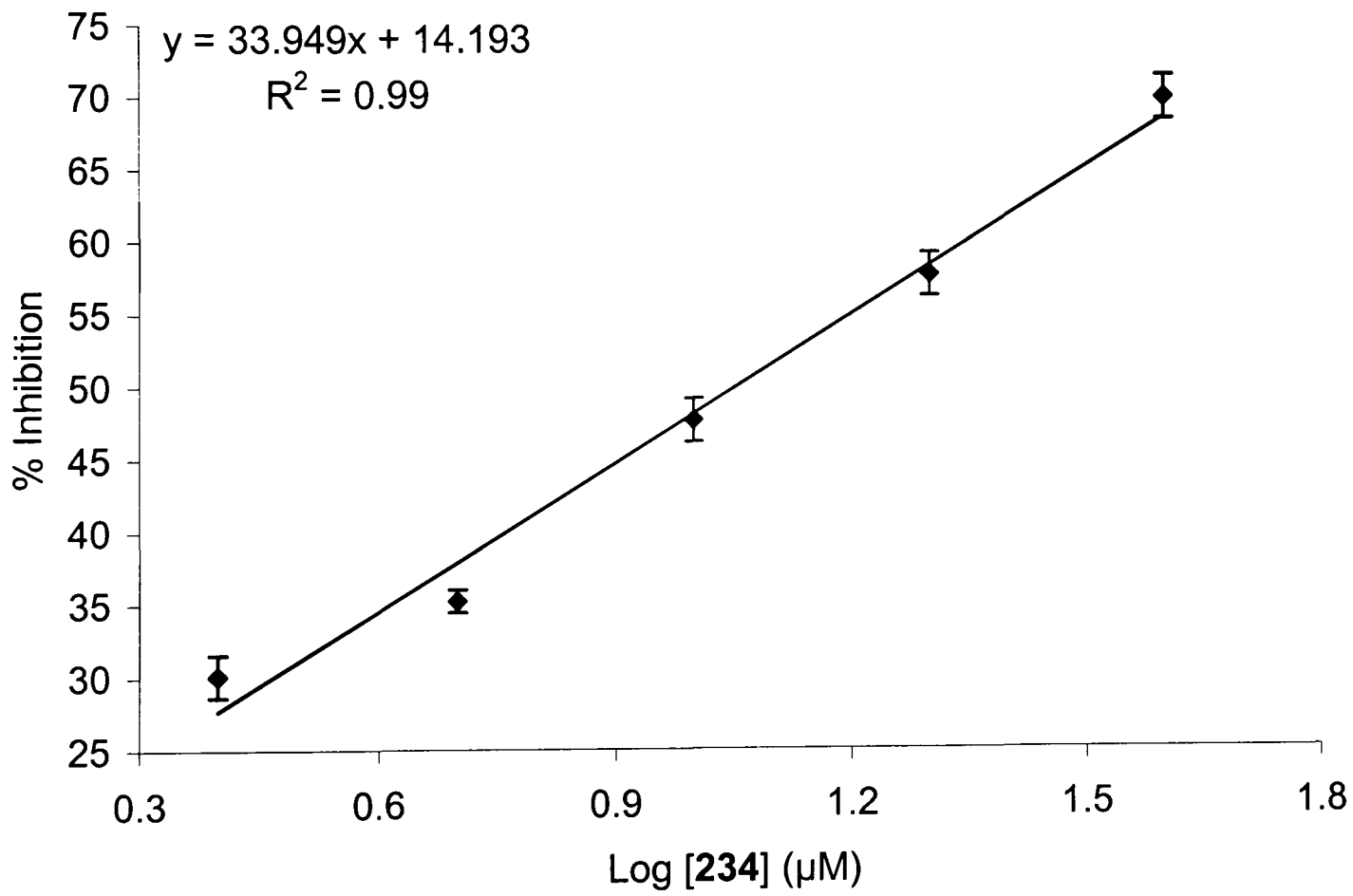

Figure 2.86 Plot of percentage inhibition versus log [**234**] for 1-(3,4-dichloro-benzyl)-1*H*-imidazole (**234**) against 17α-hydroxylase.

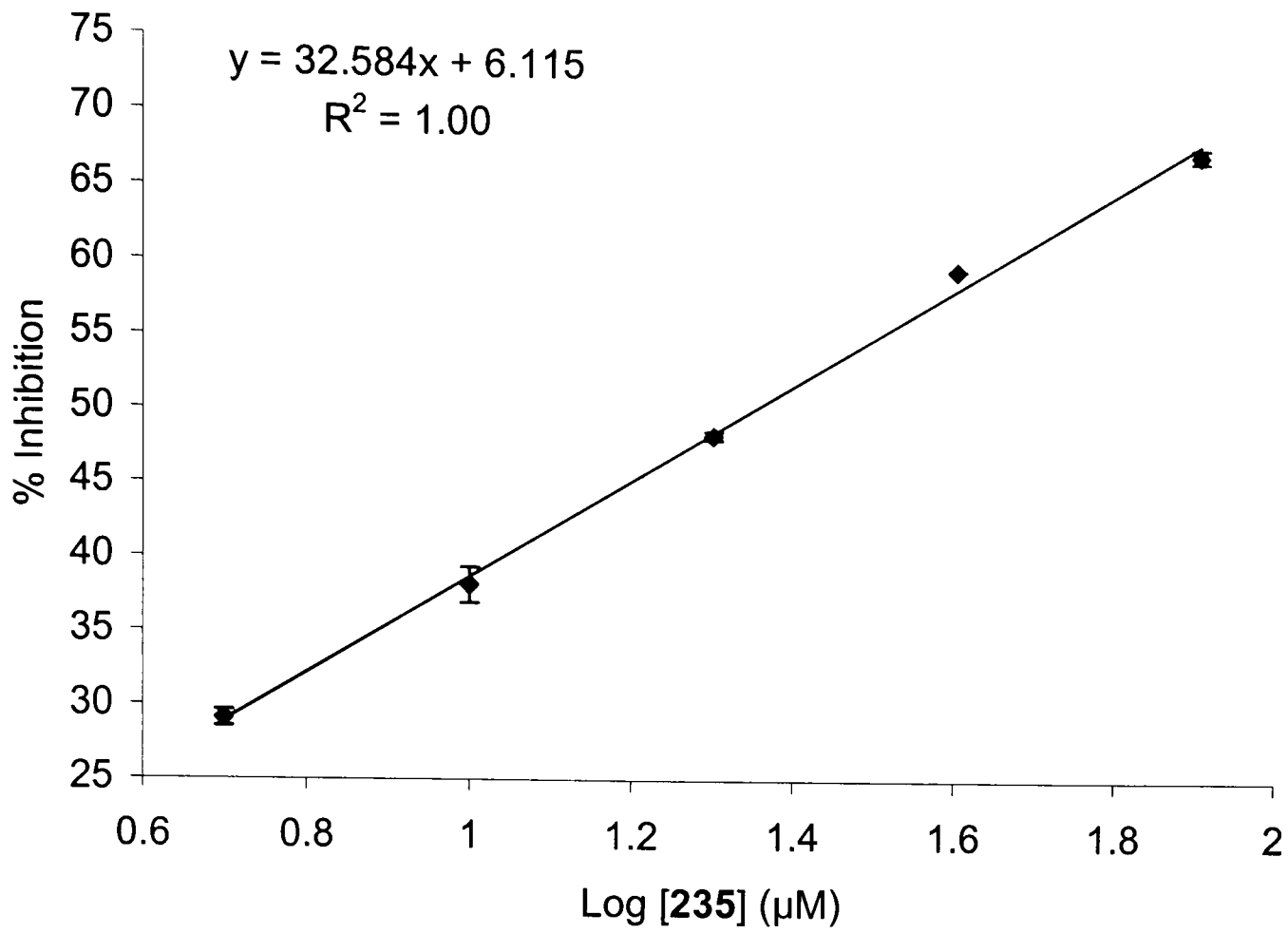

Figure 2.87 Plot of percentage inhibition versus log [**235**] for 1-(3,5-dichloro-benzyl)-1*H*-imidazole (**235**) against 17α-hydroxylase.

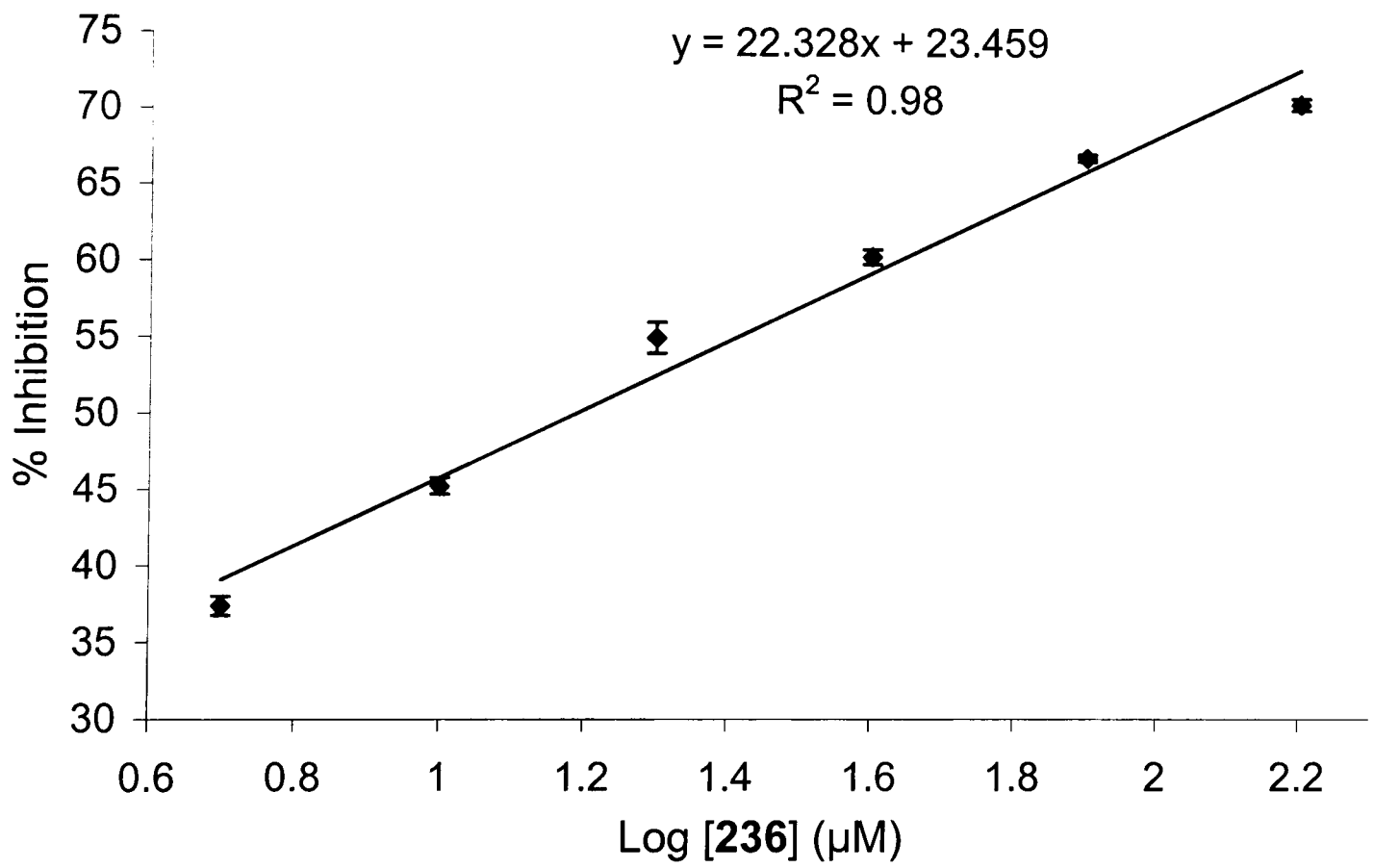

Figure 2.88 Plot of percentage inhibition versus log [**236**] for 1-(2-bromo-benzyl)-1*H*-imidazole (**236**) against 17α-hydroxylase.

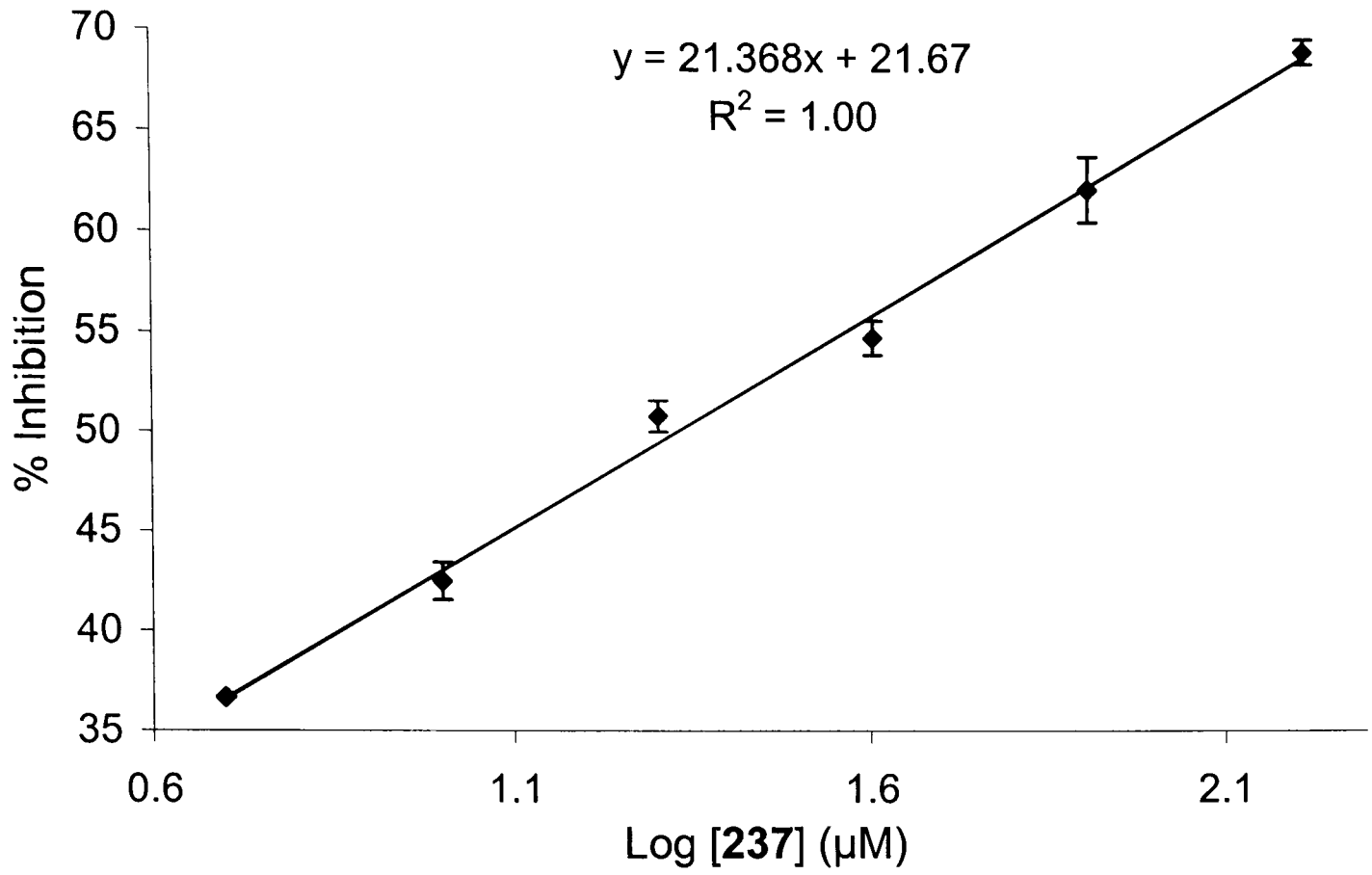

Figure 2.89 Plot of percentage inhibition versus log [**237**] for 1-(3-bromo-benzyl)-1*H*-imidazole (**237**) against 17α-hydroxylase.

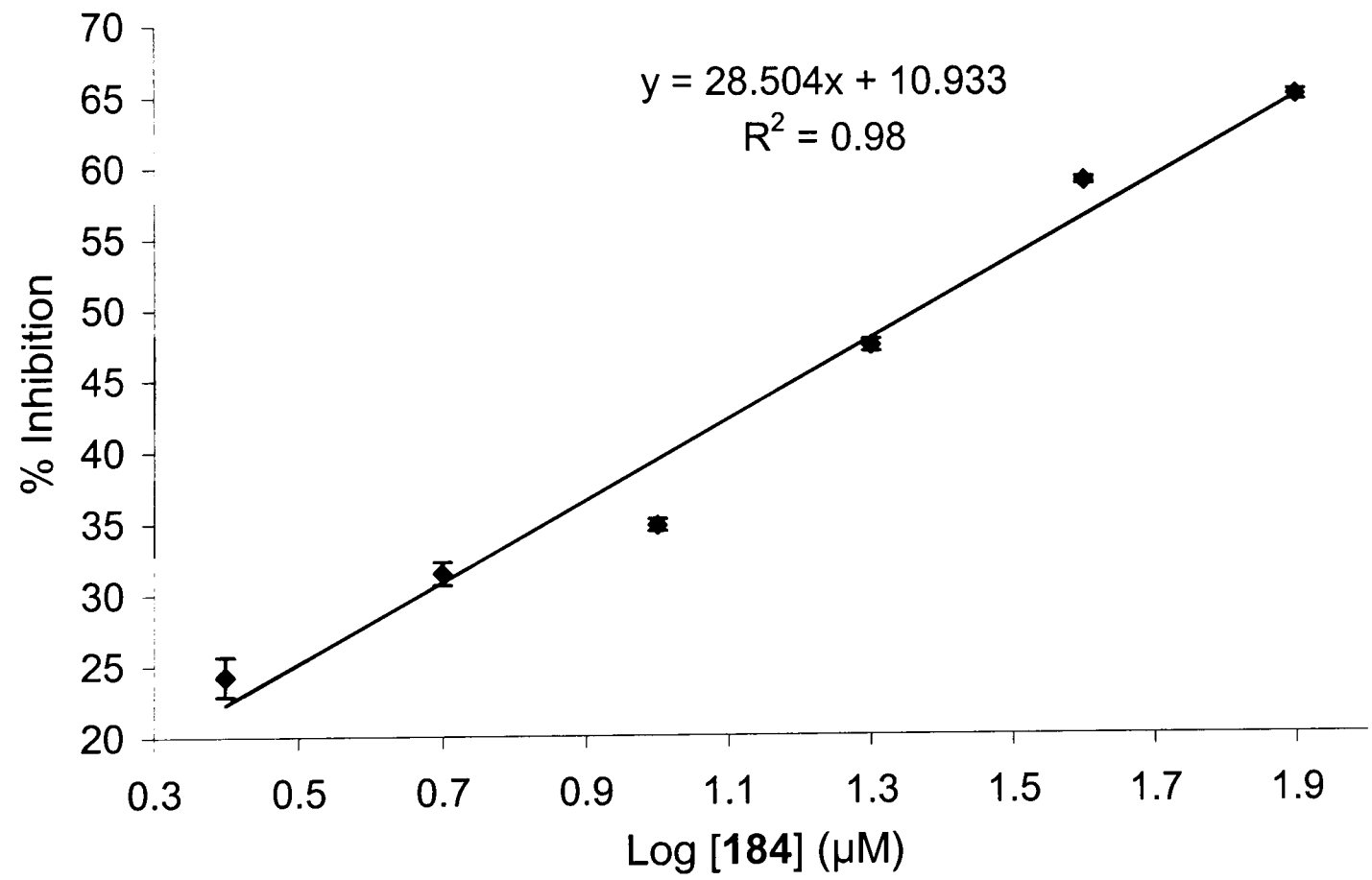

Figure 2.90 Plot of percentage inhibition versus log [**184**] for 1-(4-bromo-benzyl)-1*H*-imidazole (**184**) against 17α-hydroxylase.

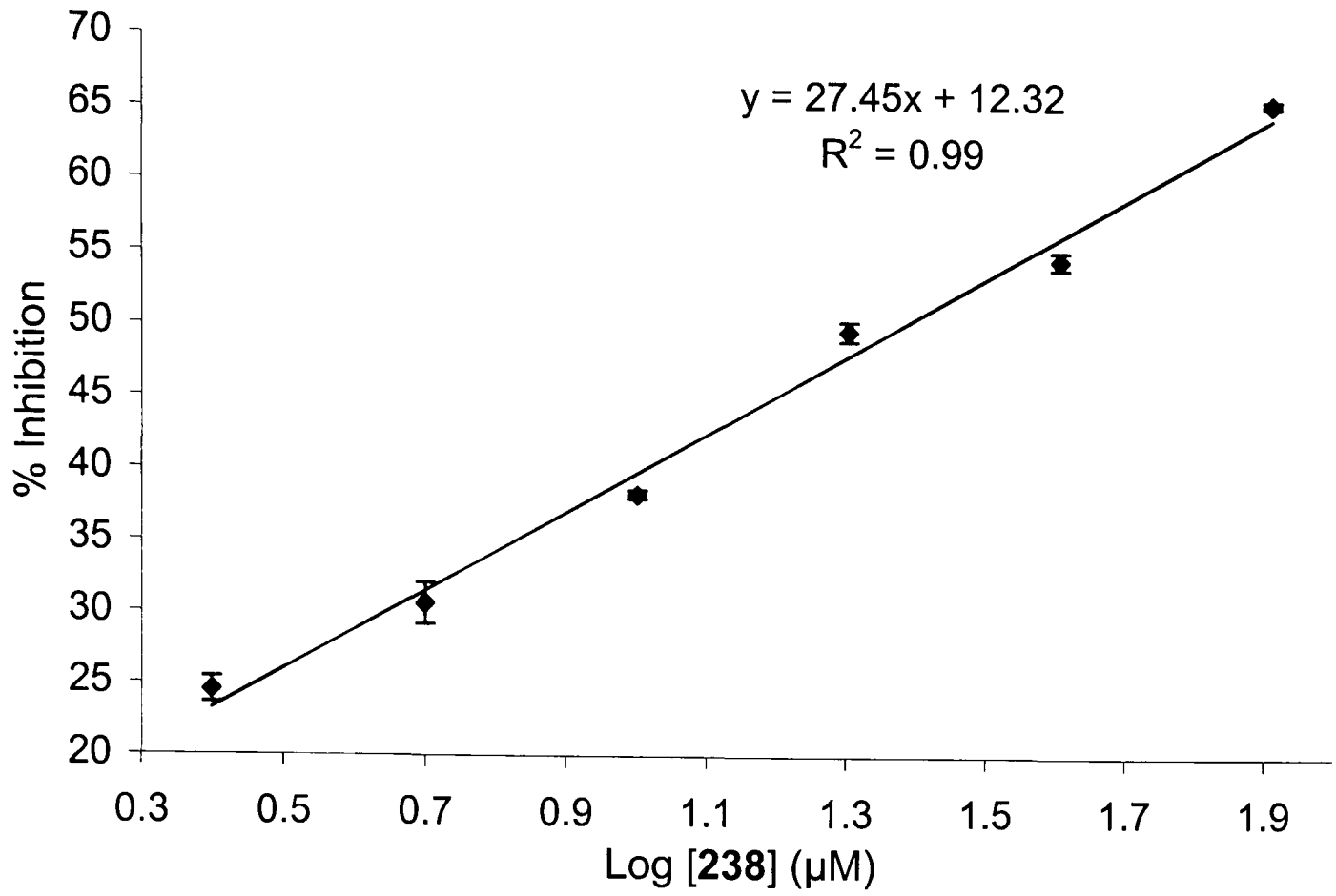

Figure 2.91 Plot of percentage inhibition versus log [**238**] for 1-(3,5-dibromo-benzyl)-1*H*-imidazole (**238**) against 17α-hydroxylase.

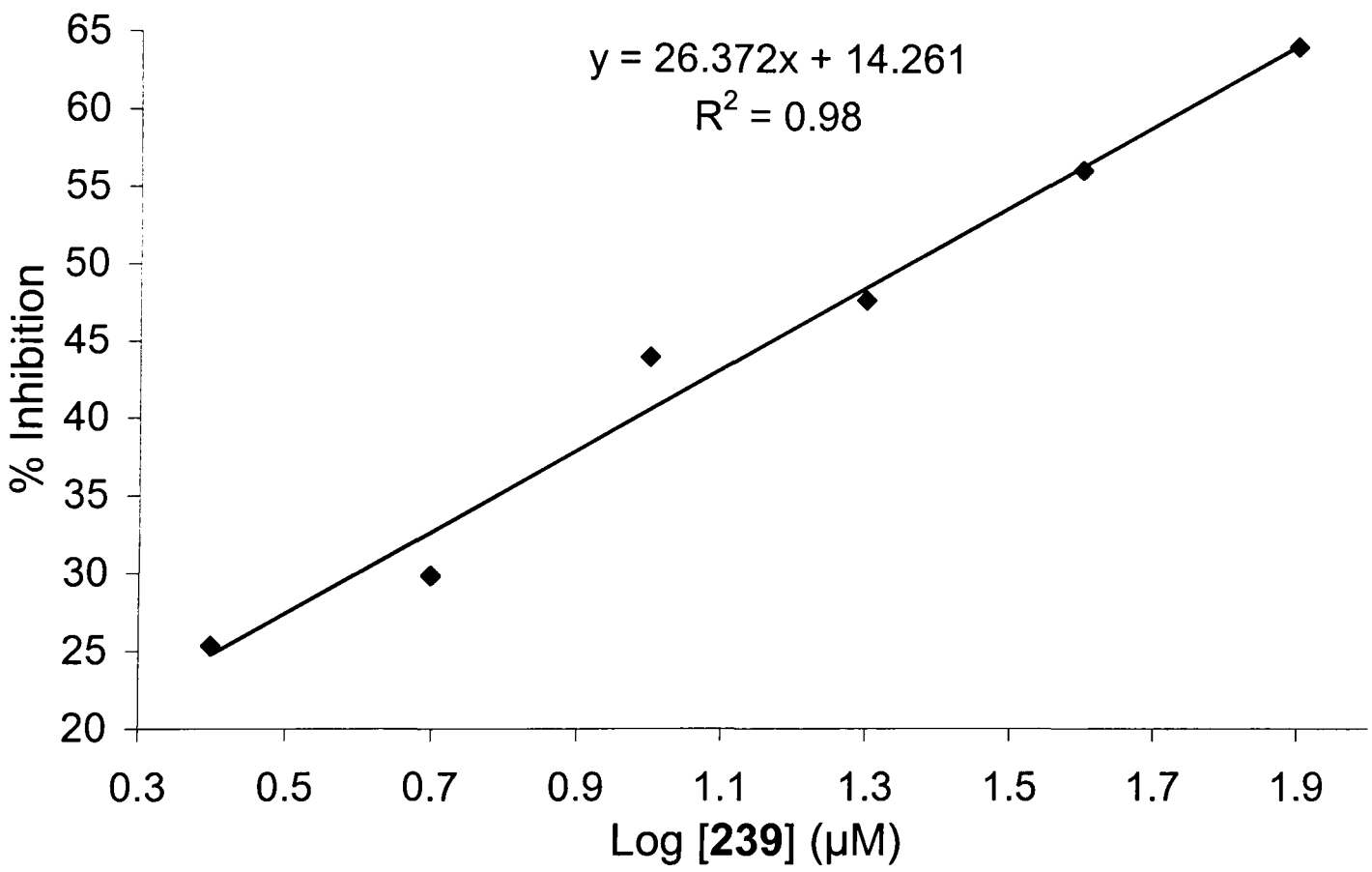

Figure 2.92 Plot of percentage inhibition versus log [**239**] for 1-(2-iodo-benzyl)-1*H*-imidazole (**239**) against 17α-hydroxylase.

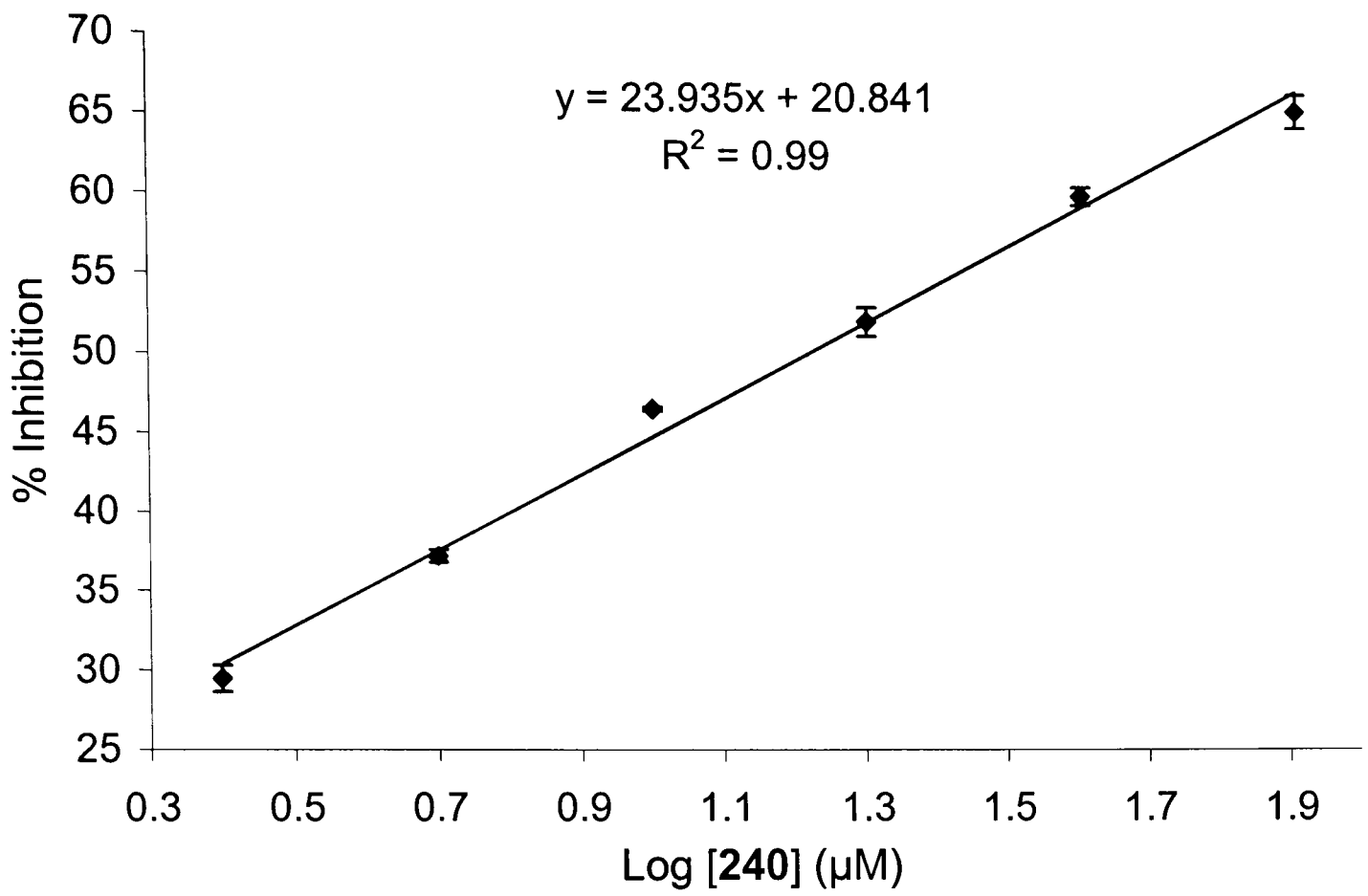

Figure 2.93 Plot of percentage inhibition versus log [**240**] for 1-(3-iodo-benzyl)-1*H*-imidazole (**240**) against 17α-hydroxylase.

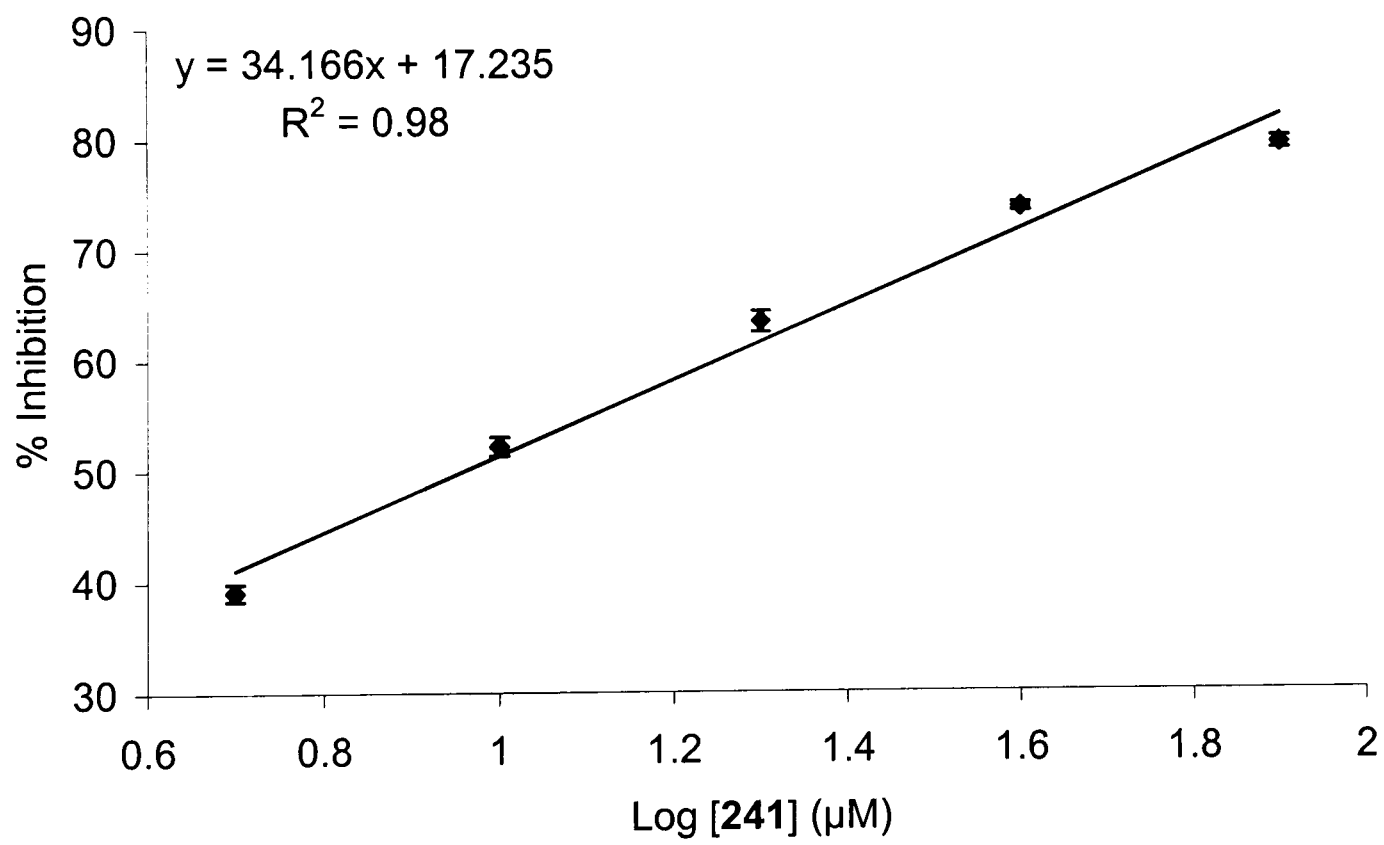

Figure 2.94 Plot of percentage inhibition versus log [**241**] for 1-(4-iodo-benzyl)-1*H*-imidazole (**241**) against 17α-hydroxylase.

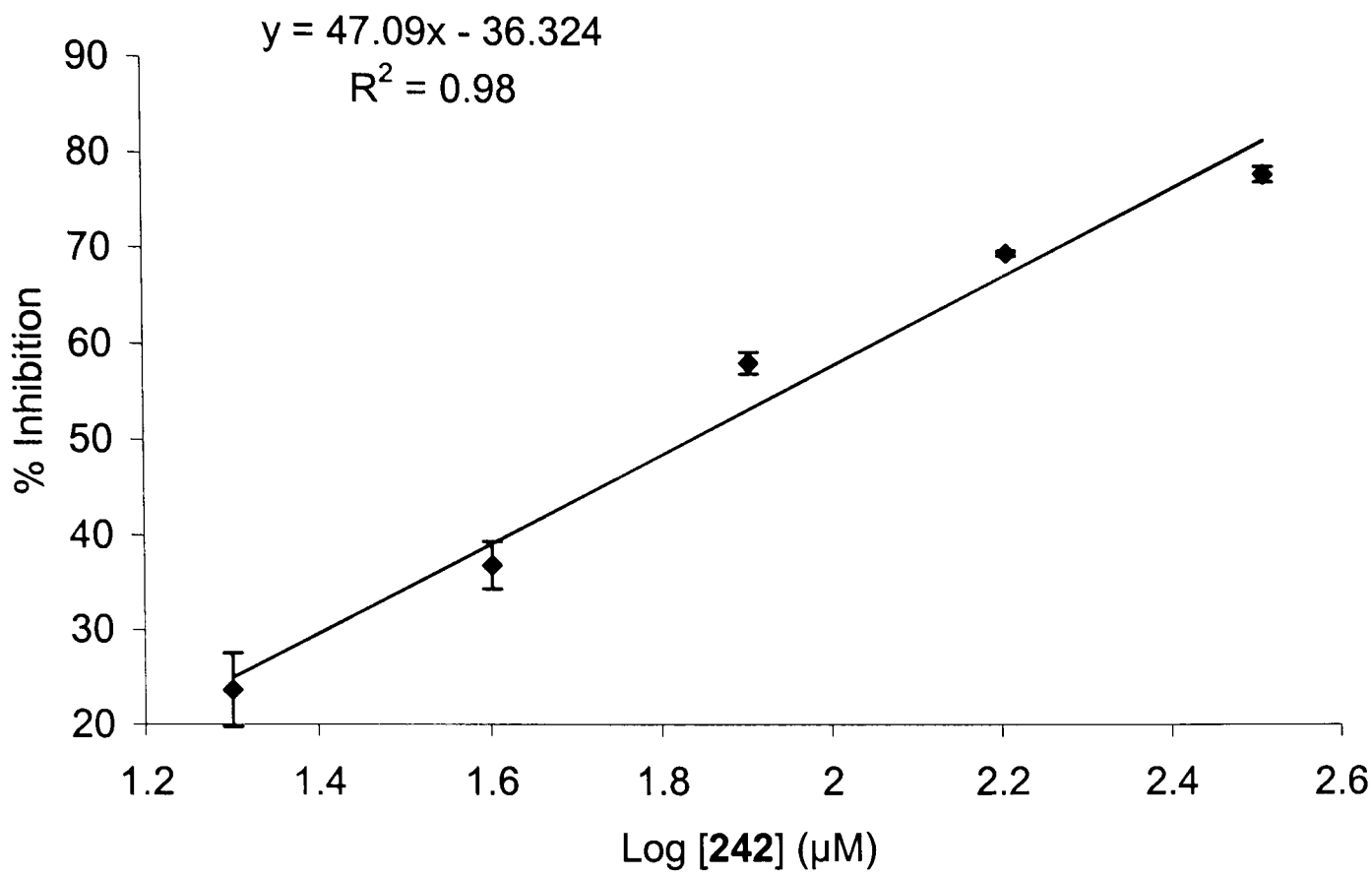

Figure 2.95 Plot of percentage inhibition versus log [**242**] for 4-imidazol-1-ylmethyl-phenol (**242**) against 17α-hydroxylase.

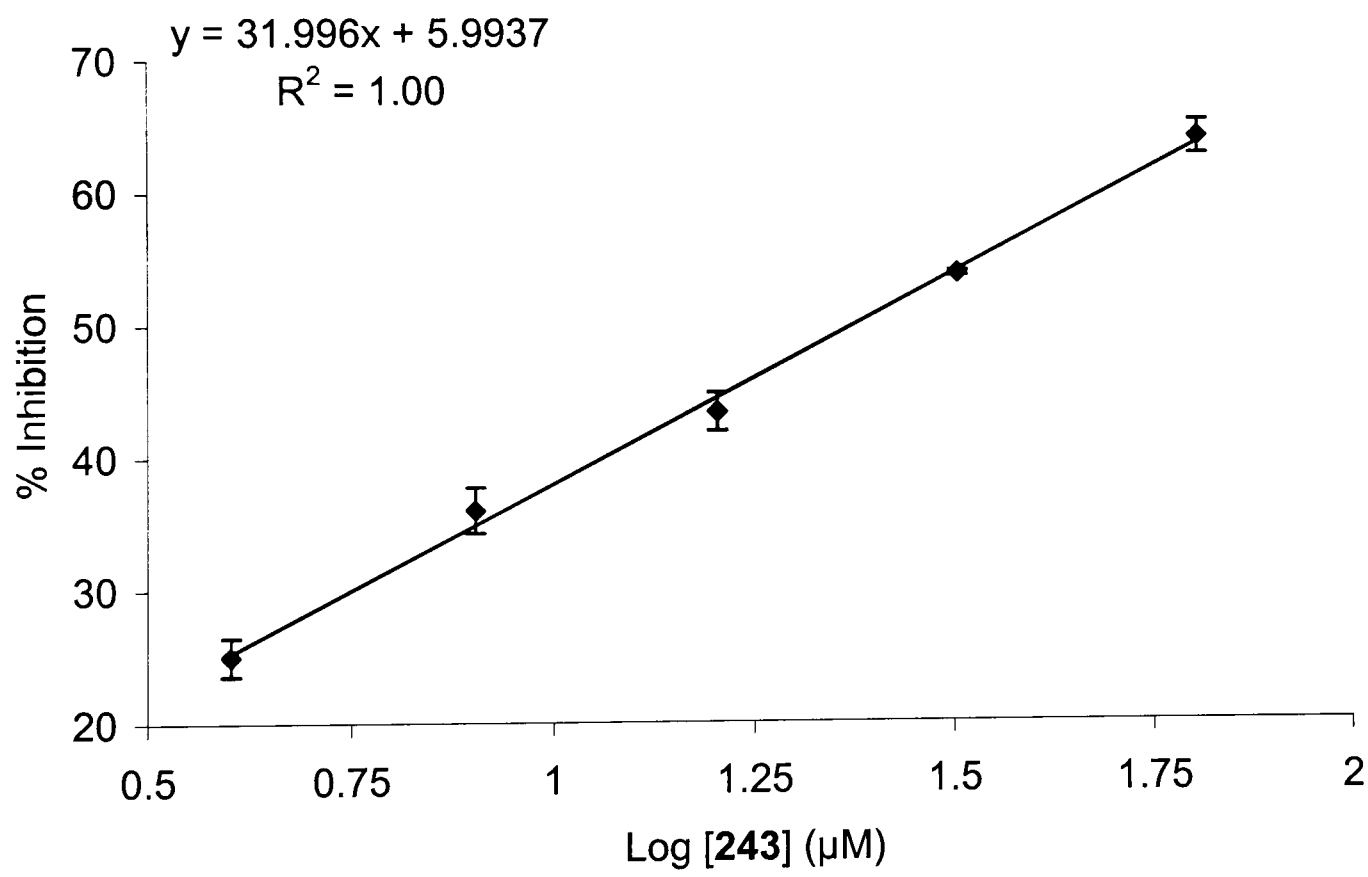

Figure 2.96 Plot of percentage inhibition versus log [**243**] for 1-(4-Nitro-benzyl)-4*H*-imidazole (**243**) against 17α-hydroxylase.

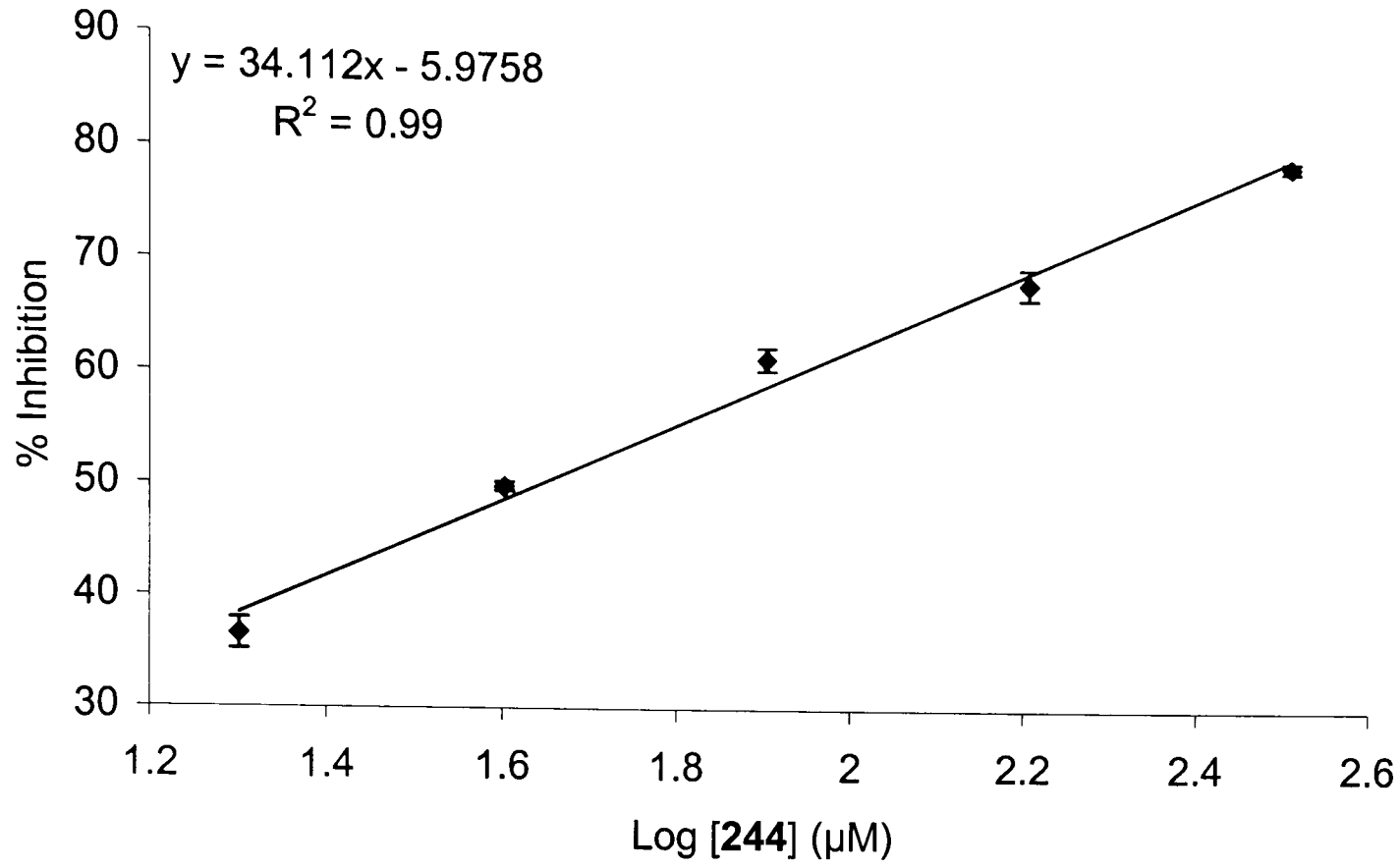

Figure 2.97 Plot of percentage inhibition versus log [**244**] for 4-imidazol-1-ylmethyl-benzonitrile (**244**) against 17α-hydroxylase.

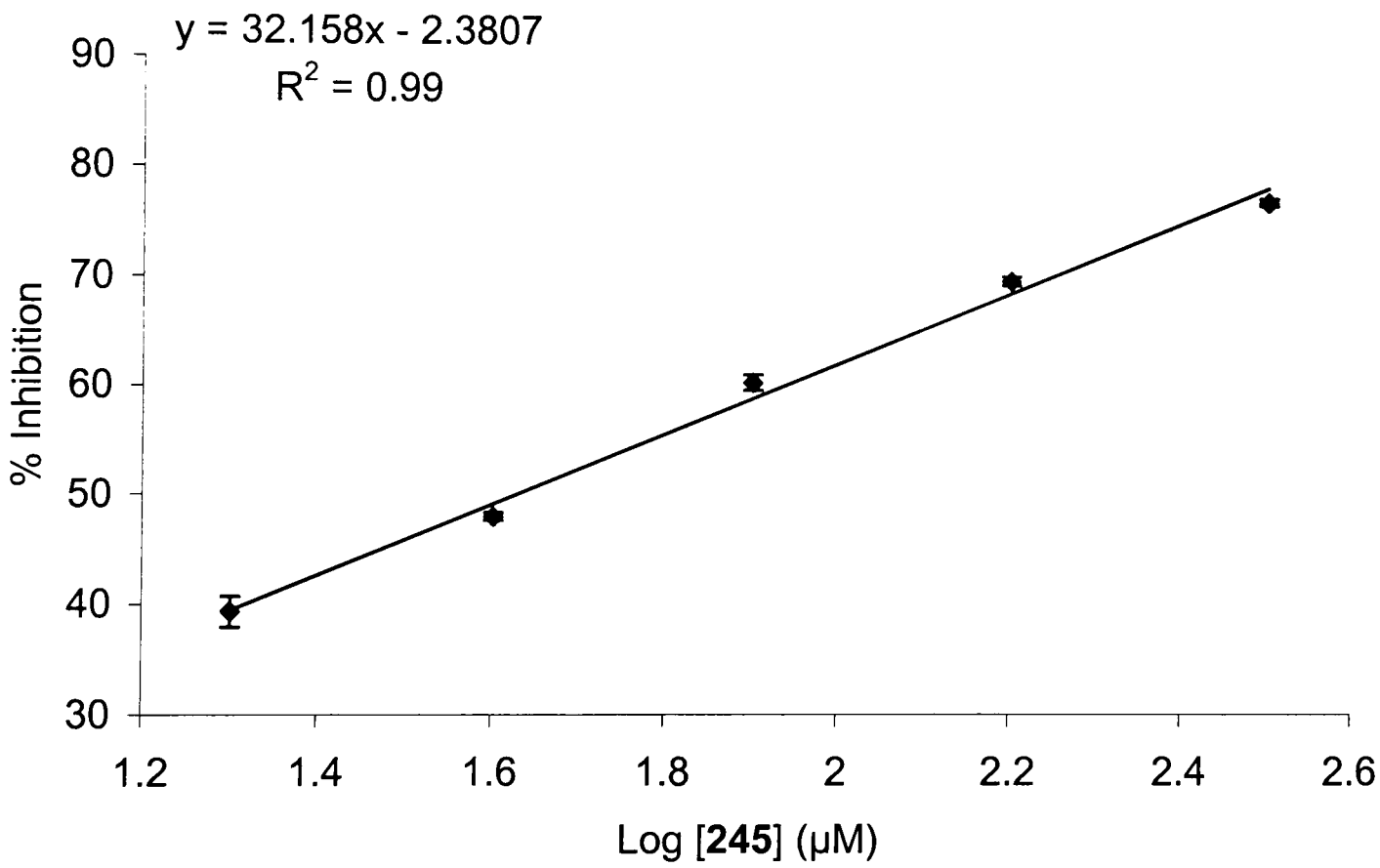

Figure 2.98 Plot of percentage inhibition versus log [**245**] for 1-(4-methyl-benzyl)-1*H*-imidazole (**245**) against 17α-hydroxylase.

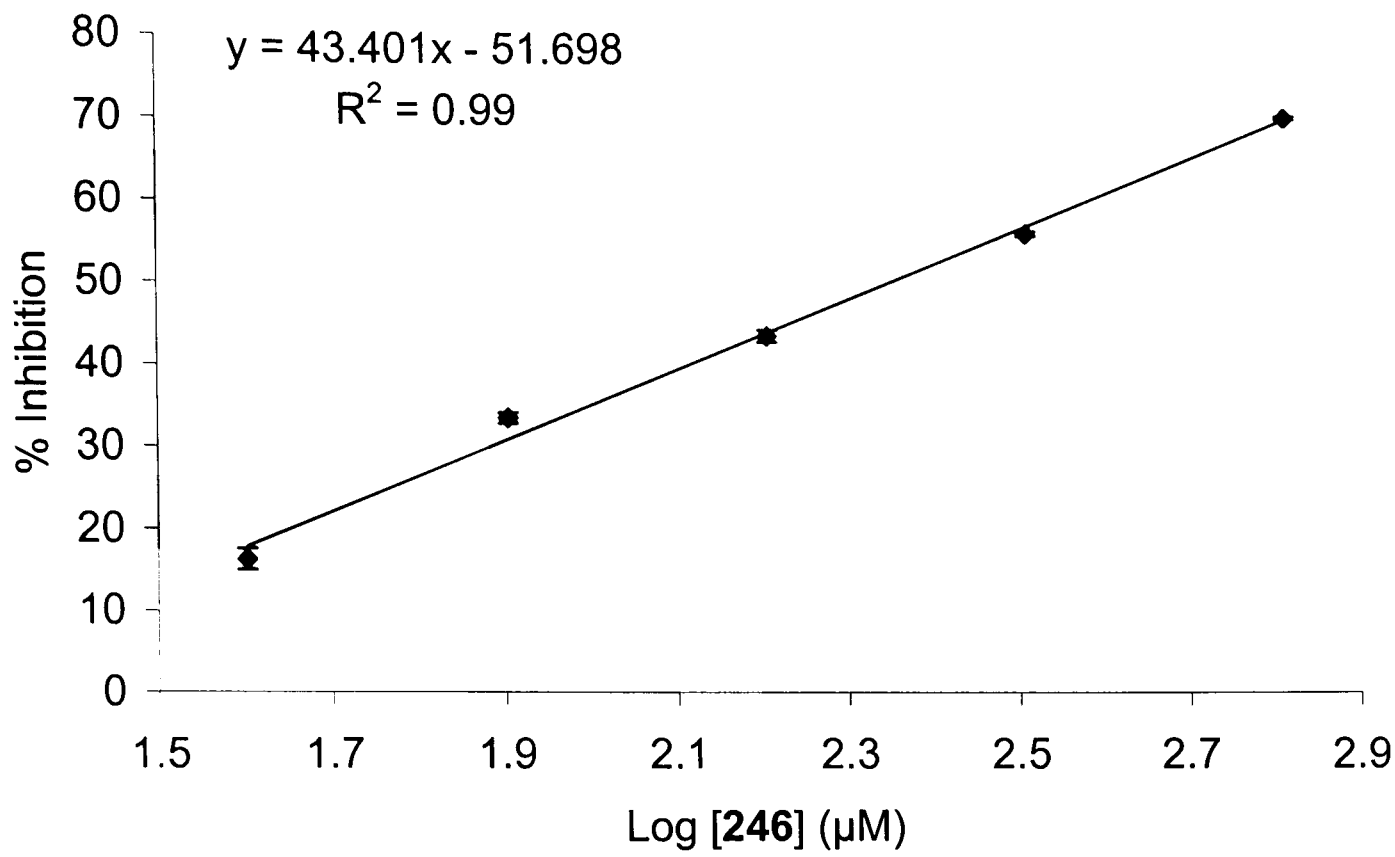

Figure 2.99 Plot of percentage inhibition versus log [**246**] for 1-(3,5-Bis-trifluoromethyl-benzyl)-1*H*-imidazole (**246**) against 17α-hydroxylase.

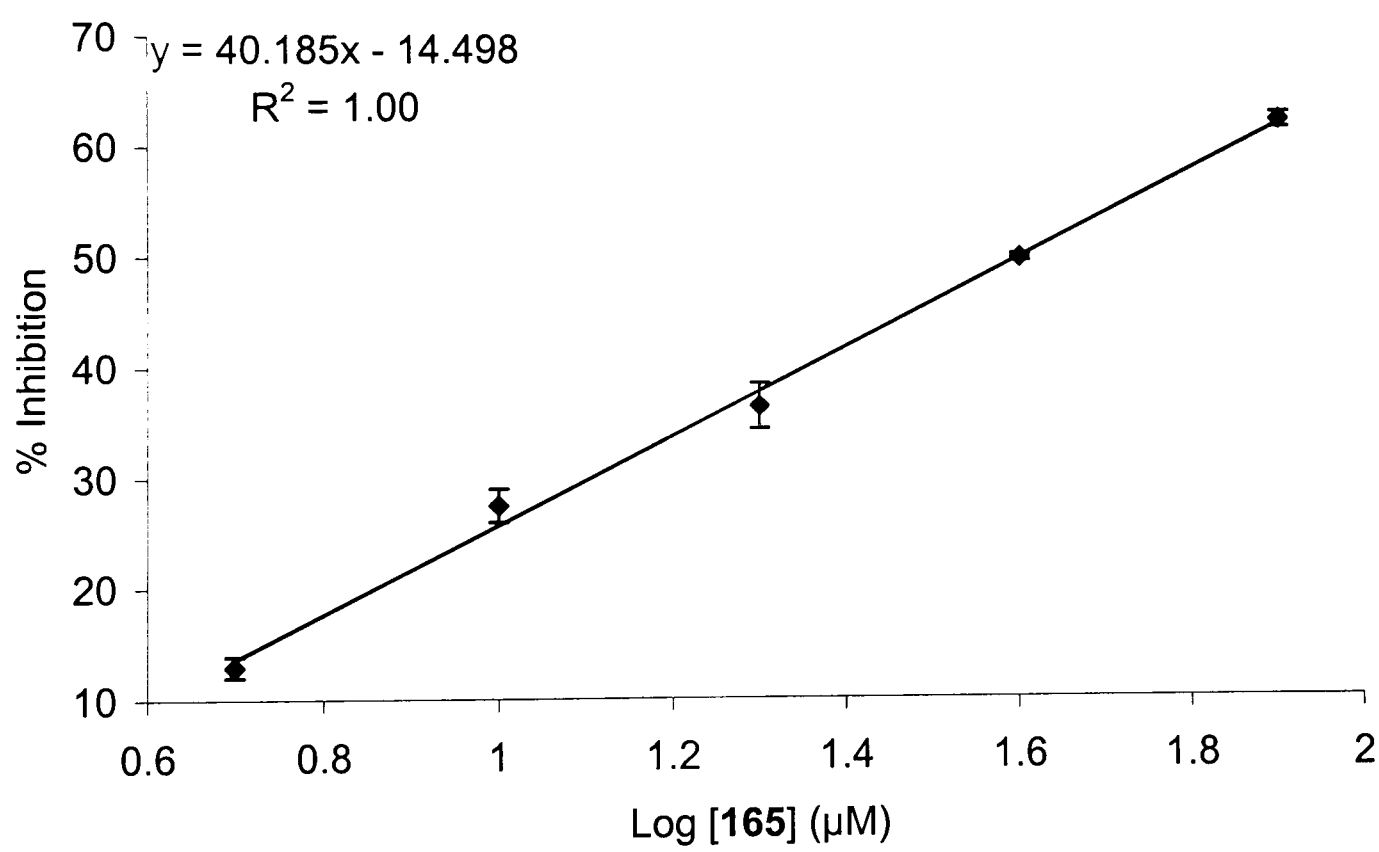

Figure 2.100 Plot of percentage inhibition versus log [**165**] for 1-benzyl-1*H*-imidazole (**165**) against 17,20-lyase.

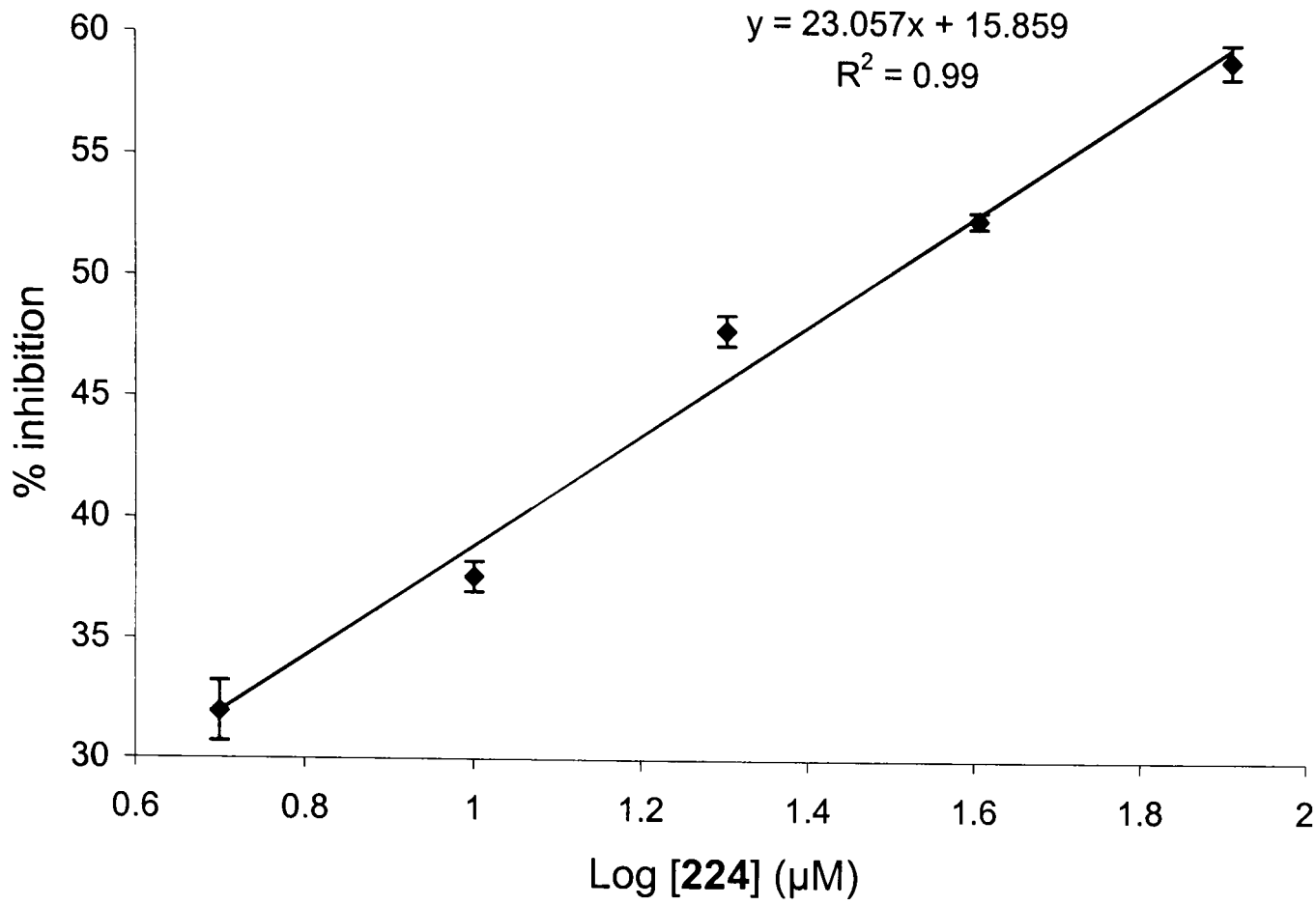

Figure 2.101 Plot of percentage inhibition versus log [**224**] for 1-(2-fluoro-benzyl)-1*H*-imidazole (**224**) against 17,20-lyase.

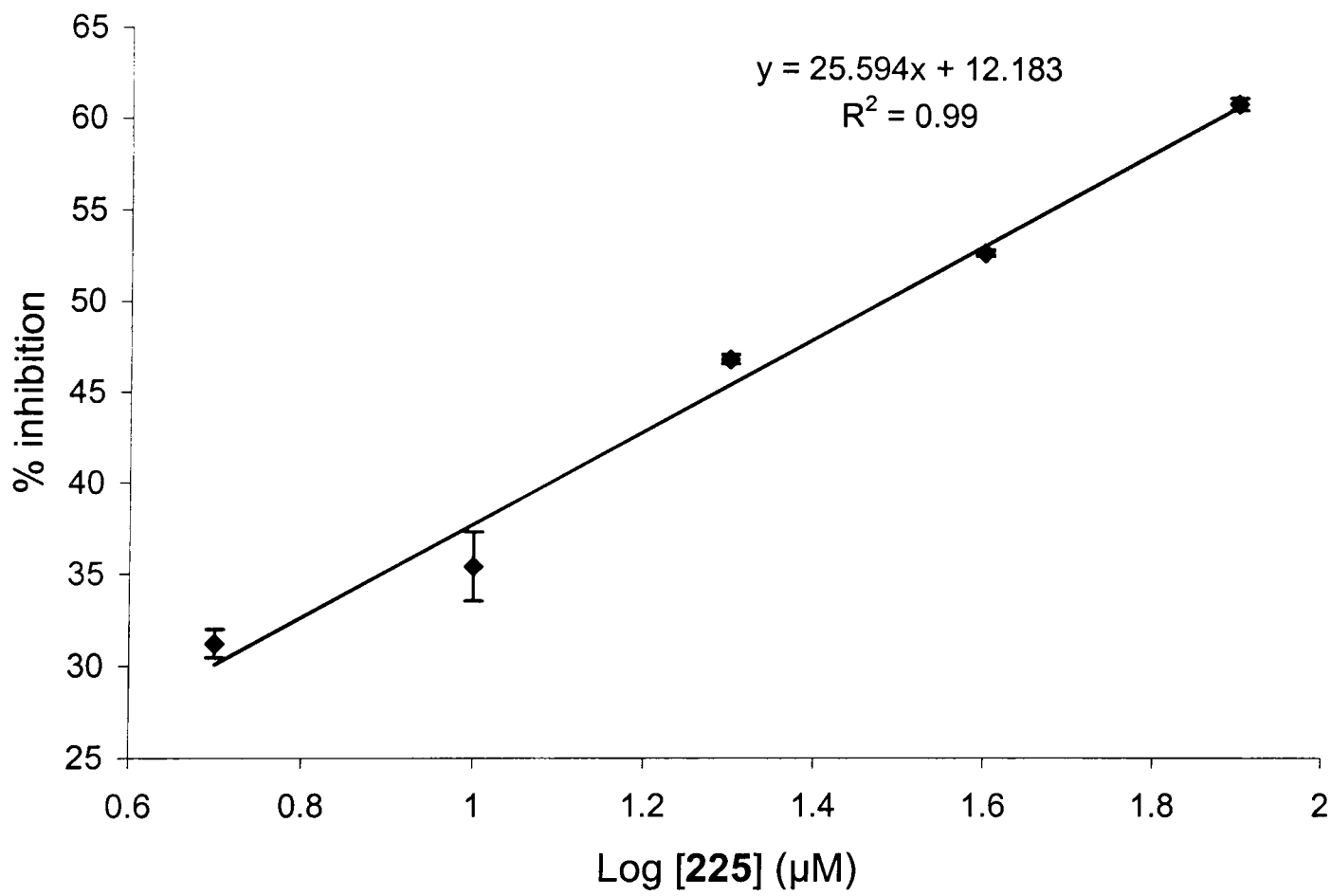

Figure 2.102 Plot of percentage inhibition versus log [**225**] for 1-(3-fluoro-benzyl)-1*H*-imidazole (**225**) against 17,20-lyase.

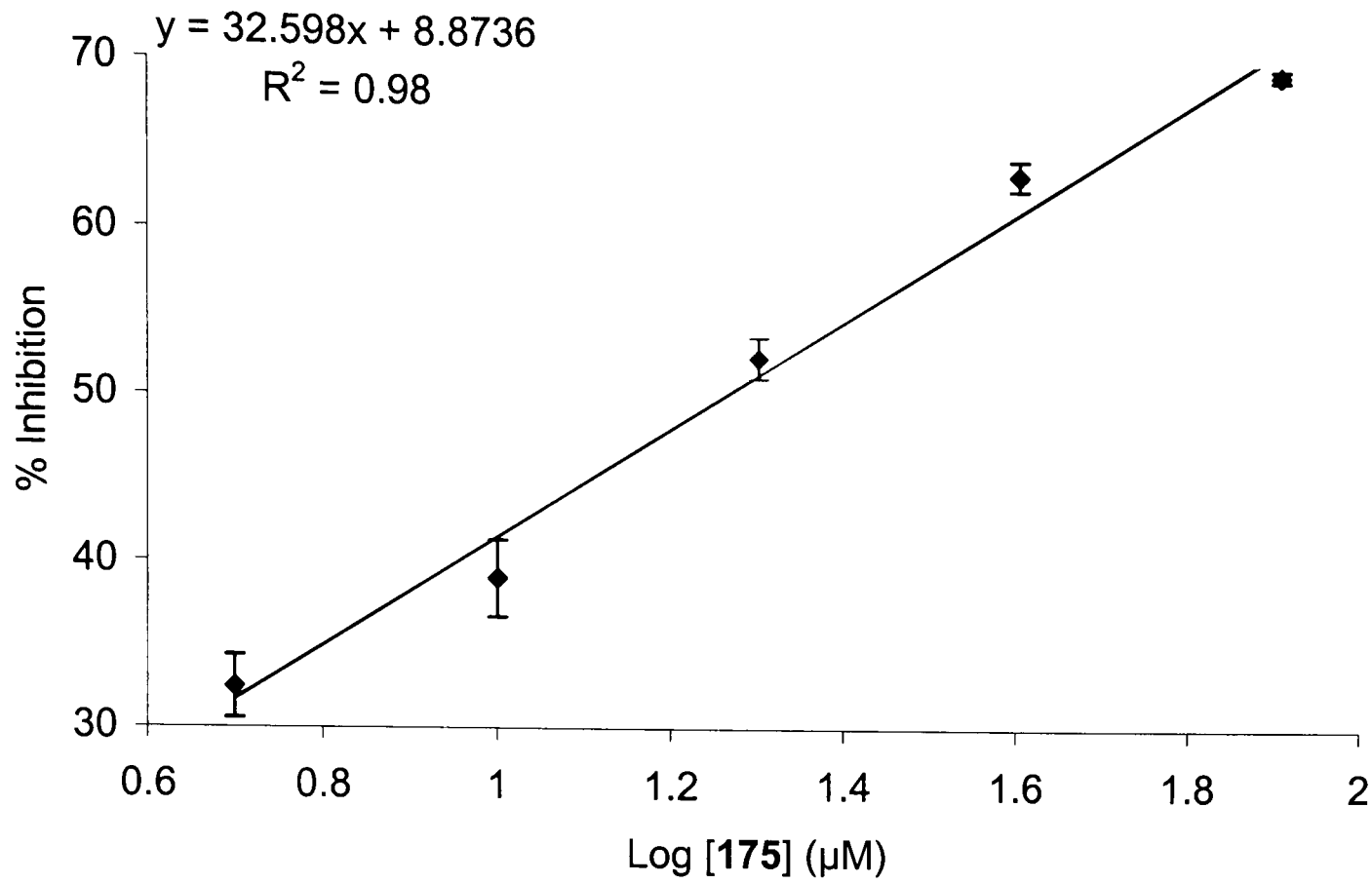

Figure 2.103 Plot of percentage inhibition versus log [**175**] for 1-(4-fluoro-benzyl)-1*H*-imidazole (**175**) against 17,20-lyase.

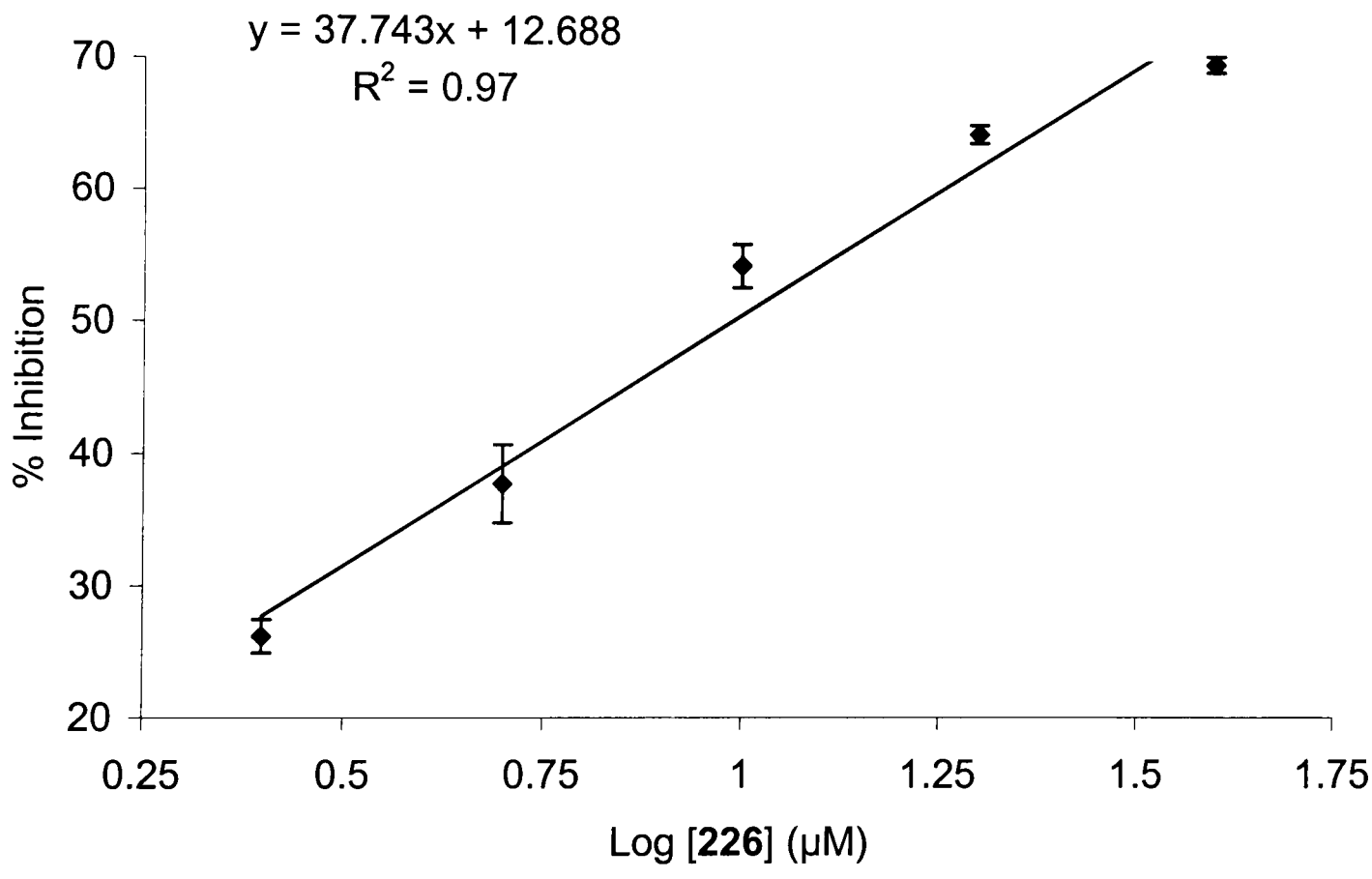

Figure 2.104 Plot of percentage inhibition versus log [**226**] for 1-(3,4-difluoro-benzyl)-1*H*-imidazole (**226**) against 17,20-lyase.

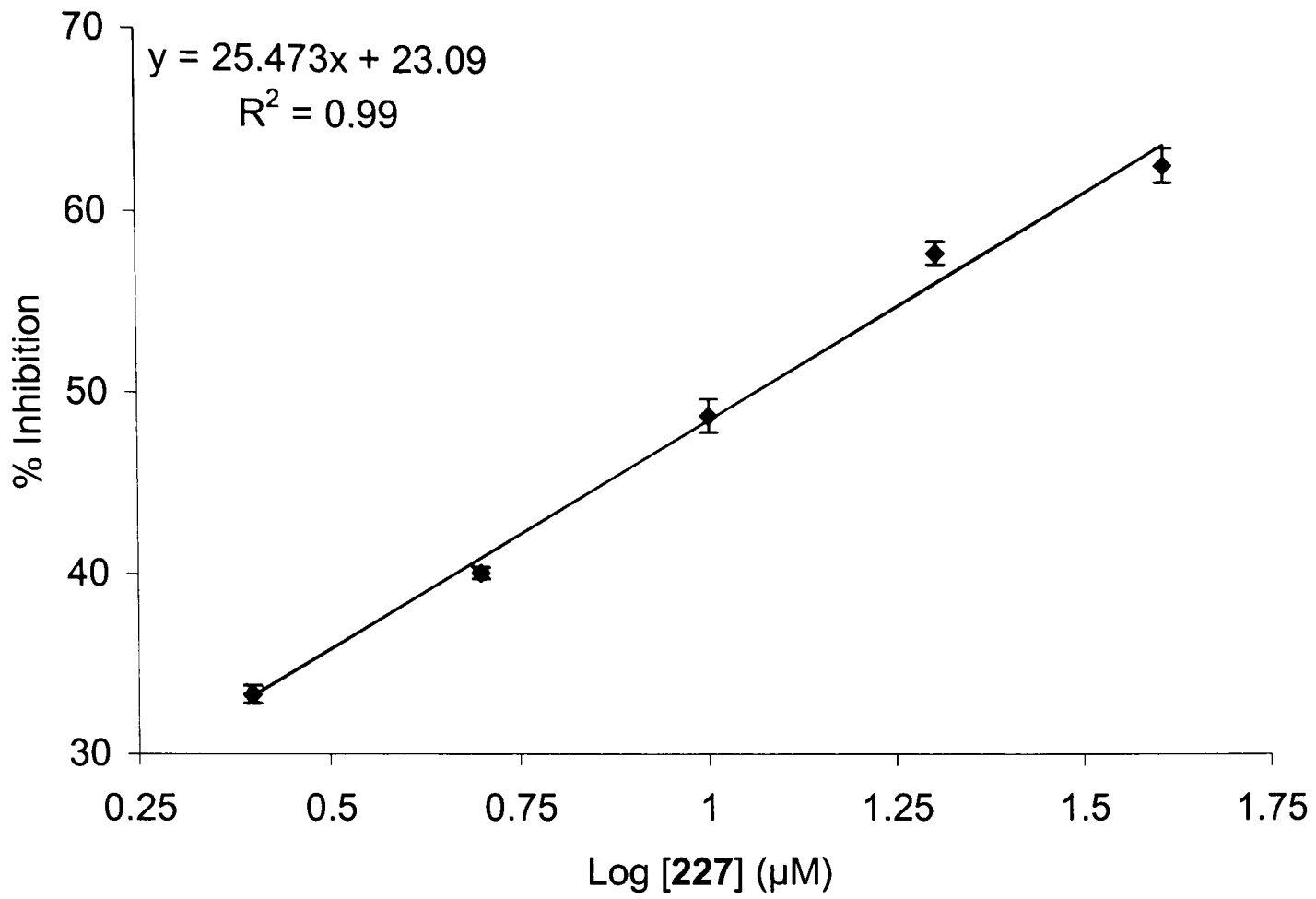

Figure 2.105 Plot of percentage inhibition versus log [**227**] for 1-(3,5-difluoro-benzyl)-1*H*-imidazole (**227**) against 17,20-lyase.

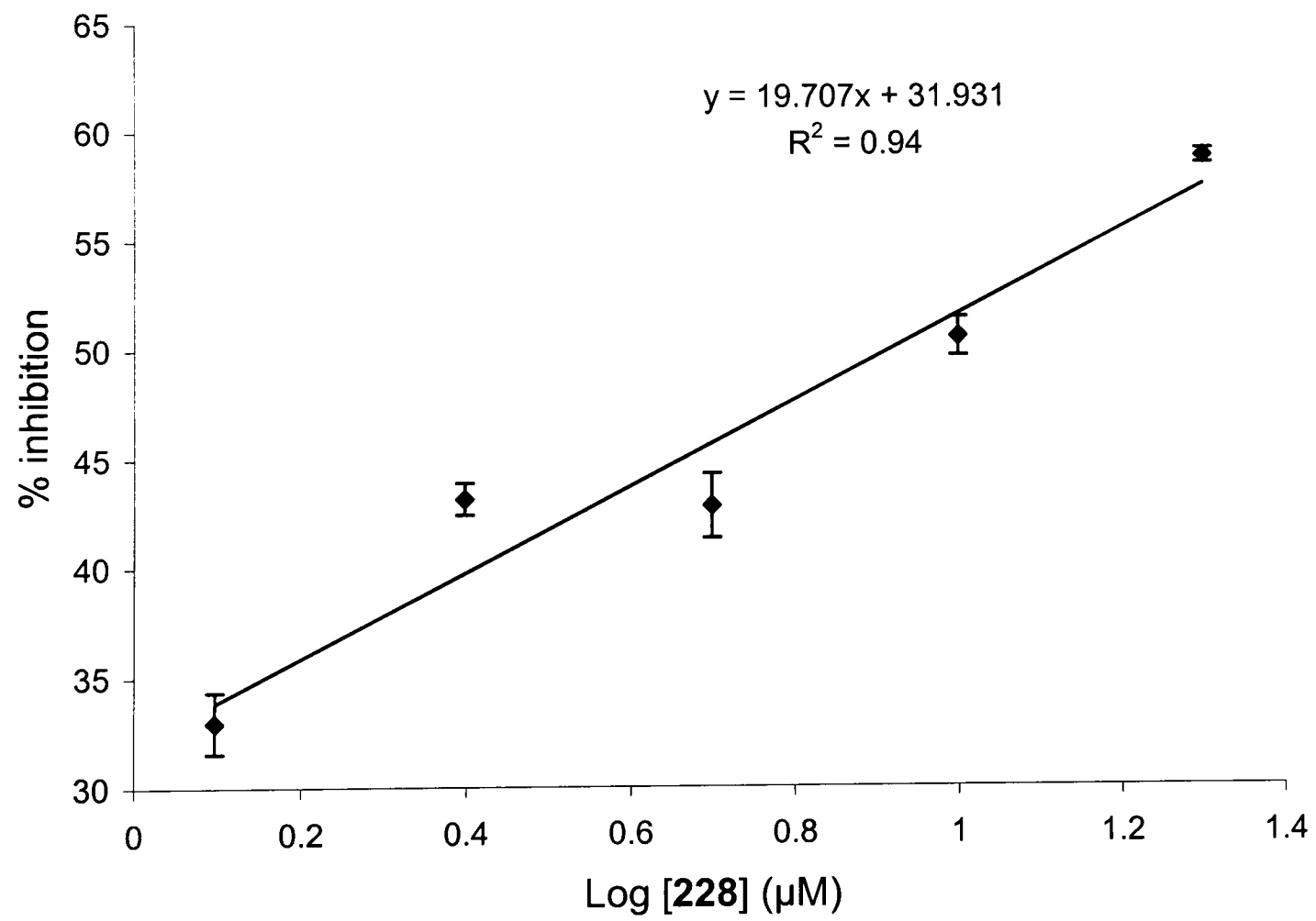

Figure 2.106 Plot of percentage inhibition versus log [**228**] for 1-(2-chloro-benzyl)-1*H*-imidazole (**228**) against 17,20-lyase.

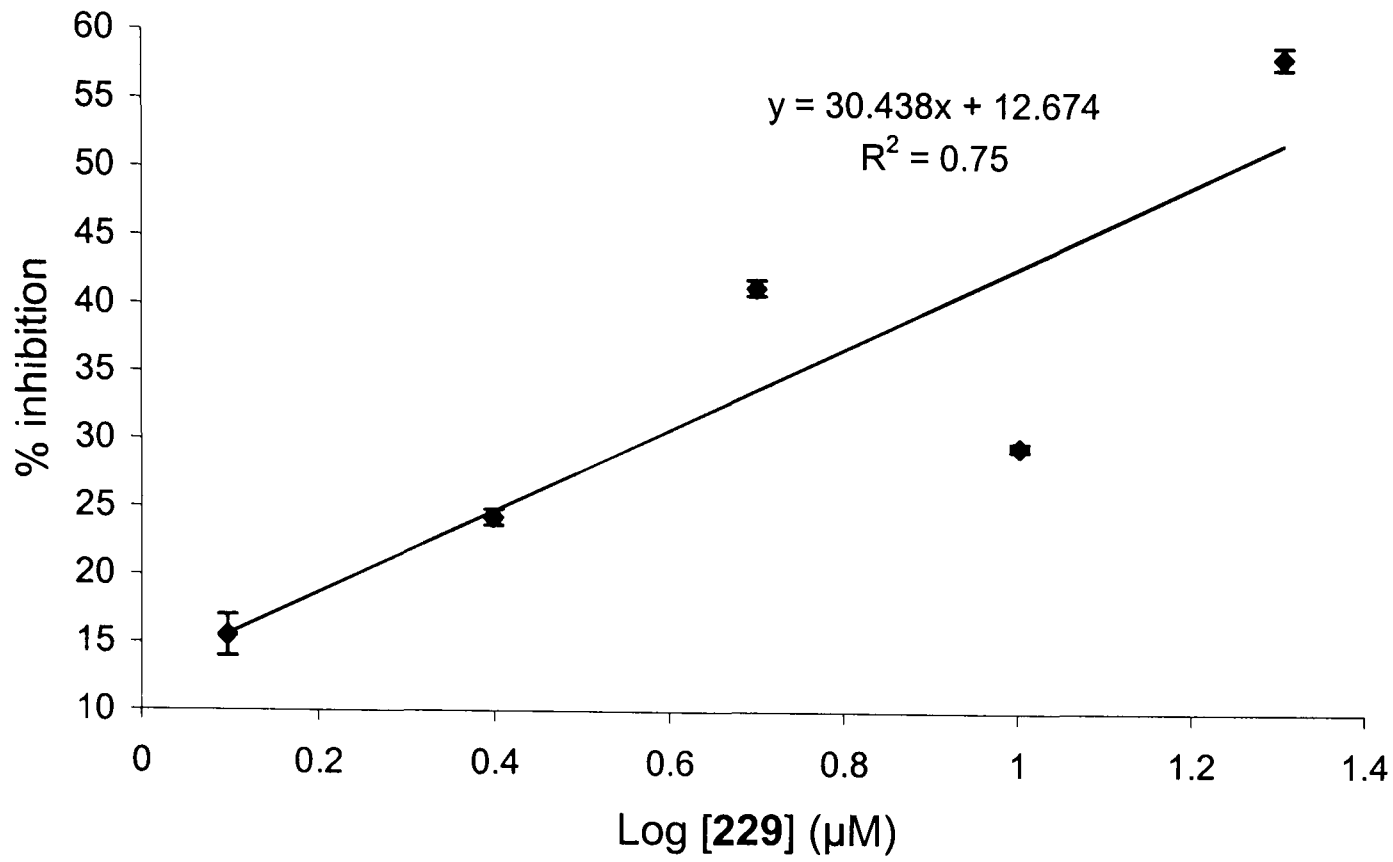

Figure 2.107 Plot of percentage inhibition versus log [**229**] for 1-(3-chloro-benzyl)-1*H*-imidazole (**229**) against 17,20-lyase.

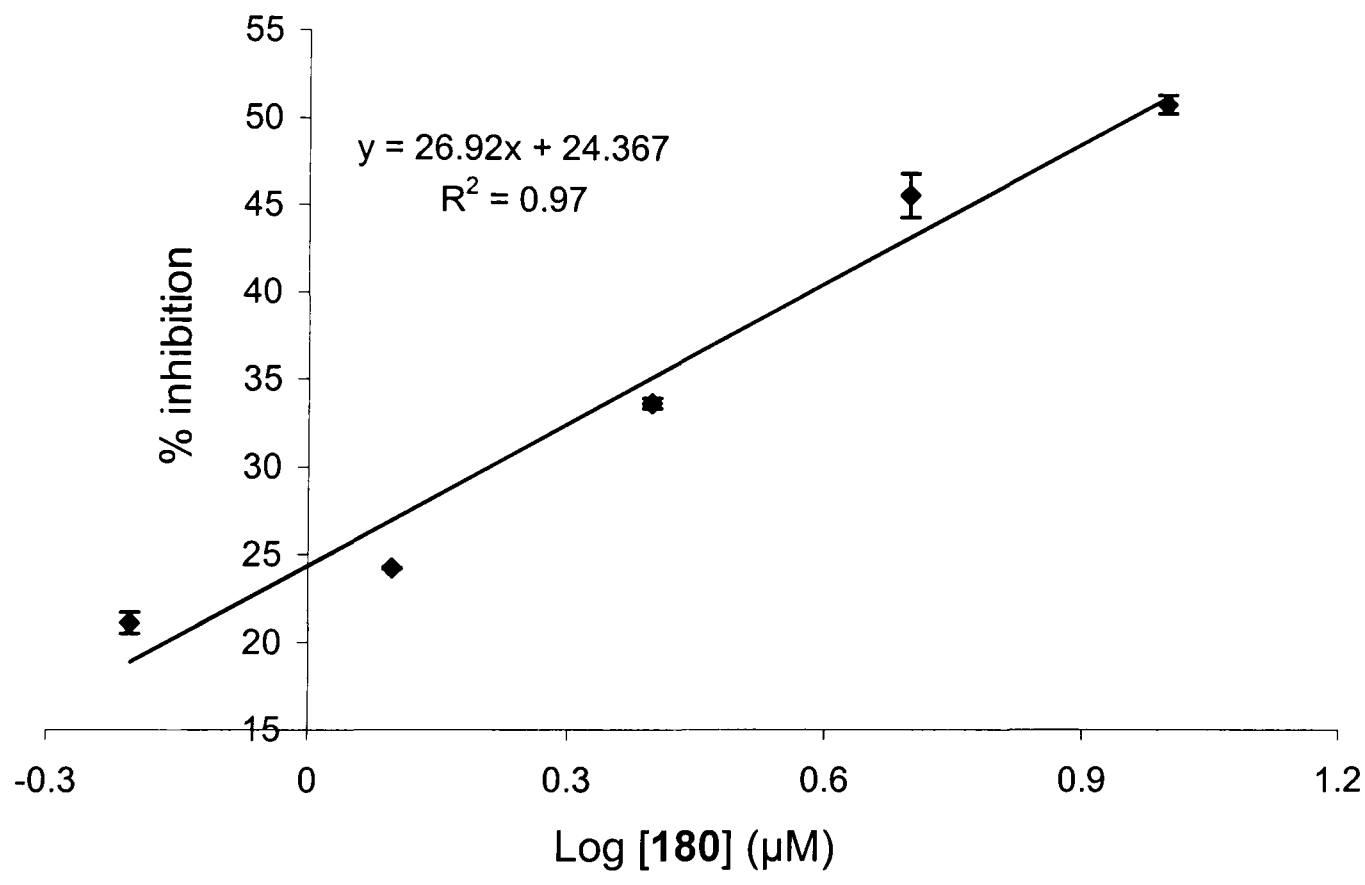

Figure 2.108 Plot of percentage inhibition versus log [**180**] for 1-(4-chloro-benzyl)-1*H*-imidazole (**180**) against 17,20-lyase.

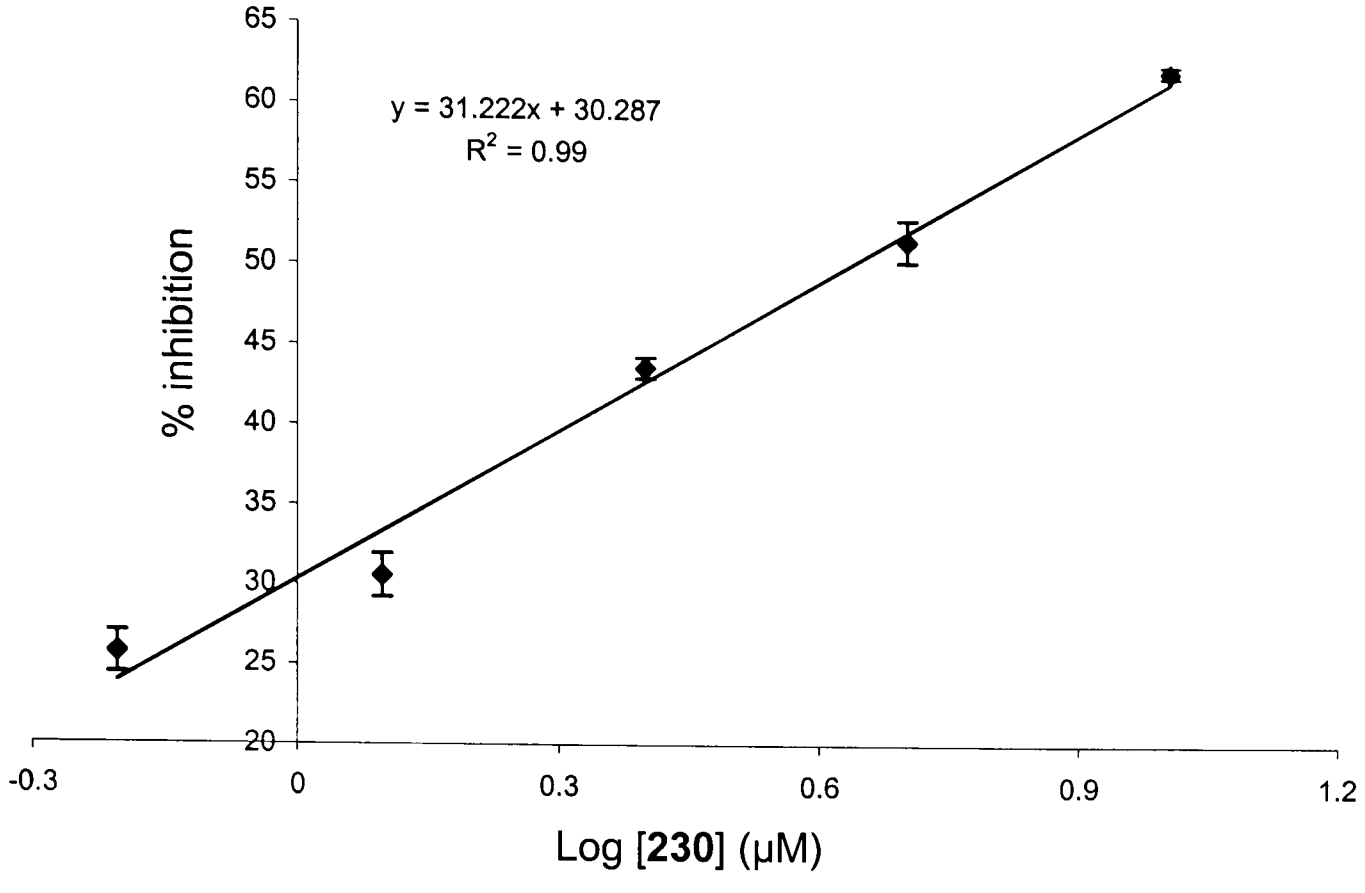

Figure 2.109 Plot of percentage inhibition versus log [**230**] for 1-(2,3-dichloro-benzyl)-1*H*-imidazole (**230**) against 17,20-lyase.

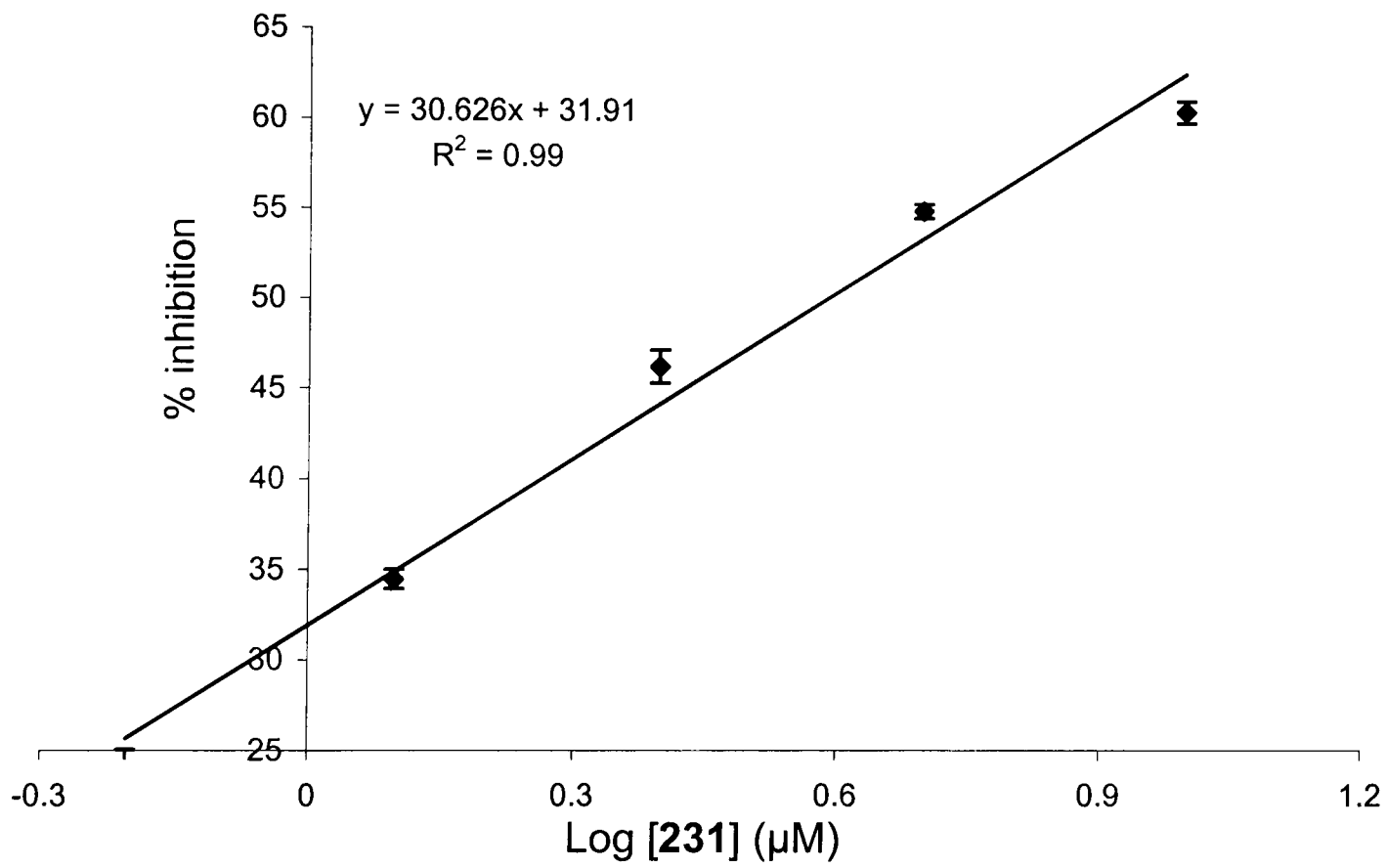

Figure 2.110 Plot of percentage inhibition versus log [**231**] for 1-(2,4-dichloro-benzyl)-1*H*-imidazole (**231**) against 17,20-lyase.

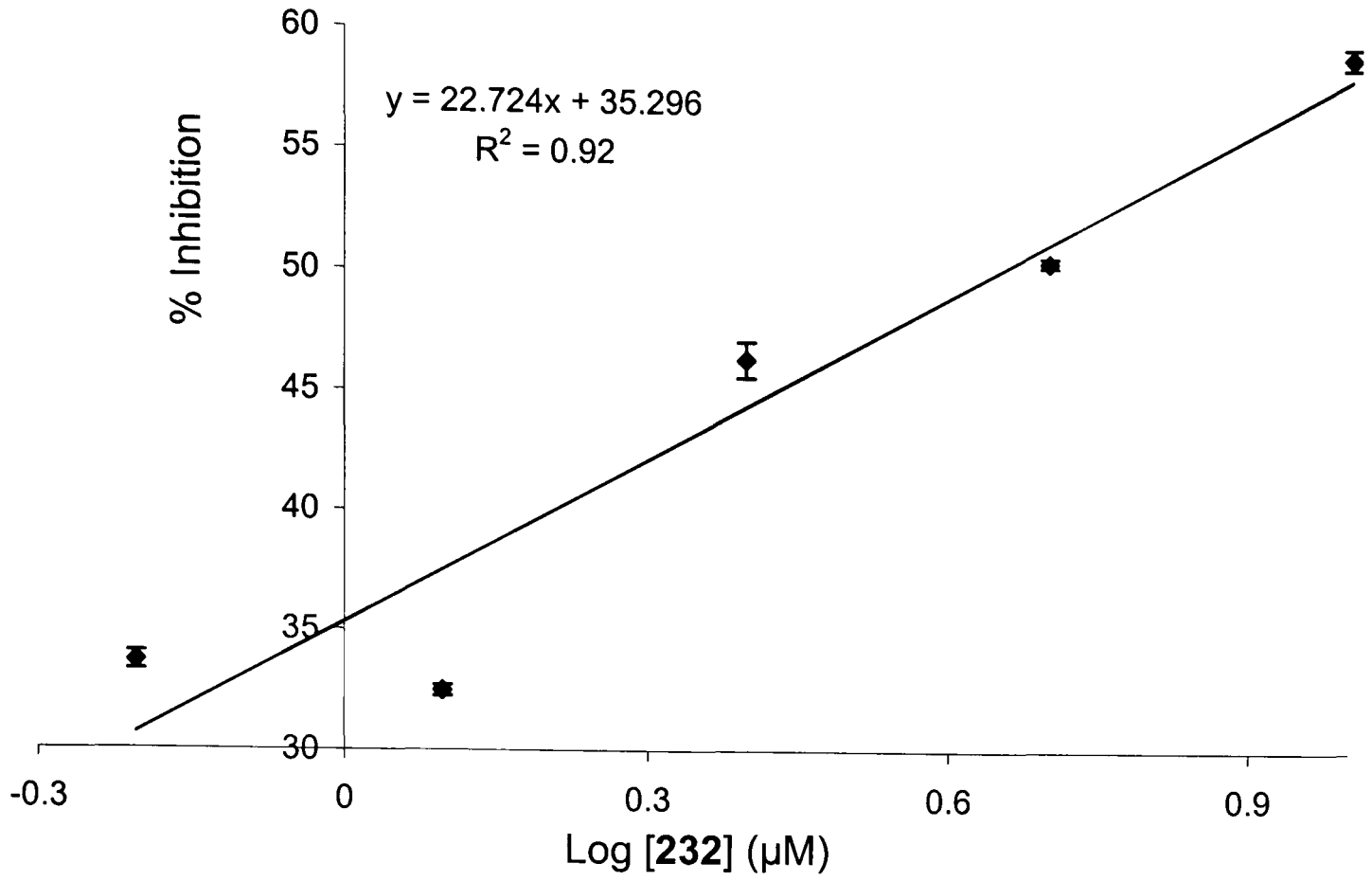

Figure 2.111 Plot of percentage inhibition versus log [**232**] for 1-(2,5-dichloro-benzyl)-1*H*-imidazole (**232**) against 17,20-lyase.

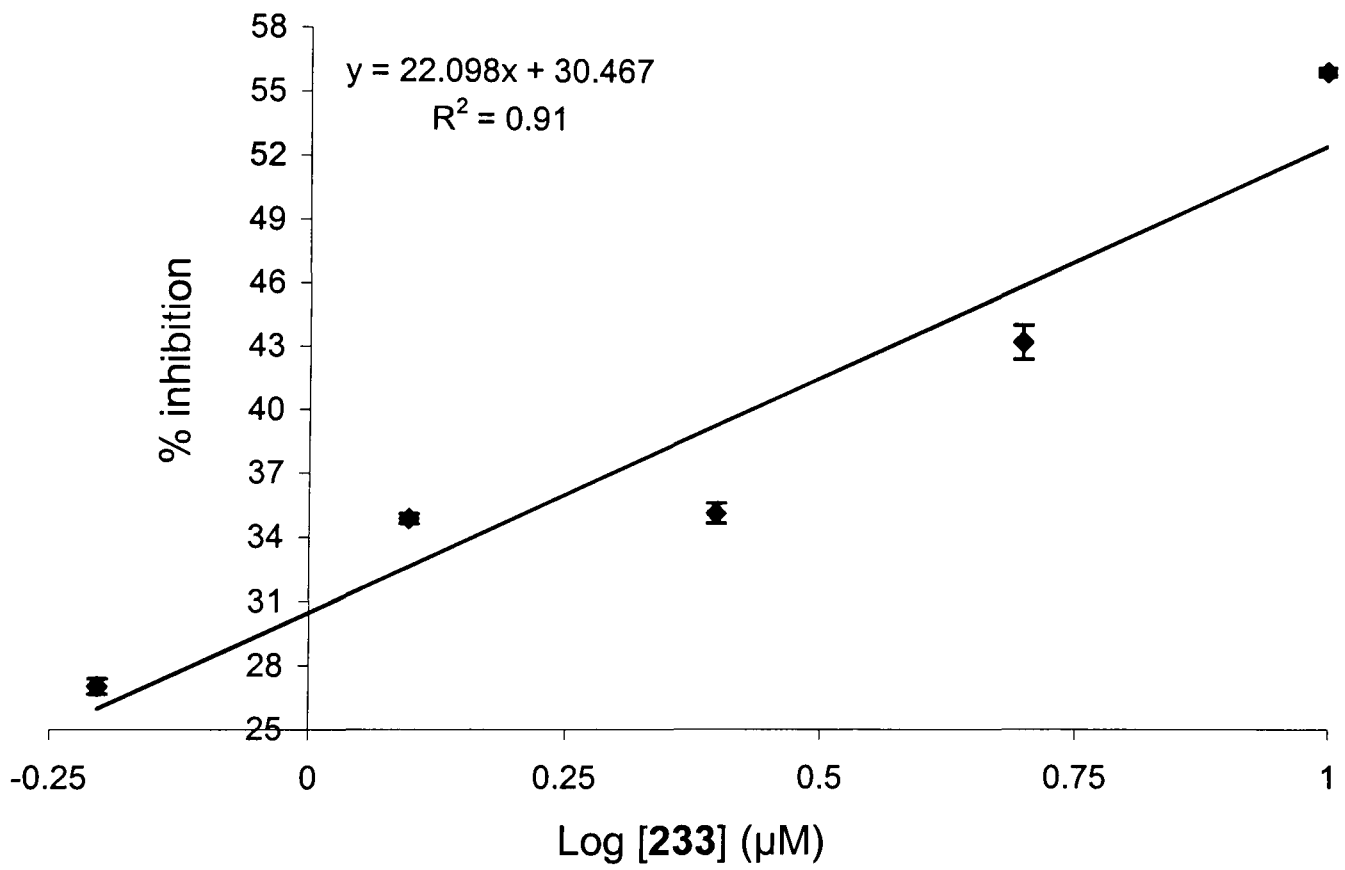

Figure 2.112 Plot of percentage inhibition versus log [**233**] for 1-(2,6-dichloro-benzyl)-1*H*-imidazole (**233**) against 17,20-lyase.

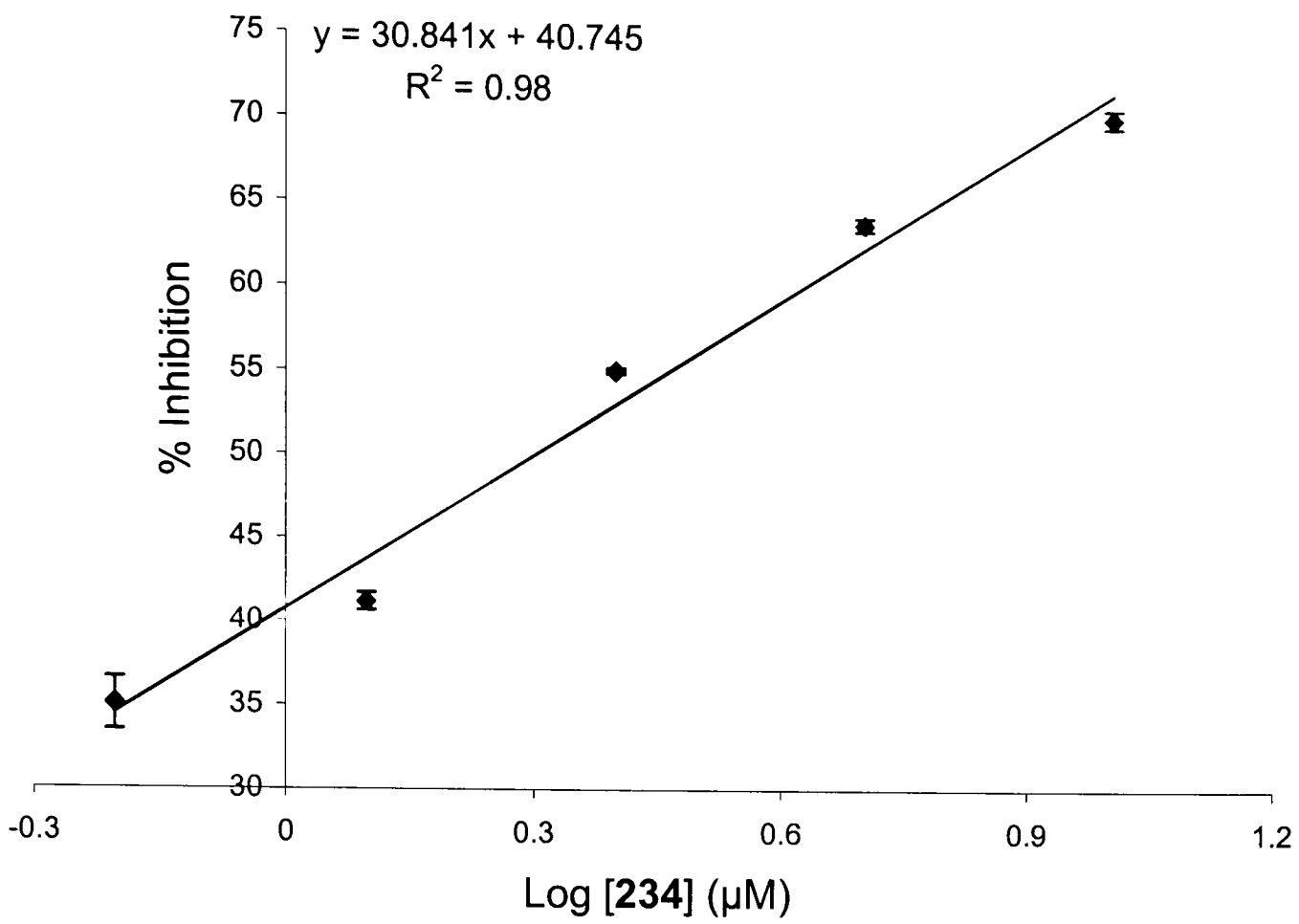

Figure 2.113 Plot of percentage inhibition versus log [**234**] for 1-(3,4-dichloro-benzyl)-1*H*-imidazole (**234**) against 17,20-lyase.

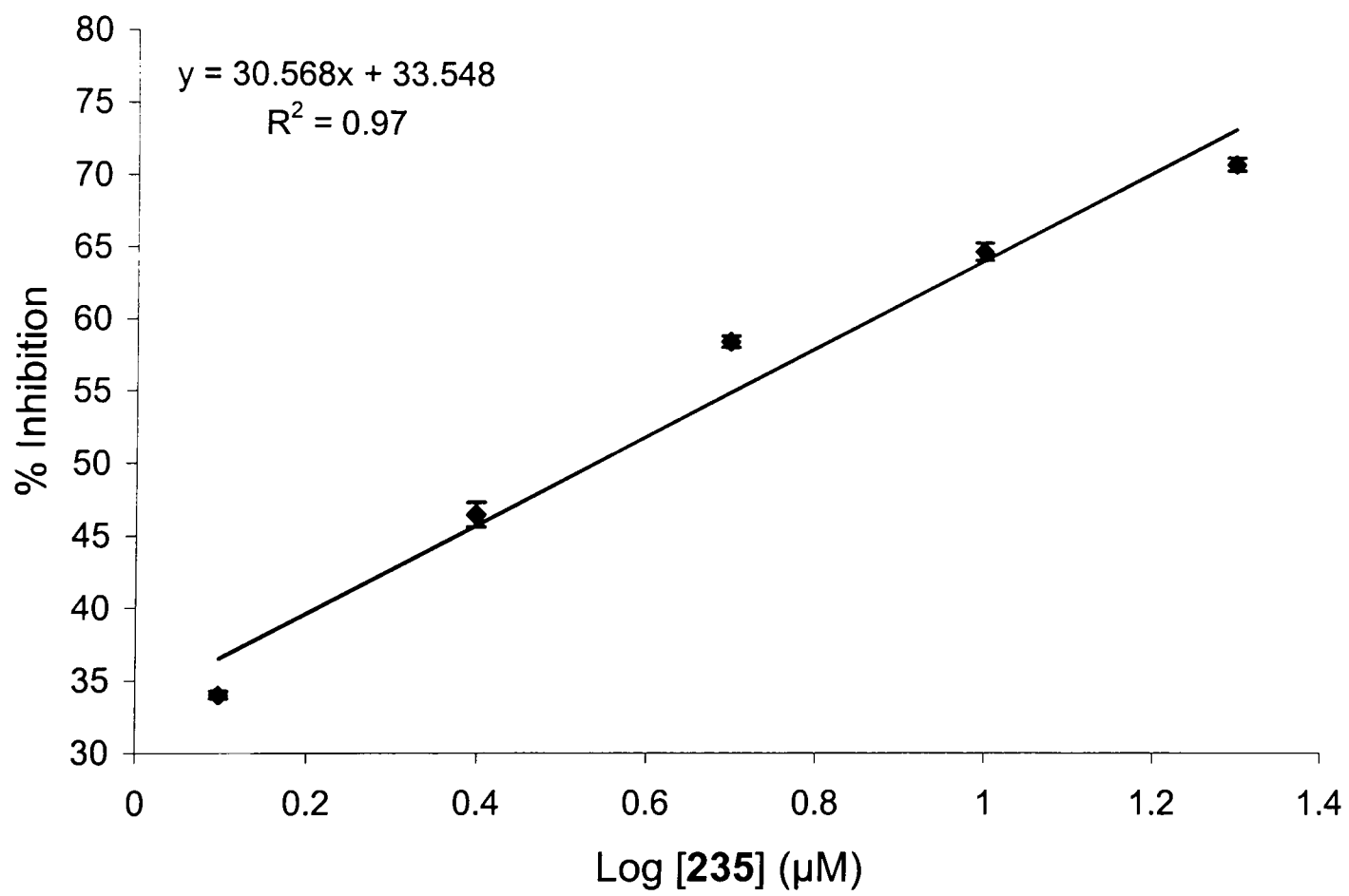

Figure 2.114 Plot of percentage inhibition versus log [**235**] for 1-(3,5-dichloro-benzyl)-1*H*-imidazole (**235**) against 17,20-lyase.

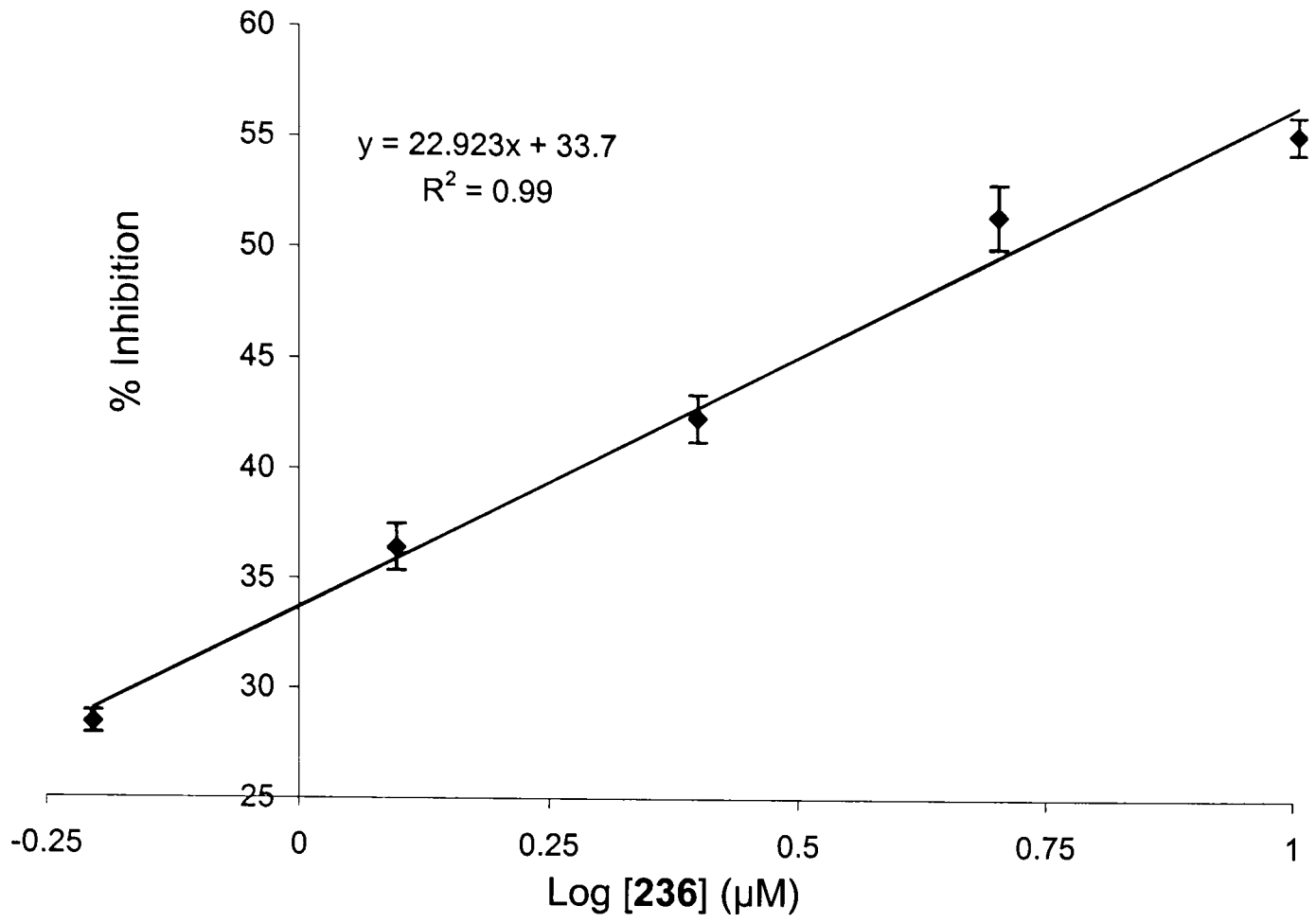

Figure 2.115 Plot of percentage inhibition versus log [**236**] for 1-(2-bromo-benzyl)-1*H*-imidazole (**236**) against 17,20-lyase.

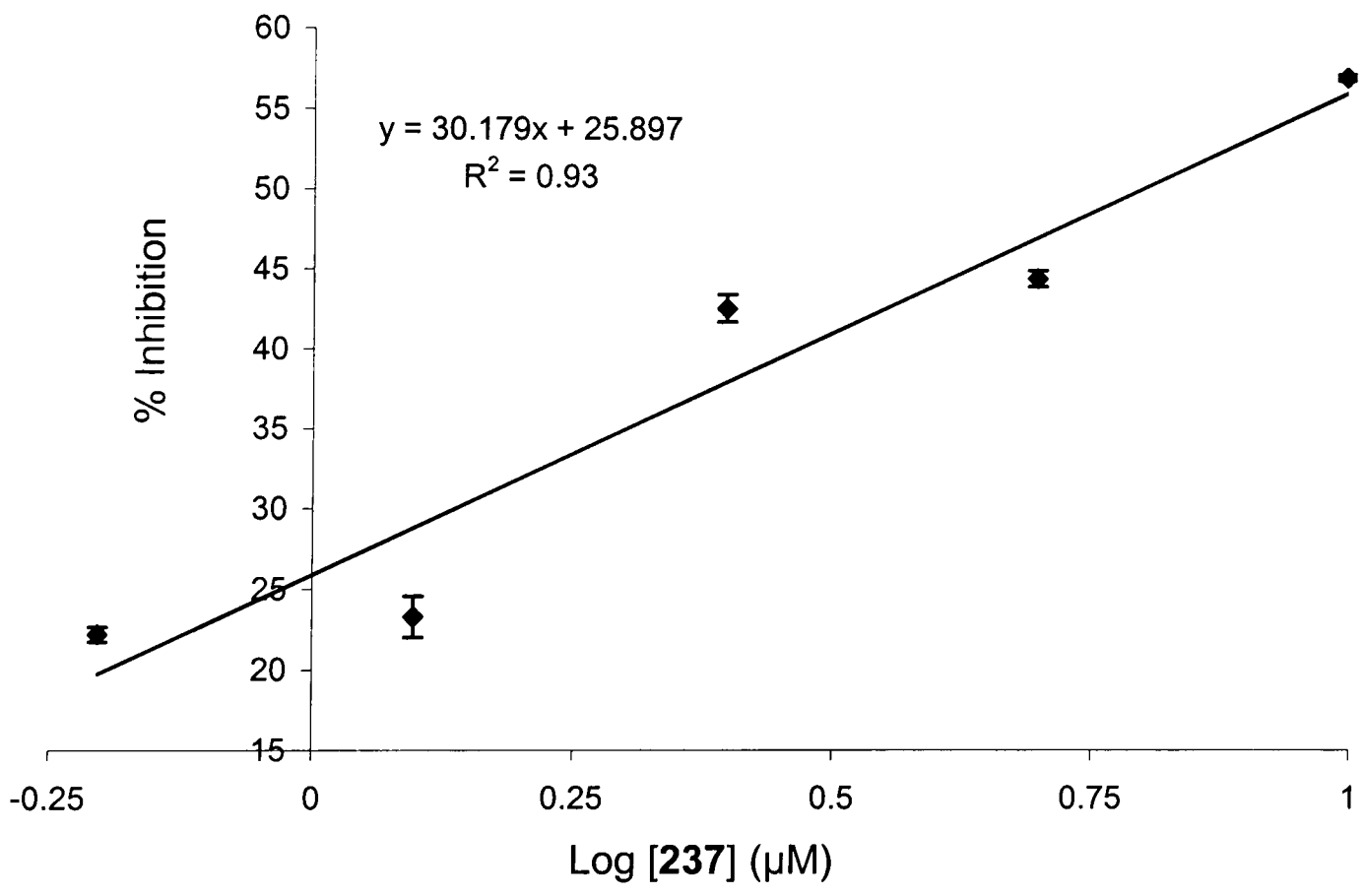

Figure 2.116 Plot of percentage inhibition versus log [**237**] for 1-(3-bromo-benzyl)-1*H*-imidazole (**237**) against 17,20-lyase.

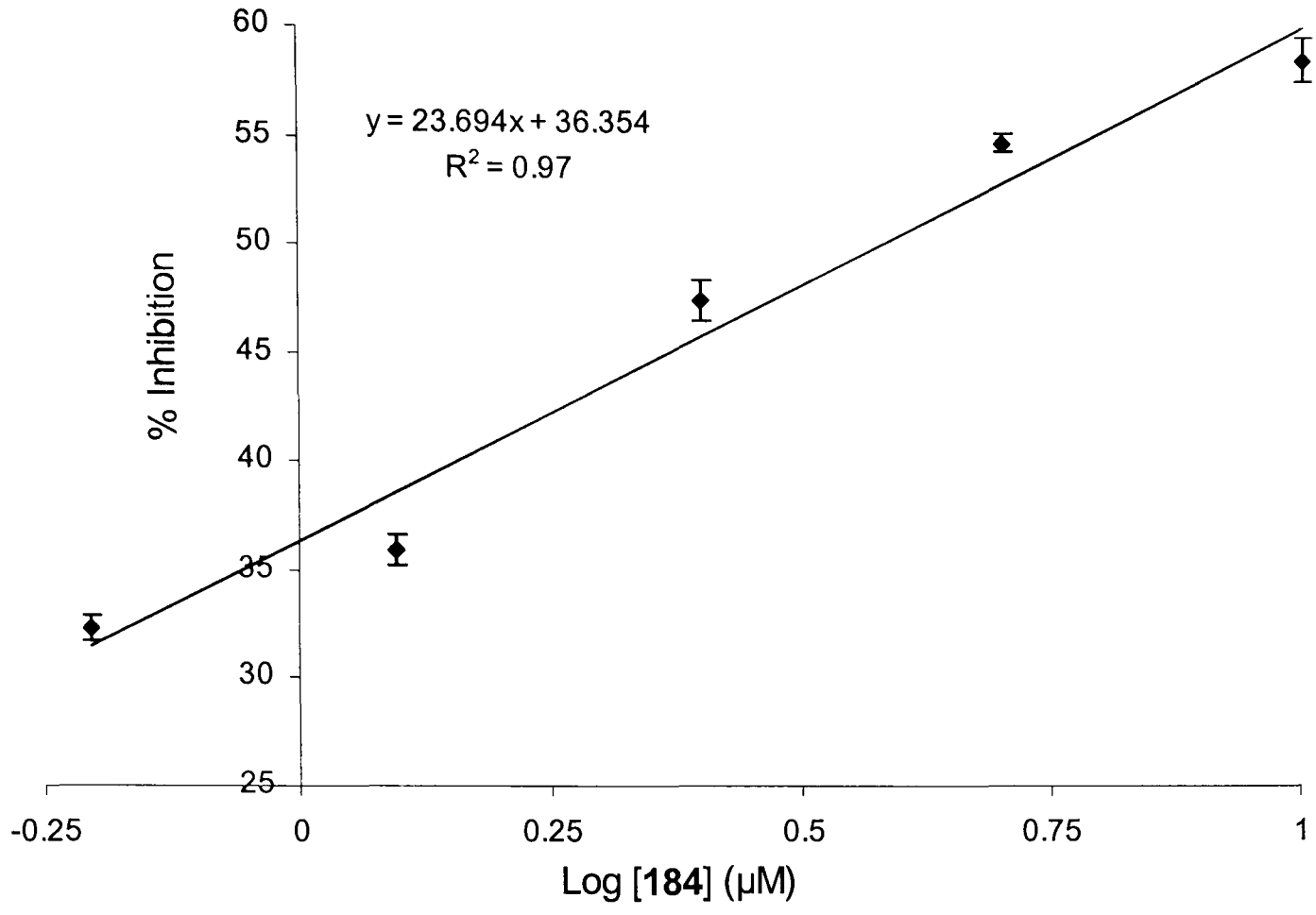

Figure 2.117 Plot of percentage inhibition versus log [**184**] for 1-(4-bromo-benzyl)-1*H*-imidazole (**184**) against 17,20-lyase.

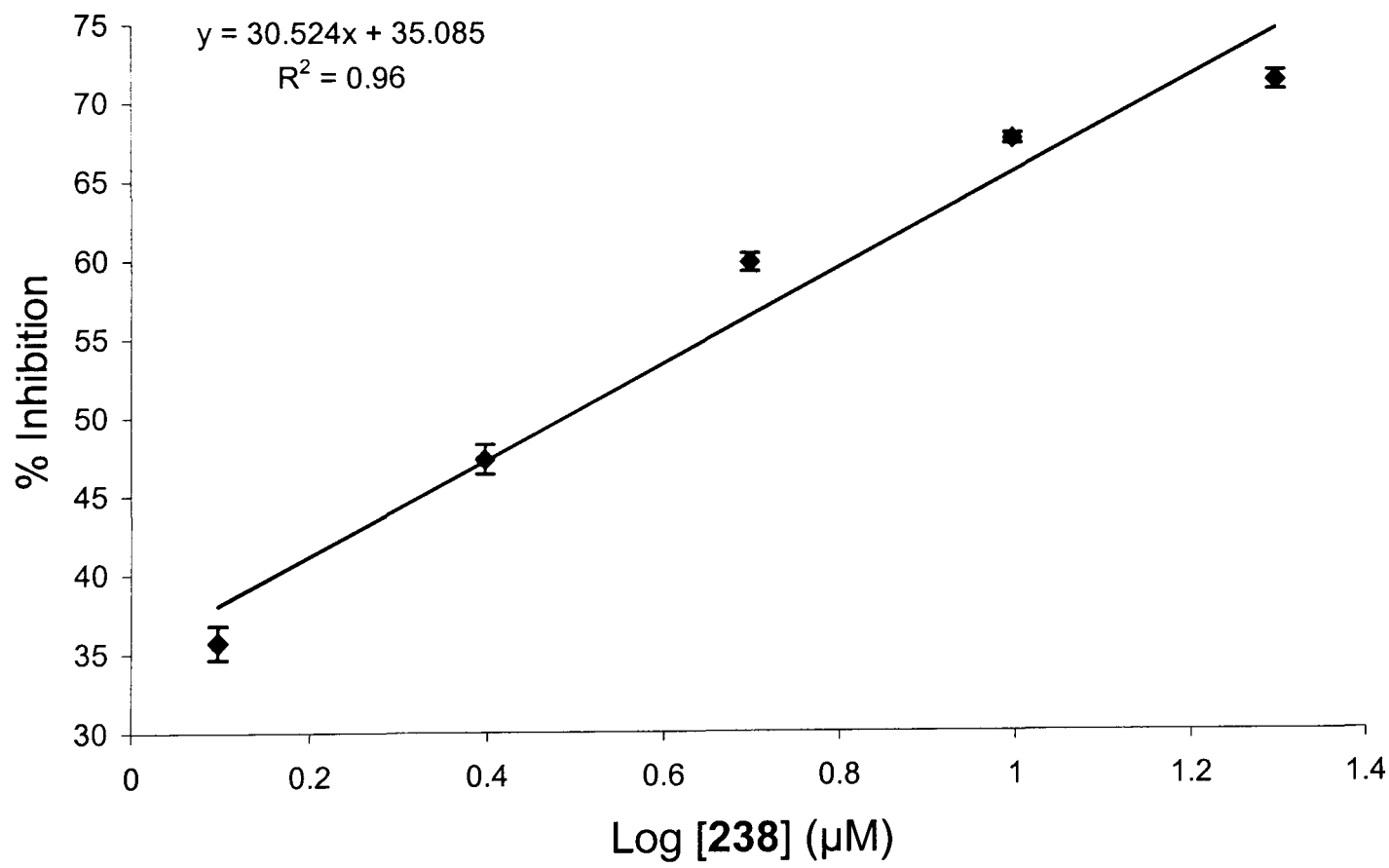

Figure 2.118 Plot of percentage inhibition versus log [**238**] for 1-(3,5-dibromo-benzyl)-1*H*-imidazole (**238**) against 17,20 lyase.

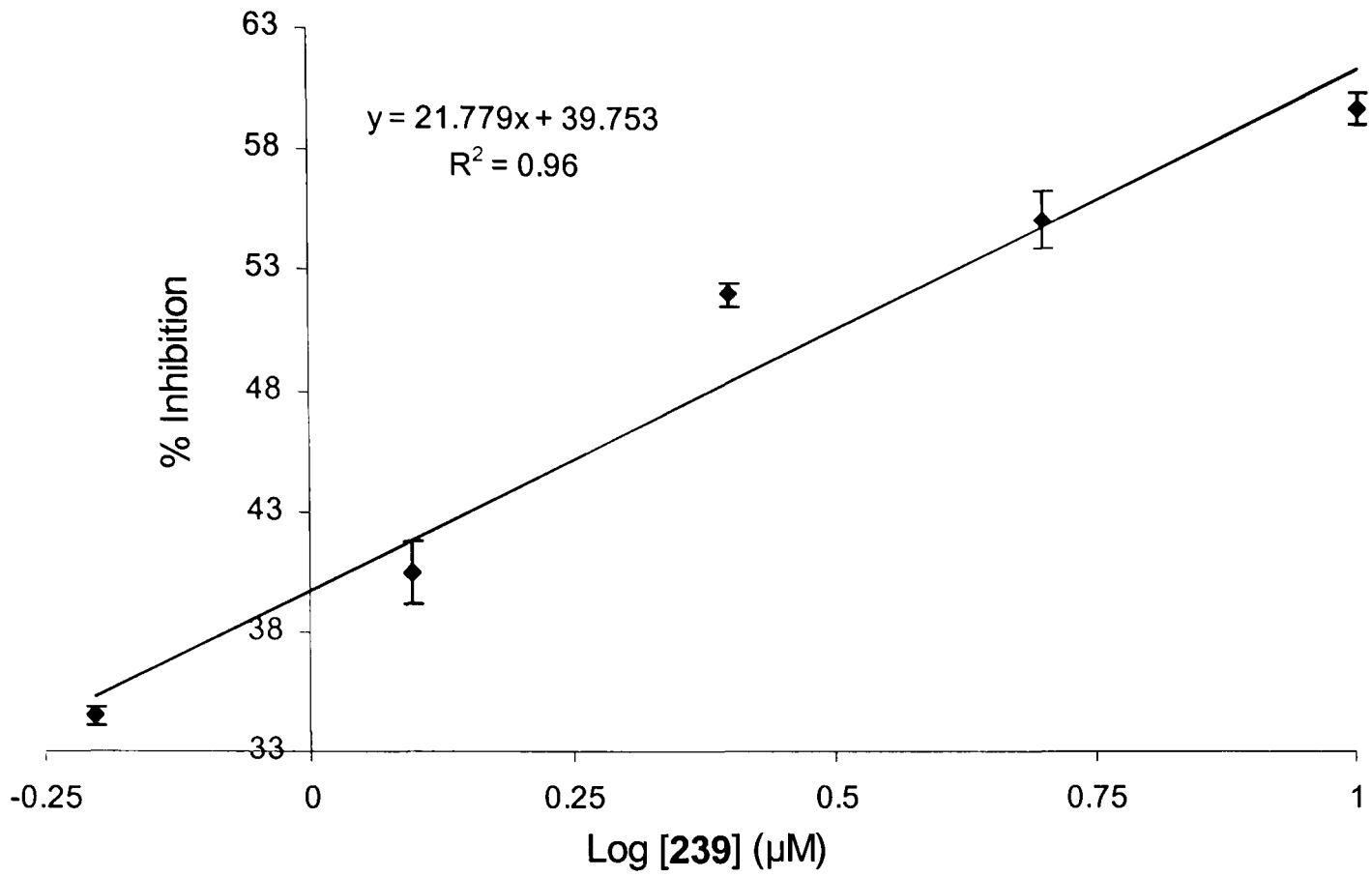

Figure 2.119 Plot of percentage inhibition versus log [**239**] for 1-(2-iodo-benzyl)-1*H*-imidazole (**239**) against 17,20-lyase.

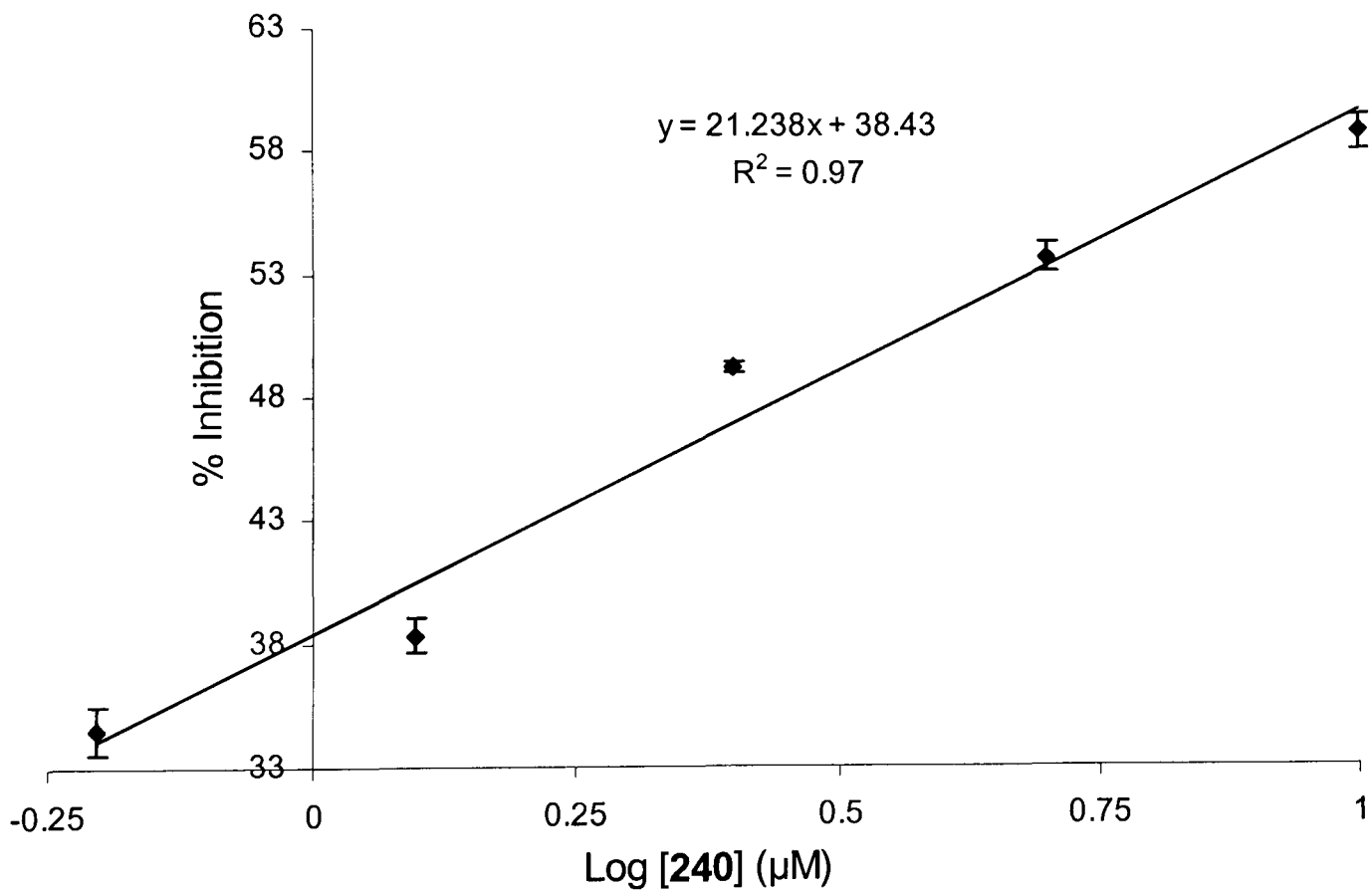

Figure 2.120 Plot of percentage inhibition versus log [**240**] for 1-(3-iodo-benzyl)-1*H*-imidazole (**240**) against 17,20-lyase.

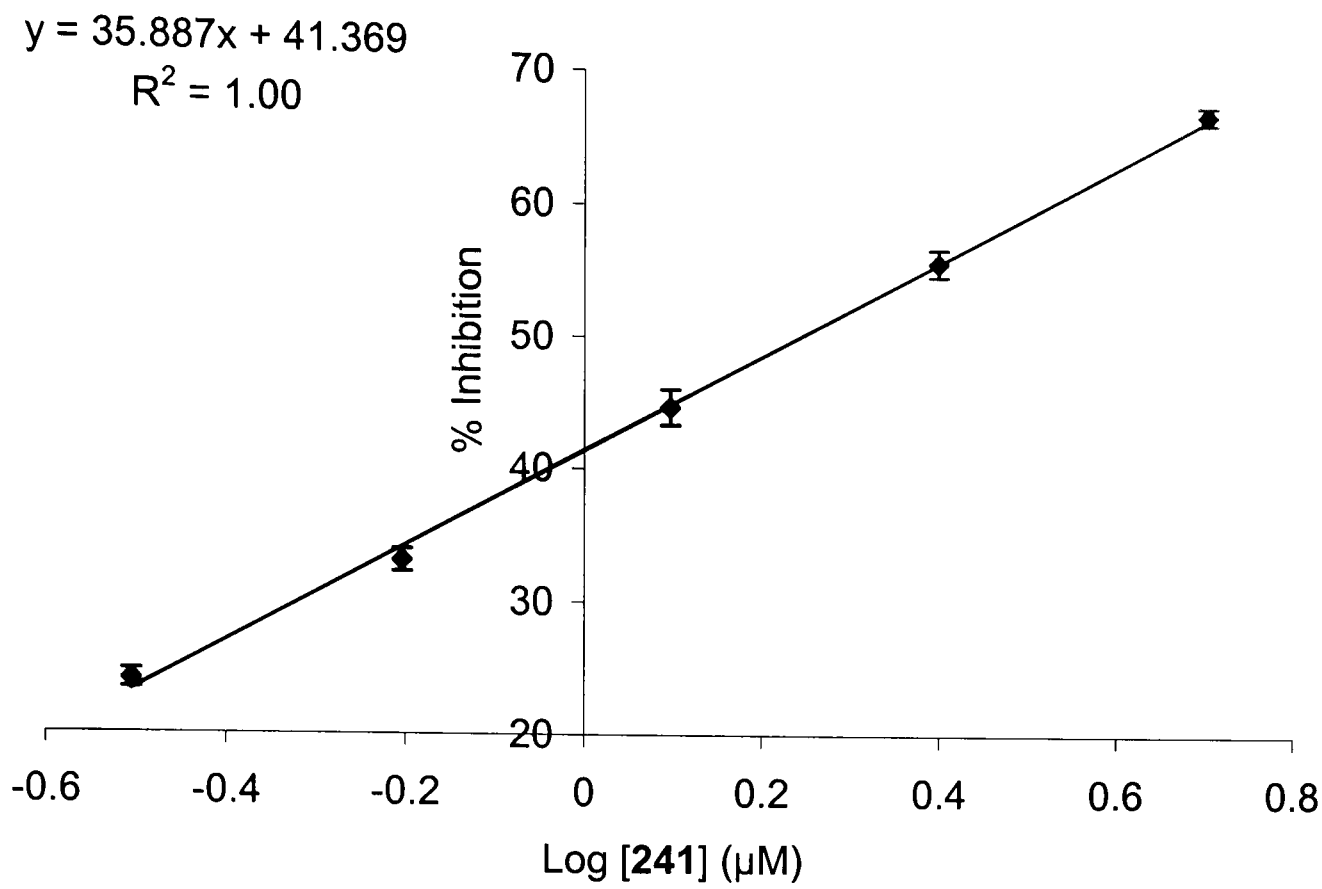

Figure 2.121 Plot of percentage inhibition versus log [**241**] for 1-(4-iodo-benzyl)-1*H*-imidazole (**241**) against 17,20-lyase.

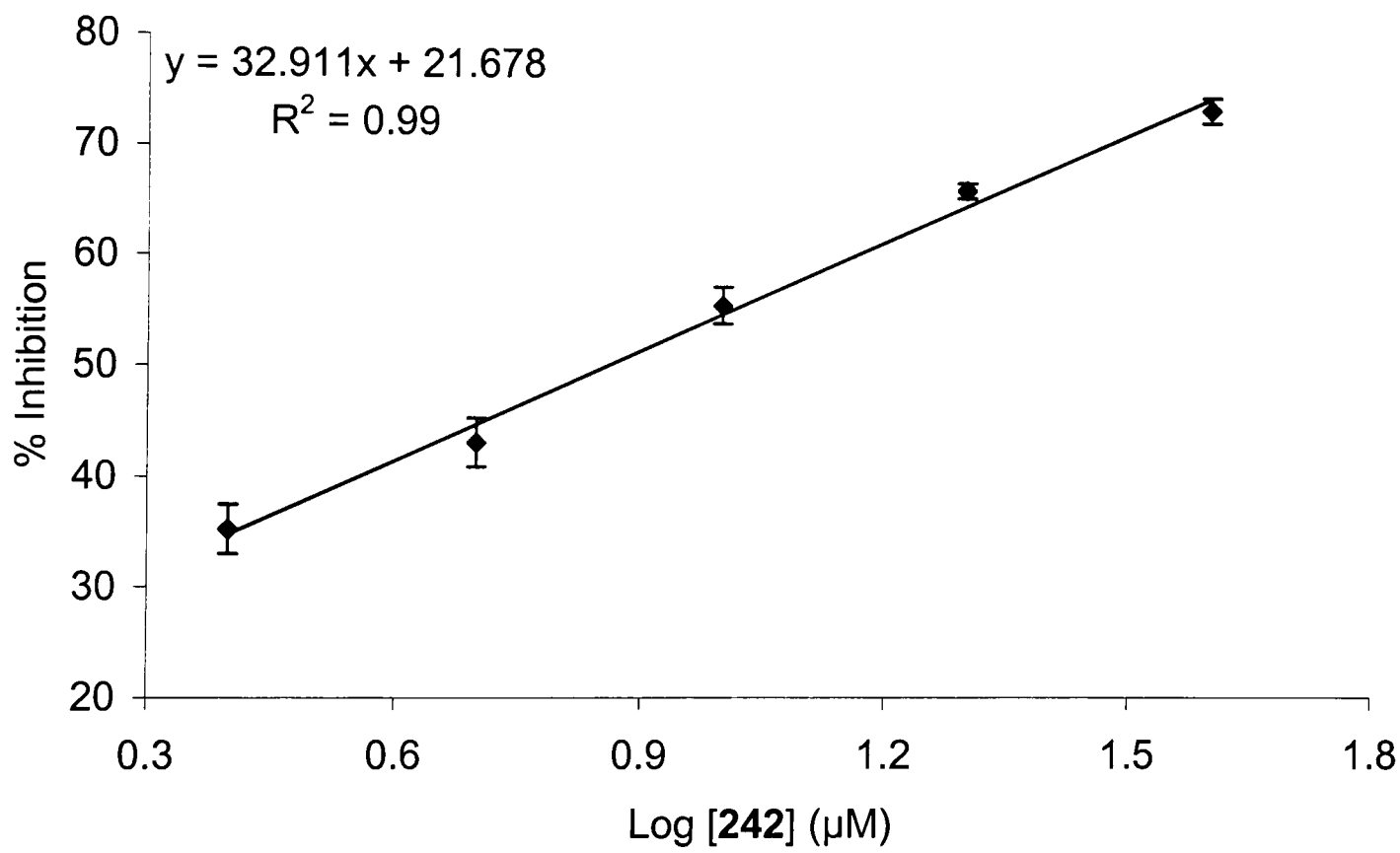

Figure 2.122 Plot of percentage inhibition versus log [**242**] for 4-imidazol-1-ylmethyl-phenol (**242**) against 17,20-lyase.

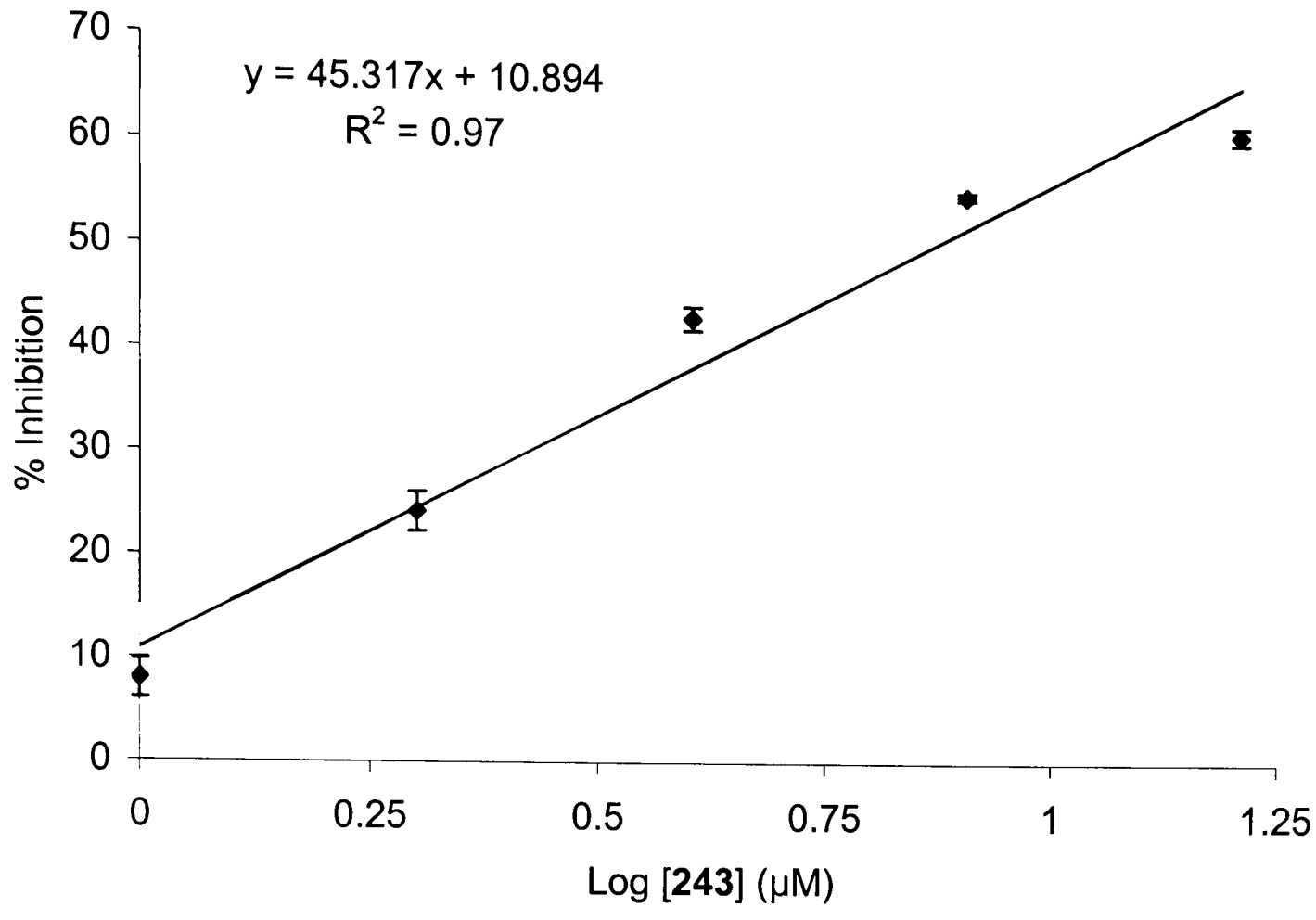

Figure 2.123 Plot of percentage inhibition versus log [**243**] for 1-(4-Nitro-benzyl)-4*H*-imidazole (**243**) against 17,20-lyase.

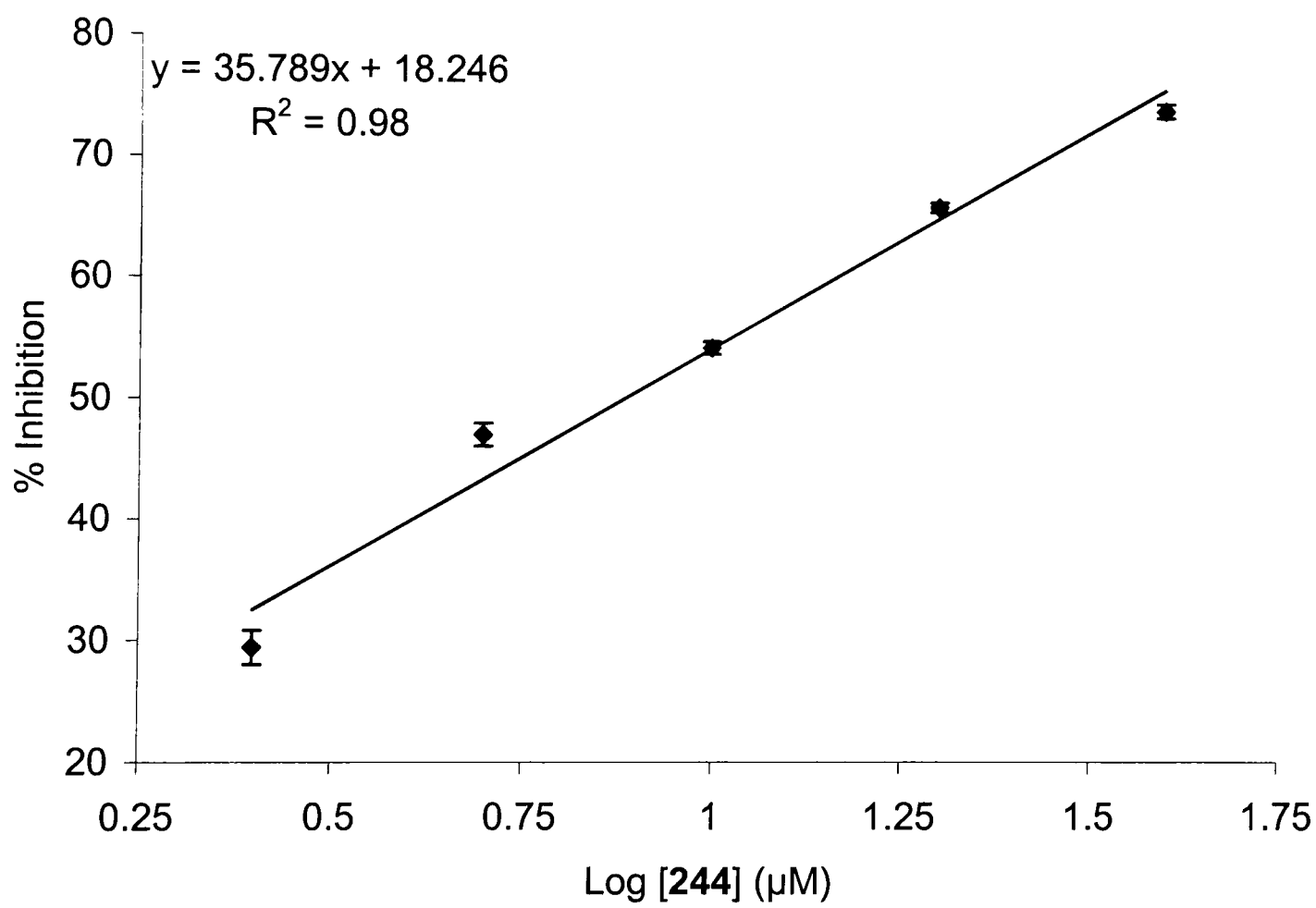

Figure 2.124 Plot of percentage inhibition versus log [**244**] for 4-imidazol-1-ylmethyl-benzonitrile (**244**) against 17,20-lyase.

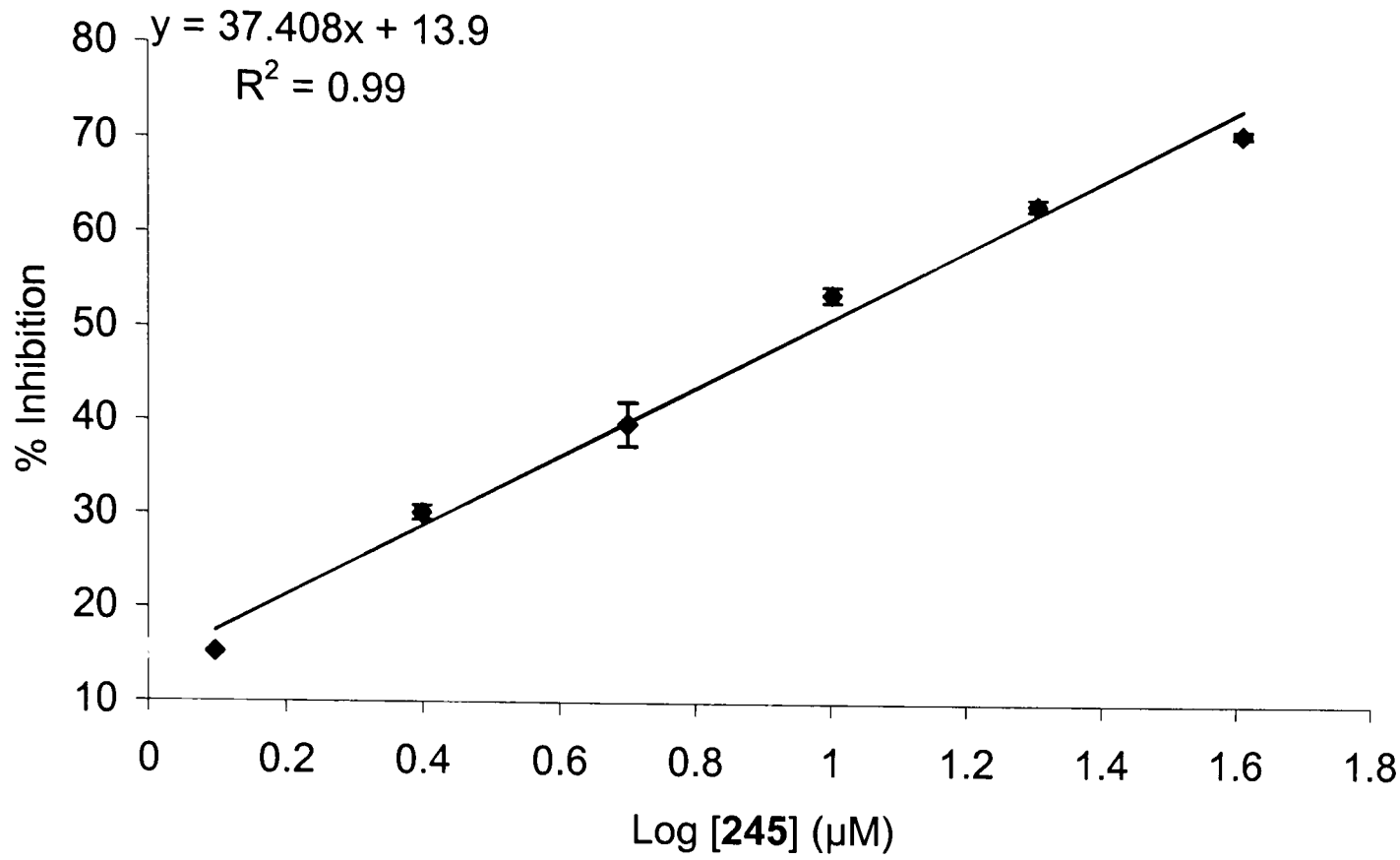

Figure 2.125 Plot of percentage inhibition versus log [**245**] for 1-(4-methyl-benzyl)-1*H*-imidazole (**245**) against 17,20-lyase.

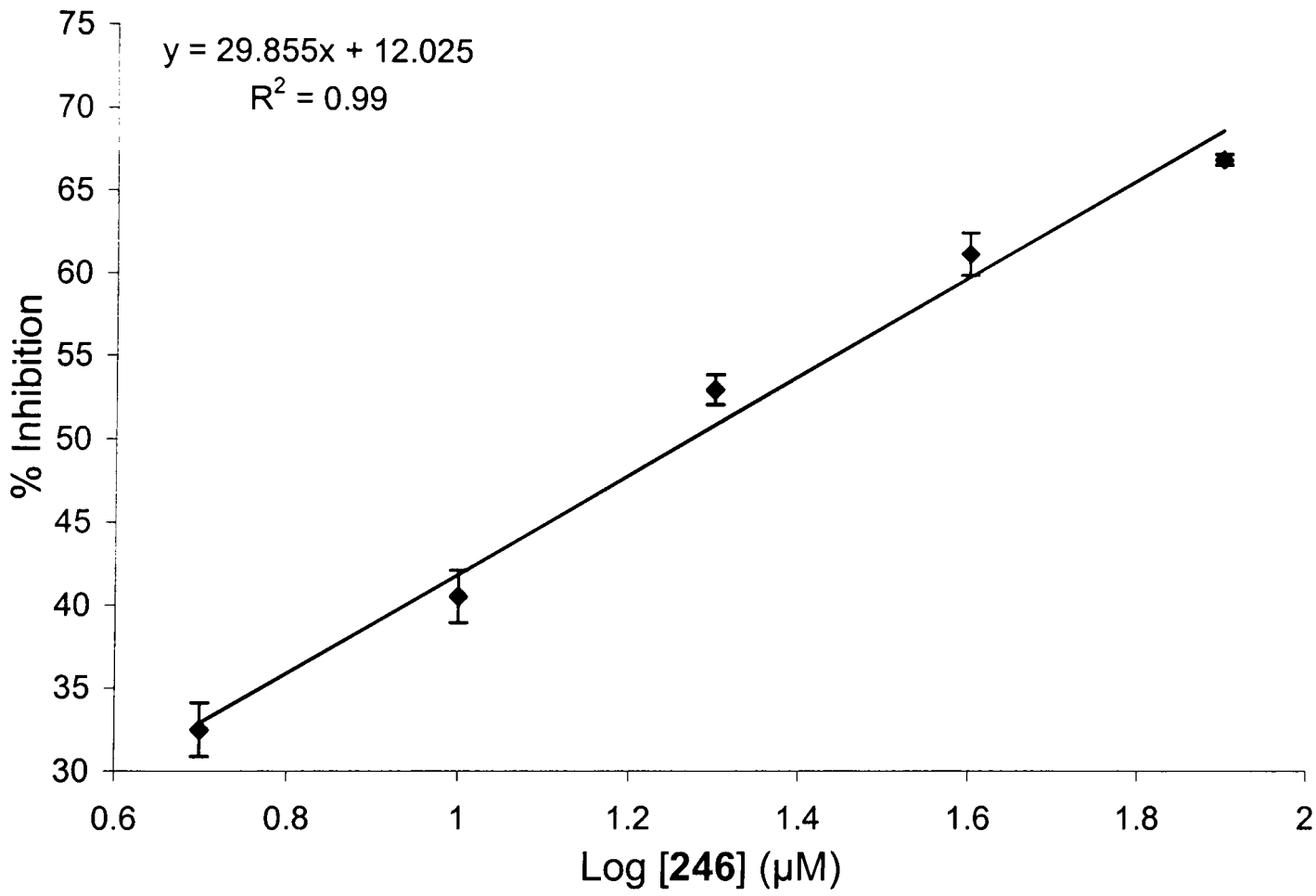

Figure 2.126 Plot of percentage inhibition versus log [**246**] for 1-(3,5-Bis-trifluoromethyl-benzyl)-1*H*-imidazole (**246**) against 17,20-lyase.

2.47 Determination of the Dissociation Constant of the Enzyme-Inhibitor Complex (K_i) for a number of Inhibitors against 17α-Hydroxylase

K_i is the dissociation constant of the enzyme-inhibitor complex and is thus used to compare the affinity of the inhibitor for the enzyme. K_i determination was carried out for ketoconazole and also for those compounds that had a lower IC_{50} than ketoconazole.

The assay involved the incubation, in triplicate, of varying inhibitor concentrations at varying final substrate concentrations. Each assay tube contained substrate (of varying final concentration, 15μL), NADPH-generating system (25μL), phosphate buffer (445μL), enzyme (0.10mg/mL final concentration, 5μL) and inhibitor (of varying final concentration, 10μl). The procedure was otherwise as that described earlier (Section 2.38).

2.48 Determination of the K_i values for a number of Inhibitors against 17,20-Lyase

K_i determination was carried out for ketoconazole and also for those compounds that had a higher potency than that of ketoconazole. The assay involved the incubation, in triplicate, of varying inhibitor concentrations at varying final substrate concentrations. Each assay tube contained substrate (of varying final concentration, 10μL), NADPH-generating system (10μL), phosphate buffer (174μL), enzyme (0.19mg/mL final concentration, 2μL) and inhibitor (of varying final concentration, 4μL). The procedure was otherwise as that described earlier (Section 2.44).

2.49 Results – Graphical Determination of K_i

The K_i for each inhibitor was calculated by two different graphical methods:

(1) The velocity, v, for each reaction at each inhibitor concentration was determined in a similar manner to that described in Section 2.10/2.23

(equation 2.2/2.4) and a Dixon plot carried out to determine (i) the K_i value, and (ii) the type of reversible inhibition occuring, for each inhibitor. In the Dixon plots of 1/v versus [I], the point of intersection of the lines at different substrate concentration gives the K_i value on the [I] ordinate. In cases where the lines cross at two or more points, the values are averaged to give a mean value for K_i.

(2) A Lineweaver-Burk plot of 1/v versus 1/[S] for each inhibitor concentration was obtained and the slope of each plot plotted against the inhibitor concentration. The K_i was obtained by extrapolation of the line to the negative abscissa intercept.

The results and plots are shown in Table 2.14 and Figures 2.127 – 2.168.

2.49.1 Discussion

K_i values for ketoconazole obtained by other workers within the field against rat microsomes was 39.5μM (Li et al, 1992) and 160 ± 4.92nM (Ayub and Levell, 1987a) for 17α-hydroxylase and 3.6μM (Li et al, 1992) and 84 ± 3.5nM (Ayub and Levell, 1987a) for $C_{17,20}$-lyase where Km for 17α-hydroxylase was 33.85μM (Li et al, 1992) and 89 ± 0.65nM (Ayub and Levell, 1987a) and Km for $C_{17,20}$-lyase was 4.55μM (Li et al, 1992) and 250 ± 0.75nM (Ayub and Levell, 1987a). the K_i value we obtained for ketoconazole was 1.24 ± 0.01μM and 0.67 ± 0.02μM for 17α-hydroxylase and 17,20-lyase respectively. Compounds that showed more potency than ketoconazole were evaluated for K_i along with ketoconazole. K_i was also conducted on compounds **221** and **228** which were amongst the most potent benzyl imidazoles but with lower potency than ketoconazole. The Lineweaver-Burk plots seemed to indicate that the type of inhibition is mixed inhibition for all the compounds tested apart from ketoconazole which showed competitive inhibition.

Compound No.	Compound	17α-hydroxylase		17,20-lyase	
		K_i values (nM)	IC_{50} (nM)	K_i values (nM)	IC_{50} (nM)
1	**Ketoconazole**	1240.0 ± 10.0	3760.0 ± 10.0	665.0 ± 15.0	1660.0 ± 150.0
171	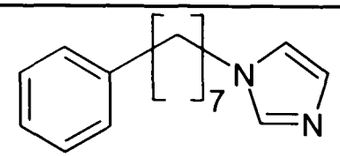	207.0 ± 11.0	320.0 ± 50.0	55.3 ± 3.4	99.0 ± 16.0
178	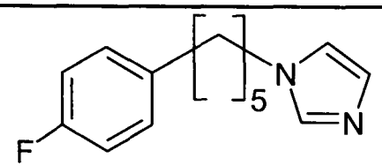	265.0 ± 13.0	750.0 ± 5.0	52.0 ± 2.0	100.0 ± 10.0
179	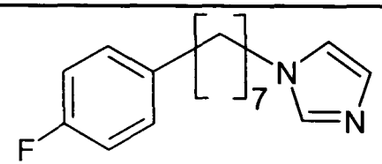	77.5 ± 2.5	173.62 ± 7.0	21.5 ± 0.1	57.5 ± 1.5
183	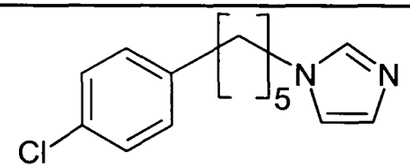	208.0 ± 6.0	570.0 ± 30.0	40.0 ± 2.0	86.0 ± 6.0
234	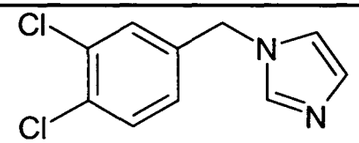	4740.0 ± 200.0	12220.0 ± 880.0	1855.0 ± 135.0	2065.5 ± 69.5
241	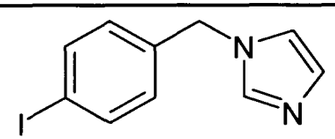	3930.0 ± 120.0	10060.0 ± 960.0	735.0 ± 55.0	1580.0 ± 170.0

Table 2.14 Results from IC_{50} and K_i data of some imidazoles for 17α-hydroxylase and 17,20-lyase activity.

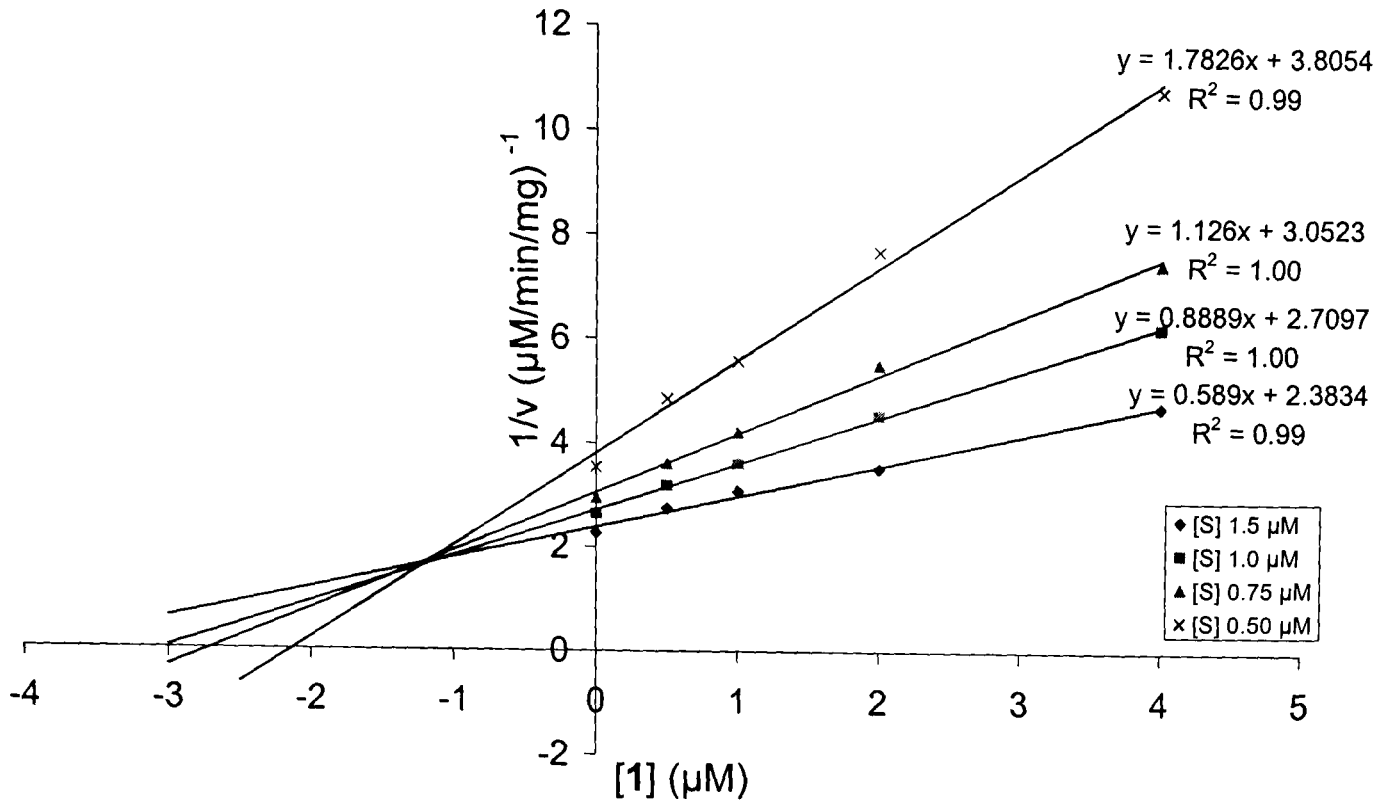

Figure 2.127 Dixon plot of 1/v versus [**1**] for ketoconazole (**1**) against 17α-hydroxylase giving a K_i value of 1230nM.

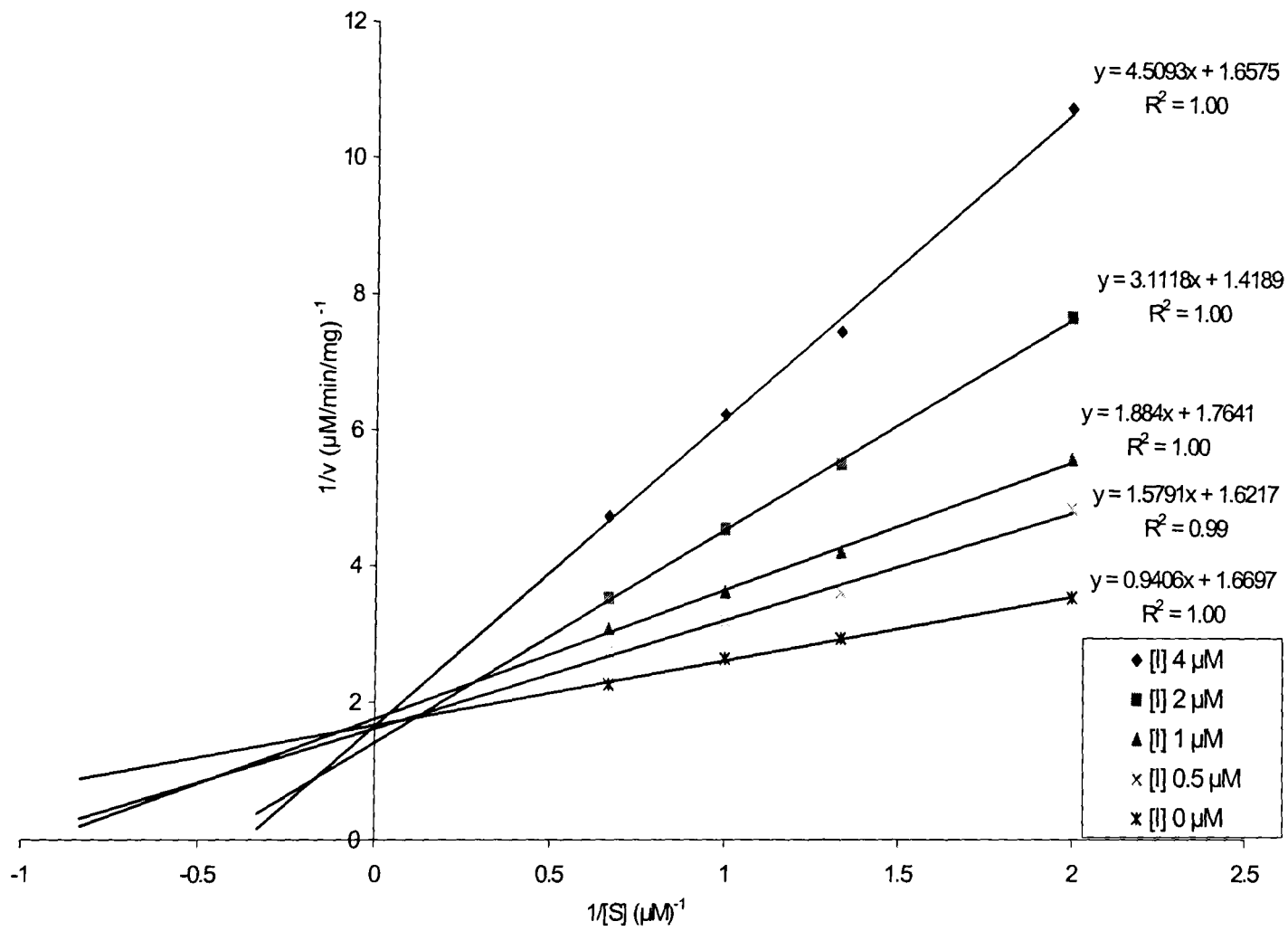

Figure 2.128 Lineweaver-Burk plots of 1/v versus 1/[S] for ketoconazole (**1**) against 17α-hydroxylase.

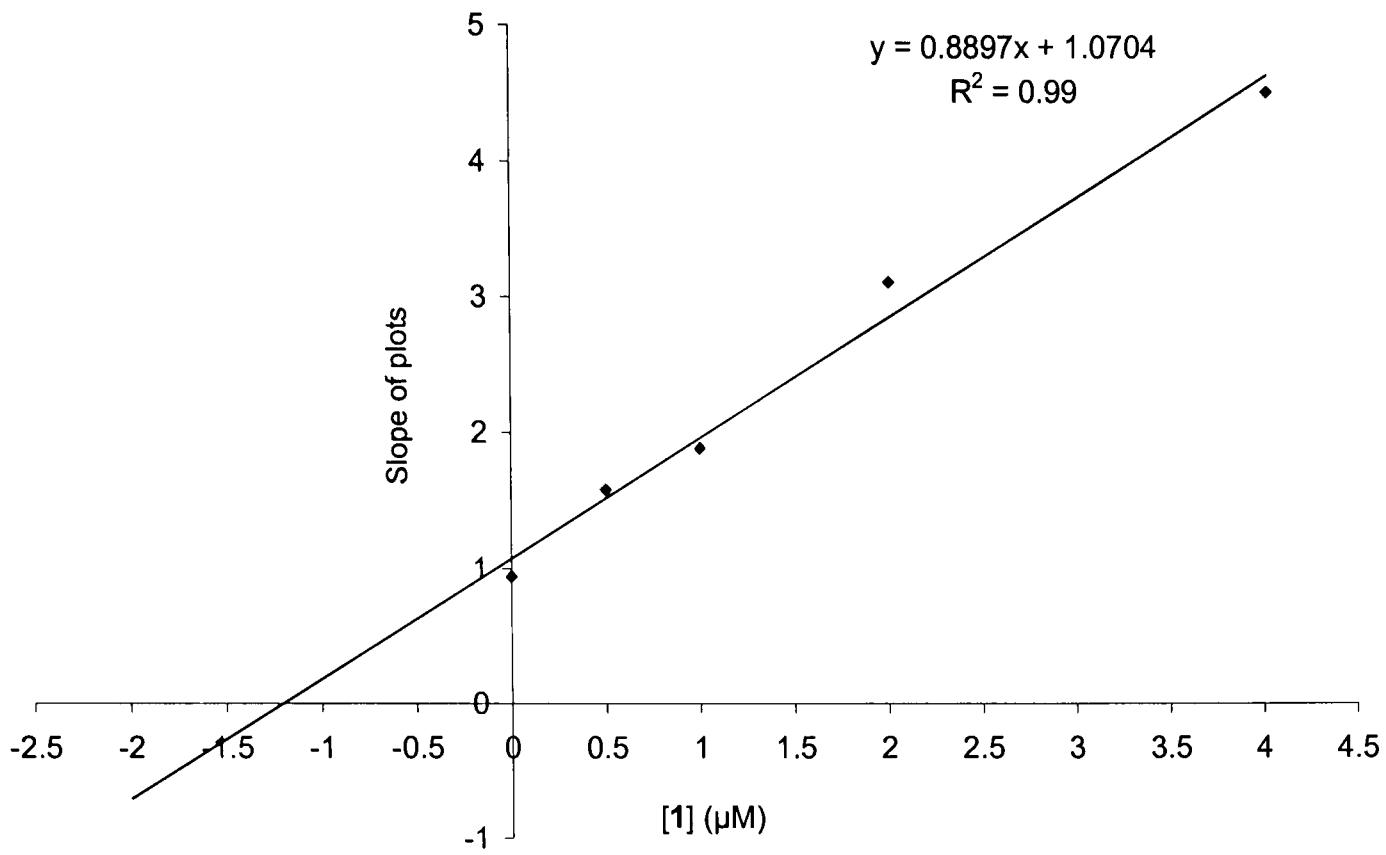

Figure 2.129 Plot of slope of Lineweaver-Burk plots versus the concentration of ketoconazole (**1**) against 17α-hydroxylase showing a K_i of 1250nM.

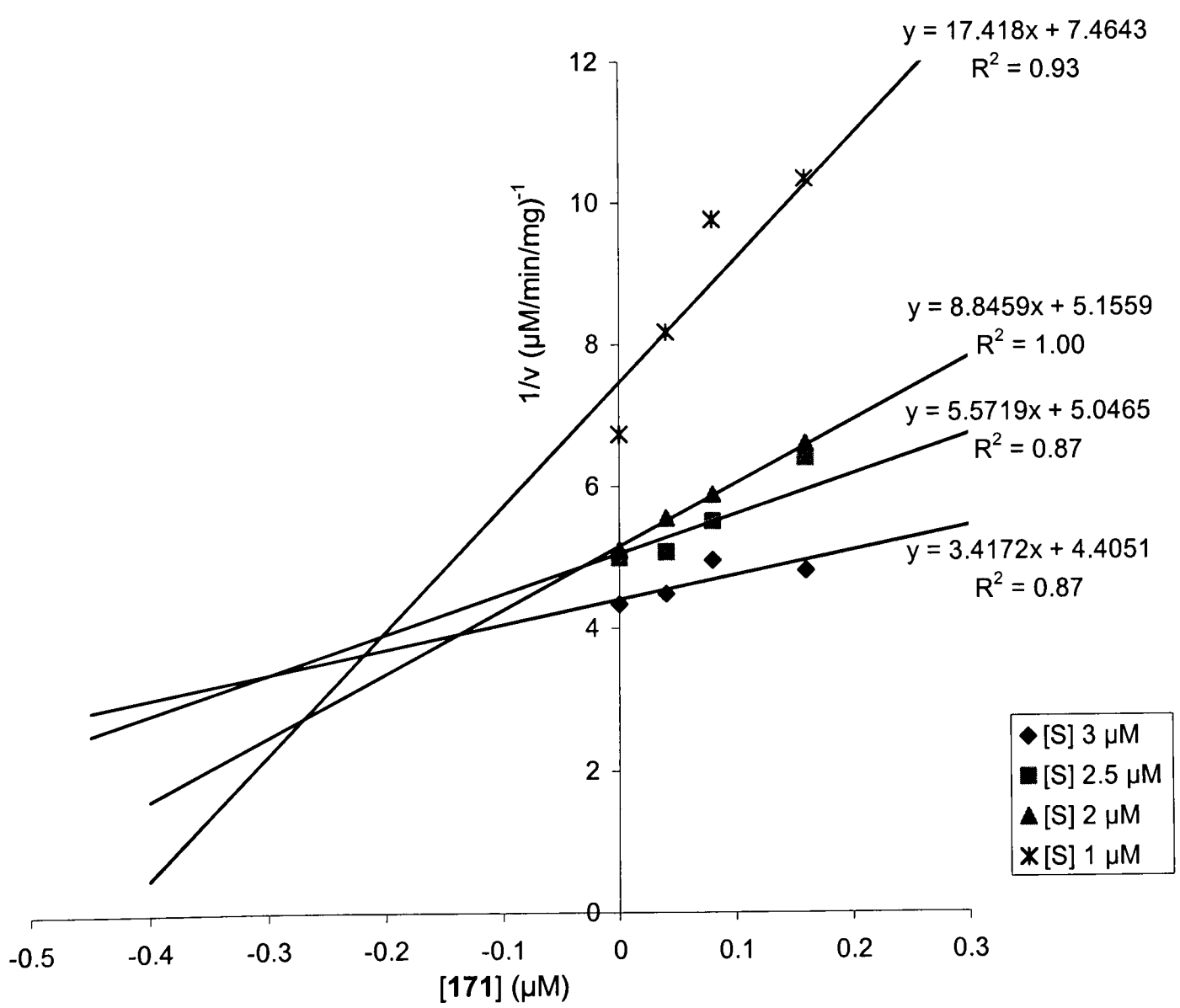

Figure 2.130 Dixon plot of 1/v versus [**171**] for 1-(7-phenyl-heptyl)-1*H*-imidazole (**171**) against 17α-hydroxylase giving a K_i value of 195nM.

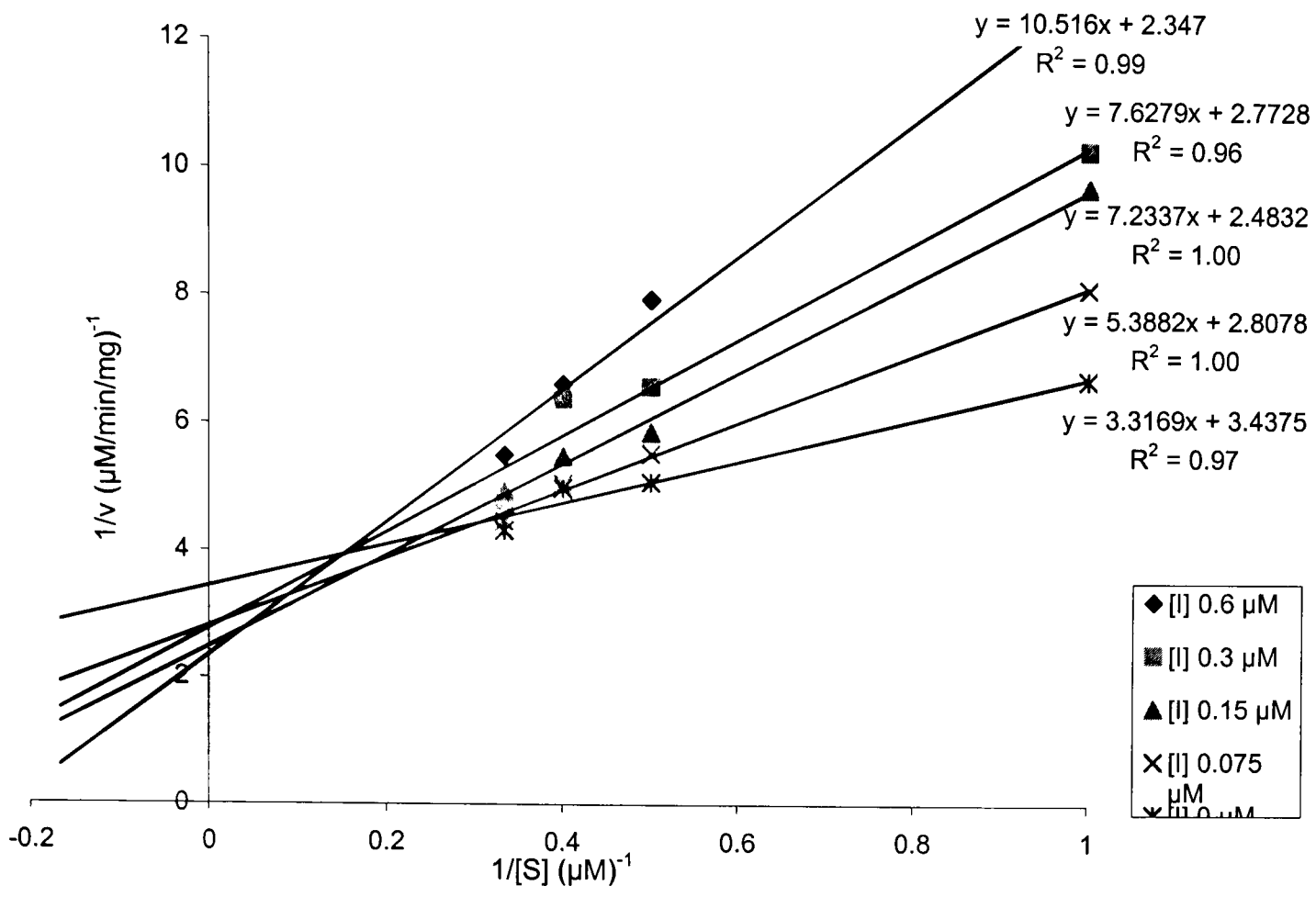

Figure 2.131 Lineweaver-Burk plots of 1/v versus 1/[S] for 1-(7-phenyl-heptyl)-1*H*-imidazole (**171**) against 17α-hydroxylase.

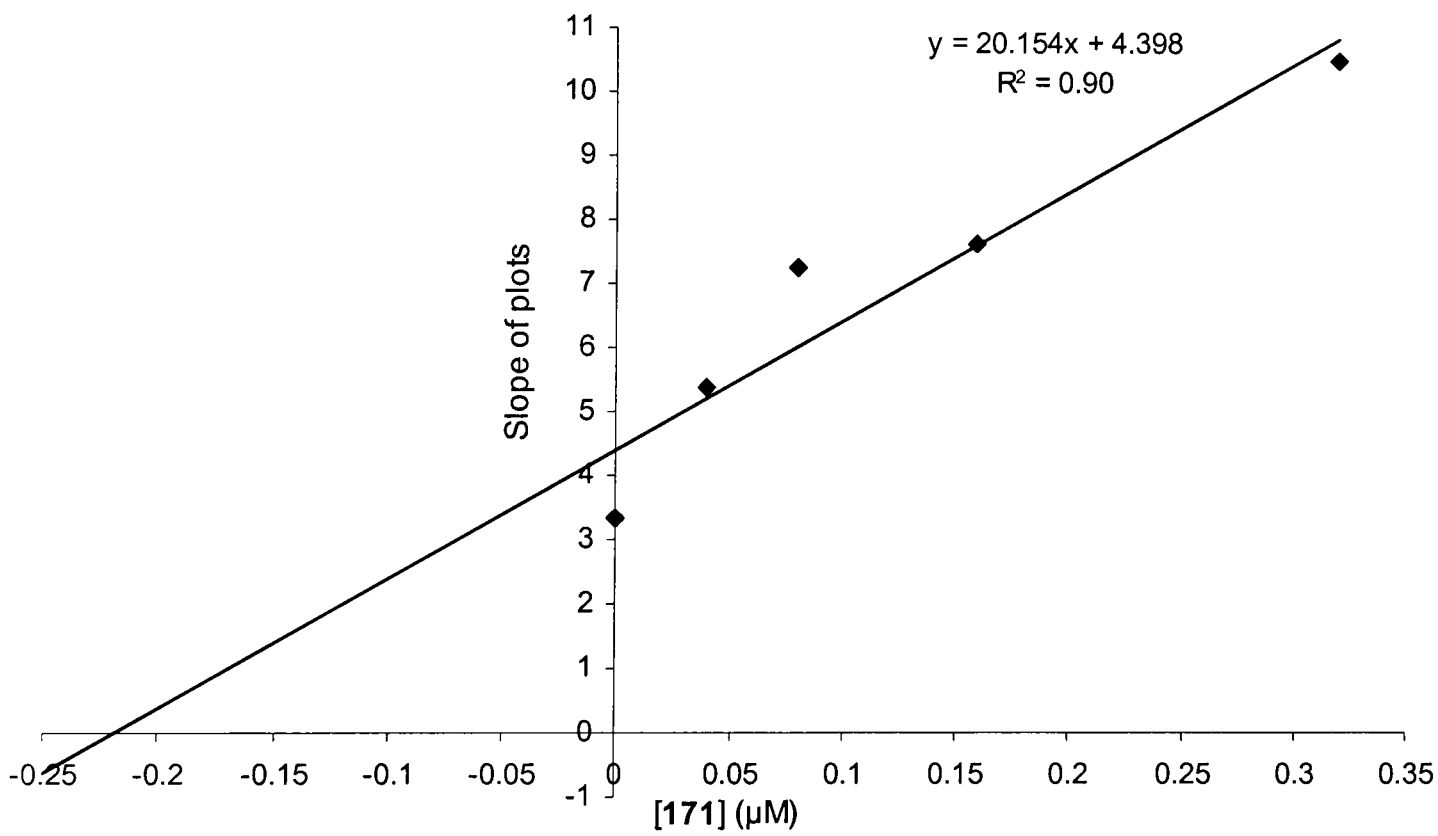

Figure 2.132 Plot of slope of Lineweaver-Burk plots versus the concentration of 1-(7-phenyl-heptyl)-1*H*-imidazole (**171**) against 17α-hydroxylase showing a K_i of 218nM.

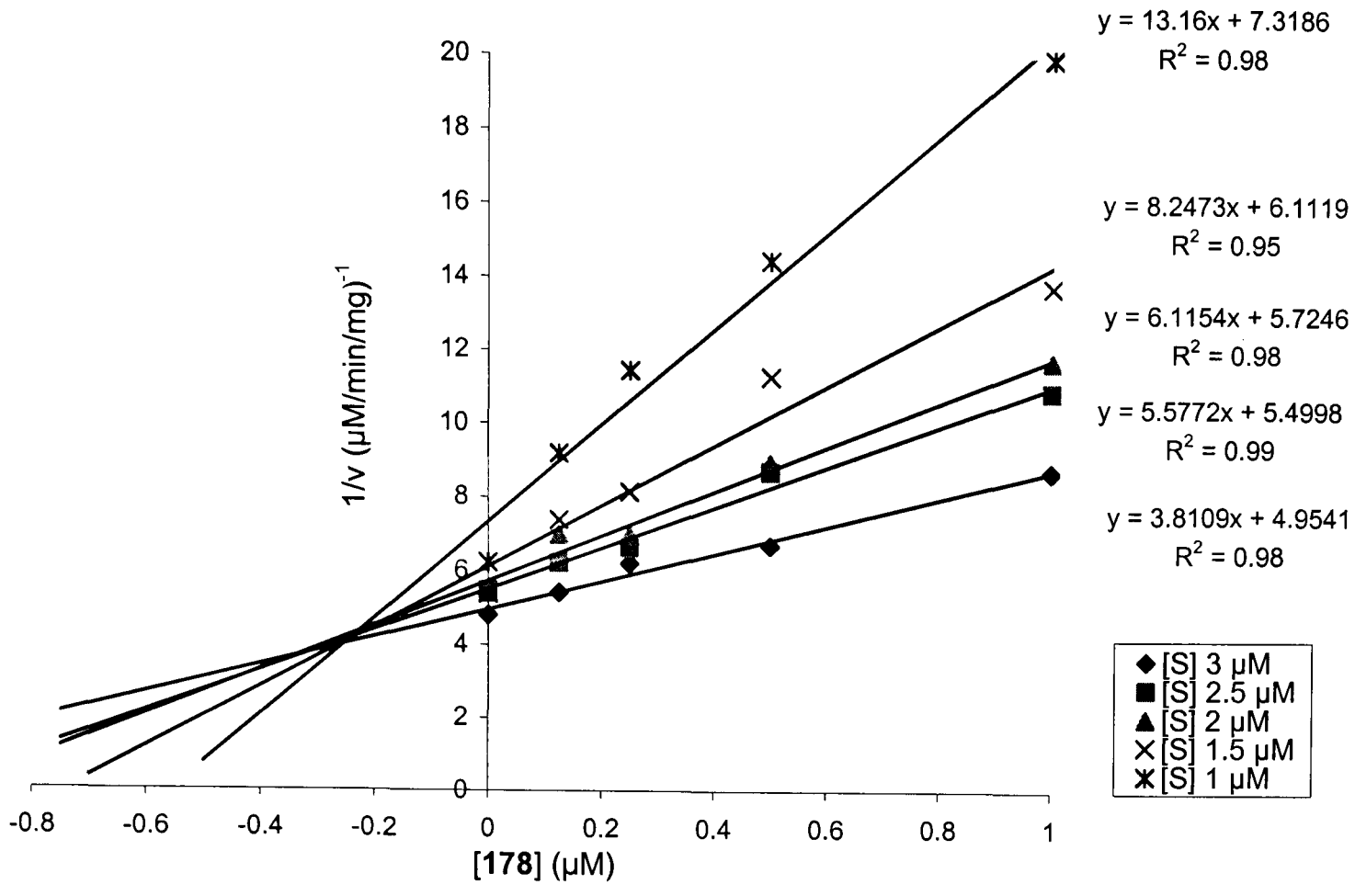

Figure 2.133 Dixon plot of 1/v versus [**178**] for 1-[5-(4-fluoro-phenyl)-pentyl]-1*H*-imidazole (**178**) against 17α-hydroxylase giving a K_i value of 278nM.

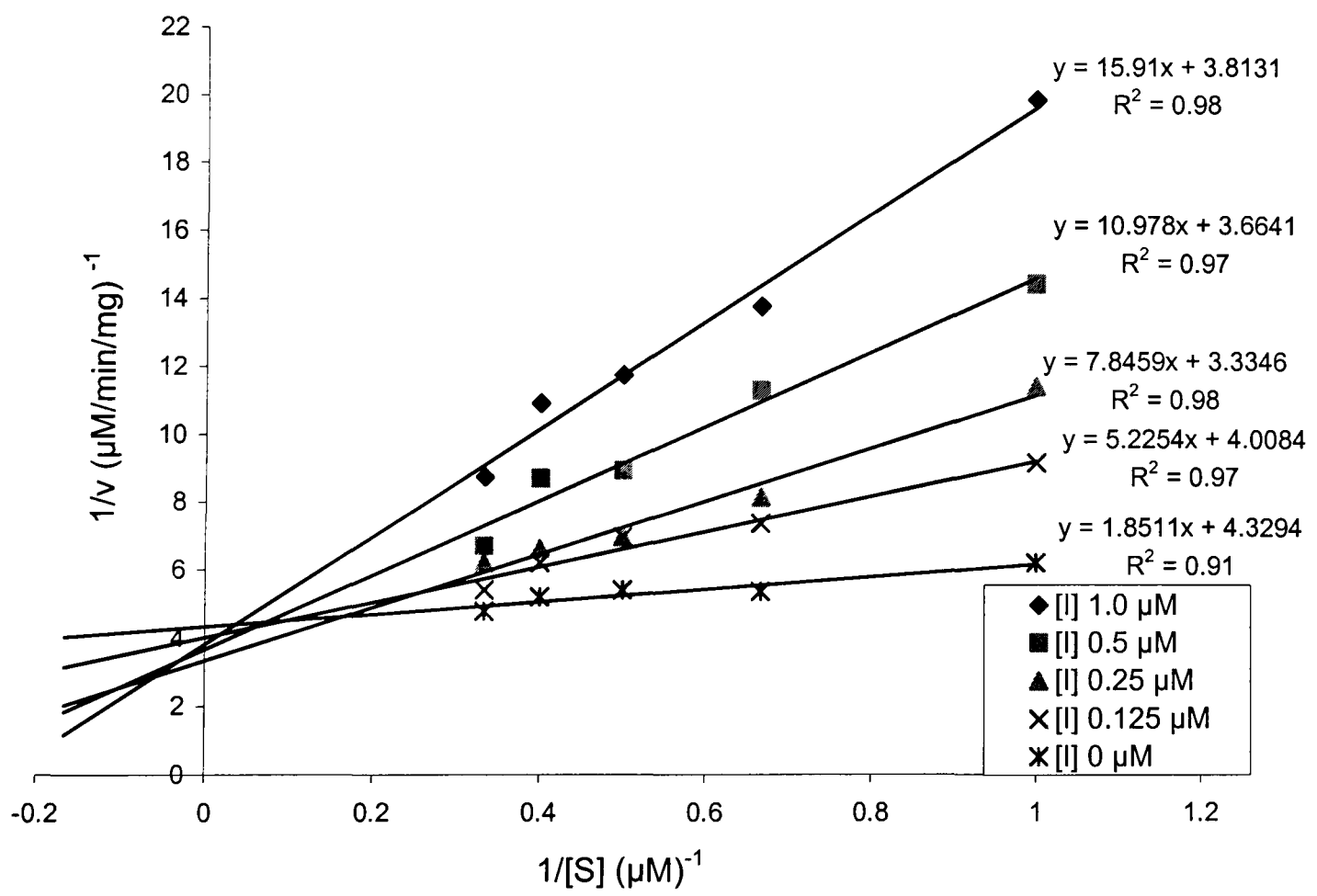

Figure 2.134 Lineweaver-Burk plots of 1/v versus 1/[S] for 1-[5-(4-fluoro-phenyl)-pentyl]-1*H*-imidazole (**178**) against 17α-hydroxylase.

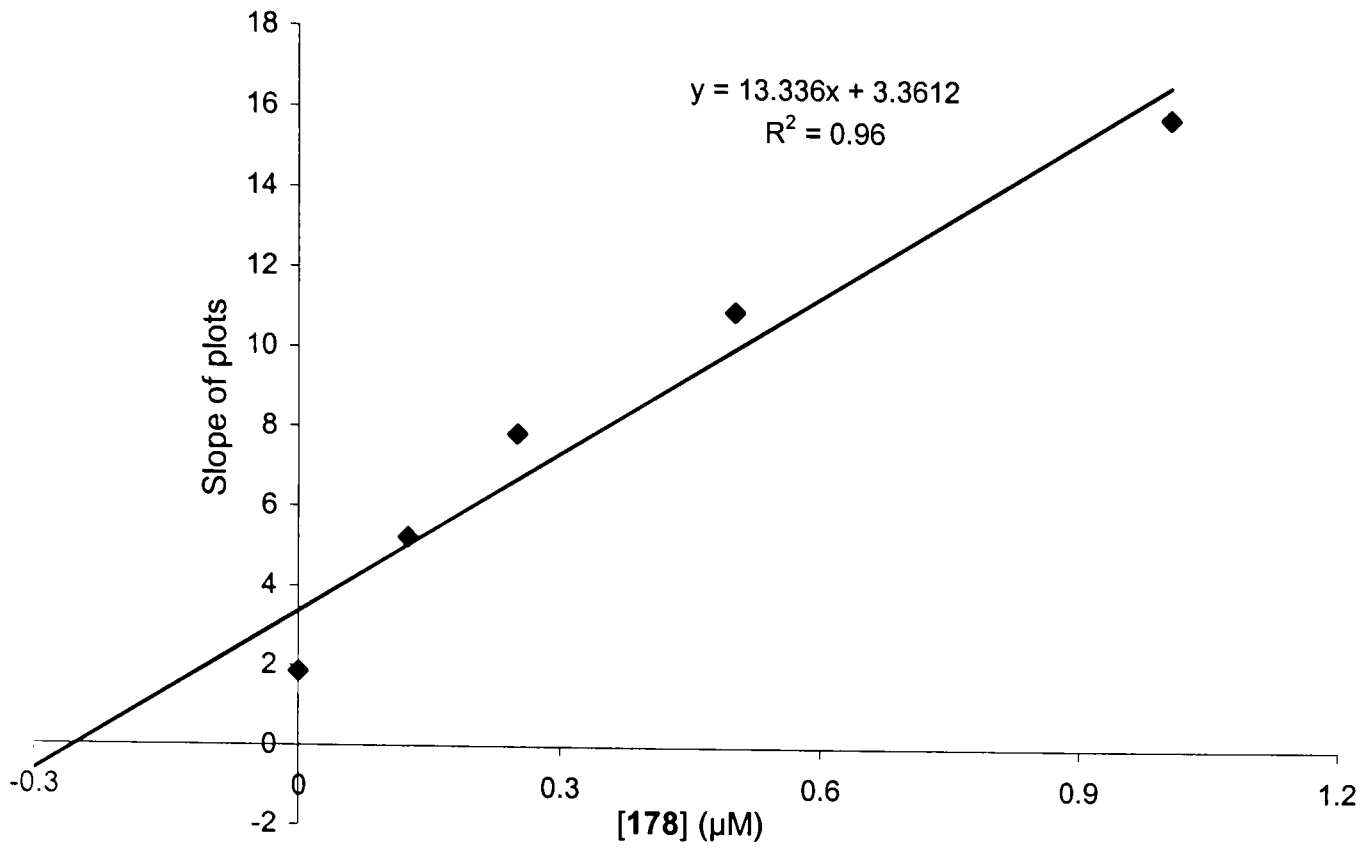

Figure 2.135 Plot of slope of Lineweaver-Burk plots versus the concentration of 1-[5-(4-fluoro-phenyl)-pentyl]-1*H*-imidazole (**178**) against 17α-hydroxylase showing a K_i of 252nM.

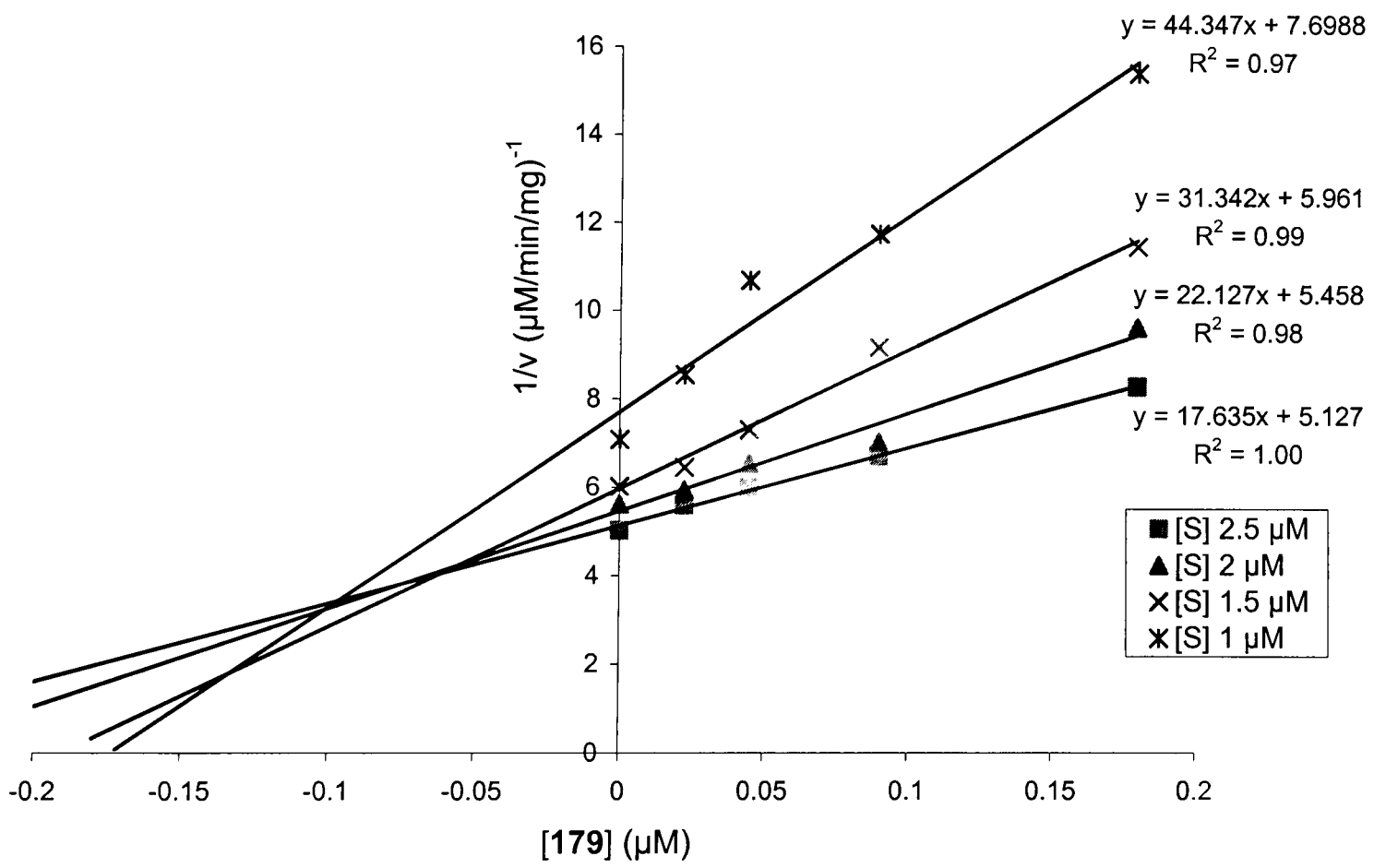

Figure 2.136 Dixon plot of 1/v versus [**179**] for 1-[7-(4-fluoro-phenyl)-heptyl]-1*H*-imidazole (**179**) against 17α-hydroxylase giving a K_i value of 80nM.

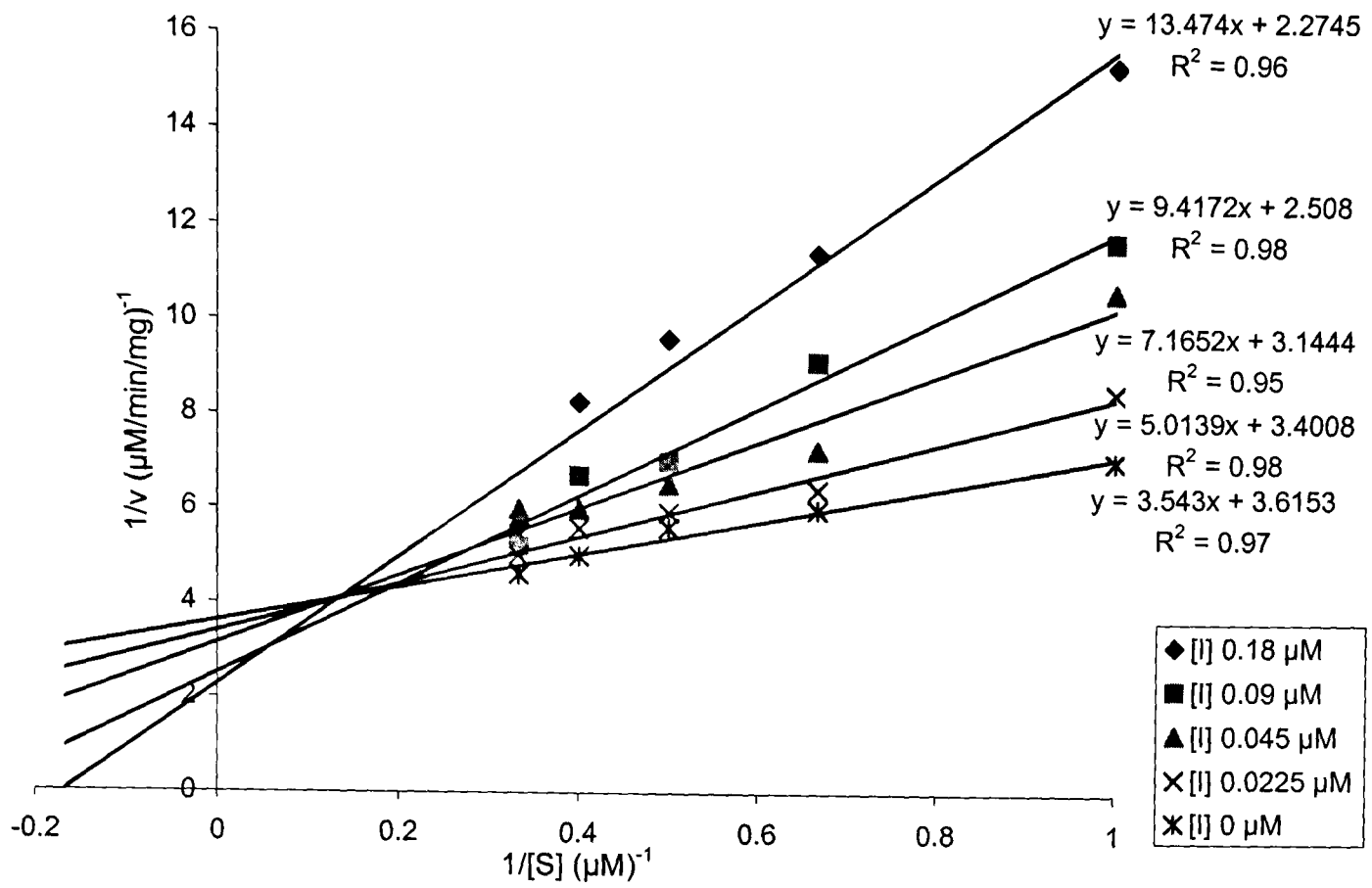

Figure 2.137 Lineweaver-Burk plots of 1/v versus 1/[S] for 1-[7-(4-fluoro-phenyl)-heptyl]-1*H*-imidazole (**179**) against 17α-hydroxylase.

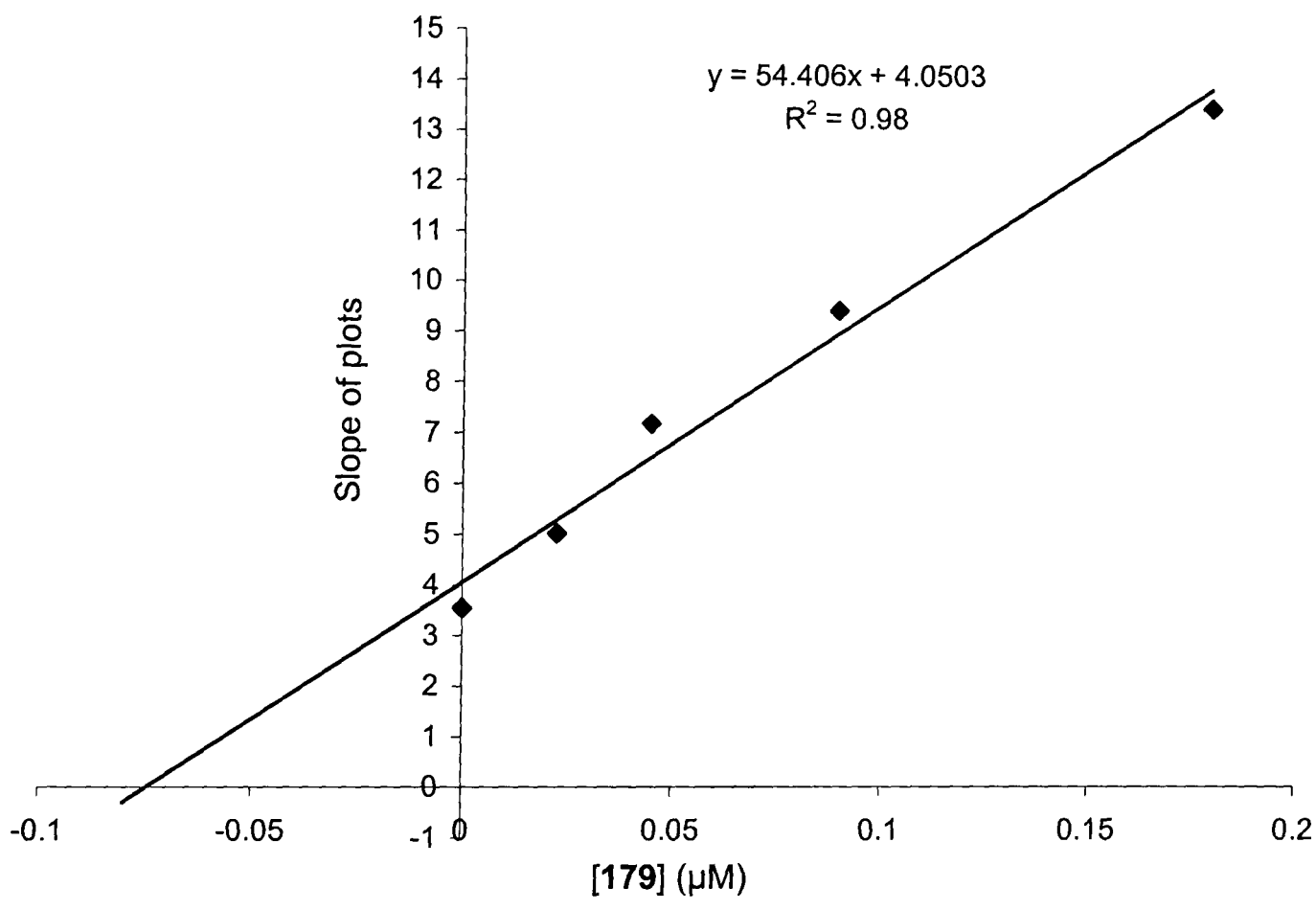

Figure 2.138 Plot of slope of Lineweaver-Burk plots versus the concentration of 1-[7-(4-fluoro-phenyl)-heptyl]-1*H*-imidazole (**179**) against 17α-hydroxylase showing a K_i of 75nM.

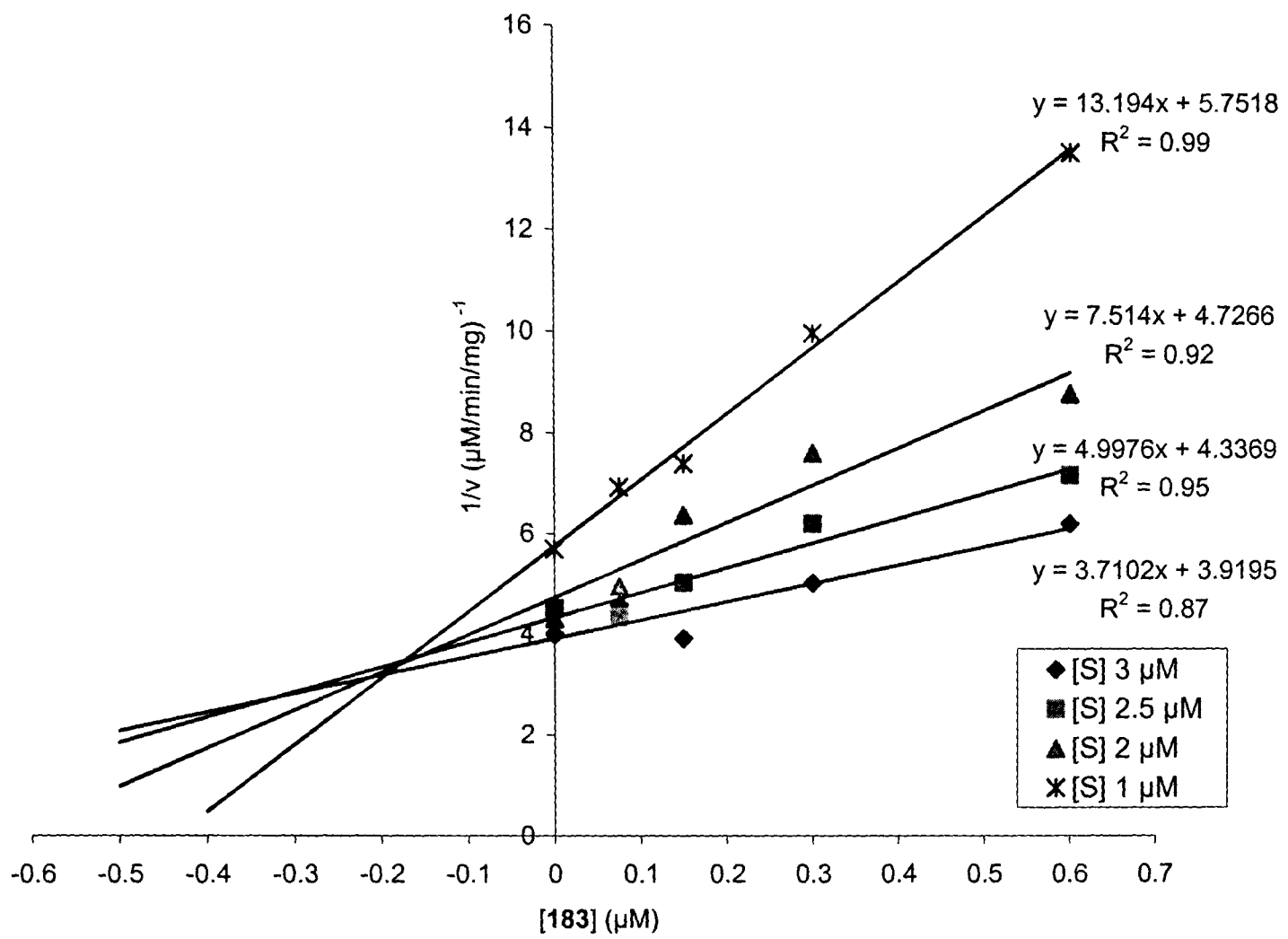

Figure 2.139 Dixon plot of 1/v versus [**183**] for 1-[5-(4-chloro-phenyl)-pentyl]-1*H*-imidazole (**183**) against 17α-hydroxylase giving a K_i value of 214nM.

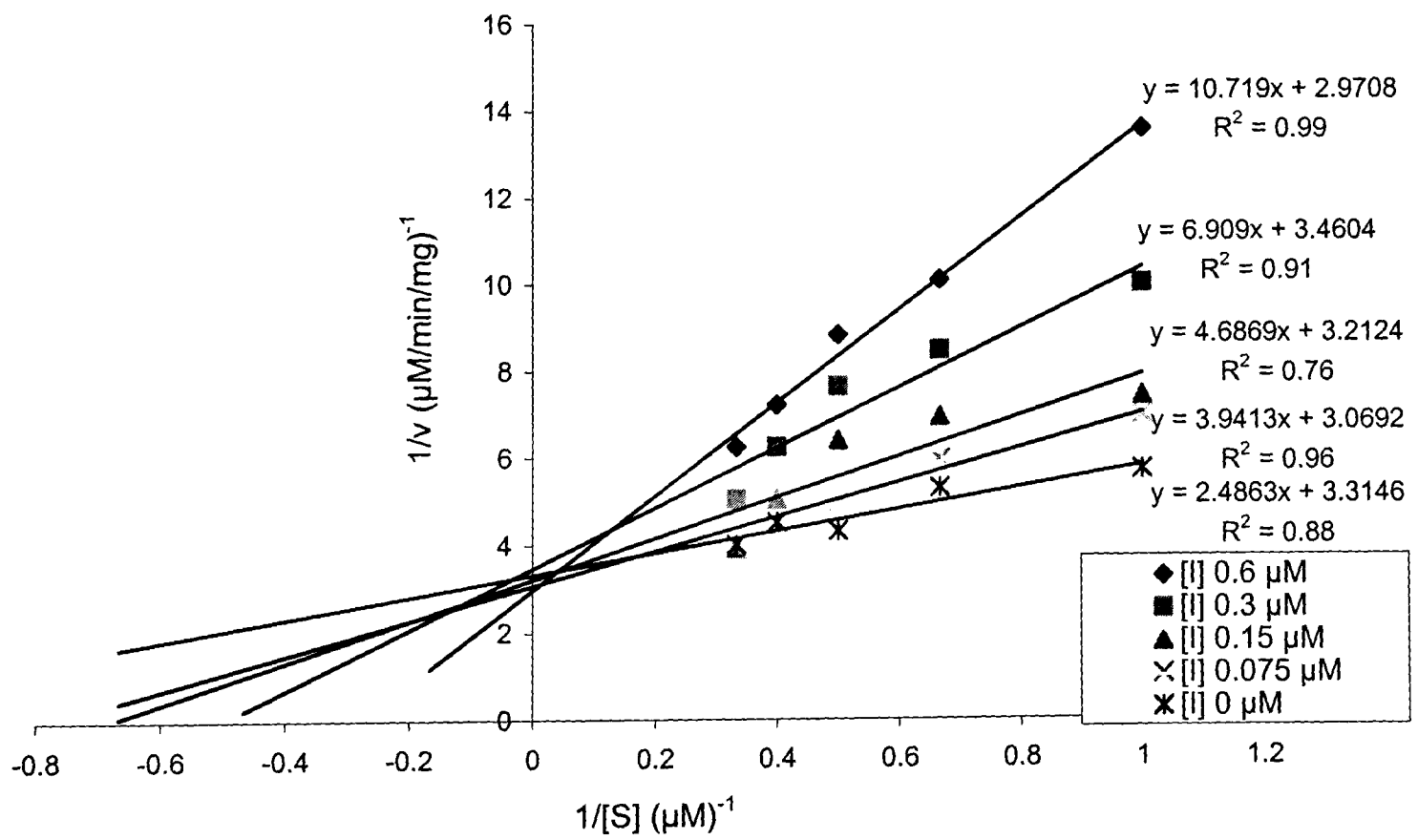

Figure 2.140 Lineweaver-Burk plots of 1/v versus 1/[S] for 1-[5-(4-chloro phenyl)-pentyl]-1*H*-imidazole (**183**) against 17α-hydroxylase.

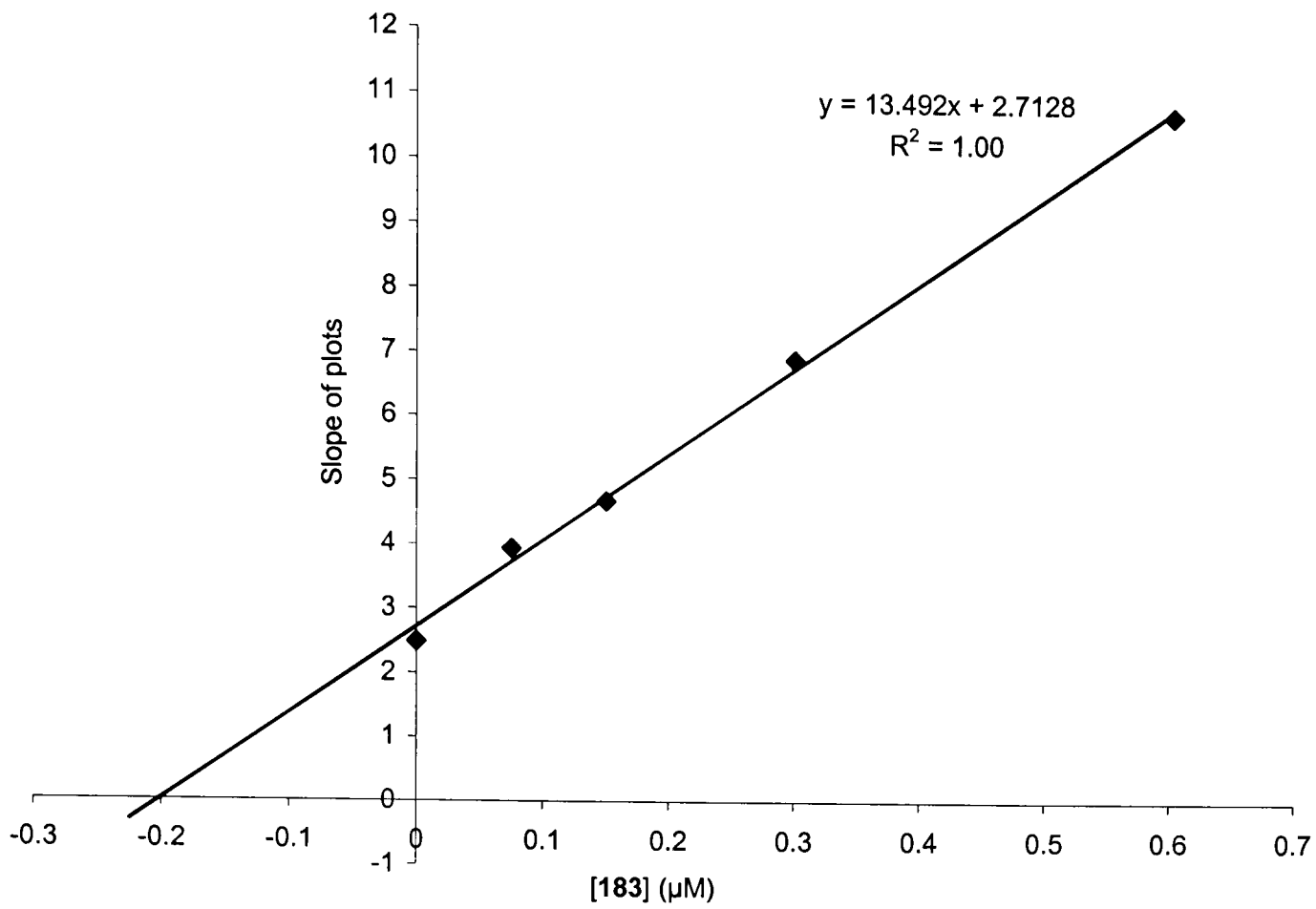

Figure 2.141 Plot of slope of Lineweaver-Burk plots versus the concentration of 1-[5-(4-chloro-phenyl)-pentyl]-1*H*-imidazole (**183**) against 17α-hydroxylase showing a K_i of 202nM.

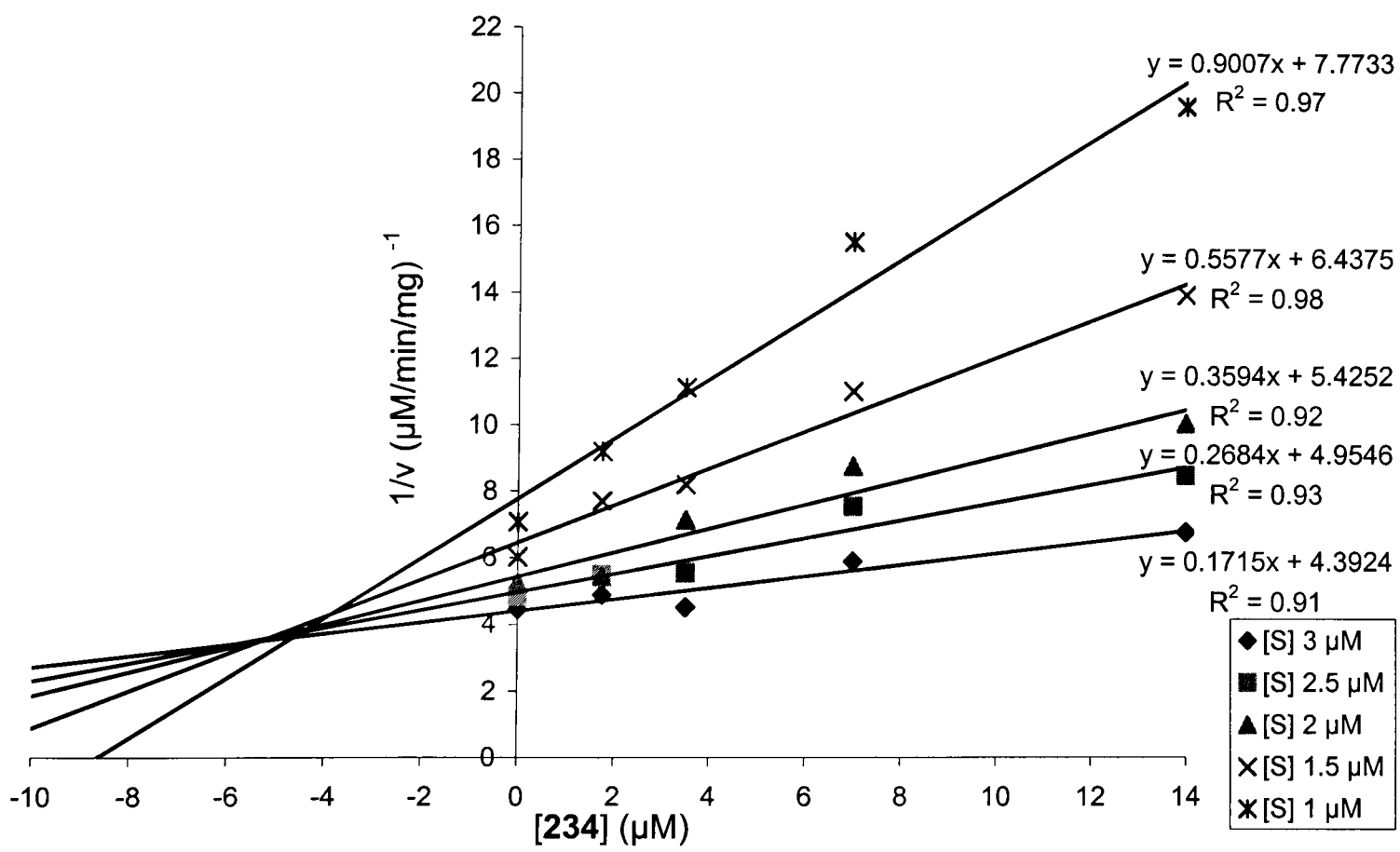

Figure 2.142 Dixon plot of 1/v versus [**234**] for 1-(3,4-dichloro-benzyl)-1*H*-imidazole (**234**) against 17α-hydroxylase giving a K_i value of 4940nM.

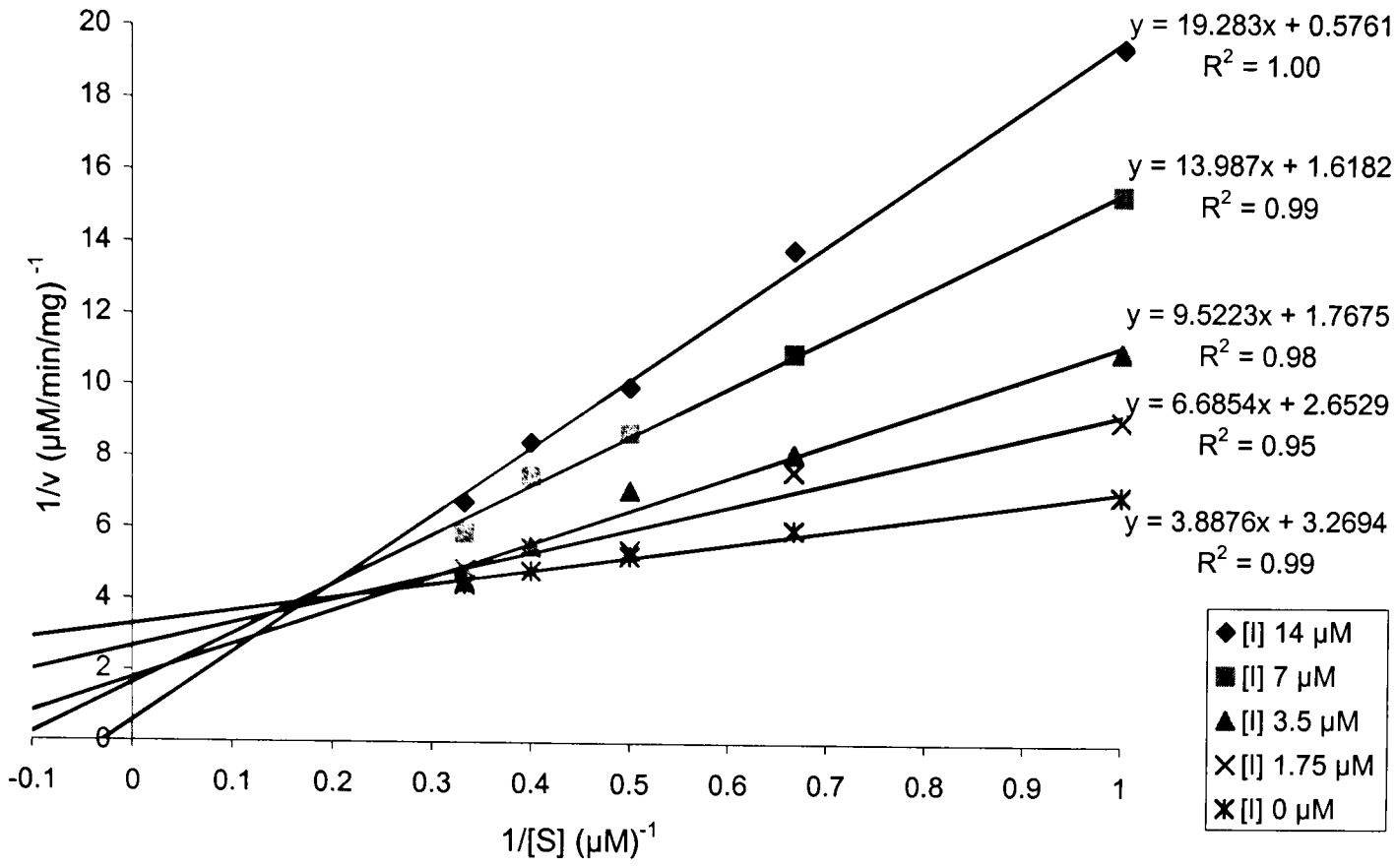

Figure 2.143 Lineweaver-Burk plots of 1/v versus 1/[S] for 1-(3,4-dichloro-benzyl)-1*H*-imidazole (**234**) against 17α-hydroxylase.

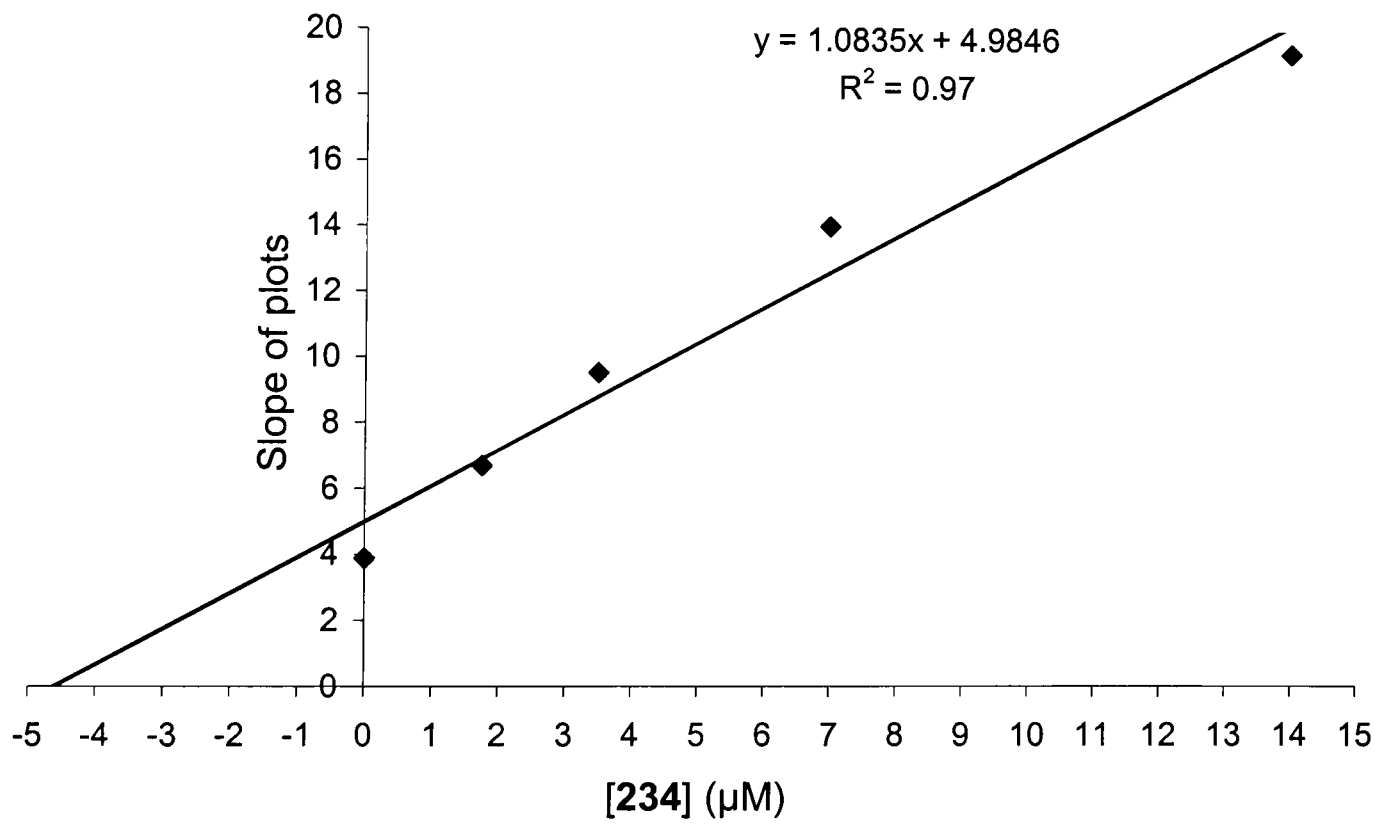

Figure 2.144 Plot of slope of Lineweaver-Burk plots versus the concentration of 1-(3,4-dichloro-benzyl)-1*H*-imidazole (**234**) against 17α-hydroxylase showing a K_i of 4600nM.

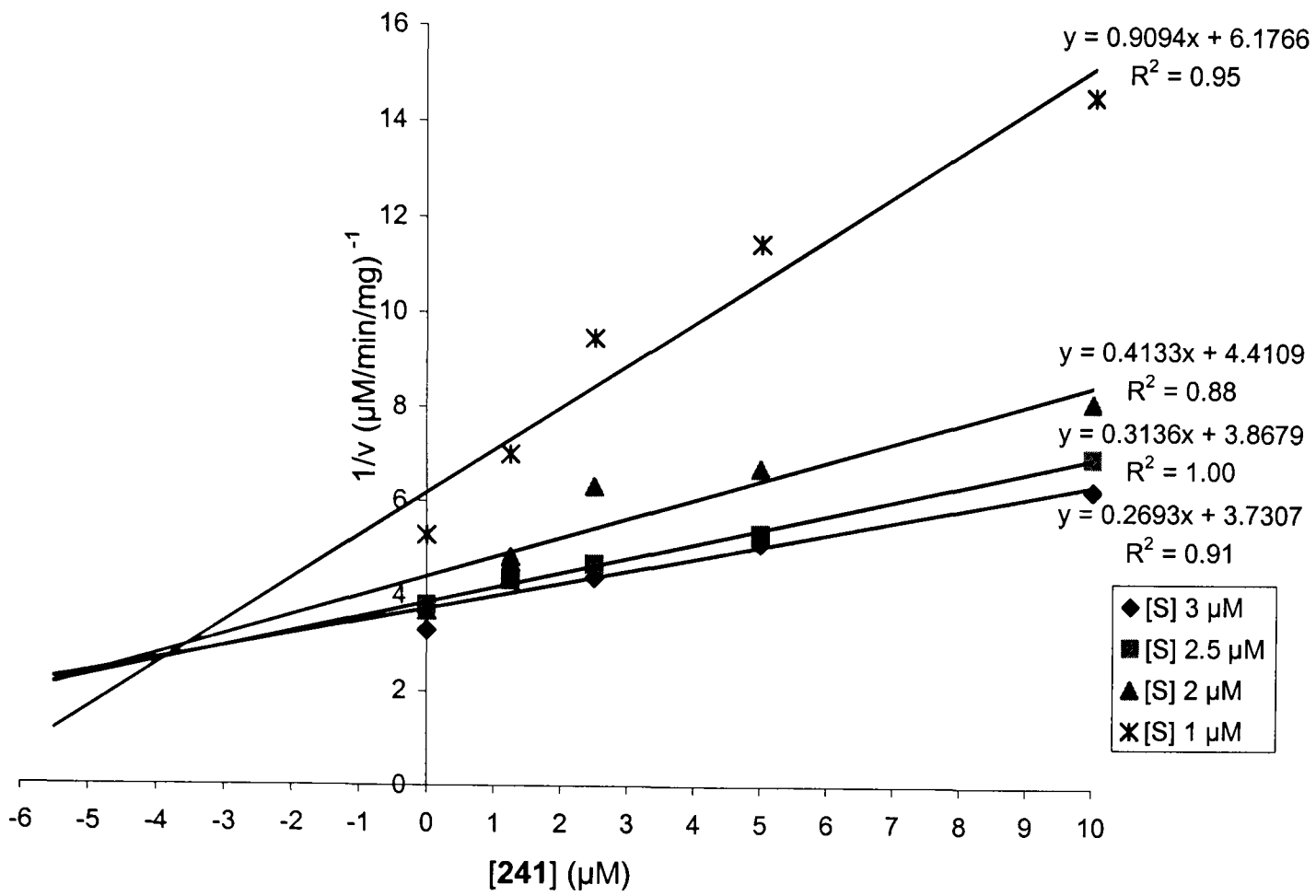

Figure 2.145 Dixon plot of 1/v versus **[241]** for 1-(4-iodo-benzyl)-1*H*-imidazole (**241**) against 17α-hydroxylase giving a K_i value of 4050nM.

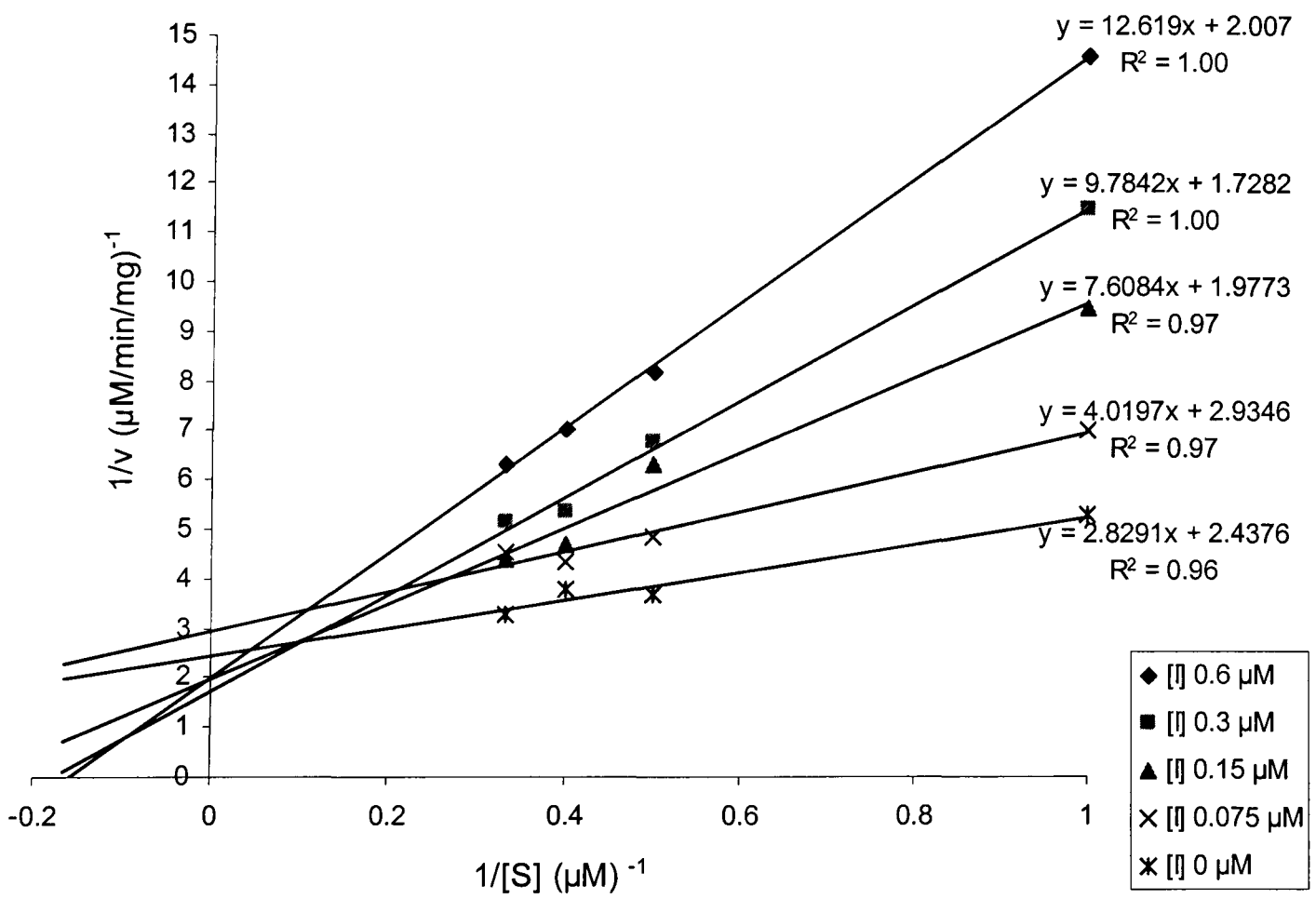

Figure 2.146 Lineweaver-Burk plots of 1/v versus 1/[S] for 1-(4-iodo-benzyl)-1*H*-imidazole (**241**) against 17α-hydroxylase.

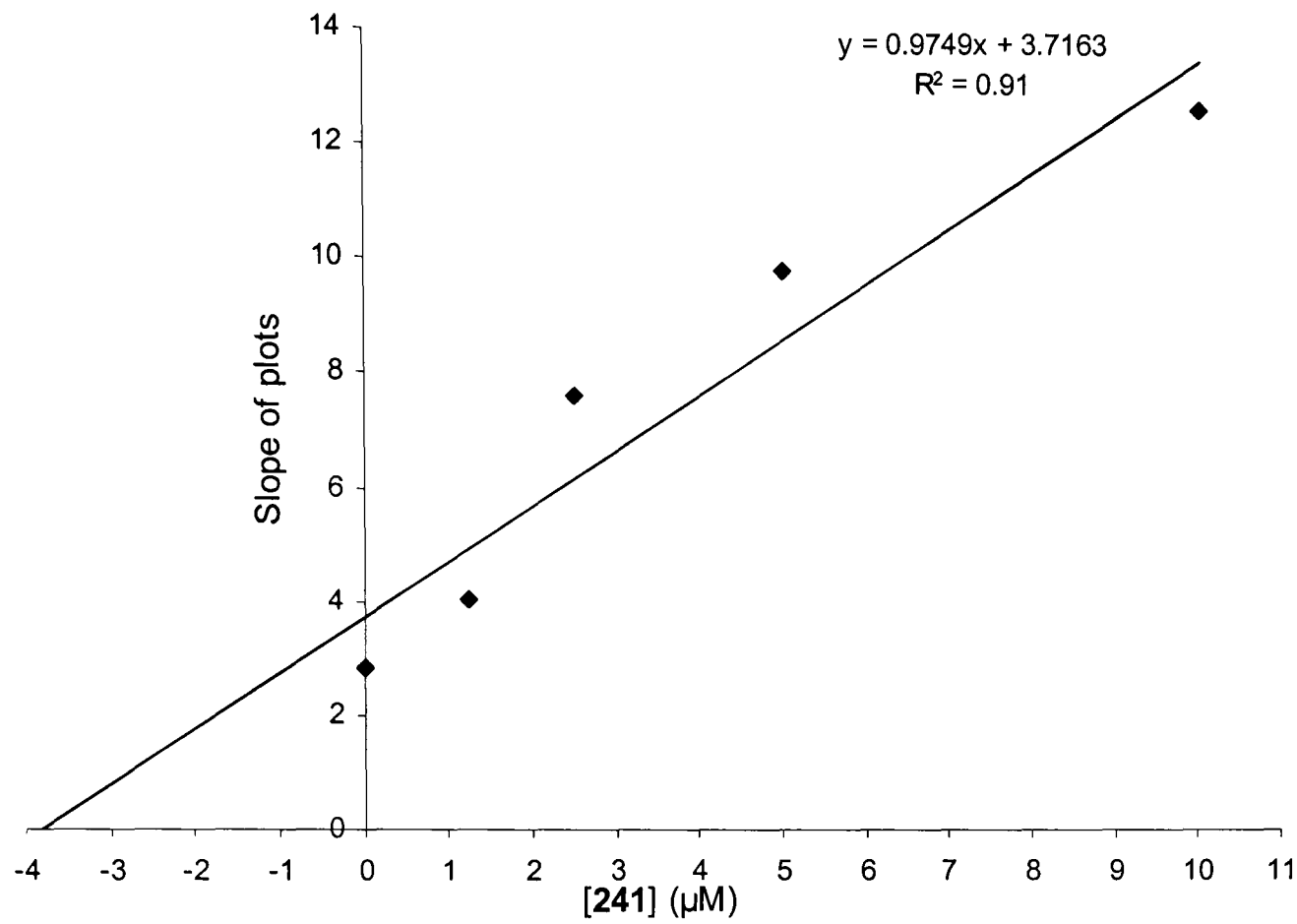

Figure 2.147 Plot of slope of Lineweaver-Burk plots versus the concentration of 1-(4-iodo-benzyl)-1*H*-imidazole (**241**) against 17α-hydroxylase showing a K_i of 3810nM.

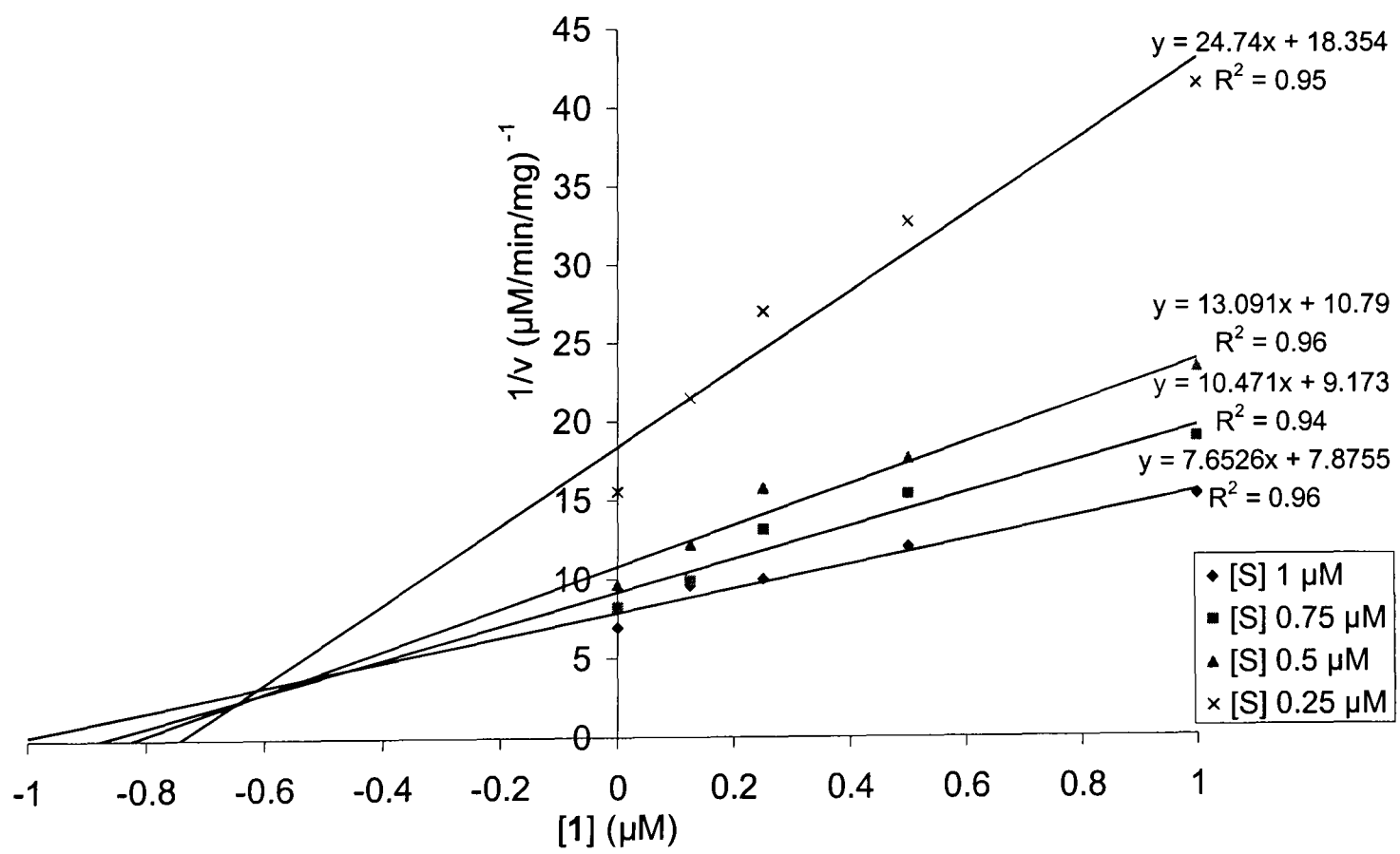

Figure 2.148 Dixon plot of 1/v versus [**1**] for ketoconazole (**1**) against 17,20-lyase giving a K_i value of 680nM.

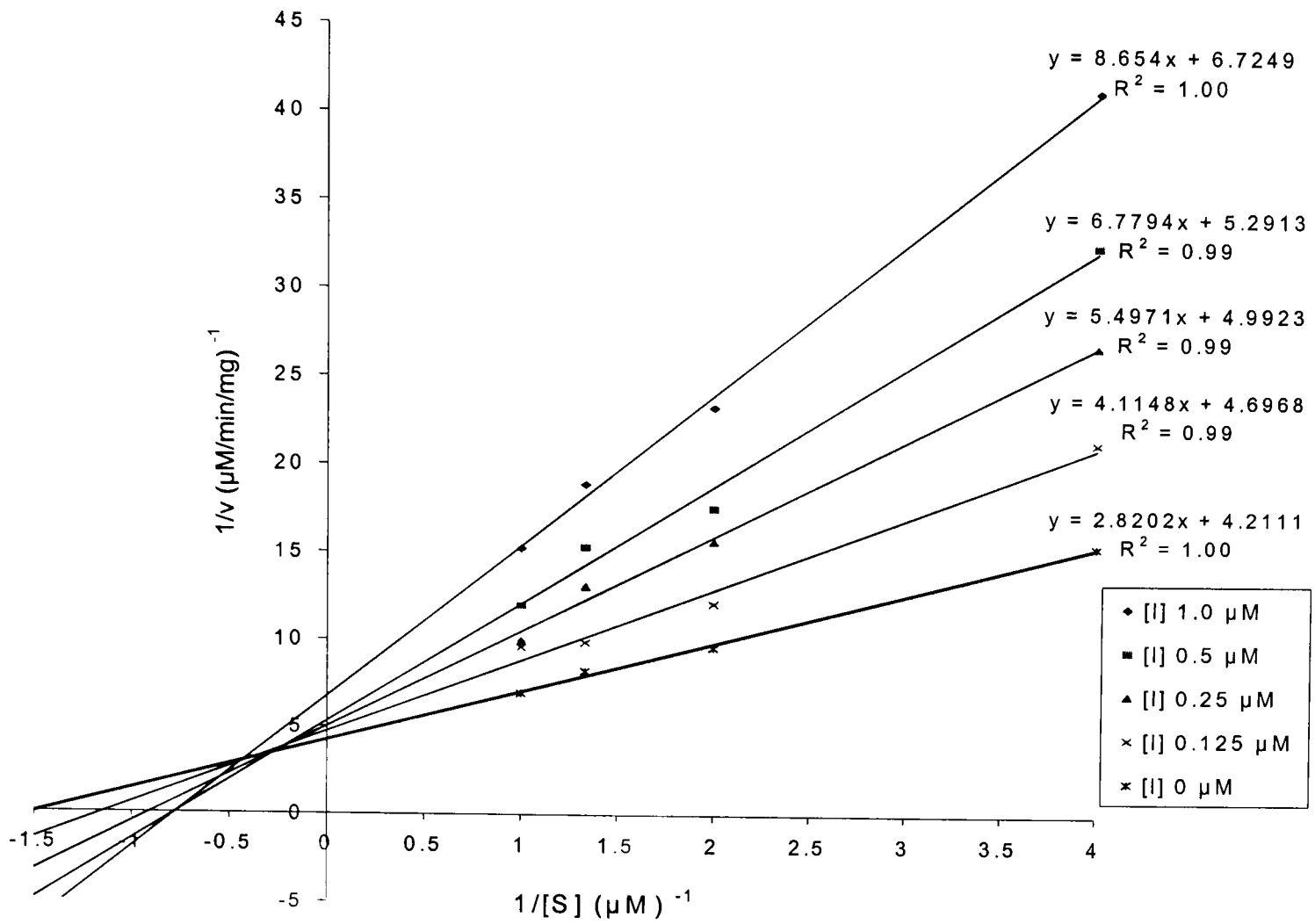

Figure 2.149 Lineweaver-Burk plots of 1/v versus 1/[S] for ketoconazole (**1**) against 17,20-lyase.

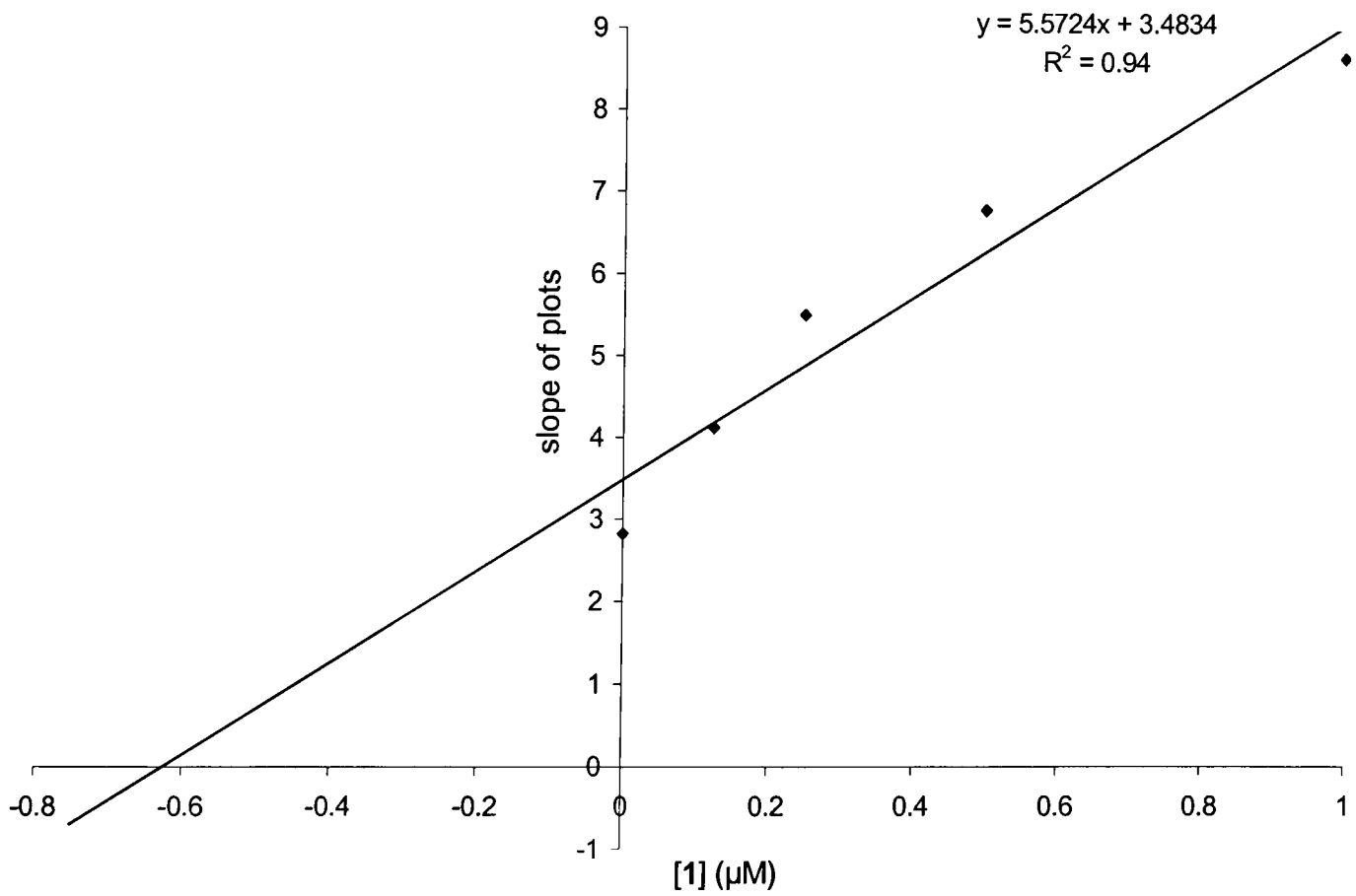

Figure 2.150 Plot of slope of Lineweaver-Burk plots versus the concentration of ketoconazole (**1**) against 17,20-lyase showing a K_i of 650nM.

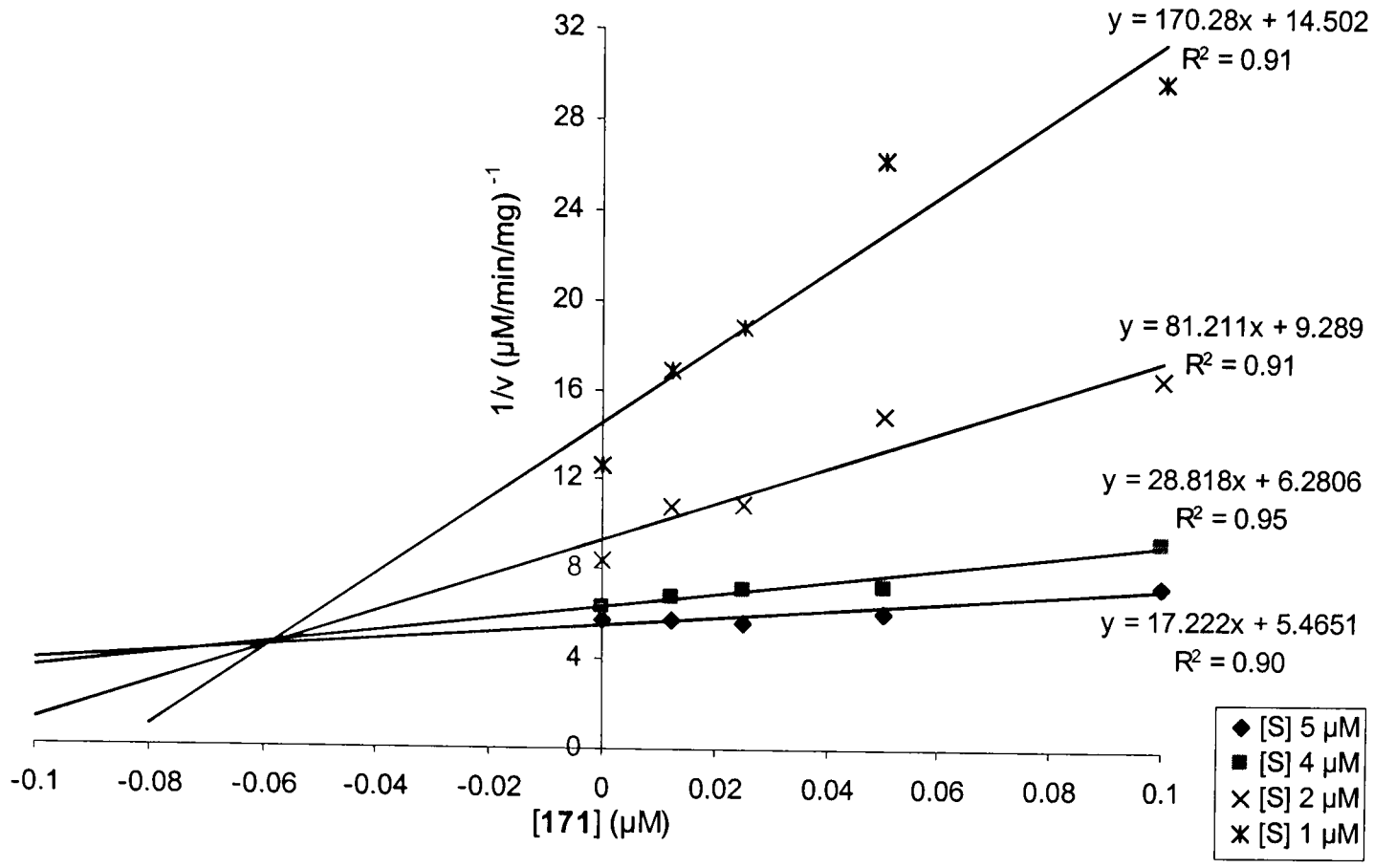

Figure 2.151 Dixon plot of 1/v versus [**171**] for 1-(7-phenyl-heptyl)-1*H*-imidazole (**171**) against 17,20-lyase giving a K_i value of 51.88nM.

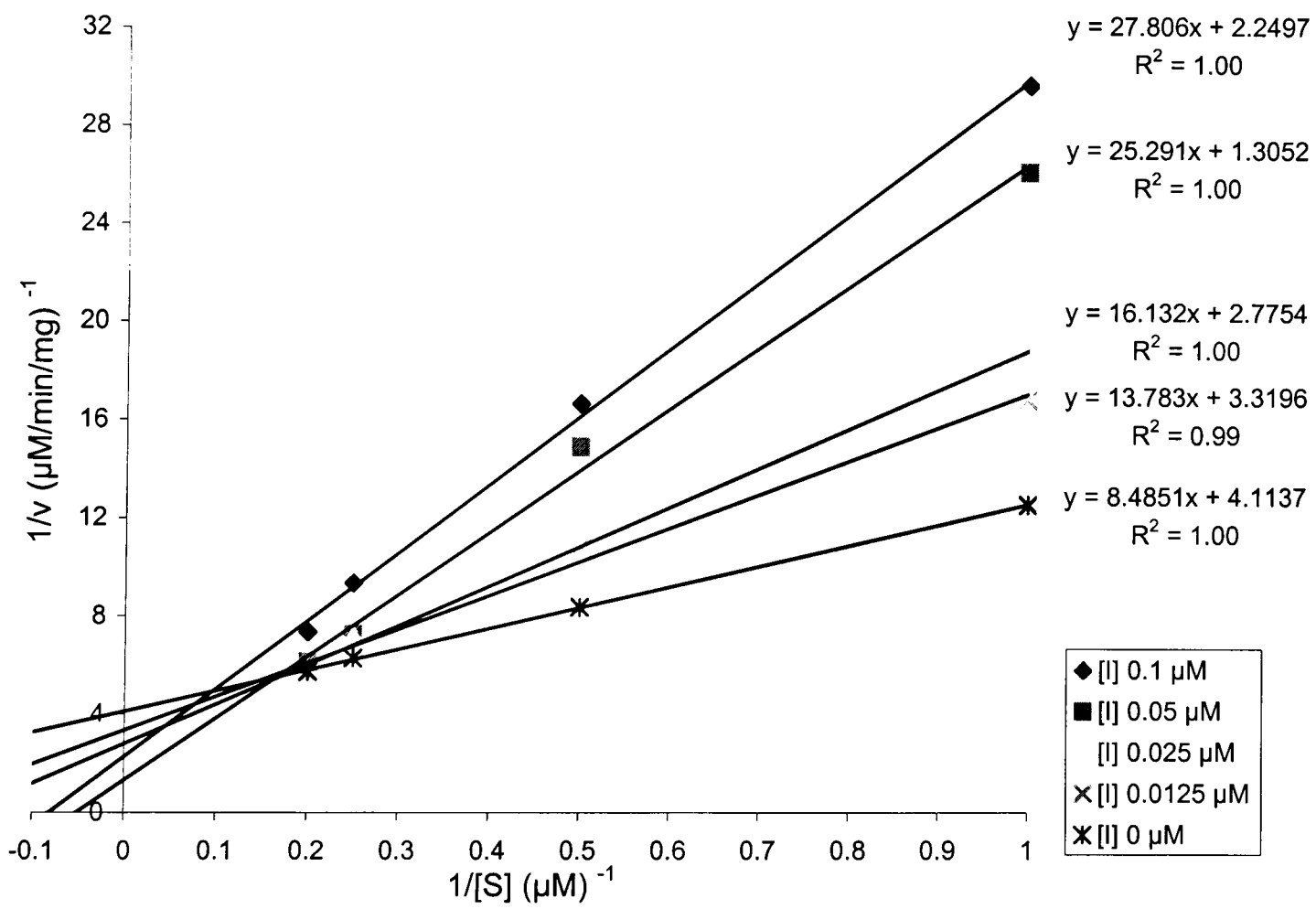

Figure 2.152 Lineweaver-Burk plots of 1/v versus 1/[S] for 1-(7-phenyl-heptyl)-1*H*-imidazole (**171**) against 17,20-lyase.

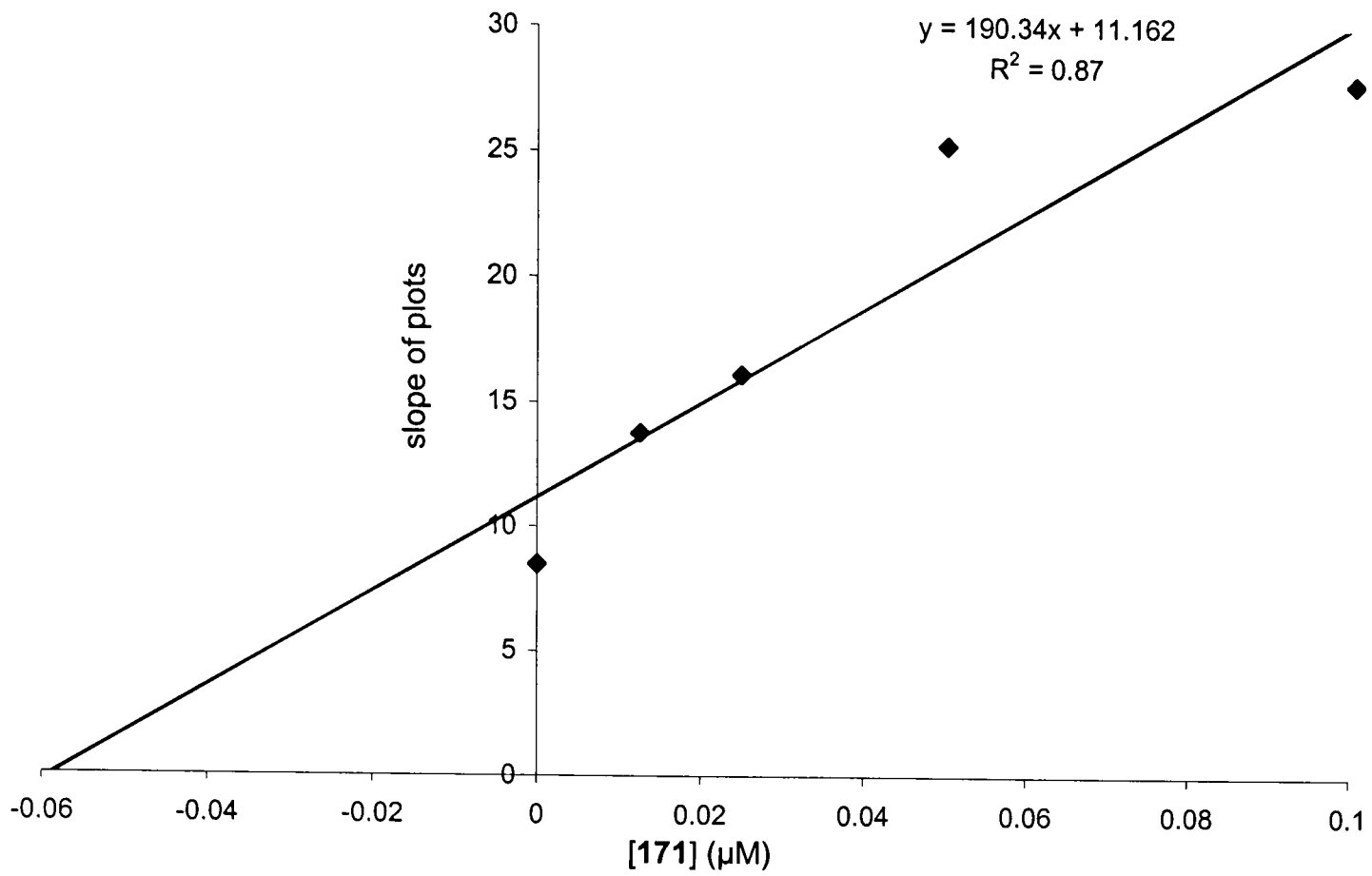

Figure 2.153 Plot of slope of Lineweaver-Burk plots versus the concentration of 1-(7-phenyl-heptyl)-1*H*-imidazole (**171**) against 17,20-lyase showing a K_i of 58.64nM.

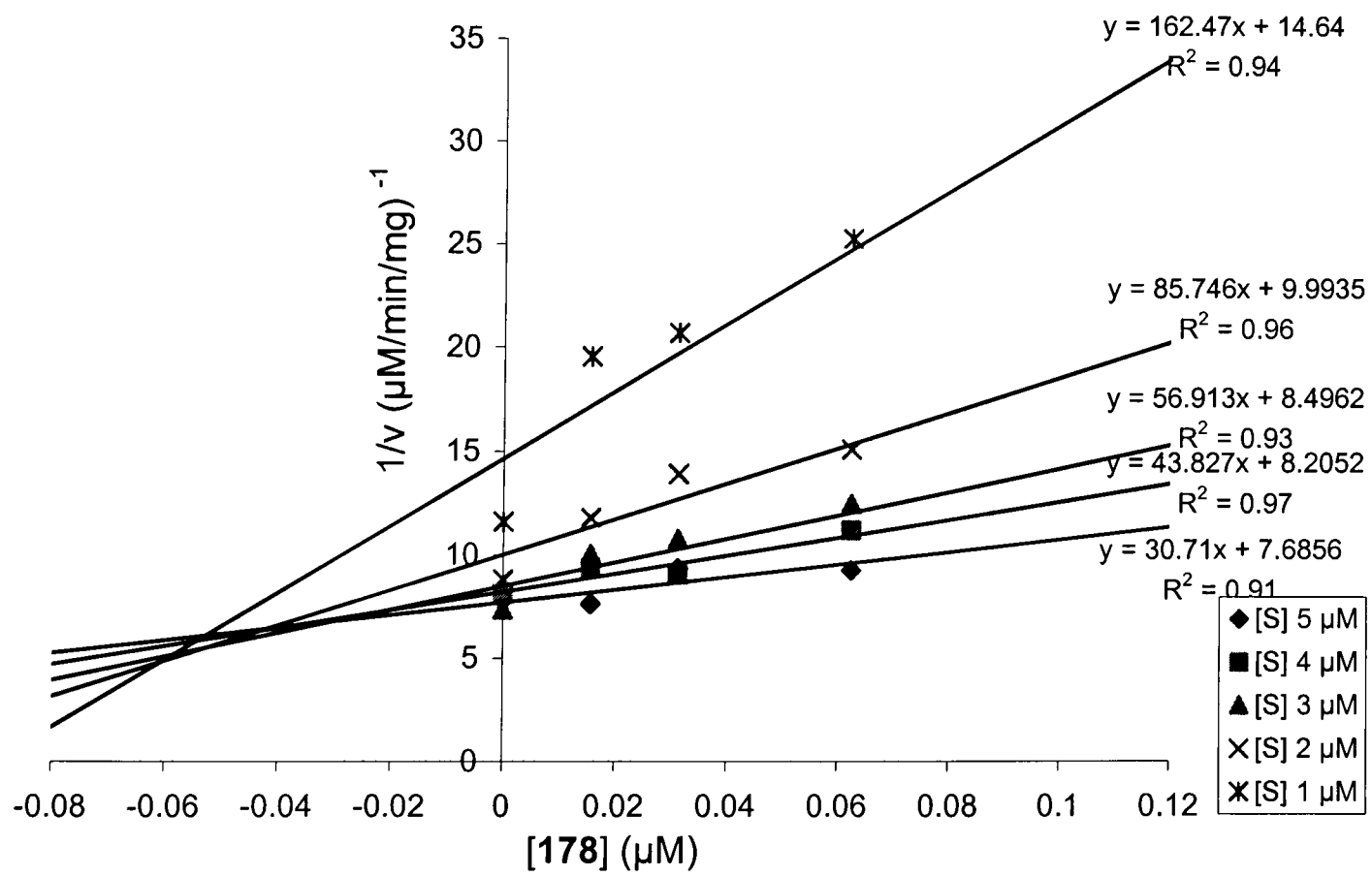

Figure 2.154 Dixon plot of 1/v versus [**178**] for 1-[5-(4-fluoro-phenyl)-pentyl]-1*H*-imidazole (**178**) against 17,20-lyase giving a K_i value of 54nM.

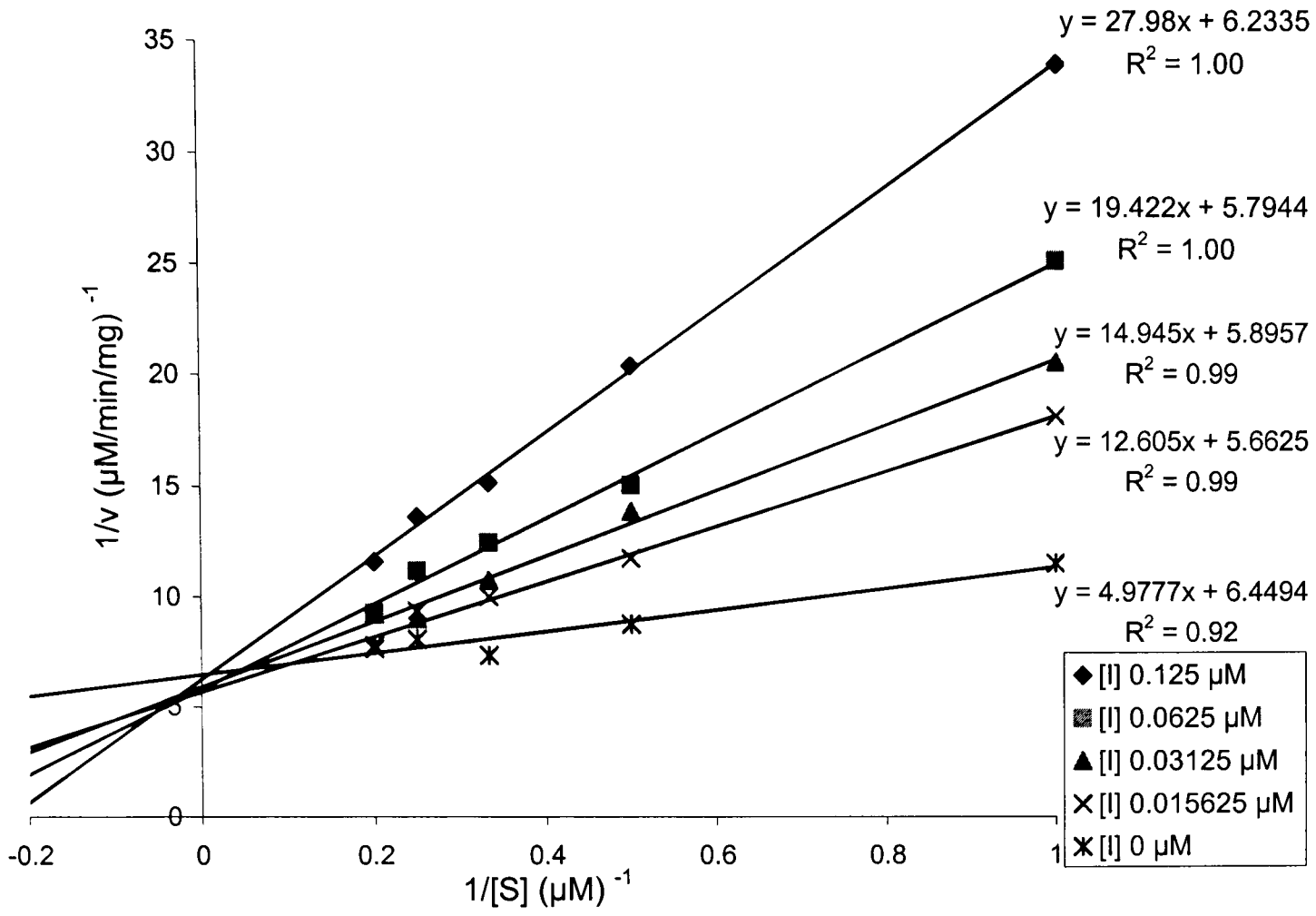

Figure 2.155 Lineweaver-Burk plots of 1/v versus 1/[S] for 1-[5-(4-fluoro-phenyl)-pentyl]-1*H*-imidazole (**178**) against 17,20-lyase.

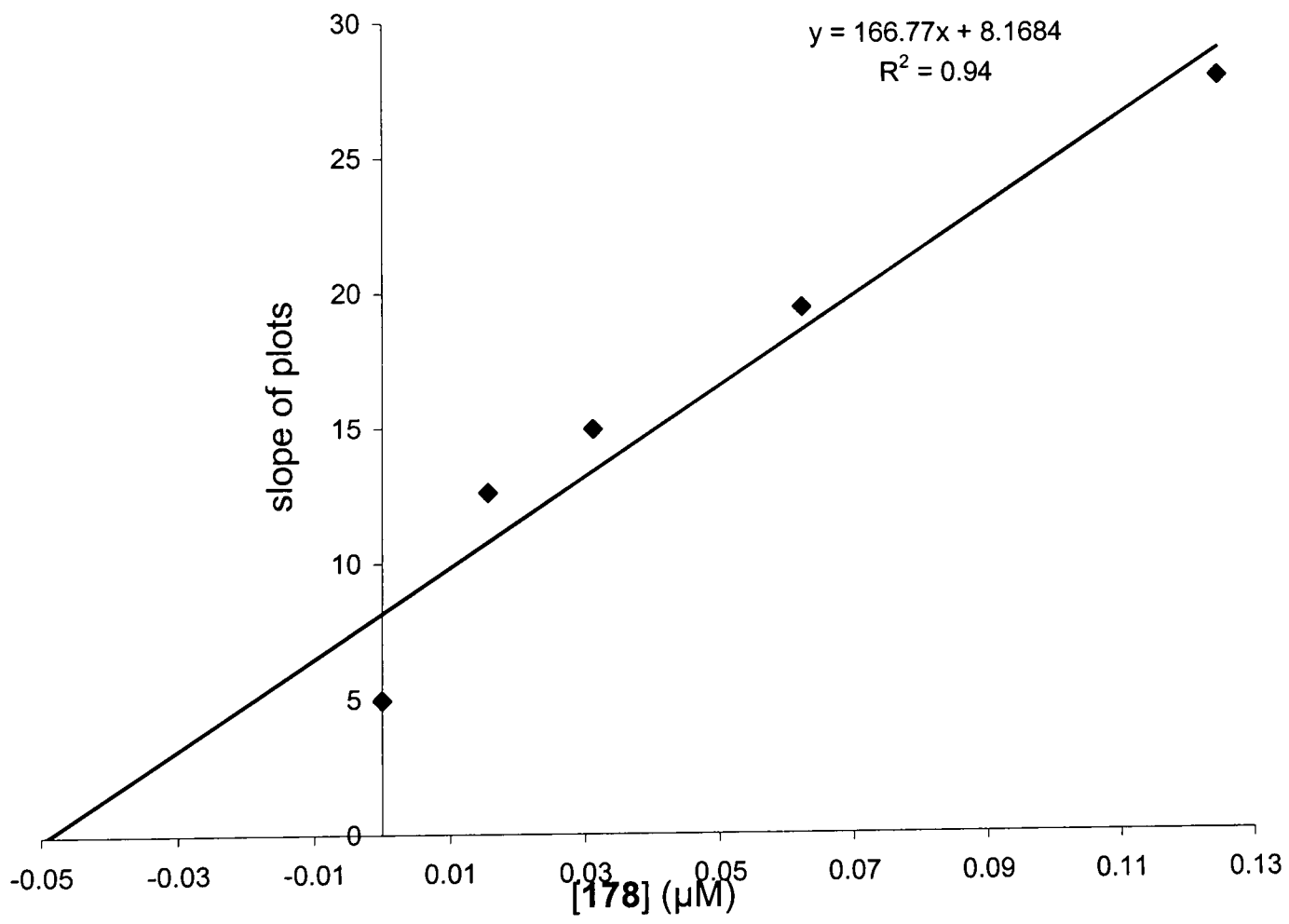

Figure 2.156 Plot of slope of Lineweaver-Burk plots versus the concentration of 1-[5-(4-fluoro-phenyl)-pentyl]-1*H*-imidazole (**178**) against 17,20-lyase showing a K_i of 50nM.

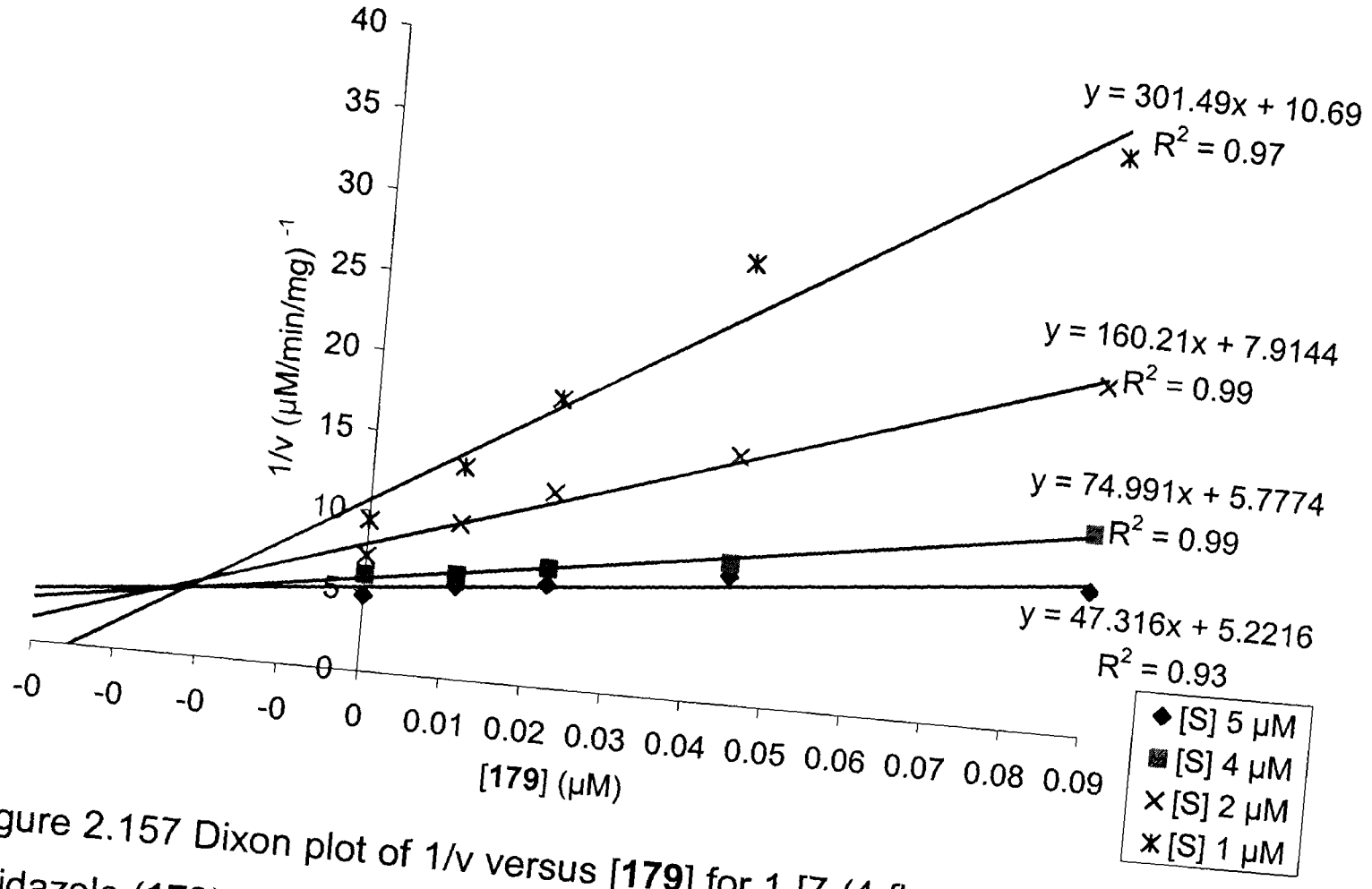

Figure 2.157 Dixon plot of 1/v versus [**179**] for 1-[7-(4-fluoro-phenyl)-heptyl]-1*H*-imidazole (**179**) against 17,20-lyase giving a K_i value of 21.40nM.

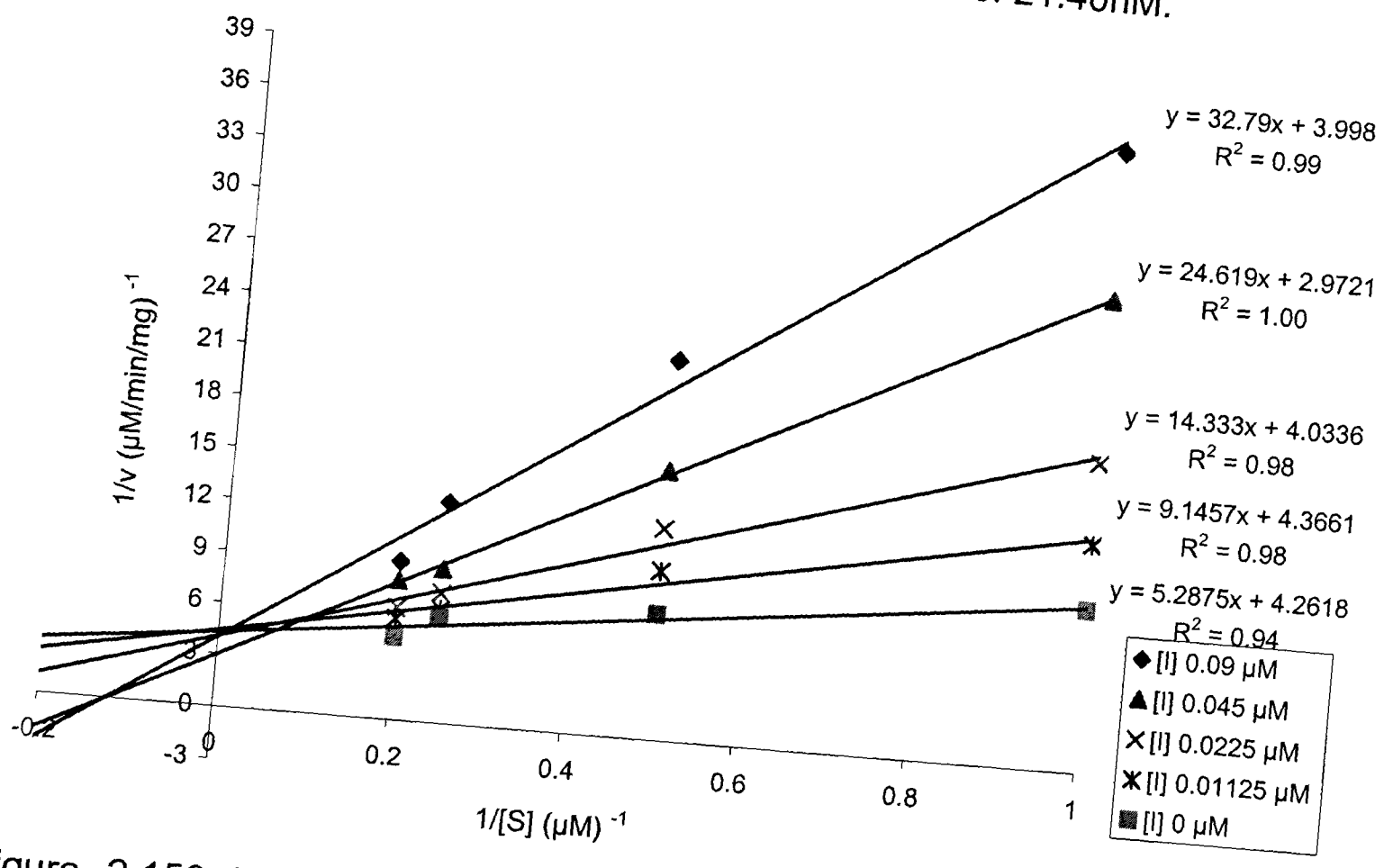

Figure 2.158 Lineweaver-Burk plots of 1/v versus 1/[S] for 1-[7-(4-fluoro-phenyl)-heptyl]-1*H*-imidazole (**179**) against 17,20-lyase.

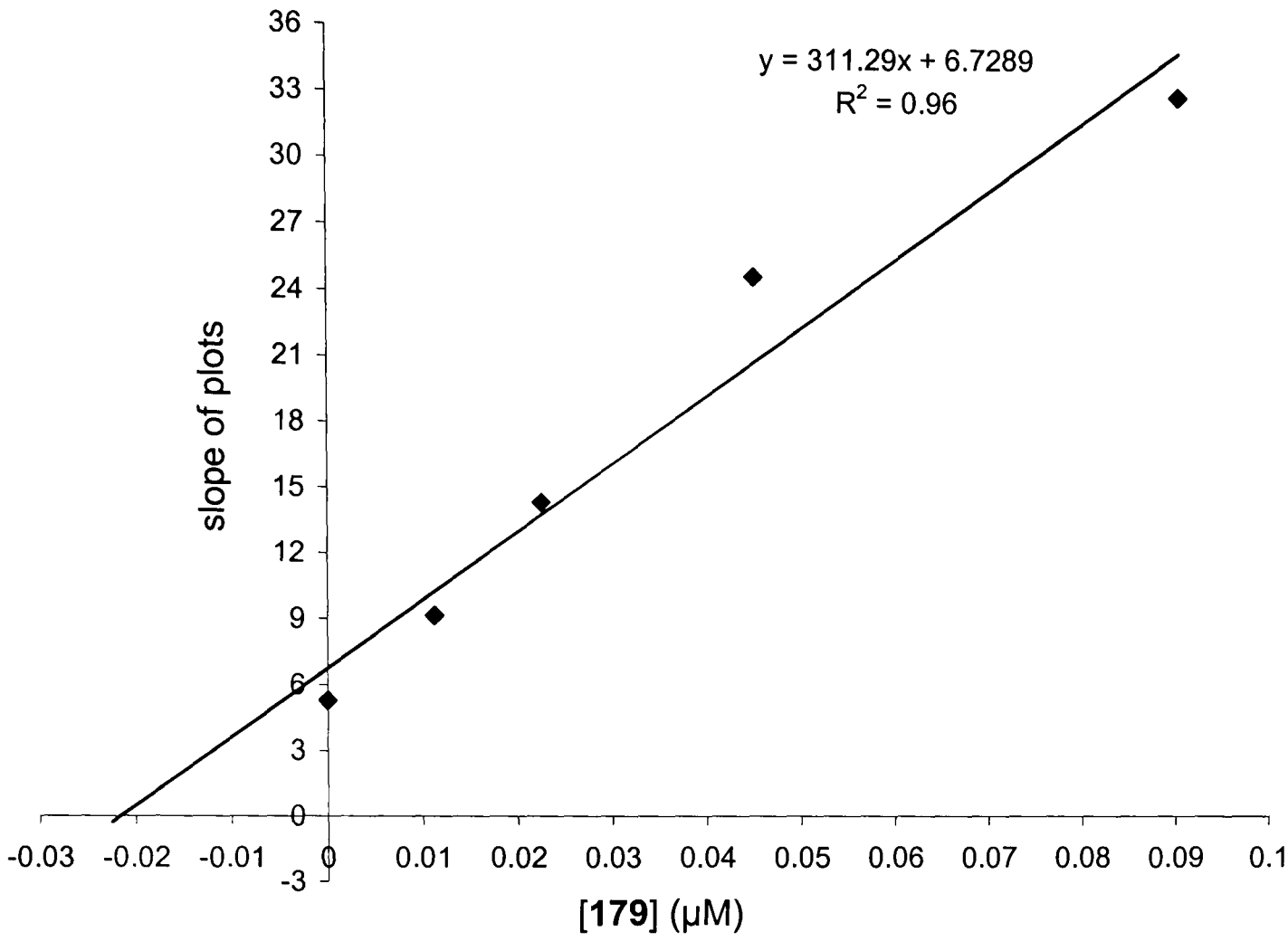

Figure 2.159 Plot of slope of Lineweaver-Burk plots versus the concentration of 1-[7-(4-fluoro-phenyl)-heptyl]-1*H*-imidazole (**179**) against 17,20-lyase showing a K_i of 21.60nM.

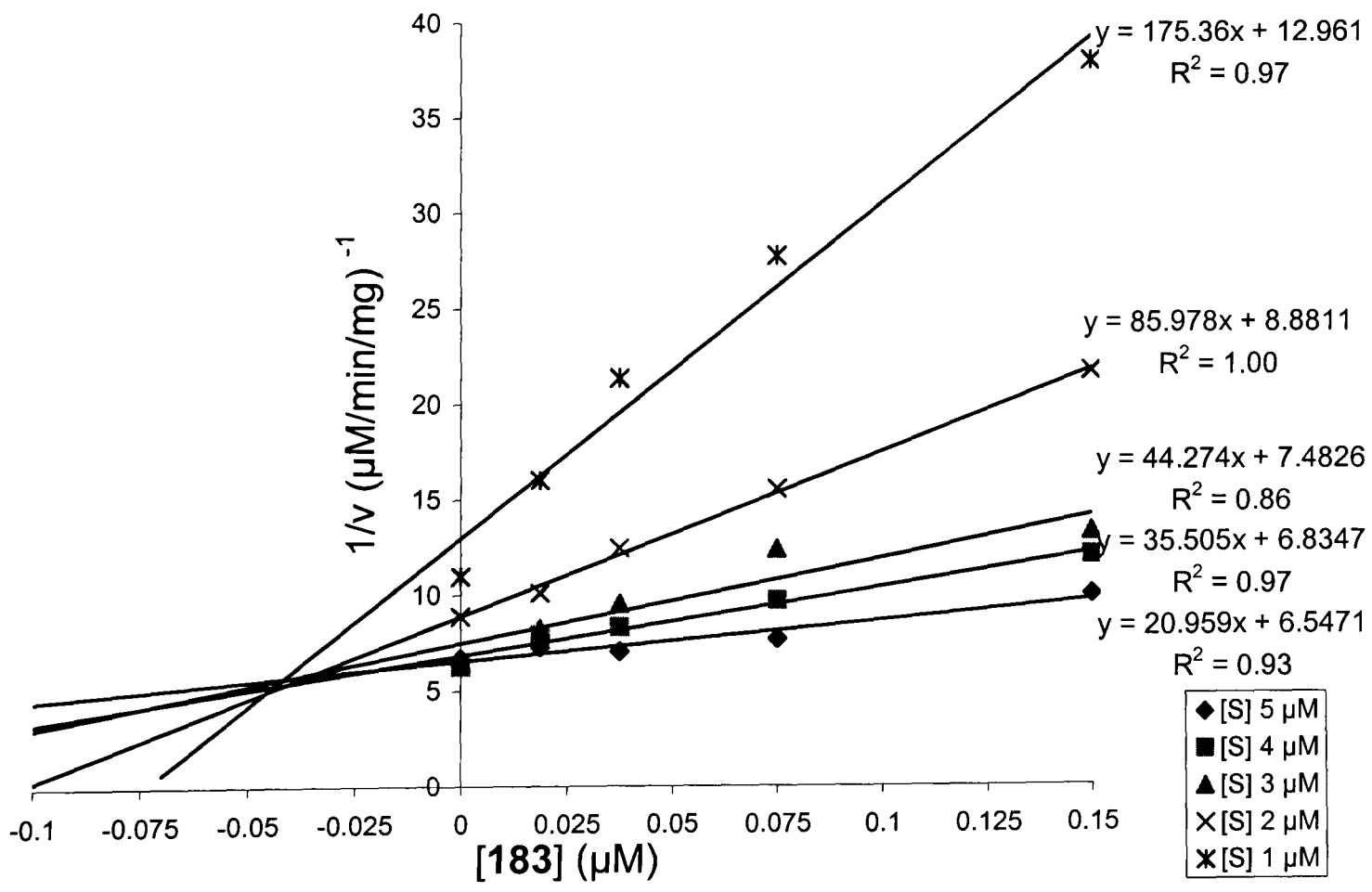

Figure 2.160 Dixon plot of 1/v versus [**183**] for 1-[5-(4-chloro-phenyl)-pentyl]-1*H*-imidazole (**183**) against 17,20-lyase giving a K_i value of 38nM.

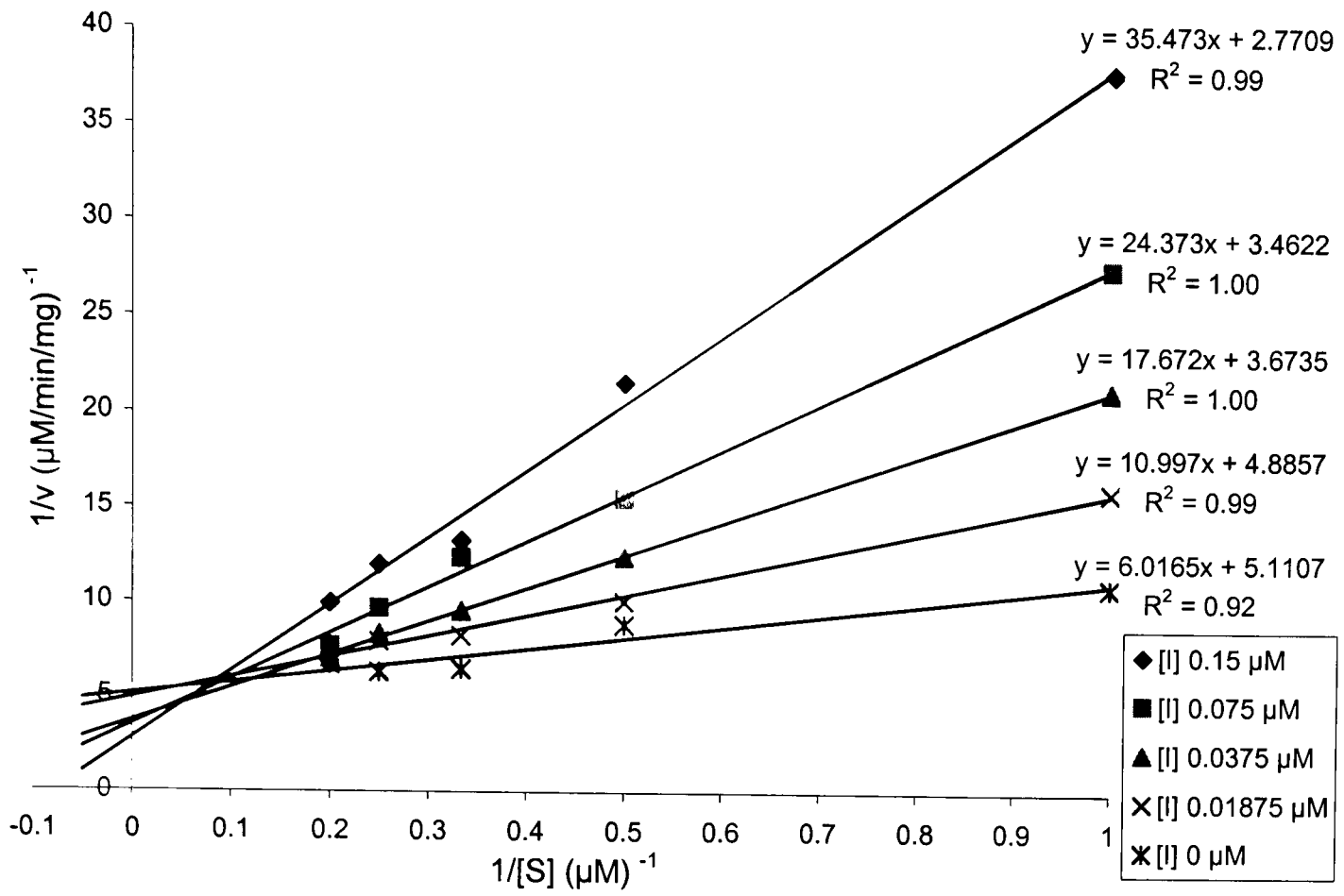

Figure 2.161 Lineweaver-Burk plots of 1/v versus 1/[S] for 1-[5-(4-chloro-phenyl)-pentyl]-1*H*-imidazole (**183**) against 17,20-lyase.

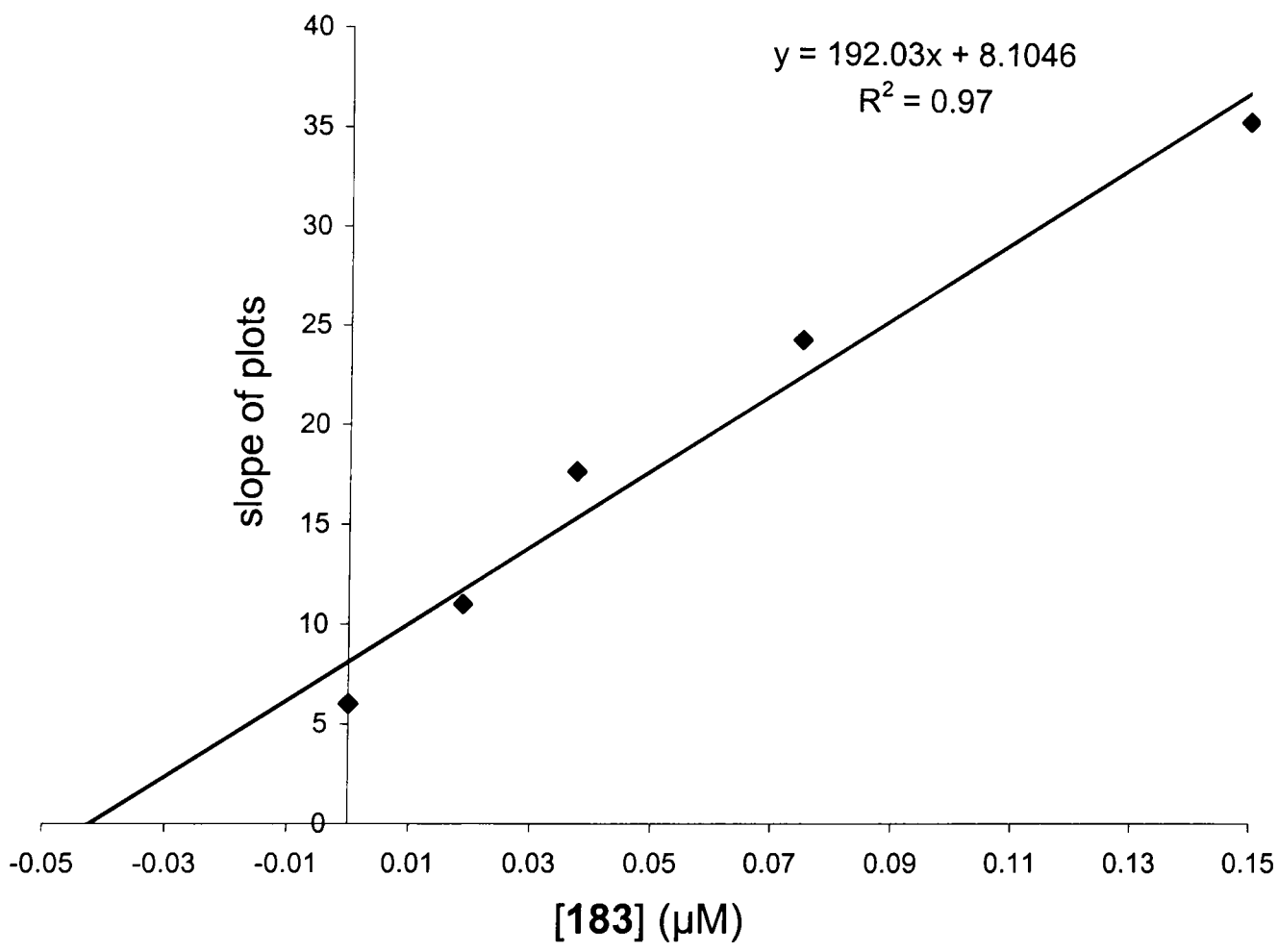

Figure 2.162 Plot of slope of Lineweaver-Burk plots versus the concentration of 1-[5-(4-chloro-phenyl)-pentyl]-1*H*-imidazole (**183**) against 17,20-lyase showing a K_i of 42nM.

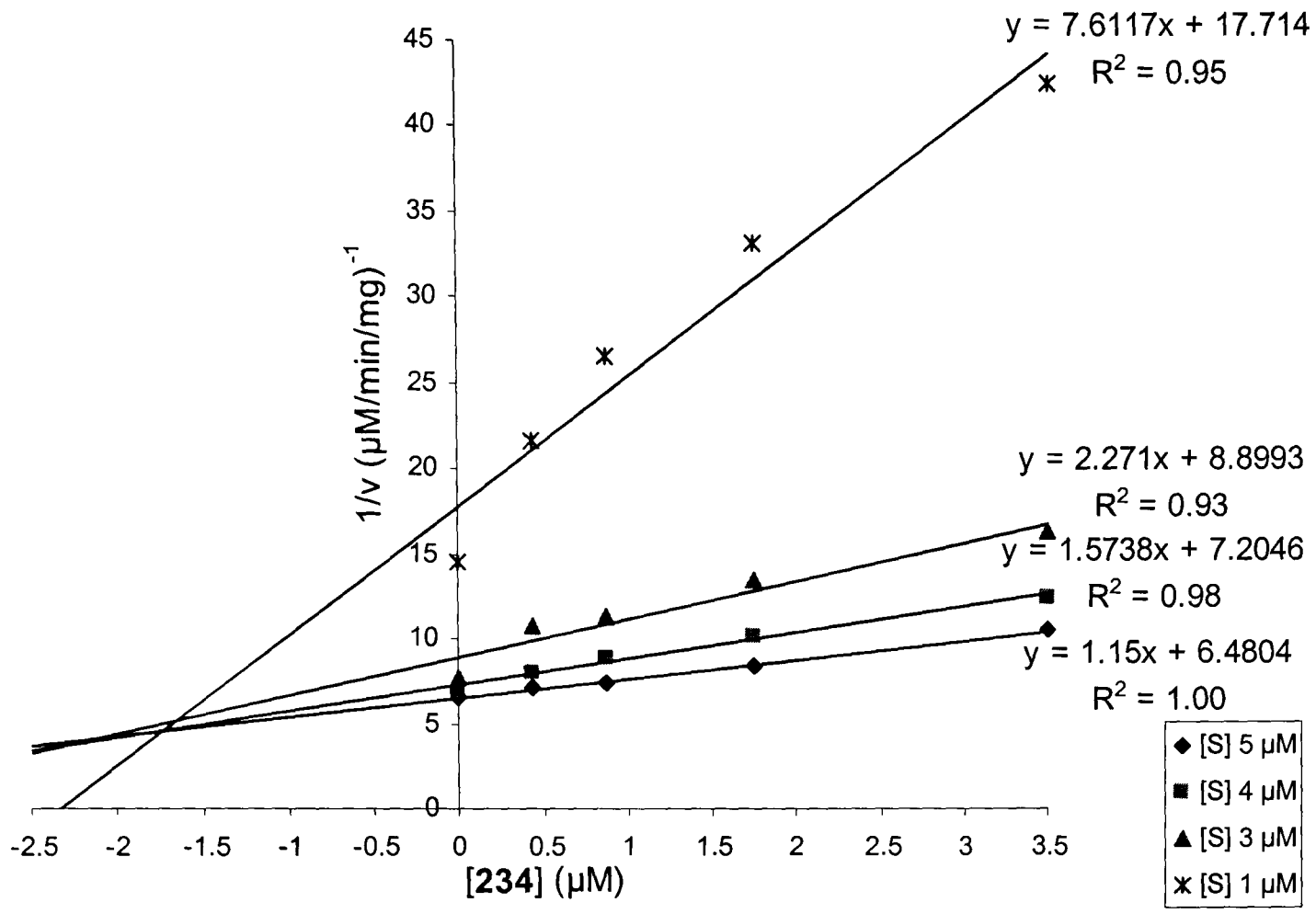

Figure 2.163 Dixon plot of 1/v versus **[234]** for 1-(3,4-dichloro-benzyl)-1*H*-imidazole (**234**) against 17,20-lyase giving a K_i value of 1990nM.

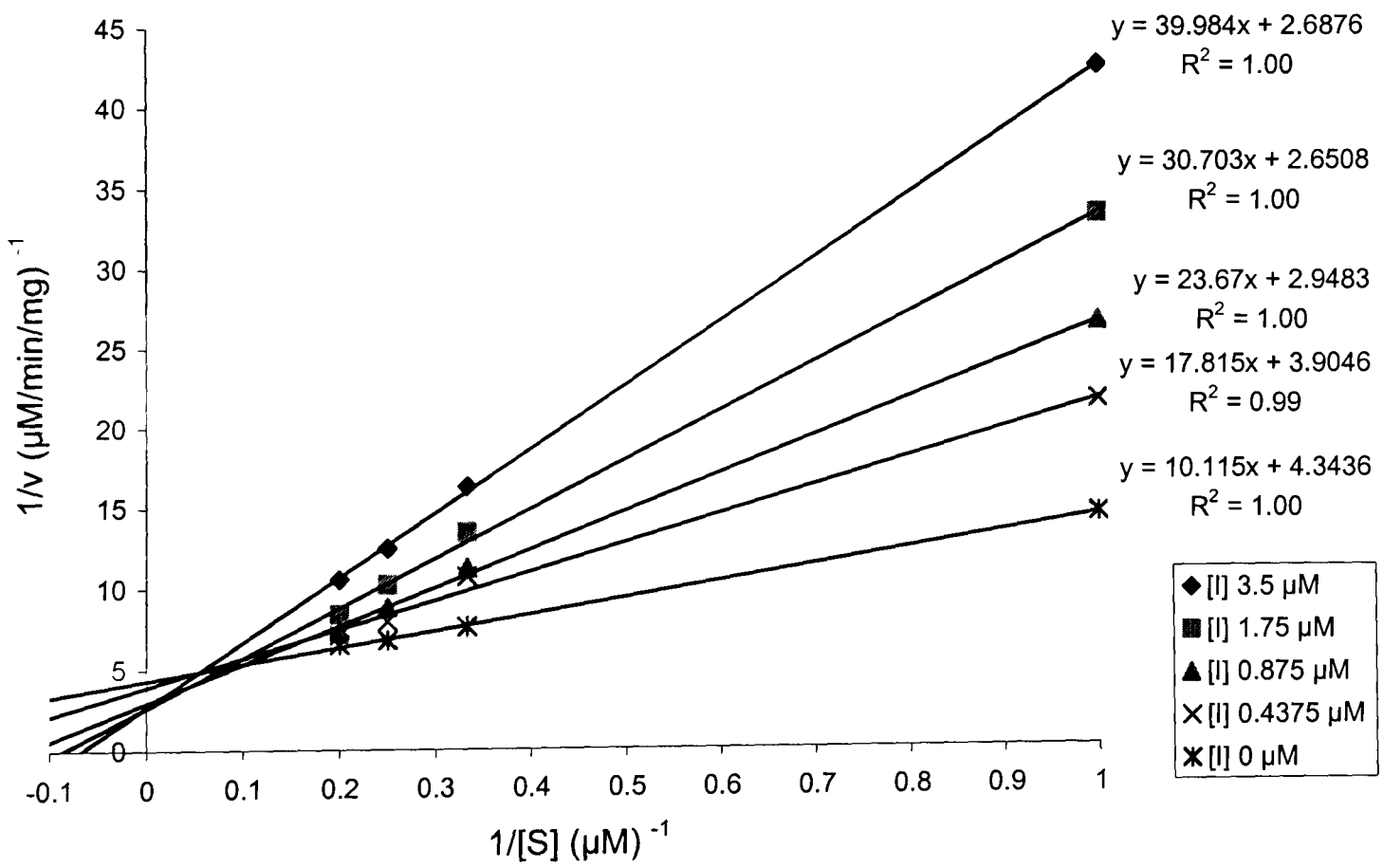

Figure 2.164 Lineweaver-Burk plots of 1/v versus 1/[S] for 1-(3,4-dichloro-benzyl)-1*H*-imidazole (**234**) against 17,20-lyase.

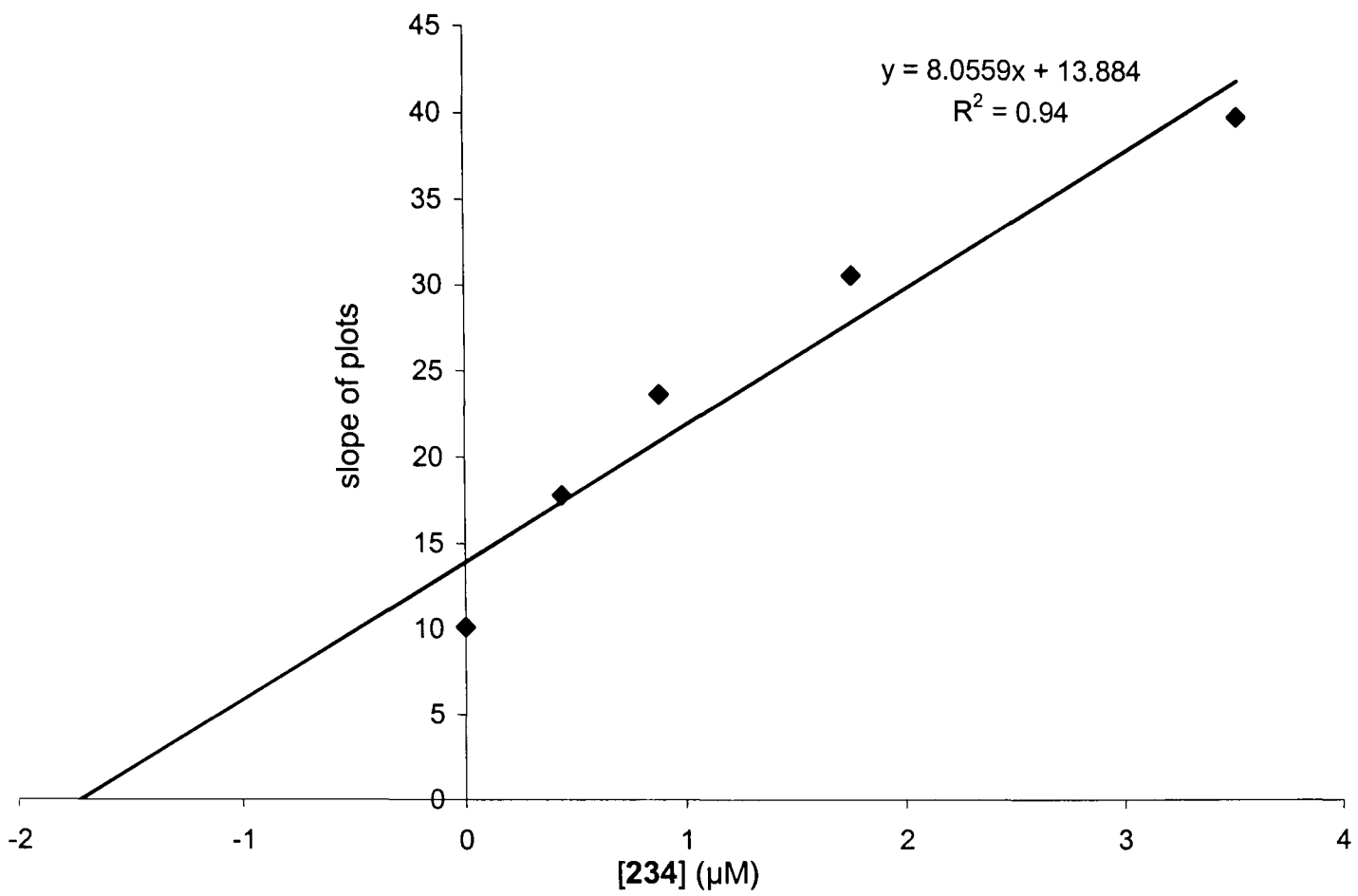

Figure 2.165 Plot of slope of Lineweaver-Burk plots versus the concentration of 1-(3,4-dichloro-benzyl)-1*H*-imidazole (**234**) against 17,20-lyase showing a K_i of 1720nM.

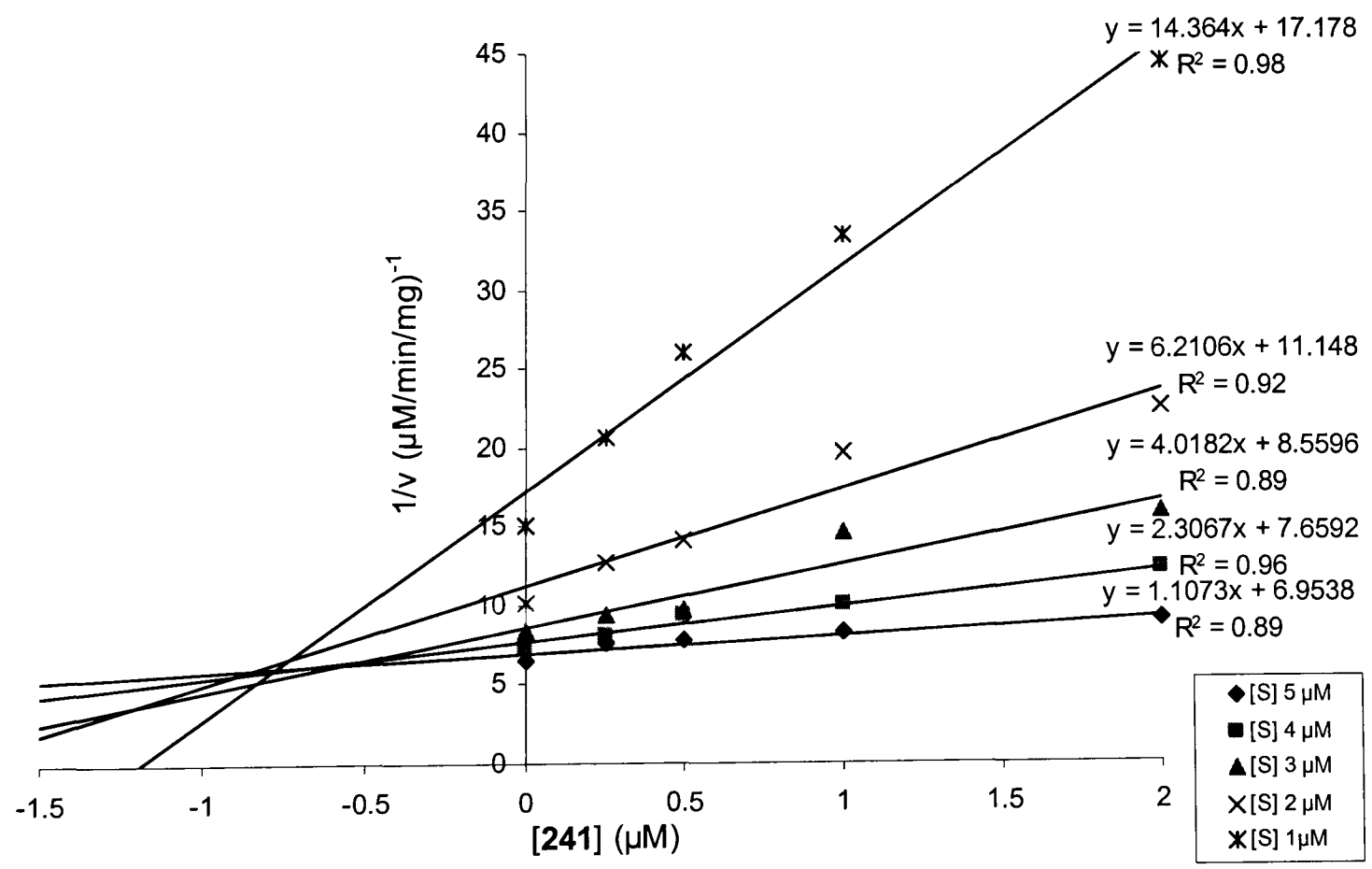

Figure 2.166 Dixon plot of 1/v versus [**241**] for 1-(4-iodo-benzyl)-1*H*-imidazole (**241**) against 17,20-lyase giving a K_i value of 680nM.

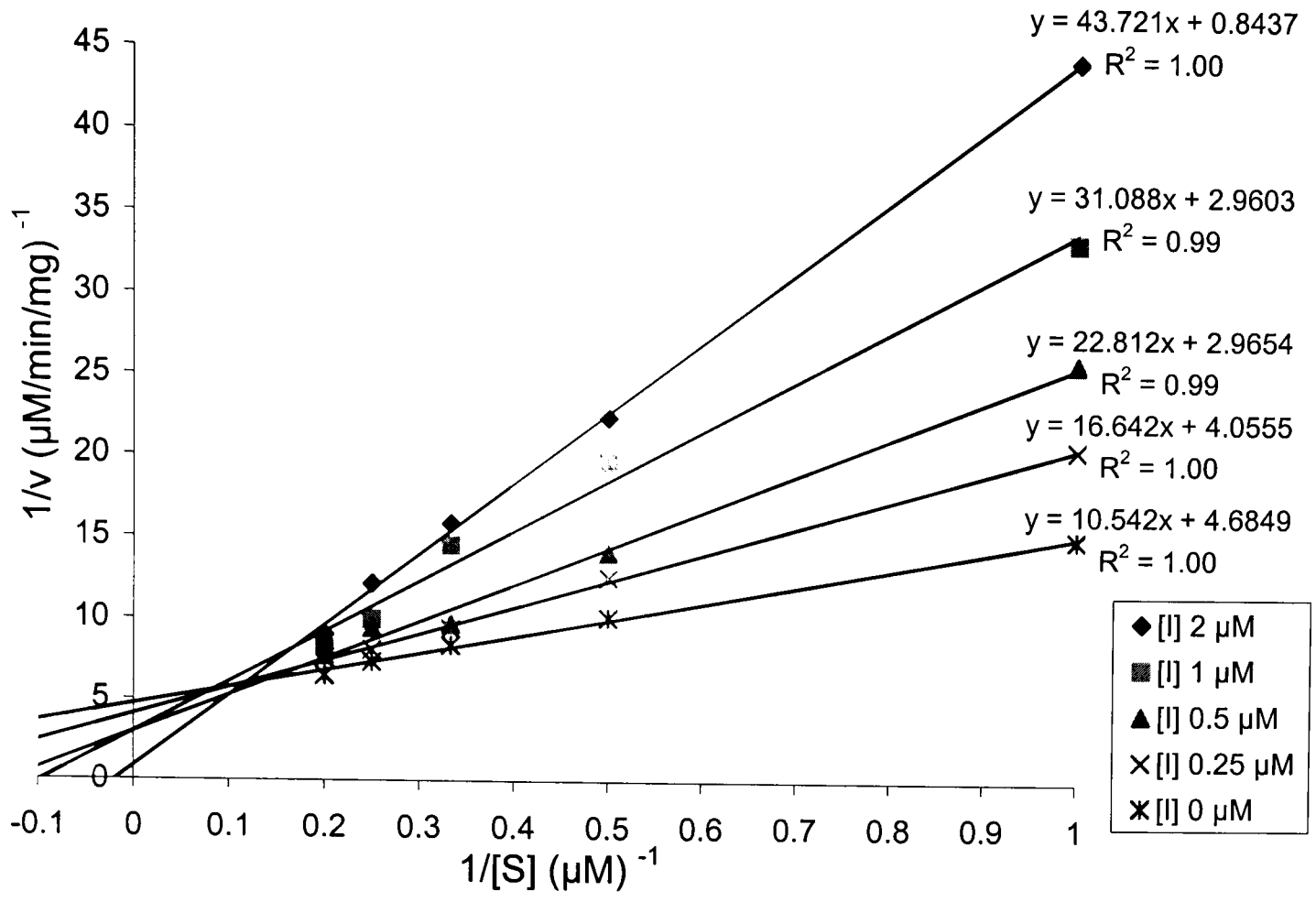

Figure 2.167 Lineweaver-Burk plots of 1/v versus 1/[S] for 1-(4-iodo-benzyl)-1*H*-imidazole (**241**) against 17,20-lyase.

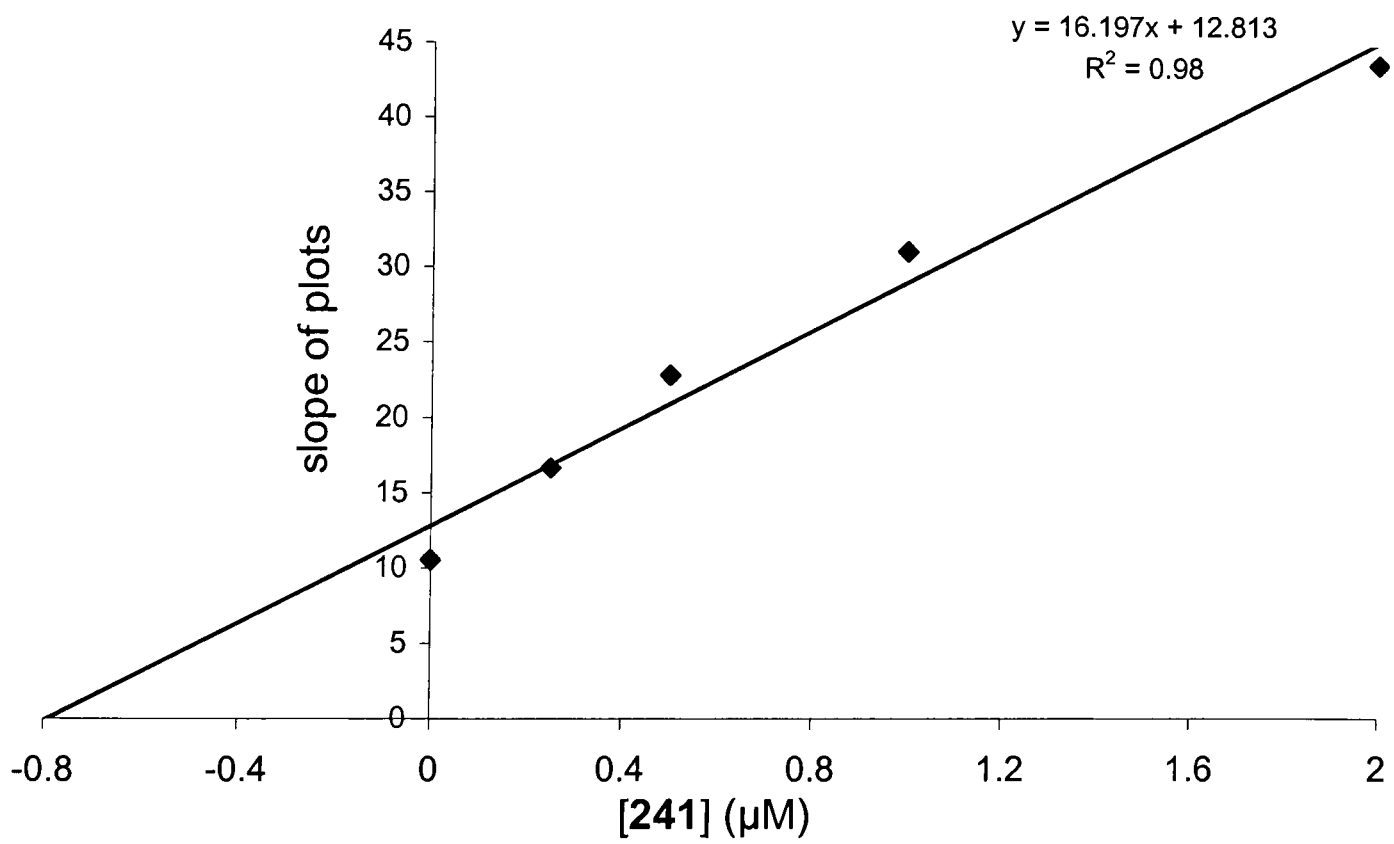

Figure 2.168 Plot of slope of Lineweaver-Burk plots versus the concentration of 1-(4-iodo-benzyl)-1*H*-imidazole (**241**) against 17,20-lyase showing a K_i of 790nM.

Chapter 3

3.0 HSDs

3.1 Type 3 17β-HSD Enzyme Assay (A to T)

3.2 Introduction

Compounds synthesised within the research group (by Miss Rupinder Lota) were evaluated for type 3 17β-HSD inhibitory activity using the microsomal fraction obtained from Sprague Dawley rat testicular tissue. The assay used was based on that of Le Lain et al (2001) and measures the effect of potential inhibitors on the rate of conversion of radiolabelled A to T.

To separate A and T from the reaction mixture, the method of TLC was employed. The extracts, together with the carrier steroids (5mg/mL), were applied to TLC plates (the carrier steroids were used to identify the radiolabelled steroids from the assay mixture). The mobile phase used was that developed as mentioned in Chapter 2, Section 2.2.

After elution and identification using UV light, each steroid was cut out and counted for 4min per tube in a cocktail of scintillation fluid and acetone. The percentage conversion of A to T was determined by the division of the CPM for the product from the total CPM of both steroids.

3.3 Methods, Materials and Instruments

All methods, materials and instruments used were as mentioned in Chapter 2, Section 2.3. [1,2,6,7-^{3}H]A was obtained from Amersham Pharmacia Biotech UK Limited, Buckinghamshire.

3.4 Buffer, Solution and Substrate Preparation

Buffers and solutions used in the assay were as described in Chapter 2, Section 2.4.

Substrate preparation of [1,2,6,7-^{3}H]A (100μM)

A stock solution of substrate was prepared by transferring radiolabelled [1,2,6,7-^{3}H]A (0.22μM, 20μL) to a glass vial and removing the toluene:ethanol mixture under a stream of nitrogen. Unlabelled substrate in propane-1,2-diol (99.78μM, 1mL) was added to the radiolabelled residue and mixed thoroughly to give a final concentration of 100μM.

3.5 Preparation of Testicular Microsomes

The microsomes were prepared as previously described in Chapter 2, Section 2.5.

3.6 Protein Assay

The protein concentration of the testicular microsomes was determined as previously described in Chapter 2, Section 2.6. The results are shown in Figure 3.1.

The protein concentration of the testicular microsomes was determined from the standard protein calibration curve (Figure 3.1) and was found to be 9.74mg/mL.

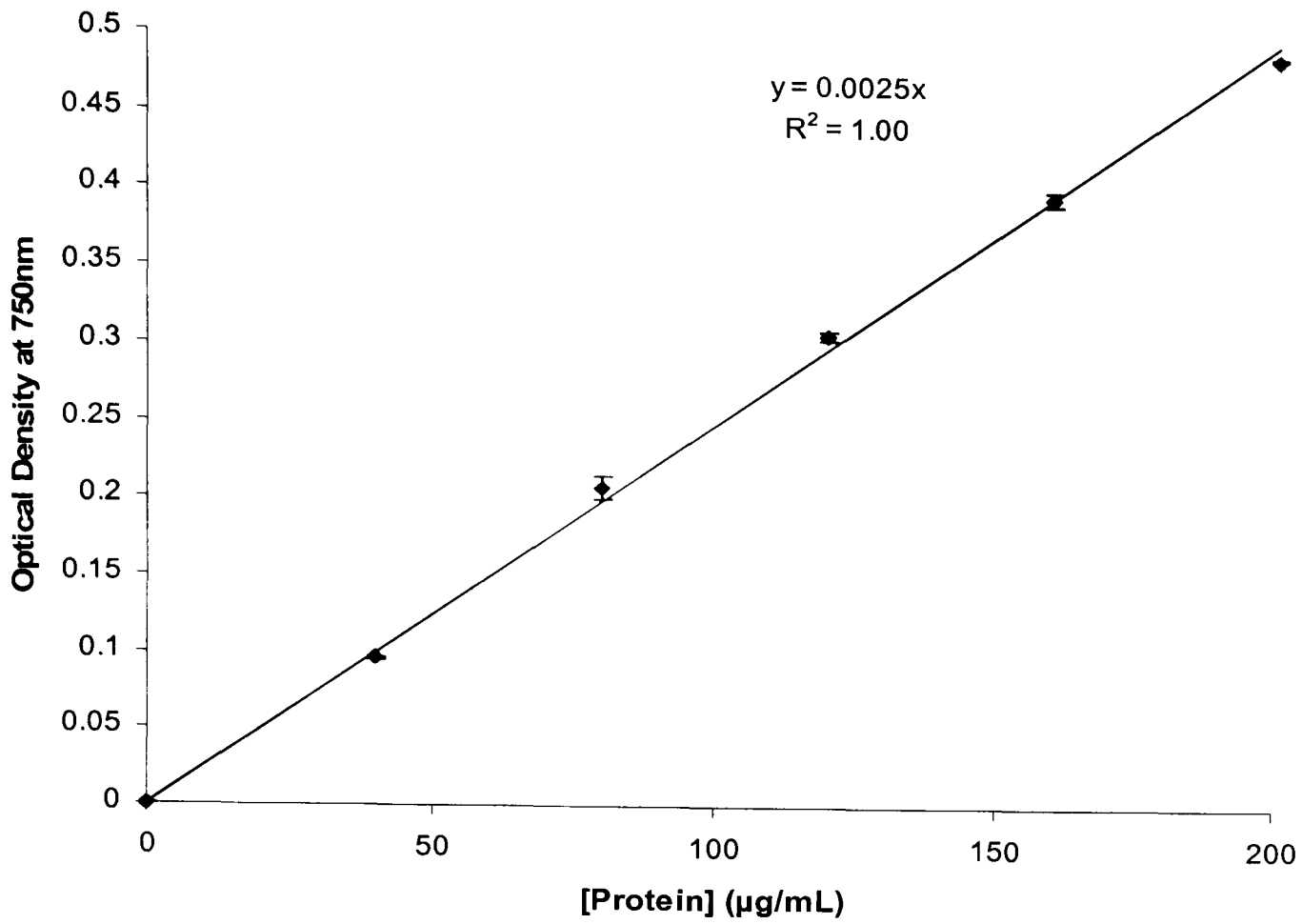

Figure 3.1 Calibration graph for protein assay for type 3 17β-HSD.

3.7 Validation of the 17β-HSD Assay for Conversion of A to T

To validate the 17β-HSD assay, it was necessary to determine the quantity of non-enzymatic product formation. Assay conditions were set so that the prepared substrate, A (1µM final concentration), was incubated for 30min at 37°C in the following solutions:

i. Sodium phosphate buffer (50mM, pH7.4)
ii. Testicular microsomes (0.097mg/mL, 10µL) and sodium phosphate buffer, lacking NADPH-generating system
iii. Testicular microsomes, denatured by addition of ether (2mL), sodium phosphate buffer and NADPH-generating system.

After incubation, the assay mixtures were treated, except (iii), with ether (2mL). The solutions were vortexed, then left to stand over ice for 15min. The organic phase was extracted into a separate clean tube. The assay mixture was further extracted with ether (2x2mL), and the organic layers combined. The solvent

was removed under a stream of nitrogen, acetone (30μl) was added to each tube and the solution spotted onto silica based TLC plates along with carrier steroids (A and T, 5mg/mL, approximately 10μL) were spotted onto TLC plates and run, using a mobile phase consisting of dichloromethane (70mL) and ethyl acetate (30mL). After development, the separated steroids were identified, using an UV lamp, cut from the plate and placed into scintillation vials. Acetone (1mL) was added to each vial in order to dissolve the steroid from the silica plate and then scintillation fluid (Optiscint HiSafe, 3mL) was added. The samples were vortexed and then read for radioactivity (4min). None of the samples showed detectable quantities of T, indicating that (a) testicular microsomes and (b) NADPH are both essential requirements for the conversion of A to T.

3.8 Protein Dependency for Type 3 17β-HSD

An experiment was performed to establish whether the rate of appearance of T, produced during the enzymatic reaction, was proportional to the protein concentration.

Incubations were carried out (in triplicate) using protein concentrations 0.097, 0.244, 0.487, 0.731 and 0.974mg/mL (final concentration), prepared substrate, A (1μM final concentration, 10μL), NADPH-generating system (50μL) and phosphate buffer (pH7.4, to 1mL). The solutions were incubated for 30min at 37°C and the reaction was quenched by the addition of ether (2mL) and placed on ice. The assay was completed as previously described (Section 3.7) and the percentage conversions determined using equation 3.1. The results are shown in Figure 3.2

$$\text{Percentage Conversion} = \left(\frac{T}{A + T}\right) \times 100$$

Equation 3.1 Percentage conversion of A to T.

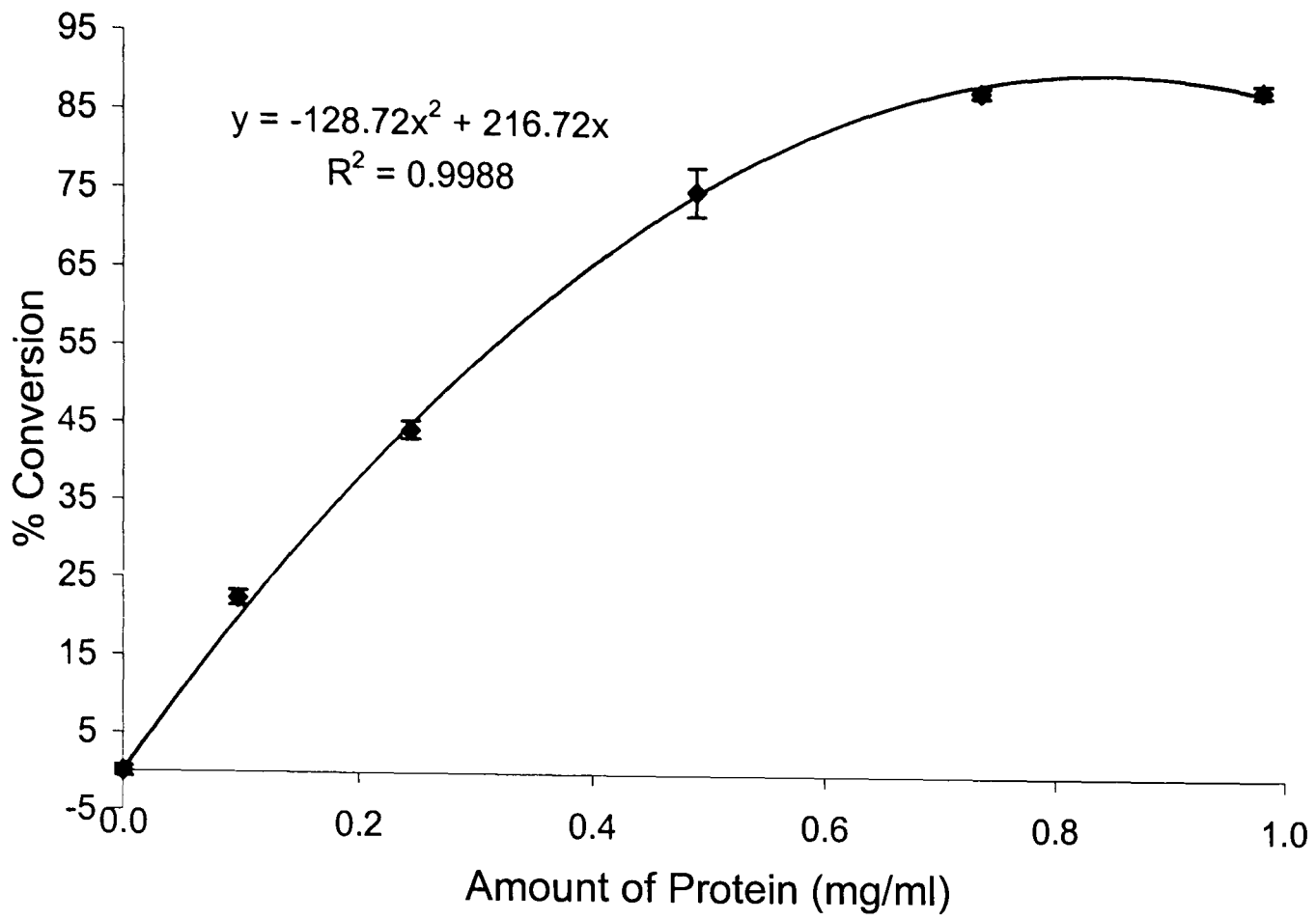

Figure 3.2 Plot to show percentage conversion of A to T at varying protein concentrations.

At 1μM substrate concentration, it can be concluded that the kinetics of the reaction are linear for concentrations up to 0.49mg/mL protein.

3.9 Time Dependency for Type 3 17β-HSD

Time dependency experiments were performed to ensure that the assays were within the linear phase of the enzyme reaction.

Incubations were carried out (in triplicate) using prepared substrate, A (1μM final concentration, 10μL), NADPH-generating system (50μL) and sodium phosphate buffer (pH7.4, 930μL). The samples were warmed to 37°C in a shaking water bath before the addition of the testicular microsomes (0.097mg/mL final concentration, 10μL), at differing time intervals (15, 30, 45, 60, 90 and 120min). The reaction was quenched by the addition of ether (2mL) and placed on ice. The assay was completed as previously described (Section 3.7). A graph was then plotted for percentage conversion versus time (Figure 3.3).

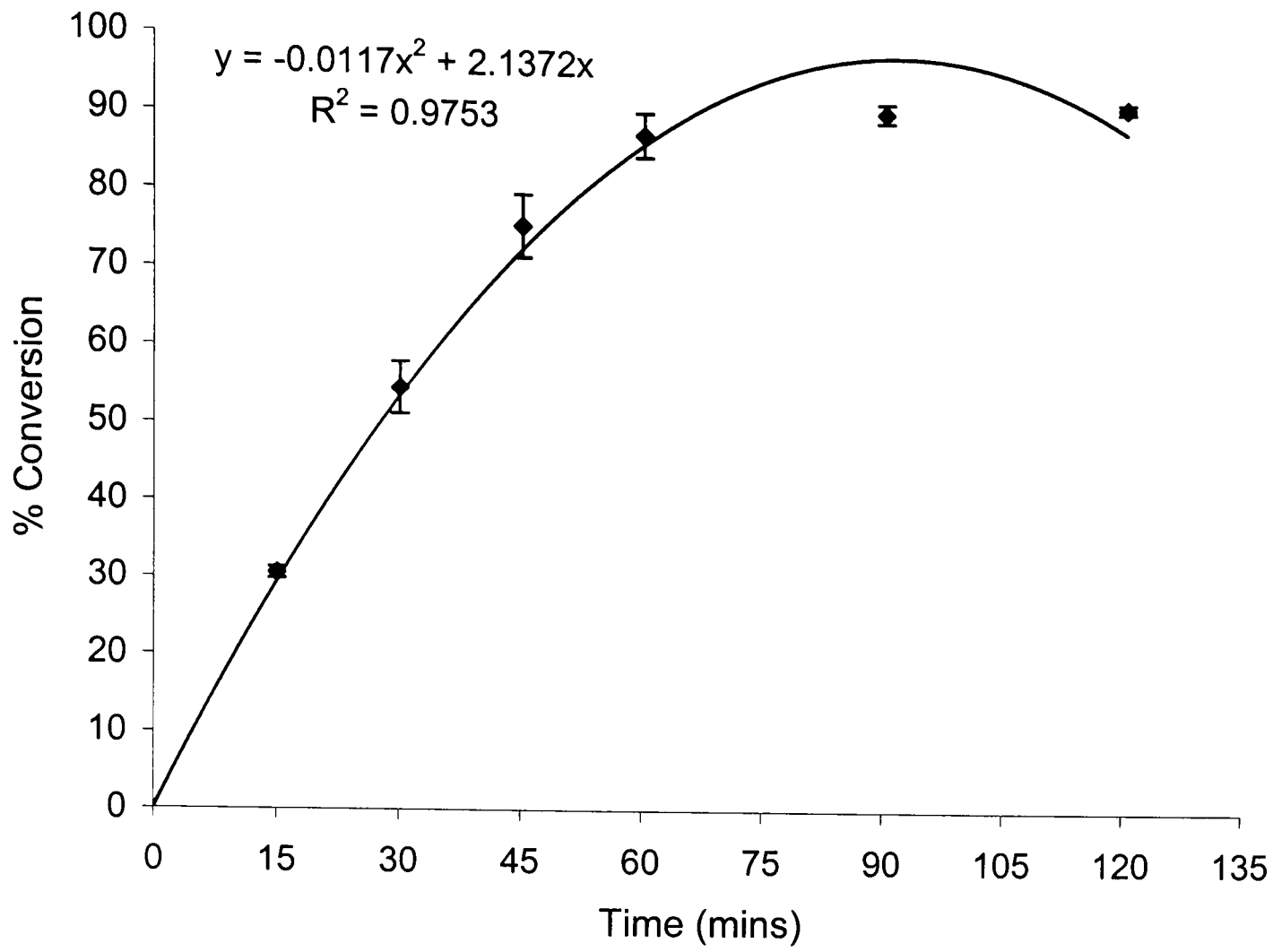

Figure 3.3 Plot to show percentage conversion of A to T at varying time intervals.

At 0.097mg/mL protein concentration and 1μM substrate concentration, it can be concluded that the kinetics of the reaction are linear up to 60min.

3.10 Determination of K_m for Type 3 17β-HSD

The prepared substrate, A (100μM) was serially diluted, using propane-1,2-diol, to give a range of final incubation concentrations of substrate (0.2 to 1.5μM). All incubations were carried out in triplicate at 37°C in a shaking water bath. Incubation mixtures (1mL), containing NADPH-generating system (50μL) and prepared substrate A (of varying concentration, 10μL), in sodium phosphate buffer (930μL, pH7.4), were allowed to warm to 37°C. The testicular microsomes were thawed and warmed to 37°C before addition (0.097mg/mL final concentration, 10μL) to the assay mixture. The solutions were incubated for 30min at 37°C and the reaction was quenched by the addition of ether (2mL)

and placed on ice. The assay was completed as previously described (Section 3.7). The velocity, v, for each substrate concentration was calculated using Equation 3.2, where units for v are: μM/min/mg.

$$v = \frac{\text{CPM (T) x substrate concentration [S] (}\mu\text{M)}}{\text{CPM (A+T) x protein concentration (mg/ml) x time (min)}}$$

Equation 3.2 Velocity calculation for each substrate concentration

3.11 Results – Graphical Determination of K_m

The K_m and V_{max} were determined from five different general methods for A, as previously described in Chapter 2, Section 2.11, and are shown in Figures 3.4 to 3.8 and the averages of three assays are summarised in Table 3.1

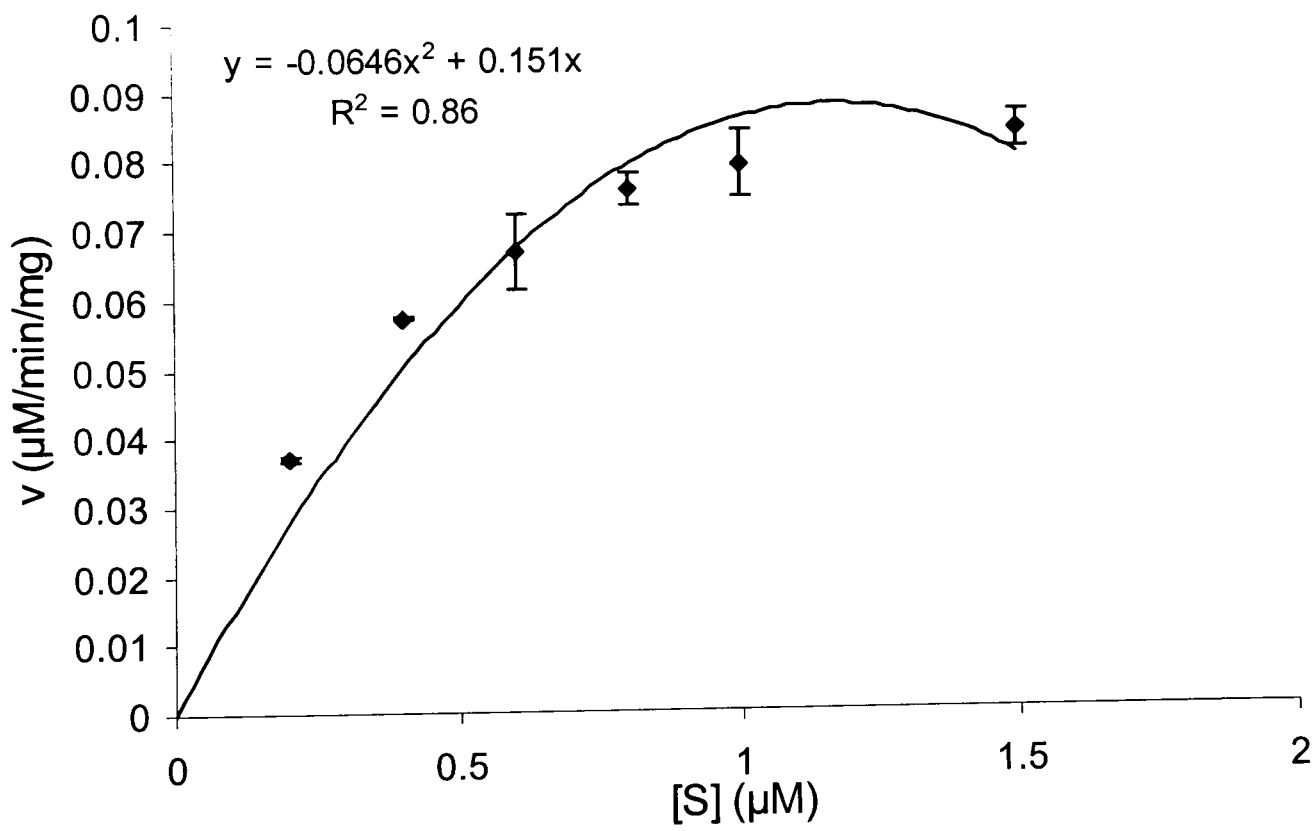

Figure 3.4 Michaelis Menten plot for type 3 17β-HSD.

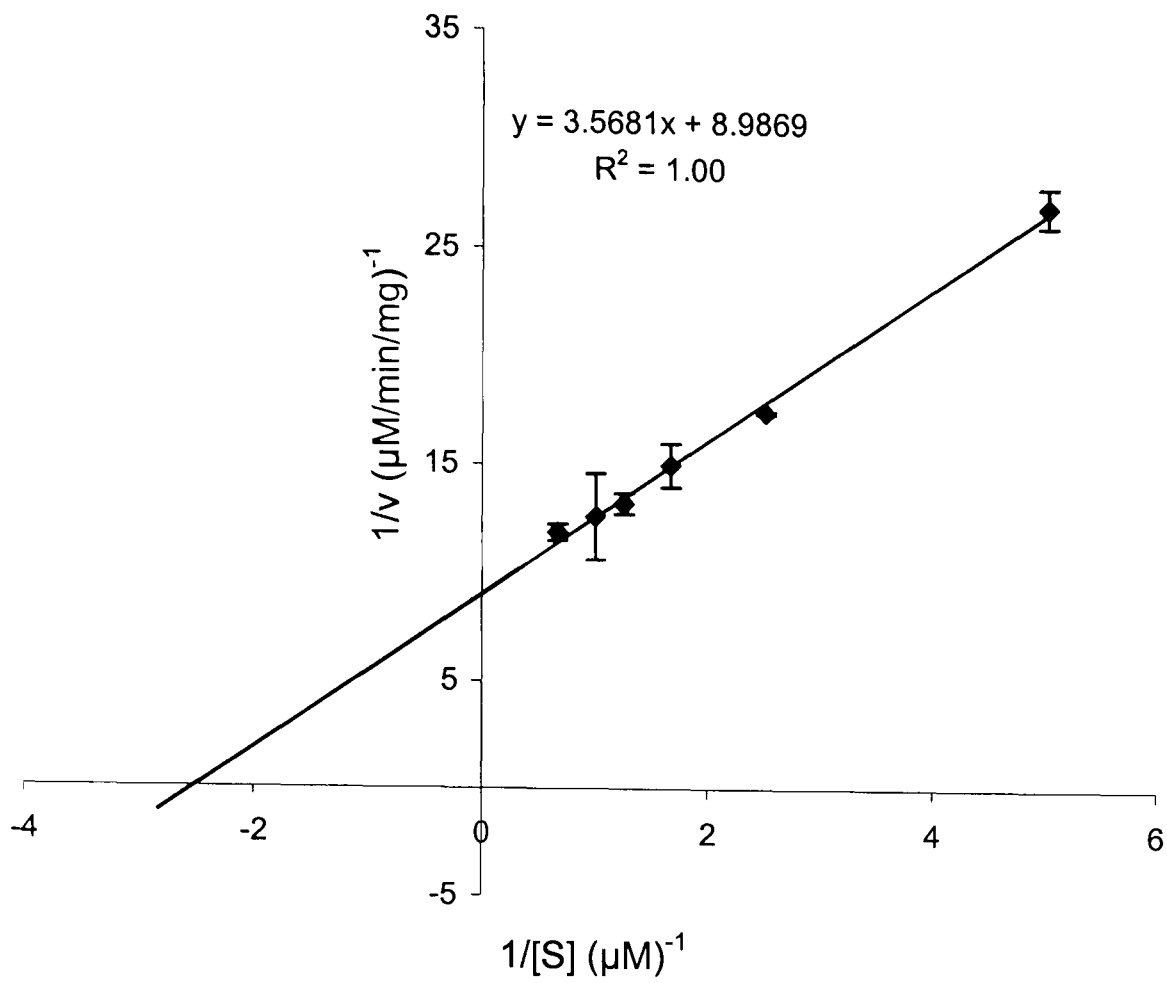

Figure 3.5 Lineweaver-Burk plot for type 3 17β-HSD.

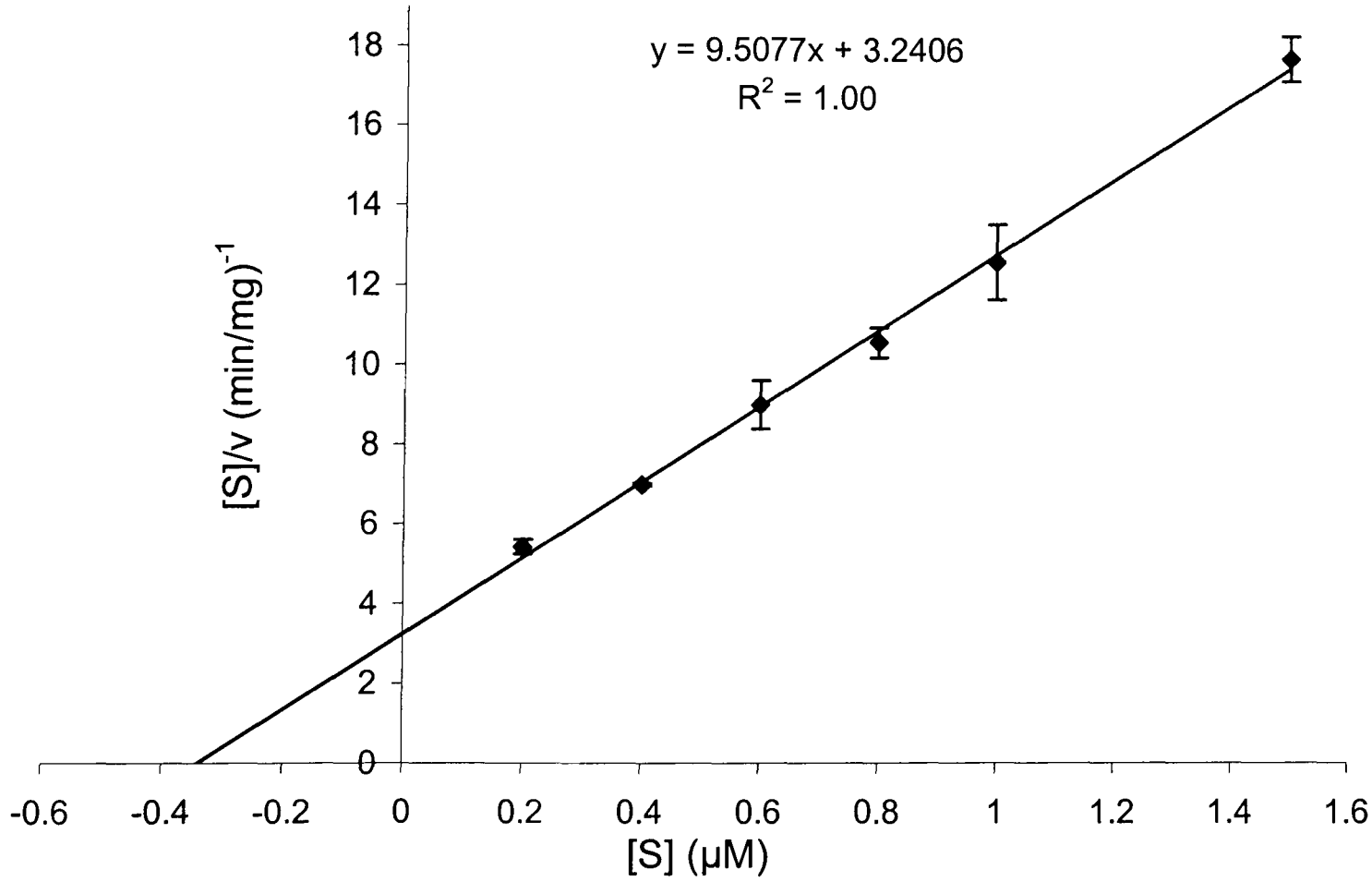

Figure 3.6 Hanes-Woolf plot for type 3 17β-HSD.

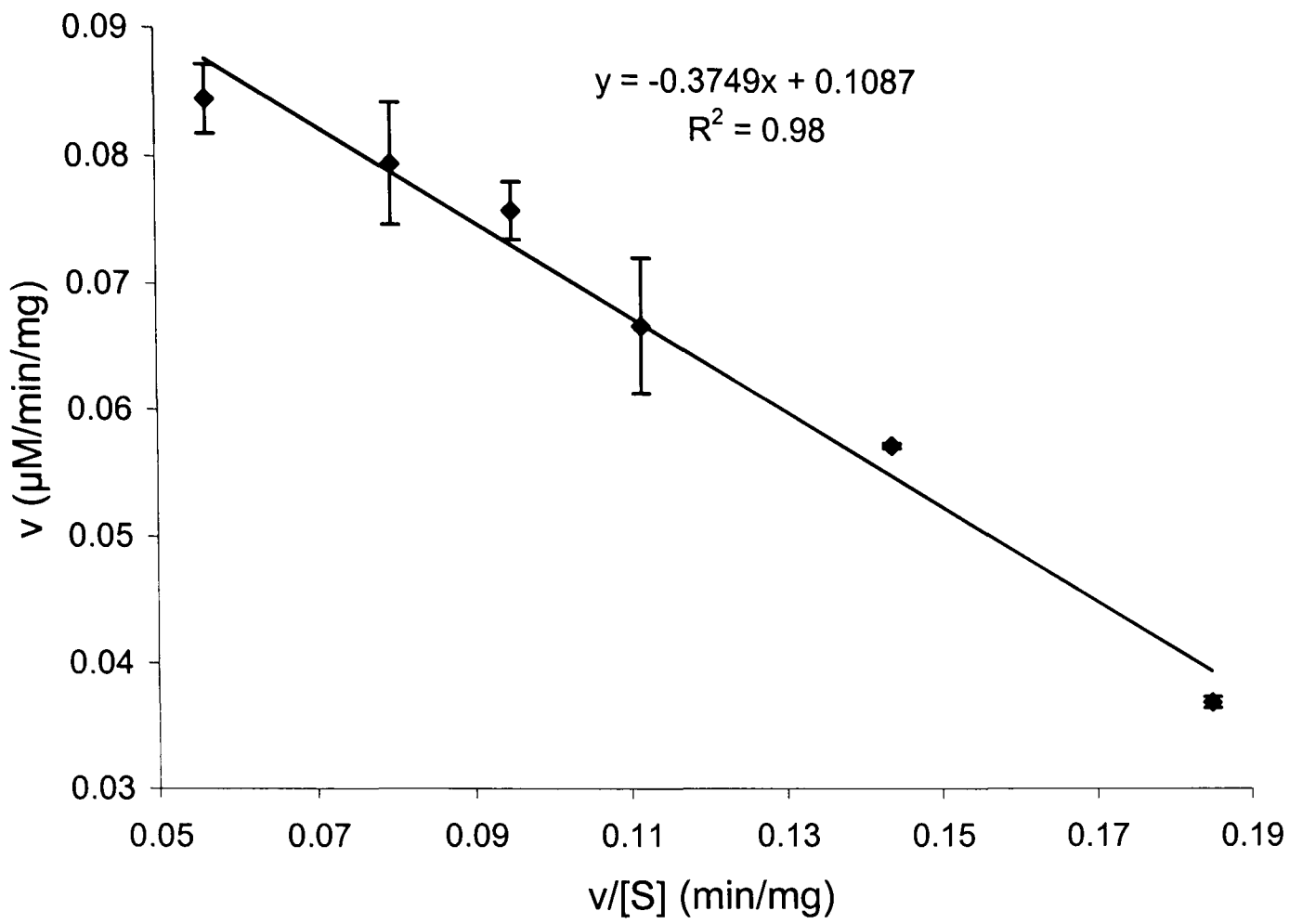

Figure 3.7 Eadie-Hofstee plot for type 3 17β-HSD.

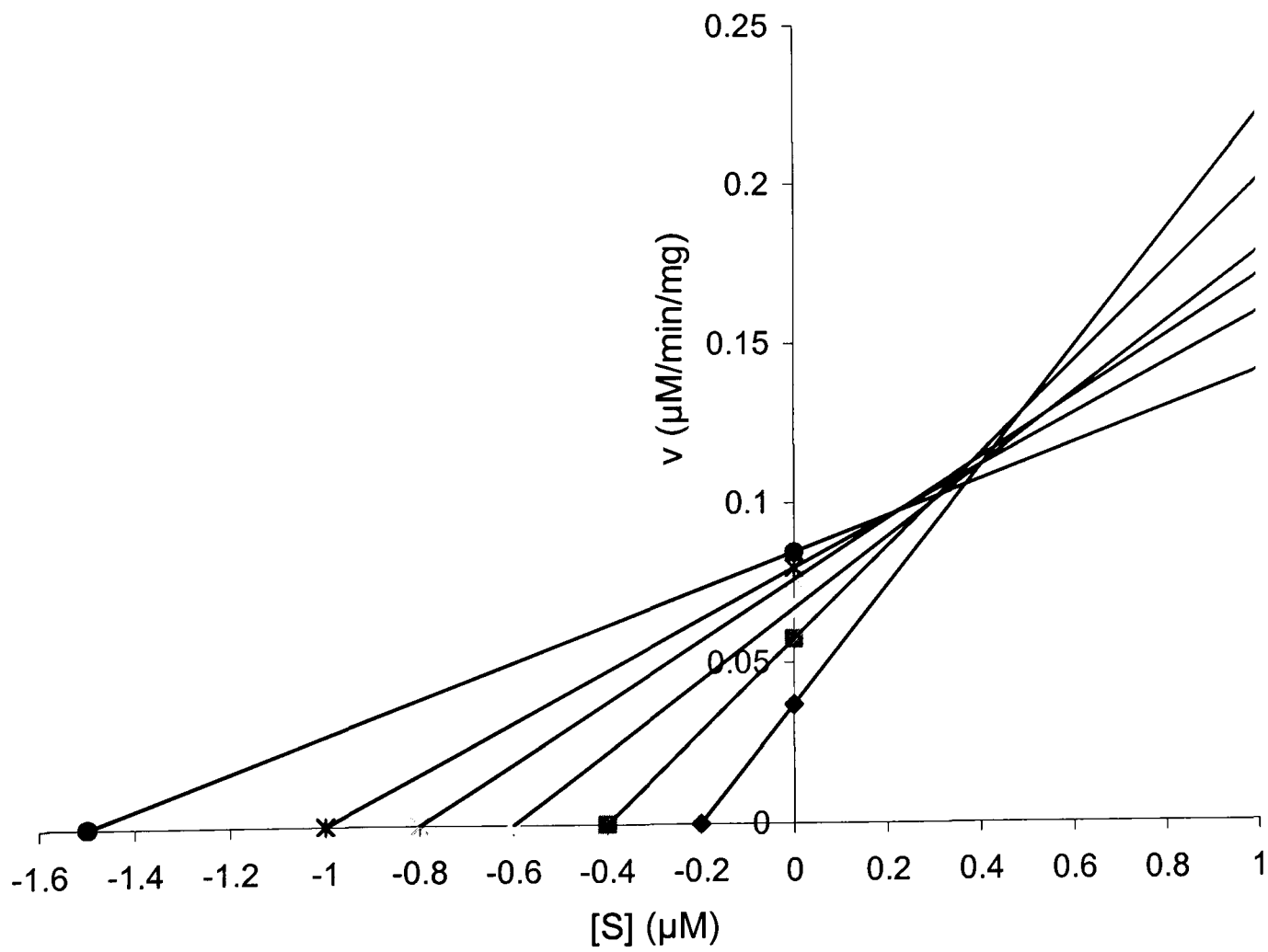

Figure 3.8 Direct linear plot for type 3 17β-HSD

Plot	K_m (μM)
Michalis Menten plot	0.35 ± 0.03
Lineweaver-Burk plot	0.44 ± 0.05
Hanes-Woolf plot	0.34 ± 0.04
Eadie-Hofstee plot	0.37 ± 0.03
Direct linear plot	0.35 ± 0.01
Average K_m	0.37 ± 0.03

Table 3.1 Summary of K_m plots for type 3 17β-HSD.

3.12 Discussion

The average K_m value for type 3 17β-HSD with the substrate A using Sprague-Dawley testicular microsomes was found to be 0.37 ± 0.03μM, compared to K_m values obtained by other workers i.e., K_m = 0.77 ± 0.26μM (Le Lain et al, 2001).

3.13 Preliminary Screening of Compounds for Type 3 17β-HSD Activity

The assay procedure for screening involved inhibitors and standards (baicalein and 7-hydroxyflavone) dissolved in absolute ethanol and diluted to give the required final incubation concentration. The assay was carried out (in triplicate) at 37°C in a shaking water bath. The total assay volume was 1mL. Prepared substrate A (1.5μM/tube, 15μL), NADPH-generating system (50μL) and Inhibitor (100μM, 20μL), in sodium phosphate buffer (905μL, pH7.4), were allowed to warm to 37°C. The testicular microsomes were thawed and warmed to 37°C before addition (0.097mg/mL final concentration, 10μL) to the assay mixture. The solutions were incubated for 30min at 37°C and the reaction was quenched by the addition of ether (2mL) and placed on ice. The assay was completed as previously described (Section 3.7). Control samples with no inhibitor were incubated simultaneously. The results were determined by using equation 3.1 to determine the percentage conversion of A to T and then comparing the conversion in the presence of inhibitors to that of the controls. Results are shown in Tables 3.2a – 3.4b.

3.14 IC_{50} of Compounds for Type 3 17β-HSD activity

IC_{50} determination was carried out on baicalein and 7-hydroxyflavone and all inhibitors which showed significant 17β-HSD inhibitory activity. The assay was carried out in the same manner as described in Section 3.13, except that each inhibitor (20μL) was tested over a range of final assay concentrations depending on its preliminary screening result. The IC_{50} was determined from plots of percentage inhibition versus Log [I] (Figures 3.9 – 3.24).

3.15 Results for 4-Hydroxyphenyl Ketones

The results are shown in Tables 3.2a – 3.2d

3.15.1 Discussion

Good inhibitory activity has been found by the evaluation of flavonoid-based compounds and due to a lack of compounds in the clinic it was found that evaluation against a single standard was not possible, as such baicalein (**113**) and 7-hydroxyflavone (**97**) were used. All compounds were screened against type 3 17β-HSD and it was found that compounds **248** – **260** showed more potency than the standards and thus IC_{50s} were conducted on the whole range **247** – **260.** It was found that compounds **252** – **262** were more potent than both standards but **248** and **249** were equipotent and more potent than baicalein respectively but less potent than 7-hydroxyflavone while **250** was equipotent to 7-hydroxyflavone.

Compound No.	Structure	% Inhibition at 100μM	IC_{50} Value (μM)
113 Baicalein	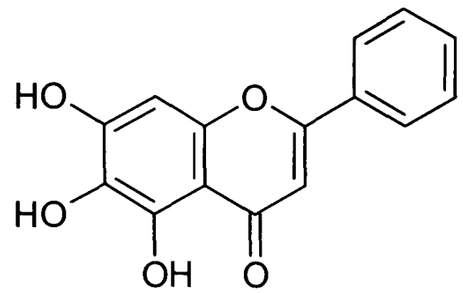	38.78 ± 1.36	185.92 ± 12.70
97 7-hydroxyflavone	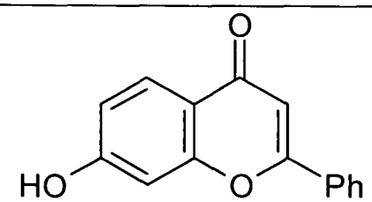	53.93 ± 1.07	66.98 ± 0.95
247	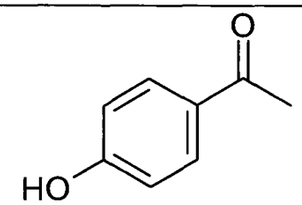	36.59 ± 0.52	1708.92 ± 170.71
248	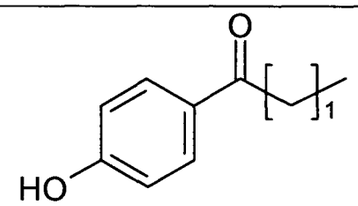	39.04 ± 0.42	150.56 ± 12.21

Table 3.2a Results from preliminary screening and IC_{50} data of some 4-hydroxyphenyl ketones for type 3 17β-HSD activity.

Compound No.	Structure	% Inhibition at 100μM	IC_{50} Value (μM)
249	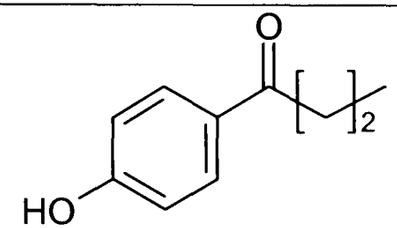	60.18 ± 0.77	89.51 ± 6.73
250	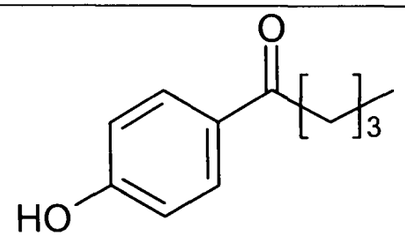	61.81 ± 0.89	60.52 ± 5.83
251	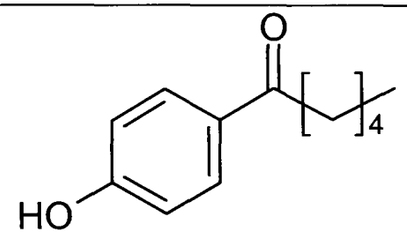	76.40 ± 0.18	18.02 ± 0.96
252	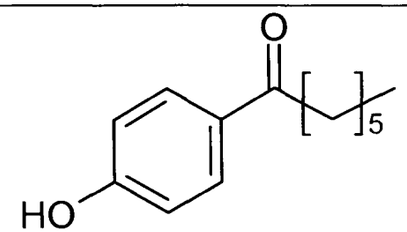	80.26 ± 0.20	7.84 ± 0.36
253	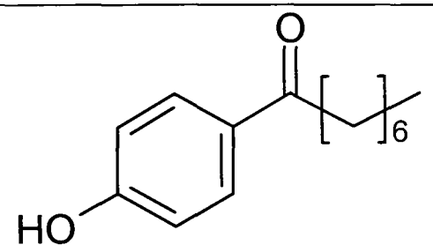	82.58 ± 0.49	6.52 ± 0.18

Table 3.2b Results from preliminary screening and IC_{50} data of some 4-hydroxyphenyl ketones for type 3 17β-HSD activity.

Compound No.	Structure	% Inhibition at 100μM	IC_{50} Value (μM)
254	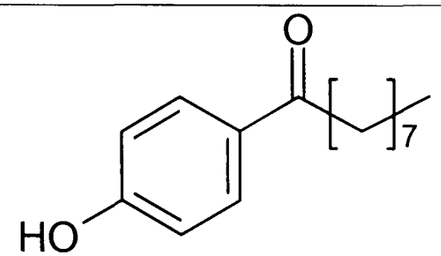	83.53 ± 0.48	2.86 ± 0.03
255	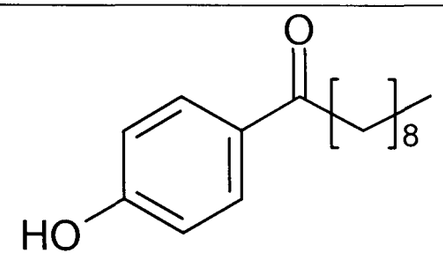	81.39 ± 0.09	4.97 ± 0.25
256	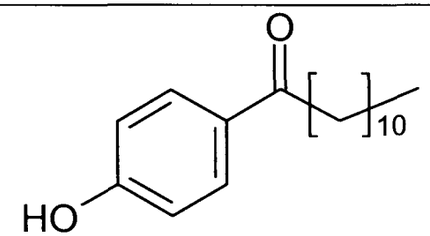	78.92 ± 0.58	7.55 ± 0.32
257	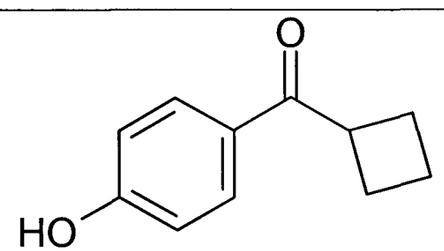	65.88 ± 0.42	27.15 ± 2.23

Table 3.2c Results from preliminary screening and IC_{50} data of some 4-hydroxyphenyl ketones for type 3 17β-HSD activity.

Compound No.	Structure	% Inhibition at 100μM	IC_{50} Value (μM)
258	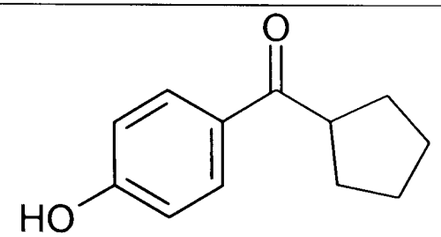	64.77 ± 0.40	33.19 ± 1.62
259	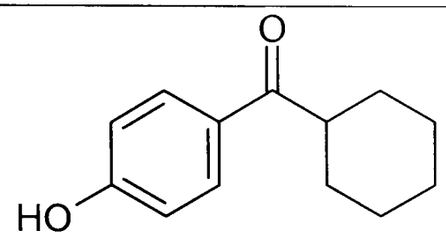	62.94 ± 0.82	36.16 ± 2.45
260	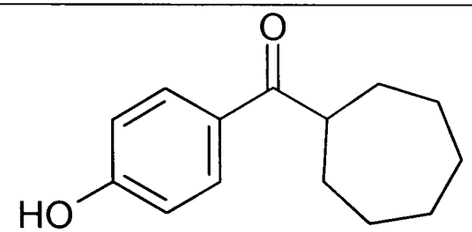	63.62 ± 0.78	29.66 ± 0.76

Table 3.2d Results from preliminary screening and IC_{50} data of some 4-hydroxyphenyl ketones for type 3 17β-HSD activity.

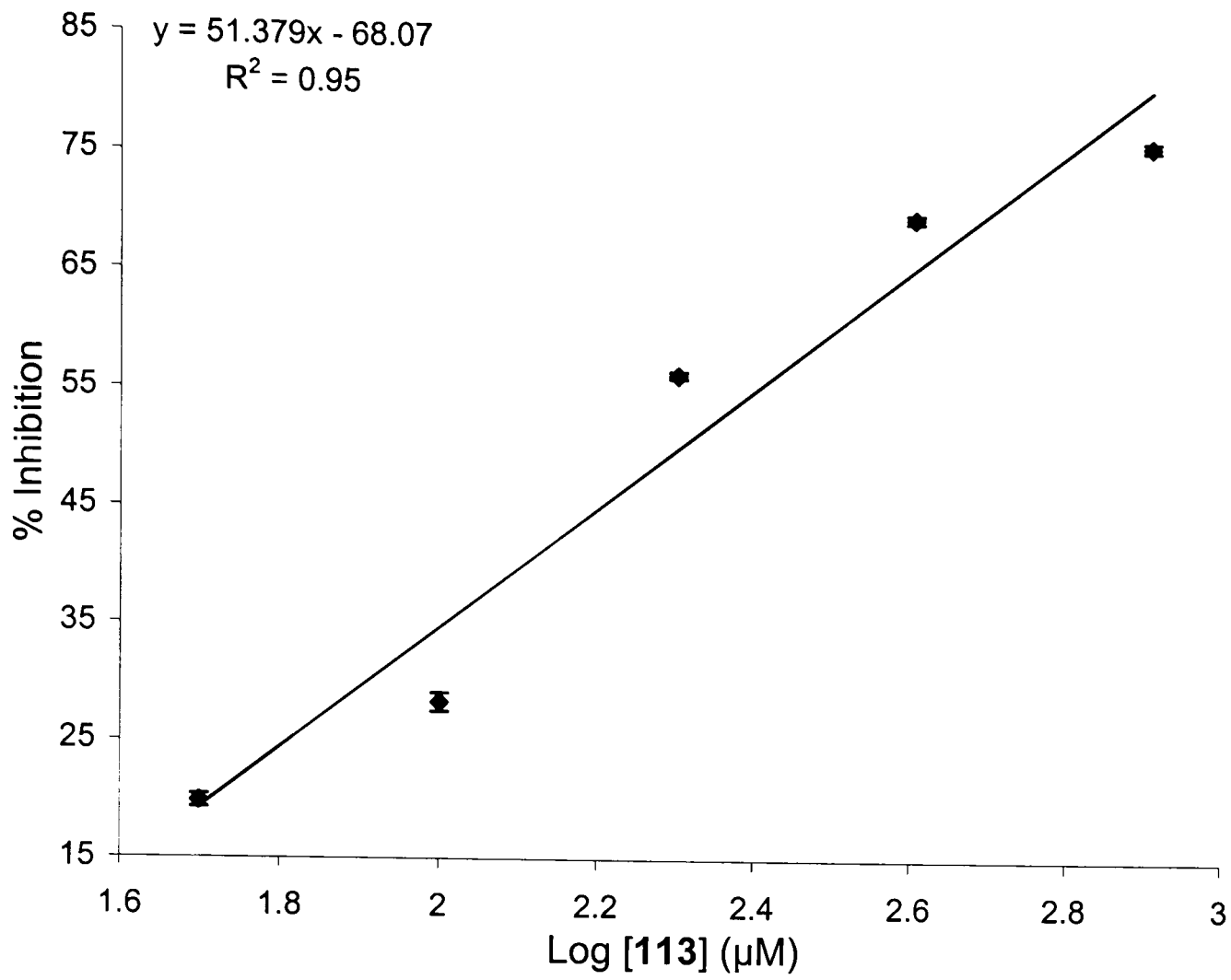

Figure 3.9 Plot of percentage inhibition versus log [**113**] for baicalein (**113**) against type 3 17β-HSD.

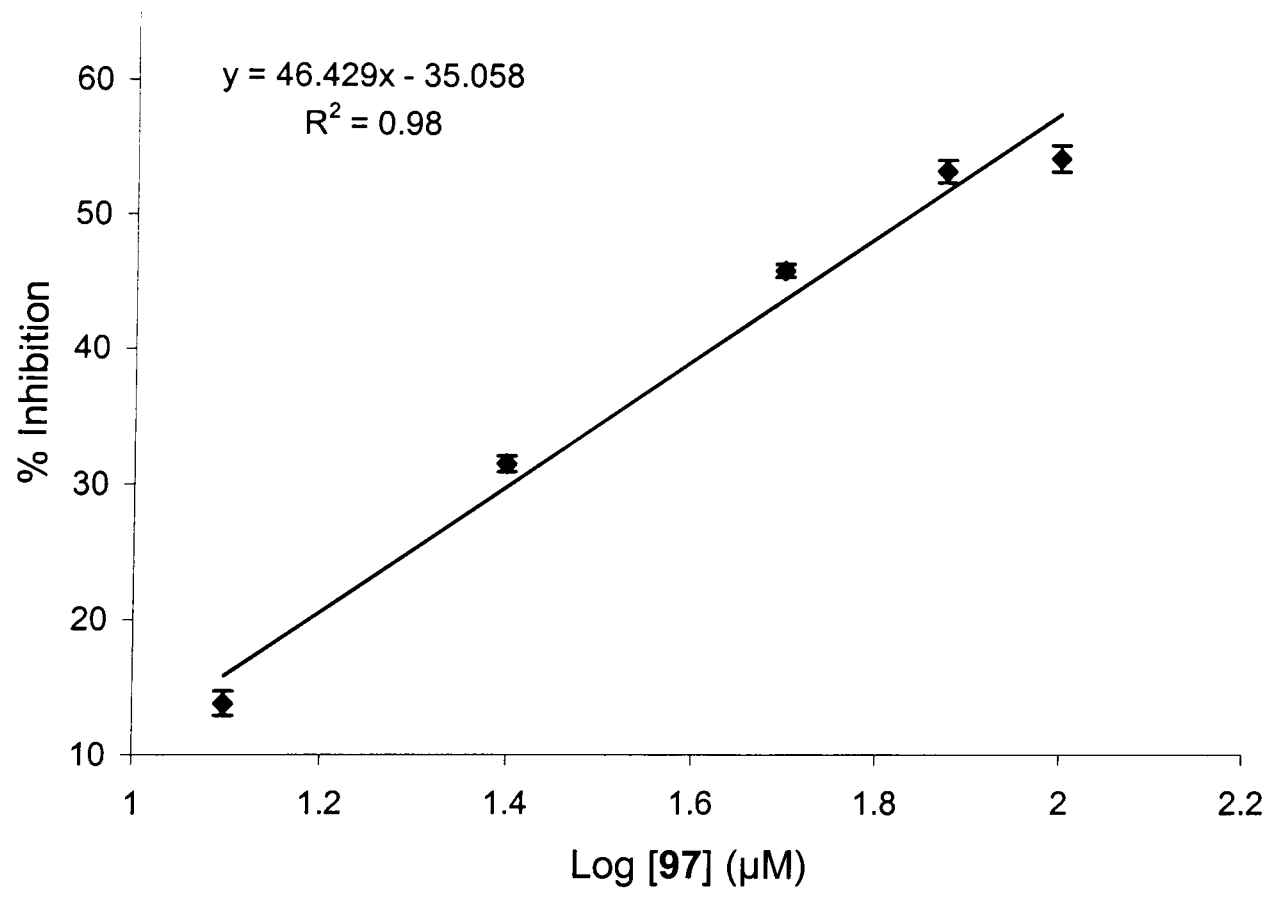

Figure 3.10 Plot of percentage inhibition versus log [**97**] for 7-hydroxyflavone (**97**) against type 3 17β-HSD.

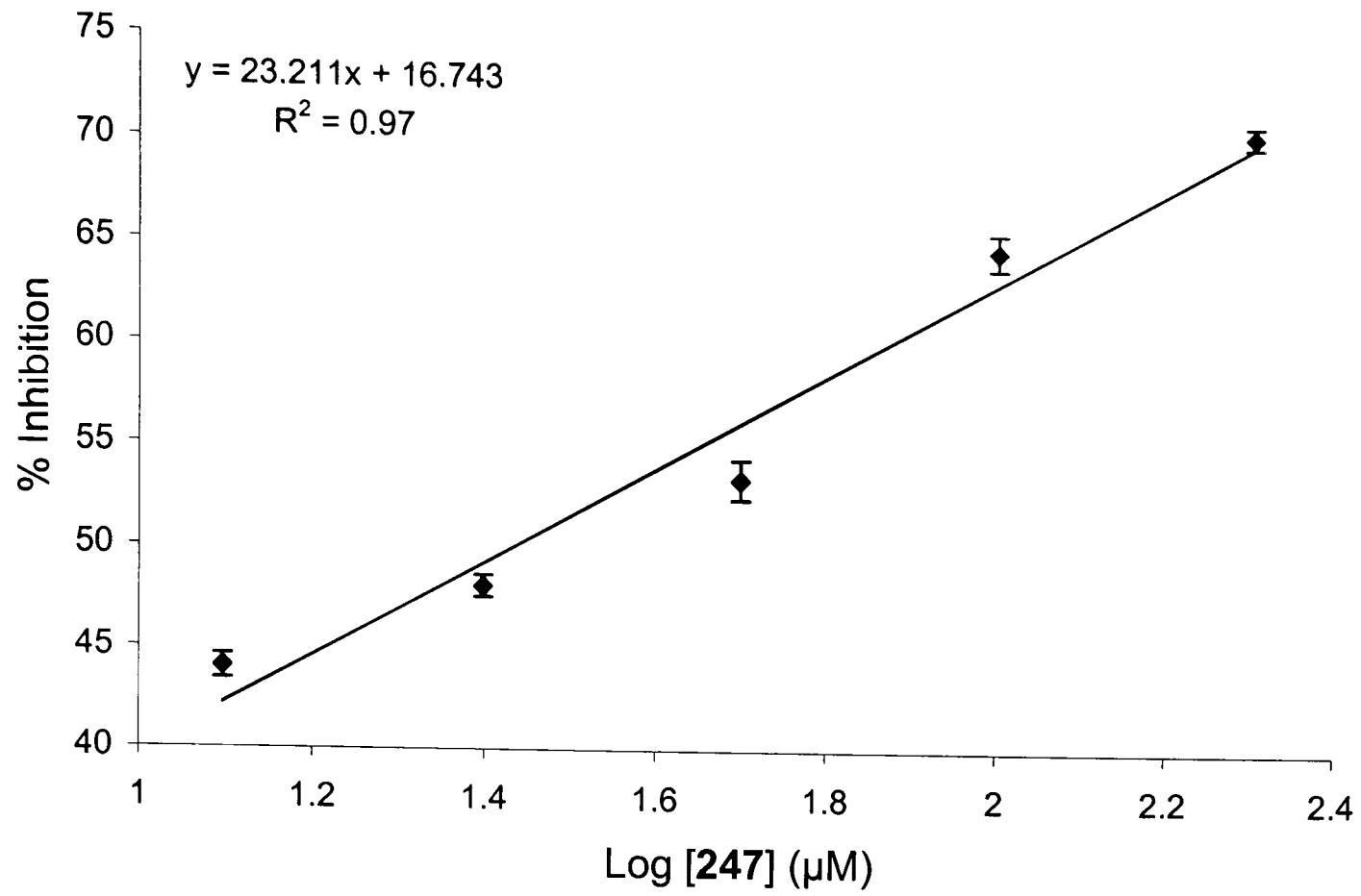

Figure 3.11 Plot of percentage inhibition versus log [**247**] for 1-(4-hydroxy-phenyl)-ethanone (**247**) against type 3 17β-HSD.

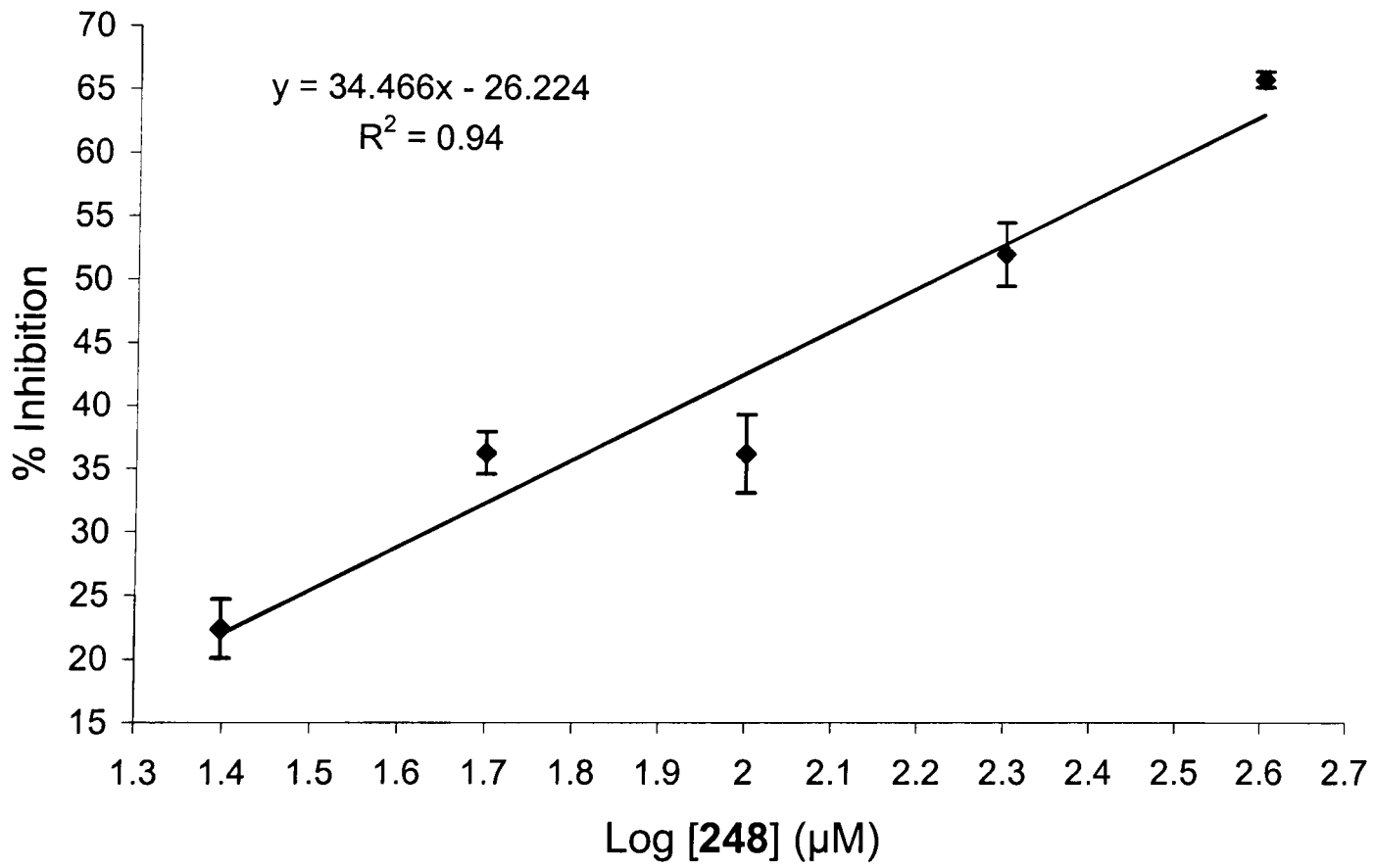

Figure 3.12 Plot of percentage inhibition versus log [**248**] for 1-(4-hydroxy-phenyl)-propan-1-one (**248**) against type 3 17β-HSD.

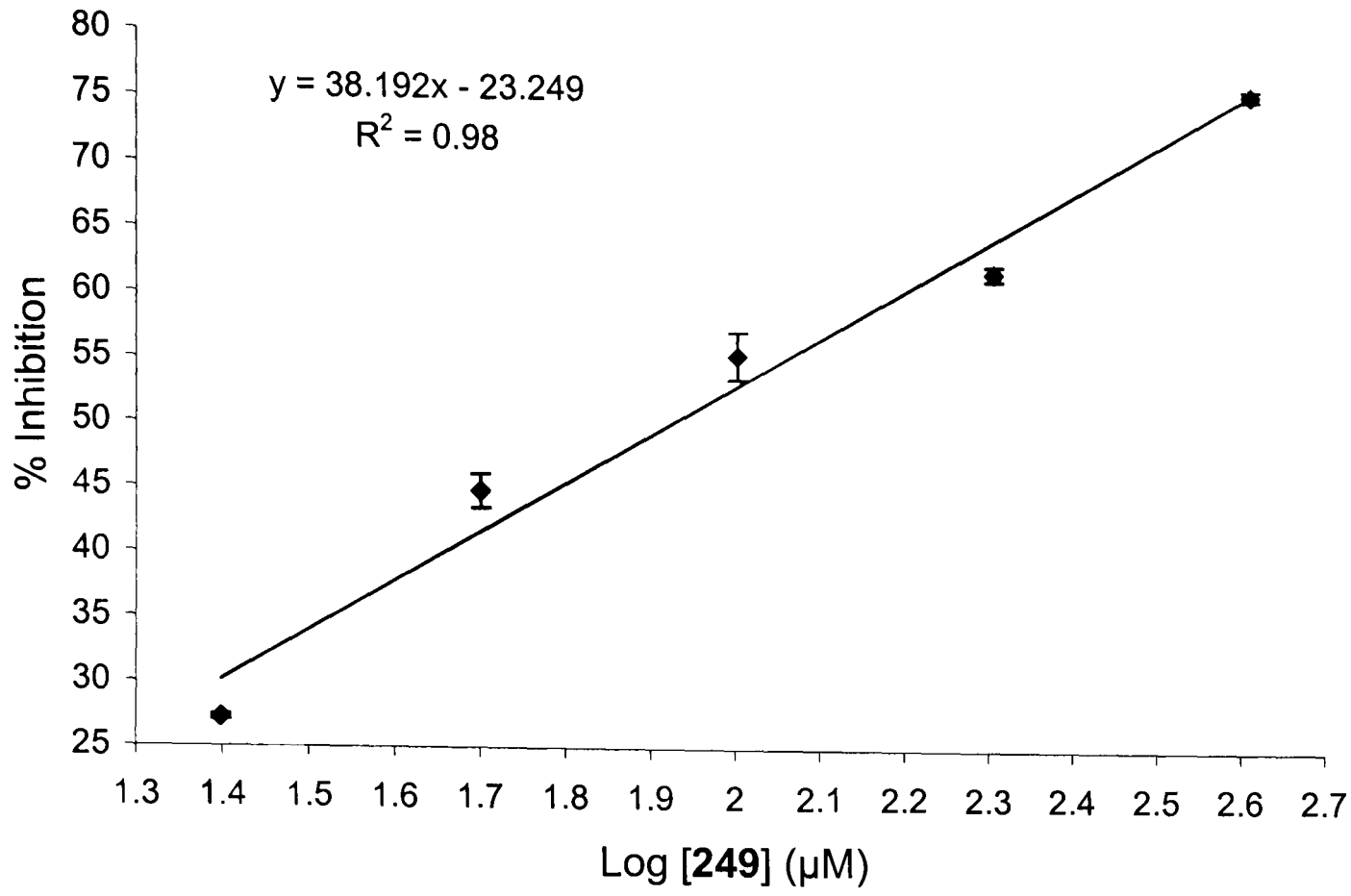

Figure 3.13 Plot of percentage inhibition versus log [**249**] for 1-(4-hydroxy-phenyl)-butan-1-one (**249**) against type 3 17β-HSD.

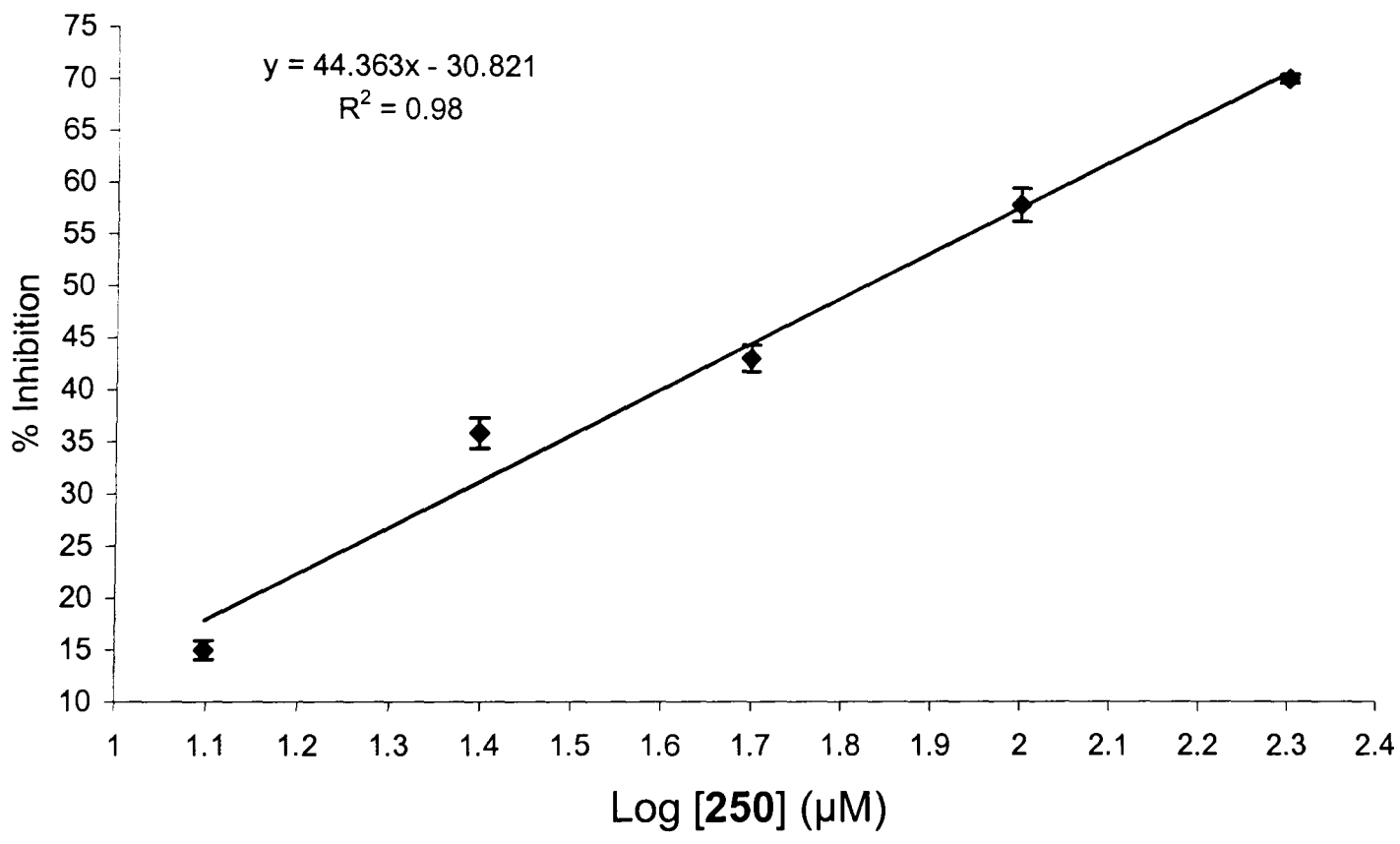

Figure 3.14 Plot of percentage inhibition versus log [**250**] for 1-(4-hydroxy-phenyl)-pentan-1-one (**250**) against type 3 17β-HSD.

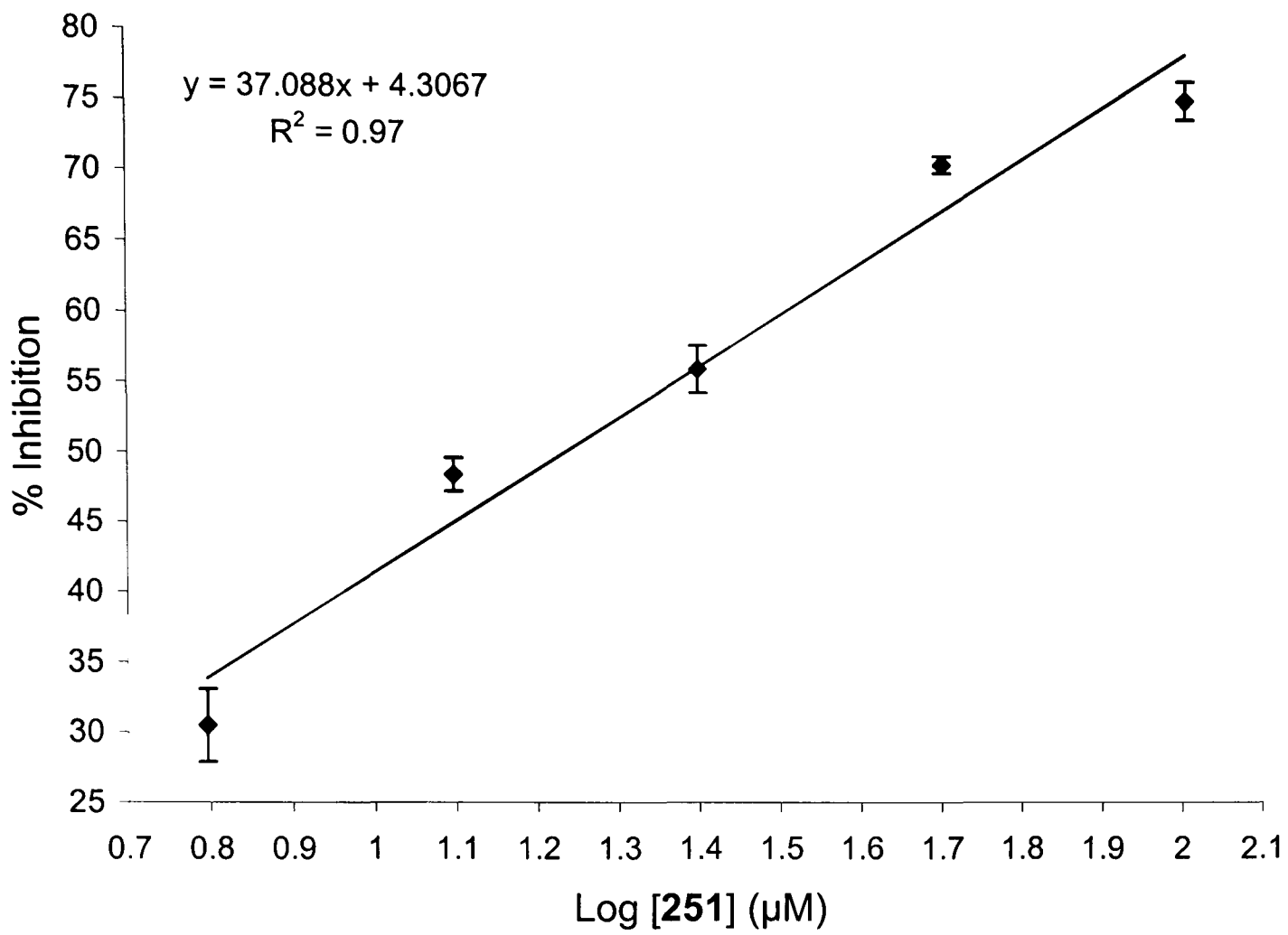

Figure 3.15 Plot of percentage inhibition versus log [**251**] for 1-(4-hydroxy-phenyl)-hexan-1-one (**251**) against type 3 17β-HSD.

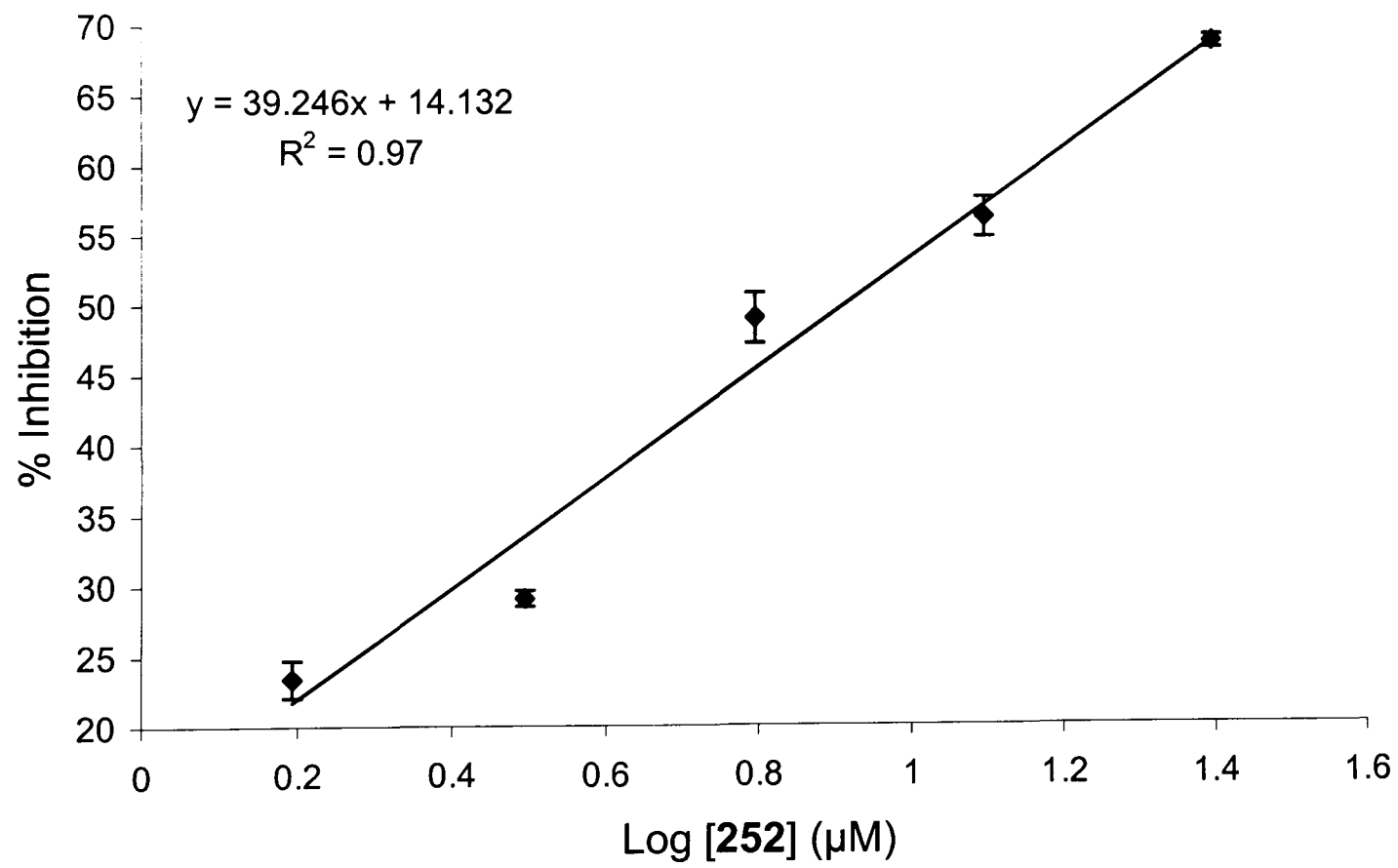

Figure 3.16 Plot of percentage inhibition versus log [**252**] for 1-(4-hydroxy-phenyl)-heptan-1-one (**252**) against type 3 17β-HSD.

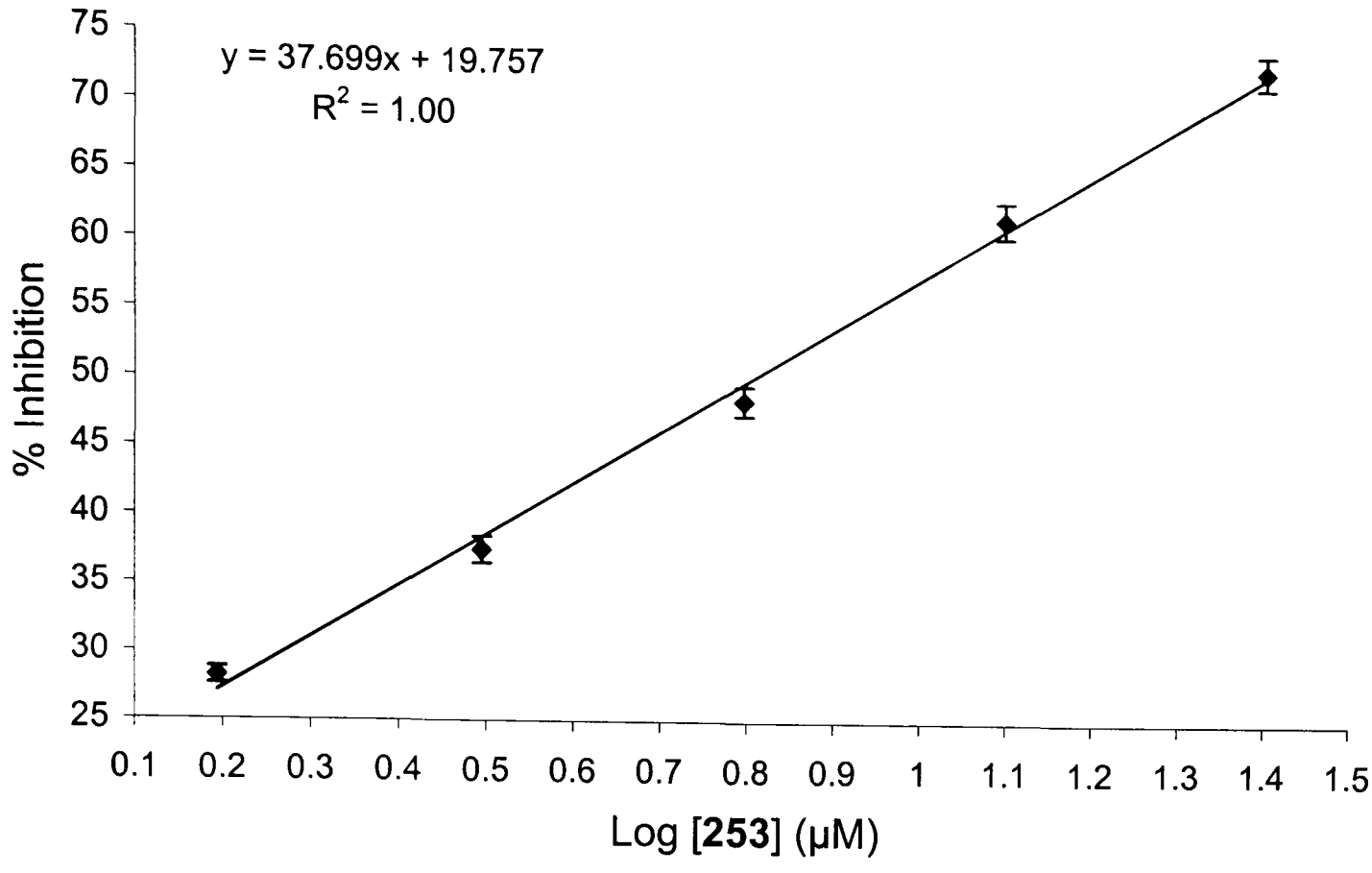

Figure 3.17 Plot of percentage inhibition versus log [**253**] for 1-(4-hydroxy-phenyl)-octan-1-one (**253**) against type 3 17β-HSD.

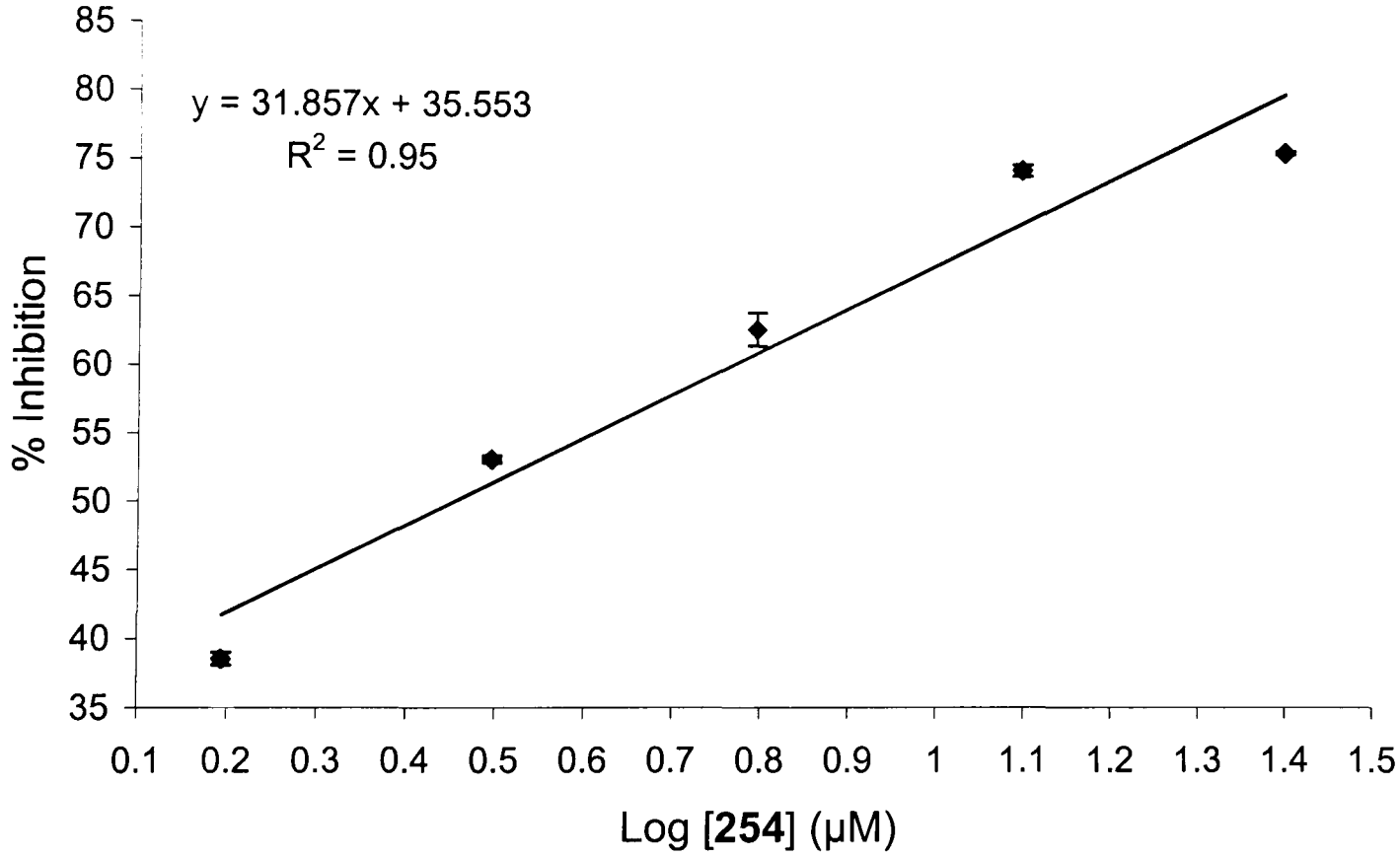

Figure 3.18 Plot of percentage inhibition versus log [**254**] for 1-(4-hydroxy-phenyl)-nonan-1-one (**254**) against type 3 17β-HSD.

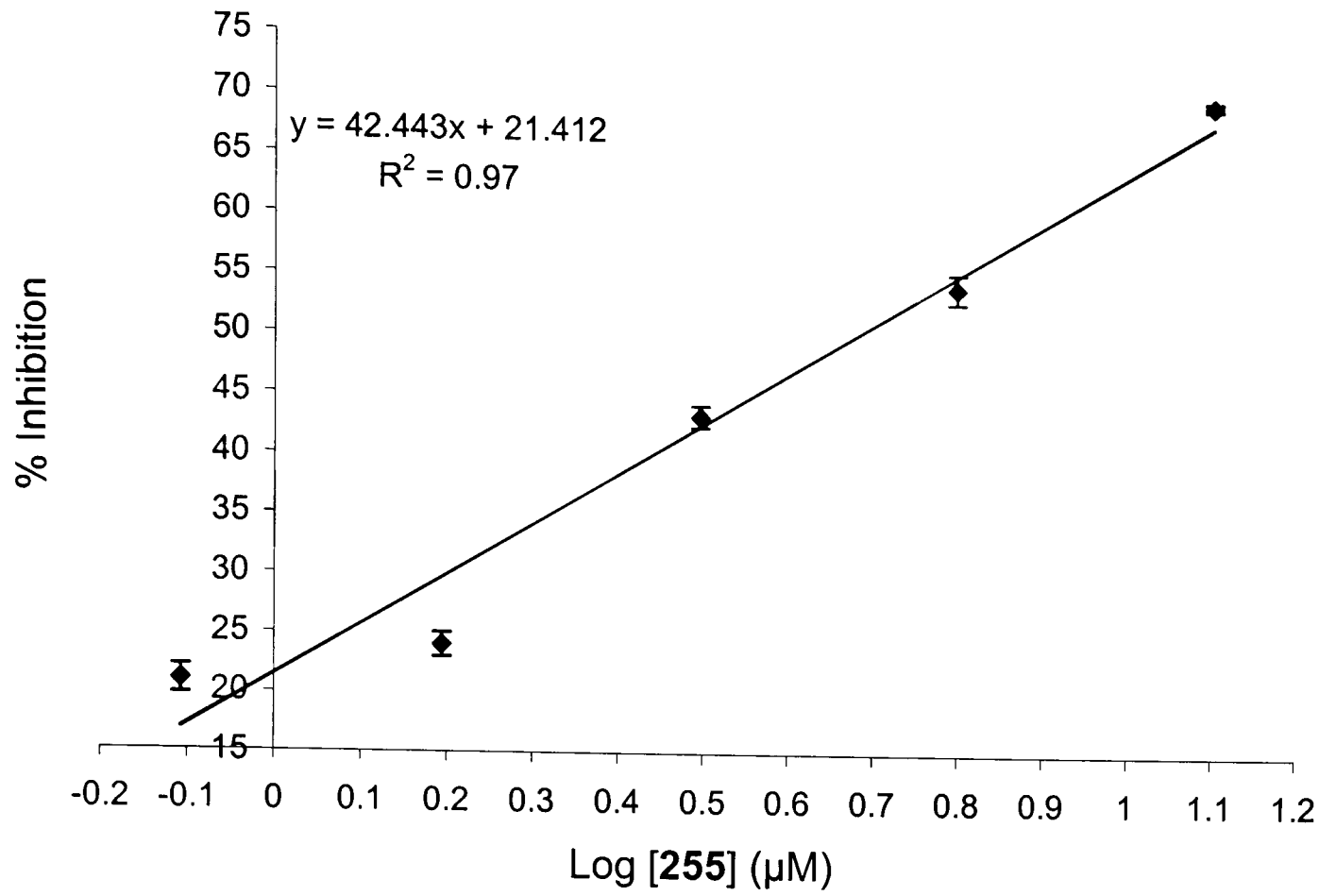

Figure 3.19 Plot of percentage inhibition versus log [**255**] for 1-(4-hydroxy-phenyl)-decan-1-one (**255**) against type 3 17β-HSD.

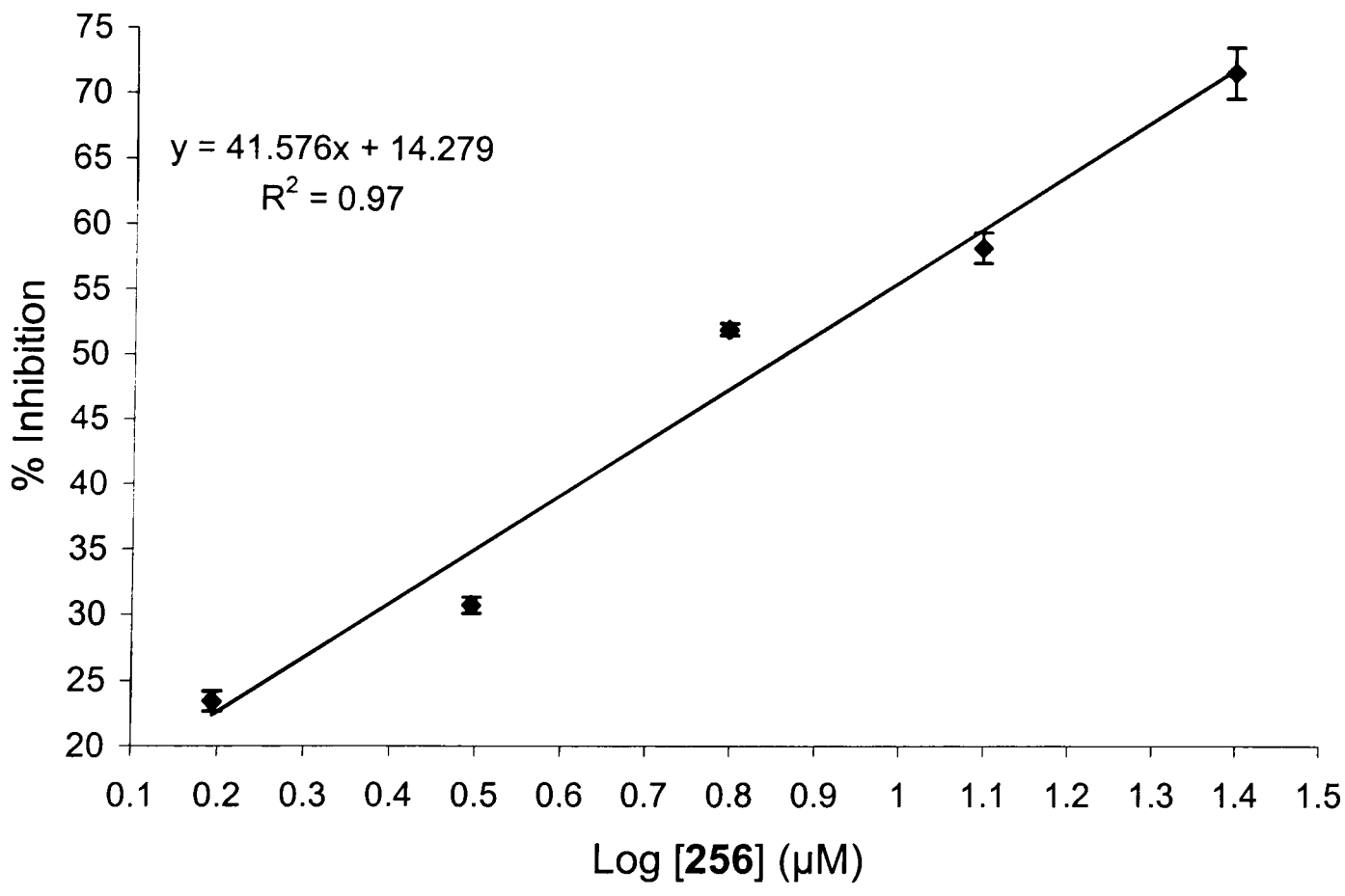

Figure 3.20 Plot of percentage inhibition versus log [**256**] for 1-(4-hydroxy-phenyl)-dodecan-1-one (**256**) against type 3 17β-HSD.

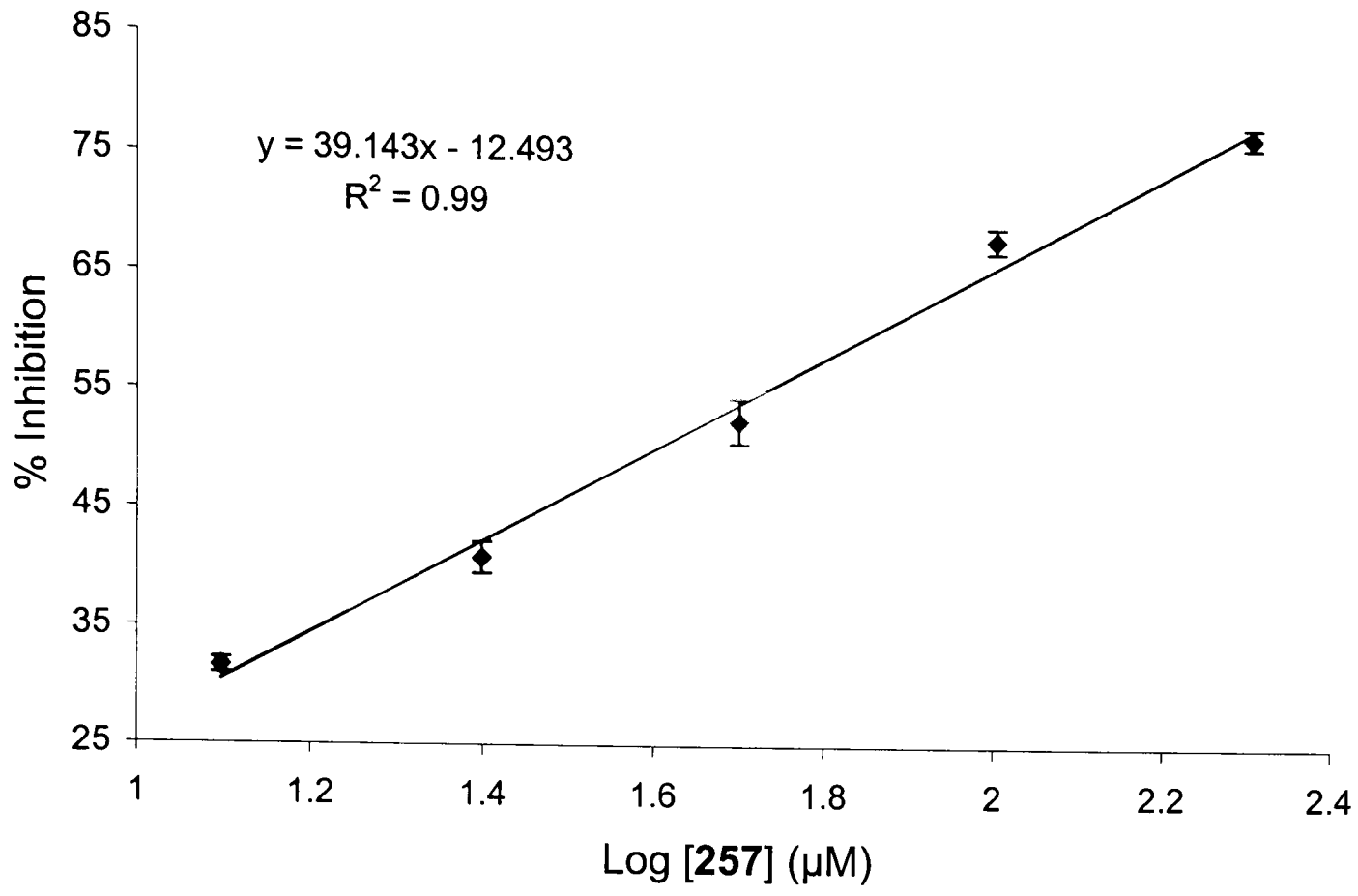

Figure 3.21 Plot of percentage inhibition versus log [**257**] for cyclobutyl-(4-hydroxy-phenyl)-methanone (**257**) against type 3 17β-HSD.

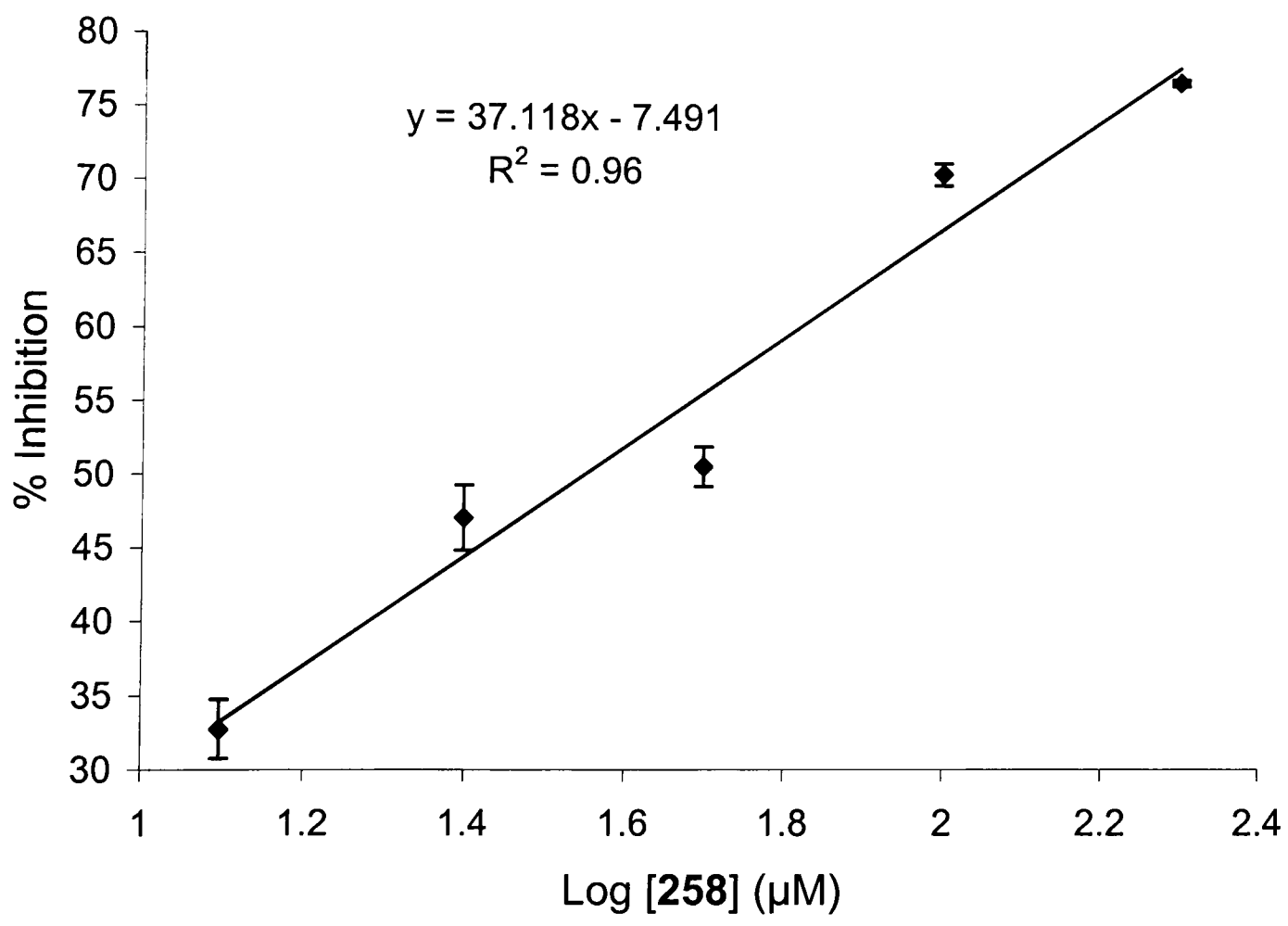

Figure 3.22 Plot of percentage inhibition versus log [**258**] for cyclopentyl-(4-hydroxy-phenyl)-methanone (**258**) against type 3 17β-HSD.

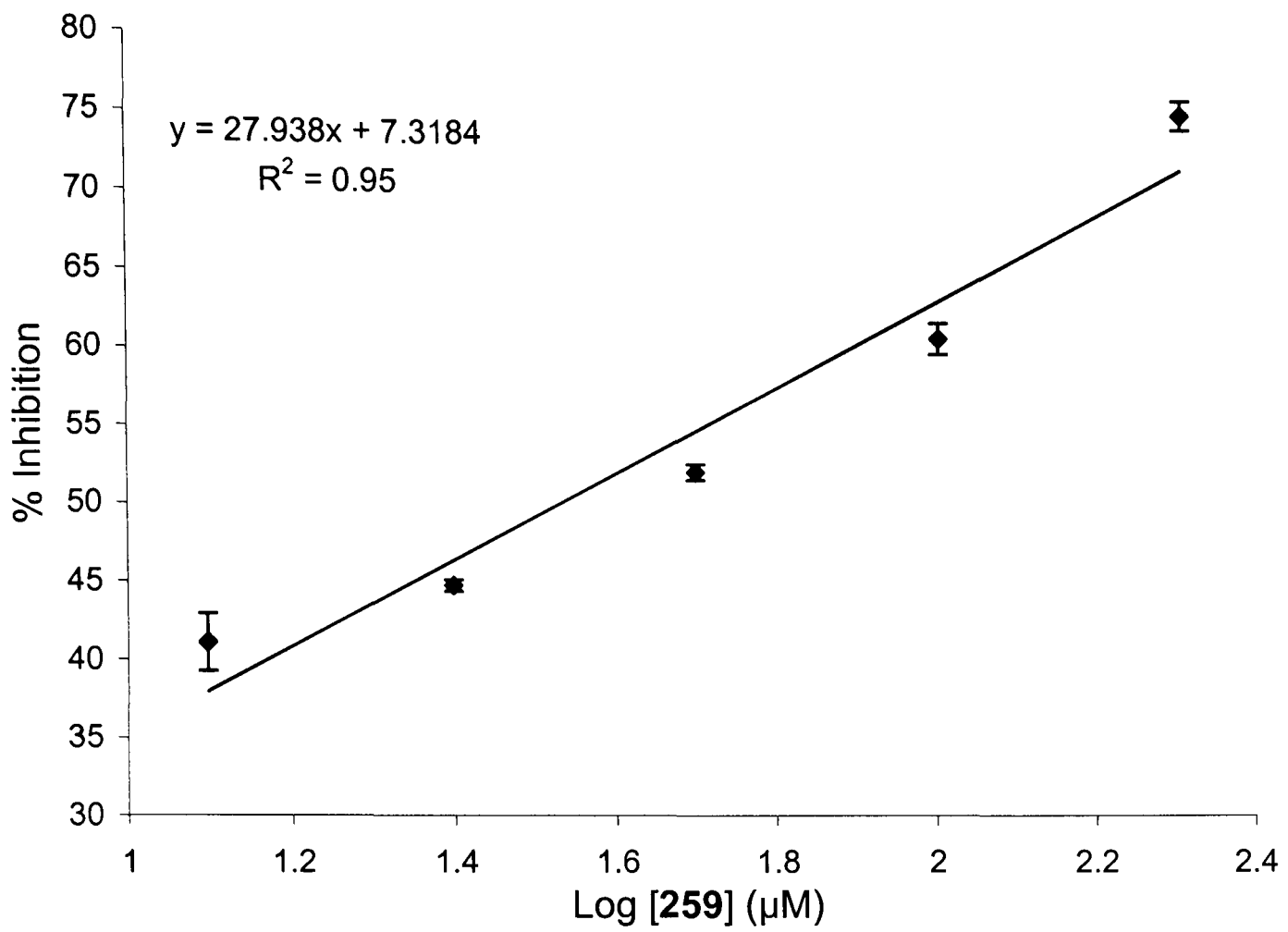

Figure 3.23 Plot of percentage inhibition versus log [**259**] for cyclohexyl-(4-hydroxy-phenyl)-methanone (**259**) against type 3 17β-HSD.

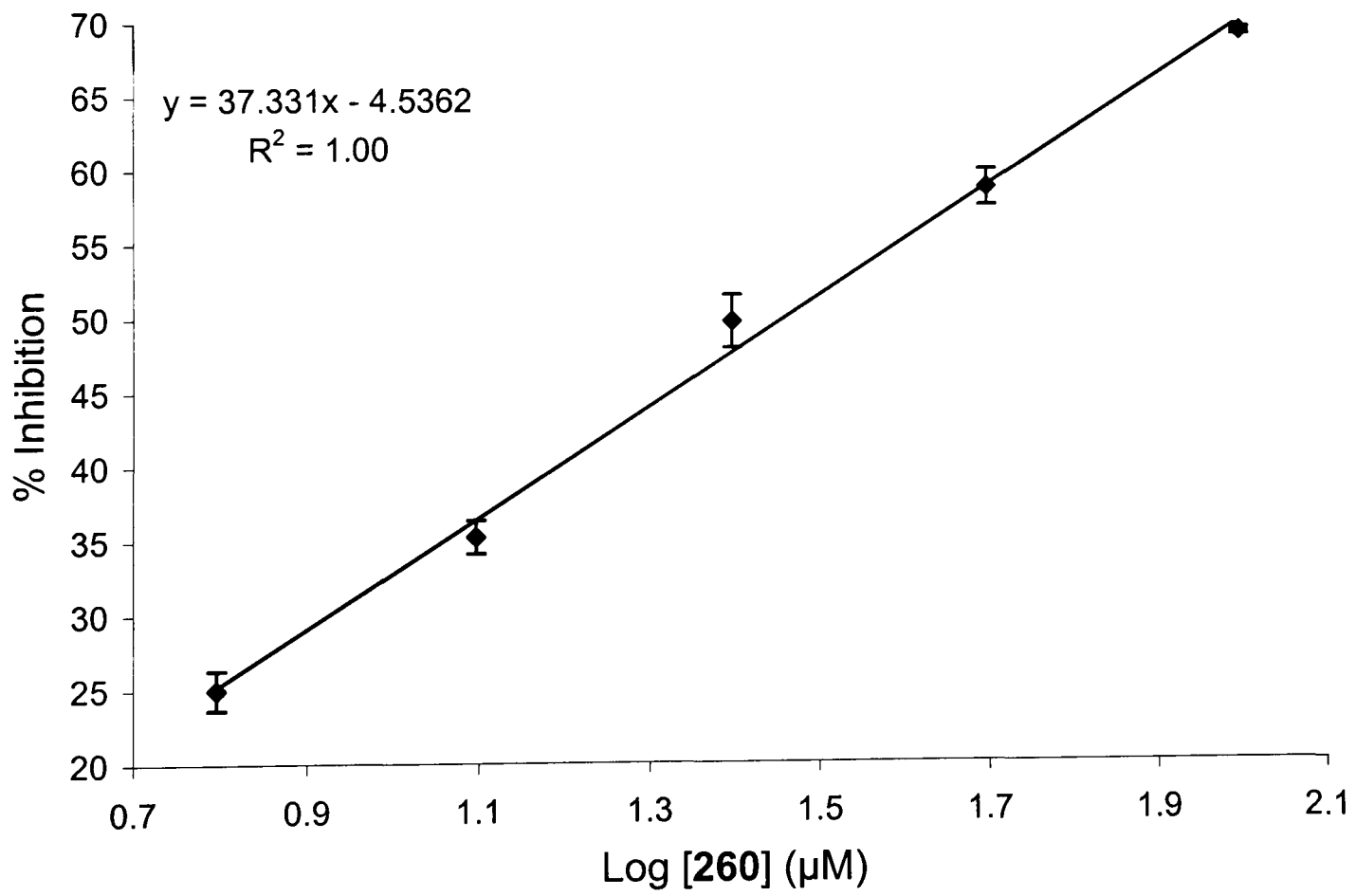

Figure 3.24 Plot of percentage inhibition versus log [**260**] for cycloheptyl-(4-hydroxy-phenyl)-methanone (**260**) against type 3 17β-HSD.

3.16 Results for the Biphenyl Ketones

The results are shown in Tables 3.3a – 3.3b

3.16.1 Discussion

All compounds were screened against type 3 17β-HSD and it was found that they were in general weaker than the standards baicalein and 7-hydroxyflavone.

Compound No.	Structure	% Inhibition at 100μM
113 Baicalein	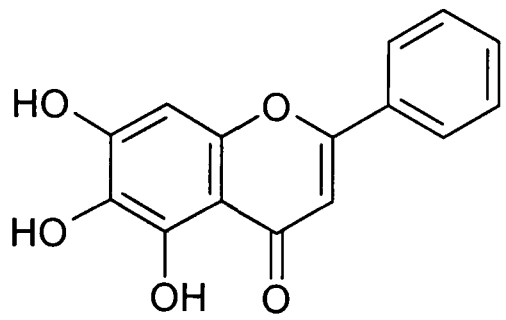	49.43 ± 1.16
97 7-Hydroxyflavone	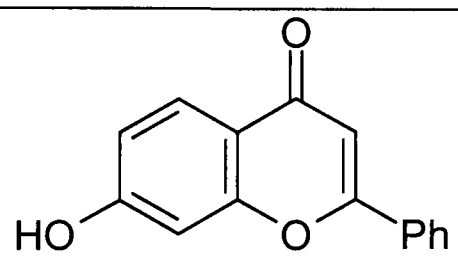	66.42 ± 2.05
261	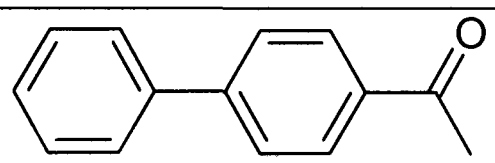	0
262	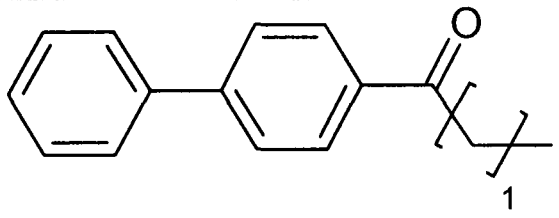	0
263	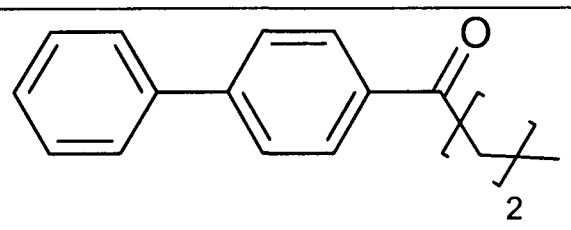	20.36 ± 1.74
264	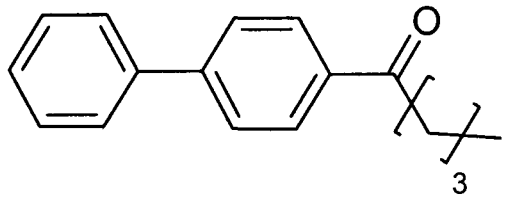	8.55 ± 1.00

Table 3.3a Results from preliminary screening data of some biphenyl ketones for type 3 17β-HSD activity.

Compound No.	Structure	% Inhibition at 100μM
265	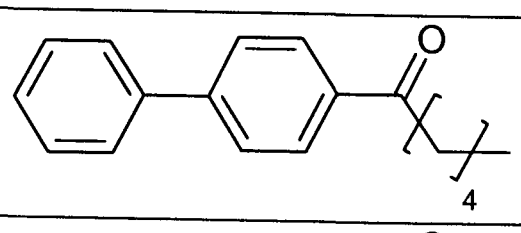	10.22 ± 1.72
266	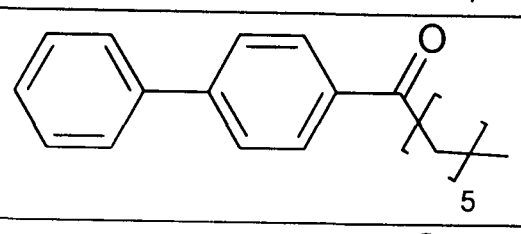	1.18 ± 0.30
267	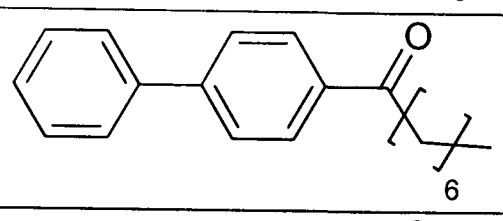	0
268	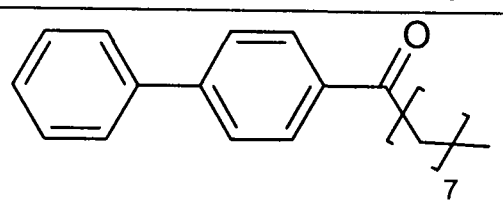	13.29 ± 0.26
269	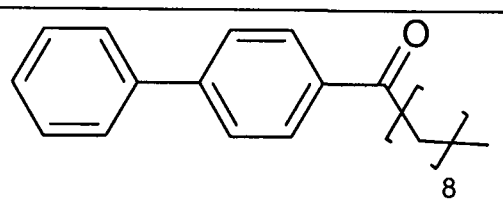	17.86 ± 1.14
270	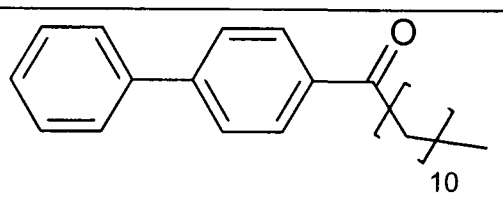	16.52 ± 0.91
271	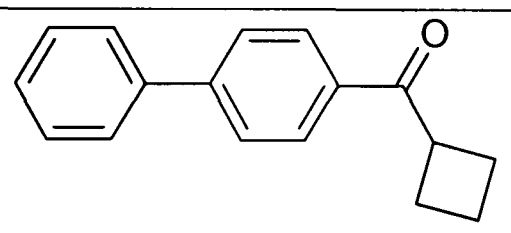	4.30 ± 0.40
272	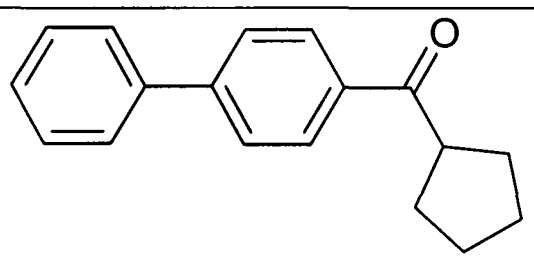	15.22 ± 1.64
273	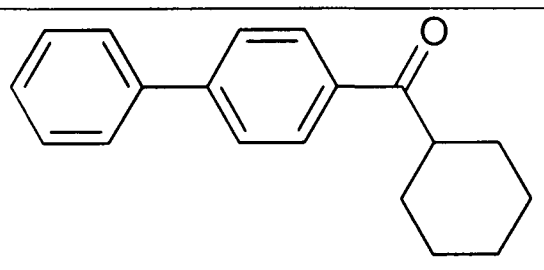	23.48 ±0.35

Table 3.3b Results from preliminary screening data of some biphenyl ketones for type 3 17β-HSD activity.

3.17 Results for Commercially Available Compounds

The results are shown in Tables 3.4a – 3.4b

3.17.1 Discussion

A number of commercially available compounds containing phenyl and carboxyl groups were screened for inhibitory activity against type 3 17β-HSD and it was found that they were, in general, weaker than the standards baicalein and 7-hydroxyflavone.

Compound No.	Structure	% Inhibition at 100μM
113	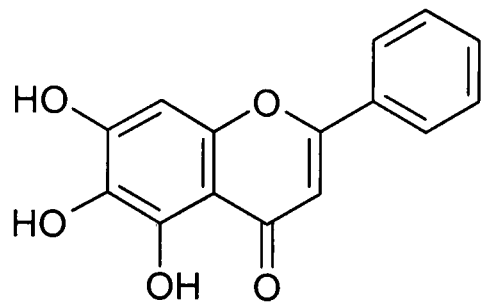	49.43 ± 1.16
97	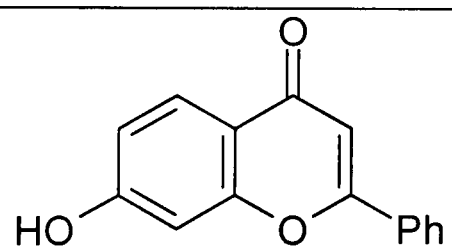	66.42 ± 2.05
274	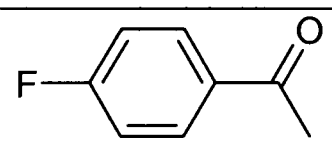	12.00 ± 1.51
275	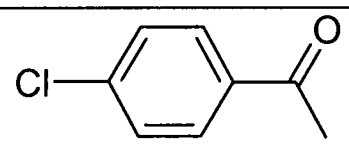	18.17 ± 1.17
276	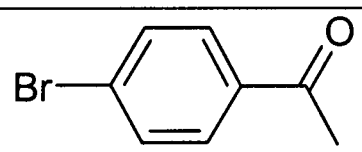	11.22 ± 0.97
277	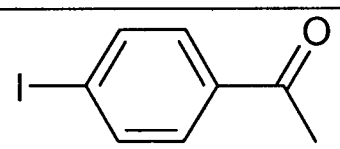	20.16 ± 2.51
278	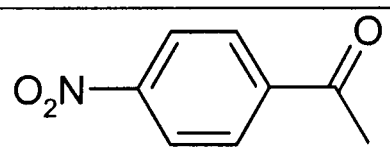	35.71 ± 1.29

Table 3.4a Results from preliminary screening data of some commercially available compounds for type 3 17β-HSD activity.

Compound No.	Structure	% Inhibition at 100μM
279	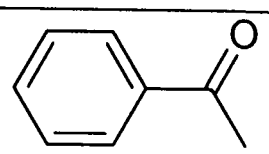	15.34 ± 2.35
280	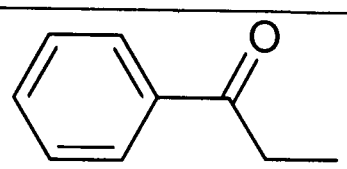	16.33 ± 1.39
281	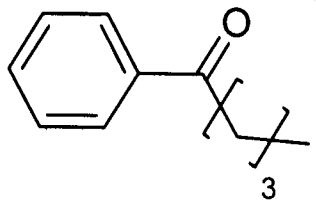	23.01 ± 2.06
282	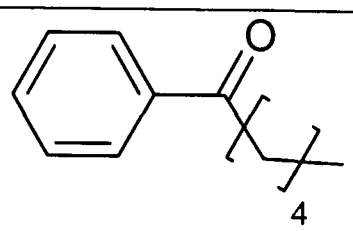	18.38 ± 0.32
283	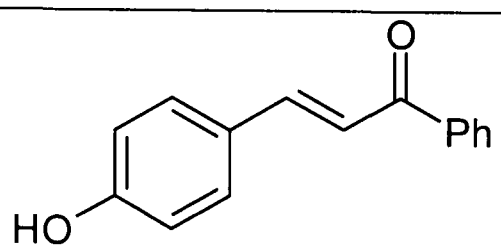	49.70 ± 0.06
284	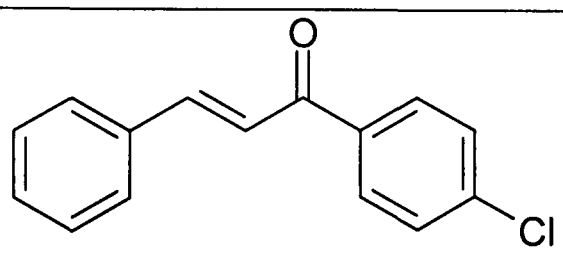	19.64 ± 0.30
285	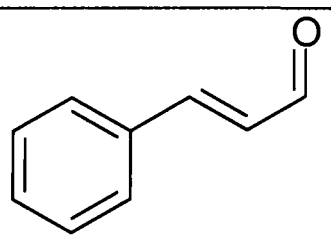	35.35 ± 1.55
286	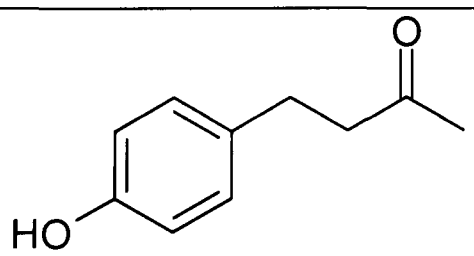	41.45 ± 0.71
287	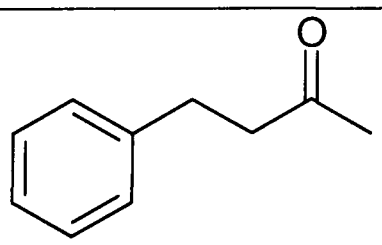	23.29 ± 1.06

Table 3.4b Results from preliminary screening data of some commercially available compounds for type 3 17β-HSD activity.

3.18 Type 1 17β-HSD Enzyme Assay (E1 to E2)

3.19 Introduction

Compounds previously tested against type 3 17β-HSD were evaluated for type 1 17β-HSD inhibitory activity using the microsomal fraction obtained from Sprague Dawley rat testicular tissue. The assay used was based on that of Le Lain et al (2001) and measures the effect of potential inhibitors on the rate of conversion of radiolabelled E1 to E2.

To separate E1 and E2 from the reaction mixture, the method of TLC was employed, where extracts, together with the carrier steroids (5mg/mL), were applied to TLC plates. The mobile phase used was that of Tremblay et al (1999) and was a mixture of dichloromethane (90mL) and ethyl acetate (10mL).

After elution and identification using UV light, each steroid was cut out and counted for 4 min per tube in a cocktail of scintillation fluid and acetone. The percentage conversion of E1 to E2 was determined by the division of the CPM for the product by the total CPM of both steroids. As such, there is no requirement for quantitative recovery of all the reactants and products from the assay mixture in this study.

3.20 Methods, Materials and Instruments

All methods, materials and instruments used were as mentioned in Chapter 2, Section 2.3. [2,4,6,7-^{3}H]E1 was obtained from Amersham Pharmacia Biotech UK Limited, Buckinghamshire.

3.21 Buffer, Solution and Substrate Preparation

Buffers and solutions used in the assay were as for those in Chapter 2, Section 2.4.

Substrate preparation of [2,4,6,7-^{3}H]E1 (100μM)

A stock solution of substrate was prepared by transferring radiolabelled [2,4,6,7-^{3}H]E1 (0.305μM, 20μL) to a glass vial and removing the toluene:ethanol mixture under a stream of nitrogen. Unlabelled substrate in propane-1,2-diol (99.695μM, 1mL) was added to the radiolabelled residue and mixed thoroughly to give a final concentration of 100μM.

3.22 Preparation of Testicular Microsomes

The microsomes were prepared as previously described in Chapter 2, Section 2.5.

3.23 Protein Assay

The protein concentration of the testicular microsomes was determined as previously described in Chapter 2, Section 2.6. The results are shown in Figure 3.25.

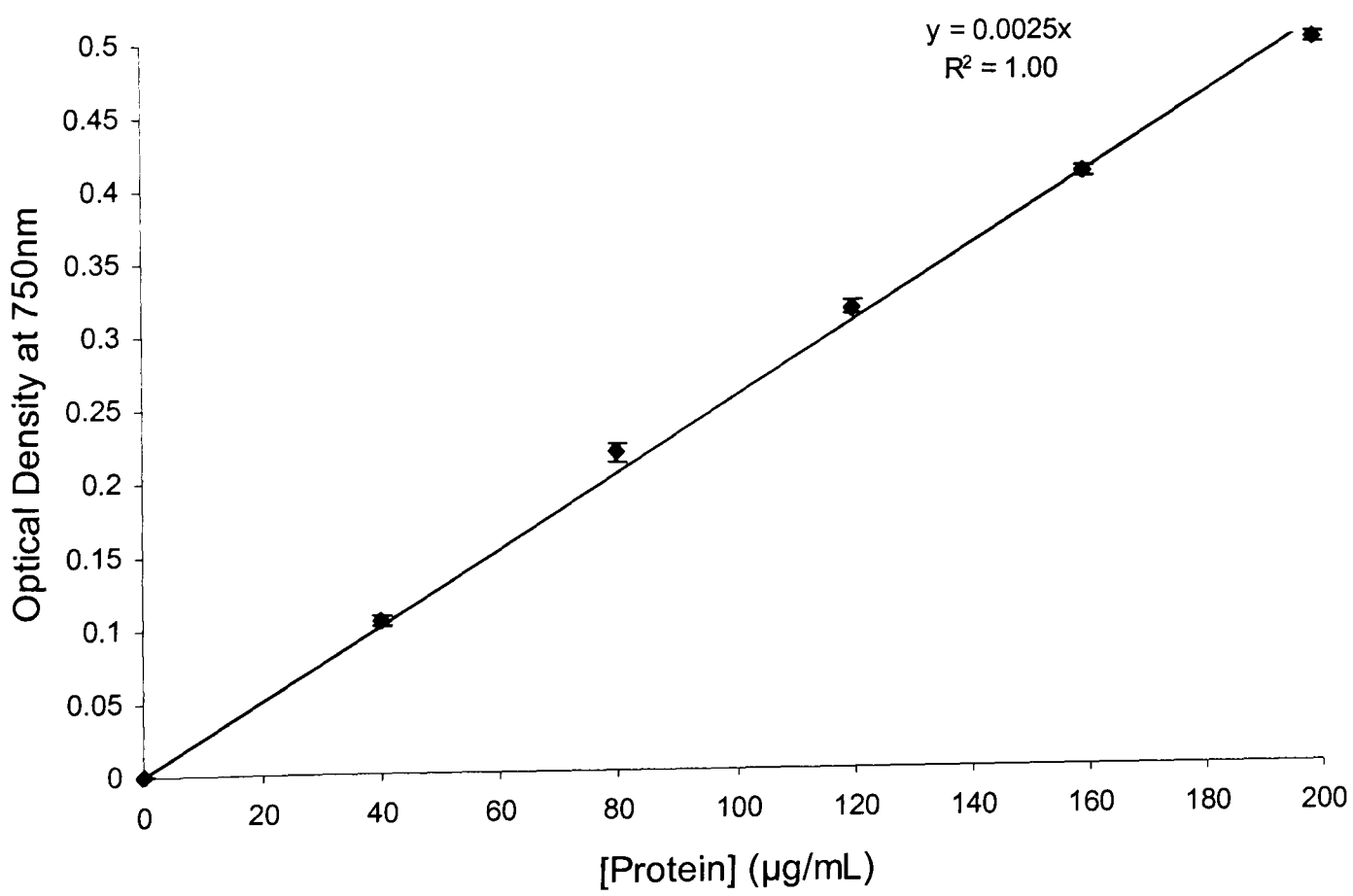

Figure 3.25 Calibration graph for protein assay for type1 17β-HSD

The protein concentration of the testicular microsomes was determined from the standard protein calibration curve (Figure 3.25) and was found to be 11.74mg/mL.

3.24 Validation of the 17β-HSD Assay for Conversion of E1 to E2

To validate the 17β-HSD assay, it was necessary to determine the quantity of non-enzymatic product formation. Assay conditions were set so that the prepared substrate, E1 (1μM final concentration), was incubated for 30min at 37°C in the following solutions:

i. Sodium phosphate buffer (50mM, pH7.4)
ii. Testicular microsomes (0.15mg/mL, 10μL) and sodium phosphate buffer, lacking NADPH-generating system
iii. Testicular microsomes, denatured by addition of ether (2mL), sodium phosphate buffer and NADPH-generating system

After incubation, the assay mixtures were treated, except (iii), with ether (2mL). The solutions were vortexed, then left to stand over ice for 15min. The organic phase was extracted into a separate clean tube. The assay mixture was further extracted with ether (2x2mL), and the organic layers combined. The solvent was removed under a stream of nitrogen, acetone (30μl) was added to each tube and the solution spotted onto silica based TLC plates along with carrier steroids (E1 and E2, 5mg/mL, approximately 10μL) were spotted onto TLC plates and run, using a mobile phase consisting of dichloromethane (90mL) and ethyl acetate (10mL). After development, the separated steroids were identified, using an UV lamp, cut from the plate and placed into scintillation vials. Acetone (1mL) was added to each vial in order to dissolve the steroid from the silica plate and then scintillation fluid (Optiscint HiSafe) was added. The samples were vortexed and read for radioactivity (4min). None of the samples showed detectable quantities of E2, indicating that (a) testicular microsomes and (b) NADPH are both essential requirements for the conversion of E1 to E2.

3.25 Protein Dependency for Type 1 17β-HSD

An experiment was performed to establish whether the rate of appearance of E2, produced during the enzymatic reaction, was proportional to the protein concentration.

Incubations were carried out (in triplicate) using protein concentrations 0.00, 0.12, 0.29, 0.59, 0.88 and 1.17mg/mL (final concentration), prepared substrate, E1 (1μM final concentration, 10μL), NADPH-generating system (50μL) and sodium phosphate buffer (pH7.4, to 1mL). The solutions were incubated for 30min at 37°C and the reaction was quenched by the addition of ether (2mL) and placed on ice. The assay was completed as previously described (Section 3.24) and the percentage conversion determined using Equation 3.3. The results are shown in Figure 3.26.

$$\text{Percentage Conversion} = \left(\frac{E2}{E1 + E2} \right) \times 100$$

Equation 3.3 Percentage conversion of E1 to E2

At 1μM substrate concentration, it can be concluded that the kinetics of the reaction are linear for protein concentrations up to 0.6mg/mL.

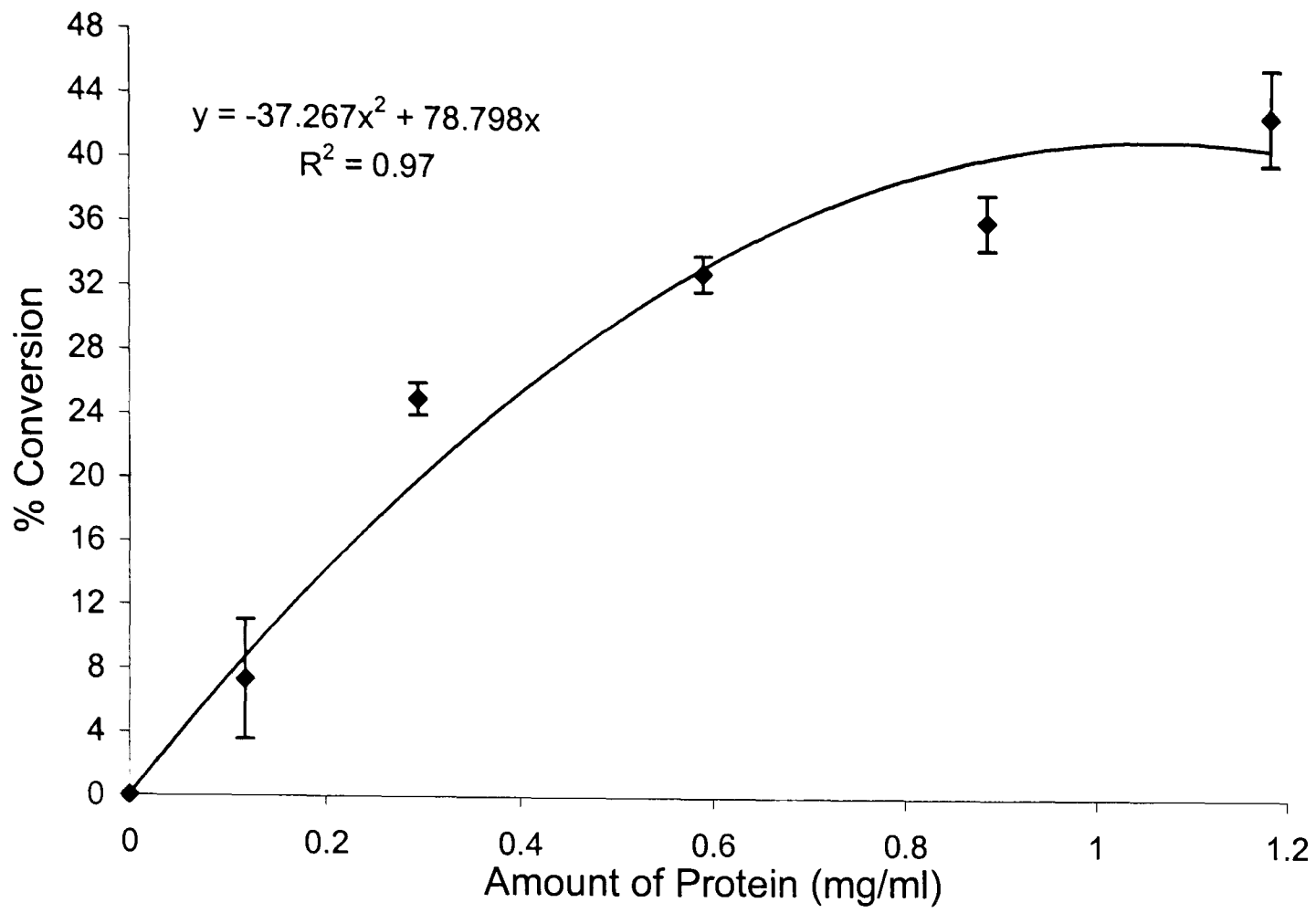

Figure 3.26 Plot to show percentage conversion of E1 to E2 at varying protein concentrations.

3.26 Time Dependency for Type 1 17β-HSD

Time dependency experiments were performed to ensure that the assays were within the linear phase of the enzyme reaction.

Incubations were carried out (in triplicate) using a final concentration of prepared substrate, E1 (1μM, 10μL), NADPH-generating system (50μL) and sodium phosphate buffer (910μL, pH7.4). The samples were warmed to 37°C in a shaking water bath before the addition of the testicular microsomes (0.35mg/mL final concentration, 30μl), were added at differing time intervals (30, 45, 60, 75, 90, 120 and 180min). The reaction was quenched by the addition of ether (2mL) and placed on ice. The assay was completed as previously described (Section 3.24). A graph was then plotted for percentage conversion versus time (Figure 3.27).

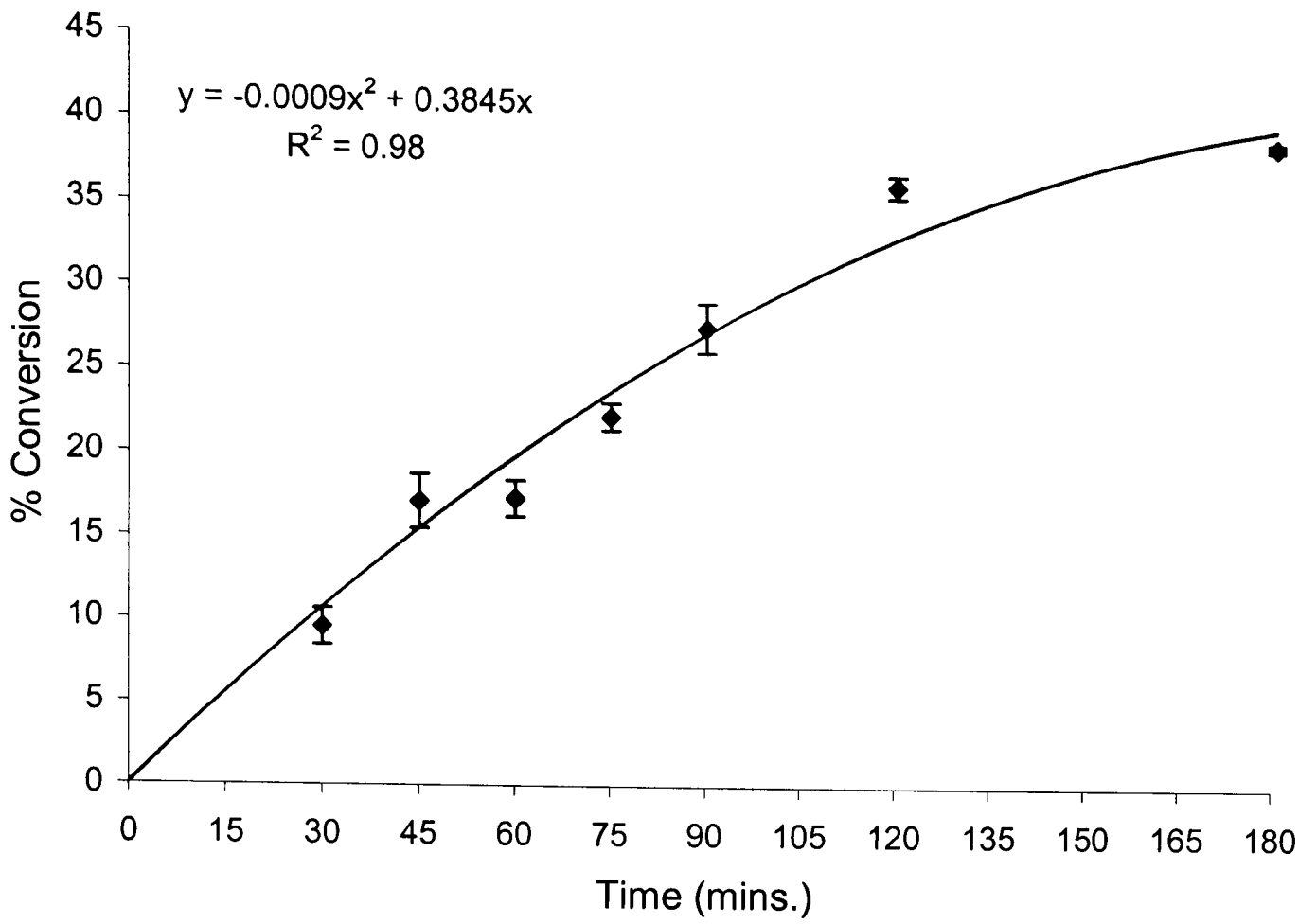

Figure 3.27 Plot to show percentage conversion of E1 at varying time intervals.

At 0.35mg/mL protein concentration, and 1μM substrate concentration, it can be concluded that the kinetics of the reaction are linear up to 120min.

3.27 Determination of K_m for Type 1 17β-HSD

The prepared substrate, E1 (100μM) was serially diluted, using propane-1,2-diol, to give a range of final incubation concentrations of substrate (0.2 to 1.0μM). All incubations were carried out in triplicate at 37°C in a shaking water bath. Incubation mixtures (1mL), containing NADPH-generating system (50μL) and prepared substrate (of varying concentration, 10μL), in sodium phosphate buffer (910μL, pH7.4), were allowed to warm to 37°C. The testicular microsomes were thawed and warmed to 37°C before addition (0.35mg/mL final concentration, 30μL) to the assay mixture. The solutions were incubated for 90min at 37°C and the reaction was quenched by the addition of ether (2mL) and placed on ice. The assay was completed as previously described (Section 3.24). The velocity, v, for each substrate concentration was calculated using equation 3.4, where units for v are: μM/min/mg.

$$v = \frac{\text{CPM (E2) x substrate concentration [S] } (\mu M)}{\text{CPM (E1+E2) x protein concentration (mg/ml) x time (min)}}$$

Equation 3.4 Velocity calculation for each substrate concentration

3.28 Results – Graphical Determination of K_m

The K_m and V_{max} were determined from five different general methods for E1, as previously described in Chapter 2, Section 2.11, and are shown in Figures 3.28 to 3.32 and the averages of three assays are summarised in Table 3.5

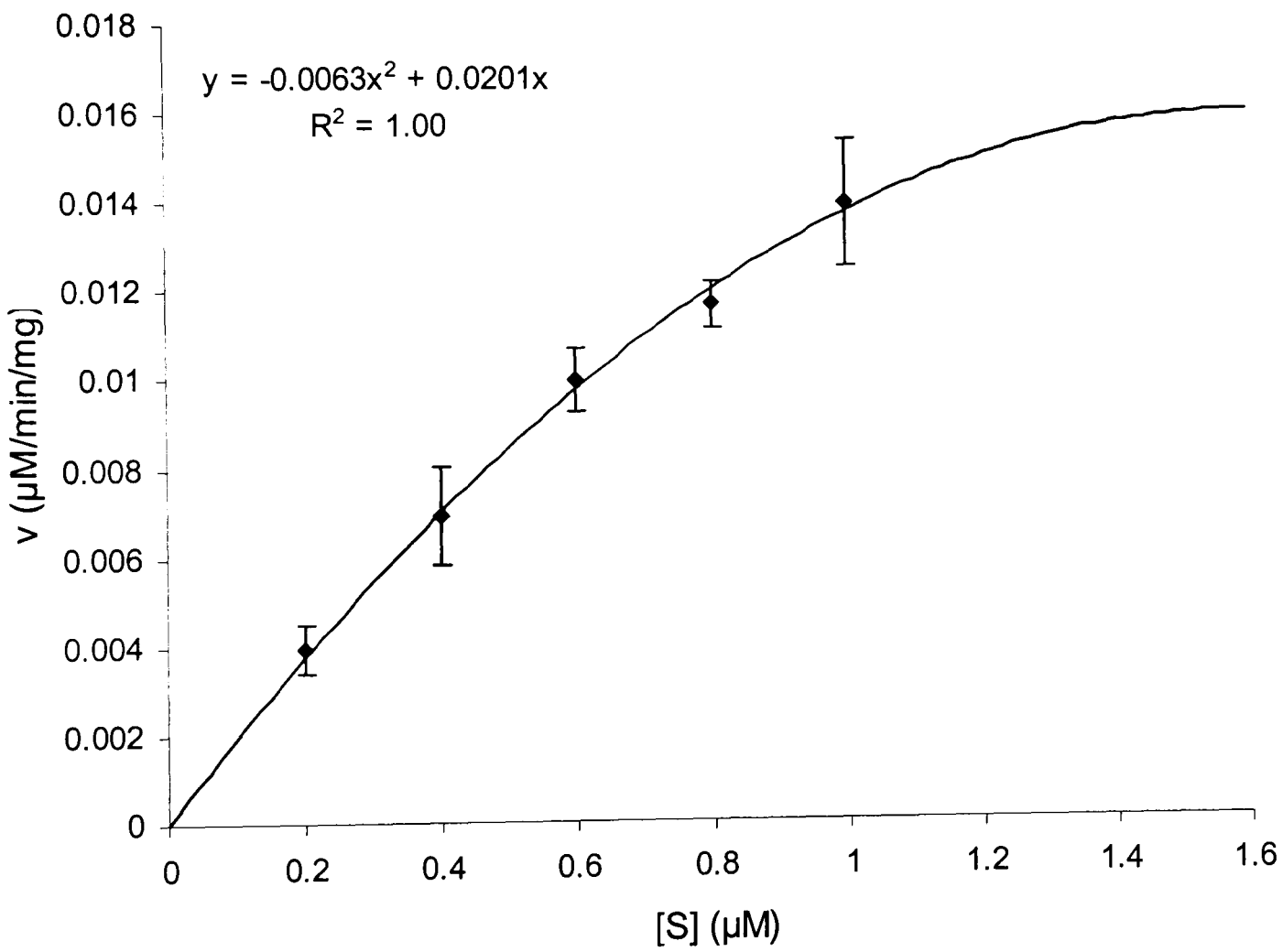

Figure 3.28 Michaelis-Menten plot for type 1 17β-HSD.

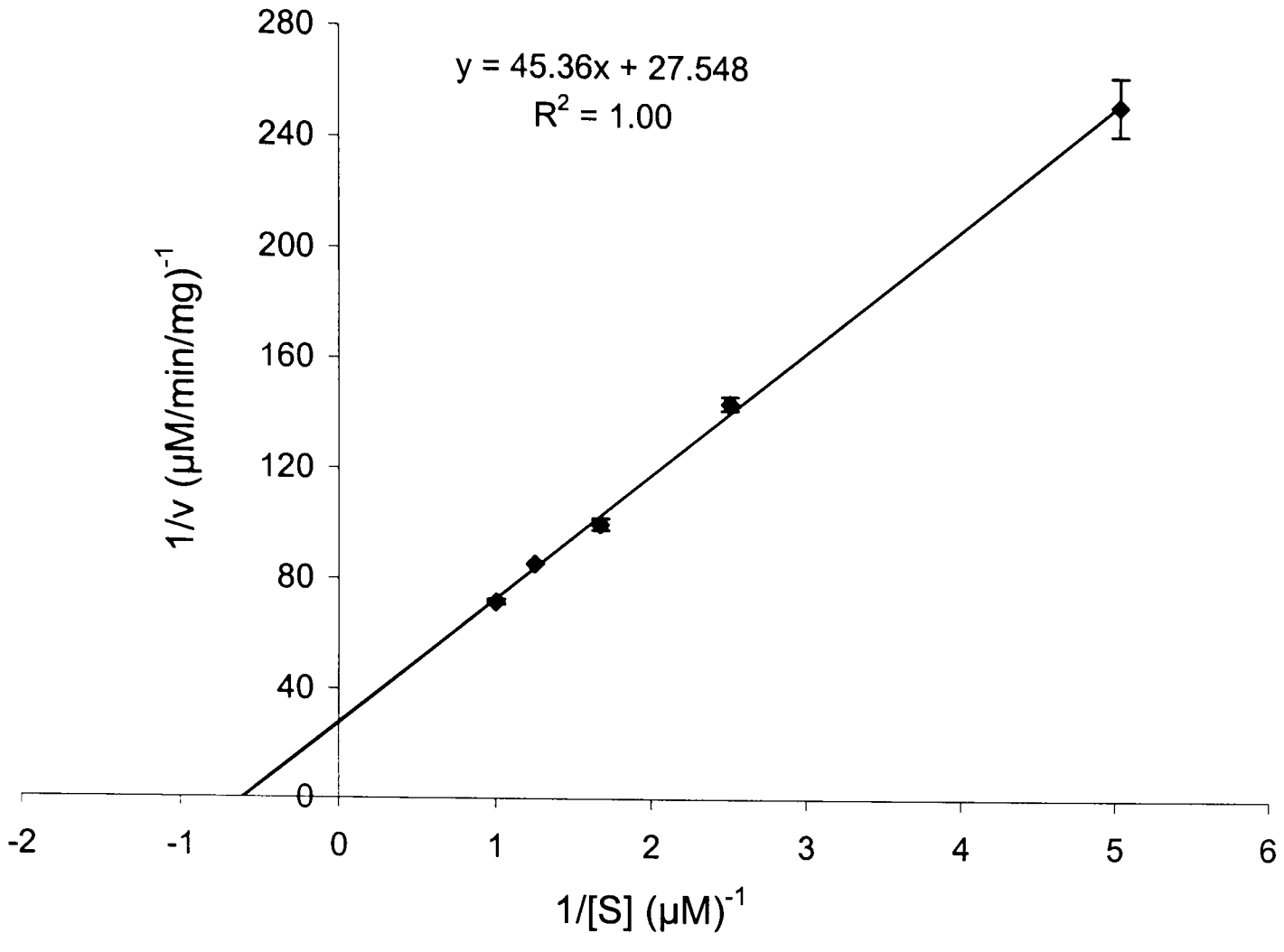

Figure 3.29 Lineweaver-Burk plot for type 1 17β-HSD.

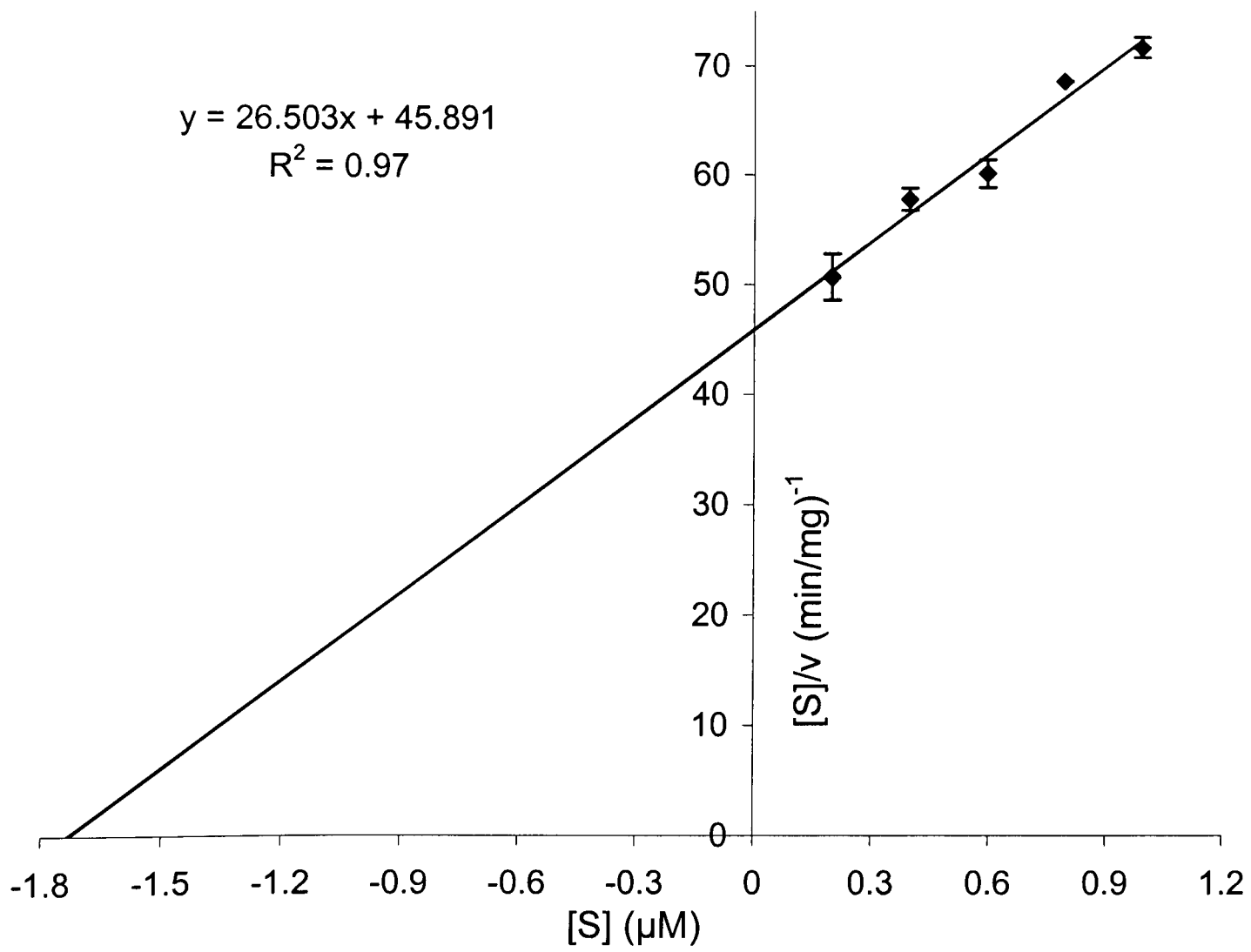

Figure 3.30 Hanes-Woolf plot for type 1 17β-HSD.

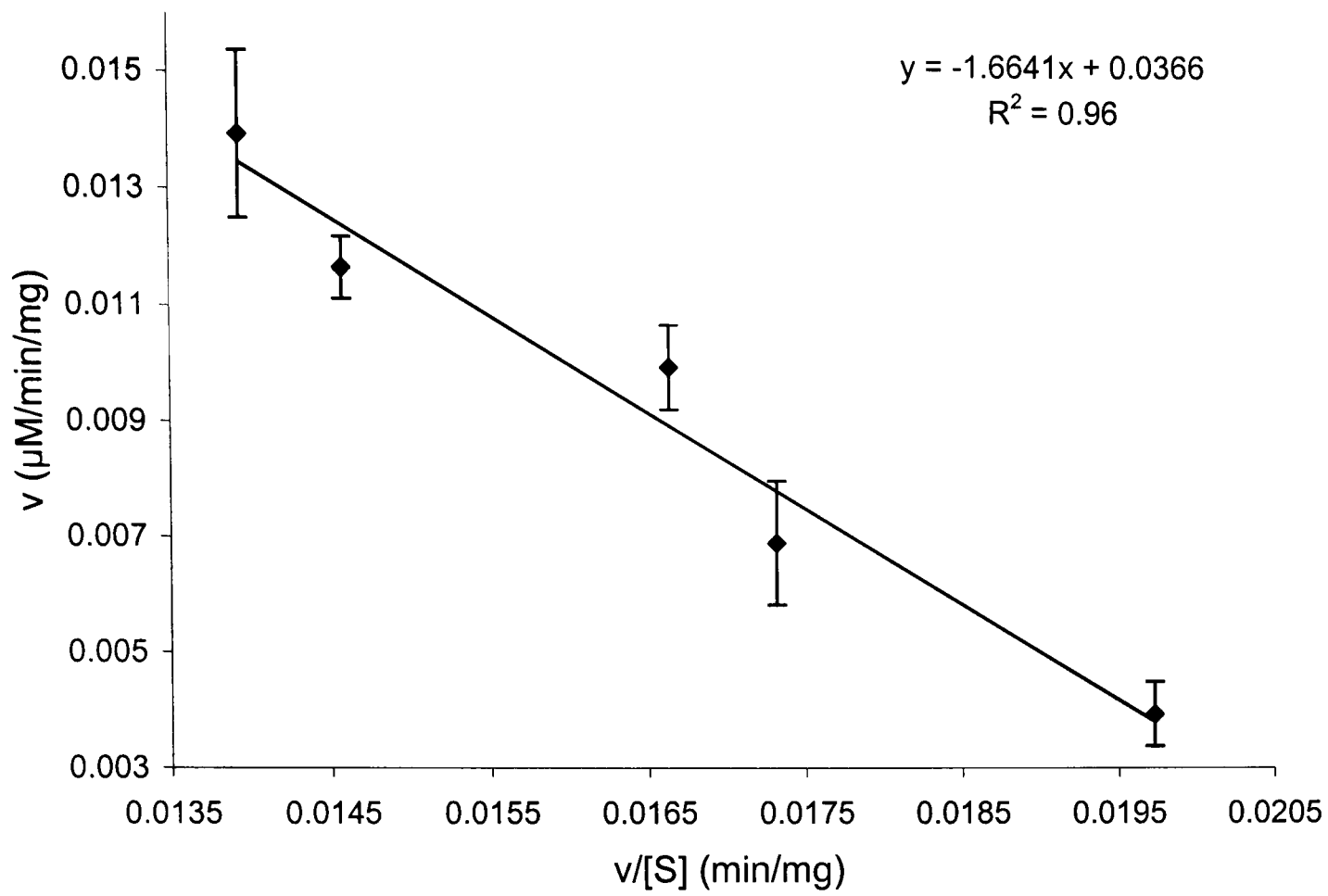

Figure 3.31 Eadie-Hofstee plot for type 1 17β-HSD.

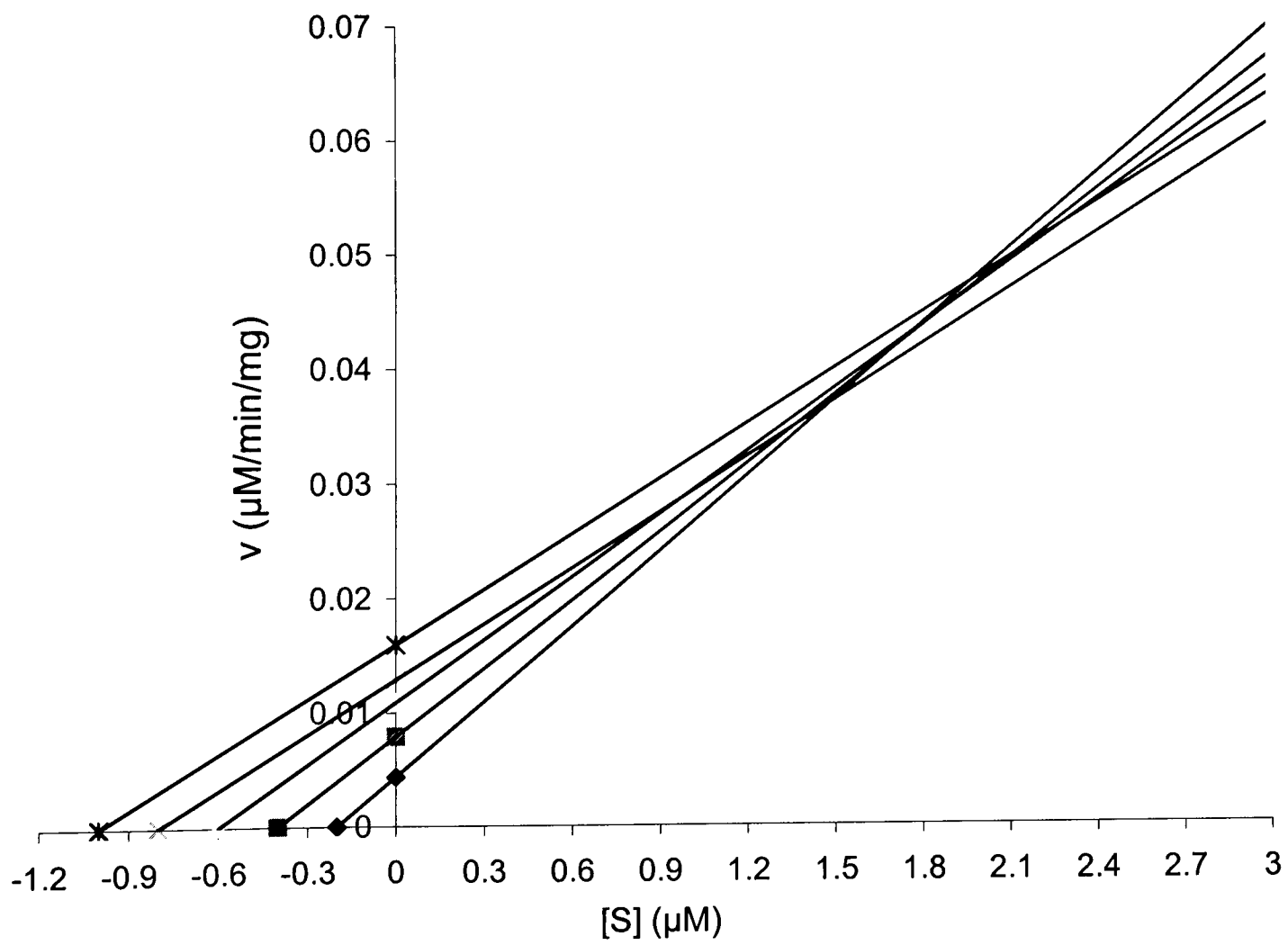

Figure 3.32 Direct linear plot for type 1 17β-HSD

Plot	K_m (μM)
Michalis Menten plot	0.47 ± 0.03
Lineweaver-Burk plot	1.68 ± 0.44
Hanes-Woolf plot	1.76 ± 0.45
Eadie-Hofstee plot	1.63 ± 0.36
Direct linear plot	1.67 ± 0.50
Average K_m	1.44 ± 0.36

Table 3.5 Summary of K_m plots for type 1 17β-HSD.

3.29 Discussion

The average K_m value for 17β-HSD with the substrate E1 using Sprague-Dawley testicular microsomes was found to be 1.44 ± 0.36μM, compared to K_m values obtained by other workers i.e., K_m = 3.3 ± 0.9μM (Le Lain et al, 2001).

3.30 Preliminary Screening of Compounds for Type 1 17β-HSD Activity for the Conversion of E1 to E2

The assay procedure for screening involved inhibitors and standards (baicalein and 7-hydroxyflavone) dissolved in absolute ethanol and diluted to give the required final incubation concentration. The assay was carried out (in triplicate) at 37°C in a shaking water bath. The total assay volume was 200μL. Prepared substrate, E1 (5μM/tube, 10μL), NADPH-generating system (10μL) and inhibitor (100μM, 4μL), in sodium phosphate buffer (pH7.4, 170μL), were allowed to warm to 37°C. The testicular microsomes were thawed and warmed to 37°C before addition (0.35mg/mL final concentration, 6μL) to the assay mixture. The solutions were incubated for 90min at 37°C and the reaction was quenched by the addition of ether (2x2mL) and placed on ice. The assay was completed as previously described (Section 3.24). Control samples with no inhibitor were incubated simultaneously. The results were determined by using equation 3.3 to determine the percentage conversion of E1 to E2 and then comparing the

conversion in the presence of inhibitors to that of the controls. Results are shown in Tables 3.6 – 3.8.

3.31 Results – Preliminary Screening

The results are shown in Tables 3.6a – 3.8b

3.31.1 Discussion

The compounds, in general, showed equipotency to the standards for both the 4-hydroxyphenyl ketones as well as the biphenyl ketones. The commercially available compounds were in general weak inhibitors in comparison to the standards.

Compound No.	Structure	% Inhibition at 100μM
113 Baicalein	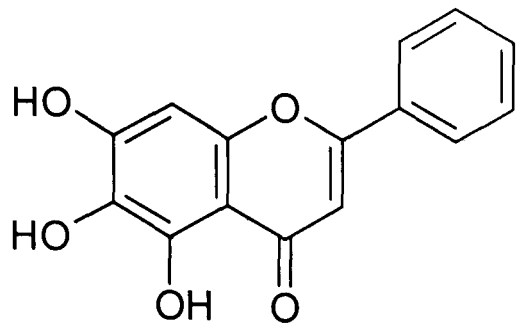	31.63 ± 4.91
97 7-hydroxyflavone	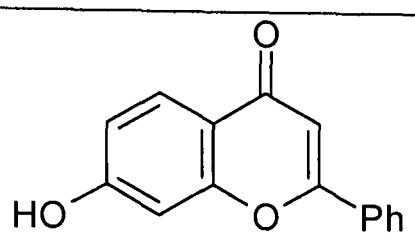	25.63 ± 2.94
247	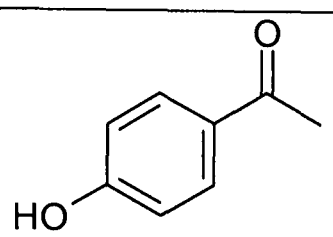	20.83 ± 0.91
248	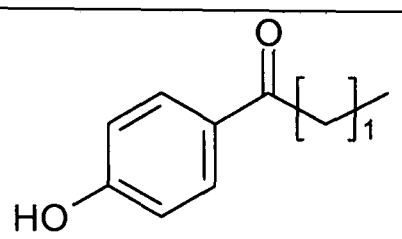	17.47 ± 0.91
249	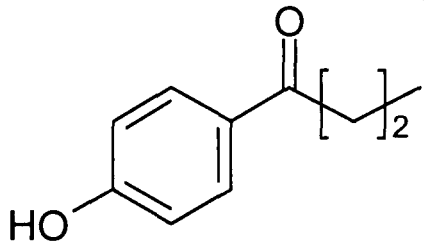	35.11 ± 2.92
250	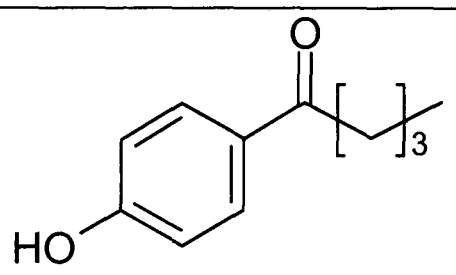	39.76 ± 1.31
251	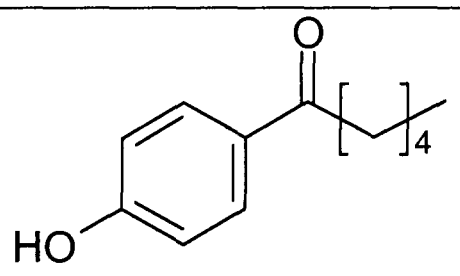	45.68 ± 1.34
252	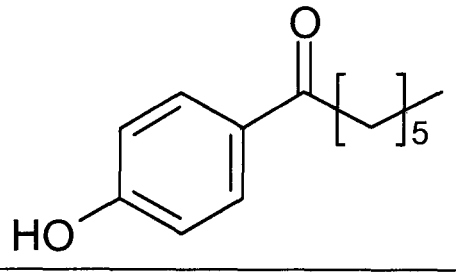	47.58 ± 2.60

Table 3.6a Results from preliminary screening data of some 4-hydroxyphenyl ketones for type 1 17β-HSD activity.

Compound No.	Structure	% Inhibition at 100μM
253	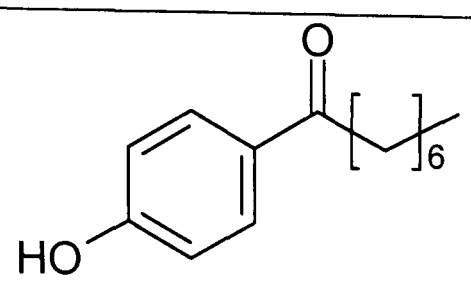	36.87 ±0.89
254	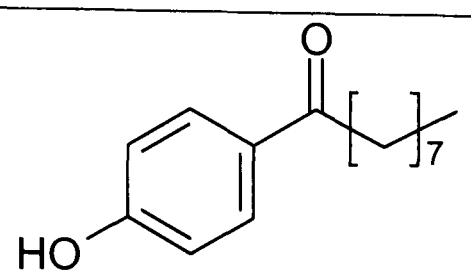	36.32 ± 0.33
255	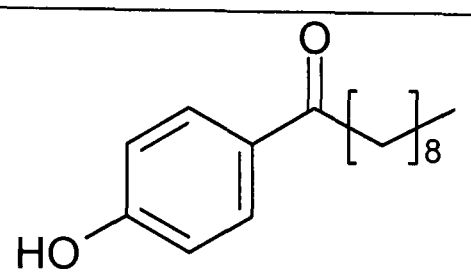	28.15 ± 3.46
256	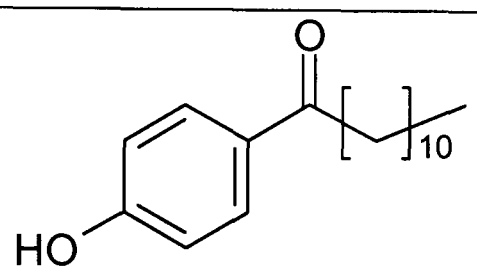	30.61 ± 3.78
257	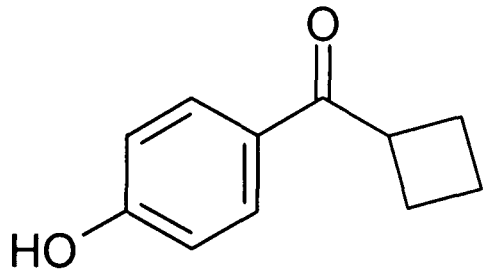	42.47 ± 2.66
258	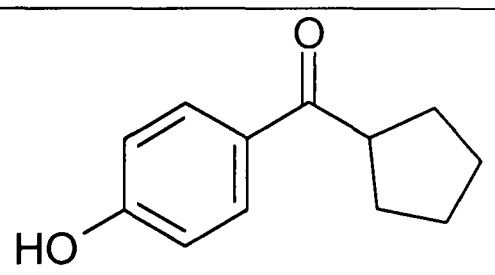	43.97 ± 0.78
259	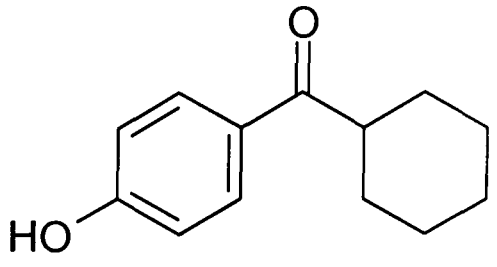	49.54 ± 2.57
260	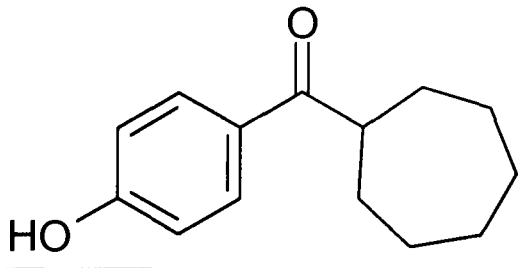	47.23 ± 2.41

Table 3.6b Results from preliminary screening data of some 4-hydroxyphenyl ketones for type 1 17β-HSD activity.

Compound No.	Structure	% Inhibition at 100μM
113 Baicalein	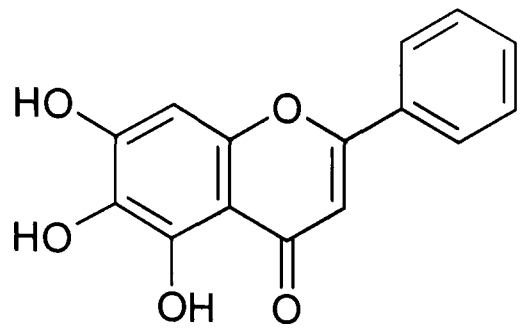	31.63 ± 4.91
97 7-hydroxyflavone	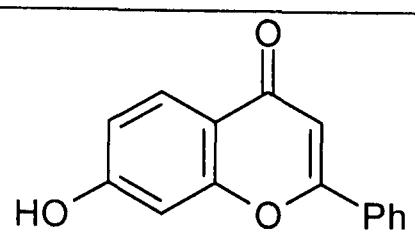	25.63 ± 2.94
261	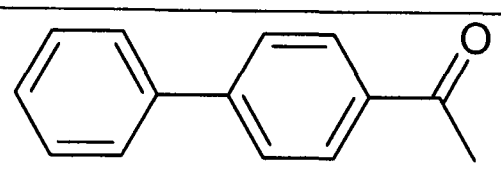	31.24 ± 2.79
262	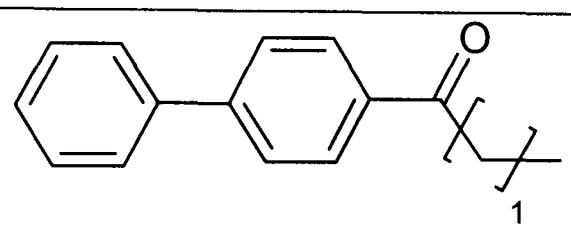	33.50 ± 2.73
263	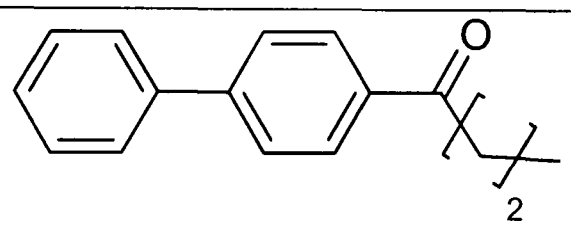	36.59 ± 0.56
264	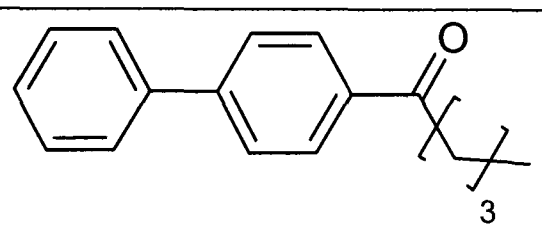	45.49 ± 0.53
265	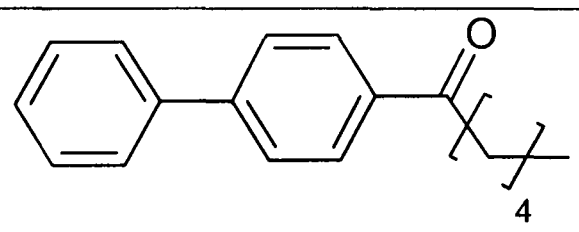	33.55 ± 0.73
266	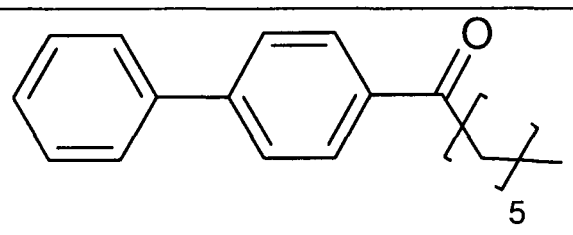	36.05 ± 0.66
267	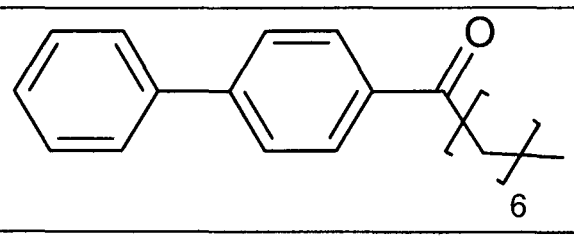	34.79 ± 0.25

Table 3.7a Results from preliminary screening data of some biphenyl ketones for type 1 17β-HSD activity.

Compound No.	Structure	% Inhibition at 100μM
268	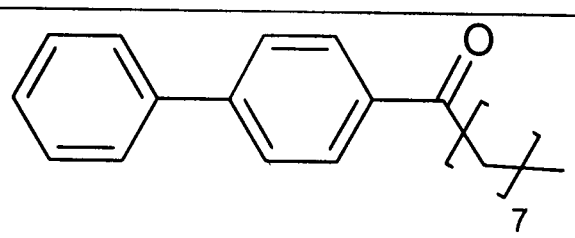	31.26 ± 0.28
269	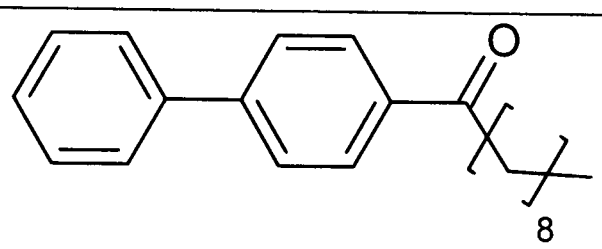	28.23 ± 1.64
270	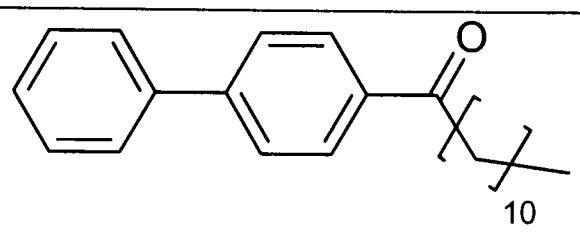	29.43 ± 0.37
271	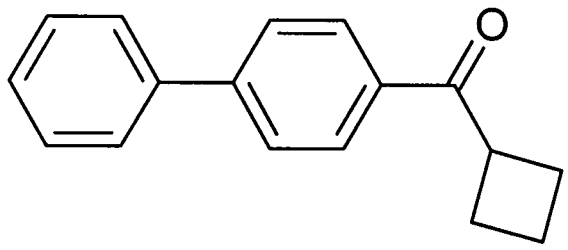	34.47 ± 0.10
272	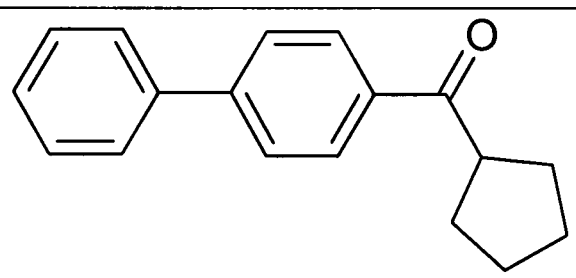	44.04 ± 1.72
273	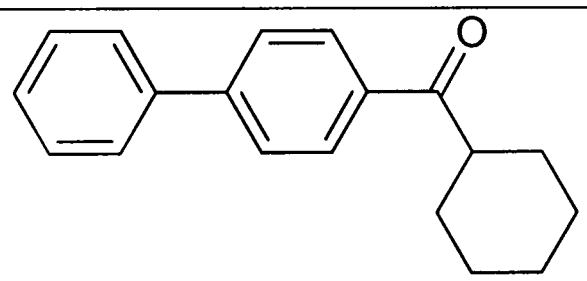	48.79 ± 0.22

Table 3.7b Results from preliminary screening data of some biphenyl ketones for type 1 17β-HSD activity.

Compound No.	Structure	% Inhibition at 100μM
113 Baicalein	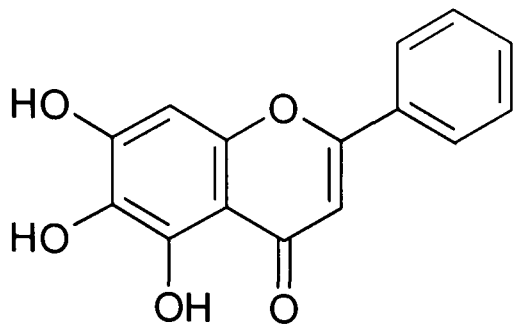	12.34 ± 1.46
97 7-hydroxyflavone	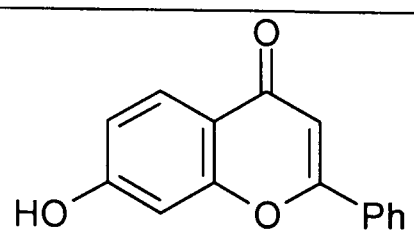	5.73 ± 0.16
274	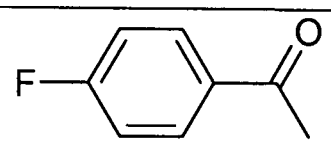	3.65 ± 0.41
275	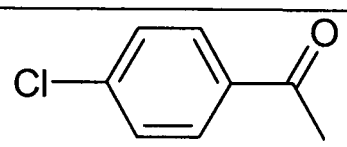	8.31 ± 0.91
276	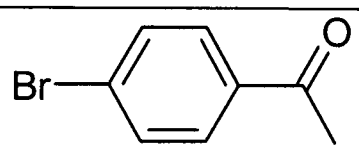	6.45 ± 0.29
277	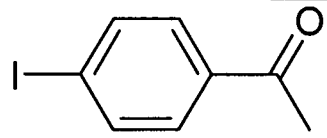	0
278	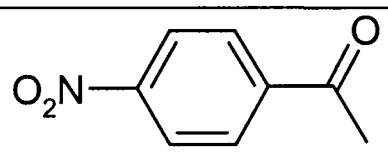	13.80 ± 2.52
279	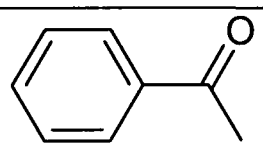	5.12 ± 3.45
280	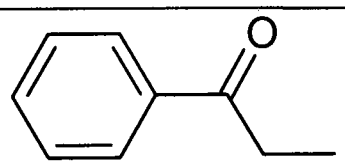	5.09 ± 3.90
281	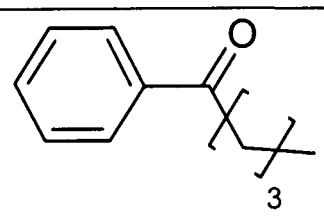	30.73 ± 1.59
282	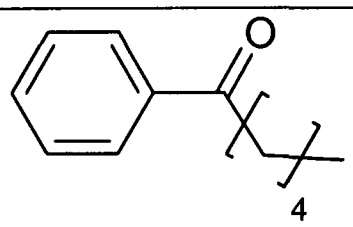	23.73 ± 2.85

Table 3.8a Results from preliminary screening data of some commercially available compounds for type 1 17β-HSD activity.

Compound No.	Structure	% Inhibition at 100μM
283	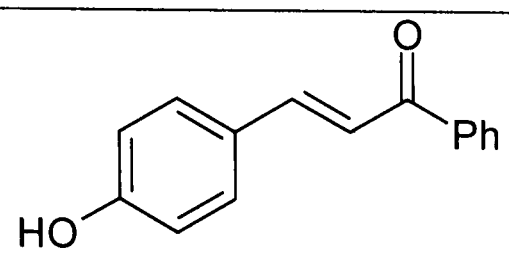	23.14 ± 0.20
284	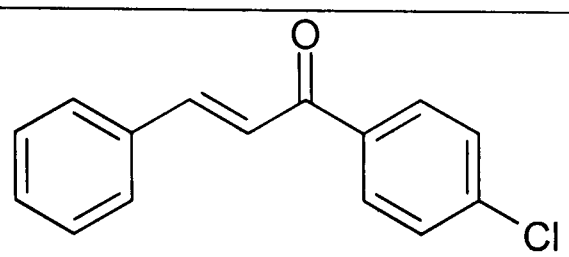	4.92 ± 1.14
285	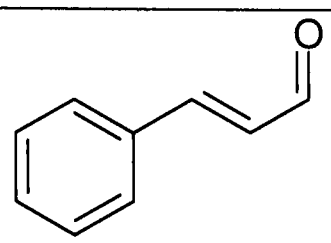	14.43 ± 1.05
286	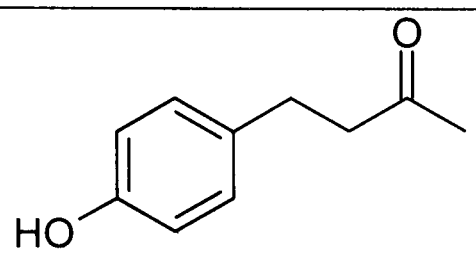	17.75 ± 2.34
287	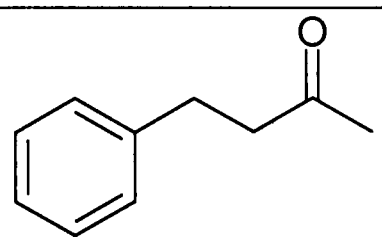	23.33 ± 2.77

Table 3.8b Results from preliminary screening data of some commercially available compounds for type 1 17β-HSD activity.

3.32 3β-HSD Enzyme Assay

3.33 Introduction

Compounds evaluated against 17β-HSD were also evaluated against 3β-HSD using the microsomal fraction obtained from Sprague Dawley rat testicular tissue. The assay used was modified from assays of Cooke and Robaire (1986) and Cooke et al (1998) and measures the effect of novel compounds on the rate of conversion of radiolabelled DHEA to A mediated by the action of 3β-hydroxysteroid dehydrogenase (3β-HSD), followed by the conversion to T mediated by the action of 17β-HSD (type 3). This assay was conducted to determine whether the inhibitors were specific for 17β-HSD or inhibitors of HSDs in general.

To separate DHEA, A and T from the reaction mixture, TLC was employed. The extracts, together with the carrier steroids (5mg/mL), were applied to TLC plates. The mobile phase used consisted of a mixture of dichloromethane (80mL) and ethyl acetate (20mL).

After elution and identification using iodine vapour and UV light, each steroid was cut out and counted for 4min per tube in a cocktail of scintillation fluid and acetone. The percentage conversion of DHEA to A and then to T, was determined by the division of the CPM for both products from the total CPM of all three steroids.

3.34 Methods, Materials and Instruments

All methods, materials and instruments used were as mentioned in Chapter 2, Section 2.3. [1,2,6,7-^{3}H]DHEA was obtained from Amersham Pharmacia Biotech UK Limited, Buckinghamshire.

3.35 Buffer, Solution and Substrate Preparation

Buffers and solutions used in the assay were as for those in Chapter 2, Section 2.4.

Except:-

Tris-HCl Buffer pH8.4 (50mM)

A: Tris(hydroxymethyl)aminomethane ($NH_2C(CH_2OH)_3$) (mW – 121.14) (6.057g) dissolved in distilled water (500mL)

B: Hydrochloric acid (0.1M)

Solution B was added to solution A (500mL) until a pH of 8.4 was reached. The solution was made up to 1L with distilled water.

Substrate preparation of [1,2,6,7-^{3}H]DHEA (100μM)

A stock solution of substrate was prepared by transferring radiolabelled [1,2,6,7-^{3}H]DHEA (0.333μM, 20μL) to a glass vial and removing the toluene:ethanol mixture under a stream of nitrogen. Unlabelled substrate in propane-1,2-diol (99.667μM, 1mL) was added to the radiolabelled residue and mixed thoroughly to give a final concentration of 100μM.

3.36 Preparation of Testicular Microsomes

The microsomes were prepared as previously described in Chapter 2, Section 2.5

3.37 Protein Assay

The protein concentration of the testicular microsomes was determined as previously described in Chapter 2, Section 2.6. The results are shown in Figure 3.33.

The protein concentration of the testicular microsomes was determined from the standard protein calibration curve (Figure 3.33) and was found to be 11.74mg/mL.

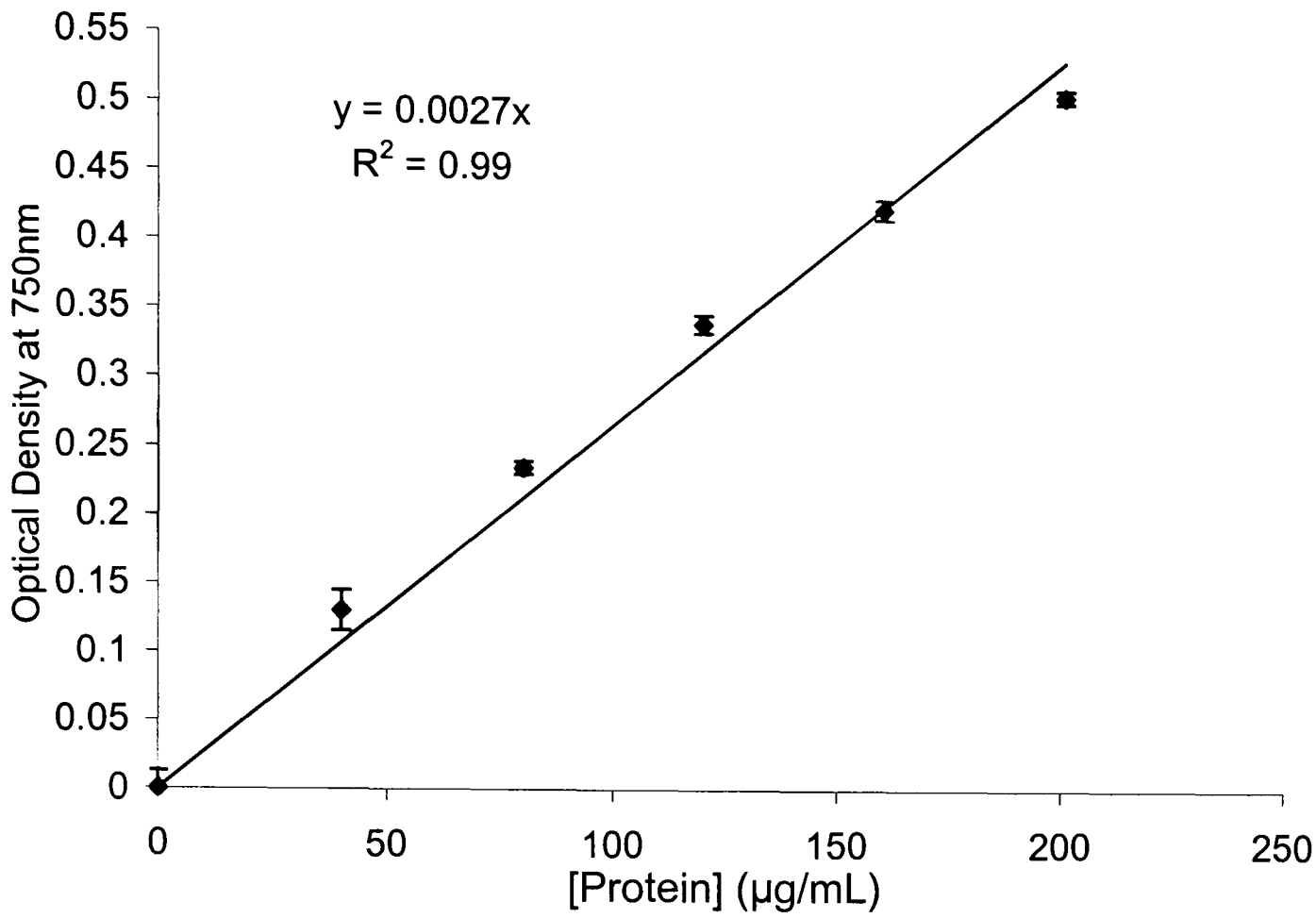

Figure 3.33 Calibration graph for protein assay for 3β-HSD

3.38 Validation of the 3β-HSD Assay

To validate the 3β-HSD assay, it was necessary to determine the quantity of non-enzymatic product formation. Assay conditions were set so that the prepared substrate, DHEA (1µM final concentration), was incubated for 30min at 37°C in the following solutions:

i. Tris-HCl buffer (50mM, pH8.4)
ii. Testicular microsomes (0.29mg/mL, 25µL) and Tris-HCl buffer, lacking NADPH-generating system
iii. Testicular microsomes, denatured by addition of ether (2mL), Tris-HCl buffer and NADPH-generating system

After incubation, the assay mixtures were treated, except (iii), with ether (2mL). The solutions were vortexed, then left to stand over ice for 15min. The organic phase was extracted into a separate clean tube. The assay mixture was further extracted with ether (2x2mL), and the organic layers combined. The solvent was removed under a stream of nitrogen, acetone (30μl) was added to each tube and the solution spotted onto silica based TLC plates along with carrier steroids (DHEA, A and T, 5mg/mL, approximately 10μL) were spotted onto TLC plates and run, using a mobile phase consisting of dichloromethane (80mL) and ethyl acetate (20mL). After development, the separated steroids were identified, using iodine vapours and UV lamp, cut from the plate and placed into scintillation vials. Acetone (1mL) was added to each vial in order to dissolve the steroid from the silica plate and then scintillation fluid (Optiscint HiSafe, 3mL) was added. The samples were vortexed and read radioactivity. None of the samples showed detectable quantities of T and A, indicating that (a) testicular microsomes and (b) NADPH are both essential requirements for the conversion of DHEA to its subsequent products.

3.39 Protein Dependency for 3β-HSD

An experiment was performed to establish whether the rate of appearance of A and T, produced during the enzymatic reaction, was proportional to the protein concentration.

Incubations were carried out (in triplicate) using protein concentrations 0.00, 0.12, 0.29, 0.59, 0.88 and 1.17mg/mL (final concentration), prepared substrate, DHEA (1μM final concentration, 10μL), NADPH-generating system (50μL) and Tris-HCl buffer (pH8.4, to 1mL). The solutions were incubated for 30min at 37°C and the reaction was quenched by the addition of ether (2mL) and placed on ice. The assay was completed as previously described (Section 3.38) and the percentage conversions determined using equation 3.5

$$\text{Percentage Conversion} = \left(\frac{A + T}{DHEA + A + T} \right) \times 100$$

Equation 3.5 Percentage conversion of DHEA to A and T.

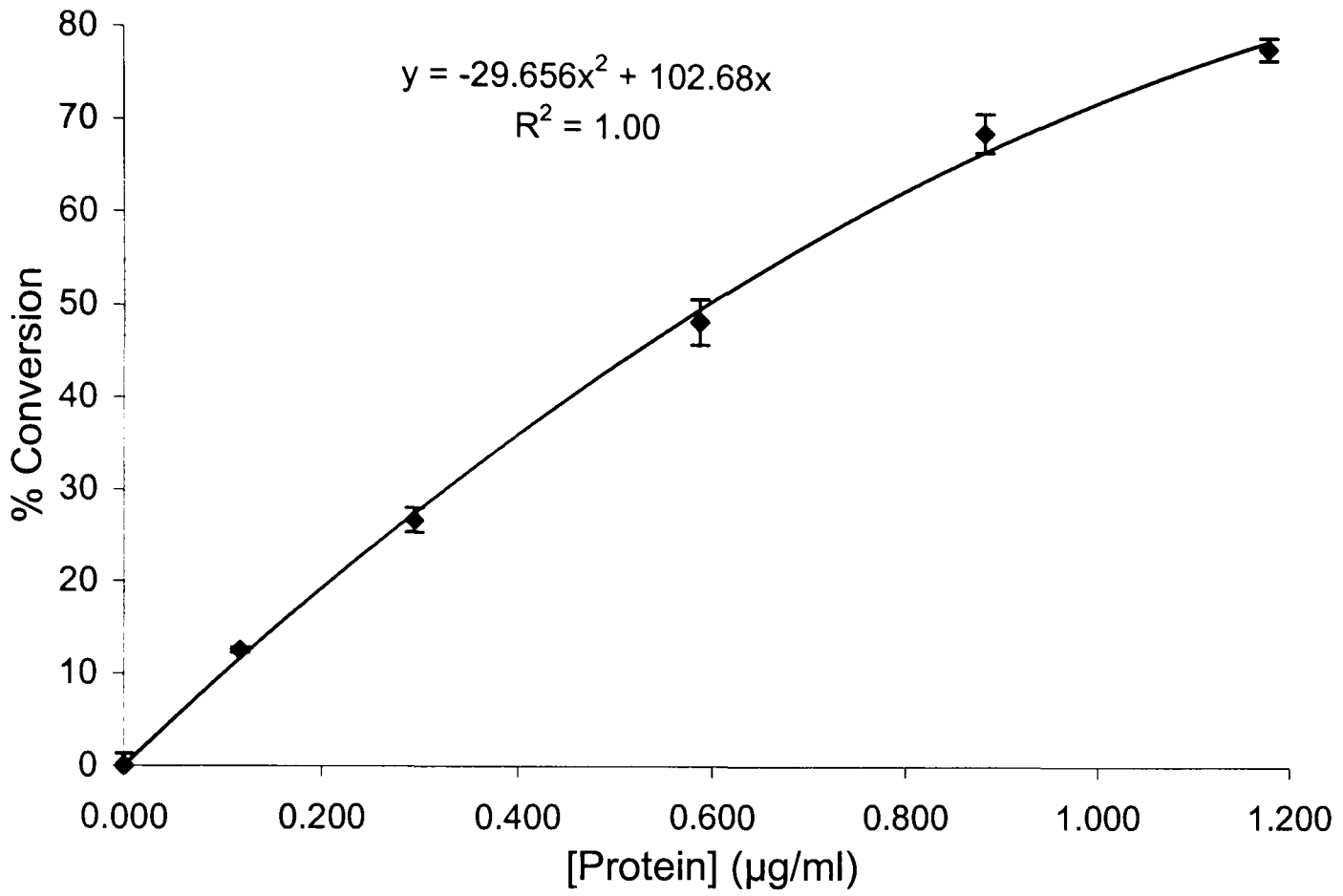

Figure 3.34 Plot to show percentage conversion of DHEA at varying protein concentrations.

At 1µM substrate concentration, it can be concluded that the kinetics of the reaction are linear for protein concentrations up to 0.88mg/mL.

3.40 Time Dependency for 3β-HSD

Time dependency experiments were performed to ensure that the assays were within the linear phase of the enzyme reaction.

Incubations were carried out (in triplicate) using a final concentration of prepared substrate, DHEA (1µM, 10µL), NADPH-generating system (50µL) and Tris-HCl buffer (920µL, pH8.4). The samples were warmed to 37°C in a shaking

water bath before the addition of the testicular microsomes (0.23mg/mL final concentration, 20μL), added at differing time intervals (15, 30, 45, 60, 90 and 120min). The reaction was quenched by the addition of ether (2mL) and placed on ice. The assay was completed as previously described (Section 3.38). A graph was then plotted for percentage conversion versus time (Figure 3.35).

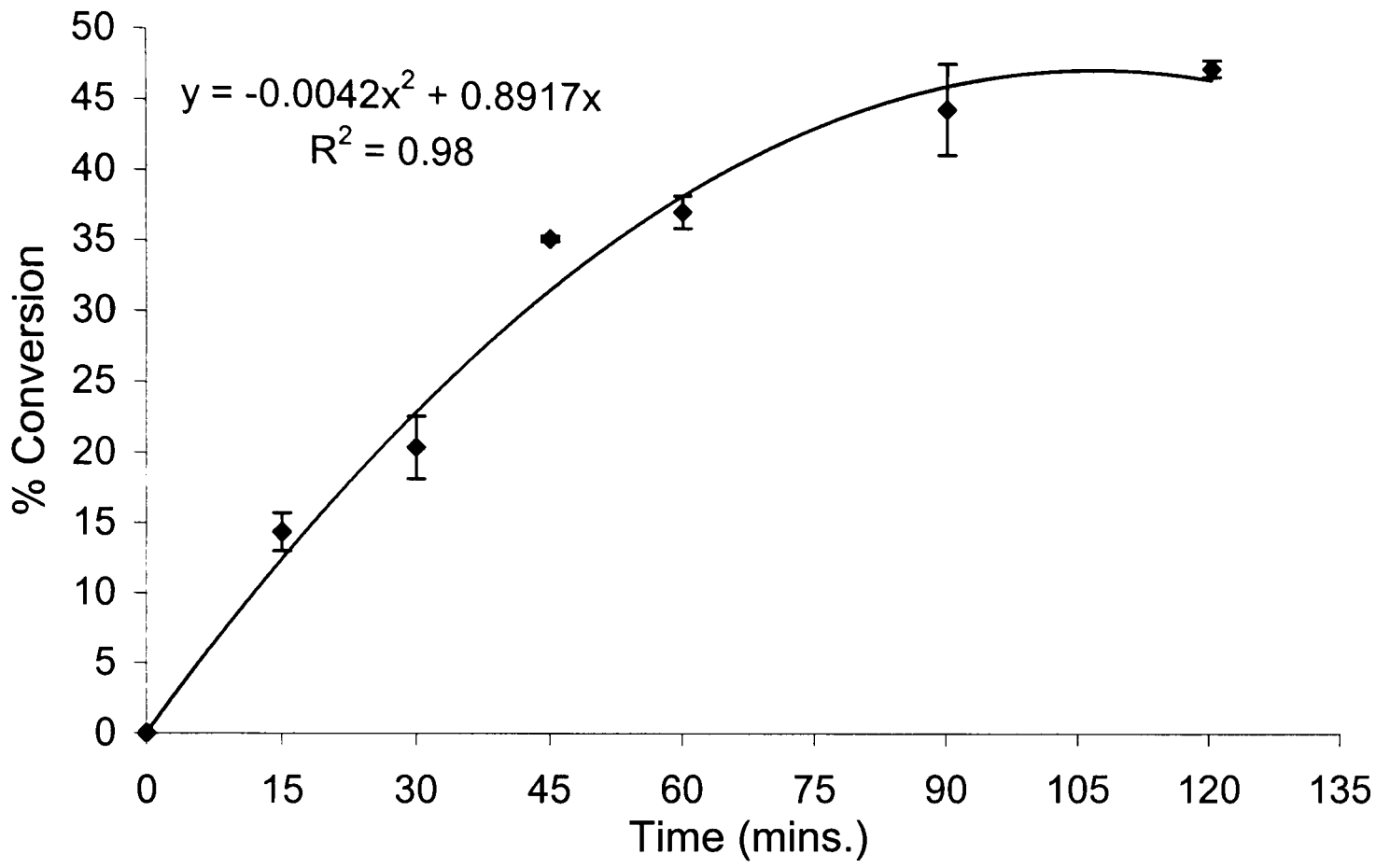

Figure 3.35 Plot to show percentage conversion of DHEA at varying time intervals.

At 0.23 mg/mL of protein concentration and 1μM substrate concentration, it can be concluded that the kinetics of the reaction are linear for time intervals up to 60min.

3.41 Determination of K_m for 3β-HSD

The prepared substrate, DHEA (100μM) was serially diluted, using propane-1,2-diol, to give a range of final incubation concentrations of substrate (0.8 to 4.0μM). All incubations were carried out in triplicate at 37°C in a shaking water bath. Incubation mixtures (1mL), containing NADPH-generating system (50μL) and prepared substrate (of varying concentration, 40μL), in Tris-HCl buffer

(890µL, pH8.4), were allowed to warm to 37°C. The testicular microsomes were thawed and warmed to 37°C before addition (0.23mg/mL final concentration, 20µL) to the assay mixture. The solutions were incubated for 40min at 37°C and the reaction was quenched by the addition of ether (2mL) and placed on ice. The assay was completed as previously described (Section 3.38). The velocity, v, for each substrate concentration was calculated using the equation 3.6, where units for v are: µM/min/mg.

$$v = \frac{\text{CPM (A + T) x substrate concentration [S] (µM)}}{\text{CPM (DHEA + A + T) x protein concentration (mg/ml) x time (min)}}$$

Equation 3.6 Velocity calculation for each substrate concentration

3.42 Results – Graphical Determination of K_m

The K_m and maximum velocity (V_{max}) were determined from five different general methods for DHEA, as previously described in Chapter 2, Section 2.11, and are shown in Figures 3.36 to 3.39 and the average of three assays are summarised in Table 3.9

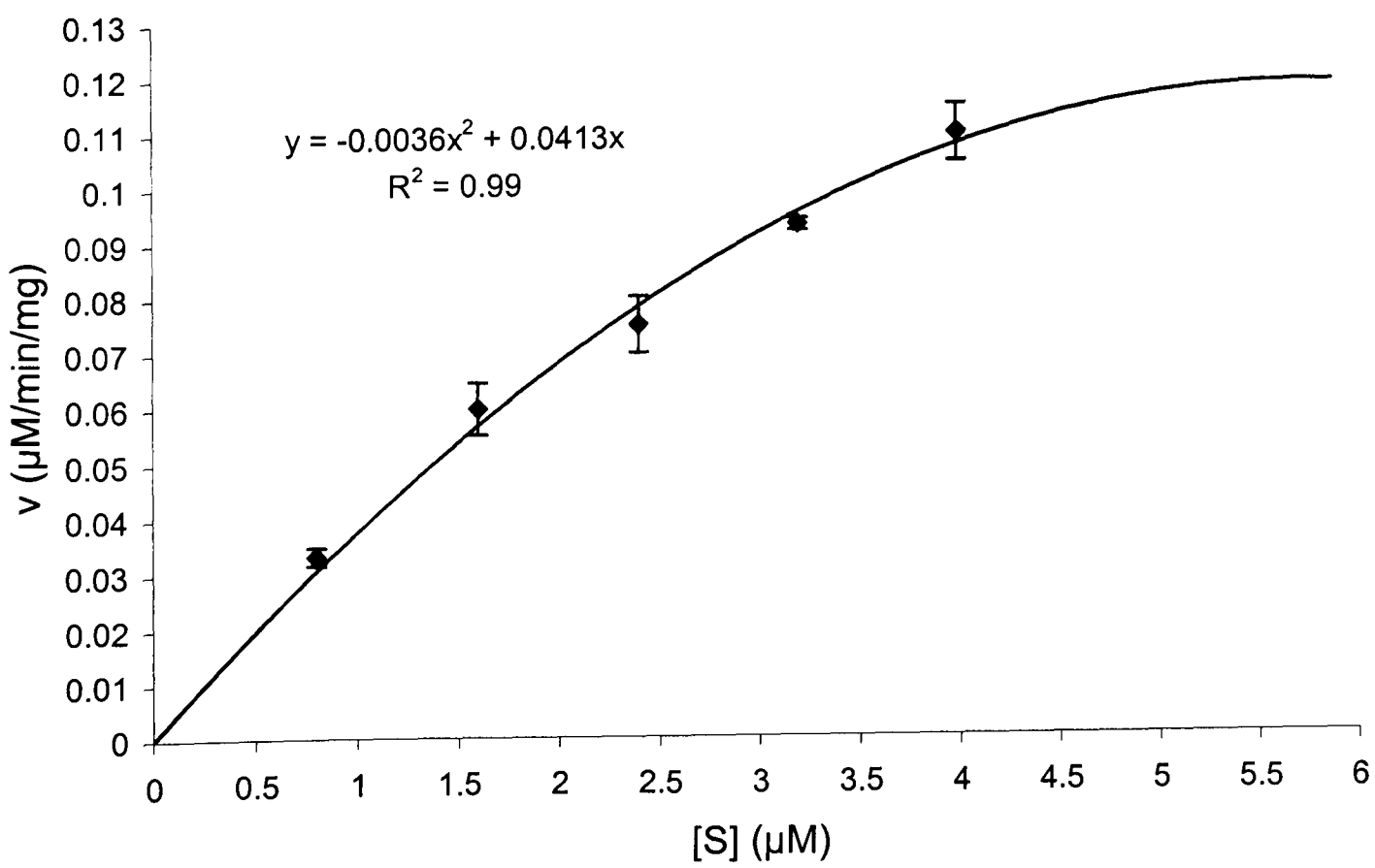

Figure 3.36 Michaelis Menten plot for 3β-HSD.

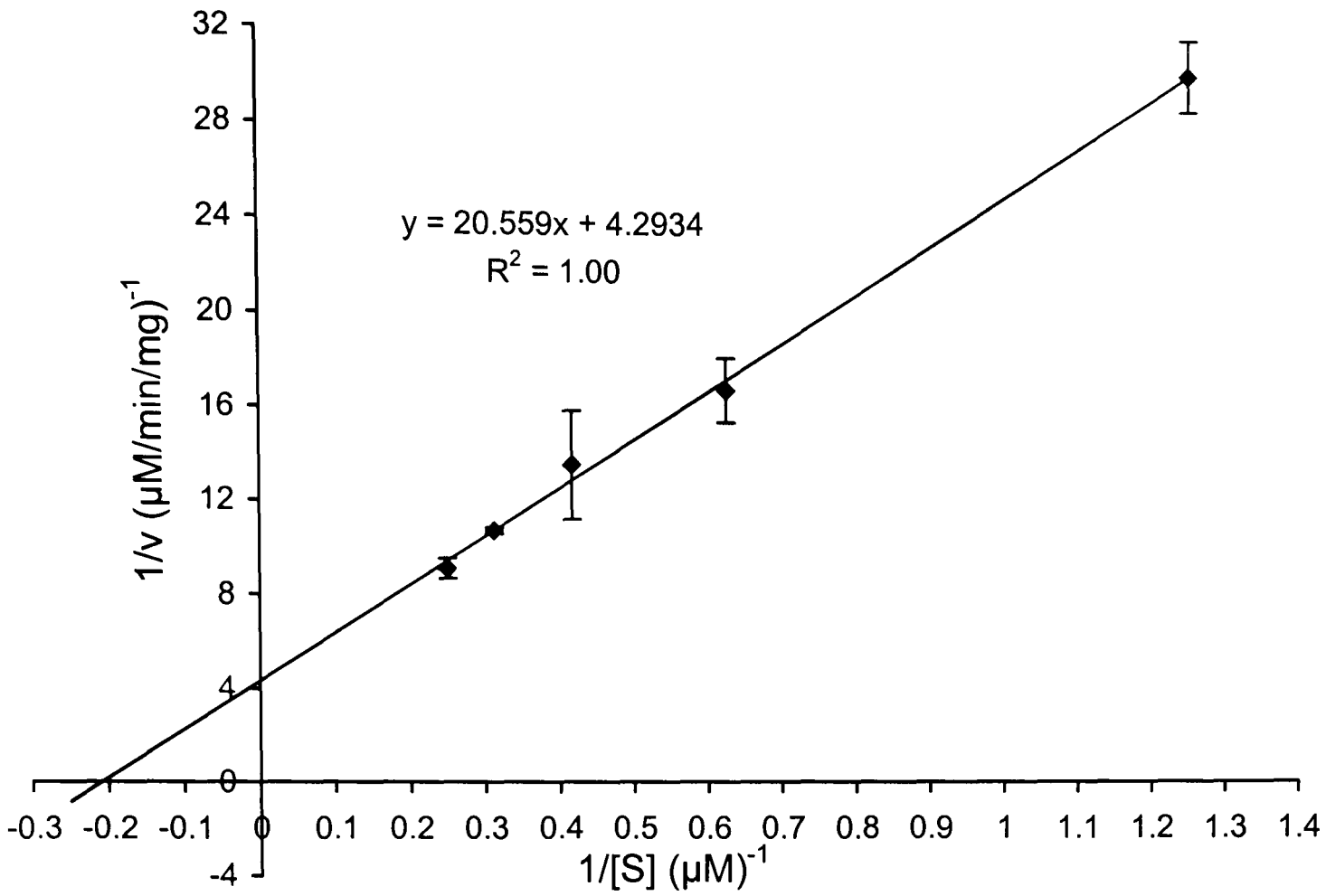

Figure 3.37 Lineweaver-Burk plot for 3β-HSD.

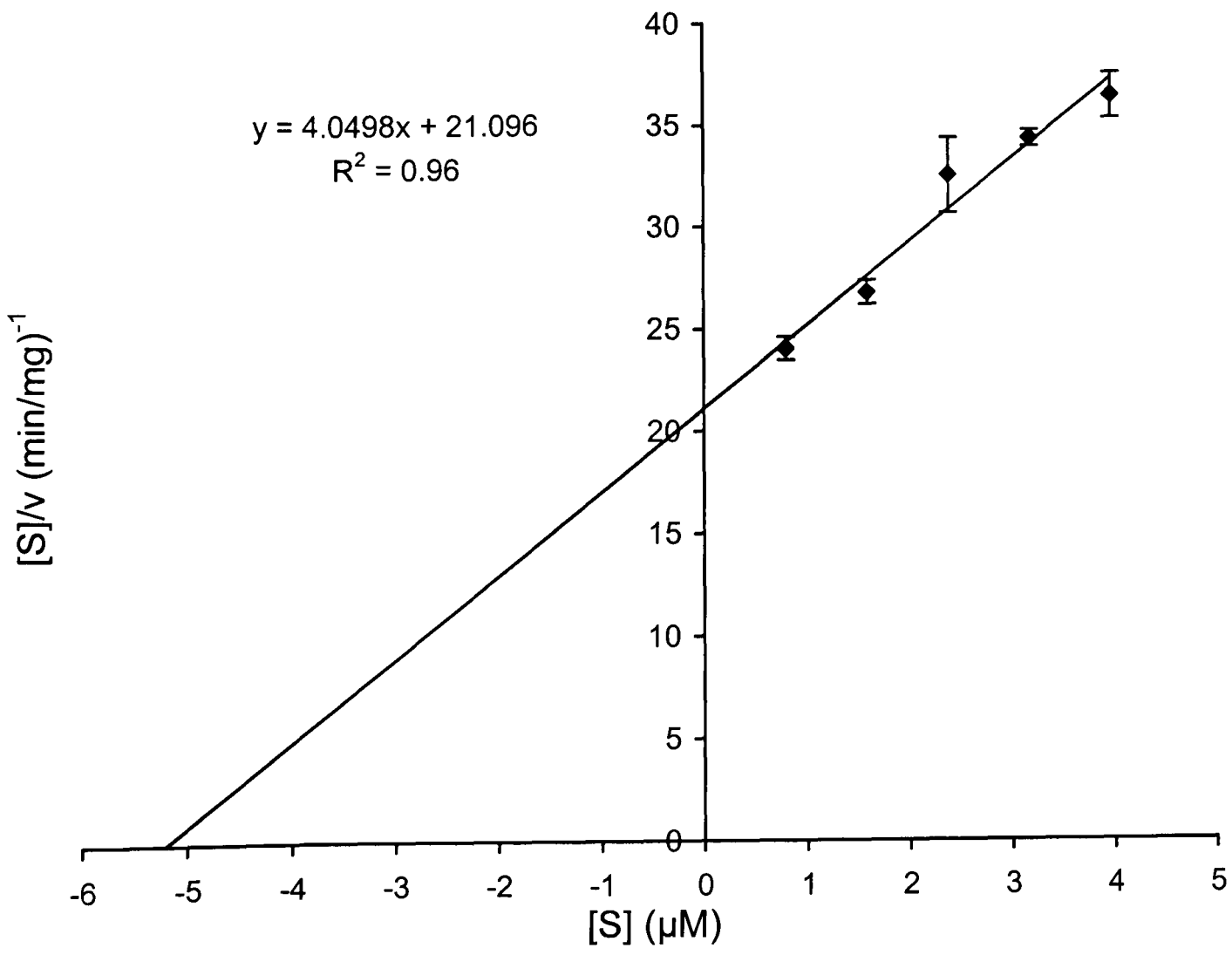

Figure 3.38 Hanes-Woolf plot for 3β-HSD.

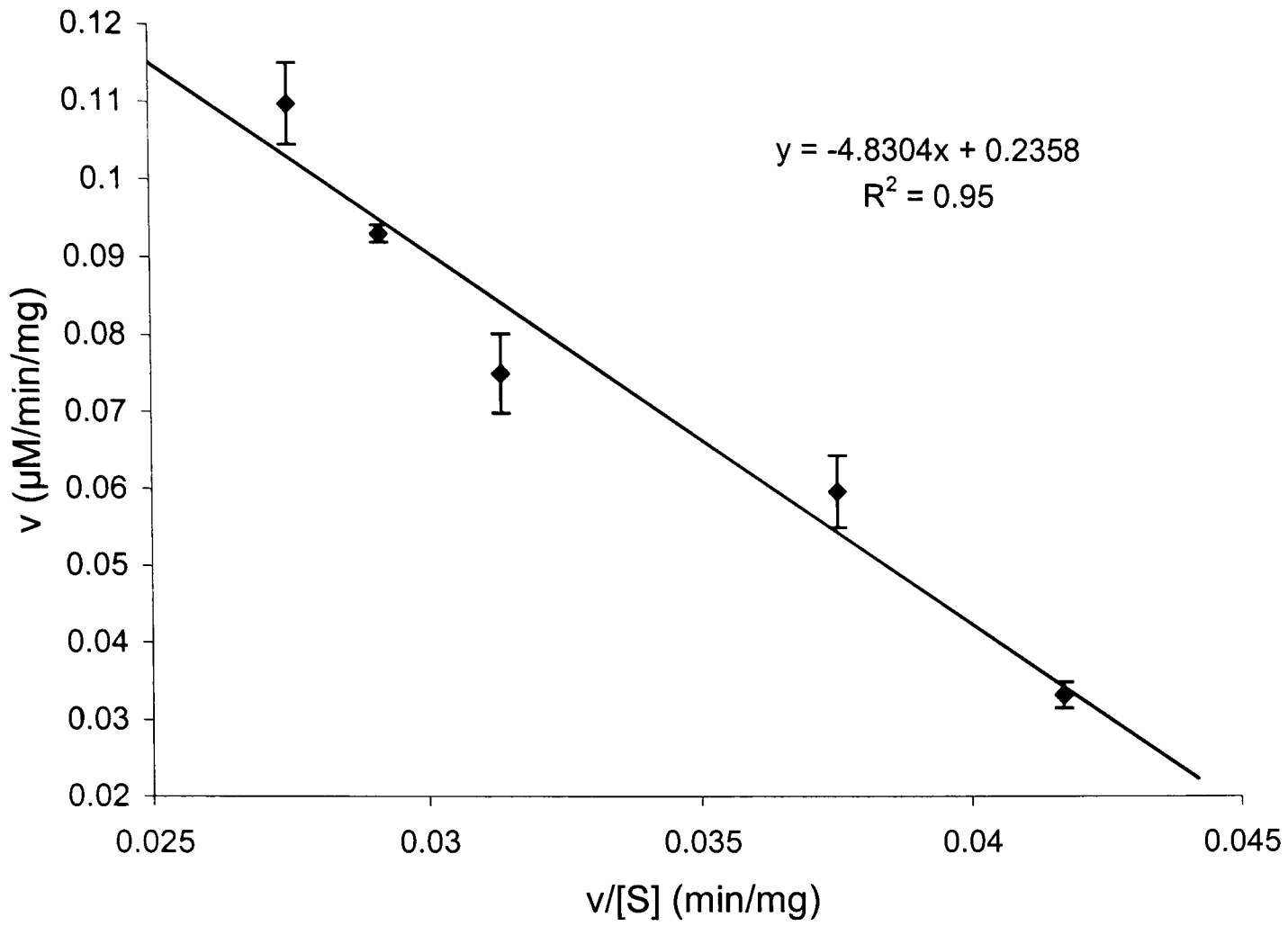

Figure 3.39 Eadie-Hofstee plot for 3β-HSD.

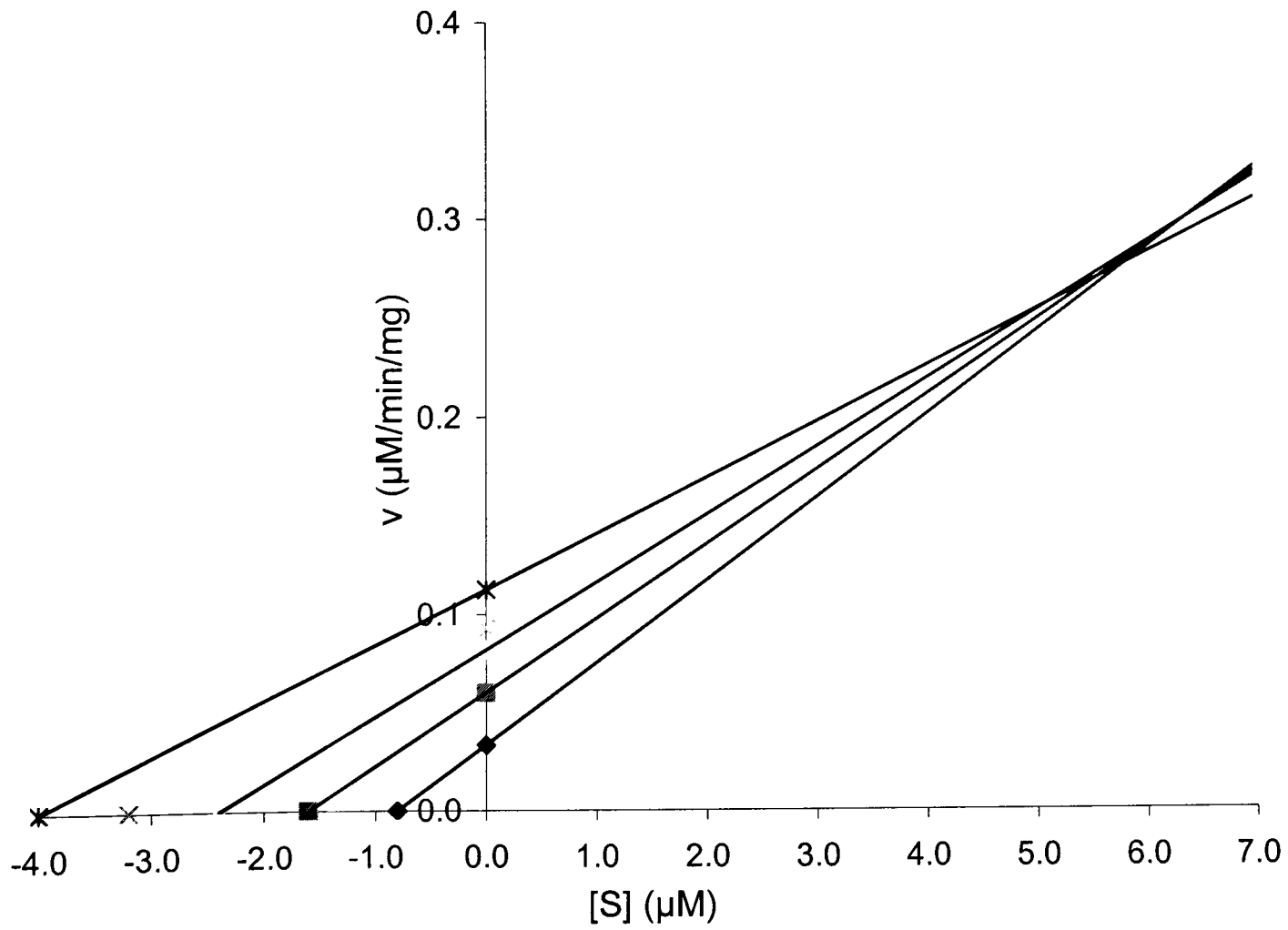

Figure 3.40 Direct linear plot for 3β-HSD

Plot	K_m (μM)
Michalis Menten plot	1.77 ± 0.31
Lineweaver-Burk plot	4.85 ± 0.55
Hanes-Woolf plot	5.22 ± 0.71
Eadie-Hofstee plot	4.45 ± 0.35
Direct linear plot	5.83 ± 0.54
Average K_m	4.87 ± 0.70

Table 3.9 Summary of K_m plots for 3β-HSD.

3.43 Discussion

The average K_m value for 3β-HSD with the substrate DHEA using Sprague-Dawley testicular microsomes was found to be 4.76 ± 0.63μM, compared to K_m values obtained by other workers i.e., K_m = 0.71μM (Simard et al, 1993) and K_m = 420nM (Cooke and Robaire, 1986).

3.44 Preliminary Screening of Compounds for 3β-HSD Activity

The assay procedure for screening involved inhibitors and standards (baicalein and 7-hydroxyflavone) dissolved in absolute ethanol and diluted to give the required final incubation concentration. The assay was carried out (in triplicate) at 37°C in a shaking water bath. The total assay volume was 200μL. Prepared substrate DHEA (15μM/tube, 30μL), NADPH-generating system (10μL) and Inhibitor (100μM or 500μM, 20μL), in Tris-HCl buffer (136μL, pH8.4), were allowed to warm to 37°C. The testicular microsomes were thawed and warmed to 37°C before addition (0.23mg/mL final concentration, 4μL) to the assay mixture. The solutions were incubated for 40min at 37°C and the reaction was quenched by the addition of ether (2mL) and placed on ice. The assay was completed as previously described (Section 3.38). Control samples with no inhibitor were incubated simultaneously. The results were determined by using equation 2.1 to determine the percentage conversion of P and then comparing the conversion in the presence of inhibitors to that of the controls.

3.45 Results – Preliminary screening

The results are shown in Tables 3.10 – 3.12

3.45.1 Discussion

The compounds in general showed very poor potency or were inactive for this enzyme at both 100μM and 500μM inhibitor concentration.

Compound No.	Structure	% Inhibition
113 Baicalein	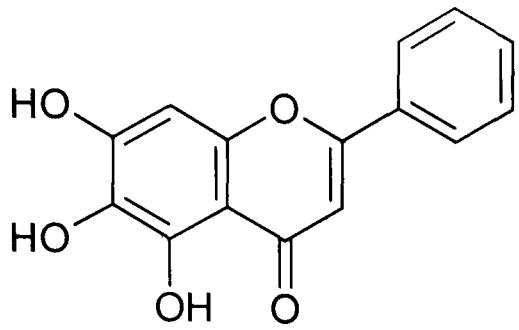	28.26 ± 0.79[a], 24.01 ± 2.44[b]
97 7-hydroxyflavone	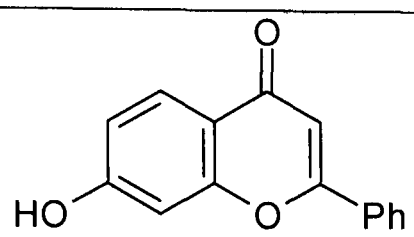	0[b]
247	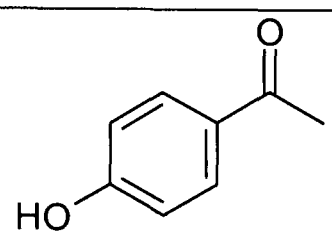	4.72 ± 1.10[b]
248	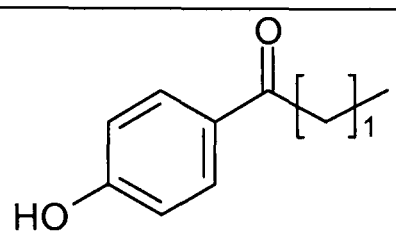	0[b]
249	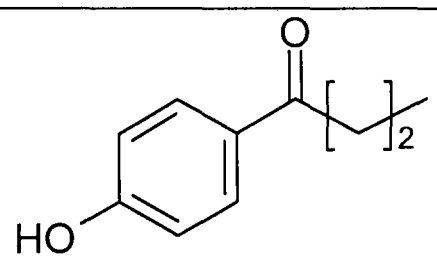	0[b]
250	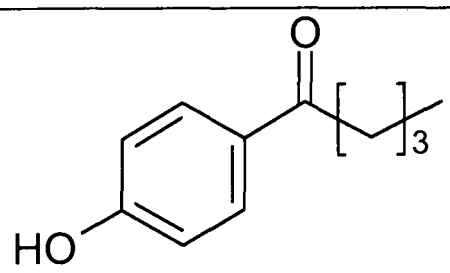	0[b]
251	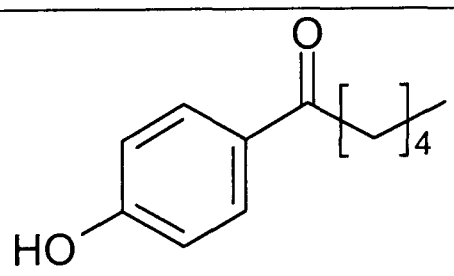	0[b]
252	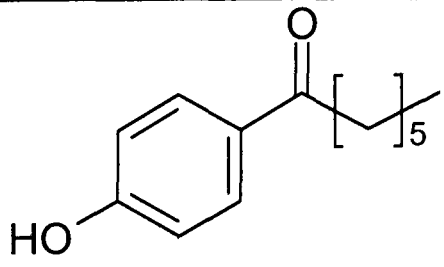	3.08 ± 1.02[b]

Table 3.10a Results from preliminary screening data of some 4-hydroxyphenyl ketones for 3β-HSD activity, (where [a][I]=100μM and [b][I]=500μM).

Compound No.	Structure	% Inhibition
253	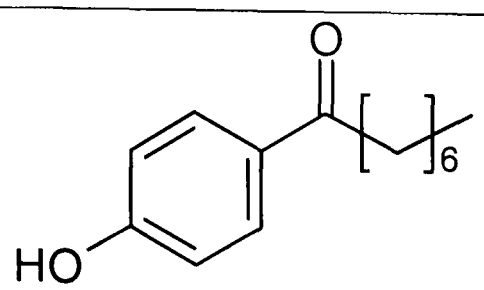	5.71 ± 0.30[b]
254	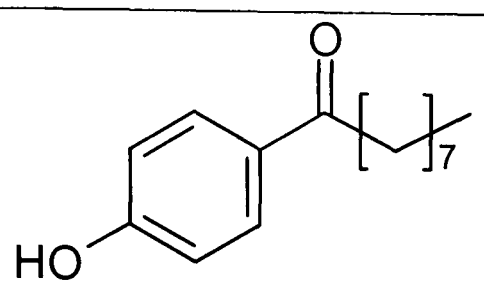	9.02 ± 0.41[b]
255	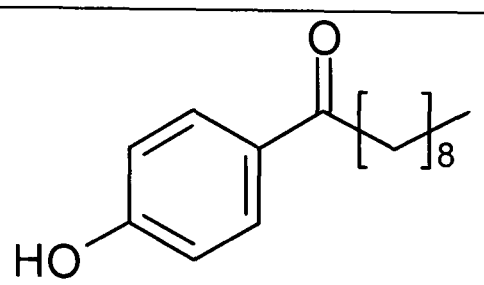	4.23 ± 0.59[a], 21.08 ± 2.08[b]
256	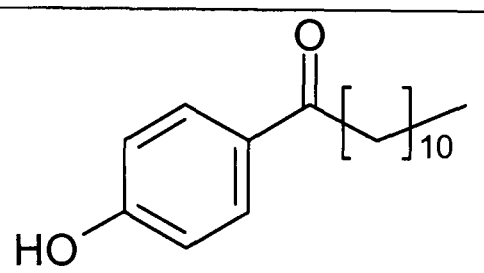	20.11 ± 0.73[a], 40.68 ± 1.09[b]
257	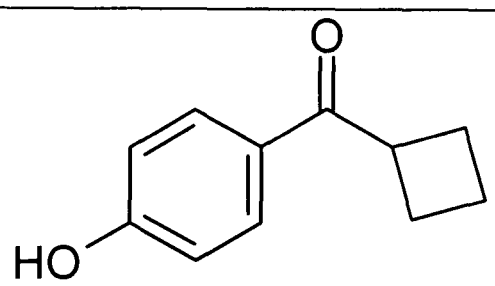	21.47 ± 1.17[b]
258	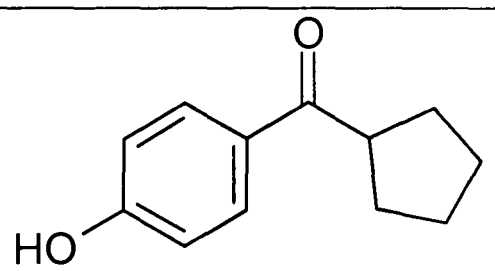	33.59 ± 1.03[b]
259	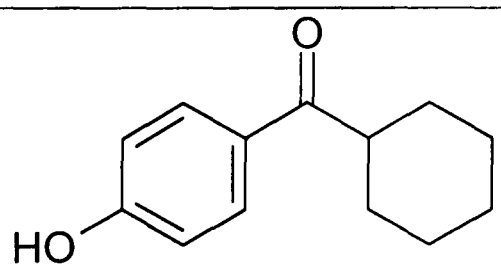	4.31 ± 2.35[a], 34.56 ± 1.26[b]
260	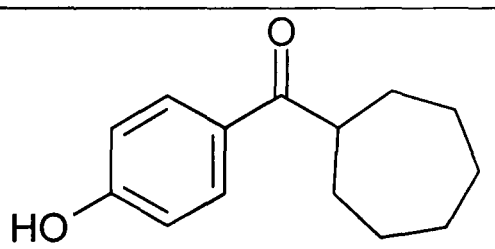	9.83 ± 1.43[a], 47.42 ± 0.47[b]

Table 3.10b Results from preliminary screening data of some 4-hydroxyphenyl ketones for 3β-HSD activity, (where [a][I]=100μM and [b][I]=500μM).

Compound No.	Structure	% Inhibition at 100μM	% Inhibition at 500μM
113 Baicalein	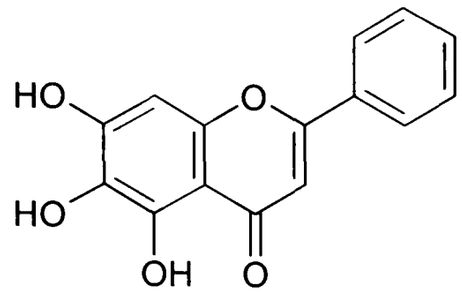	28.26 ± 0.79	24.01 ± 2.44
97 7-hydroxyflavone	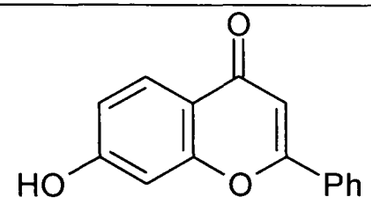	0	0
261	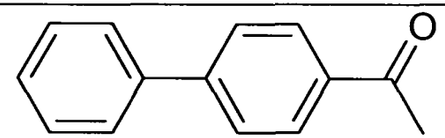	5.56 ± 0.08	12.91 ± 0.21
262	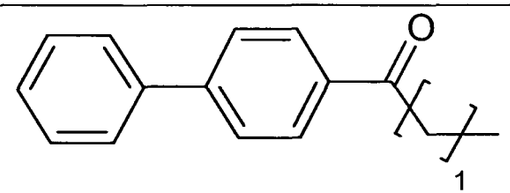	10.63 ± 0.70	5.35 ± 0.07
263	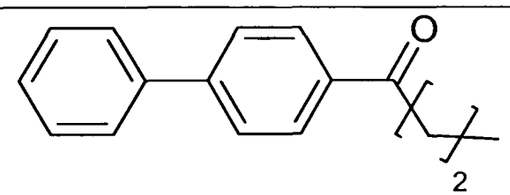	9.72 ± 0.03	12.40 ± 0.22

Table 3.11a Results from preliminary screening data of some biphenyl ketones for 3β-HSD activity.

Compound No.	Structure	% Inhibition at 100μM	% Inhibition at 500μM
264	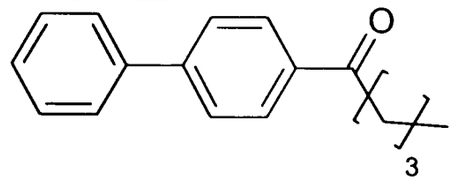	25.51 ± 0.08	10.33 ± 0.33
265	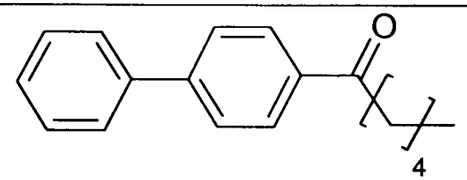	4.34 ± 0.95	24.10 ± 0.07
266	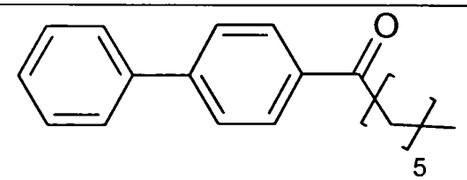	7.68 ± 0.78	22.97 ± 0.51
267	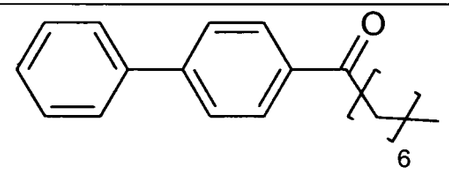	0	24.72 ± 0.97
268	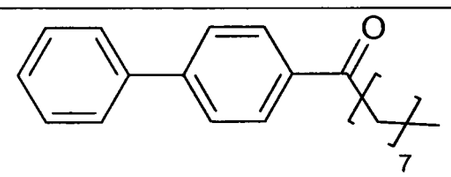	0	0
269	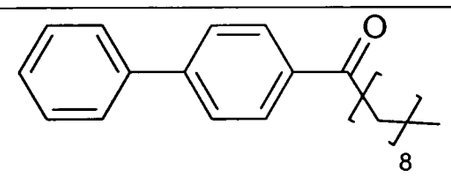	0	0

Table 3.11b Results from preliminary screening data of some biphenyl ketones for 3β-HSD activity.

Compound No.	Structure	% Inhibition at 100μM	% Inhibition at 500μM
270	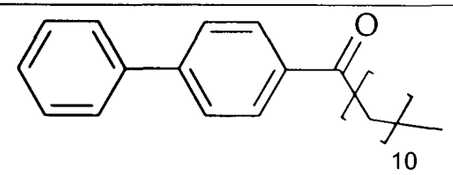	4.38 ± 0.63	0
271	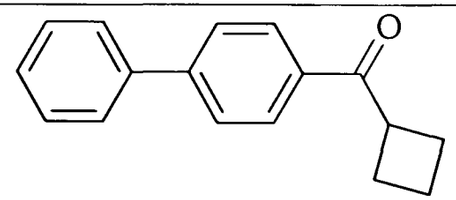	0	4.36 ± 0.68
272	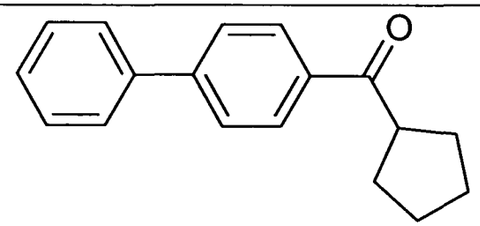	19.81 ± 0.76	23.38 ± 0.12
273	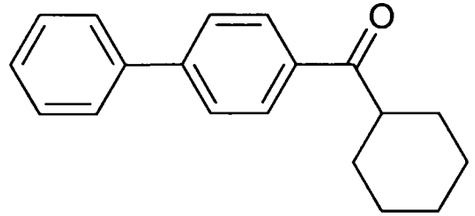	21.80 ± 0.26	22.37 ± 1.13

Table 3.11 Results from preliminary screening data of some biphenyl ketones for 3β-HSD activity.

Compound No.	Structure	% Inhibition at 100μM
113 Baicalein	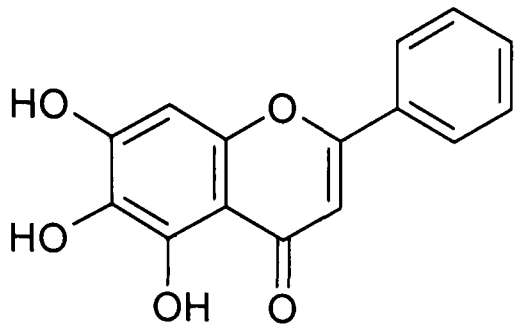	28.26 ± 0.79
97 7-hydroxyflavone	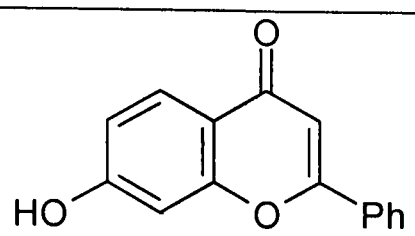	0
274	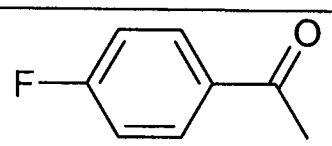	2.37 ± 1.12
275	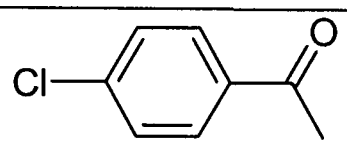	0
276	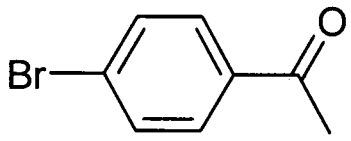	0
277	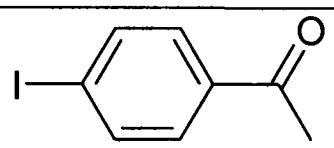	0
278	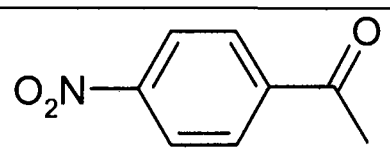	11.49 ± 0.61
279	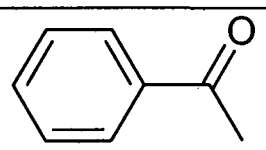	0
280	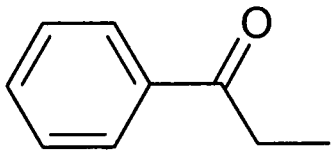	0
281	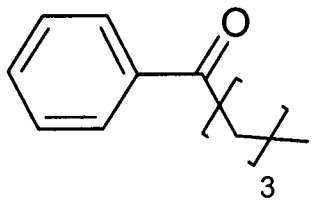	0
282	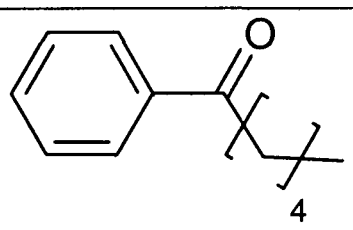	0

Table 3.12a Results from preliminary screening data of some commercially available compounds for 3β-HSD activity.

Compound No.	Structure	% Inhibition at 100μM
283	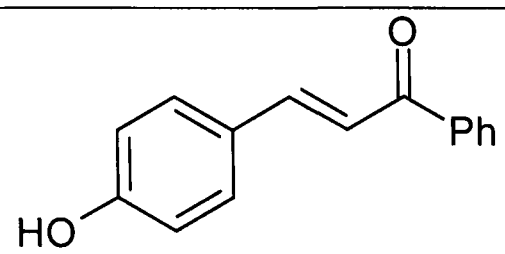	5.59 ± 2.11
284	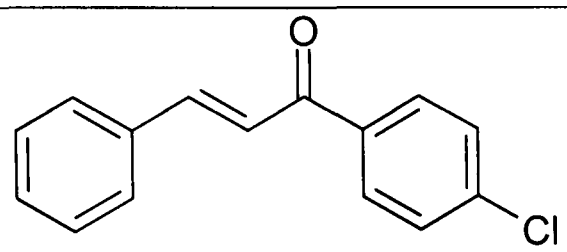	0
285	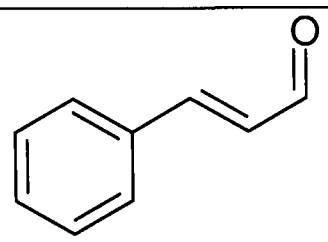	0
286	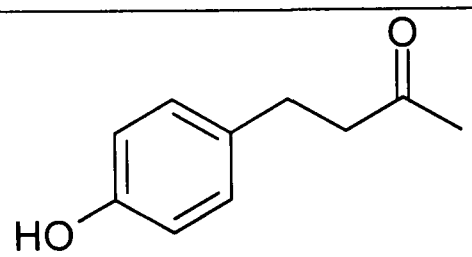	0
287	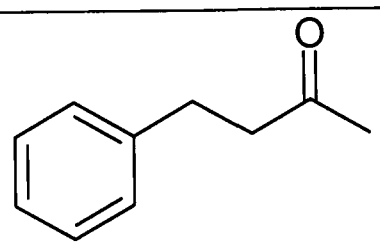	0

Table 3.12b Results from preliminary screening data of some commercially available compounds for 3β-HSD activity.

Chapter 4

4.0 DISCUSSION

4.1 Inhibition of $P450_{17\alpha}$

Consideration of the inhibitory activity possessed by the range of synthesised compounds considered within the current study shows that, in general, the azole-based inhibitors are more potent than the phenylamine-based compounds (the latter possessing very poor inhibitory activity even at [I]=100μM). Within the azole-based compounds, the imidazole-based inhibitors are more potent than the triazole-based compounds.

Furthermore, we observe that the inhibitory activity is strongly correlated with the ability of the ligating species to donate a lone pair of electrons. The weakest ligating group is the phenylamine and we observe that extremely weak binding amine group result in the inhibitors based on this functionality to possess the weakest inhibitory activity. The imidazole functionality, however, being a stronger base than either triazole or the phenylamine-based compounds, is able to donate its lone pair of electrons more readily, resulting in the increased inhibitory activity of the imidazole-based compounds. The lack of inhibition within the phenylamine based compounds is particularly surprising since inhibitors using the phenylamine functional group to bind to the haem whilst using a pyrrolidine-2,5-dione ring system to interact with the enzyme active site have previously shown some good inhibitory activity (Ahmed, 1990), the binding mode of these compounds have been rationalised previously using the substrate-haem complex approach (Ahmed and Davis, 1995; Ahmed and Keane, 1998). It should be noted that the substrate-haem complex approach was used as the start point for the design (by Professor Ahmed) of compounds based on the Evan's chiral auxiliary (Figure 4.1) and in the design of all of the compounds considered within this study - the development of the substrate-haem complex approach has been well documented and will not be discussed here.

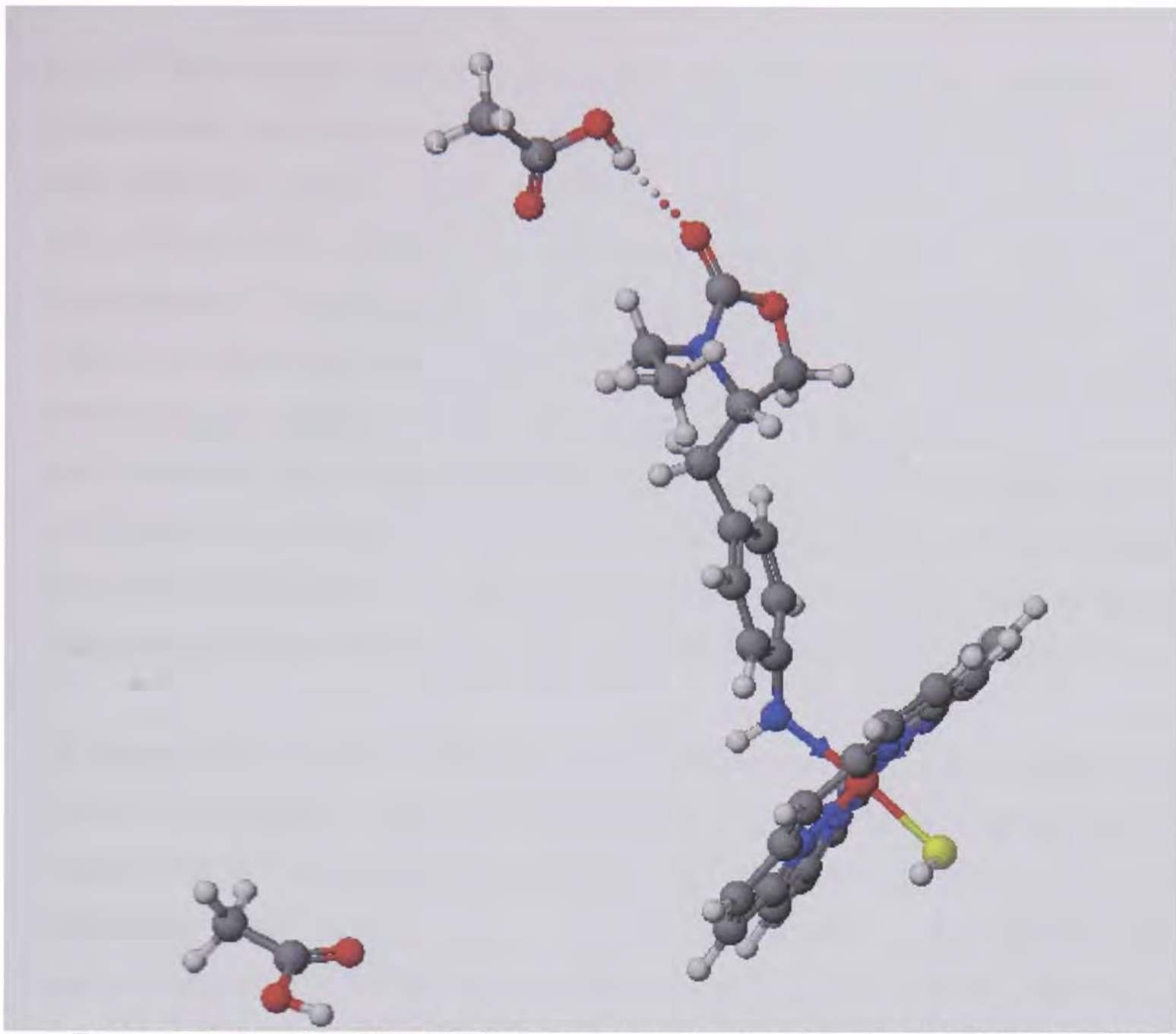

Figure 4.1 To show the binding of a phenylamine-based inhibitor within the overall representation of the 17α-hydroxylase/17,20-lyase active site.

A detailed consideration of the inhibitory data displayed by the synthesised azole-based inhibitors suggest that the inhibitory activity is related to the overall length of the alkyl chain (spacer) group, which separates the phenyl ring from the imidazole moiety. For example, from considering the inhibitory data for the non-substituted phenyl alkyl imidazoles, we observe that on going from the phenyl butyl imidazole (**167**) to the phenyl nonyl imidazole (**173**), there is a marked decrease in the IC_{50} value (against lyase) from 2.23±0.38μM to 0.35±0.01μM respectively – a less dramatic decrease is also observed when the IC_{50} values against 17α-hydroxylase for the same range of compounds is considered.

A similar trend is also observed for the 4-substituted phenyl alkyl azole-based compounds, that is, inhibitory data shows that compound **177**

(IC_{50}=1.96±0.01μM against lyase and IC_{50}=27.81±1.44μM against 17α-hydroxylase) possesses greatly reduced inhibitory activity compared to the corresponding larger alkyl chain inhibitors, such as compound **179** (IC_{50}=57.5±1.5nM against lyase and IC_{50}=173.62±7.00nM against 17α-hydroxylase). This increase in inhibitory activity with increasing length of the alkyl chain has been rationalised using the substrate-haem complex approach which suggests that the ability of the inhibitors to bind to the complex increases (and therefore the inhibitory activity) with the ability of the 4-substituted phenyl ring system to undergo more effective interaction(s) with appropriate amino acid group(s) at the active site, thereby leading to a more stable enzyme-inhibitor complex and thus resulting in potent inhibitory activity (Figures 4.2 and 4.3).

A similar trend is also observed within the series of compounds which do not contain a heteroatom within the phenyl ring system. That is, consideration of tables 2.3a to 2.3b shows us that there is an increase in inhibitory activity with increasing alkyl chain length. Due to the lack of a heteroatom, these compounds would not be expected to undergo any polar-polar interaction(s) postulated for the 4-substituted inhibitors. A detailed consideration of the non-substituted compounds together with their physicochemical properties, in particular, logP, shows that a non-linear correlation appears to exist between the hydrophobicity of the inhibitors and the observed inhibitory activity (Figure 4.4). Although, the increasing inhibitory activity with increasing alkyl chain length within the non-substituted azoles may initially appear to weaken the hypothesis used to rationalise the inhibitory activity observed within the 4-substituted compounds above, we suggest that the correlation observed between the inhibitory activity of the non-substituted compounds and their physicochemical properties suggests that other parameters play a major role in determining the overall inhibitory activity of this enzyme.

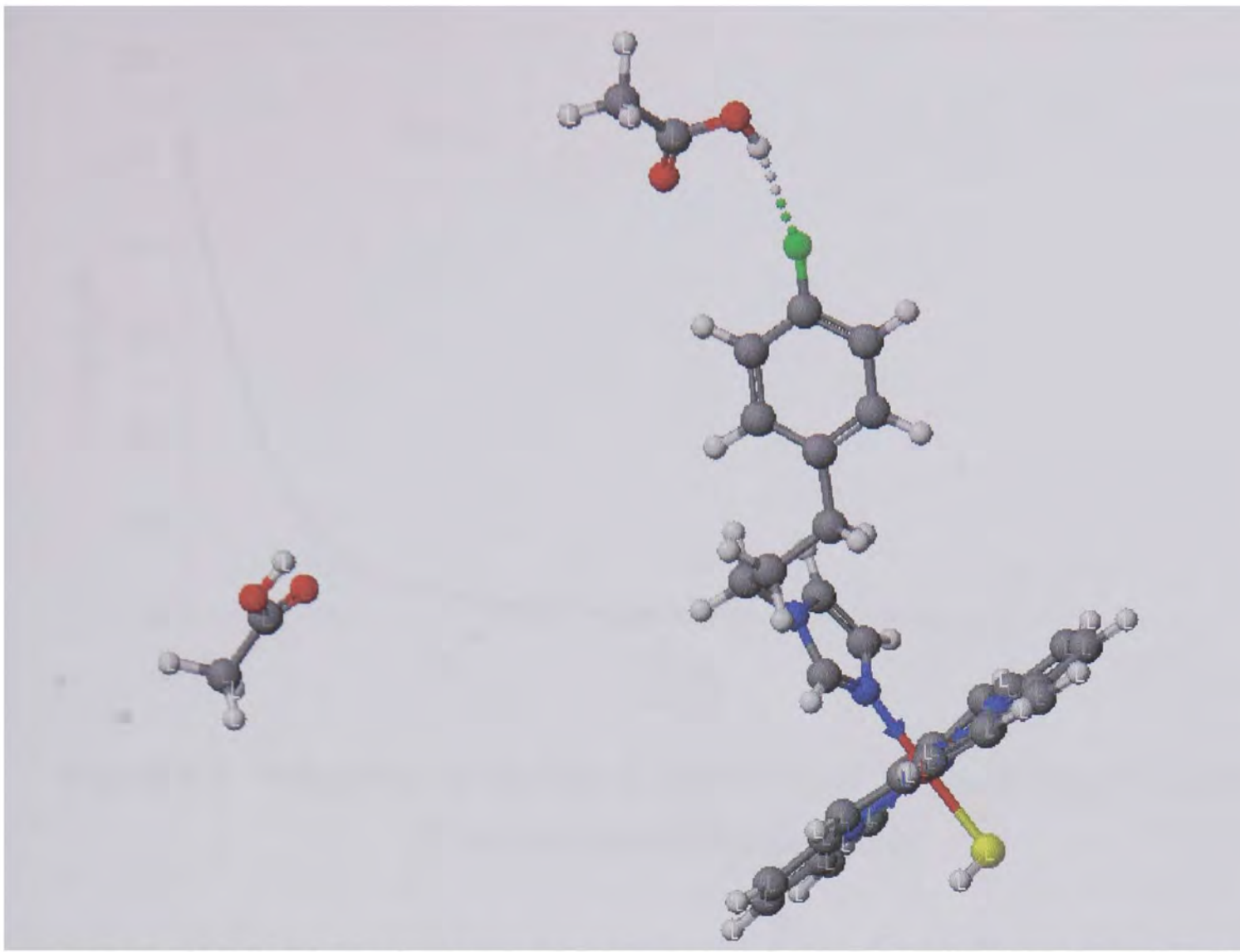

Figure 4.2 To show the binding of compound **177** bound within the overall representation of the 17α-hydroxylase/17,20-lyase active site.

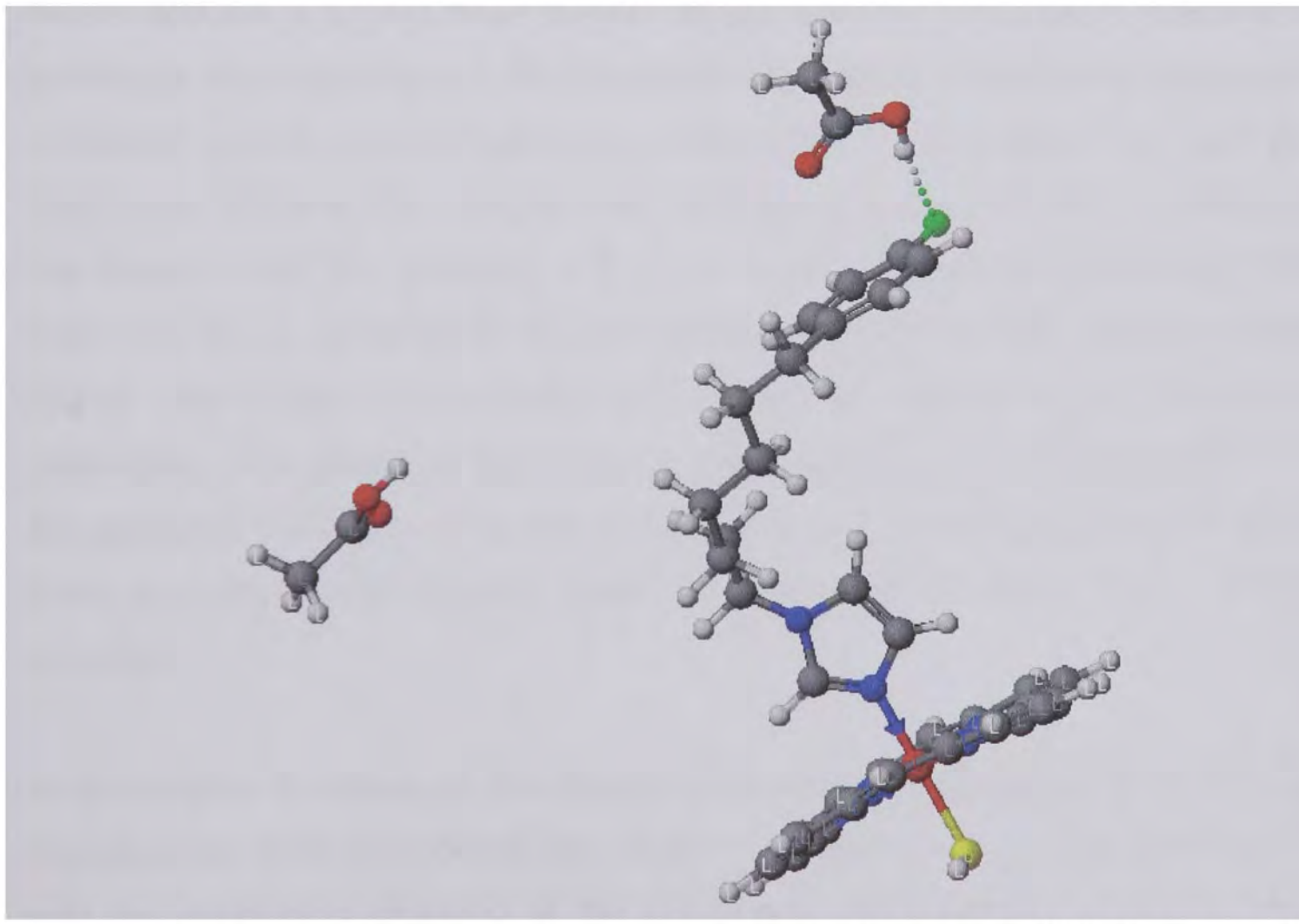

Figure 4.3 To show the binding of compound **179** bound within the overall representation of the 17α-hytdroxylase/17,20-lyase active site.

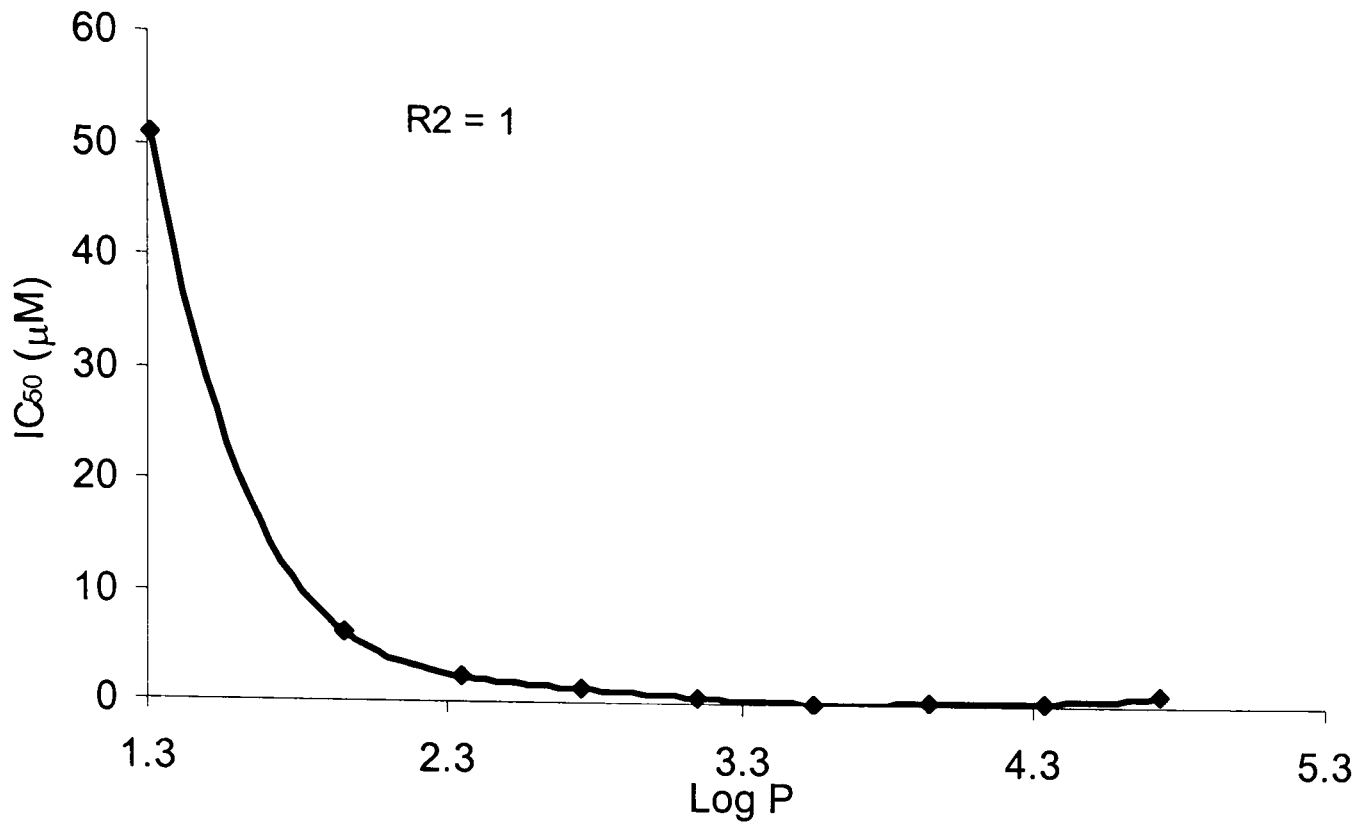

Figure 4.4. Polynomial (n=6) plot of LogP versus IC_{50} values (against lyase) for the non-substituted imidazole

Another trend which is observed is the effect of the substitution on the inhibitory activity of the compounds. For example, consider the range of compounds which contain a pentyl alkyl spacer group between the phenyl ring and the imidazole ring systems and the observed IC_{50} values. Detailed consideration of inhibitory activity shows that these compounds depend upon the polar-polar interaction between the inhibitor and the enzyme active site wall. Furthermore, we observe that the inhibitory activity of these compounds increase on going from the fluoro substituted (which possesses the weakest inhibitory activity within the range of 4-substituted derivatives considered) to the bromo derivative. We postulate that the observed structure-activity relationship may be related to the ability of the heteroatom to 'donate' electrons, as such, fluorine being a highly electronegative atom does not share its electrons as readily as bromine.

In conclusion therefore, in the design of further novel inhibitors of $P450_{17\alpha}$, two factors need to be considered: the ability of a polar group to undergo interaction with corresponding group(s) at the active site (for example, a halogen group such as a bromine atom); and a logP factor, which would appear to aid the stabilisation of the inhibitor-enzyme complex. These two factors are clearly

present in steroidal inhibitors which are able to ligate to the haem iron atom through the formation of a dative covalent bond, as such, these compounds possess highly potent inhibitory activity in comparison to the non-steroidal inhibitors considered here.

4.2 Inhibition of isozymes of 17β-HSD

As previously mentioned, due to a lack of compounds in the clinic for 17β-HSD, it was not possible to compare the biological activity (and therefore relative potency) of the synthesised compounds within the current study against a single and well defined standard compound. However, a number of workers within the field have previously undertaken biochemical evaluation of flavonoid-based compounds, in particular, Baicalein (**113**) and 7-hydroxyflavone (**97**). We have therefore also evaluated our novel inhibitors using these two compounds for comparison.

17β-HSD3

In general, the results of the study shows that the 4-hydroxyphenyl ketone-based compounds are potent inhibitors of 17β-HSD3, with only two inhibitors showing poor inhibitory activity and IC_{50} values. Detailed consideration of the inhibitory activity shows that compounds **254** (IC_{50}=2.86μM) and **255** (IC_{50}=4.97μM) are highly potent inhibitors of this isozyme of 17β-HSD. As such, **254** is some 65 and 23 times more potent than Baicalein (IC_{50}=185.92μM) and 7-hydroxyflavone (IC_{50}=66.98μM) respectively. Compounds **252** (IC_{50}=7.84μM), **253** (IC_{50}=6.52μM) and **256** (IC_{50}=7.55μM) have also been shown to be extremely good inhibitors in comparison to the two standard compounds.

A detailed consideration of the inhibitory activity observed within this series of compounds show that the potency of the compounds appear to increase with increasing alkyl chain length and therefore the logarithm of the calculated partition coefficient (logP). A plot of logP (calculated using Quantum CaChe

Project Leader) versus IC_{50} shows a very good correlation (R^2=0.95) (Figure 4.5), with an optimum logP of approximately 3.8 and 4.3, corresponding to compound **254**.

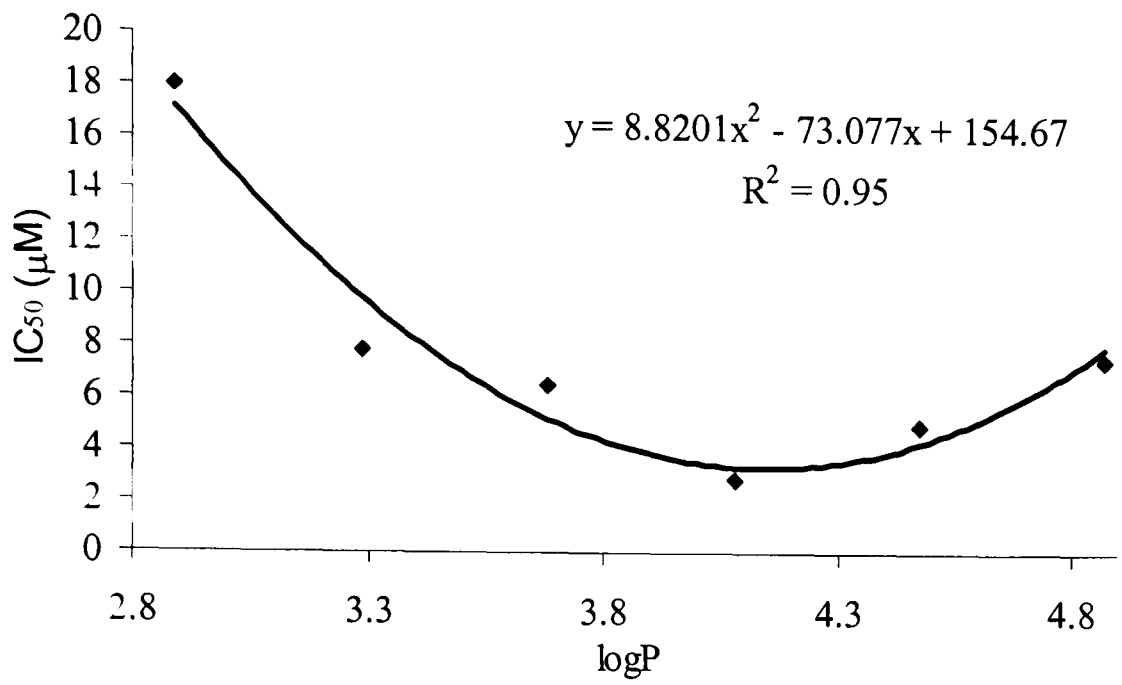

Figure 4.5. Plot of IC_{50} versus calculated logP for a small range of the compounds (carbon chain length from 5 to 10) synthesised within the current study (Lota et al, 2006).

Molecular modelling of these compounds were undertaken (by Professor Ahmed) which suggested that the 4-hydroxyphenyl ketone-based inhibitors may possess two modes of binding to the active when compared to the steroid backbone. That is, the inhibitors are presumed to bind to the active site such that the carbonyl moiety within the inhibitor mimics the C(17)=O of the substrate, however, in one scenario the alkyl chain extends towards the area of space normally occupied by the rings A, B and C of the steroid substrate, placing the 4-hydroxyphenyl moiety beyond the (C15) and C(16) position of the steroid backbone (Figure 4.6a). The alternative mode of superimpositioning involves the 4-hydroxyphenyl being positioned towards the steroid backbone whilst the alkyl chain is now positioned such that it extends far beyond the D-ring (Figure 4.6b).

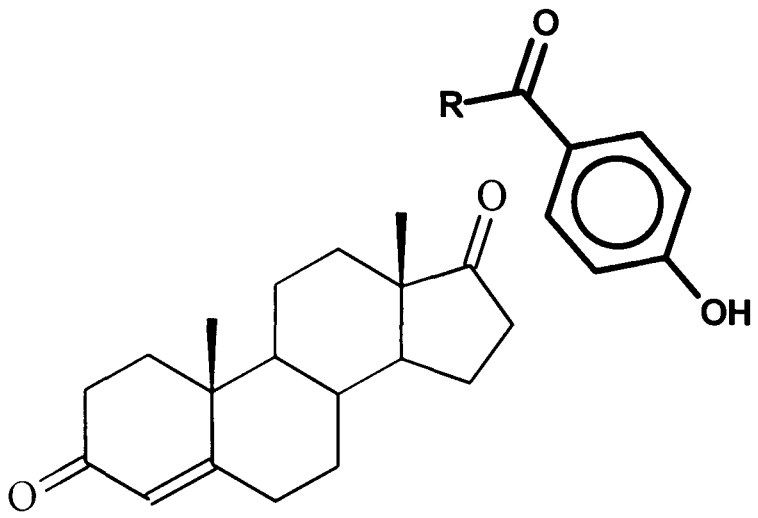

Figure 4.6a. Superimposing of novel inhibitor onto the backbone of A

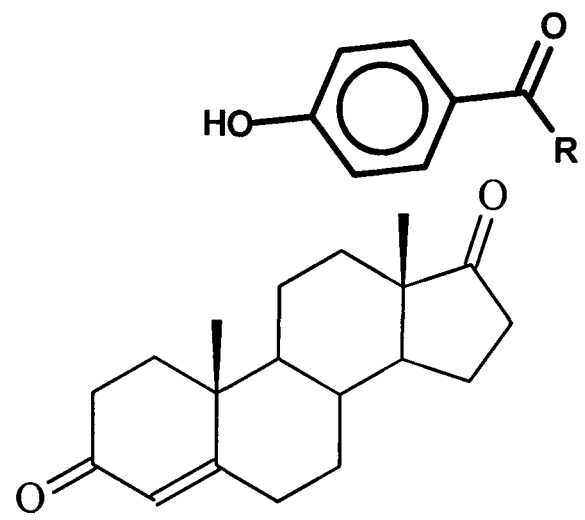

Figure 4.6b Alternative mode of superimposing of novel inhibitor onto the backbone of A

Owen and Ahmed (2004) have previously suggested that the area of the enzyme active site corresponding to the D-ring of the natural substrate may be populated with hydrogen donor and bonding groups as well as NADPH. This area of the active site would therefore be expected to be constrained and the volume of space available for the acyl chains to be restricted, in particular for the larger alkyl chain containing compunds. As such, binding in such a manner where the alkyl chain extends out beyond the D-ring as suggested by Figure 4.6b is highly unlikely due to steric interactions which would therefore lead to reduced inhibitory activity. We therefore suggest that the mode of binding suggested in Figure 4.6a is more preferable and is the mode of binding for the majority of the compounds – Figure 4.7 shows the binding of one of the inhibitors in such a manner whilst Figure 4.8 shows the alternative mode of binding which is suggested to be undertaken by the small alkyl chain containing compounds. Furthermore, from the consideration of the potency of the larger alkyl chain containing compounds, we suggest that the 4-hydroxyphenyl moiety may be involved in hydrogen bonding interactions with the active site about the C(15) and C(16) area of the steroid backbone and which would result in stronger binding and therefore increased inhibitory activity.

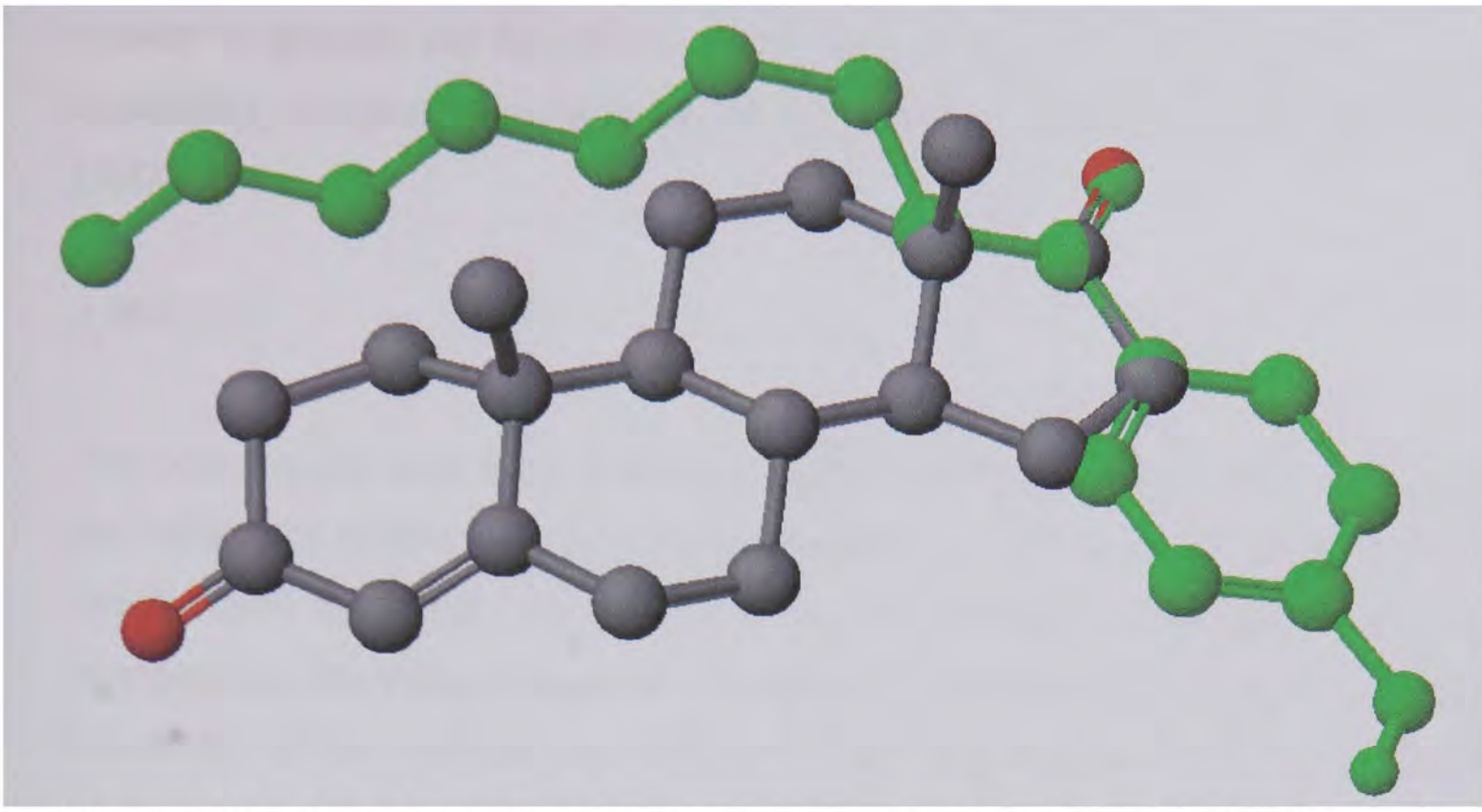

Figure 4.7. Superimpositioning of a low energy conformer of **254** (in ball and stick representation) onto the backbone of A (Lota et al, 2006).

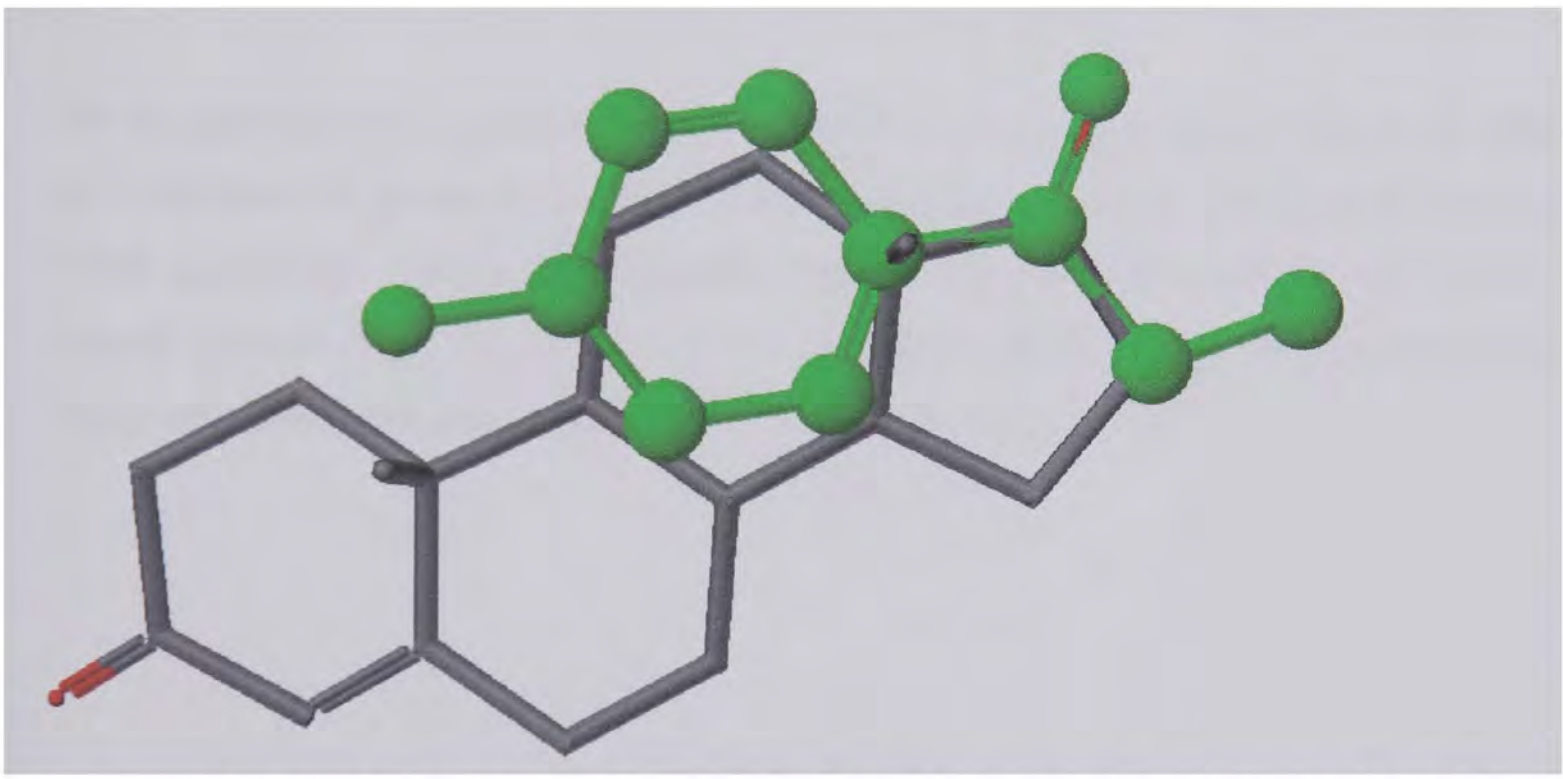

Figure 4.8. Superimpositioning of **248** (in ball and stick representation) onto the backbone of A (Lota et al, 2006).

That the 4-hydroxy moiety is able to undergo this favourable hydrogen bonding interaction, resulting in the increased potent inhibitory activity observed within the larger inhibitors of 17β-HSD3, is supported by the observation that when compounds lacking hydrogen bonding groups are evaluated against this enzyme they showed poor inhibitory activity. That is, the poor inhibitory activity

observed within the biphenyl and non-hydroxy containing compounds would appear to support our hypothesis regarding the ability of the larger alkyl chain containing compounds to hydrogen bond to groups within the active site of 17β-HSD3.

17β-HSD1

The compounds were also evaluated against 17β-HSD1 in an effort to evaluate the selectivity of the 4-hydroxyphenyl ketones. From the consideration of the results (and the small range of isozymes considered), we observe that these compounds are indeed selective inhibitors of the 17β-HSD family of enzymes. However, of the compounds evaluated, only the biphenyl-based compounds showed any level of potency against this isozyme.

3β-HSD

All the compounds synthesised were also evaluated against 3β-HSD in an effort to evaluate the general potency of the comounds against the overall family of HSD enzymes. From the consideration of the inhibitory activity obtained, it would appear that, in general, all of the compounds are non-inhibitors of 3β-HSD and therefore would appear to be specific inhibitors of 17β-HSD3.

Chapter 5

5.0 REFERENCES

A

Ahmed, S., Synthesis and Evaluation of Inhibitors of 17α-Hydroxylase/17,20-Lyase as Potential Anti-tumour Agents, University of Wales College of Cardiff, 1990.

Ahmed, S. and Davis, P. J., The mechanism of aromatase — a molecular modelling perspective, Bioorg. Med. Chem. Lett., 1995, 5, 2789-2794.

Ahmed, S., Smith, J. H., Nicholls, P. J., Whomsley, R. and Cariuk, P., Synthesis and biological evaluation of imidazole based compounds as cytochrome P-450 inhibitors, Drug Des. Discovery, 1995, 13, 27-41.

Ahmed, S., A novel molecular modelling study of Inhibitors of the 17α-Hydroxylase component of the enzyme system 17α-Hydroxylase/17,20-Lyase ($P\text{-}450_{17\alpha}$), Bioorg. Med. Chem., 7, 1999, 1487-1496.

Ahmed, S. and Keane, J., Modeling Study of Some Inhibitors of 17,20-Lyase, a Component of the Enzyme 17α-Hydroxylase/17,20-Lyase: A Novel Approach, Biochem. Biophys. Res. Comm., 1998, 253, 273–276.

Akhtar, M., LeeRobichaud, P., Akhtar, M. E. and Wright, J. N., The impact of aromatase mechanism on other P450s, J. Steroid Biochem. Mol. Biol., 1997, 61, 127-132.

Allsbrook, W. C. Jr, and Simms W. W., 1992, Histochemistry of the prostate, Hum. Pathol., 1992, 23, 297-305.

Angelastro, M. R., Laughlin, M. E., Schatzman, G. L., Bey, P. and Blohm, T. R., 17β-(cyclopropylamino)-androst-5-en-3β-ol, a selective mechanism-

based inhibitor of cytochrome P450(17α) (steroid 17α-hydroxylase/C17-20 lyase), Biochem. Biophys. Res. Commun., 1989, 162,1571-1577.

Arrighi, H. M., Metter, E. J., Guess, H. A. and Fozzard, J. L., Natural-history of benign prostatic hyperplasia and risk of prostatectomy – the Baltimore longitudinal-study of aging, Urology, 1991, 38 (supplement), 4-8.

Auzeby, A., Bogdan, A. and Touitou, Y., An alternate pathway to androstenedione synthesis by human adrenals: evidence of a balance in 11β-hydroxylase and 17,20-lyase activities leading to androstenedione, J. Clin. Endocrinol. Metab., 1995, 80, 1706-1711.

Ayub, M. and Levell, M. J., Inhibition of testicular 17α-hydroxylase and 17,20-lyase but not 3β-hydroxysteroid dehydrogenase-isomerase or 17β-hydroxysteroid oxidoreductase by ketoconazole and other imidazole drugs, J. Steroid Biochem., 1987a, 28, 521-531.

Ayub, M. and Levell, M. J., Inhibition of rat testicular 17α-hydroxylase and 17,20-lyase activities by anti-androgens (flutamide, hydroxyflutamide, ru23908, cyproterone acetate) in vitro, J. Steroid Biochem., 1987b, 28, 43-47.

B

Barrie, S. E., Rowlands, M. G., Foster, A. B. and Jarman, M., Inhibition of 17α-hydroxylase/C17,20 lyase by bifluranol and its analogues, J. Steroid Biochem., 1989, 33, 1191-1195.

Barrie, S. E. and Jarman, M., Inhibitors of cytochrome P450(17α) (17α-hydroxylase/C17,20 lyase), Endocr.-Relat. Cancer, 1996, 3, 25-39.

Barrie, S. E., Haynes, B. P., Potter, G. A., Chan, F. C. Y., Goddard, P. M., Dowsett, M. and Jarman, M., Biochemistry and pharmacokinetics of potent

non-steroidal cytochrome $P450_{17\alpha}$ inhibitors, J. Steroid Biochem. Mol. Biol., 1997, 60, 347-351.

Betz, G. and Michels, D., Steroid 17,20-lyase: The effect of detergents on enzymatic activity and microsomal composition, Steroids, 1973, 21, 785-800.

Bratoeff, E., Ramírez, E., Murillo, E., Flores, G. and Cabeza, M., Steroidal Antiandrogens and 5α-Reductase Inhibitors, Curr. Med. Chem., 1999, 6, 1107-1123.

C

Cairns, P., Okami, K., Halachmi, N., Esteller, M., Herman, J. G., Jen, J., Isaacs, W. B., Bova, G. S., and Sidransky, D., Frequent inactivation of PTEN/MMAC1 in primary prostate cancer, Cancer Res., 1997, 57, 4997-5000.

Catalona, W. J., Scott, W. W., Walsh, P. C., Gittes, R. F., Perlmuter, A. D., Stamley, T. A., In Campbell's Urology ; 5th edition ; W.B. Saunders Co. , Philadelphia, 1986, 1463.

Chabre, O., Defaye, G. and Chambaz, E. M., Oxygen availability as a regulatory factor of androgen synthesis by adrenocortical cells, Endocrinology, 1993, 132, 255-260.

Chan, F. C. Y., Potter, G. A., Barrie, S. E., Haynes, B. P., Rowlands, M. G., Houghton, J. and Jarman, M., 3- and 4-Pyridylalkyl Adamantanecarboxylates: Inhibitors of Human Cytochrome $P450_{17\alpha}$ (17α-Hydroxylase/$C_{17,20}$-Lyase). Potential Nonsteroidal Agents for the Treatment of Prostatic Cancer, J. Med. Chem., 1996b, 39, 3319-3323.

Chan, J. M., Stampfer, M. J., Ma, J., Gann, P. H., Gaziano, J. M. and Giovannucci, E. L., Dairy products, calcium, and prostate cancer risk in the Physicians' Health Study, Am. J. Clin. Nutr., 2001, 74, 549-554.

Chang, B., Zheng, S. L., Hawkins, G. A., Isaacs, S. D., Wiley, K. E., Turner, A., Carpten, J. D., Bleecker, E. R., Walsh, P. C., Trent, J. M., Meyers, D. A., Isaacs, W. B. and Xu, J., Polymorphic GGC repeats in the androgen receptor gene are associated with hereditary and sporadic prostate cancer risk, Hum. Genet., 2002, 110, 122-129.

Chasalow, F. I., Marr, H. and Taylor, G., A new assay and solubilization procedure for steroid 17,20-lyase from rat testes, Steroids, 1982, 39, 617-630.

Chen, L., Stacewicz-Sapuntzakis, M., Duncan, C., Sharifi, R., Ghosh, L., van Breemen, R., Ashton, D. and Bowen, P. E., Oxidative DNA Damage in Prostate Cancer Patients Consuming Tomato Sauce-Based Entrees as a Whole-Food Intervention, J. Natl. Cancer Inst., 2001, 93, 1872-1879.

Chung, L. W., Gleave, M. E., Hsieh, J. T., Hong, S. J. and Zhau, H. E., Reciprocal mesenchymal-epithelial interaction affecting prostate tumor growth and hormonal responsiveness, Cancer Surv., 1991, 11, 91-121.

Cooke, G. M. and Robaire, B., The effect of diethyl-4-methyl-3-oxo-4-aza-5α-androstane-17β-carboxamide (4-MA) and (4R)-5,10-seco-19-norpregna-4,5-diene-3,10,20-trione (SECO) on androgen biosynthesis in the rat testis and epididmis, J. Steroid Biochem., 1986, 24, 877-886.

Cooke, G. M., Price, C. A. and Oko, R. J., Effects of *in utero* and lactational exposure to 2,3,7,8-tetrachlorodibenzo-*p*-dioxin (TCDD) on serum androgens and steroidogenic enzyme activities in the male rat reproductive tract, J. Steroid Biochem. Mol. Biol., 1998, 67, 347-354.

Crawford, E. D., Epidemiology of prostate cancer, Urology, 2003, 62, 3-12.

Cunha, G. R., Chung, L. W. K., Sannon, J. M., Taguihi, O., Fujii, H., Hormone induced morphogenesis and growth: role of mesenchymal interactions, Recent Prog. Horm. Res., 1983, 39, 559-598.

D

Dalla Valle, L., Ramina, A., Vianello, S., Belvedere, P. and Colombo, L., Kinetic analysis of duodenal and testicular cytochrome P450c17 in the rat., J. Steroid Biochem. Mol. Biol., 1996, 58, 577-584.

Denis, L. and Mahler, C., Prostatic-cancer-An overview, Acta Oncol., 1990, 29, 665-677.

Duffield-Lillico, A. J., Dalkin, B. L., Reid, M. E., Turnbull, B. W., Slate, E. H., Jacobs, E. T., Marshall, J. R. and Clark, L. C., Selenium supplementation, baseline plasma selenium status and incidence of prostate cancer: an analysis of the complete treatment period of the Nutritional Prevention of Cancer Trial, BJU Int., 2003, 91, 608-612.

E

Eales, L. -J., Immunology for life scientists: A basic introduction, 215, 1997, John Wiley & Sons, Chichester.

Egawa, T., Ogura, T., Makino, R., Ishimura, Y. and Kitagawa, T., Observation of the O-O stretching Raman band for cytochrome P-450cam under catalytic conditions, J. Biol. Chem., 1991, 266, 10246-10248.

Eisenthal, R. and Cornish-Bowden, A., The direct linear plot – A new graphical procedure for estimating enzyme kinetic parameters, Biochem. J., 1974, 139, 715-720.

F

Fink, B. E., Gavai, A. V., Tokarski, J. S., Goyal, B., Misra, R., Xiao, H. -Y., Kimball, S. D., Han, W. -C., Norris, D., Spires, T. E., You, D., Gottardis, M. M., Lorenzi, M. V. and Vite, G. D., Identification of a novel series of tetrahydrodibenzazocines as inhibitors of 17β-hydroxysteroid dehydrogenase type 3, Bioorg. Med. Chem. Lett., 2006, 16, 1532-1536.

Frye, S. V., Inhibitors of 5α-reductase, Curr. Pharm. Design, 1996, 2, 59-84.

G

Gann, P. H., Hennekens, C. H., Sacks, F. M., Grodstein, F., Giovannucci, E. L. and Stampfer, M. J., Prospective study of plasma fatty acids and risk of prostate cancer., J. Natl. Cancer Inst., 1994, 86, 281–286.

Garsky, V. M., Lumma, P. K., Feng, D. M., Wai, J., Ramjit, H. G., Sardana, M. K., Oliff, A., Jones, R. E., DeFeo-Jones, D. and Freidinger, R. M., The Synthesis of a Prodrug of Doxorubicin Designed to Provide Reduced Systemic Toxicity and Greater Target Efficacy, J. Med. Chem., 2001, 44, 4216-4224.

Geller, J., Basis for hormonal management of advanced prostate-cancer, Cancer, 1993, 3 (supplement), 1039-1045.

Georgiou, M., Perkins, L. M. and Payne, A. H., Steroid synthesis-dependent, oxygen-mediated damage of mitochondrial and microsomal cytochrome P-450 enzymes in rat Leydig cell cultures, Endocrinology, 1987, 121, 1390-1399.

Gibson, G. and Skett, P. (1994), Techniques and experiments illustrating drug metabolism, in Introduction to Drug Metabolism (Gibson G and Skett P eds) pp 220-221, Blackie Academic and Professional, London.

Giovannucci, E., Rimm, E. B., Colditz, G. A., Stampher, M. J., Ascherio, A., Chute, C. C. and Willett, W. C., A prospective study of dietary fat and risk of prostate cancer. J. Natl. Cancer. Inst., 1993, 85, 1571–1579.

Giovannucci, E., Rimm, E. B., Liu, Y., Stampfer, M. J. and Willett, W. C., A prospective study of tomato products, lycopene, and prostate cancer risk. J Natl. Cancer Inst., 2002 94, 391–398.

Gobec, S., Sova, M., Kristan, K. and Rižner, T. L., Cinnamic acid esters as potent inhibitors of fungal 17β-hydroxysteroid dehydrogenase—a model enzyme of the short-chain dehydrogenase/reductase superfamily, Bioorg. Med. Chem. Lett., 2004, 14, 3933-3936.

Gormley, G. J., 5α-reductase inhibitors in prostate cancer, Endocr.-Relat. Cancer, 1996, 3, 57-63.

Gregory, C. W., He, B., Johnson, R. T., Ford, O. H., Mohler, J. L., French, F. S., Wilson, E. M., A Mechanism for Androgen Receptor-mediated Prostate Cancer Recurrence after Androgen Deprivation Therapy, Cancer Res., 2001, 61, 4315-4319.

H

Hall, P. F., Cytochromes P-450 and the regulation of steroid synthesis, Steroids, 1986, 48, 131-196.

Hartmann, R. W., Hector, M., Haidar, S., Ehmer, P. B., Reichert, W. and Jose, J., Synthesis and evaluation of novel steroidal oxime inhibitors of P450 17 (17α-Hydroxylase/C17-20-Lyase) and 5α-Reductase types1 and 2, J. Med. Chem., 2000, 43, 4266-4277.

Harvei, S., Bjerve, K. S., Tretli, S., Jellum, E., Robsahm, T. E. and Vatten, L., Prediagnostic level of fatty acids in serum phospholipids: omega-3 and

omega-6 fatty acids and the risk of prostate cancer., Int. J. Cancer, 1997, 71, 545-551.

Huggins, C. and Hodges C. V., Studies on prostatic cancer. I. The effect of castration, of estrogen and androgen injection on serum phosphatases in metastatic carcinoma of the prostate, Cancer Res., 1941, 1, 293-297.

Hyytinen, E. -R., Thalmann, G. N., Zhau, H. E., Karhu, R., Kallioniemi, O. -P., Chung, L. W. K. and Visakorpi, T., Genetic changes associated with the acquisition of androgen-independent growth, tumorigenicity and metastatic potential in a prostate cancer model., Br. J. Cancer, 1997, 75, 190-195.

I

Ideyama, Y., Kudoh, M., Tanimoto, K., Susaki, K., Nanya, T., Nakahara, T., Ishikawa, H., Fujikura, T., Akaza, H. and Shikama, H., YM116, 2-(1H-Imidazol-4-ylmethyl)-9H-carbazole, Decreases Adrenal Androgen Synthesis by Inhibiting C17-20 Lyase Activity in NCI-H295 Human Adrenocortical Carcinoma Cells, Japan. J. Pharmacol., 1999, 79, 213-220.

Imperato-McGinley, J., Guerrero, L., Gautier, T. and Peterson, R. E., Steroid 5α-reductase deficiency in man: an inherited form of male pseudohermaphroditism, Science, 1974, 186, 1213-1215.

Isaacs, J. T., Importance of the natural-history of benign prostatic hyperplasia in the evaluation of pharmacologic intervention, Prostate, 1990, 3 (supplement), 1-7.

J

Jarman, M., Smith, H. J., Nicholls, P. J. and Simons, C., Inhibitors of enzymes of androgen biosynthesis: cytochrome $P450_{17\alpha}$ and 5α-steroid reductase, Nat. Prod. Rep., 1998, 15, 495-512.

K

Kim, I. Y., Seong, D. W., Kim, B. C., Lee, D. K., Remaley, A. T., Leach, F., Morton, R. A. and Kim, S. J., Raloxifene, a Selective Estrogen Receptor Modulator, Induces Apoptosis in Androgen-responsive Human Prostate Cancer Cell Line LNCaP through an Androgen-independent Pathway, Cancer Res., 2002, 62, 3649-3653.

Kondo, Y., Homma, Y., Aso, Y. and Kakizoe, T., Promotional effect of two-generation exposure to a high-fat diet on prostate carcinogenesis in ACI/Seg rats., Cancer Res., 1994, 54, 6129–6132.

Kristan, K., Starčević, S., Brunskole, M., Rižner, T. L. and Gobec, S., Cinnamates and cinnamamides inhibit fungal 17β-hydroxysteroid dehydrogenase, Molecular and Cellular Endocrinology, 2006, 248, 239-241.

Kühn-velten, N. and Staib, W., Distribution of progesterone-binding cytochrome P450 and steroid-17α-hydroxylase/C-17,20-lyase within different compartments of the rat testis, FEBS Lett., 1983, 154, 70-74.

L

Labrie, F., Dupont, A., Belanger, A., Lacoursiere, Y., Raynaud, J. P., Husson, J. M., Gareau, J., Fazekas, A. T. A., Sandow, J., Monfette, G., Girard, J. G., Emond, J. and Houle, J. G., New approach in the treatment of prostate cancer: complete instead of partial withdrawal of androgens, Prostate, 1983, 4, 579–594.

Laitinen, S., Karhu, R., Sawyers, C. L., Vessella, R. L. and Visakorpi, T., Chromosomal Aberrations in Prostate Cancer Xenografts Detected by

Comparative Genomic Hybridization, Gene. Chromosome. Canc., 2002, 35, 66–73.

Landis, S. H., Murray, T., Bolden, S. and Wingo, P. A., Cancer statistics, 1999, CA-A Cancer J. Clin., 1999, 49, 8-31.

Laughton, C. A., McKenna, R., Neidle, S., Jarman, M., McCague, R. and Rowlands, M. G., Crystallographic and molecular modeling studies on 3-ethyl-3-(4-pyridyl)piperidine-2,6-dione and its butyl analog, inhibitors of mammalian aromatase. Comparison with natural substrates: prediction of enantioselectivity for N-alkyl derivatives, J. Med. Chem., 1990, 33, 2673-2679.

Le Bail, J. -C., Champavier, Y., Chulia, A. -J. and Habrioux, G., Effects of phytoestrogens on aromatase, 3β and 17β-Hydroxysteroid dehydrogenase activities and human breast cancer cells, Life Sci., 2000, 66, 1281-1291.

Le Bail, J. -C., Laroche, T., Marre-Fournier, F., and Harbrioux, G., Aromatase and 17β-hydroxysteroid dehydrogenase inhibition by flavanoids, Cancer Lett., 1998, 133, 101-106.

Le Bail, J. -C., Pouget, C., Fagnere, C., Basly, J. -P., Chulia, A. -P. and Habbrioux, G., Chalcones are potent inhibitors of aromatase and 17β-hydroxysteroid dehydrogenase activities, Life Sci., 2001, 68, 751-761.

Le Lain, R., Barrell, K. J., Saeed, G. S., Nicholls, P. J., Simons, C., Kirby, A. and Smith, H. J., Some coumarins and triphenylethene derivatives as inhibitors of human testes microsomal 17β-hydroxysteroid dehydrogenase (17β-HSD type 3): further studies with tamoxifen on the rat testes microsomal enzyme, J. Enzyme Inhib. Med. Chem., 2002, 17, 93-100.

Le Lain, R., Nicholls, P. J., Smith, H. J. and Maharlouie, F. H., Inhibitors of human and rat testes microsomal 17β-Hydroxysteroid Dehydrogenase (17β-

HSD) as Potential Agents for Prostatic Cancer, J. Enzyme Inhib., 2001, 16, 35-45.

Lee-Robichaud, P., Akhtar, M. E. and Akhtar, M., An analysis of the role of active site protic residues of cytochrome *P*-450s: mechanistic and mutational studies on 17α-hydroxylase-17,20-lyase (*P*-$450_{17\alpha}$ also CYP17) Biochem. J., 1998, 330, 967-974.

Leinonen, J., Wu, P., Stenman, U. H., Koivunen, E. and Närvänen, A., Development of novel peptide ligands modulating the enzyme activity of prostate-specific antigen, Scand. J. Clin. Lab. Inv., 2000, 60, suppl.233, 59-64.

Leong, A. S., Gilham, P., Milos, J., Cytokeratin and vimentin intermediate filaments proteins in benign and neoplastic prostatic epithilium, Histopathology, 1988, 13, 435-442.

Levy, M. A., Holt, D. A., Brandt, M. and Metcalf, B. W., Inhibition of 3(17)β-hydroxysteroid dehydrogenase from Pseudomonas testosteroni by steroidal A ring fused pyrazoles, Biochemistry, 1987, 26, 2270-2279.

Li, J., Li, Y., Son, C., Banks, P. and Brodie, A., 4-pregnene-3-one-20β-carboxaldehyde: A potent inhibitor of 17α-hydroxylase/$C_{17,20}$-lyase and of 5α-reductase, J.Steroid Biochem. Mol. Biol., 1992, 42, 313-320.

Lin, D., Black, S. M., Nagahama, Y. and Miller, W.L., Steroid 17α-hydroxylase and 17,20-lyase activities of P450c17: contributions of serine106 and P450 reductase, Endocrinology, 1993, 132, 2498-2506.

Linja, M. J., Savinainen, K. J., Saramäki, O. R., Tammela, T. L. J., Vessella, R. L. and Visakorpi, T., Amplification and Overexpression of Androgen Receptor Gene in Hormone-Refractory Prostate Cancer, Cancer Res., 2001, 61, 3550-3555.

Long, B. J., Grigoryev, D. N., Nnane, I. P., Liu, Y., Ling, Y. Z. and Brodie, A., Antiandrogenic Effects of Novel Androgen Synthesis Inhibitors on Hormone-dependent Prostate Cancer, Cancer Res., 2000, 60, 6630-6640.

Lota, R. K., Dhanani, S., Owen, C. P. and Ahmed, S., Synthesis, biochemical evaluation and rationalisation of the inhibitory activity of a series of 4-hydroxyphenyl ketones as potential inhibitors of 17β-hydroxysteroid dehydrogenase type 3 (17β-HSD3), Bioorg. Med. Chem. Lett., 2006, 16, 4519-4522.

Lowry, D. H., Rosenbrough, N. J., Farr, A. L. and Randall, R., Protein measurement with folin phenol reagent, J. Biol. Chem., 1951, 193, 265–275.

Luu-The, V., Analysis and characteristics of multiple types of human 17β-hydroxysteroid dehydrogenase, J. Steroid Biochem. Mol. Biol., 2001, 76, 143-151.

Luu-The, V., Labrie, C., Simard, J., Lachance, Y., Zhao, H. F., Couet, J., Leblanc, G. and Labrie, F., Structure of two in tandem human 17β-hydroxysteroid dehydrogenase genes, Mol. Endocrinol., 1990, 4, 268-275.

Luu-The, V., Labrie, C., Zhao, H. F., Couet, J., Lachance, Y., Simard, J., Leblanc, G., Cote, J., Berube, D., Gagne, R. and Labrie, F., Characterization of cDNAs for human estradiol 17β-dehydrogenase and assignment of the gene to chromosome 17: evidence of two mRNA species with distinct 5'-termini in human placenta, Mol. Endocrinol., 1989, 3, 1301-1309.

Lynn, W. S. and Brown, R. H., The conversion of progesterone to androgens by testes, J. Biol. Chem., 1958, 232, 1015-1030.

M

Mahapokai, W., Van Sluijs F. J. and Schalken J. A., Models for studying benign prostatic hyperplasia, Prostate Cancer P. D., 2000, 3, 28-33.

Maltais, R., Luu-The, V. and Poirier, D., Parallel solid-phase synthesis of 3β-peptido-3α-hydroxy-5α-androstan-17-one derivatives for inhibition of type 3 17β-hydroxysteroid dehydrogenase, Bioorg. Med. Chem., 2001, 9, 3101-3111.

Maltais, R., Luu-The, V. and Poirier, D., Synthesis and Optimization of a new family of type 3 17β-Hydroxysteroid Dehydrogenase Inhibitors by Parallel Liquid-Phase Chemistry, J. Med. Chem., 2002, 45, 640-653.

Mason, H. S., Oxidases, Advanced Enzymology, 1957, 19, 179-233.

Mason, J. I., Carr, B. R. and Murry, B. A., Imidazole antimycotics: Selective inhibitors of steroid aromatization and progesterone hydroxylation, Steroids, 1987, 50, 179-189.

Matsunaga, N., Kaku, T., Ojida, A., Tanaka, T., Hara, T., Yamaoka, M., Kusaka, M. and Tasaka, A., $C_{17,20}$-lyase inhibitors. Part 2: Design, synthesis and structure–activity relationships of (2-naphthylmethyl)-1*H*-imidazoles as novel $C_{17,20}$-lyase inhibitors, Bioorg. Med. Chem., 2004, 12, 4313-4336.

Matteson, K. J., Picado-Leonard, J., Chung, B. C., Mohandas, T. K. and Miller, W. L., Assignment of the gene for adrenal P450c17 (steroid 17α-hydroxylase/17,20 lyase) to human chromosome 10, J. Clin. Endocrinol. Metab., 1986, 63, 789-791.

McCague, R., Rowlands, M. G., Barrie, E. and Houghton, J., Inhibiton of enzymes of estrogen and androgen biosynthesis by esters of 4-pyridylacetic acid, J. Med. Chem., 1990, 33, 3050-3055.

McNeal, J. E., Zonal anatomy of the prostate, Prostate, 1981, 2, 35-49.

Mesiano, S., Coulter, C. L. and Jaffe, R. B., Localization of cytochrome P450 cholesterol side-chain cleavage, cytochrome P450 17α–hydroxylase/17, 20-lyase, and 3β–hydroxysteroid dehydrogenase isomerase steroidogenic enzymes in human and rhesus monkey fetal adrenal glands: reappraisal of functional zonation, J. Clin. Endocrinol. Metab., 1993, 77, 1184-1189.

N

Nagai, K., Miyamori, I., Takeda, R., Suhara, K. and Katagiri, M., Effect of ketoconazole, etomidate and other inhibitors of steroidogenesis on cytochrome P-450sccII-catalyzed reactions, J. Steroid Biochem., 1987, 28, 333-336.

Nakajin, S., Shively, J. E., Yuan, P. M. and Hall, P. F., Microsomal cytochrome P-450 from neonatal pig testis - 2 enzymatic activities (17α-hydroxylase and C17,20-lyase) associated with one protein, Biochemistry, 1981, 20, 4037-4042.

Njar, V. C. O. and Brodie, A. M. H., Inhibitors of 17α-Hydroxylase/17,20-Lyase (CYP17): Potential Agents for the Treatment of Prostate Cancer, Curr. Pharm. Design, 1999, 5, 163-180.

Njar, V. C. O., Hector, M. and Hartmann, R. W., 20-Amino and 20,21-aziridinyl pregnene steroids: Development of potent inhibitors of 17α-hydroxylase/C17,20-lyase (P450 17), Bioorg. Med. Chem., 1996b, 4, 1447-1453.

Njar, V. C. O., Klus, G. T., Johnson, H. H. and Brodie, A. M. H., Synthesis of novel 21-Trifluoropregnane steroids: Inhibitors of 17α–hydroxylase/l7,20-lyase (17α-lyase), Steroids, 1997, 62, 468-473.

Nnane, I. P. , Njar, V. C. O., Liu, Y., Lu, Q. and Brodie, A. M. H., Effects of novel 17-azolyl compounds on androgen synthesis in vitro and in vivo, The J. Steroid Biochem. Mol. Biol., 1999a, 71, 145-152.

Nnane, I. P., Kato, K., Liu, Y., Long, B. J., Lu, Q., Wang, X., Ling, Y-Z. and Brodie, A., "Inhibition of androgen synthesis in testicular and prostatic microsomes and in male rats by novel steroidal compounds" Endocrinology, 1999b, 140: 2891-2897.

O

Obasaju, C. and Hudes, G. R., Paclitaxel and docetaxel in prostate cancer, Hematol. Oncol. Clin. N., 2001, 15, 525.

Oritz de Montellano, P. R., In Cytochrome P-450 Structure, Mechanism and Biochemistry, P. R., Oritz de Montellano, (ed.), New York, Plenum Press, 1986.

Owen, C. P., Synthesis and Evaluation of Inhibitors of 17α-Hydroxylase/17,20-Lyase as Potential Anti-tumour Agents, University of Wales College of Cardiff, 1995.

Owen, C. P. and Ahmed, S., The derivation of a potential transition state for the reduction reaction catalysed by 17β-hydroxysteroid dehydrogenase—an approximate representation of its active site for use in drug design and discovery, Biochem. Biophys. Res. Comm., 2004, 318, 131-134.

P

Peehl, D. M., Krishnan, A. V. and Feldman, D., Pathways Mediating the Growth-Inhibitory Actions of Vitamin D in Prostate Cancer, J. Nutr., 2003, 133, 2461S-2469S.

Penning, T. M., Molecular determinants of steroid recognition and catalysis in aldo-keto reductases. Lessons from 3α-hydroxysteroid dehydrogenase , J. Steroid Biochem. Mol. Biol., 1999, 69, 211-225.

Pentyala, S. N., Whyard, T. C., Waltzer, W. C., Meek, A. G. and Hod, Y., Androgen induction of urokinase gene expression in Incap cells is dependent on their interaction with the extracellular matrix, Cancer Lett., 1998, 130, 121-126.

Pentyala, S. N., Lee, J., Hsieh, K., Waltzer, W. C., Trocchia, A., Musacchia, L., Rebecchi, M. J. and Khan, S. A., Prostate cancer: a comprehensive review, Med. Oncol., 2000, 17, 85-105.

Perrin, A., Chambaz, E. M. and Defay, G., Modulation of hydroxylase and lyase activities of bovine cytochrome *P*-$450_{17\alpha}$ in adrenal and testicular microsomes by a tissue-specific local membrane environment, J. Steroid Biochem. Mol. Biol., 1995, 54, 121-129.

Poirier, D., Dionne, P. and Auger, S., A 6β-(Thiaheptanamide) Derivative of Estradiol as Inhibitor of 17β-Hydroxysteroid Dehydrogenase Type 1, J. Steroid Biochem. Mol. Biol., 1998, 64, 83-90.

Pollard, M. and Luckert, P. H., Promotional effects of testosterone and high fat diet on the development of autochthonous prostate cancer in rats., Cancer Lett., 1986 32, 223-227.

Potter, G. A., Barrie, S. E., Jarman, M. and Rowlands, M. G., Novel Steroidal Inhibitors of Human Cytochrome P45017α-Hydroxylase-C17,20-lyase): Potential Agents for the Treatment of Prostatic Cancer, J. Med. Chem., 1995, 38, 2463-2471.

Pour, P. M., Groot, K., Kazakoff, K., Anderson, K. and Schally, A. V., Effects of high-fat diet on the patterns of prostatic cancer induced in rats by N-nitrosobis(2-oxopropyl)amine and testosterone., Cancer Res., 1991, 51, 4757–4761.

Q

Quigley, C. A., De Bellis, A., Marschke, K. B., el-Awady, M. K., Wilson, E. M. and French, F. S., Androgen receptor defects: historical, clinical, and molecular perspectives, Endocr. Rev., 1995, 16, 271-321.

R

Rang, H. P., Dale, M. M. and Ritter, J. M., Pharmacology third edition 696-699, 1996, Churchill Livingstone, Edinburgh.

Ross, R. K., Bernstein, L., Pike, M. C., Henderson, B. E., Lobo, R. A., Stanczyk, F. Z. and Shimizu, H., 5α-reductase activity and risk of prostate cancer among Japanese and US white and black males, Lancet, 1992, 339, 887-889 .

Rotstein, D. M., Kertesz, D. J., Walker, K. A. M. and Swinney, D. C., Stereoisomers of ketoconazole: preparation and biological activity, J. Med. Chem., 1992, 35, 2818-2825.

Rovira, C., Ballone, P. and Parrinello, M., A density functional study of iron-porphyrin complexes, Chem. Phys. Lett., 1997, 271, 247-250.

Rowlands, M. G., Barrie, S. E., Chan, F., Houghton, J., Jarman, M., McCague, R. and Potter, G. A., Esters of 3-Pyridylacetic Acid That Combine Potent Inhibition of 17α-Hydroxylase/C17,20-Lyase (Cytochrome P45017α) with Resistance to Esterase Hydrolysis, J. Med. Chem., 1995, 38, 4191-4197.

S

Sartora, O., Zhenga, Q. and Easthama, J. A., Androgen receptor gene CAG repeat length varies in a race-specific fashion in men without prostate cancer, Urology, 1999, 53, 378-380.

Sasano, H., Okamoto, M., Mason, J. I., Simpson, E. R., Mendelson, C. R., Sasano, N. and Silverberg, S. G., Immunohistochemical studies of steroidogenic enzymes (aromatase, 17α-hydroxylase and cholesterol side-chain cleavage cytochromes P-450) in sex cord-stromal tumors of the ovary, Human Pathol., 1989, 20, 452-457.

Sergejew, T. and Hartmann, R. W., Pyridyl substituted benzocycloalkenes – new inhibitors of 17-alpha-hydroxylase – 17,20-lyase (P450 17-alpha), J. Enzym. Inhib., 1994, 8, 113-122.

Shen M., Robert Wood Johnson Medical School; comparative anatomy of the human and mouse prostate glands, *Comparative Mammalian Anatomy Atlas*, 2001, http://ccm.ucdavis.edu/mmhcc/prostate/comparativeindex.htm.

Shirai, T., Yamamoto, A., Iwasaki, S., Tamano, S. and Masui, T., Induction of invasive carcinomas of the seminal vesicles and coagulating glands of F344 rats by administration of *N*-methylnitrosourea or *N*-nitrosobis(2-oxopropyl) amine and followed by testosterone propionate with or without high-fat diet., Carcinogenesis, 1991, 12, 2169–2173.

Siiteri, P. K., and Wilson, J. D., Dihydrotestosterone in prostatic hypertrophy. I. The formation and content of dihydrotestosterone in hypertrophic prostate of man, J. Clin. Invest., 1970, 49, 1737-1745.

Simard, J., Couet, J., Durocher, F., Labrie, Y., Sanchez, R., Breton, N., Turgeon, C. and Labrie, F., Structure and tissue-specific expression of a novel member of the rat 3 beta-hydroxysteroid dehydrogenase/delta 5-delta 4 isomerase (3β-HSD) family. The exclusive 3 beta-HSD gene expression in the skin, J. Biol. Chem., 1993, 26, 19659-19668.

Simard, J., Dumont, M., Soucy, P. and Labrie, F., Perspective: Prostate Cancer Susceptibility Genes, Endocrinology, 2002, 143, 2029-2040.

Smith, H. J., Nicholls, P. J., Simons, C. and Lain, R. L., Inhibitors of steroidogenesis as agents for the treatment of hormone-dependent cancers, Expert Opin. Ther. Pat., 2001, 11, 789-824.

Soucy, P. and Luu-The, V., Conversion of pregnenolone to DHEA by human 17α-hydroxylase/17, 20-lyase (P450c17): evidence that DHEA is produced from the released intermediate, 17alpha-hydroxypregnenolone. Eur. J. Biochem., 2000, 267, 3243–3247.

Sparkes, R. S., Klisak, I. and Miller, W. L., Regional Mapping of genes encoding human steroidogenic enzymes - P450SCC to 15Q23-Q24, adrenodoxin to 11Q22 – adrenonodoxin reductase to 17Q24-Q25 - and P450C17 to 10Q24-Q25, DNA Cell Biol., 1991, 10, 359-365.

Spires, T. E., Fink, B. E., Kick, E. K., You, D., Rizzo, C. A., Takenaka, I., Lawrence, R. M., Ruan, Z., Salvati, M. E., Vite, G. D., Weinmann, R., Attar, R. M., Gottardis, M. M. and Lorenzi, M. V., Identification of novel functional inhibitors of 17β-hydroxysteroid dehydrogenase type III (17β-HSD3), The Prostate, 2005, 65, 159-170.

Stenman, U., Leinonen, J., Zhang, W. and Finne, P., Prostate-specific antigen, Semin. Cancer Biol, 1999, 9, 83-93.

Suzuki, S., Tadakuma, T., Asano, T., and Hayakawa, M., Coexpression of the Partial Androgen Receptor Enhances the Efficacy of Prostate-specific Antigen Promoter-driven Suicide Gene Therapy for Prostate Cancer Cells at Low Testosterone Concentrations, Cancer Res., 2001, 61, 1276-1279.

Swart, P., Swart, A. C., Waterman, M. R., Estabrook, R. W. and Mason, J. I., Progesterone 16α-hydroxylase activity is catalyzed by human cytochrome P450 17α-hydroxylase, J. Clin. Endocrinol. Metab., 1993, 77, 98-102.

Sweet, F., Boyd, J., Medina, O., Konderski, L. and Murdock, G. L., Hydrogen bonding in steroidogenesis: Studies on new heterocyclic analogs of estrone that inhibit human estradiol 17β-dehydrogenase, Biochem. Biophys. Res. Comm., 1991, 180, 1057-1063.

T

Tortora, G. J. and Anagnostakos N. P., Principles of Anatomy and Physiology, 6th Ed., 1990, 890, Harper Collins, New York.

Trachtenberg, J. and Zadra, J., Steroid-synthesis inhibition by Ketoconazole – sites of action, Clin. Invest. Med., 1988, 11, 1-5.

Tremblay, M. R., Luu-The, V., Leblanc, G., Noël, P., Breton, E., Labrie, F. and Poirier, D., Spironolactone-related inhibitors of type II 17β-hydroxysteroid dehydrogenase: chemical synthesis, receptor binding affinities, and proliferative/antiproliferative activities, Bioorg. Med. Chem., 1999, 7, 1013-1023.

V

Van Wauwe, J. P., and Janssen, P. A. J., Is There a Case for P-450 Inhibitors in Cancer Treatment?, J. Med. Chem., 1989, 32, 2231-2239.

W

Wachall, B. G., Hector, M., Zhuang, Y. and Hartmann, R. W., Imidazole substituted biphenyls: A new class of highly potent and in vivo active inhibitors of P450 17 as potential therapeutics for treatment of prostate cancer, Bioorg. Med. Chem.,1999, 7, 1913-1924.

Wächter, G. A., Hartmann, R. W., Sergejew, T., Grün, G. L. and Ledergerber, D., Tetrahydronaphthalenes: Influence of Heterocyclic Substituents on Inhibition of Steroidogenic Enzymes P450 arom and P450 17, J. Med. Chem., 1996a, 39, 834-841.

Watanabe, M., Nakayama, T., Shiraishi, T., Stemmermann, G. N. and Yatani, R., Comparative studies of prostate cancer in Japan versus the United States, Urol. Oncol., 2000, 5, 274-283.

Weusten, J. J. A. M., Smals, A. G. H., Hofman, J. A., Kloppenborg, P. W. C. and Benraad, T. J., The sex pheromone precursor androsta-5,16-dien-3β-ol is a major early metabolite in in vitro pregnenolone metabolism in human testicular homogenates, J. Clin. Endocrinol. Metab., 1987, 65, 753-756.

Y

Young, H. S., Jones, L. R. and Stokes D. L., Locating phospholamban in co-crystals with Ca2+-ATPase by cryoelectron microscopy, Biophys. J., 2001, 81, 884-894.

Zhang, W. -M., Finne, P., Leinonen, J., Salo, J. and Stenman, U. -H., Determination of prostate-specific antigen complexed to α_2-macroglobulin in serum increases the specificity of free to $total_{PSA}$ for prostate cancer, Urology, 2000, 56, 267-272.

Zhang, Y., Ni, J., Messing, E. M., Chang, E., Yang, C. -R. and Yeh, S., Vitamin E succinate inhibits the function of androgen receptor and the expression of prostate-specific antigen in prostate cancer cells, Proc. Natl. Acad. Sci. U.S.A., 2002, 99, 7408-7413.

Zhuang, Y., Wachall, B. G. and Hartmann, R. W., Novel imidazolyl and triazolyl substituted biphenyl compounds: synthesis and evaluation as nonsteroidal inhibitors of human 17α-hydroxylase-C17, 20-Lyase (P450 17), Bioorg. Med. Chem., 2000, 8, 1245-1252.